

Seventh US-Japan Workshop

on

Inertial Electrostatic Confinement Fusion

Sponsored by Alme and Associates and Los Alamos National Laboratory

March 14-16, 2005

Los Alamos, New Mexico, USA

Welcome

Seventh US-Japan Workshop on
Inertial Confinement Fusion
March 14-16, 2005
Los Alamos, NM

Seventh US-Japan Workshop
on
Inertial Electrostatic Confinement Fusion
Sponsored by Alme and Associates and Los Alamos National Laboratory
March 14-16, 2005
Los Alamos, New Mexico, USA

INDEX

[PRESENTATION LIST](#)

[ABSTRACTS](#)

[PAPERS](#)

[CONCLUDING REMARKS](#)

[PHOTOGRAPHS](#)

Seventh US-Japan Workshop on
Inertial Confinement Fusion
March 14-16, 2005
Los Alamos, NM

Seventh US-Japan Workshop
on
Inertial Electrostatic Confinement Fusion

Sponsored by Alme and Associates and Los Alamos National Laboratory

March 14-16, 2005

Los Alamos, New Mexico, USA

PRESENTATIONS

SESSION I

1) “Recent Progress in Periodically Oscillating Plasma Sphere (POPS) and Neutron Source Development at LANL”

J. Park, R. A. Nebel, S. M. Stange, and *C. R. Mansfield

*Los Alamos National Laboratory, and *Alme and Associates, Los Alamos, NM 87544*

[Abstract](#) [Paper](#)

2) “Recent Results of Energetic neutral energy measurement at an end of the cylindrical IECF device at Kyoto University”

Y. Yamamoto, Y. Ueno, K. Noborio, and S. Konishi

Institute of Advanced Energy, Kyoto University, Gokasho, Uji, Kyoto 611-0011, Japan

[Abstract](#) [Paper](#)

3) “Overview and History of the University of Wisconsin IEC Fusion Project”

R. P. Ashley

Fusion Technology Institute, Department of Engineering Physics, University of Wisconsin

[Abstract](#) [Paper](#)

SESSION II

4) “Neutron Yield in Spherical Convergent Ion Focus Fusion”

Masami Ohnishi, Hodaka Osawa, Takehiro Tabata, Shigehisa Yoshimura

*Department of Electrical Engineering and Computer Science, Kansai University 3-3-35,
Yamate-cho, Suita-shi, Osaka 564-8680*

[Abstract](#) [Paper](#)

5) “Dipole-Assisted Inertial Electrostatic Confinement”

George H. Miley, Hiromu Momota, Rob Thomas, and Yoshi Takeyama

*Department of Nuclear, Plasma and Radiological Engineering, University of Illinois,
Urbana, IL 61801, USA*

[Abstract](#) [Paper](#)

6) "Performance Characteristics of Ion-Source-Assisted Cylindrical IEC Fusion Neutron/Proton Source"

*Kunihiro Yamauchi, Atsushi Tashiro, Sonoe Ohura, Masato Watanabe, Akitoshi Okino,
Toshiyuki Kohno, Eiki Hotta, and Morimasa Yuura^{a)}

*Dept. of Energy Sciences, Tokyo Institute of Technology, Yokohama 226-8502,
Japan ^{a)}Pulse Electronic Engineering Co.,Ltd., Noda, Chiba 278-0016, Japan*

[Abstract](#) [Paper](#)

SESSION III

7) "Atomic Physics Effects on IEC Ion Radial Flow"

G.A. Emmert and J.F. Santarius

*Fusion Technology Institute, Department of Engineering Physics, University of Wisconsin
[Abstract](#) [Paper](#)*

8) "Development of Low-Energetic Metastable Helium Beam Injector for Electric Field Diagnostics through Laser-Induced Fluorescence"

K. Masuda, T. Ando, T. Nishi, H. Toku and K. Yoshikawa

Institute of Advanced Energy, Kyoto University

[Abstract](#) [Paper](#)

9) "MEIEC (Microwave Enhancement of Inertial Electrostatic Confinement) of Plasmas: Theory and Experiment"

John Brandenburg and Marin Racic

Florida Space, MS: FSI, Kennedy Space Center FL 3899

[Abstract](#) [Paper](#)

SESSION IV

10) "Progress in the Development of a ^3He Ion Source for IEC Fusion"

Gregory R. Piefer, John F. Santarius, Robert P. Ashley, Gerald L. Kulcinski

*Fusion Technology Institute—University of Wisconsin Madison: 1500 Engineering Drive,
Madison, WI, USA, 53706*

[Abstract](#) [Paper](#)

11) "Measurement of D- ^3He Protons in an Inertial Electrostatic Confinement Fusion"

S. Ogawa, T. Hama, T. Takamatsu, K. Masuda, H. Toku and K. Yoshikawa

Institute of Advanced Energy, Kyoto University

[Abstract](#) [Paper](#)

12) "Progress in Explosives Detection using D-D Fusion at the University of Wisconsin-Madison"

A.L. Wehmeyer, G.L. Kulcinski, R.P. Ashley, J.F. Santarius, G.R. Piefer, R.F. Radel,
T.E. Radel, D.R. Boris, R.C. Giar, and E.C. Alderson

Fusion Technology Institute, University of Wisconsin, Madison, WI

[Abstract](#) [Paper](#)

13) "Coaxial neutron generators using RF-driven plasmas"

Kyoung-Jae Chung, Min-Joon Park, and Yong-Seok Hwang

*Department of Nuclear Engineering, Seoul National University, San 56-1, Shillim-dong,
Gwanak-gu, Seoul 151-742, Republic of Korea, E-mail: yhwang@snu.ac.kr*

[Abstract](#) [Paper](#)

SESSION V

14) “A Magnetron Discharge Ion Source for an Inertial Electrostatic Confinement Fusion Device”

Teruhisa Takamatsu, Toshiyuki Kyunai, Satoshi Ogawa, Kai Masuda, Hisayuki Toku, and Kiyoshi Yoshikawa

Institute of Advanced Energy, Kyoto University, Uji, Kyoto 611-0011, Japan

[Abstract](#) [Paper](#)

15) “Implantation of D⁺ and He⁺ in Candidate Fusion First Wall Materials”

R.F. Radel, G.L. Kulcinski, R.P. Ashley, J.F. Santarius, G.R. Piefer, A.L. Wehmeyer, D.R. Boris, R.C. Giar, T.E. Radel, and E.C. Alderson

Fusion Technology Institute, Madison, WI<mailto:rfradel@wisc.edu>

[Abstract](#) [Paper](#)

16) “Neutron Production through Beam-Beam Collision at Low Gas Pressure and Large Current Operation”

K. Noborio, Y. Yamamoto, Y. Ueno, and S. Konishi

Institute of Advanced Energy, Kyoto University, Gokasho, Uji, Kyoto 611-0011, Japan

[Abstract](#) [Paper](#)

17) “Plasma Compression in the Periodically Oscillating Plasma Sphere”

R. A. Nebel, L. Chacon, J. Park, E. Evstati

Los Alamos National Laboratory, Los Alamos, New Mexico 87545

[Abstract](#) [Paper](#)

Session VI

18) “Numerical Study on Hollow Cathode Discharge of IEC Fusion”

Hodaka OSAWA and Masami OHNISHI

Dept. of Electrical Engineering, Kansai University. Suita ,Osaka JAPAN

osawa@kansai-u.ac.jp

[Abstract](#) [Paper](#)

19) “Kinetic Simulation of Inertial_Electrostatic Confinement Experiments at Los Alamos National Laboratory”

G. Lapenta (T_15), R.A. Nebel (X_3), J. Park (P_24): Plasma Theory Group (T_15), Integrated Physics Methods Group (X_3), Plasma Physics Group (P_24)

Los Alamos National Laboratory, University of California

[Abstract](#) [Paper](#)

Seventh US-Japan Workshop on
Inertial Electrostatic Confinement Fusion
March 14-16, 2005
Los Alamos, NM

SESSION I

Recent Progress in Periodically Oscillating Plasma Sphere (POPS) and Neutron Source Development at LANL

J. Park, R. A. Nebel, S. M. Stange, and *C. R. Mansfield

*Los Alamos National Laboratory, and *Alme and Associates, Los Alamos, NM 87544*

The inertial electrostatic confinement (IEC) system provides a favorable development path for practical fusion applications for technical simplicity, compact size, and long target lifetime. In order to improve the efficiency of the IEC system, a plasma heating concept based on a periodically oscillating plasma sphere (POPS) has been proposed theoretically¹, which may achieve breakeven. In this talk, we will describe the recent experimental measurements providing the first confirmation of the POPS mode. When an external radio-frequency oscillation is imposed at the POPS frequency, the resonance heating of ions results in enhanced ion losses and subsequent delays in virtual cathode decay. Excellent quantitative agreement between experimental results and theoretical predictions has been observed for a wide range of potential well depths and three different ion species: hydrogen, helium and neon. Furthermore, dynamic control of the virtual cathode lifetime using the POPS concept has been demonstrated by controlling the amplitude of the external rf modulation at the POPS resonance. In addition, a number of important theoretical milestones have been made; self-consistent simulation of plasma compression during POPS, two-stream stability in spherical geometry, and two-dimensional particle-in-cell simulation of gridded IEC system. The details of these findings will be discussed by Nebel and Lapenta. Separately, we will discuss about the recent collaborative efforts among LANL, Alme & Associates and U. Wisconsin in R&D of intense neutron source for nuclear assay applications.

TOP

Recent Results of Energetic neutral energy measurement at an end of the cylindrical IECF device at Kyoto University

Y. Yamamoto, Y. Ueno, K. Noborio, and S. Konishi

Institute of Advanced Energy, Kyoto University, Gokasho, Uji, Kyoto 611-0011, Japan

To estimate change of energy distribution and fusion reaction rate when operating gas pressure of the cylindrical IECF was reduced, we have been trying to measure neutral beam energy distributions at an end of the cylindrical IECF by using a re-ionization cell and an energy analyzer. In preliminary result, three energy peaks are observed at the higher pressure ($\sim 2\text{Pa}$) operation with self discharge (glow). The peaks shift to higher energy side with increase of the applied voltage to the cathode. When the plasma source is turned on, which is attached to another side anode, the higher energy peak appeared which indicates ions are generated near the anode. When the pressure is reduced to less than 0.3Pa where no self discharge occurs and IECF discharge is assisted by ion injections, three peaks are also observed, but the measured ion currents increases more than 10 times larger than these at higher pressure. This indicates the discharge phenomenon is changed.

These preliminary results were reported at the 16th TOFE meeting at Madison WI. After that meeting we have been developing a calculating code to estimate the energy distributions at the anode from the measured distribution at the analyzer. This code assumes that ion does not circulate between electrodes as the mean free path of charge exchange process is shorter than the length of the cylindrical IECF. The calculation includes neutralization, re-ionization, and dissociation processes along the beam path and can calculate change of beam energy and distribution both for forward direction and backward direction.

It is found from calculations that almost all D₂ particles dissociate to D atoms in the re-ionization cell as the pressure is higher enough. Using this result, we have reconsidered the measured results and tried to find out the relation ship between the operating gas pressure of the IECF and neutron production rate. The results will be presented at the meeting.

TOP

Overview and History of the University of Wisconsin IEC Fusion Project

R. P. Ashley

*Fusion Technology Institute, Department of Engineering Physics,
University of Wisconsin*

This past year has seen several new projects created at the UW IEC group. Testing the activation of unexploded ordinance (UXO, chemical explosives) with our steady state flux of neutrons from the D-D fusion reaction has begun. A large area gamma detector for the activation of UXO has been acquired and the shielding requirements for it are optimizing. In addition to our steady state operations, we are testing out a pulsed mode system. This is based on pulsing the source of ions rather than pulsing the high voltage on the cathode. We have also used the IEC configuration to reproduce the effects of He bombardment on tungsten samples at various temperatures. The development of a Helicon ion source to allow low pressure operation with ^3He in our second IEC chamber is continuing. A timeline of the history of the UW IEC group will also be presented.

TOP

Seventh US-Japan Workshop on
Inertial Electrostatic Confinement Fusion
March 14-16, 2005
Los Alamos, NM

SESSION II

Neutron Yield in Spherical Convergent Ion Focus Fusion

Masami Ohnishi, Hodaka Osawa, Takehiro Tabata, Shigehisa Yoshimura

*Department of Electrical Engineering and Computer Science
Kansai University 3-3-35 Yamate-cho, Suita-shi, Osaka 564-8680*

A device which causes fusion reactions by spherically converging deuterium ions into the center is paid attention because it produces anomalously more neutrons than expected. Based upon the experimental data, we identify the origin of neutron yield to be mainly fusion reactions between D_2^+ ions, not D^+ ions, and background neutral molecules D_2^0 . The unexpected high neutron production is explained by the reaction between both of D_2^+ and fast neutral D_2^0 produced by charge exchange and background molecules. At low applied voltage, the reactivity of D^+ ions and D^0 neutrals, however, plays a role in neutron production because they gain twofold higher energy per nucleon compared with D_2^+ and D_2^0 particles. In order to estimate neutron yield, we propose a physically simple model of fusion reaction in the core of the device and derive a semi-theoretical expression including the dependences of background neutral gas pressure, cathode transparency, radii of cathode and anode and applied voltage. The expression gives a neutron production rate consistent with the experiment.

TOP

Dipole-Assisted Inertial Electrostatic Confinement

*Department of Nuclear, Plasma and Radiological Engineering, University of Illinois,
Urbana, IL 61801, USA, ghmiley@uiuc.edu*

George H. Miley, Hiromu Momota, Rob Thomas, and Yoshi Takeyama

The scale-up of inertial electrostatic confinement (IEC) fusion for higher yield neutron source applications, electrical production, or spacecraft production, the IEC must overcome several crucial physics issues including electron confinement, ion loss rates, charge exchange limitations, ion collision time scales, and ion source profiling. We are currently studying one potential opportunity to enhance the IEC confinement by augmenting it with a magnetic dipole configuration. Some of the aforementioned issues and challenges may be reduced or possibly eliminated in the resulting “dipole-assisted IEC”. The theory is that the dipole fields will enhance the plasma density in the center region of the IEC and the combined IEC and dipole confinement properties will reduce plasma losses. Additionally, the dipole configuration, like the IEC, are well suited for D-³He fusion [1,2]. The levitated dipole experiment (LDX) currently being conducted at MIT and Columbia University also looks promising for future power units. However, there also exist technical issues such as fueling, heating and radiation damage of the superconducting coil, and low power density that make the LDX scale-up challenging. The dipole-assisted IEC should provide valuable additional insight into these issues and may provide a way around some.

To demonstrate that a hybrid Dipole-IEC configuration can provide an improved neutron source vs. a stand alone IEC, a first model Dipole-IEC experiment is being benchmarked against a reference IEC. Two half-bowl shaped cathode grids are put into the upper and lower sides of the dipole, to accelerate ions toward the center of the IEC. The dipole is electrically isolated from the grids, with four separate supports. The magnetic flux along the z-axis of the magnetic coil will provide a preferred path for the highly dense plasma. When the B-field lines exit the IEC grid, the electrostatic field dominates and reflects most particles back inside the grids, where the magnetic field once again dominates. Thus particles oscillate much as they would in a normal IEC with the added benefit of having a preferential particle trajectory to focus the plasma much like in an IEC based jet mode configuration. Multiple electric probe diagnostics are being used to characterize the plasma properties inside of the IEC. A triple Langmuir probe is used to find the electron temperature and density. A triple probe is advantageous over single and double Langmuir probes because it does not require a voltage sweep and the associated tedious curve fitting. An emissive probe will also be used to characterize the potential surface characteristics inside the plasma.

Initial results from these experiments will be described along with a discussion of scale-up issues.

1. Hasegawa, A., Chen, L., Mauel, M.E., Warren, H.H., Murakami, S., “A Description of a D-³He Fusion Reactor Based on a Dipole Magnetic Field,” *Fusion Technology*, Vol. 22, Aug. 1992.

2. Teller, E., Glass, A.J., Fowler, Hasegawa, A., Santarius, J.F., “Space Propulsion by Fusion in a Magnetic Dipole,” *Fusion Technology*, Vol. 22, Aug. 1992.

TOP

Performance Characteristics of Ion-Source-Assisted Cylindrical IEC Fusion Neutron/Proton Source

*Kunihiro Yamauchi, Atsushi Tashiro, Sonoe Ohura, Masato Watanabe,
Akitoshi Okino, Toshiyuki Kohno, Eiki Hotta, and Morimasa Yuura^{a)}

Dept. of Energy Sciences, Tokyo Institute of Technology, Yokohama 226-8502, Japan

^{a)}Pulse Electronic Engineering Co.,Ltd., Noda, Chiba 278-0016, Japan

Inertial electrostatic confinement (IEC) fusion has been studied for practical use as a portable neutron/proton source for various applications such as landmine detection and medical positron emission tomography. However, some problems remain for the practical use, and the most critical one is the insufficiency of absolute neutron/proton yields. In this study, a new IEC device was designed and tested to obtain high neutron/proton yields. The key features of the new device are the cylindrical electrode configuration in consideration of better electrostatic confinement of ions and extraction of protons, and an integrated bucket-type ion source which consists of sixteen ferrite magnets and sixteen filaments. To investigate the performance characteristics of the device and the effect of the ion source, three types of experimental setup were used for comparison. At first, the basic IEC setup was operated. Then a cusp magnetic field was applied by using ferrite magnets, and a thermionic cathode was added. As a result, it was confirmed that the ion source works effectively. At the same discharge condition of voltage and current, the obtained neutron production rate was about one order of magnitude higher than that of the conventional spherical IEC device.

TOP

Seventh US-Japan Workshop on
Inertial Electrostatic Confinement Fusion
March 14-16, 2005
Los Alamos, NM

SESSION III

Atomic Physics Effects on IEC Ion Radial Flow

G.A. Emmert and J.F. Santarius

Fusion Technology Institute, Department of Engineering Physics, University of Wisconsin

A simple model for the effect of charge exchange and ion impact ionization of background gas on the performance of spherical, gridded IEC devices has been developed. Ions entering the intergrid region are not only accelerated by the falling electrostatic potential, but also produce a source of cold ions through charge exchange and ion impact ionization of the background gas. Charge exchange is treated as a loss of ions with finite energy and a corresponding source of cold ions. The cold ions are also accelerated by the potential and, in turn, produce additional cold ions. A formalism has been developed which includes the bouncing motion of ions in the electrostatic potential well and sums over all generations of cold ions. This leads to a Volterra integral equation for the resulting total cold ion source function. Given the source function, the energy spectrum of the ion and fast neutral flux as a function of radius can be calculated. The integral equation has been solved numerically. Macroscopic quantities, such as the current collected by the cathode, and the fusion rate between ions and fast neutrals with the background gas, are calculated and compared with representative experimental values for the Wisconsin IEC device.

TOP

Development of Low-Energetic Metastable Helium Beam Injector for Electric Field Diagnostics through Laser-Induced Fluorescence

K. Masuda, T. Ando, T. Nishi, H. Toku and K. Yoshikawa

Institute of Advanced Energy, Kyoto University

The Laser-Induced Fluorescence (LIF) method could be an efficient tool for understanding the electric potential formation in IEC core plasmas which is no doubt one of the most intensive interests in IEC researches. Our LIF diagnostics system making use of the Stark effects in forbidden transition of He I has successfully revealed potential profiles in helium discharge IEC plasmas under relatively high operating gas pressure, where ample 2^1S metastable atoms are provided by the IEC discharge itself. In order to extend its application to lower pressure (i.e. higher voltage) operational plasmas, and deuterium plasmas as well, we intensively develop a pulsed beam injector of low-energetic 2^1S helium atoms. The key R&D issues are injection of an intense and convergent supersonic gas jet, and production of a highly efficient exciter plasma under low operational gas pressure, both of which are essential for the minimal perturbation in the objective IEC plasmas. After the last workshop, by optimal arrangement and operation of the fast electromagnetic valve and the skimmer (with a 1-2 mm diameter pin hole), almost ten times dense gas jet has been obtained. A compact magnetron-discharge-based system has also been developed which can produce a race-track-shaped plasma with a 5 cm long straight section capable of strong interaction with the injected gas jet. Its accessible helium gas pressure in preliminary dc experiments has recently reached 0.04 Pa which is as low as the achieved on-axis density in the supersonic gas jet. We are then carrying out experiments of pulsed operation of the magnetron-based excitation system by the pulsed gas jet injection. Also, spectroscopic measurements of the exciter plasma properties are being performed.

TOP

MEIEC (Microwave Enhancement of Inertial Electrostatic Confinement) of Plasmas: Theory and Experiment

John Brandenburg and Marin Racic

Florida Space, MS: FSI, Kennedy Space Center FL 3899

Recent experiments at 2.45GHz have indicated that spherical IEC (Inertial Electrostatic Confinement) plasmas can be compressed by HPM(High Power Microwaves) in a technique called MEIEC (Microwave Enhanced Inertial Electrostatic Confinement). In IEC plasma is formed and confined in a hollow porous geodesic cathode. Theory of IEC , using a form of the viral theorem, is shown to relate the confined plasma pressure to electrostatic energy density on the surface of the hollow cathode. Thus confined energy density is proportional to the voltage squared. This theory is then modified to include the “Ponderomotive Force”of microwaves on a plasma, with the result that microwave field energy density is found to contribute to electrostatic energy density in the viral expression for plasma pressure confinement. Thus , in this theory, microwaves can enhance, or even replace to a degree, the electrostatic fields used to confine the plasma. In a low cost experiment, the plasmas were created and initially heated and confined by IEC in a geodesic porous cathode and then irradiated with microwaves. The IEC plasma , generated at low voltages of approximately 500V , were observed to shrink and brighten noticeably when microwave powers of approximately 600W were introduced. Thus , these preliminary results appear to support the theory of MEIEC and suggest that further experiments may prove fruitful.

TOP

Seventh US-Japan Workshop on
Inertial Electrostatic Confinement Fusion
March 14-16, 2005
Los Alamos, NM

SESSION IV

Progress in the Development of a ${}^3\text{He}$ Ion Source for IEC Fusion

Gregory R. Piefer, John F. Santarius, Robert P. Ashley, Gerald L. Kulcinski

*Fusion Technology Institute, University of Wisconsin Madison, 1500 Engineering Drive,
Madison, WI, USA, 53706, grpiefer@wisc.edu*

Developments in ${}^3\text{He}$ ion sources at UW-Madison have produced steady state ion currents of 10 mA into IEC systems with background gas pressures as low as 200 μtorr . These developments will allow researchers to attempt observation of the ${}^3\text{He}-{}^3\text{He}$ reaction in an IEC device. Preliminary calculations of beam-background fusion rates predict that a ${}^3\text{He}-{}^3\text{He}$ spectrum should be observable in an IEC operating below 200 kV. This capability can provide valuable data regarding ${}^3\text{He}$ fusion cross sections at “low” energies with better counting statistics than accelerator measurements. Progress in source development, and preliminary results will be discussed.

TOP

Measurement of D-³He Protons in an Inertial Electrostatic Confinement Fusion

S. Ogawa, T. Hama, T. Takamatsu, K. Masuda, H. Toku and K. Yoshikawa

Institute of Advanced Energy, Kyoto University

A proton counting system was designed for a higher S/N ratio in detecting both the 3.03 and 14.7MeV protons from D-³He IECF plasmas.

The counting system is basically the same as that we have used for D-D proton measurements, and that is being used at UW Madison. We use a semiconductor diode (Solid-State Detector: SSD). A metallic foil is set up in front of the SSD to block the metallic ions due to sputtering and electrons and X rays that cause the noise. The SSD we have chosen for the scheduled D-³He experiments is Li implanted Si diode of a 27.6-mm diameter and a 2-mm thickness capable of identification of 14.7MeV proton energy.

As of the foil for shielding the SSD, we have used 25- μ m thick lead foil. However the lead foil is found to result in a poor S/N ratio in detecting 3.03MeV protons, because of too much proton energy loss through the foil. For the present counting system, we examined an optimal shielding foil thickness and material as follows.

First of all, it is found difficult to block 100keV X rays from the IECF device with a metallic foil, because 100keV X-rays have higher transmittance than the objective 3.03 MeV protons. Therefore in this design, we focus on shielding from electrons and energy loss of D-D protons. We select the foil to block 100keV electrons and to obtain least energy loss of D-D protons. Also, we consider use of deflection magnet for blocking the 100keV electrons. With the magnetic deflector, the foil is to be used only for blocking low-energetic ions by sputtering, and thus it could be much thinner. Preliminary experiments by use of this proton counting system are scheduled for this February. The results will be also presented.

TOP

Progress in Explosives Detection using D-D Fusion at the University of Wisconsin-Madison

A.L. Wehmeyer, G.L. Kulcinski, R.P. Ashley, J.F. Santarius, G.R. Piefer, R.F. Radel,
T.E. Radel, D.R. Boris, R.C. Giar, and E.C. Alderson

Fusion Technology Institute, University of Wisconsin, Madison, WI
alwehmeyer@engr.wisc.edu

Detection of explosives has been identified as a near term commercial opportunity for using a fusion plasma. Typical explosive compositions contain low Z material (C, H, N, O) which are not easily detected using conventional x-rays or metal detectors. However, 2.45 MeV neutrons produced in a D-D fusion reaction can be used for detection of explosives or other clandestine materials in suitcases, packages, or shipping containers.

Steady-state D-D operation is possible using an Inertial Electrostatic Confinement (IEC) fusion device. The University of Wisconsin IEC device has produced D-D neutrons at 1.8×10^8 neutrons/second at a true cathode voltage of 166 kV and a meter current of 68 mA. These neutron production rates are approaching the levels required for the detection of explosives. Recent progress in the experimental setup for detecting explosives utilizing prompt gamma neutron activation analysis techniques and determining the effect of neutron production rates by altering the cathode's size, geometry, and material.

TOP

Coaxial neutron generators using RF-driven plasmas

Kyoung-Jae Chung, Min-Joon Park, and Yong-Seok Hwang

*Department of Nuclear Engineering, Seoul National University, San 56-1, Shillim-dong,
Gwanak-gu, Seoul 151-742, Republic of Korea, E-mail: yhwang@snu.ac.kr*

A compact coaxial neutron generator based on RF ICP (Inductively Coupled Plasma) with radially convergent ion beam extraction system has been developed. Since the RF plasma source has high density with low gas pressure, high mono-atomic fraction and long lifetime, it is known to be suitable for generating high neutron yield with high efficiency. In order to increase neutron yield, the energy and the number of incident particles should be as large as possible. Furthermore, it is desirable to operate at the low pressure to prevent extracted ions from charge exchange with ambient neutral gases. Since the coaxial cylindrical source can be operated like a line source the extracted beam current is expected to be large. Therefore, pulsed operation is required to increase the extraction voltage without power supply current limit.

In this presentation, preliminary experimental results with coaxial neutron generator will be given for both dc and pulsed operations. Based on these data, new design of the device will be discussed to accommodate beam-plasma target operations (cylindrical IEC).

TOP

Seventh US-Japan Workshop on
Inertial Electrostatic Confinement Fusion
March 14-16, 2005
Los Alamos, NM

SESSION V

A Magnetron Discharge Ion Source for an Inertial Electrostatic Confinement Fusion Device

Teruhisa Takamatsu, Toshiyuki Kyunai, Satoshi Ogawa,
Kai Masuda, Hisayuki Toku, and Kiyoshi Yoshikawa

Institute of Advanced Energy, Kyoto University, Uji, Kyoto 611-0011, Japan

A built-in magnetron discharge ion source has been studied both experimentally and numerically for a IEC(Inertial Electrostatic Confinement) device. With the magnetron discharge, ions are produced in the vicinity of the vacuum chamber (anode) at negative electric potential. Therefore, produced ions are expected to have nearly full energy corresponding to the applied voltage to the IECF cathode but slightly smaller energy than the anode potential preventing them from hitting the anode of the opposite end, eventually improving both fusion reaction rate and ion recirculation life. Also, the magnetron ion source was found to produce ample ion current for maintaining the discharge under low pressure condition.

Ions generated in the ion source are attracted by IEC central cathode because of its high negative electric potential. Therefore, it was expected that a higher applied voltage results in a higher extraction current, and accordingly a higher IEC cathode current. However, it is found that there is a optimum voltage in terms of the high IEC cathode current. Ions supplied by the magnetron ion source are essential to maintain hybrid (glow and magnetron) discharge under low gas pressure condition in an IEC, but this hybrid discharge scheme does not work well in high cathode voltage condition for some reason.

Numerical simulations are being carried out for understanding the scheme. The preliminary results will be also presented.

TOP

Implantation of D⁺ and He⁺ in Candidate Fusion First Wall Materials

R.F. Radel, G.L. Kulcinski, R.P. Ashley, J.F. Santarius, G.R. Piefer, A.L. Wehmeyer,
D.R. Boris, R.C. Giar, T.E. Radel, and E.C. Alderson

Fusion Technology Institute, Madison, WI, rfradel@wisc.edu

The effects of high temperature (700-1200 °C) implantation of deuterium and helium in candidate fusion first wall materials were studied in the University of Wisconsin Inertial Electrostatic Confinement (IEC) device. Tungsten “foam”, single crystal tungsten, and a W-25%Re alloy were compared to previous tungsten powder metallurgy samples studied in the IEC device for the High Average Power Laser (HAPL) program. Scanning electron microscopy was performed to evaluate changes in surface morphology for various ion fluences at temperature ranges comparable to first wall temperatures in fusion reactors. Preliminary results show that no deformations occur with deuterium implantation up to 2×10^{18} D⁺/cm² at 1200 °C polycrystalline tungsten samples. However, helium fluences in excess of 4×10^{17} He⁺/cm² show extensive pore formation at 800 °C. These changes will have an impact on the lifetime of IEC cathode grids as well as thin tungsten coatings on the first walls of inertial and magnetic confinement fusion reactors.

TOP

Neutron Production through Beam-Beam Collision at Low Gas Pressure and Large Current Operation

K. Noborio, Y. Yamamoto, Y. Ueno, and S. Konishi

Institute of Advanced Energy, Kyoto University, Gokasho, Uji, Kyoto 611-0011, Japan

We have developed a 1-D PIC simulation code including atomic and molecular processes, and simulated low pressure operation assisted by an external ion source in an IECF device. As we reported at the last Workshop, when the pressure decreases, neutron production caused by the beam (energetic) particle's colliding with the background gas particle is reduced because of the decrease in target density. Therefore, in order to gain more neutron yield, it is necessary to extend fusion reaction caused by beam-beam collision, and to reduce the pressure and enlarge the current of circulating ions. We have simulated low pressure and large current discharge to investigate whether the neutron production through beam-beam collision increases.

We have improved the 1-D code to calculate the fusion reaction rate through beam-beam collision more accurately. And to evaluate confinement level of ion, each particle's life span (the total length from its generation to disappearance) was recorded.

Previous results calculating at the pressure range from 0.01Pa to 0.1Pa and the current range of injected ion below 10mA show that beam-background collision dominates neutron yield. We tried to simulate cases injecting more ions at lower pressure, but space charge of ions restricted injecting new ions. In order to inject larger current than 100mA by applying high electric field, diameter of the device was reduced from 34cm to 20cm. From these calculations, it becomes clear that the life-span of injected ions increase and that this improves confinement level of ion as the pressure decreases. This extends neutron production through beam-beam collision. However, it is limited to the value estimated from the geometrical transparency of the cathode, reducing the pressure under 0.001Pa is not effective. Though enlarging the current of injected ions disturbs convergence of ions within the cathode because of high potential of virtual anode created by the space charge of the ions, it is confirmed that operation points where the neutron production through beam-beam collision is larger than that through beam-background collision exist.

TOP

Plasma Compression in the Periodically Oscillating Plasma Sphere

R. A. Nebel, L. Chacon, J. Park, E. Evstati

Los Alamos National Laboratory, Los Alamos, New Mexico 87545

The oscillating ion cloud (referred to as the Periodically Oscillating Plasma Sphere or POPS) is in local thermodynamic equilibrium at all times independent of the collisionality of the plasma (i.e. these self-similar solutions are exact solutions of the Vlasov equation). POPS is stable to multidimensional perturbations, while its self-similar solutions appear to be attractors.^{P³P} Theoretical projections have indicated that such a system may have net fusion gain even for an advanced fuel such as D-D. In addition, these systems have very favorable reactor attributes in that the total power scales inversely with the size, leading naturally to a modular, high mass power density device.

Recent experimental work has demonstrated the existence of the POPS resonance.^{P⁴P} However, there are several issues that need to be resolved in order to determine the efficacy of this scheme. Perhaps the most important issue is the effect of space charge neutralization on the plasma compression. An analytic formalism has shown that it is possible to program the distribution function of the injected electrons to completely mitigate space charge effects during the ion cloud collapse. If this can be achieved, the required compression ratios for POPS can be drastically reduced. This also eliminates the requirement that the average electron density must be much greater than the average ion density (i.e. POPS may now be possible in quasi-neutral plasmas). However, it is still likely that there will be an ultimate stability limit imposed by the two-stream instability.^{P^{5,6}P} This new formalism is presently being incorporated into the 1-D particle simulation code.^{P⁶P} Results will be presented.

1. R. A. Nebel, D. C. Barnes, *Fusion Technology* 38, 28 (1998).
2. D. C. Barnes, R. A. Nebel, *Physics of Plasmas* 5, 2498 (1998).
3. R. A. Nebel, J. M. Finn, *Physics of Plasmas* 7, 839 (2000)
4. J. Park, R. A. Nebel, S. Stange, S. K. Murali, accepted for publication in *Physics of Plasmas*, 2/05
5. R. A. Nebel, J. M. Finn, *Physics of Plasmas* 8, 1505 (2001).
6. R. A. Nebel, S. Stange, J. Park, J. M. Taccetti, S. K. Murali, C. E. Garcia, *Physics of Plasmas* 12, 12701 (2005).

TOP

Seventh US-Japan Workshop on
Inertial Electrostatic Confinement Fusion
March 14-16, 2005
Los Alamos, NM

SESSION VI

Numerical Study on Hollow Cathode Discharge of IEC Fusion

Hodaka OSAWA and Masami OHNISHI

Dept. of Electrical Engineering, Kansai University. Suita ,Osaka JAPAN
osawa@kansai-u.ac.jp

We make the three-dimensional Monte Carlo PIC code in order to investigate the discharge characteristics in the IEC. The code includes 12 kinds of atomic processes and elastic collisions among electrons, D⁺ ions, D₂⁺ ions and D₃⁺ ions as well as the effects of the electric field deformed by the existence of the current feed through and the cathode structure. The code is initialized by the seed electrons existing between electrodes. The motions of each particle are traced by the Runge-Kutta method. During tracing the particles, atomic collisions are taken into account and new ions and electrons are generated by the collisions. The time behaviors of number of ion and electrons are observed. When the particles continue to increase, we identify that the glow discharge occurs.

We have the following results from the computations.

1. The glow discharge pattern with several light spokes called “star mode” observed in the experiments is numerically demonstrated.
2. The main reaction which plays a main role of the discharge is the combination of self-multiplication reactions which produce D₂⁺ ions and electrons.
3. The fact that the discharge at a low pressure is unstable is explained by the less multiplication rate of ions and electrons.

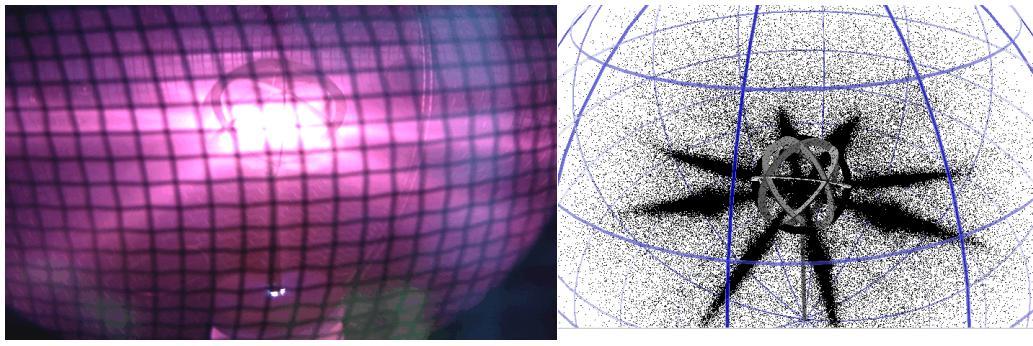


Fig.1. “Star mode” (a) Experiment. (b) Simulation

TOP

Kinetic Simulation of Inertial_Electrostatic Confinement Experiments at Los Alamos National Laboratory

G. Lapenta (T_15), R.A. Nebel (X_3), J. Park (P_24): Plasma Theory Group (T_15),
Integrated Physics Methods Group (X_3), Plasma Physics Group (P_24)

Los Alamos National Laboratory, University of California

We discuss the application of the DEMOCRITUS simulation package to the simulation of experiments conducted at the Los Alamos Inertial_Electrostatic Confinement (IEC) device [1,2]. Recently considerable new experimental advances have been made [3], particularly with regards to the study of the stability of the electron population in the virtual cathode [4] and on proving experimentally the POP solutions predicted theoretically [5,6].

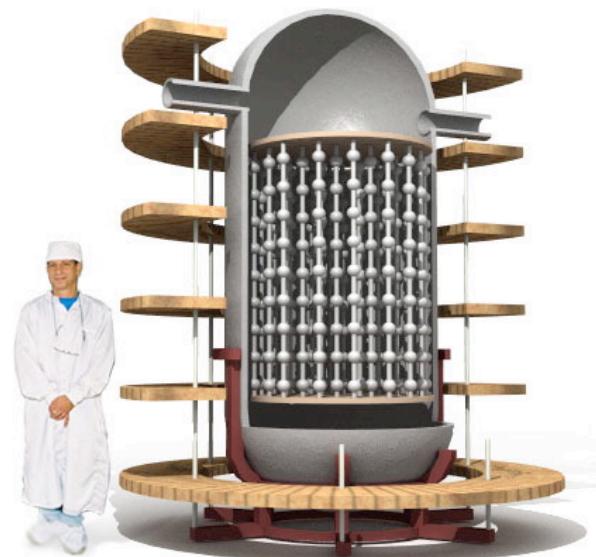
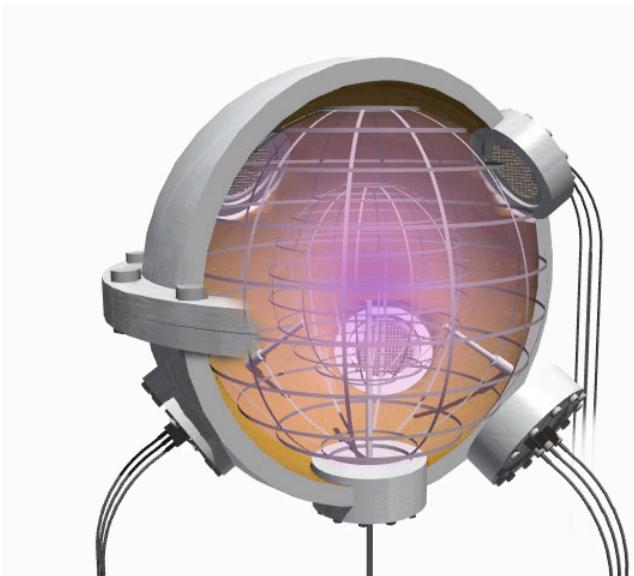
The momentous advance made experimentally requires a new simulation effort for explaining and interpreting some of the experimental finding, particularly in the area of the stability of the configurations obtained experimentally. To this end we have recently started a new effort to apply the existing DEMOCRITUS package [7] to the simulation of the IEC device at Los Alamos.

DEMOCRITUS is a 2D general geometry electrostatic PIC code. Three fundamental ingredients compose the package. First, we have a selection of different particle solvers including the explicit Boris algorithm, the implicit predictor_corrector scheme and a new fully implicit particle mover based on a Newton non_linear solver. Second, we use an adaptive grid with a general geometry discretization of the Poisson equation and we use a multigrid preconditioned Krylov solver for its solution [8]. Third, we use the immersed boundary method to handle complex geometric features (e.g. the presence of the grids to accelerate the particle in the IEC device) [9].

In the present poster we describe the method, we present a number of validation and verification results where we compare our simulation results with previous 1D simulations and with the experiment.

- [1] http://www.lanl.gov/physics/projects/pds_ps01.shtml
- [2] R.A. Nebel, D.C Barnes, Fusion Technology 38, 28 (1998).
- [3] R. A. Nebel, S. Stange, J. Park, J. M. Taccetti, S. K. Murali, and C. E. Garcia, Phys. Plasmas 12, 012701 (2005).
- [4] J. Park, R. A. Nebel, W. G. Rellergert, M. D. Sekora, Phys. Plasmas 10, 3841 (2003).
- [5] D. C. Barnes, R. A. Nebel, Phys. Plasmas 5, 2498 (1998).
- [6] R. A. Nebel, J. M. Finn, Phys. Plasmas 7, 839 (2000).
- [7] G. Lapenta, Phys. Plasmas 6, 1442 (1999).
- [8] D.A. Knoll, G. Lapenta, J. Brackbill, J. Comput. Phys. 149 377 (1999).
- [9] G. Lapenta and JU Brackbill, IEEE Trans. Plasma Sci. 24, 105 (1996).

Recent Progress in Periodically Oscillating Plasma Sphere (POPS) and Neutron Source Development at LANL



Jaeyoung Park
Plasma Physics Group (P-24)
Los Alamos National Laboratory

Acknowledgement

- Many people contributed to this talk
- LANL: Rick Nebel, Martin Taccetti, Martin Schauer, Carter Munson, Carlos Garcia, others
- Alme & Associates: Charles Mansfield, Rosemary Alme.
- U. Wisconsin: K.M. Subramanian, Gerald Kulcinski, John Santarius, Bob Ashley, many students.
- Coronado Consulting: Dan Barnes
- Summer students: W. Rellergert (Yale) and M. Sekora (MIT)
- Other IEC institutions: U. Illinois, Kyoto Univ., Kansai Univ., Tokyo Institute of Technology, Seoul National Univ.
- Support from DOE OFES ICC program greatly appreciated and POPS project at LANL is renewed for 4 more years
- DOE STTR program with Alme & Associates
- Work supported by DOE contract W-7405-ENG-36.



Outline

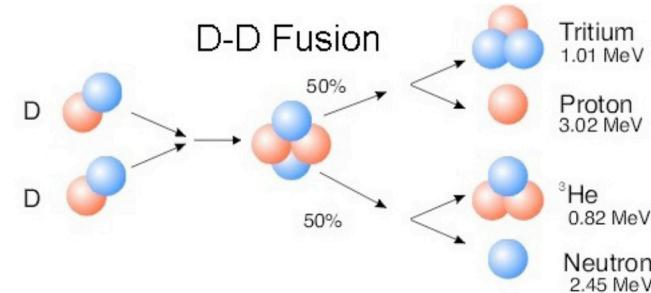
- I. Fusion and Inertial Electrostatic Confinement (IEC)**
- II. Periodically Oscillating Plasma Sphere (POPS)**
- III. Experimental Confirmation of POPS**
- IV. Neutron Source Development at LANL**
- V. Summary and Future Plan**



Fusion Reactions and its applications

- Low mass fusion reactions

- D + D \rightarrow T (1 MeV) + p (3 MeV) or He³ (0.8 MeV) + n (2.45 MeV)
- D + T \rightarrow He⁴ (3.5 MeV) + n (14.1 MeV)
- D + He³ \rightarrow He⁴ (3.6 MeV) + p (14.7 MeV)



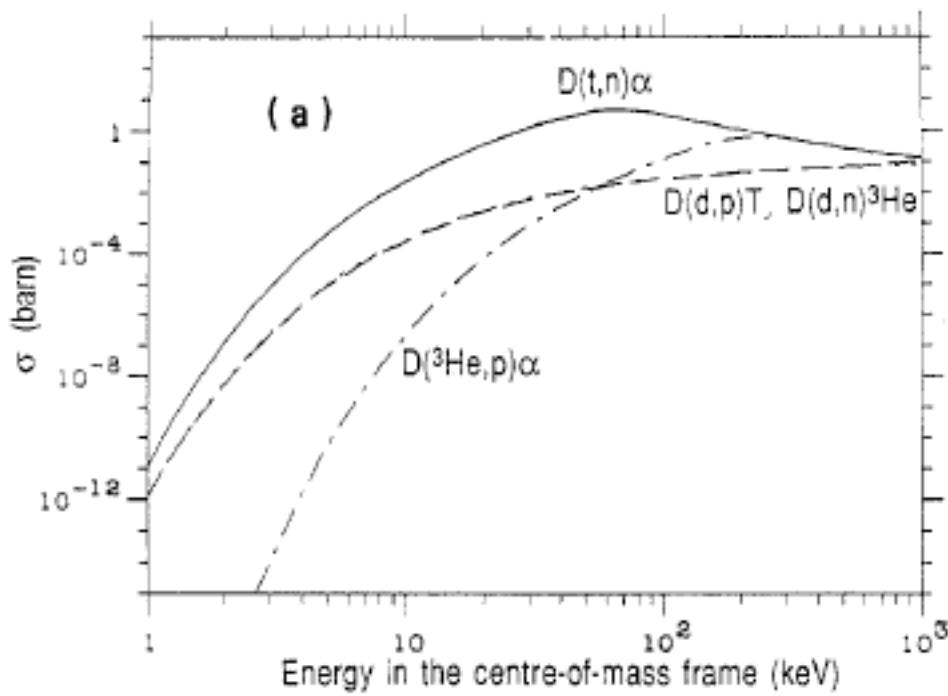
- Potential fusion applications

Fusion rate (reactions/s)	Application	Expected Apparatus	Required Fusion Efficiency
$1-10 \times 10^{10}$	Nuclear Assay	IEC or Beam-target device	10^{-5} or higher
$1-100 \times 10^{13}$	PET Isotope & Materials testing	None promising at present	0.1% or higher
$\sim 3.6 \times 10^{20}$	Fusion Power (1GWth)	Tokamak, Laser target fusion Magnetized target fusion, and IEC	10-20

Q(Fusion efficiency) = Fusion energy output /Total input Power to the device
Assuming D-T fuel, 1W D-T fusion = 3.6×10^{11} fusions/s

Requirement of Fusion Device

- Fusion require high energy collisions (10keV - 1000 keV)
 - high energy to overcome Coulomb repulsion
 - that's why we need high temperature plasma
- Unfortunately, fusion collision is hard to come by (~ 0.01 - 8 barn)



- **Technical Challenges**
 - Plasma Confinement
 - Minimize the power loss: Ion loss to the grid, CX loss, Radiation, Coulomb collisions, etc.

Scaling of IEC Fusion Efficiency

- D - T reaction at 100 keV
 - fusion cross section: $\sim 8 \times 10^{-24} \text{ cm}^2$
 - charge-exchange cross section: $\sim 1 \times 10^{-17} \text{ cm}^2$
- Beam-gas target scenario (at 1 mtorr, 7×10^{13} target particle/cm³)
 - frequency of fusion reactions: 0.25 Hz
 - frequency of CX: 3.1×10^5 Hz
 - beam-gas target IEC: $Q \sim 10^{-6}$ (**low gas pressure does not improve Q**)
- Ion loss to the grid: In gridded IEC, typically ions can make multiple transit before hitting grid and getting lost.
 - ion loss frequency: 8.8×10^4 Hz at 50 transit of 1m trajectory
 - gridded IEC (with beam-gas target at 1 mtorr): $Q \sim 3 \times 10^{-6}$
 - beam ion confinement in Tokamak: ~ 1 sec $\rightarrow Q \sim 0.25$
- If $Q \sim 3 \times 10^{-6}$, it will take ~ 100 kW to produce 1×10^{11} D-T neutrons
- D-T beam-solid target: $Q \sim 2 \times 10^{-4}$ (3×10^{10} neutrons/s at 500 W)
 - for a very short target lifetime (~ 100 hours)
 - LBNL now has a longer lifetime beam-target source (for D-D at probably lower Q value)



Opportunities of IEC Fusion Research

- Beam-beam target scenario: increase ion current
 - Pulsed high current operation of IEC in Japan and U. Illinois
 - Planned pulsed IEC operation at LANL
- Minimize CX loss: low gas pressure or high ionization fraction
 - Ion beam source development at most IEC research groups
 - High ionization fraction (10-100%) may improve the efficiency
- Minimize ion loss to grid: Penning trap, Polywell™ (and other ideas, e.g. insulating grid)
- If $Q \sim 1 \times 10^{-5}$, it will take ~ 33 kW to produce 1×10^{11} D-T neutrons for nuclear assay applications (HEU or UXO detection)
 - Reasonable power consumption
 - Can have long lifetime (critical for low cost operation)
- Periodically Oscillating Plasma Sphere (POPS): low gas pressure, compatible with Penning trap and may even achieve $Q > 1$.



Examples of Nuclear Assay Applications

- **Special Nuclear Materials Detection**

- $D + T \rightarrow He^4 + n$ (14.1 MeV)
- $D + D \rightarrow He^3$ (0.8 MeV) + n (2.45 MeV)
- $U^{235} + n \rightarrow$ fission product (FP) + $3n$ (fission and neutron multiplication or delayed neutrons).
- Fast neutrons penetrate better than thermal neutron, thus making shielding difficult.

- **High Explosives Detection**

- UXO, Landmines, Chemical Weapons Dispersant, Truck Bombs, etc.
- $N^{14} + n \rightarrow N^{15} + \gamma$ (10.8 MeV)
- $S^{32} + n \rightarrow S^{33} + \gamma$ (8.64 MeV)
- $Cl^{35} + n \rightarrow Cl^{36} + \gamma$ (7.97 MeV)

- **Spent Fuel Assay**

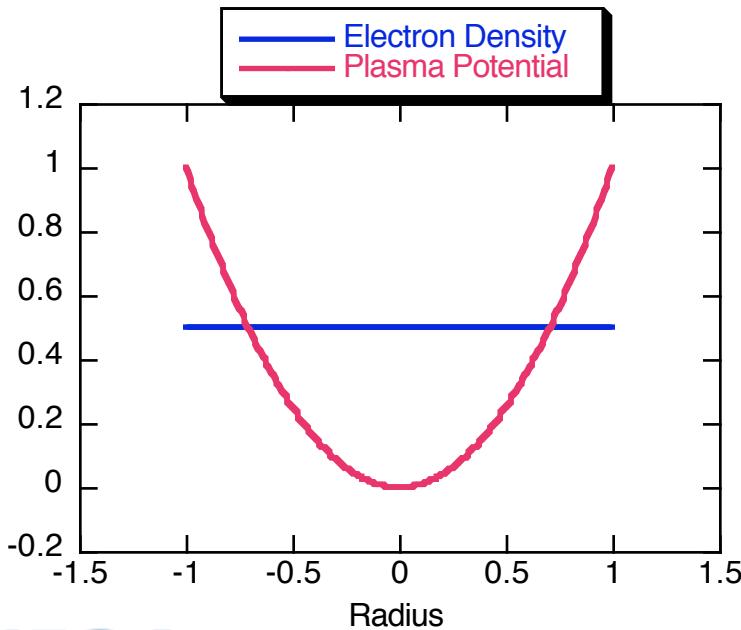
- $U^{235} + n \rightarrow$ FP + $3n$ (fission and neutron multiplication)
- $Pu^{239} + n \rightarrow$ FP + $3n$ (fission and neutron multiplication)



Periodically Oscillating Plasma Sphere (POPS)

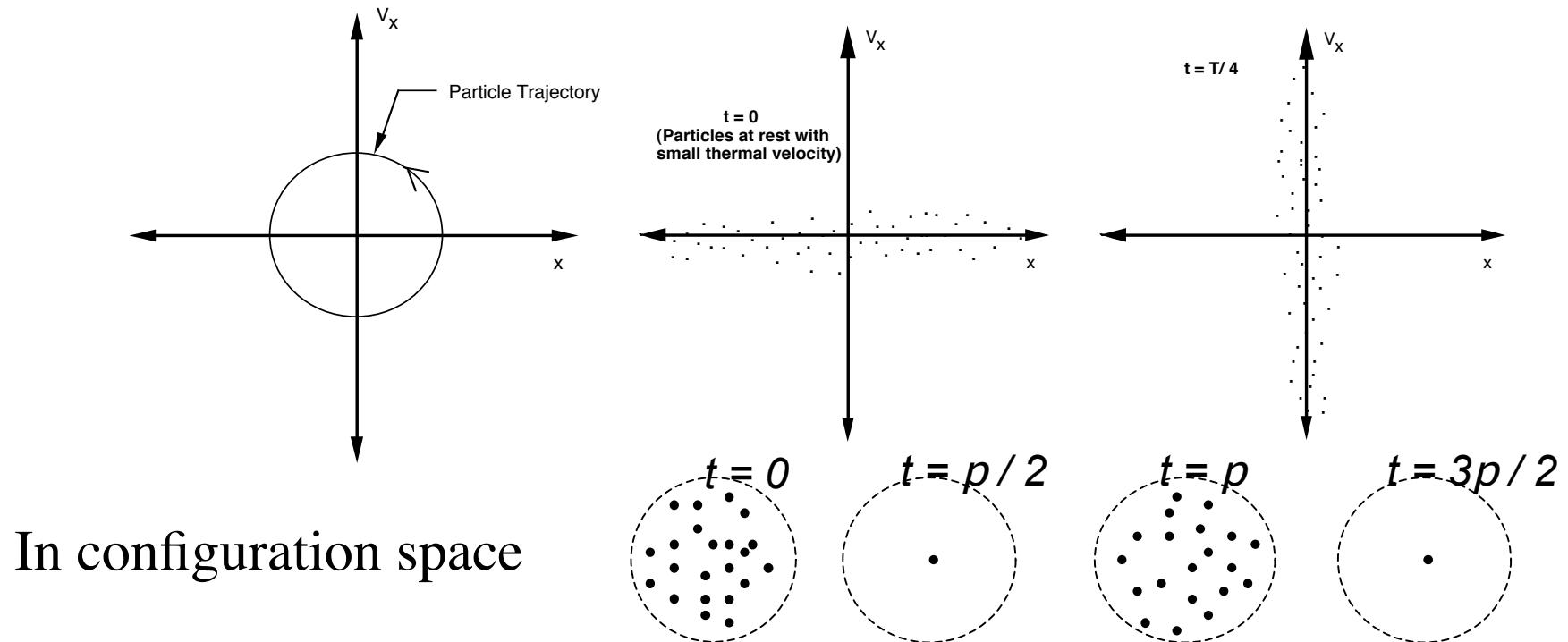
- Barnes and Nebel (circa 1997): Constant density electron background in a sphere (**by external electron injection**) --> spherical harmonic potential well for ions
- Ions created by ionization and oscillate radially in the well
- Harmonic oscillator - same freq. regardless of amplitude --> converge to the center at the same time with maximum kinetic energy
- POPS frequency for singly charged ions:

$$f_{POPS} = \frac{\sqrt{2V_{well} / M_{ion}}}{2\pi r_{VC}}$$



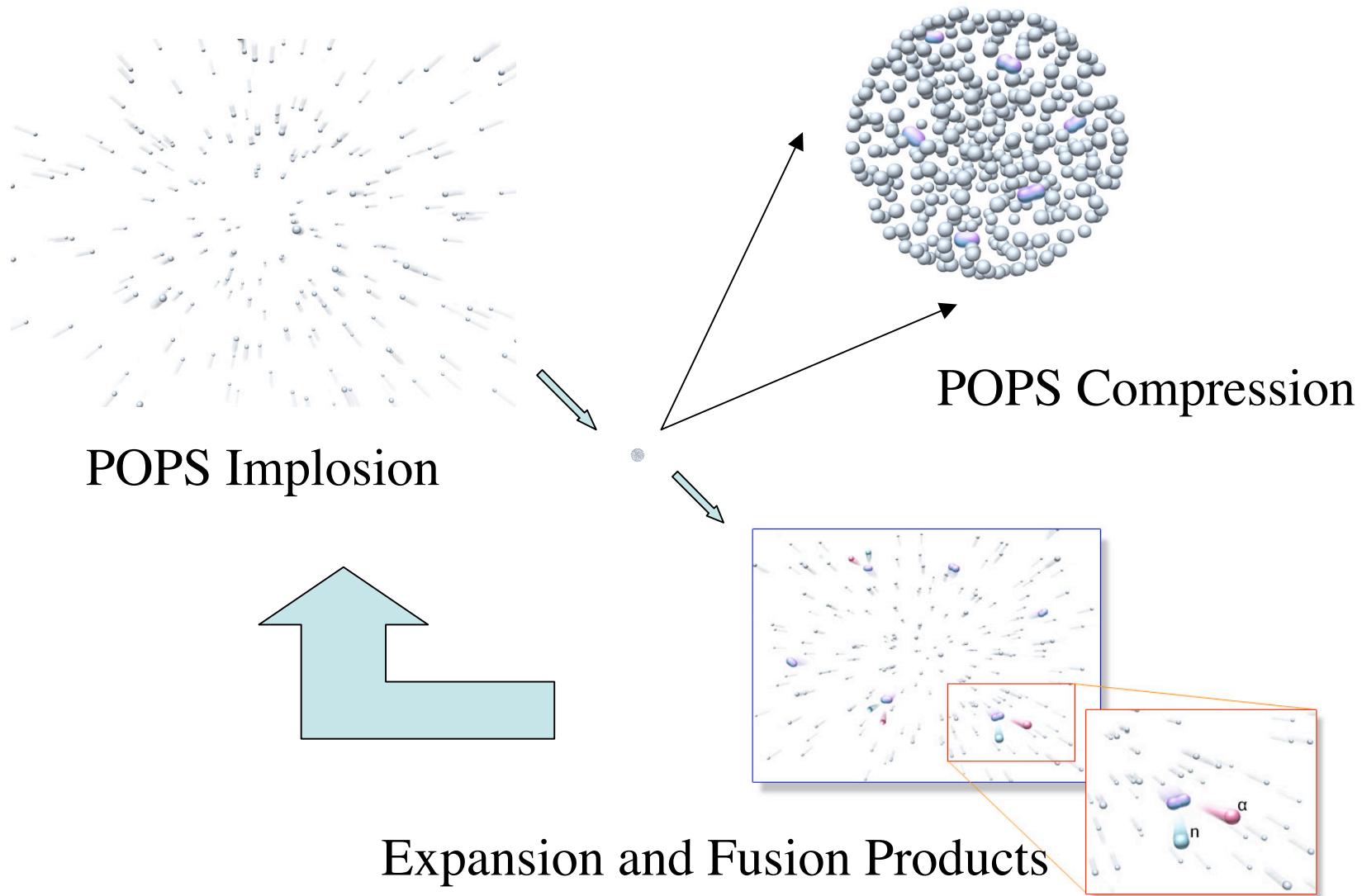
- Characteristics of POPS solutions:
 - **Ion distribution remain LTE throughout oscillation - solves ion thermalization problem**
 - **Practical embodiment based on Penning trap**
 - **Can increase fusion yields and may achieve breakever**

Ion Phase Space Motion in a Harmonic Oscillator

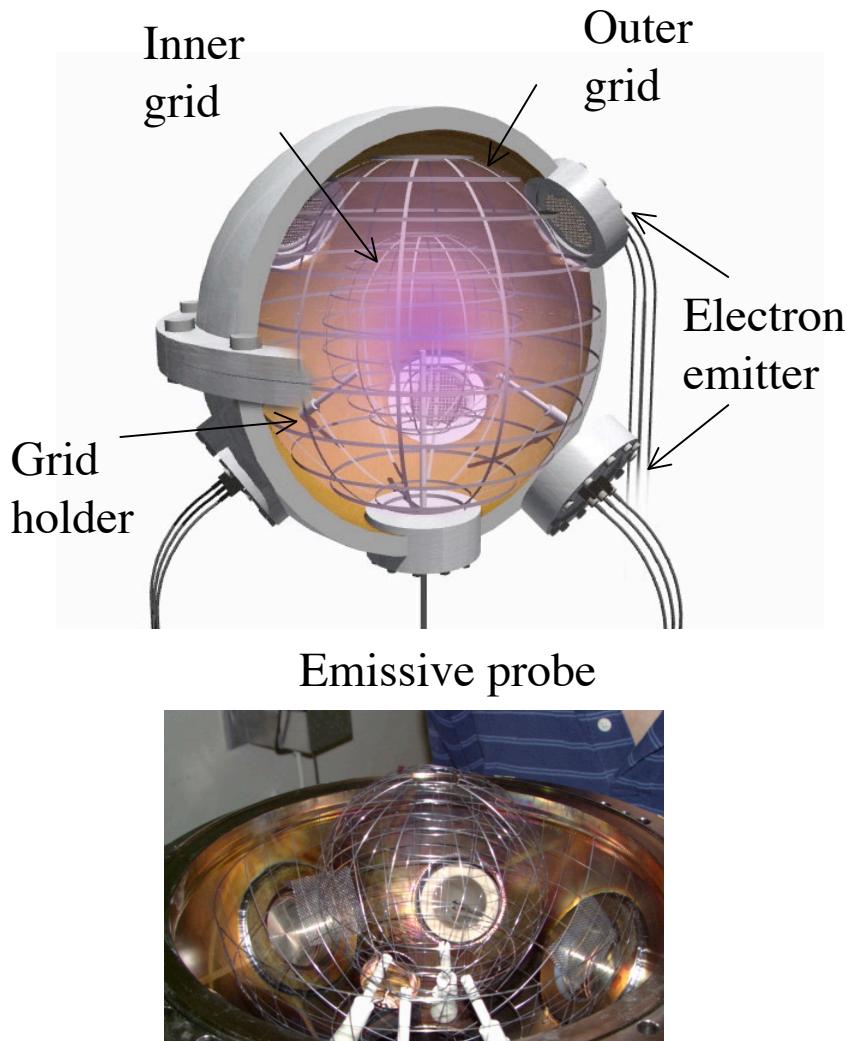


- Ion distribution function moves as a rigid rotor in phase space
- Maxwellian velocity distribution \leftrightarrow Gaussian density profile
- Particle convergence from harmonic oscillation (not from beam focusing)
- High fusion power density without beam ion distribution

Phase of POPS Oscillation



Experimental Setup - INS-e Device at LANL

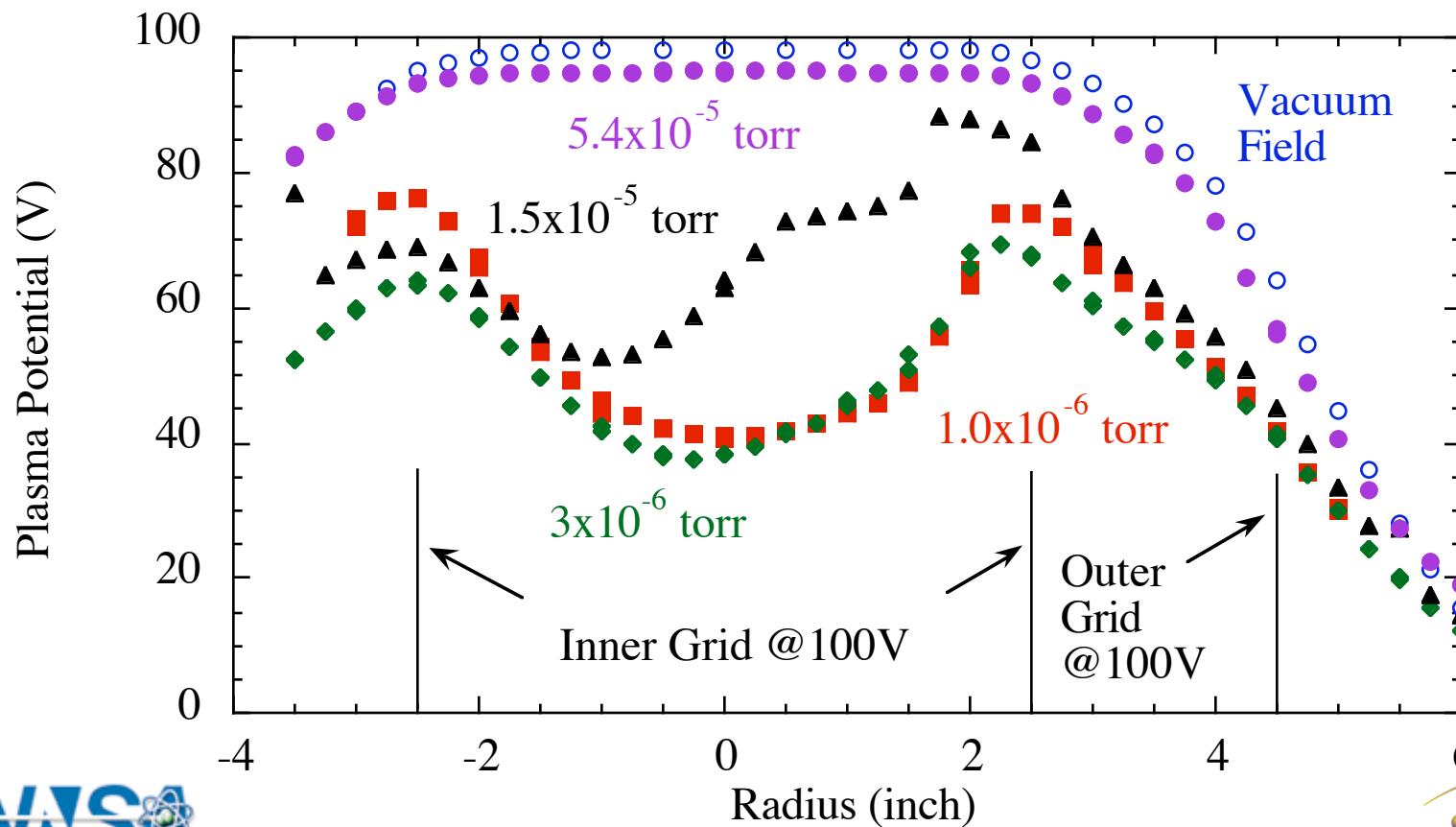


Intense Neutron Source- Electron (INS-e)

- **Electron injection:** 6 electron emitters --> create harmonic potential well (i.e. virtual cathode) - low operating pressure $\sim 10^{-6}$ torr
- **Outer grid:** controls the electron flux
- **Inner grid:** B.C. for potential well
- Grid spacing: 1 cm for inner grid (vs. Debye length ~ 1.8 cm)
- **rf modulation:** to inner grid to excite POPS oscillation and phase-lock.
- **Emissive probe:** plasma potential and its time variation
- Fill gas: H₂ (H₂⁺), He, Neon, (and D₂)

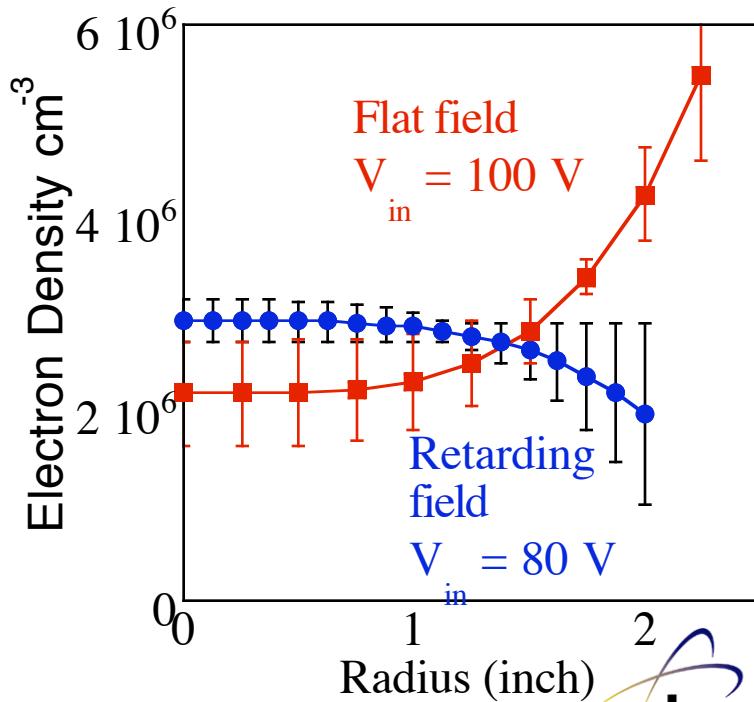
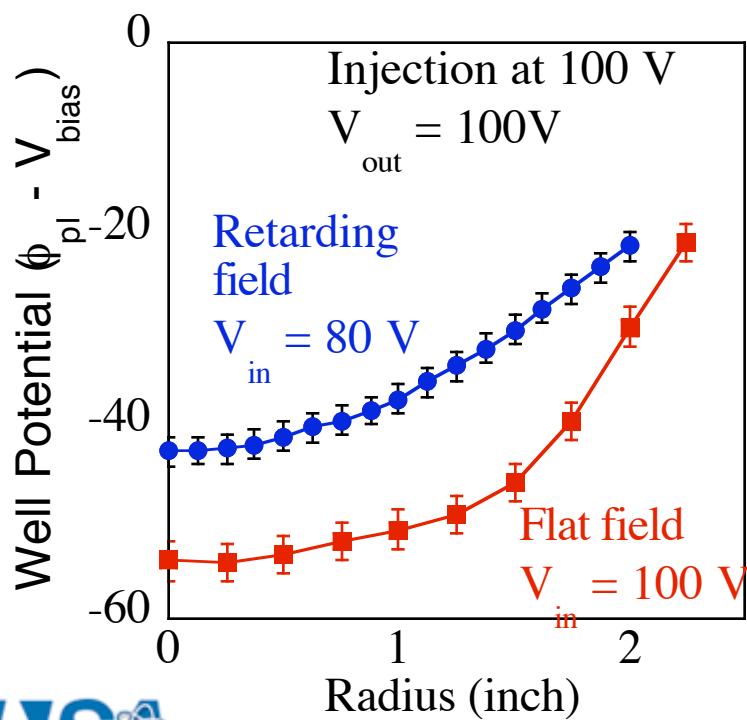
Potential Well (Virtual Cathode) Formation

- Electron injection at low gas pressure
- Stable potential wells have been created



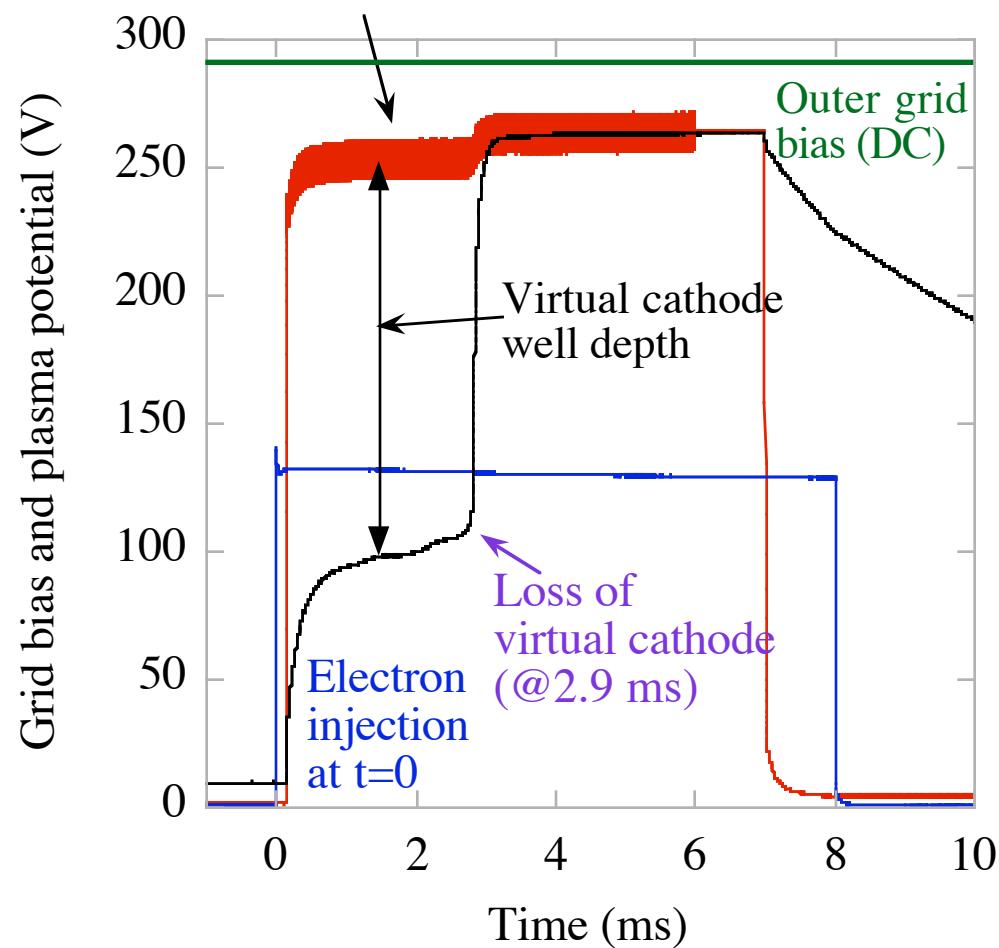
Control of Radial Plasma Profile (Potential and Density)

- Emitter bias - control of injection current and electron self-repulsion
- Relative bias voltage for inner and outer grid
 - $V_{in} < V_{out}$: retarding field --> less angular momentum spread in the center
 - $V_{in} > V_{out}$: accelerating field --> preserve angular momentum
- Flat radial electron density profile (harmonic potential well- POPS potential)
-



Excitation of POPS and virtual cathode dynamics

Inner grid bias with rf modulation



ulsed operation: necessary due to VC loss by ionization

modulation to inner grid bias --> excite POPS oscillation

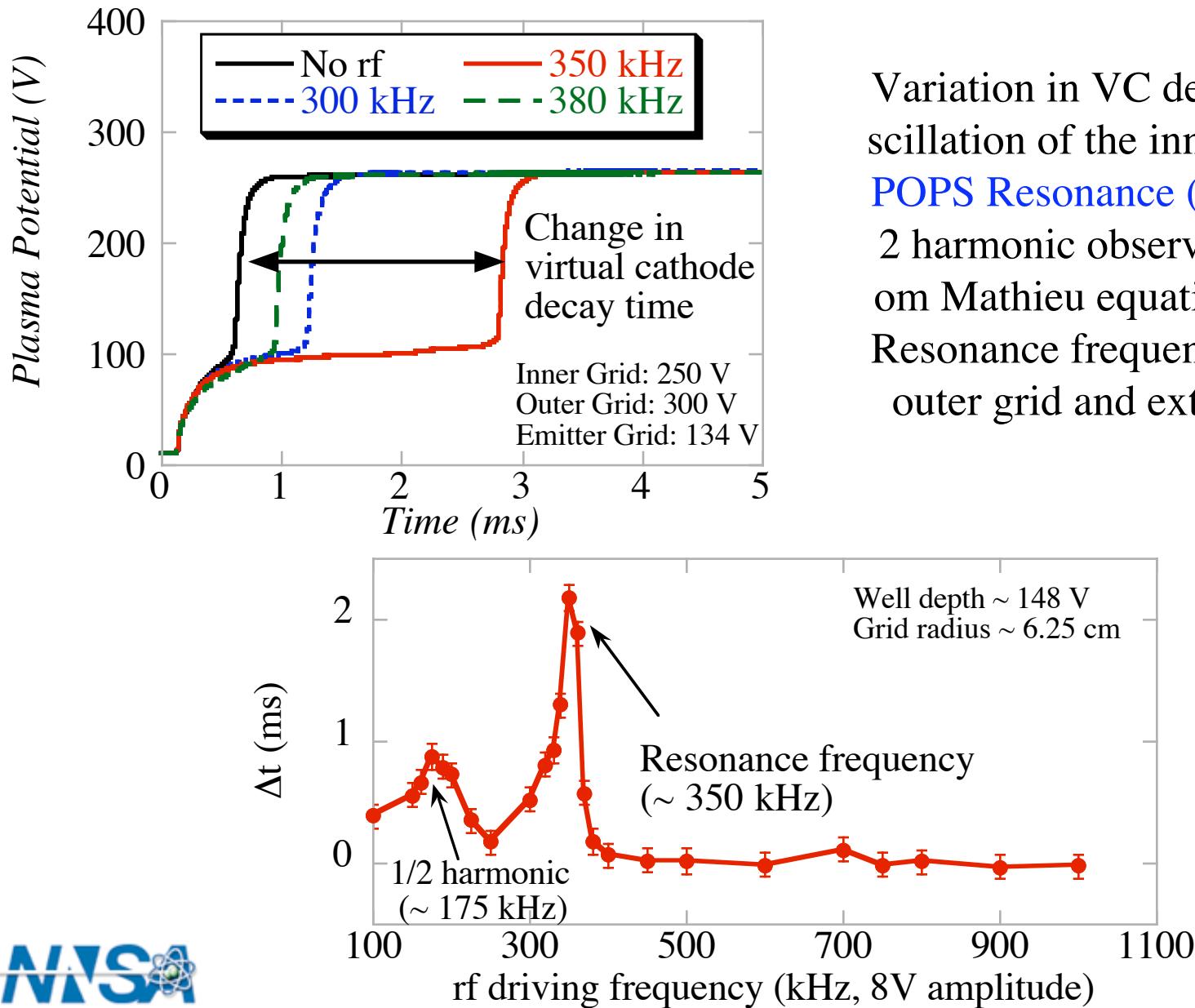
Driven POPS oscillation: forced harmonic oscillator - mathematically equivalent to **Mathieu Equation**

ons gain energy from resonant POPS oscillation

- Increase the ion loss from VC
- Delay virtual cathode loss

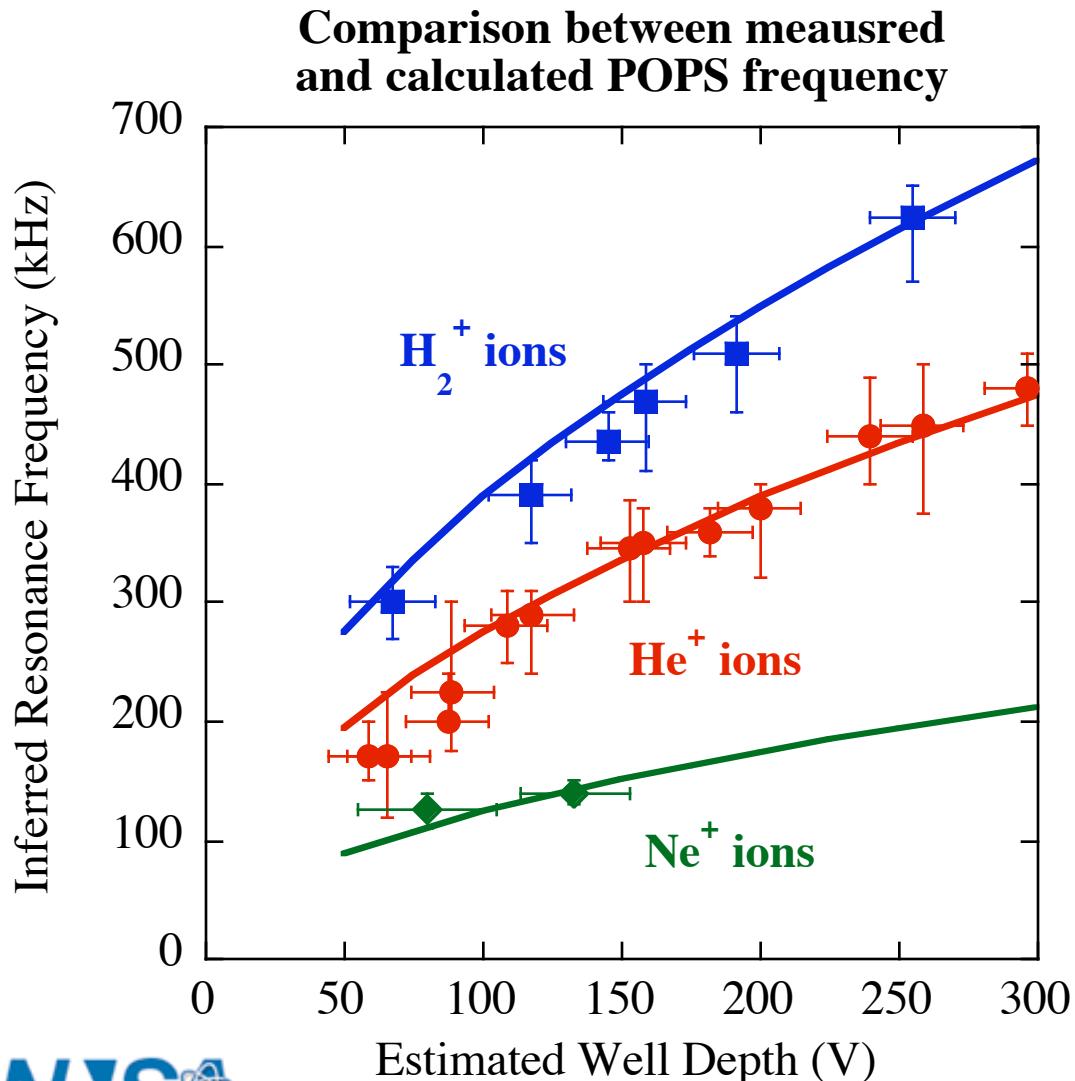
Measure the virtual cathode decay using emissive probe.

nance



Variation in VC decay time with rf oscillation of the inner grid bias.
POPS Resonance (@350 kHz) and 2 harmonic observed (expected from Mathieu equation).
Resonance frequency independent of outer grid and extractor grid bias.

Scaling of POPS frequency



on species (H_2^+ , He^+ and Ne^+) have been used.

Resonance frequency exhibit $\frac{1}{2}$ scaling

Resonance frequency exhibit $(n \text{ mass})^{1/2}$ scaling

$$f_{res} = 2 f_{POPS} = \frac{\sqrt{8V_{well} / M_{ion}}}{2\pi r_{VC}}$$

PS frequency calculation

$$r_{VC} = r_{grid} + \lambda_{debye}$$

Excellent agreement with theoretical calculations (in absolute values)

Recent Theoretical Progress of POPS

- 1D Particle Code (talk by Rick Nebel): virtual cathode stability, self-consistent POPS compression and space-charge neutralization issues, D-T hybrid POPS operation.
- 2D Particle Code (talk by Gianni Lapenta): Successfully implemented for IEC system and verified a similarity solution.



POPS Compression and Potential Applications

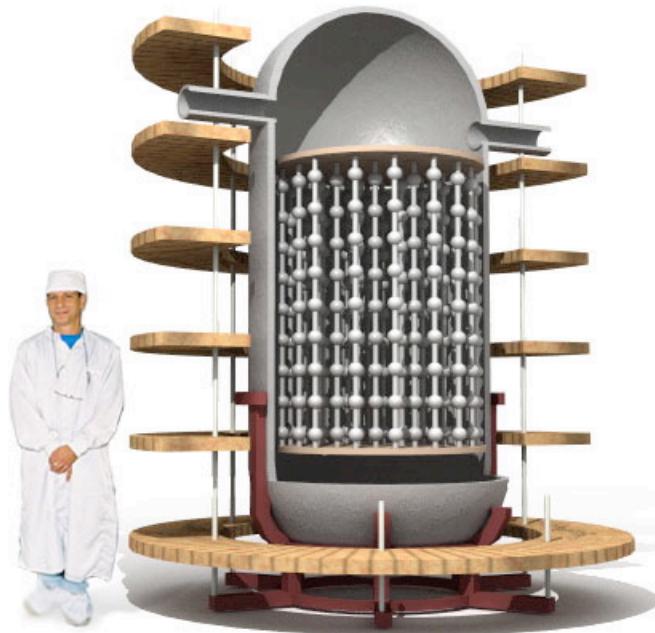
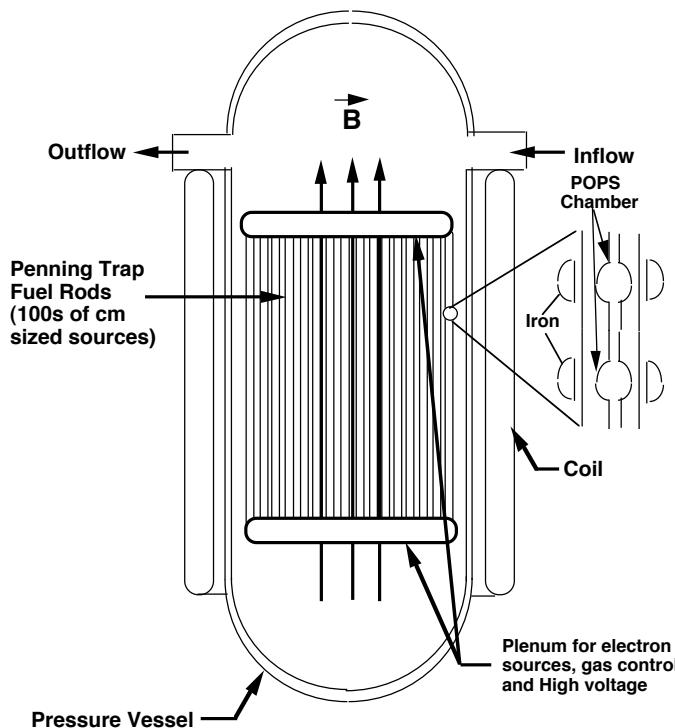
- Two factors for practical fusion devices based on POPS
 - Fusion efficiency ($Q = P_{\text{fusion}}/P_{\text{input}}$)
 - Fusion power density $\sim \text{compression}^2$
- Higher compression --> higher fusion power density --> more practical
- Various potential applications based on achievable compression ratio
- D-T mixed fuel --> lower compression requirement

Fuel	Application	Compression ratio (r_{\max}/r_{\min})	Neutron rate	Number of Modules
D-D	Nuclear Assay (HEU, HE, CW)	26 or 10 for 7 module	$\sim 1.0 \times 10^{11} \text{n/s}$	1
D-D	Neutron Tomography	17	$\sim 1.0 \times 10^{12} \text{n/s}$	25
D-D	PET Isotope Production	70	$\sim 1.0 \times 10^{15} \text{n/s}$	1400
D-D	Fusion(100MW)	1000	$\sim 1.6 \times 10^{20} \text{n/s}$	$\sim 1.1 \times 10^7$
D-T	Fusion (100MW)	86	$\sim 1.6 \times 10^{21} \text{n/s}$	$\sim 2.8 \times 10^6$



Reactor Path for POPS IEC system

Penning Trap Reactor Vessel



1. Penning trap --> Reduce the electron loss to the grid
2. Small device size --> Massively Modular System
 - Confinement doesn't depend on size and Power $\sim 1/r_{\text{tube}}$
3. Mass Power Density(MPD) for Modular IEC Reactors has a favorable scaling
4. High MPD (\sim Light Water Reactor) can be achieved with conventional wall

Intense Neutron Source R&D

- Collaboration among LANL, U. Wisconsin and Alme & Associates
- Nuclear Assay applications for HEU and UXO detection
- 1st stage: High voltage pulsed power operation
 - U. Wisconsin constructed a HV feedthru (tested up to 110 kV), two W/Re alloy grids (high temperature materials for radiative cooling)
 - LANL is nearing completion of HV pulsed power system (1 to 5 A at 75 kV)
 - Ion source development using microwave discharge
- 2nd stage(contingent on future funding): focus on shielded HEU detection in a container
 - D-T operation in 2-3 year
 - For 1×10^{11} neutrons/s source: fast, accurate and cost-efficient HEU detection in a container is feasible
 - May include fast inductive ionization or other high efficient plasma source
 - Complete system development including detection technology.



Various components of LANL pulsed IEC system



HV feedthru
with inner grid



HV pulsed power system

Various components of LANL pulsed neutron system



100 kV
Jenning Switch



HV pulsed power system

Summary

- **Inertial Electrostatic Confinement Concept**
 - Simple concept: Modest fusion rates in small devices
 - Generally low efficiency - R&D opportunities for improving Q.
 - Current focuses on nuclear assay applications - HEU and UXO detection
- **Periodically Oscillating Plasma Sphere (POPS)**
 - New approach to improve fusion efficiency IEC device
 - Can achieve fusion power at least in theory
 - POPS oscillation has been confirmed experimentally
 - Significant progress in POPS theory: see Nebel and Lapenta
 - Economical fusion reactors (= high fusion power density & high POPS compression) can generate a wide range of applications
- **Intense Neutron Source Development at LANL**
 - Collaboration with Alme & Associates and U. Wisconsin.
 - HV pulsed power system is close to operation.
 - Neutron rate study is planned for a high ion current (1-5 Aa@75 kV) operation on a single pulse base.





Measurement of Neutral Beam Energy Distribution in the C-IECF Device

Yasushi YAMAMOTO, Yukihisa UENO,
Kazuyuki NOBORIO, Satoshi KONISHI

Inst. of advanced Energy, Kyoto Univ.

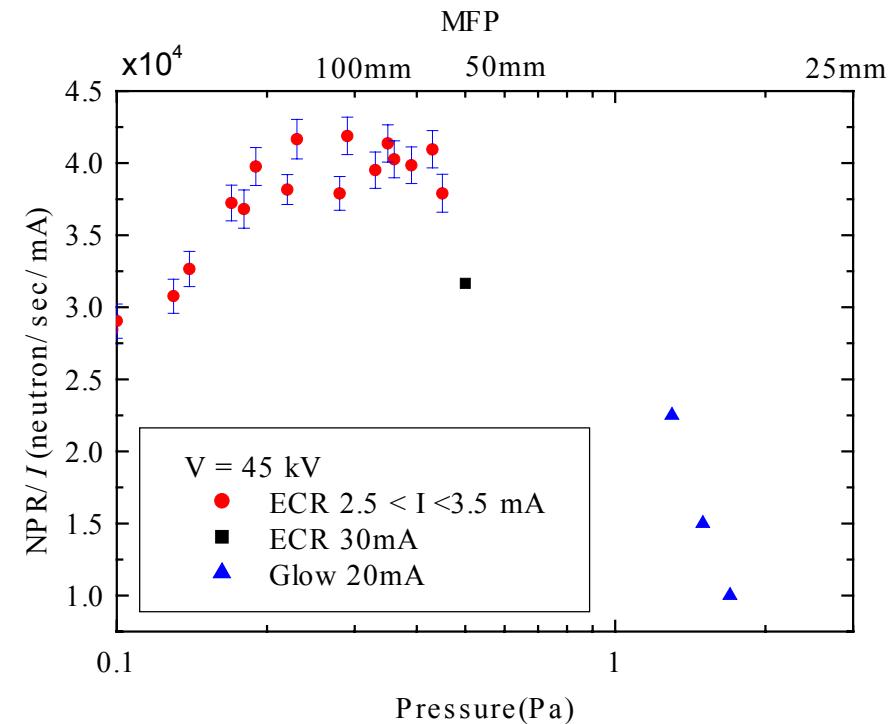
Objective

In the experiments, we have observed increase of Neutron production rate (NPR) with reduction of gas pressure.

We have tried to explain by increase of averaged ion energy through increase of mean-free-path of the charge exchange process between energetic ion and background gas as the remarkable increase of D-D fusion cross section remarkably in this energy range.



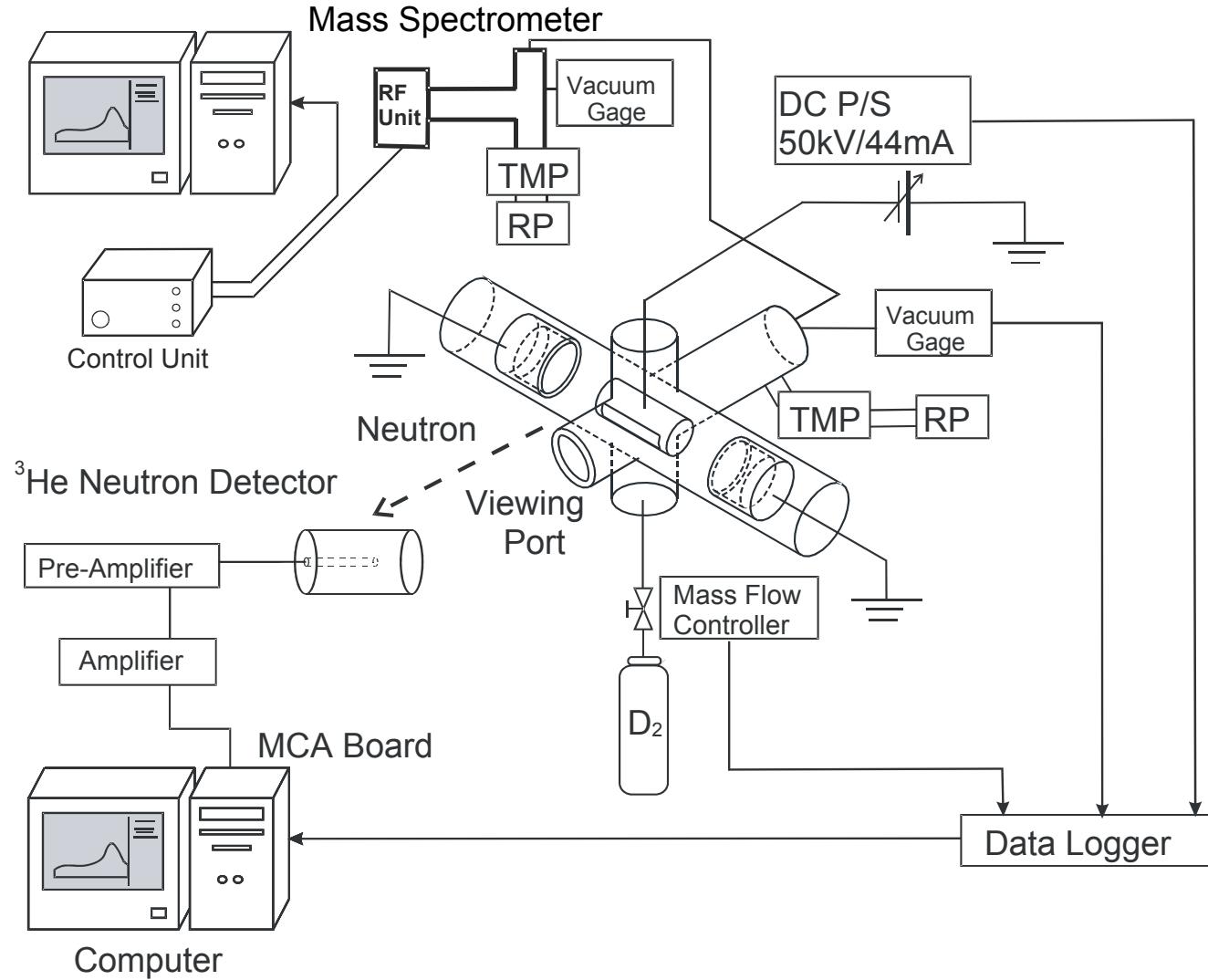
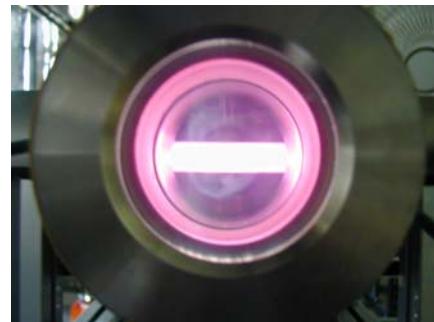
To confirm this assumption, measurements of neutral beam energy distribution at the anode of the C-IECF device was attempted to estimate ion energy distribution change with reduction of gas pressure.



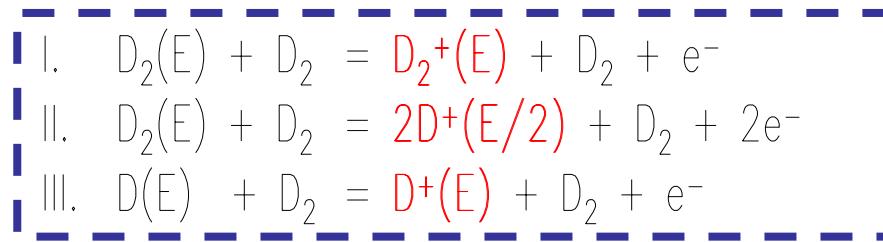
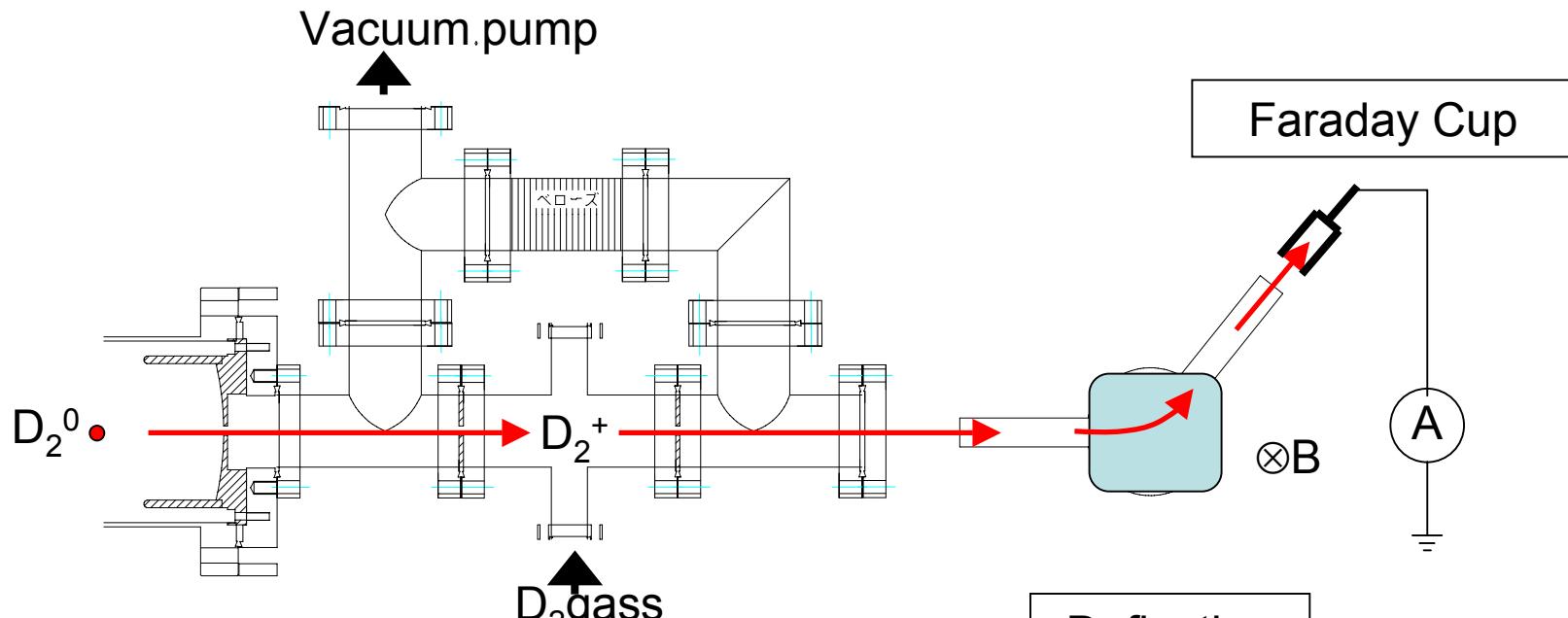
**Change of Neutron Production Rate (NPR)
with Operation Gas pressure**

Schematic of Experimental Setup

Base gas pressure
 2.5×10^{-5} [Pa]

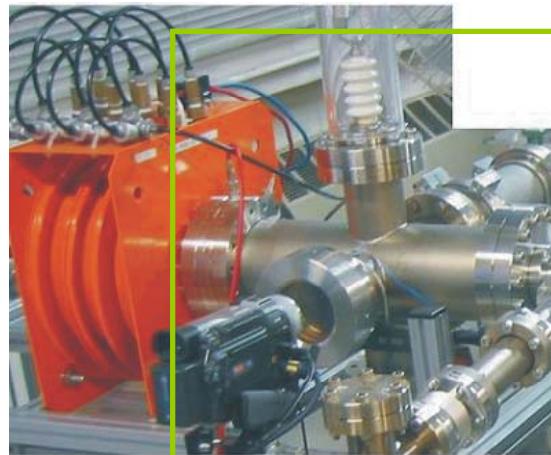


Schematic of Experimental Setup



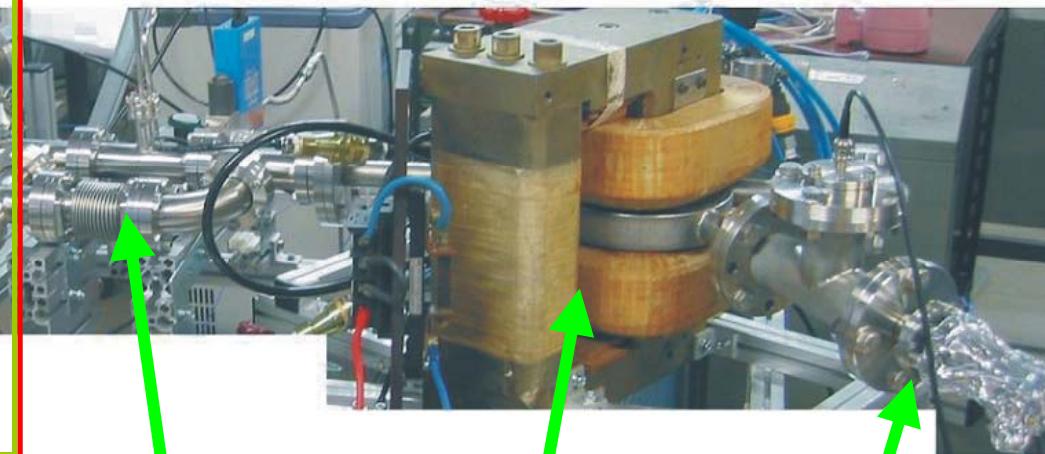
Photograph of C-IECF Device

ECR on Source



C-IECF Device

Neutral Beam Energy
Measurement Section

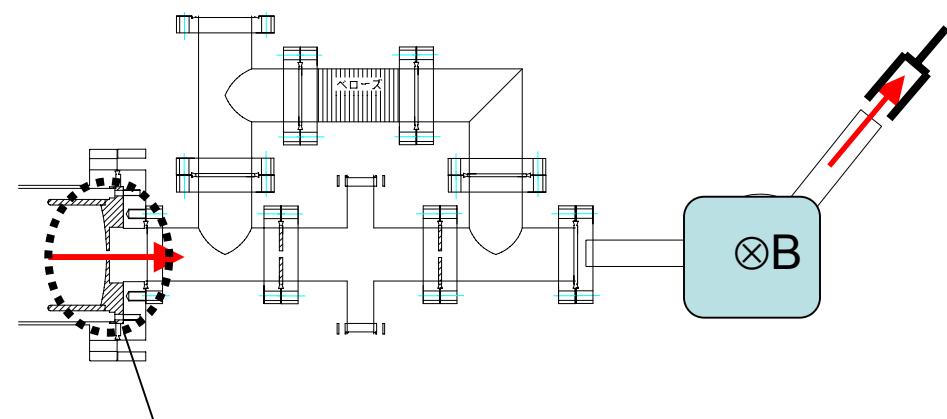
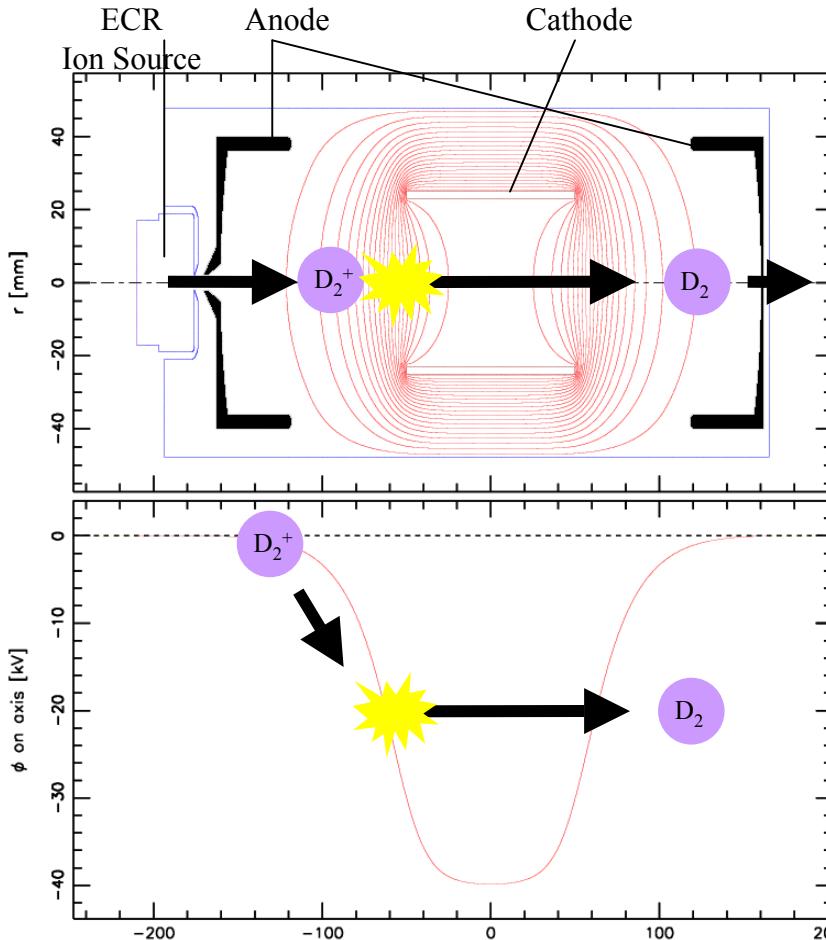


Re-ionization Cell

Deflection Magnet

Faraday Cup

Neutral beam energy distribution



Energy distribution prediction for neutral beam at the anode

Calculation is made by considering...

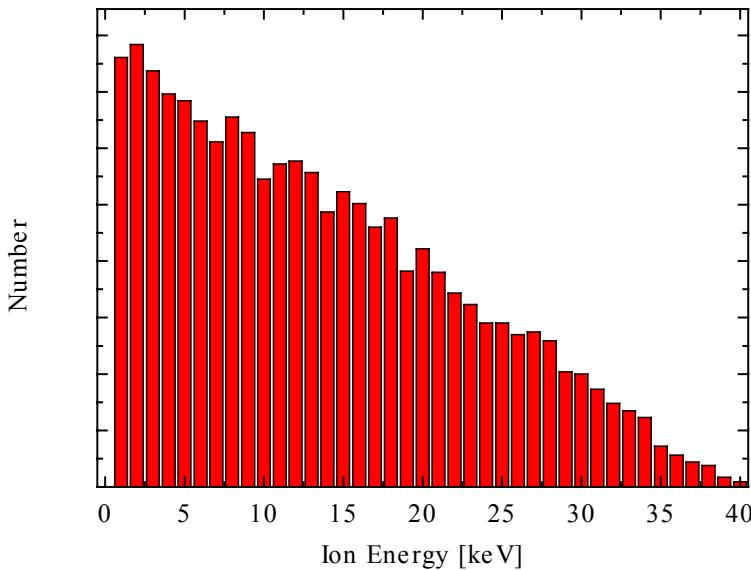
- Charge exchange reactions
- Acceleration by electric fields

Electric field strength in the C-IECF device

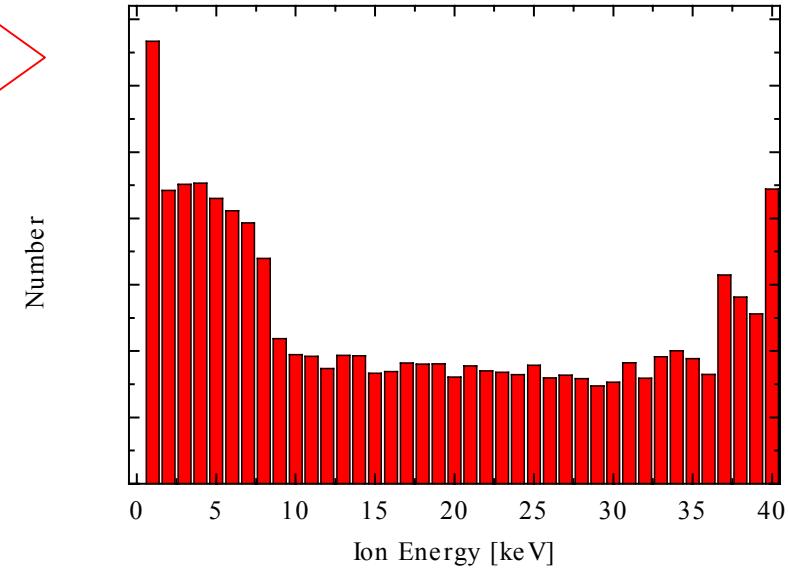
Calculation results of NBE

Calculation results for pressure change

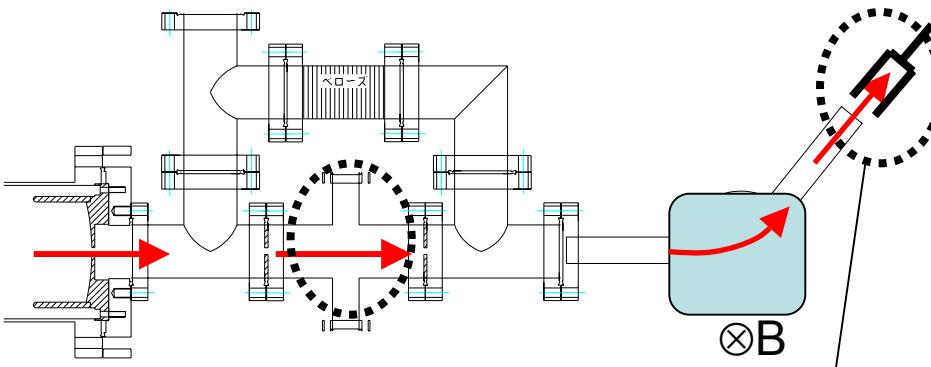
0.9Pa



0.3Pa



Collisions in the re-ionization cell

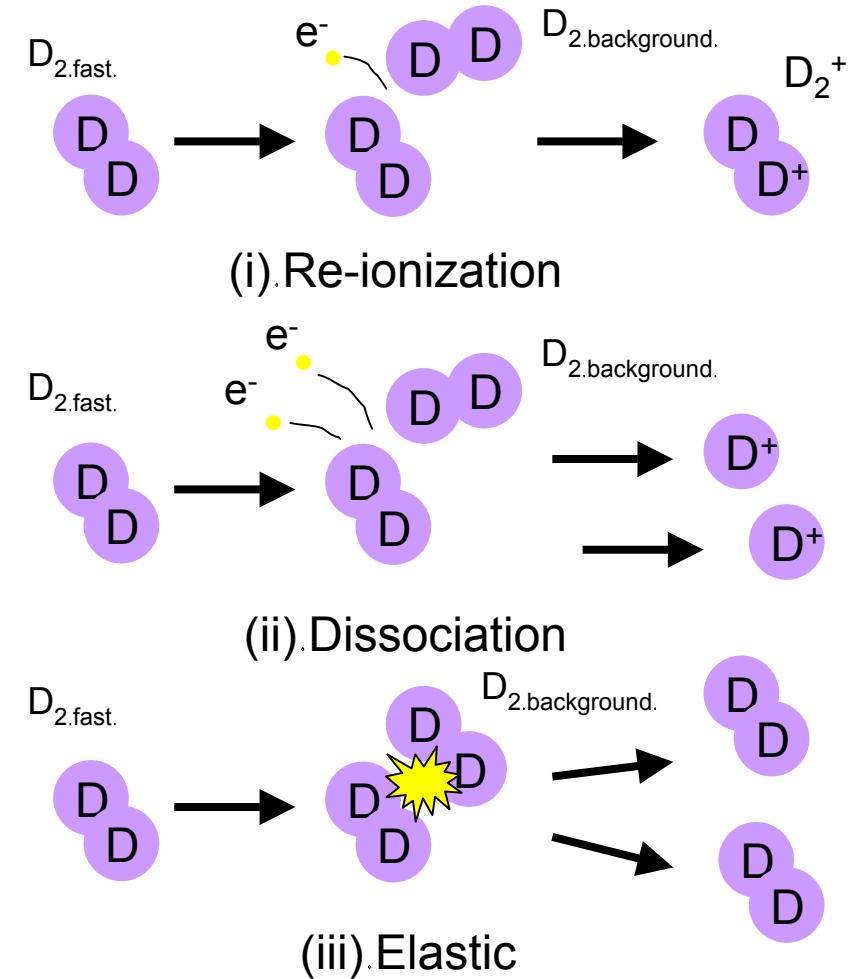


Energy distribution prediction of
Re-ionized ion Beam (RPB)

Neutral Particles . Ions

Calculation is made by considering...

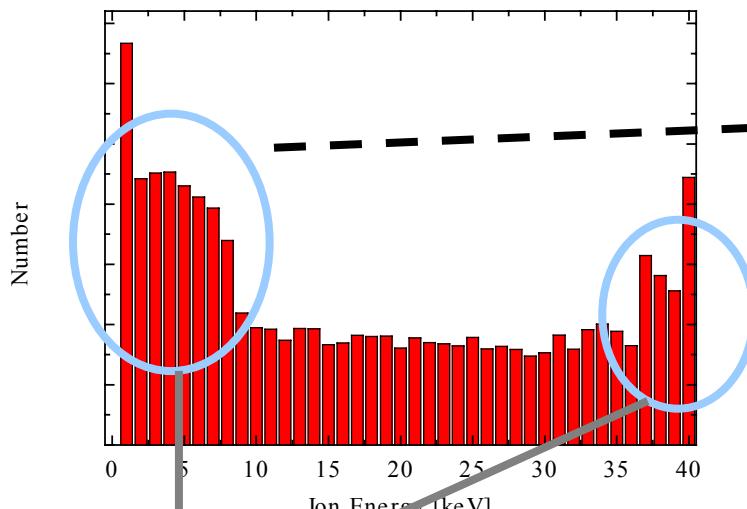
- Composition of fast particles
- Change in energy



Calculation results in the re-ionization cell

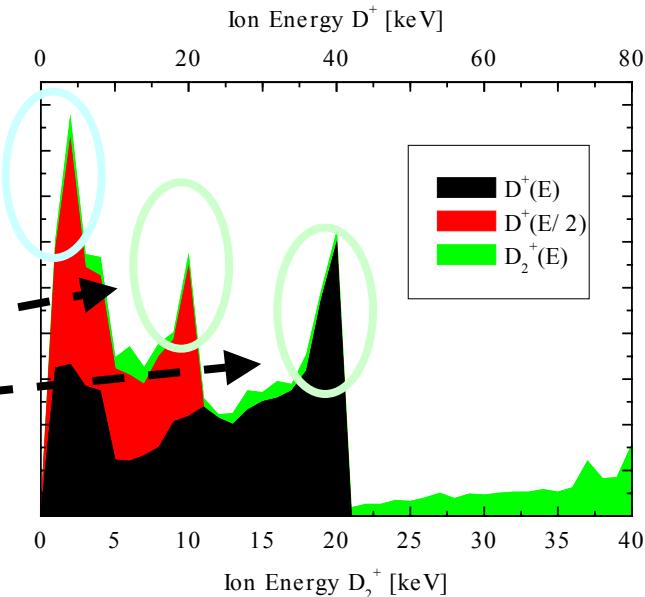
Operation gas pressure 0.3 [Pa]

Energy distribution of NPB at the anode

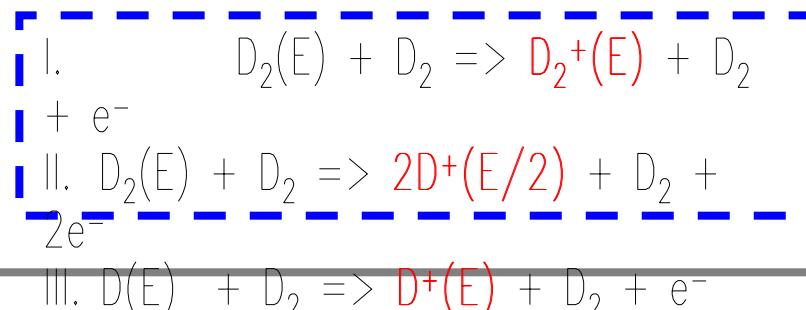


Pass the
stripping
cell

Energy distribution of RPB at faraday cup

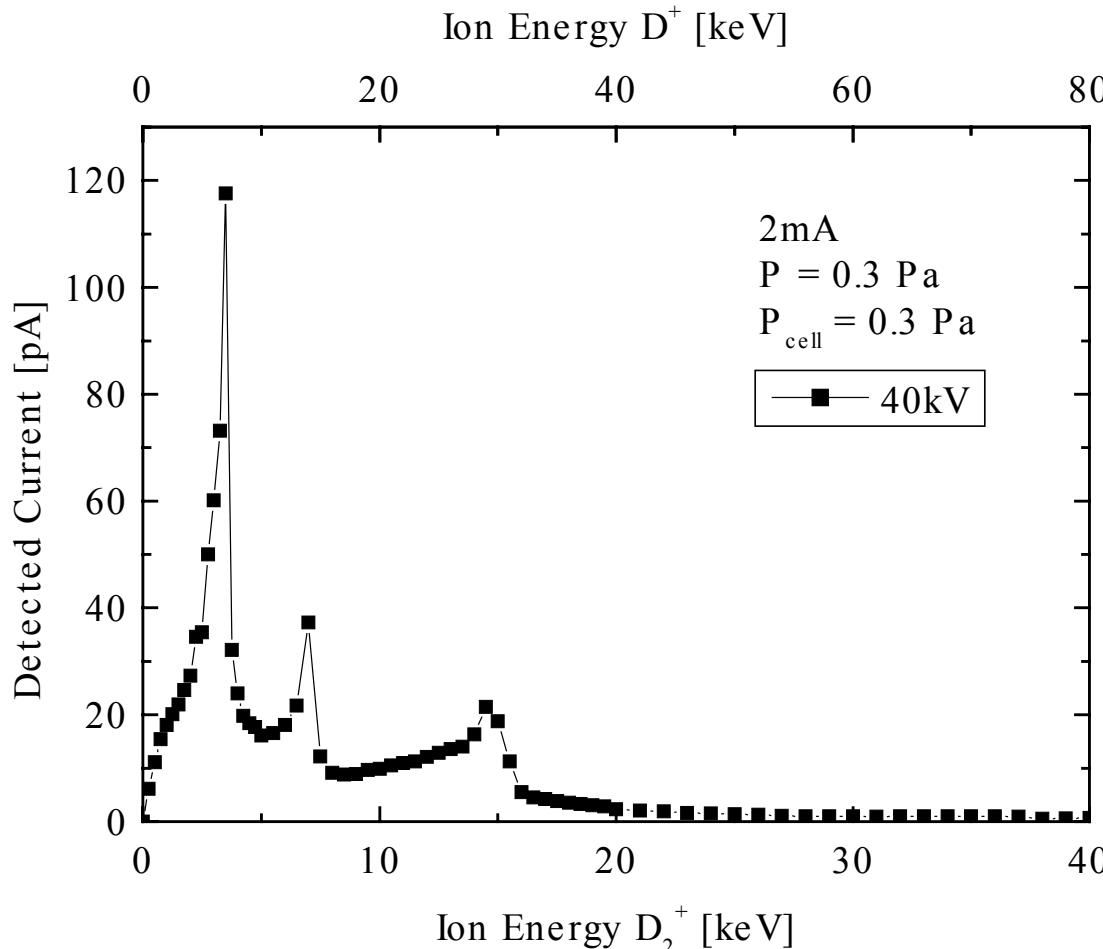


Energy peaks



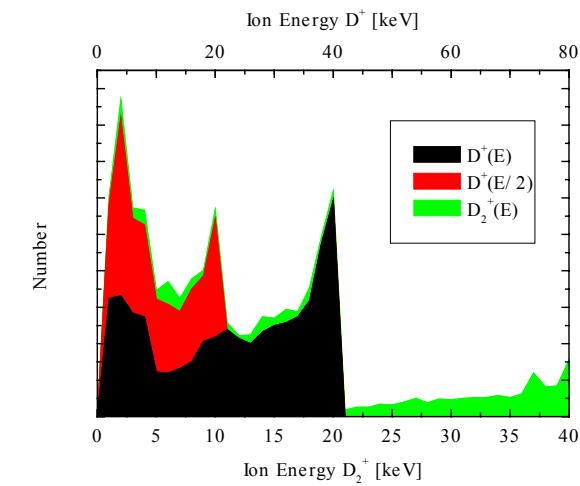
Almost all particles
are D^+

Comparison of experimental results with calculation results



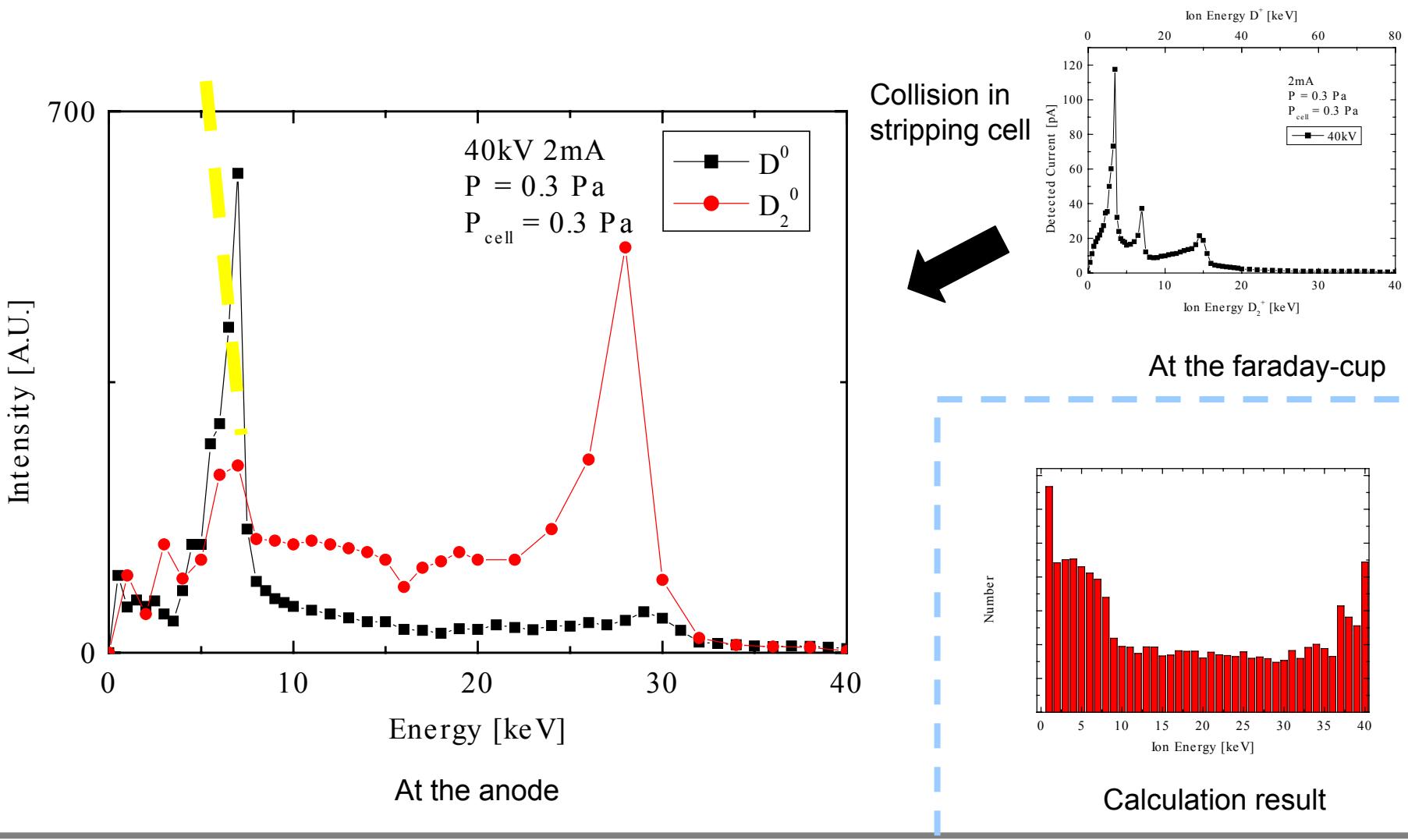
Energy measurement results of Re-ionized particles at 0.3Pa

- Tendency of the experimental results is well matched with the simulation result in the low pressure case.
- Therefore ion species composition of the experiments is expected to be similar to the calculation results.

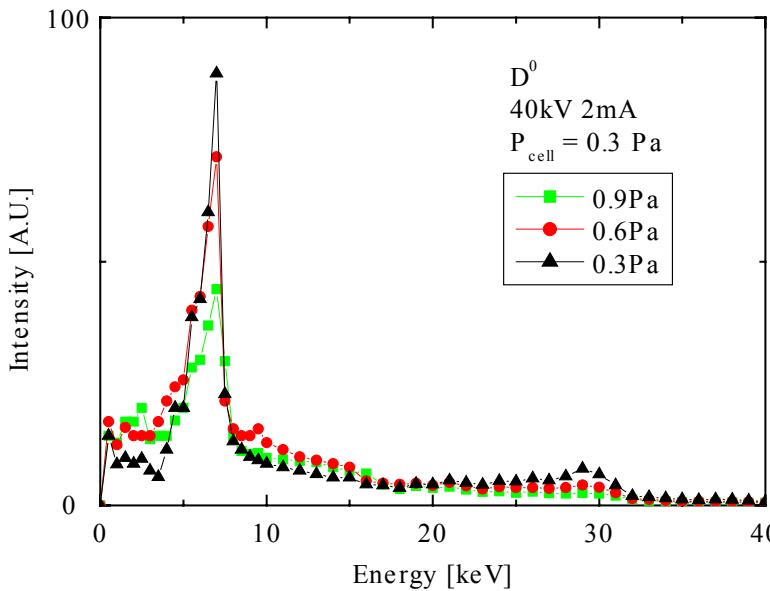


Calculation results

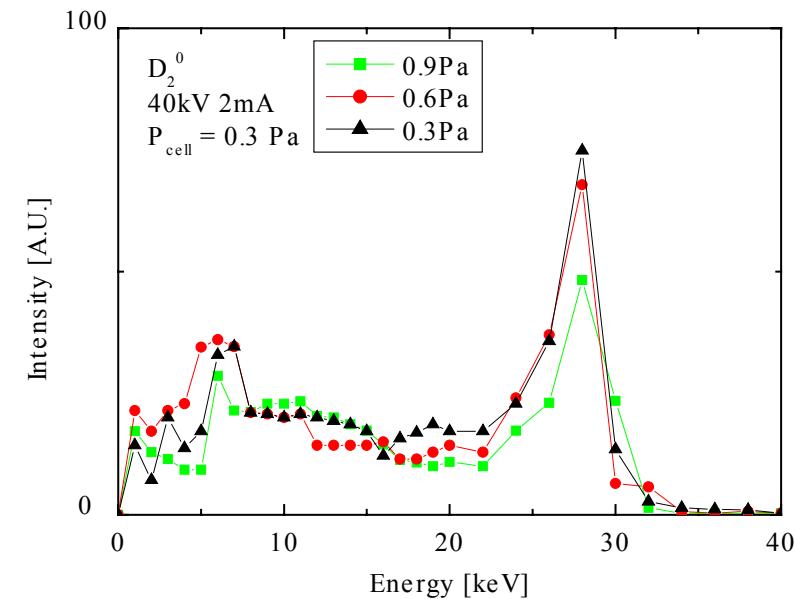
Backward calculation -Neutral beam energy distribution at the anode-



Effects of operation gas pressure



Energy distribution of D^0 at the anode

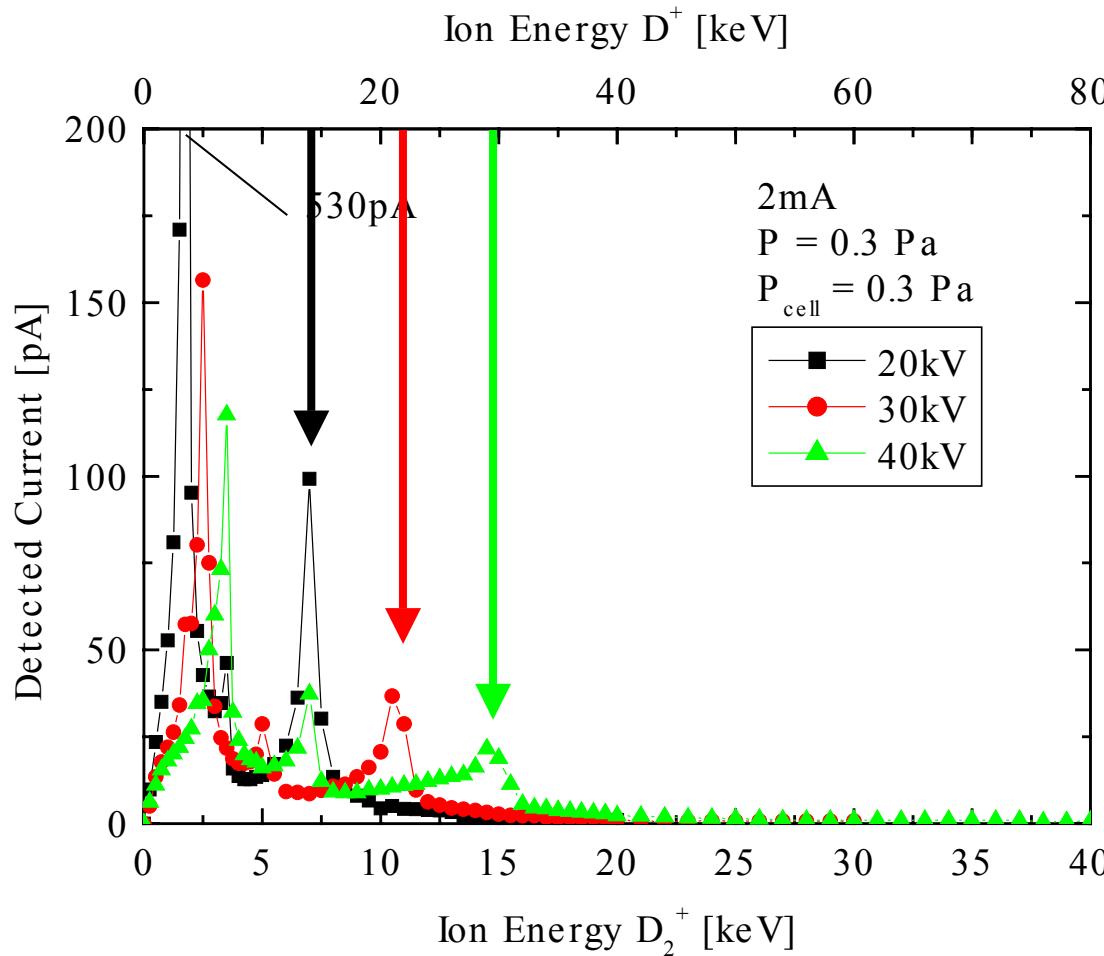


Energy distribution of D_2^0 at the anode

- A peak exists at ~ 30 keV in all gas pressure.
- Number of high energy particles increases with decrease pressure from 0.9Pa to 0.6Pa.
- There is no big change between 0.3 Pa and 0.6 Pa.

	0.9Pa	0.6Pa	0.3Pa
NPR	$2.6 \cdot 10^4$	$3.6 \cdot 10^4$	$3.6 \cdot 10^4$

Effects of the applied voltage



- Peaks move to high energy side with increase of applied voltage.
 - In all case, the highest peak is around $\frac{3}{4}$ of applied energy, and there may be some voltage loss in the system.



Summary

- Tendency of the experimental results is well matched with the simulation results in the low pressure case.
- An increase in the high energy element of the particles in the device was observed when gas pressure was decrease from 0.9Pa to 0.3Pa.
- In the pressure range lower than 1 Pa, the position of highest energy peak is not changed when operation gas pressure is changed, and the value is ~3/4 of applied voltage in the experiments using the cylindrical IECF device at Kyoto Univ.
- Energy distribution of neutral beam is found to have two peaks at the low energy part and the high energy side.
- Almost all of neutral particles drawn out from the C-IECF device are found to be D_2 , therefore, most of ions in the C-IECF device are expected to be D_2^+ .

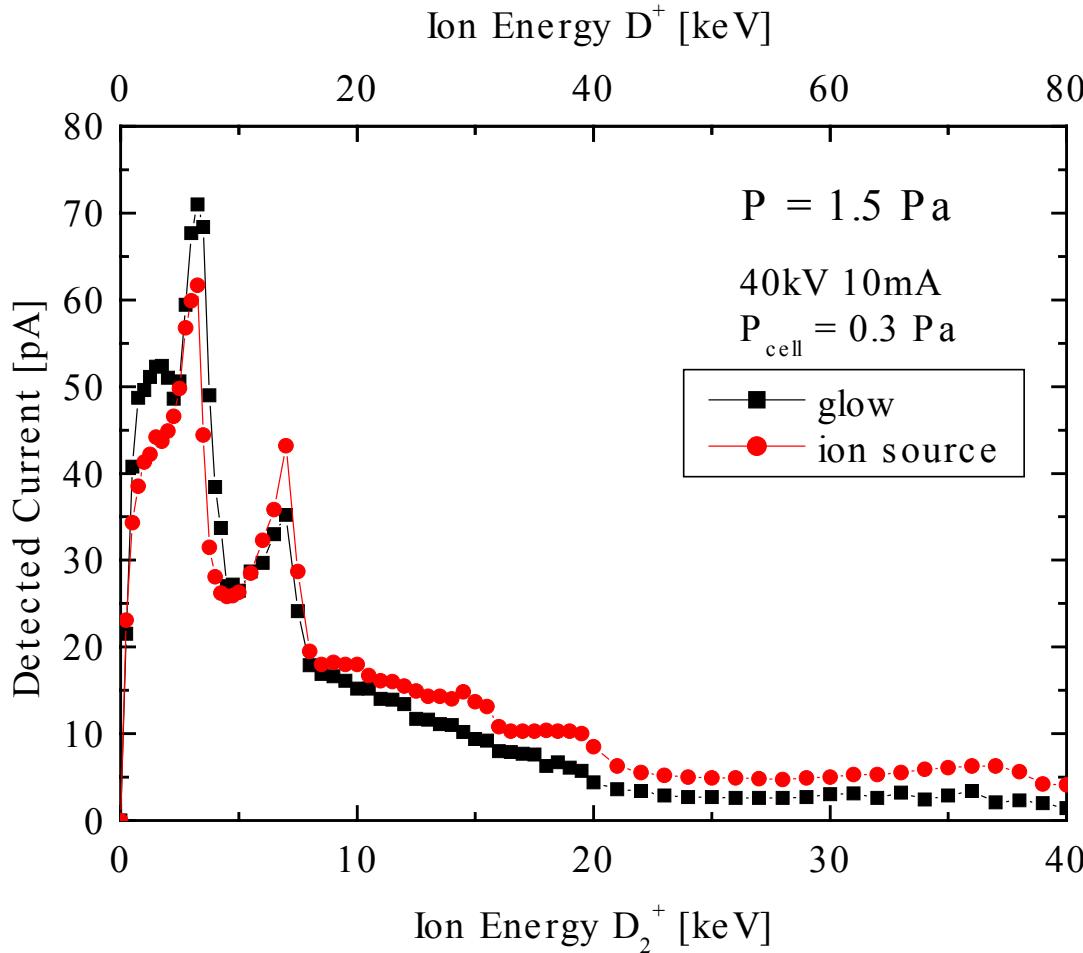


Conclusion

- From the current experimental results, it is confirmed that the number of high energy ions is increased with decrease of gas pressure. Therefore, increase of neutron production rate with decrease of gas pressure can be explained by increase of high energy ions.
- However, the number of low energy ions is still larger than that of high energy ions, and further decrease of gas pressure is requested.
- From the experiments, most of ions in the device is estimated to be D_2^+ . For that reason, it is expected to be effective to increase applied voltage or injection of D^+ ion for increase of the NPR.

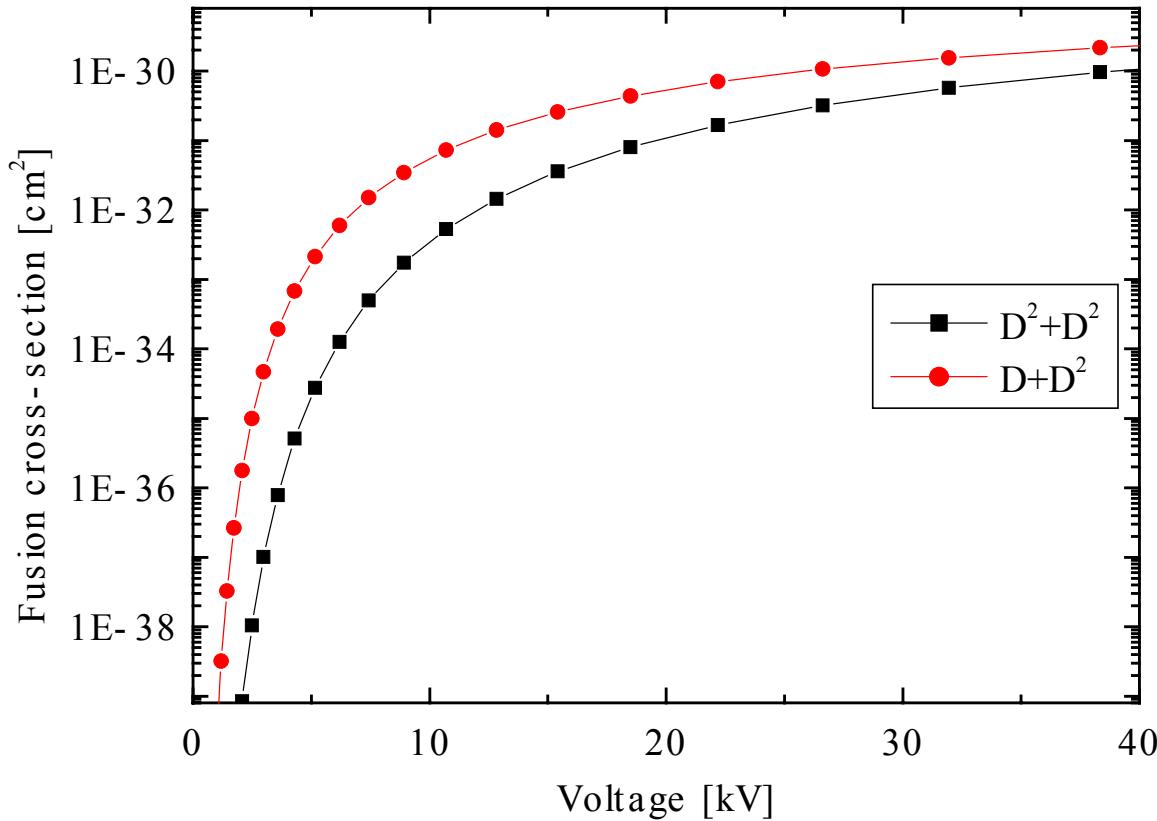
Effect of Ion Source

1.5Pa..Glow discharge domain.



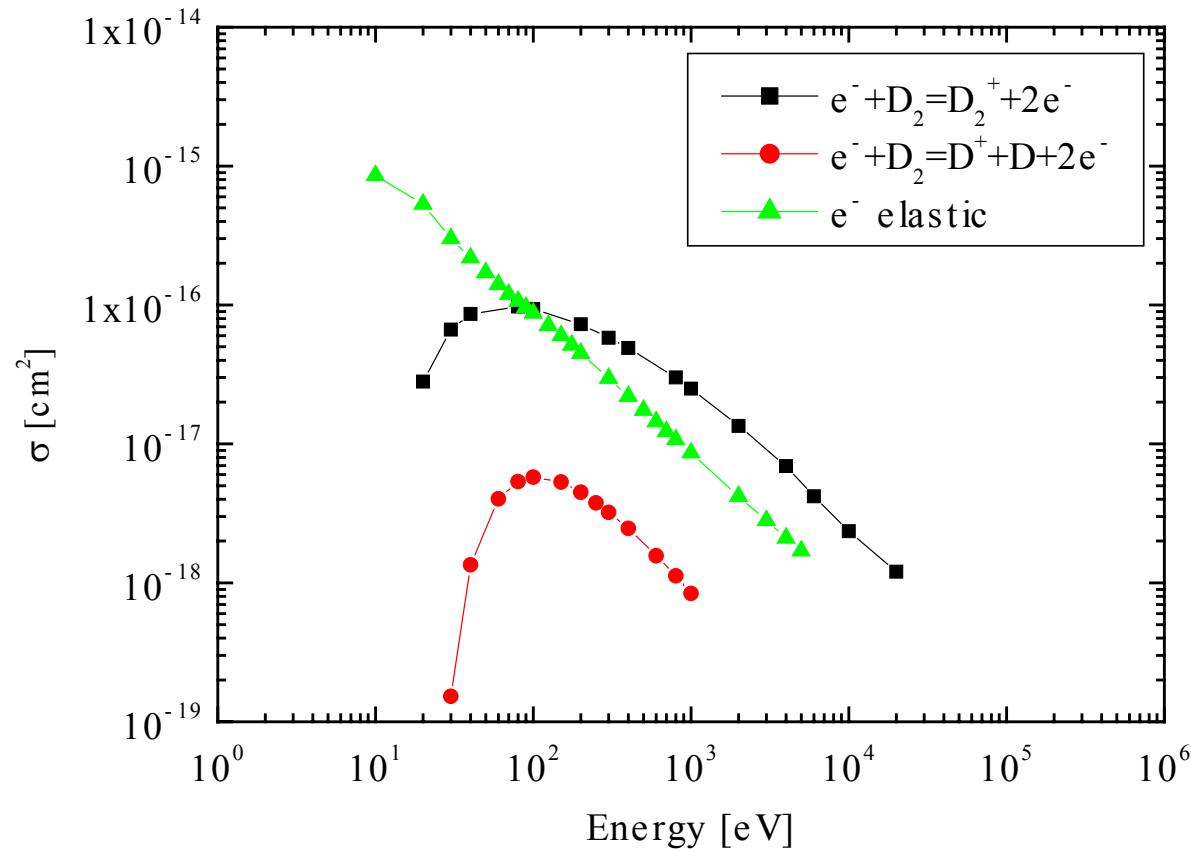
	Glow	Ion Source
NPR	8.20×10^4	9.21×10^4

Fusion Cross-Section

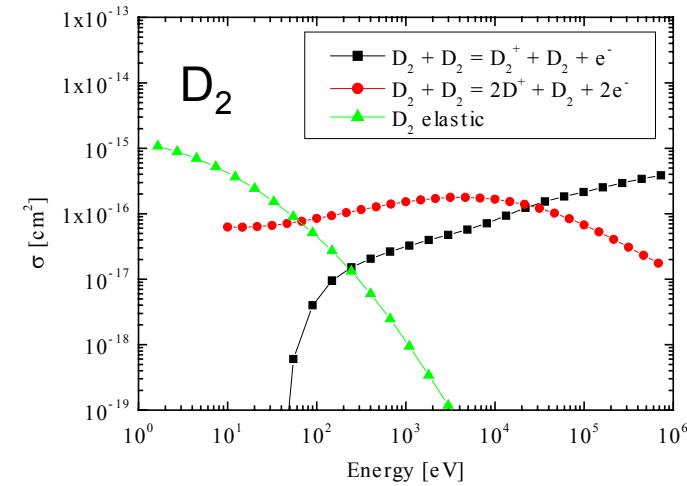
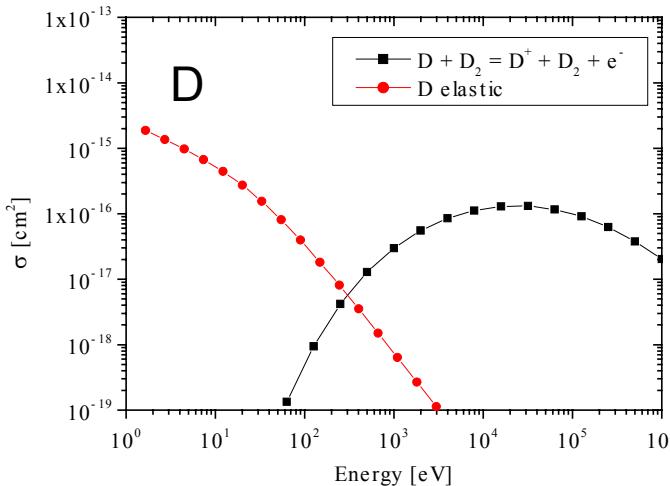
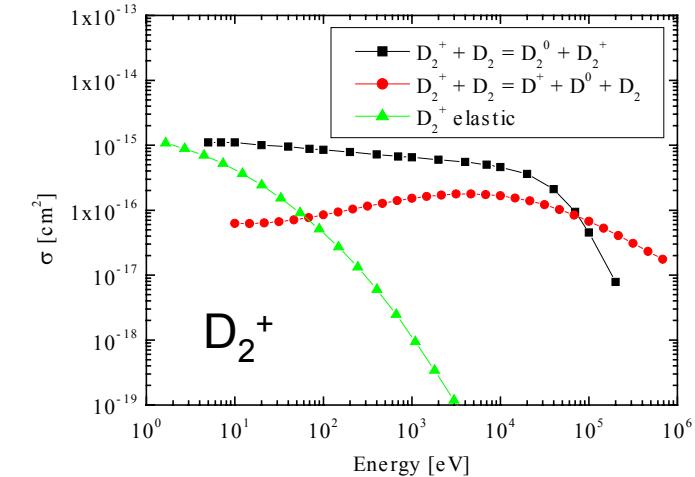
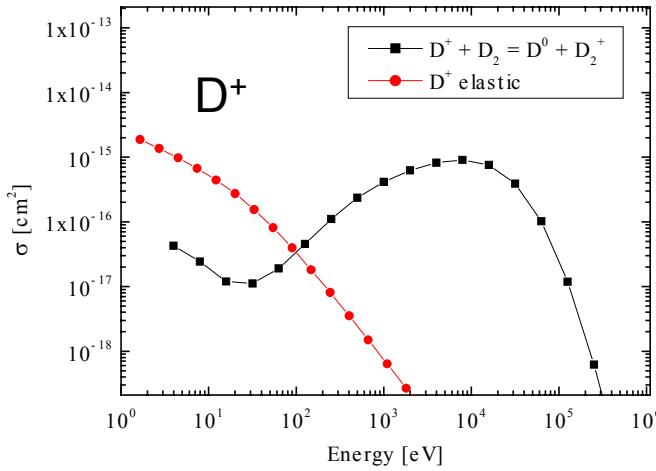




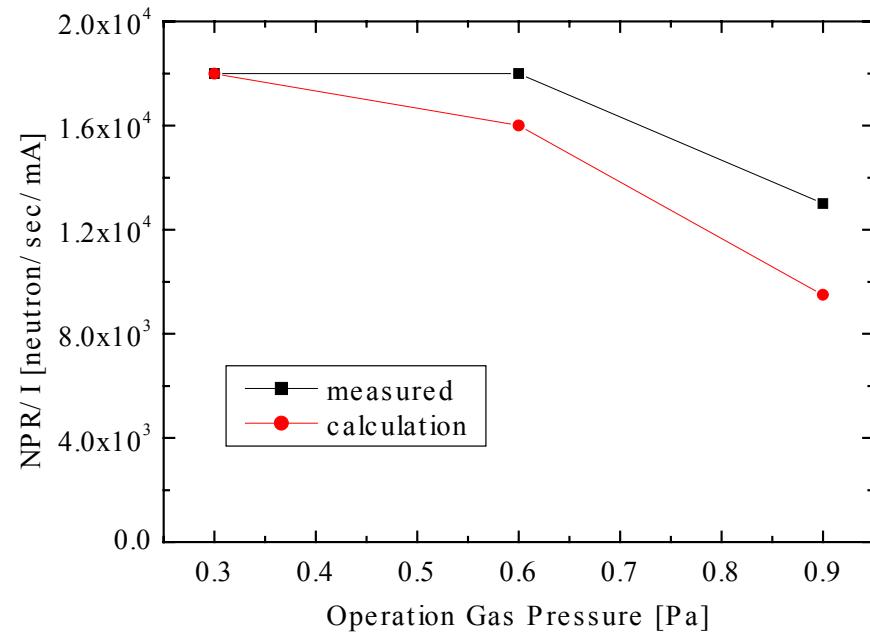
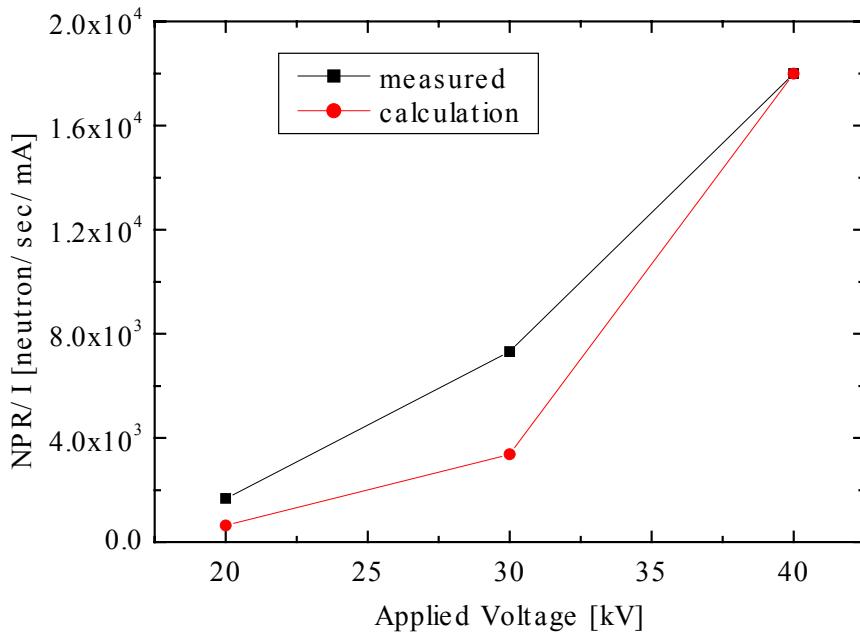
Electron Cross-Section



Cross-Section



NPR



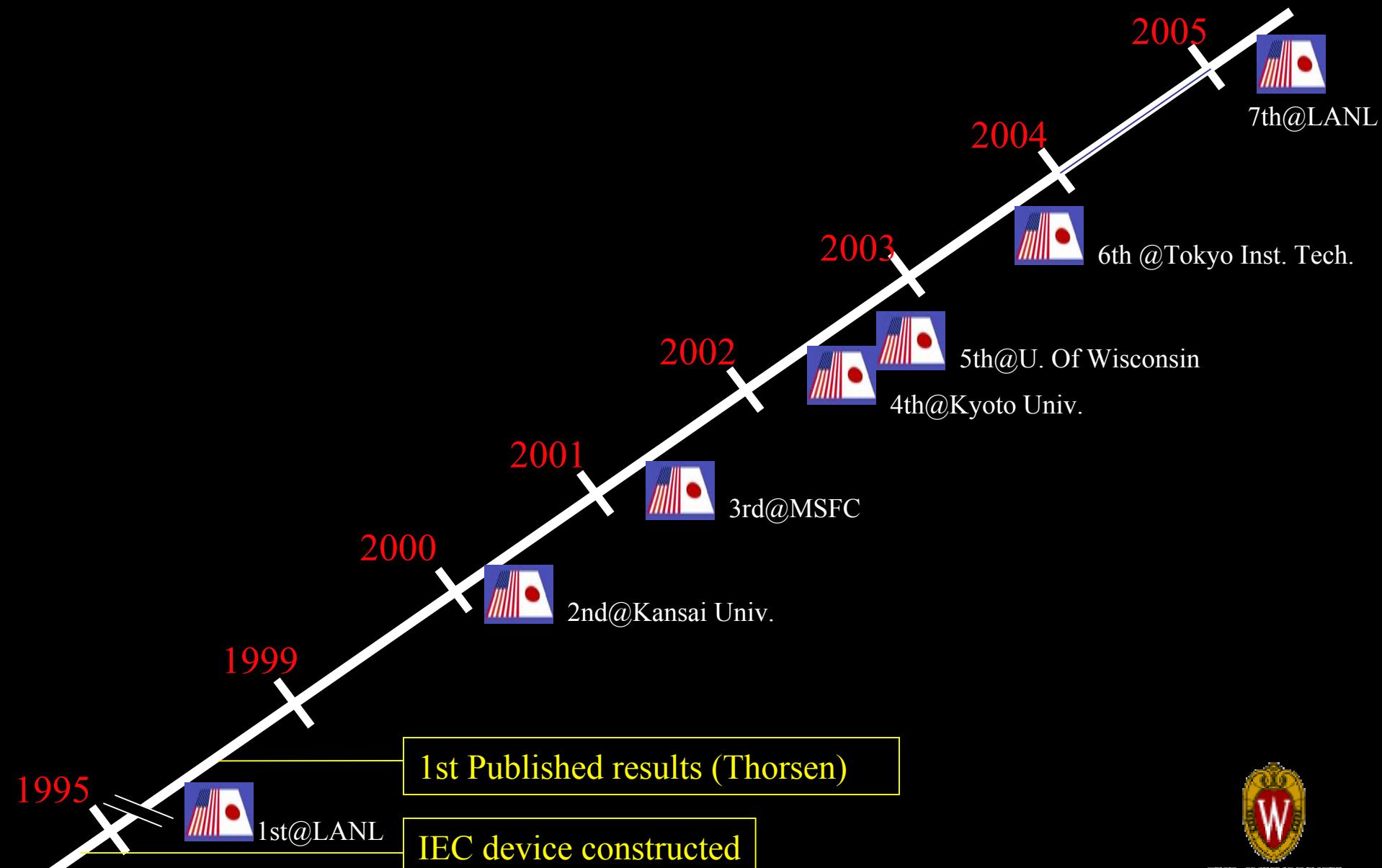
A Decade of IEC Research at the University of Wisconsin

R.P. Ashley

E.C. Alderson, D.R. Boris, R.C. Giar, G.L. Kulcinski, G.R. Piefer,
R.F. Radel, T.E. Radel, J.F. Santarius, and A.L. Wehmeyer

*University of Wisconsin-Madison, Fusion Technology Institute
1500 Engineering Drive
Madison WI 53706
(608) 265-3098*

UW IEC History Timeline



Thorsen et. al. Begin UW IEC Work in 1994

1st Paper published in 1997

Convergence, electrostatic potential, and density measurements in a spherically convergent ion focus

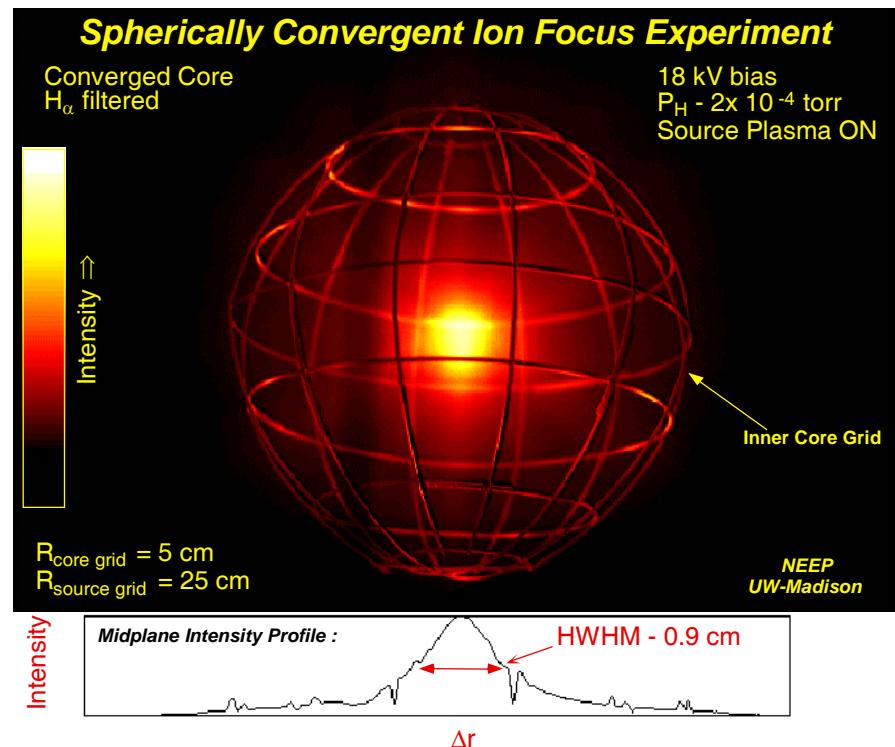
T. A. Thorson,^{a)} R. D. Durst, R. J. Fonck, and L. P. Wainwright
University of Wisconsin—Madison, 1500 Engineering Drive, Madison, Wisconsin 53706

Phys. Plasmas **4** (1), January 1997

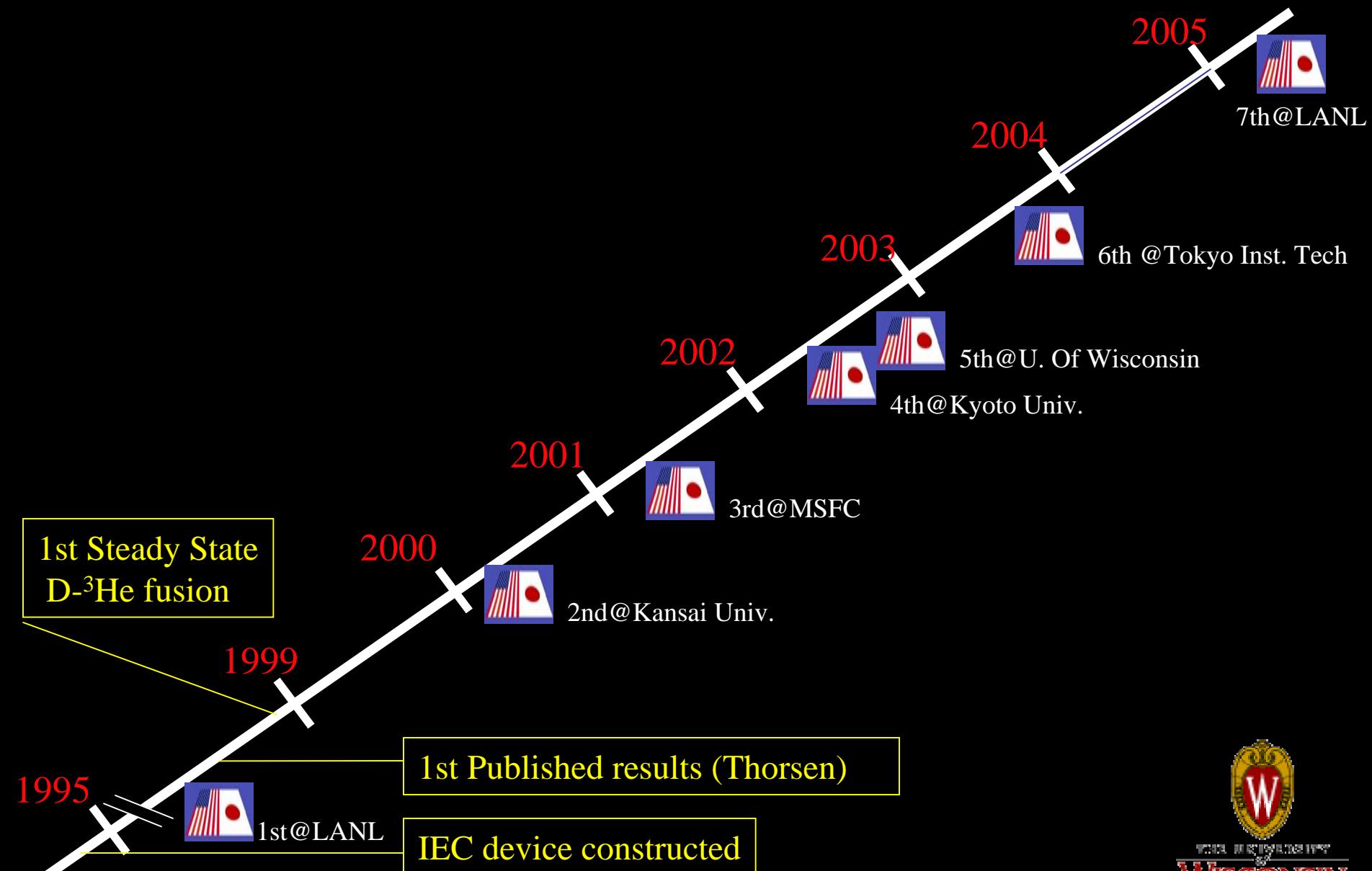
FUSION REACTIVITY CHARACTERIZATION
OF A SPHERICALLY CONVERGENT ION FOCUS

T.A. THORSON, R.D. DURST, R.J. FONCK, A.C. SONTAG
University of Wisconsin-Madison,

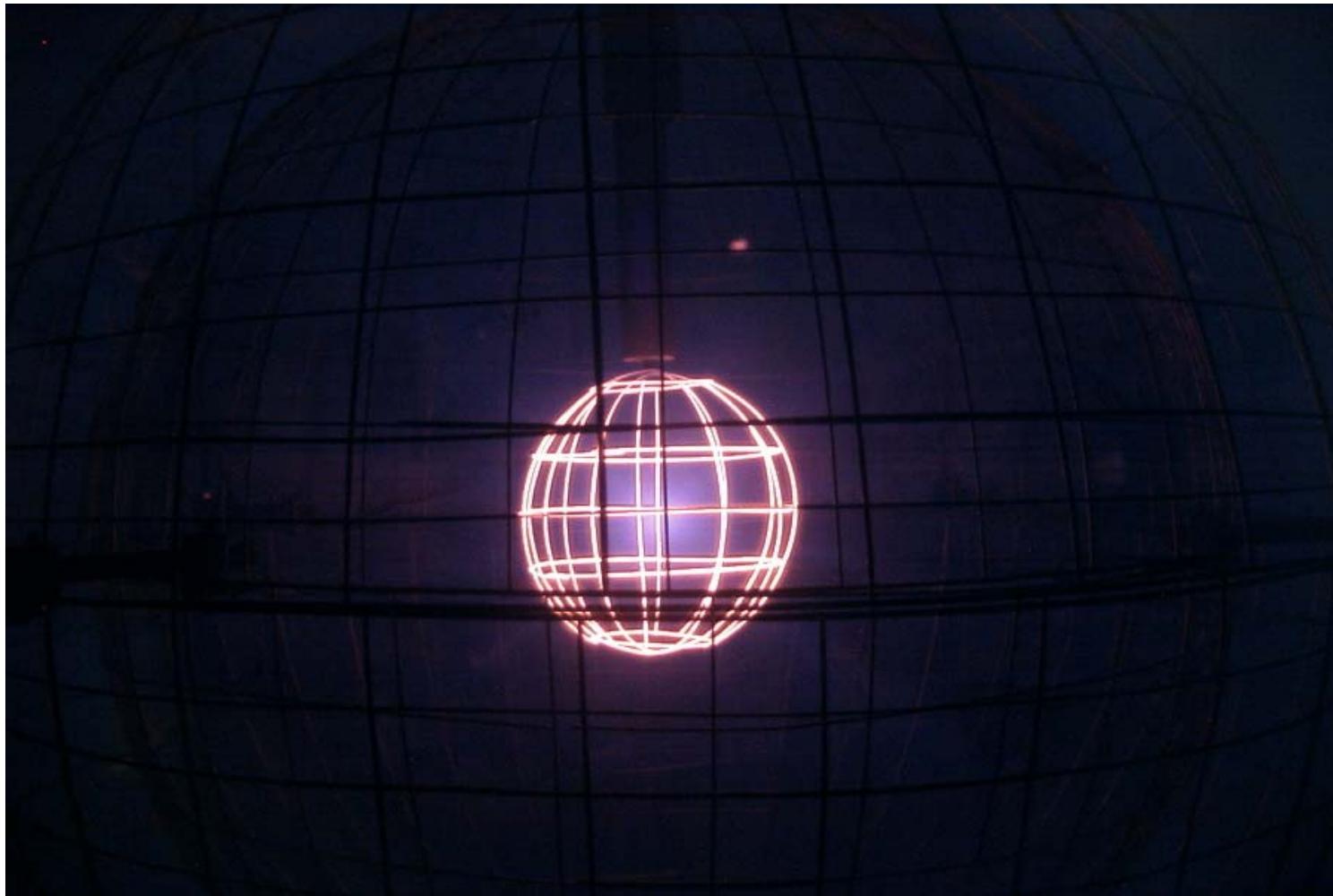
NUCLEAR FUSION, Vol. 38, No. 4 (1998)



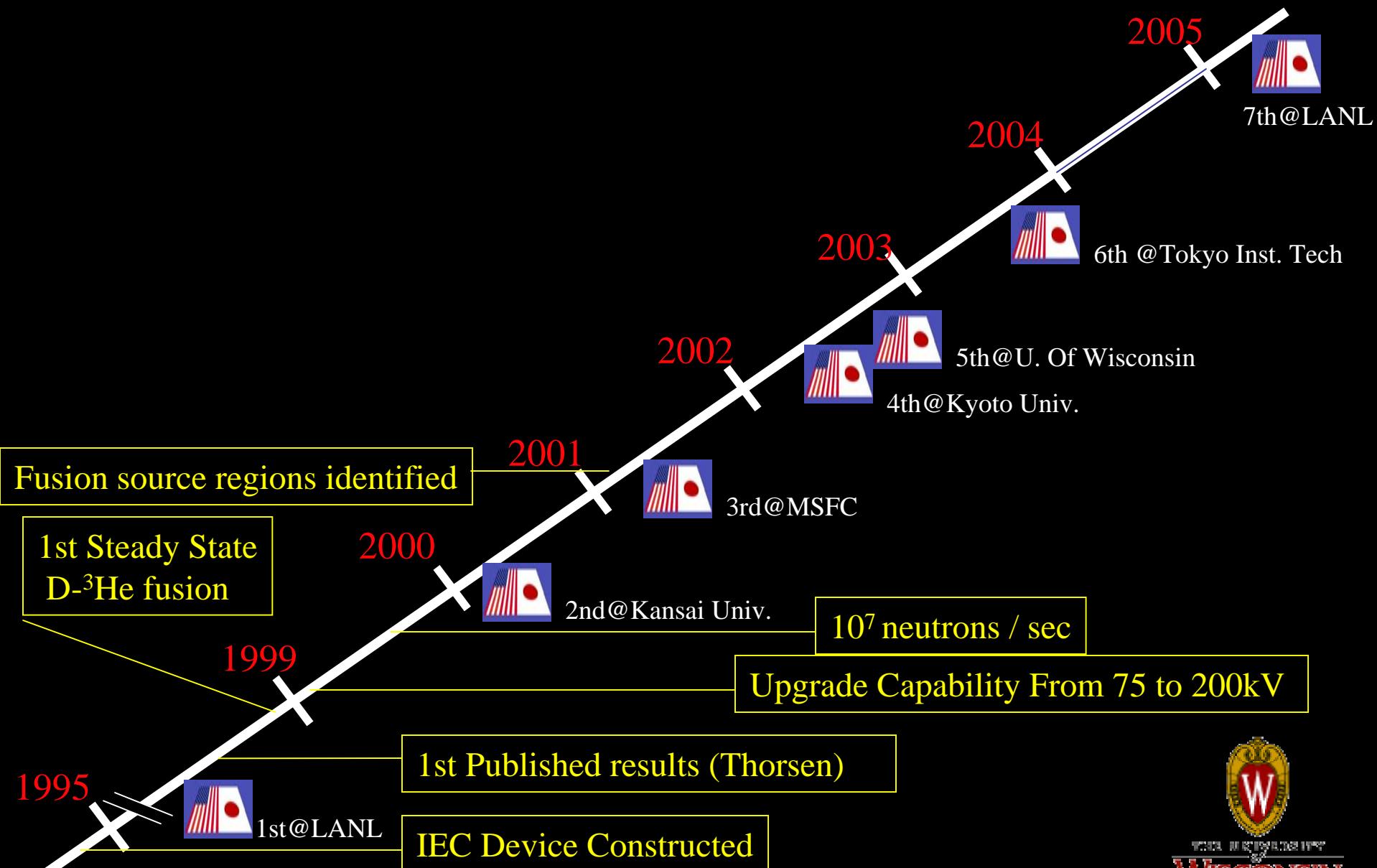
UW IEC History Timeline



1st Steady State D-³He Fusion Produced on 25 Oct 1998

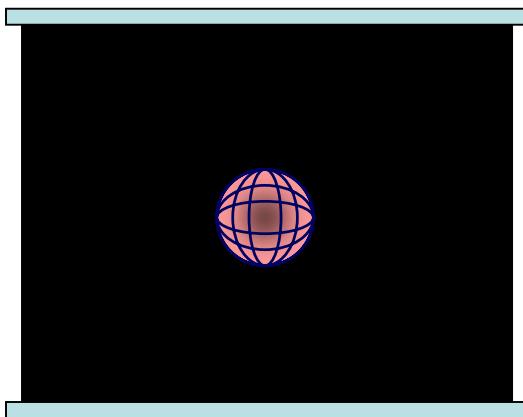


UW IEC History Timeline



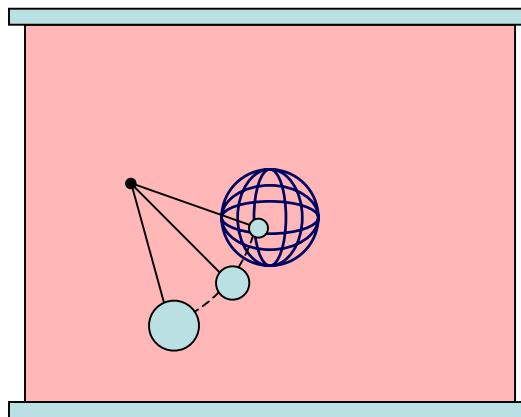
Three Sources of Fusion Reactions in an IEC Device Were Identified Using a Variable Size Eclipse Disk

Converged Core



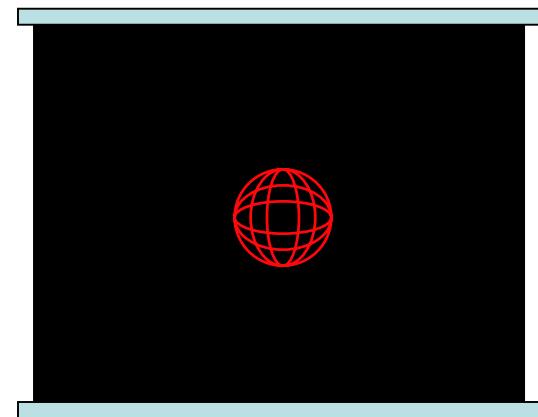
Fusion Occurs
Inside the Cathode

Charge Exchange



Fusion Occurs Throughout
Entire Volume of the Chamber

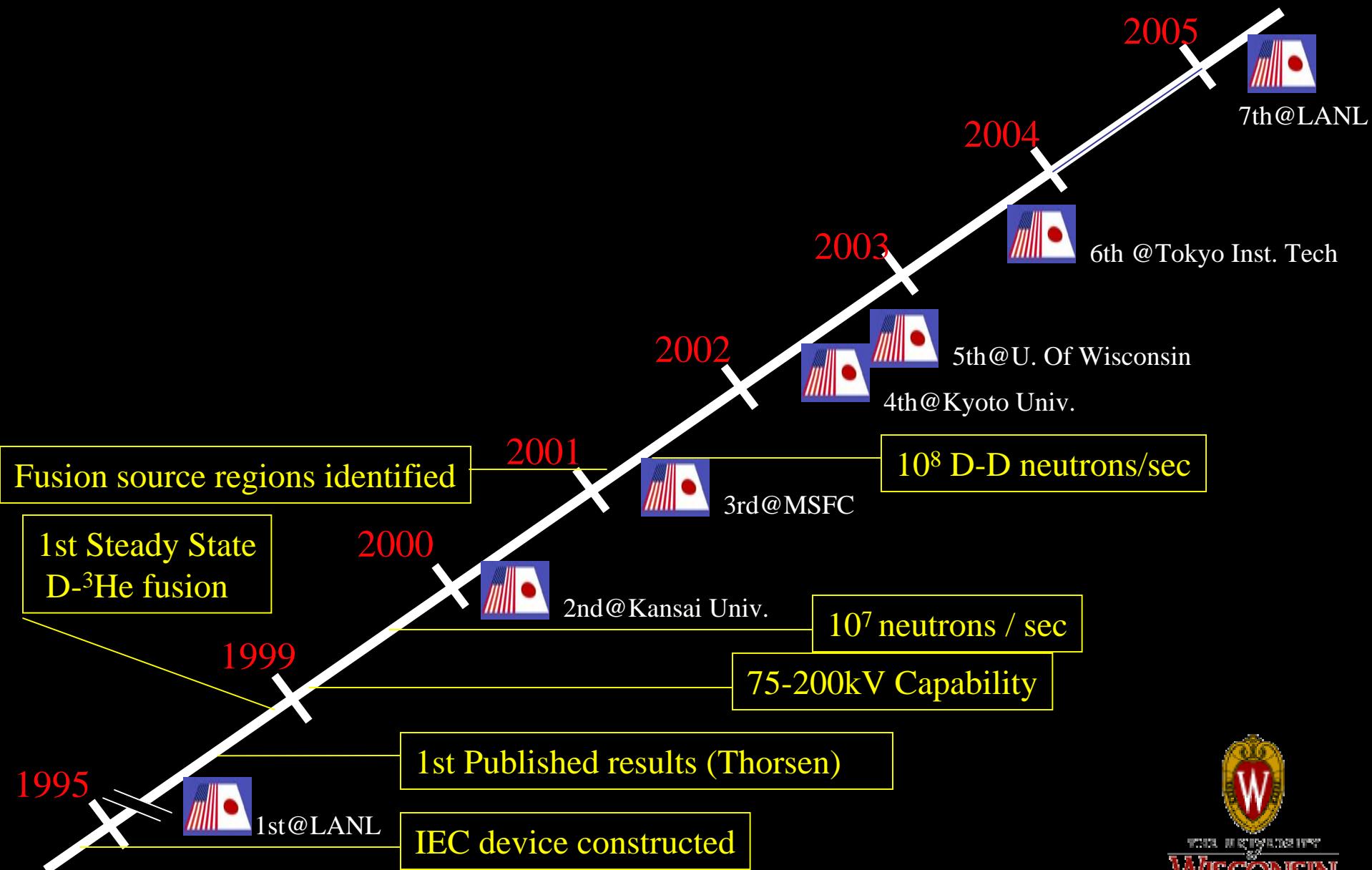
Embedded Ion



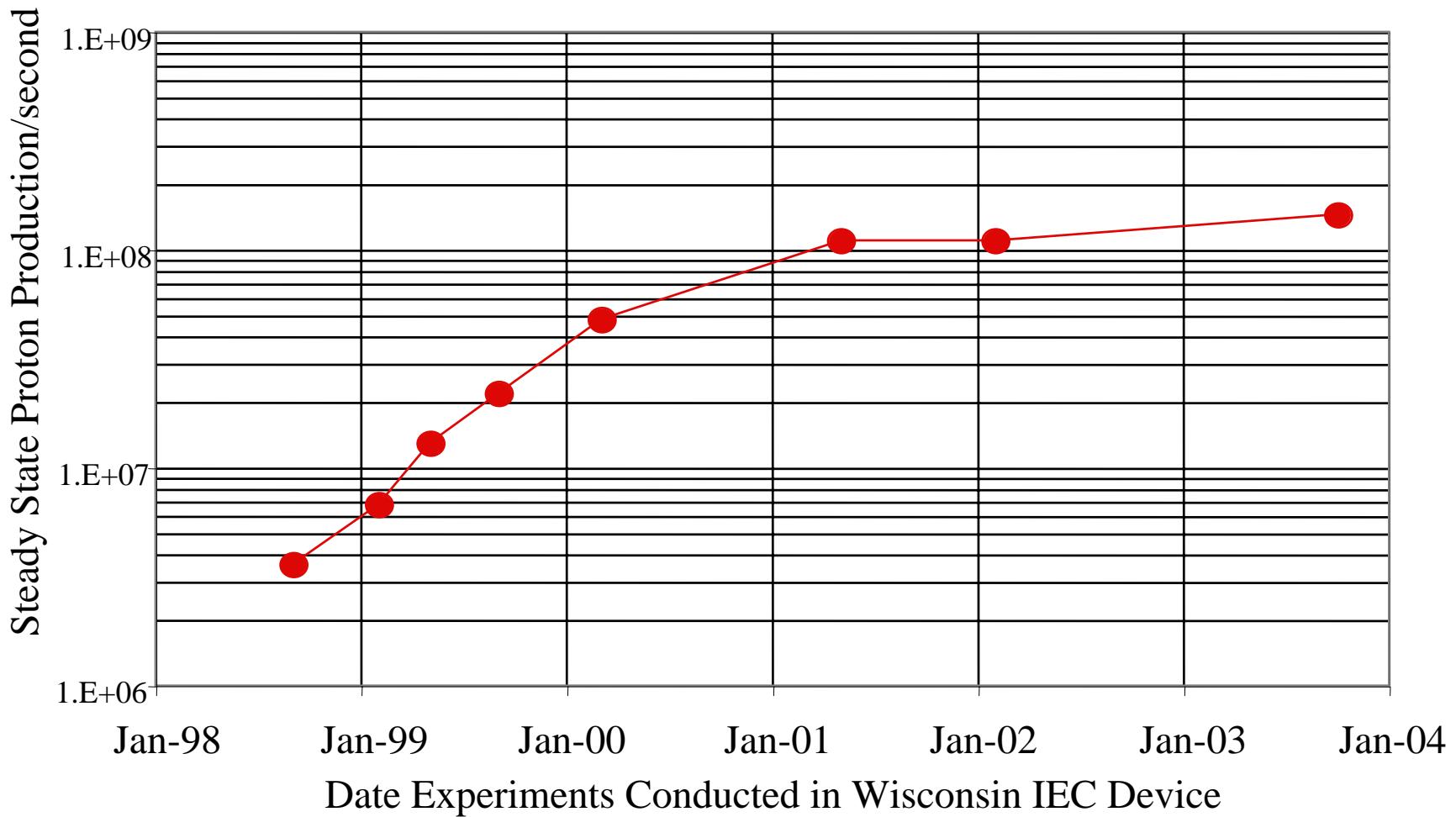
Fusion Occurs on the Surface
of the Cathode Grid Wires

- All three sources can be present at the same time
- Fraction depends on voltage, fuel, pressure, and past history

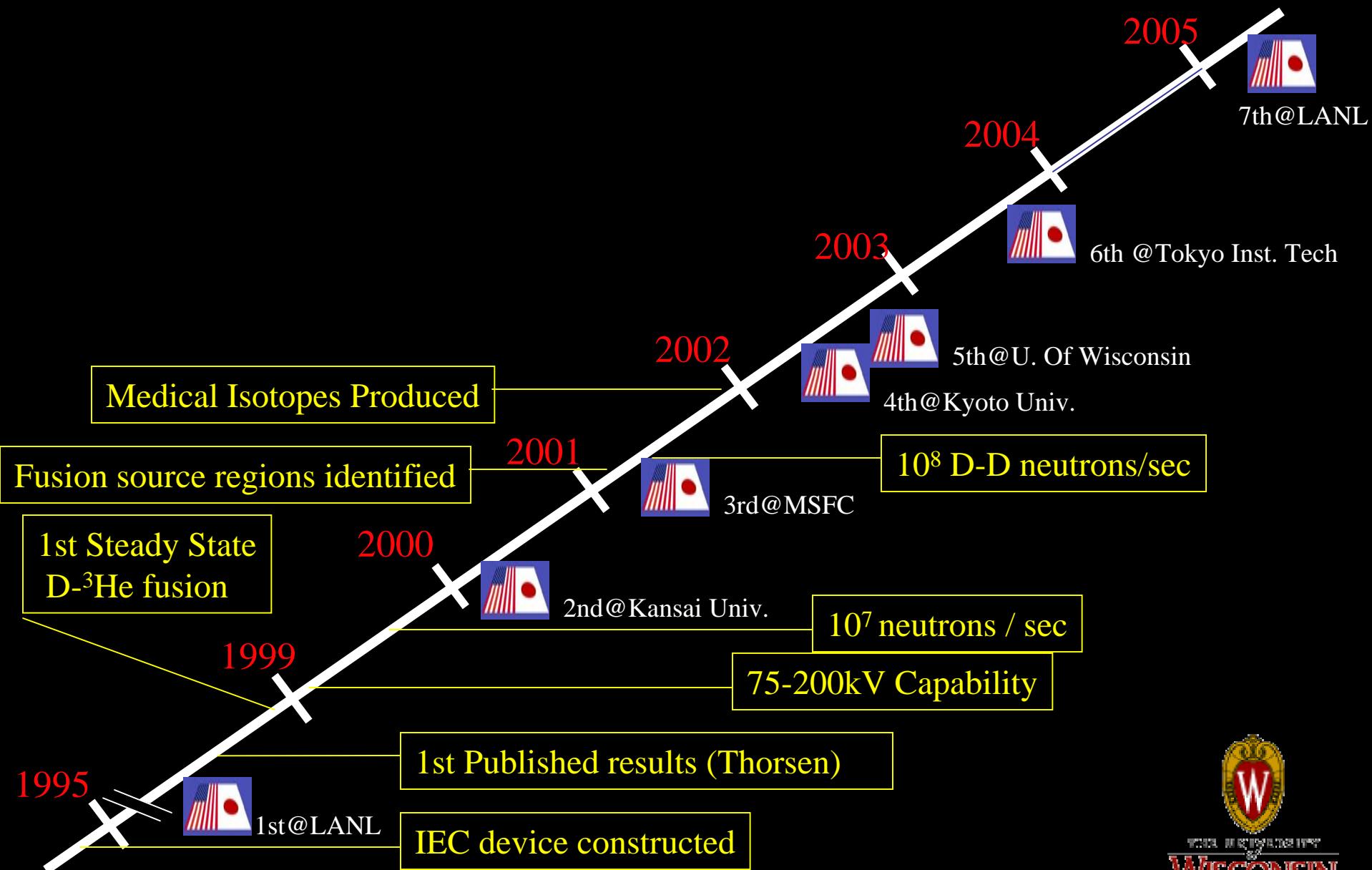
UW IEC History Timeline



Steady State D-D Neutron Records

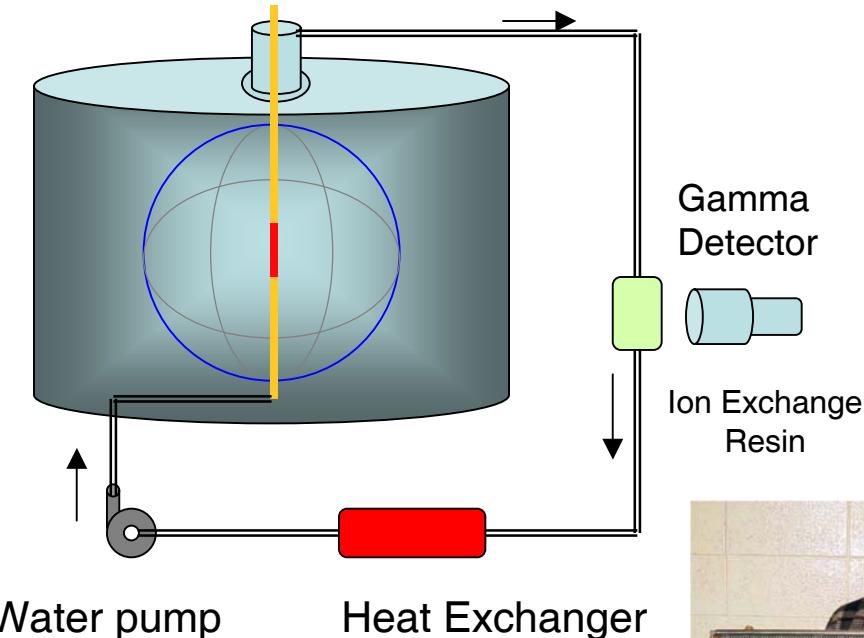


UW IEC History Timeline

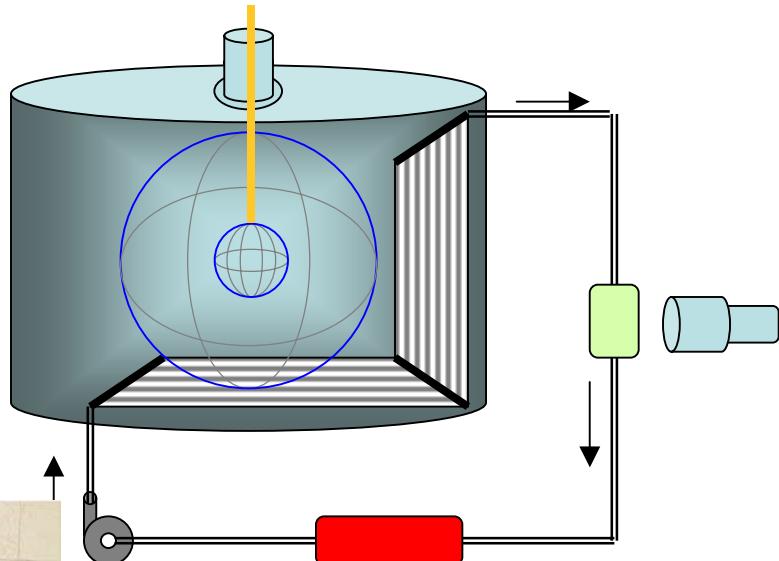


^{94m}Tc & ^{13}N Medical Isotopes Produced With D- ^3He Protons

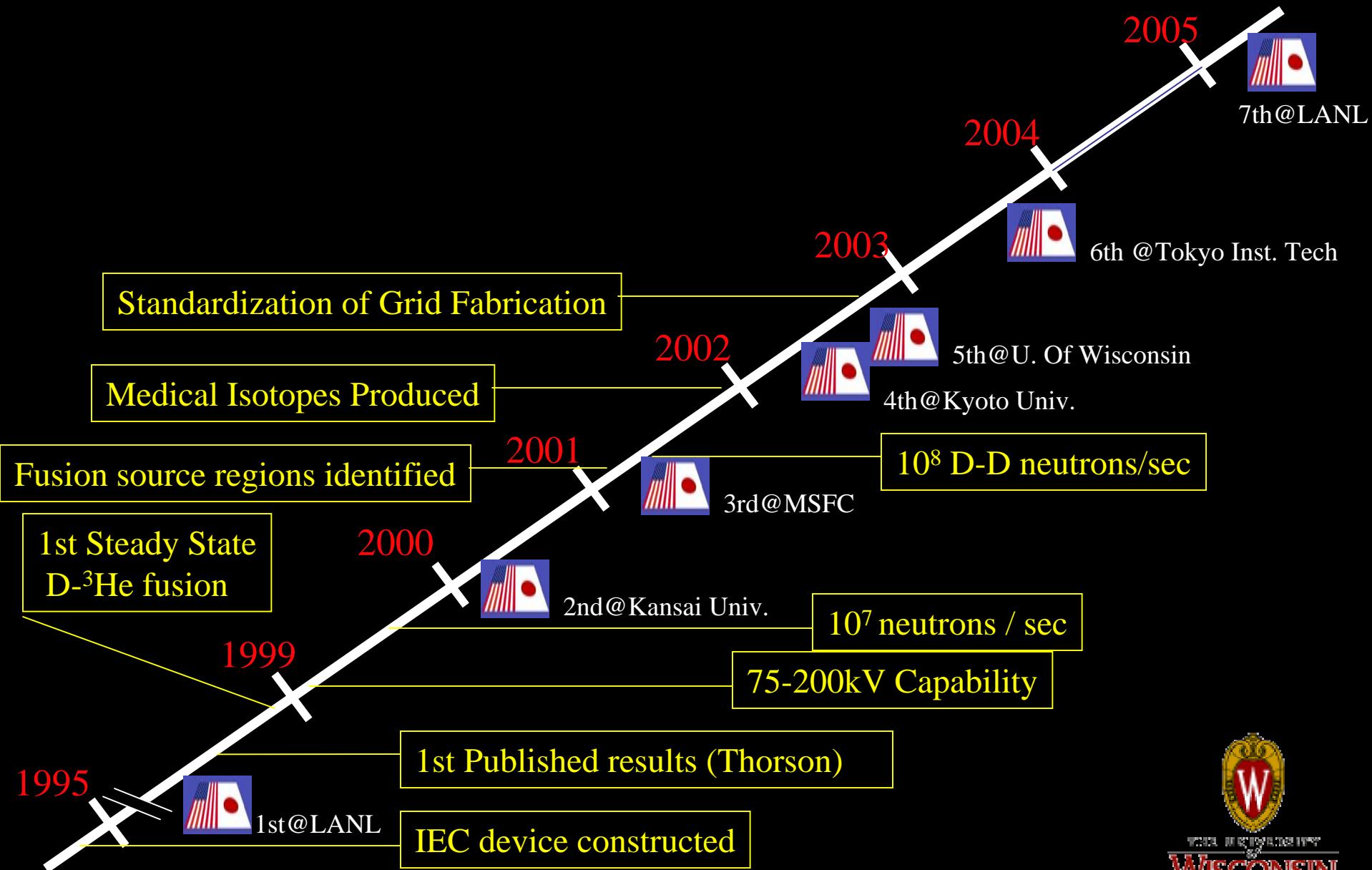
Water Cooled Cathode Target for ^{13}N



Water Cooled Wall Target for ^{13}N



UW IEC History Timeline



Grid Fabrication System



1. Mold produced from prototype

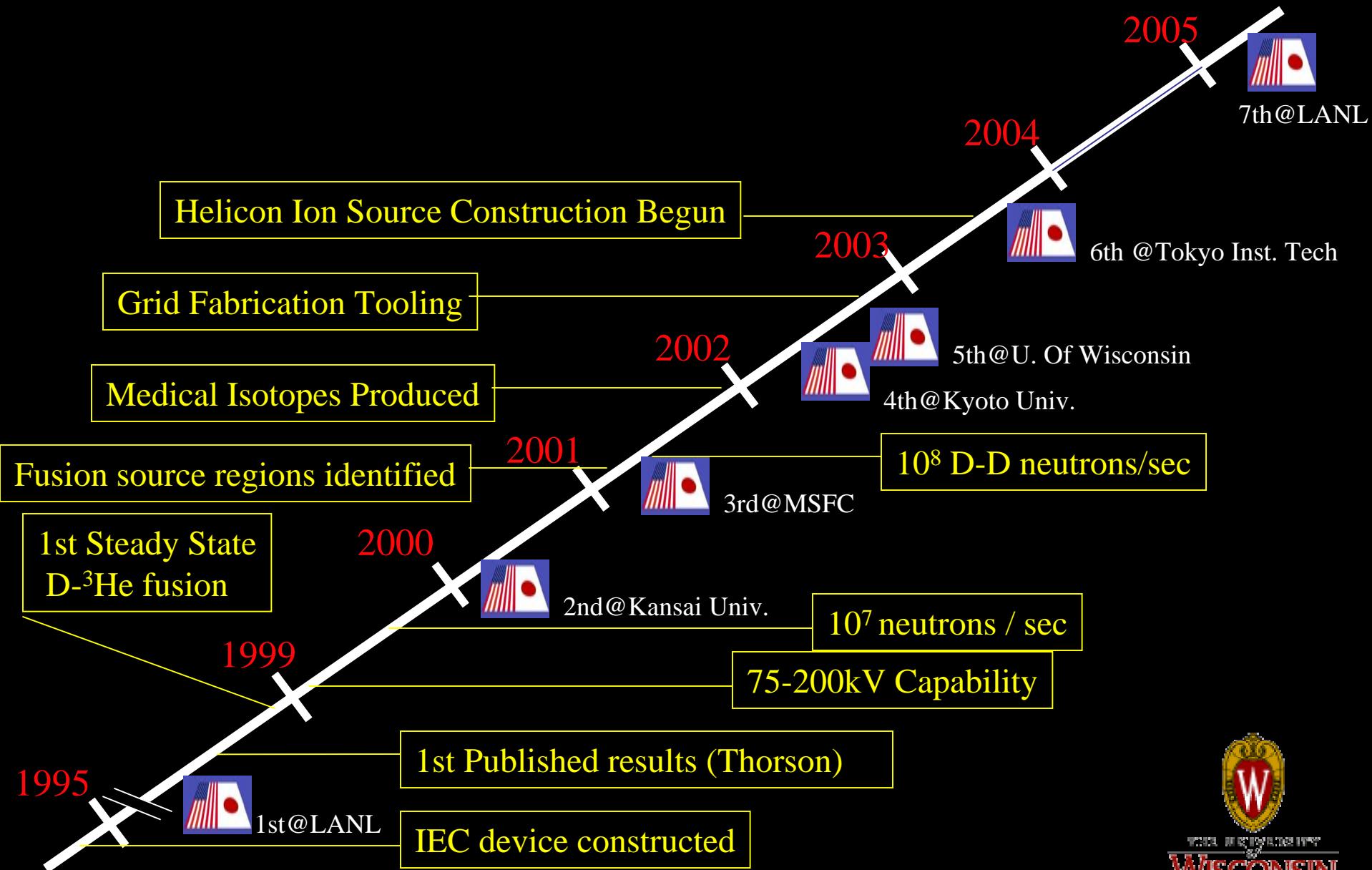


2. Wires wound around wax form

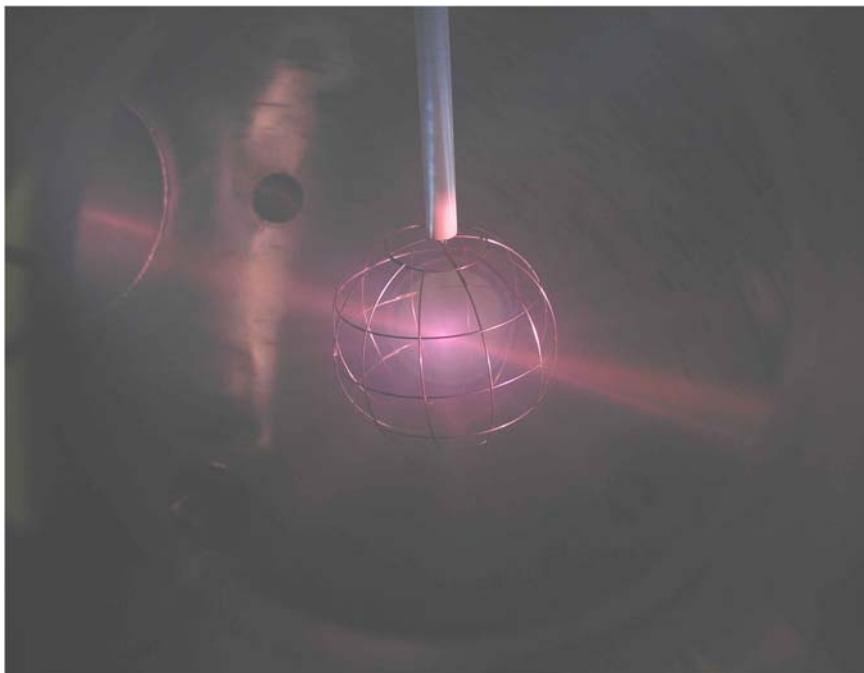


3. Finished grid cathode

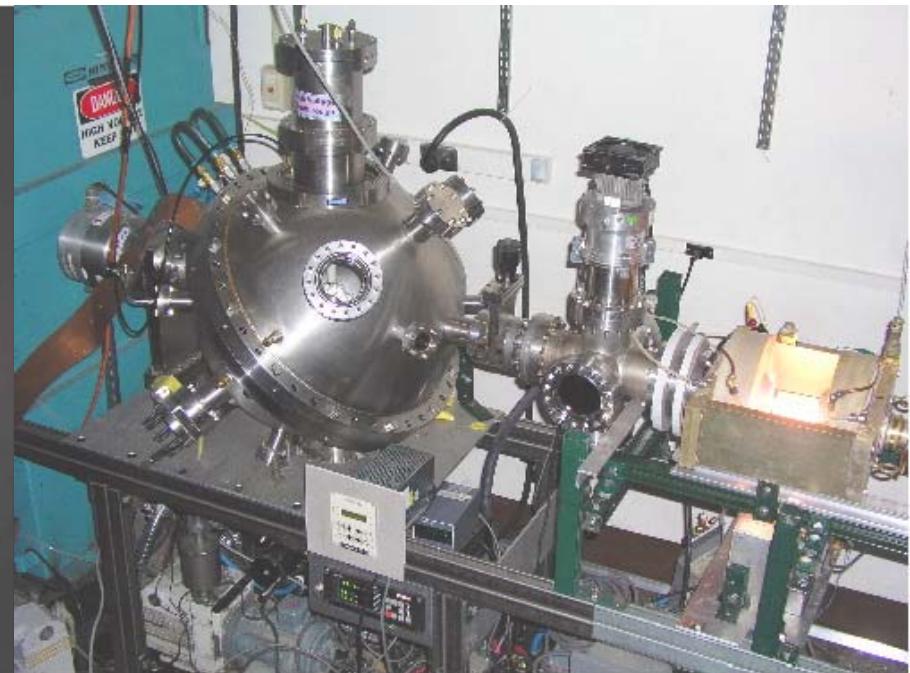
UW IEC History Timeline



Ion Gun Constructed to Study Converged Core Operation

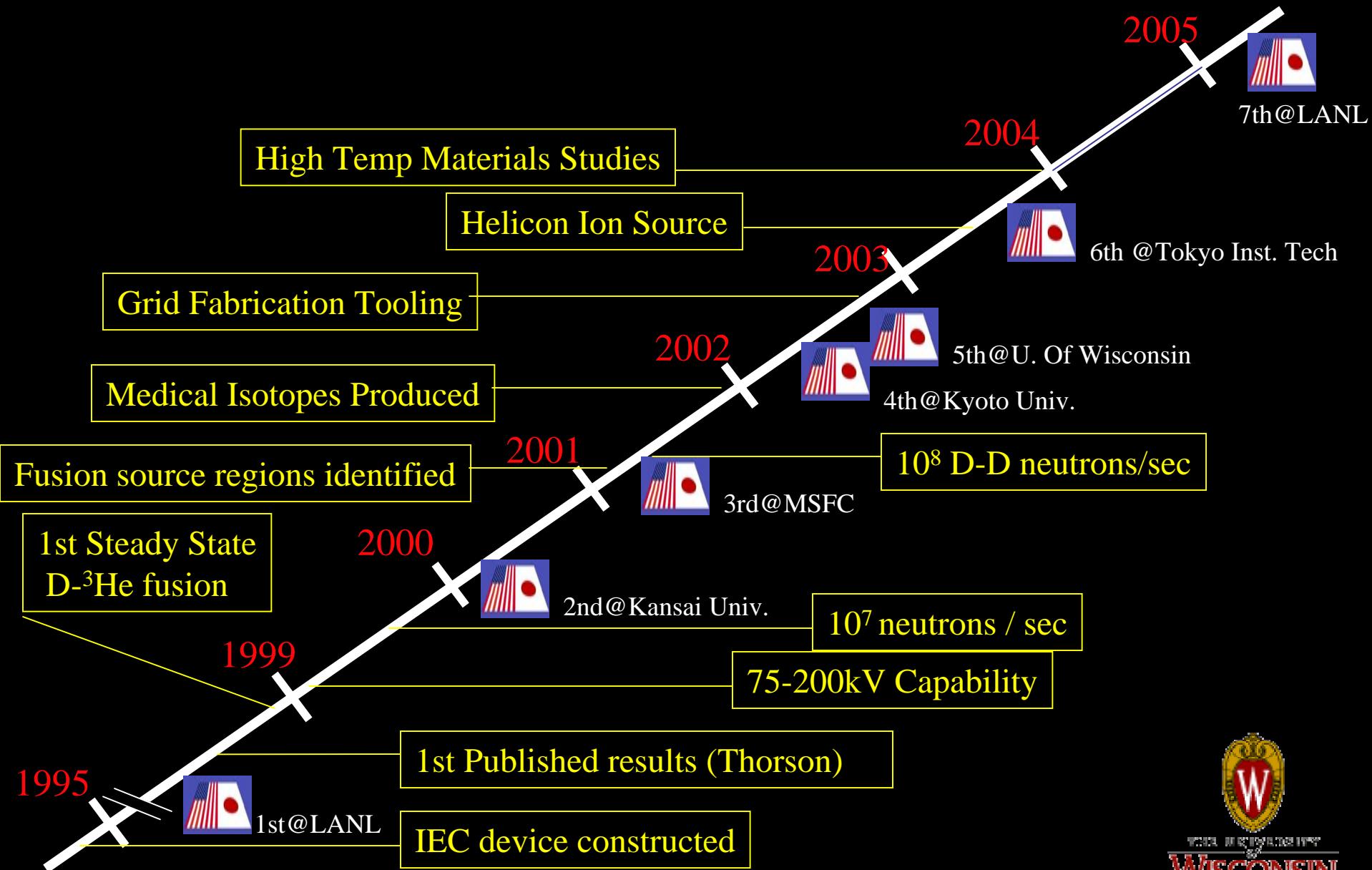


$^4\text{He}^+$ Beam Injected at 30 kV



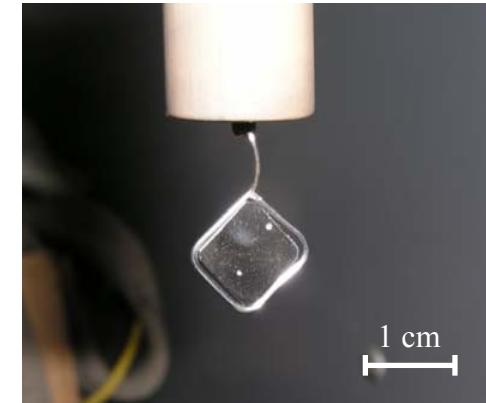
Helicon Source Coupled
to IEC Chamber

UW IEC History Timeline

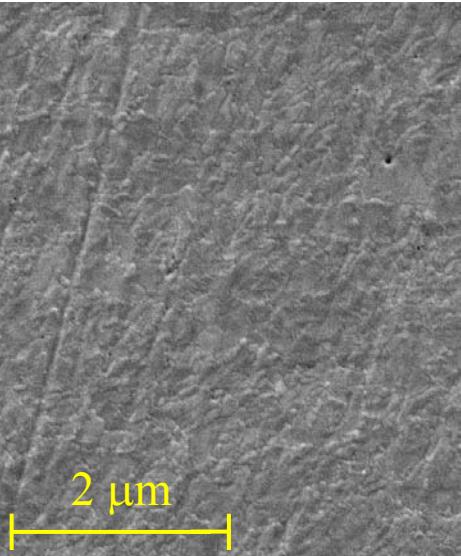


UW-IEC Has Been Used to Irradiate Tungsten Samples With D & He

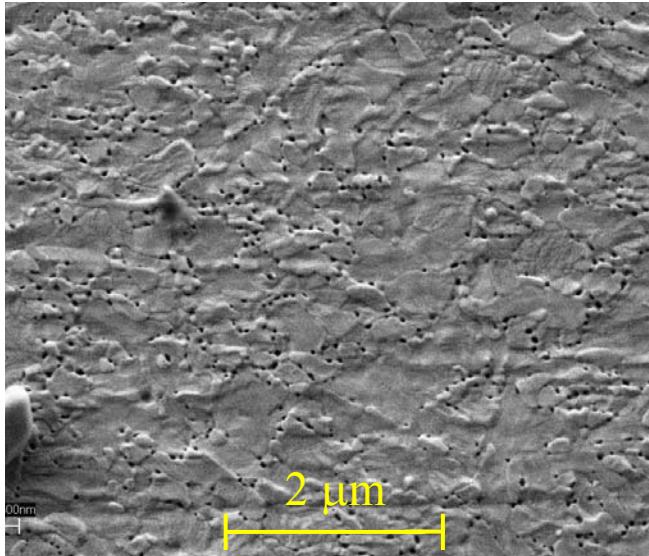
- Polycrystalline
- Single Crystal
- Tungsten “Foam”
- 800-1200 °C



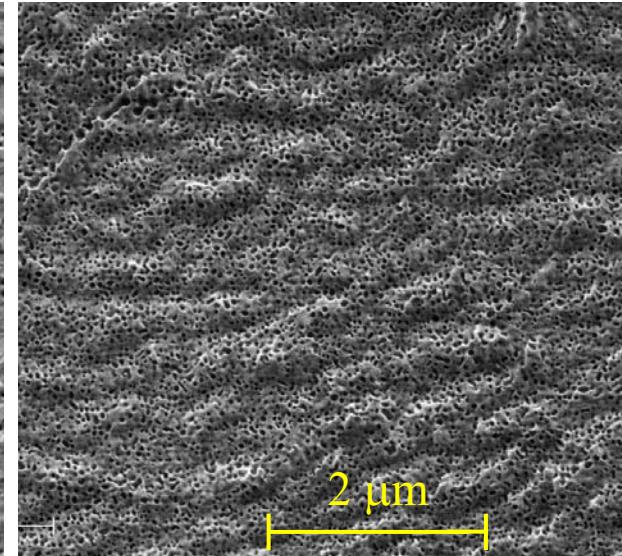
As Received



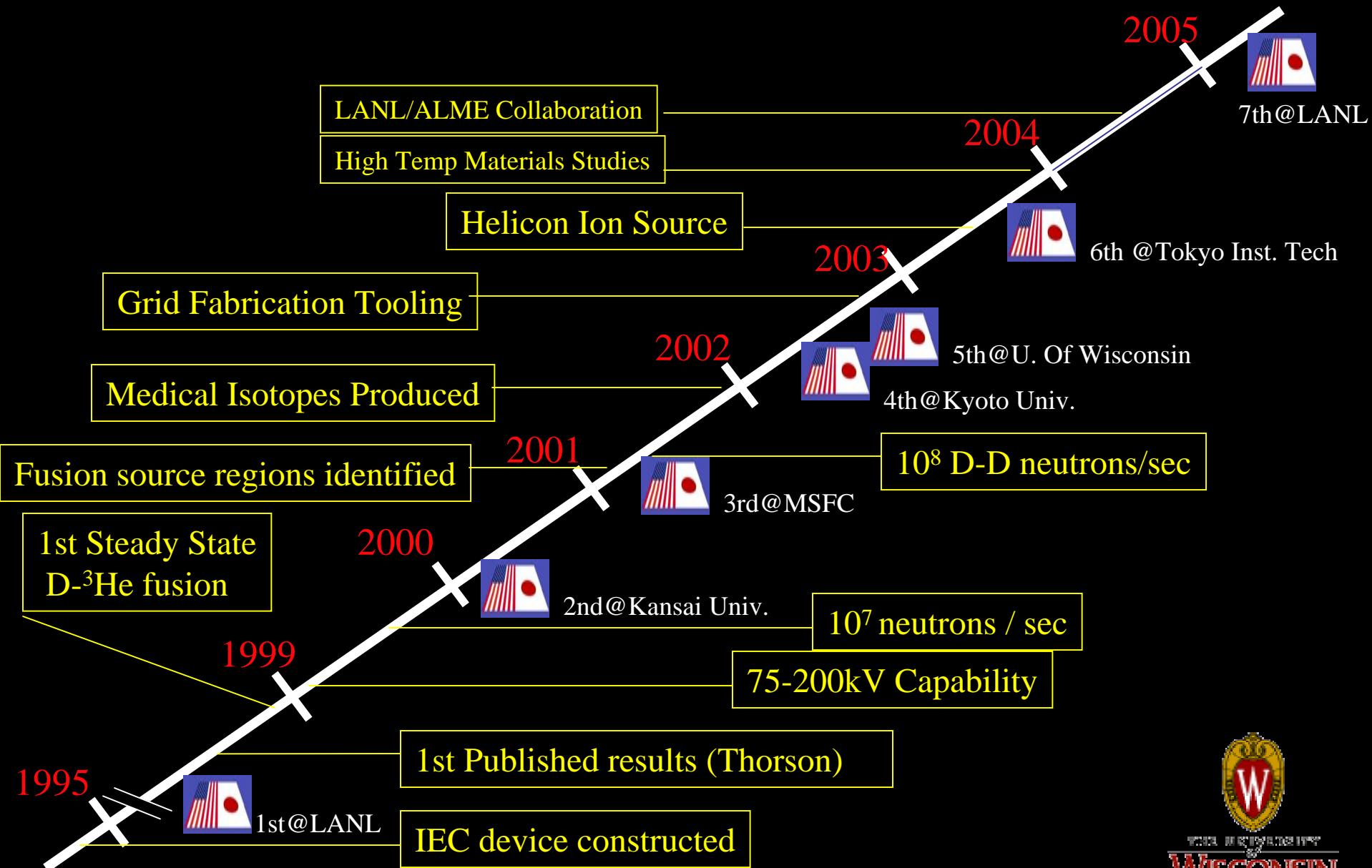
1×10^{18} He /cm², 850 °C



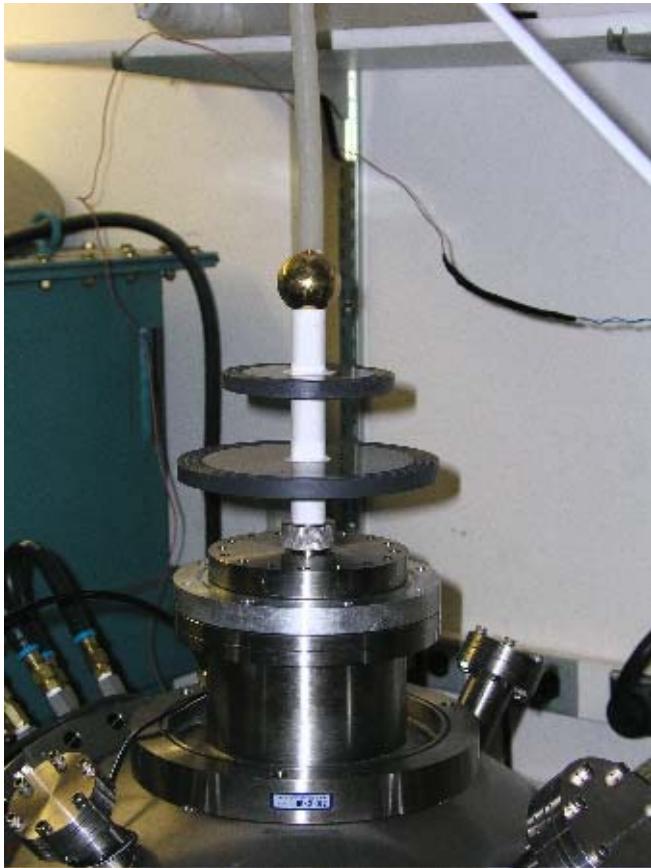
1×10^{19} He /cm², 850 °C



UW IEC History Timeline



Stalk and Grid Fabrication For Other IEC Groups

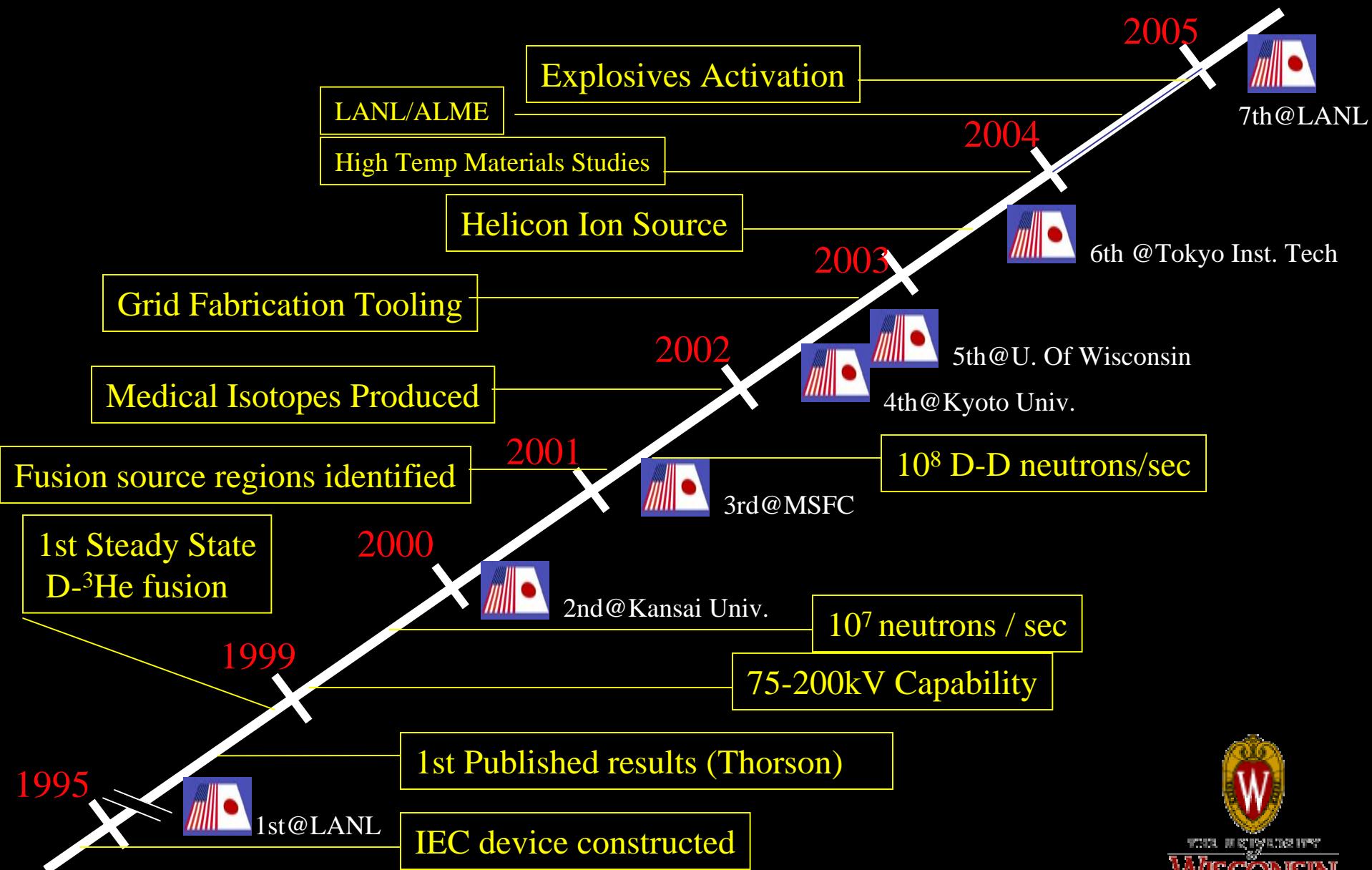


Stalk under high voltage test



A Happy Customer

UW IEC History Timeline

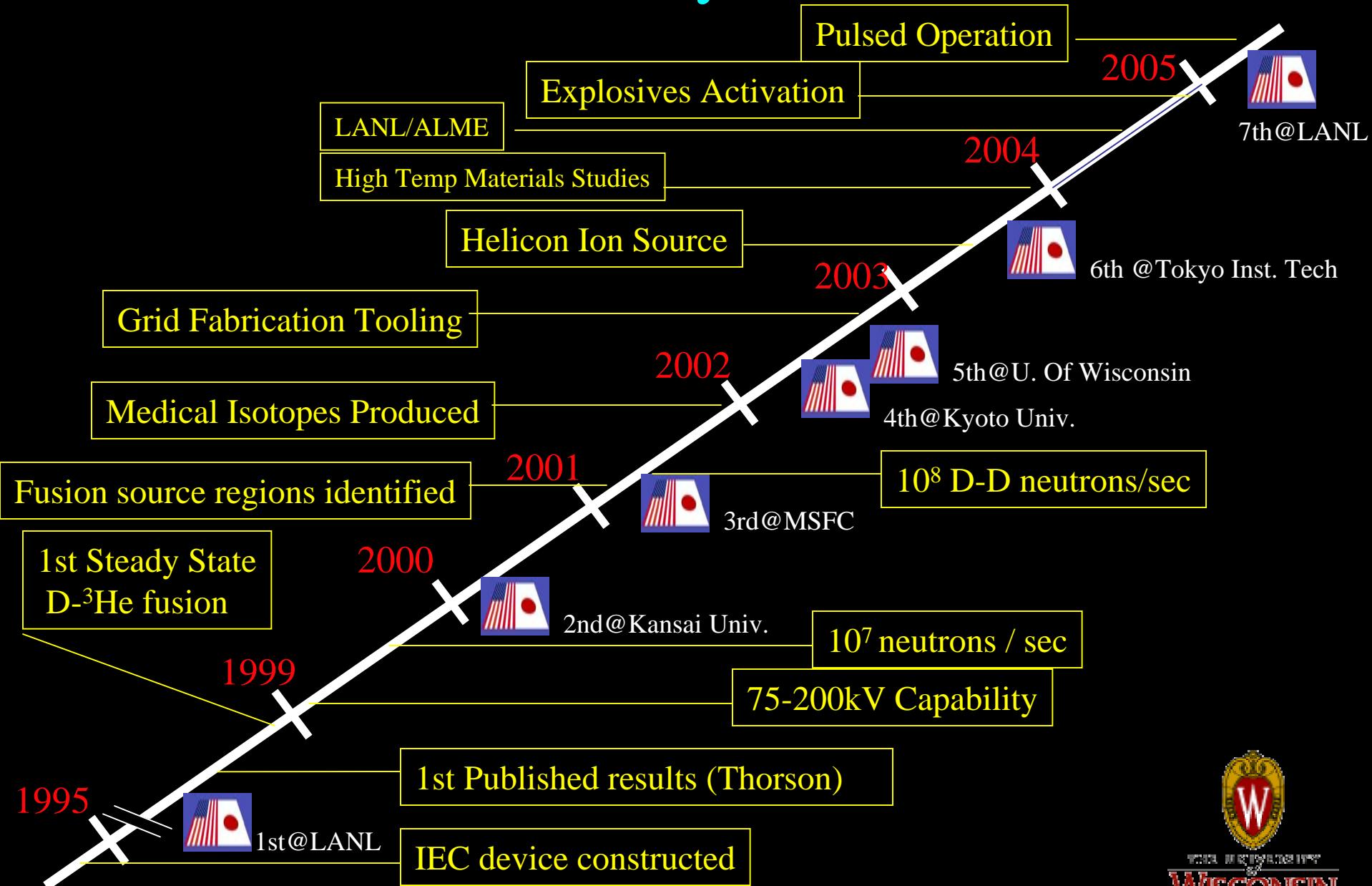


Neutron Activation of Explosives Explored

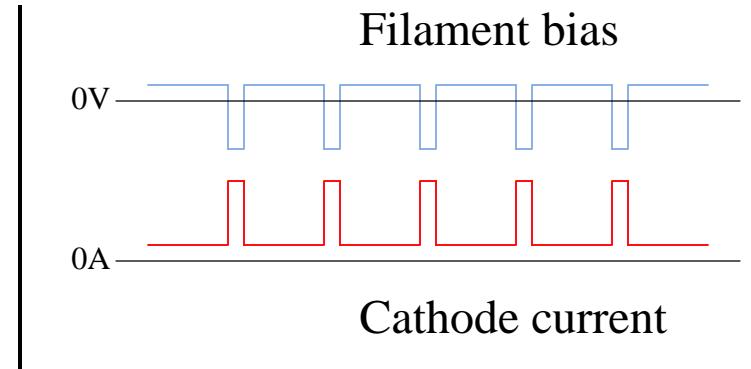
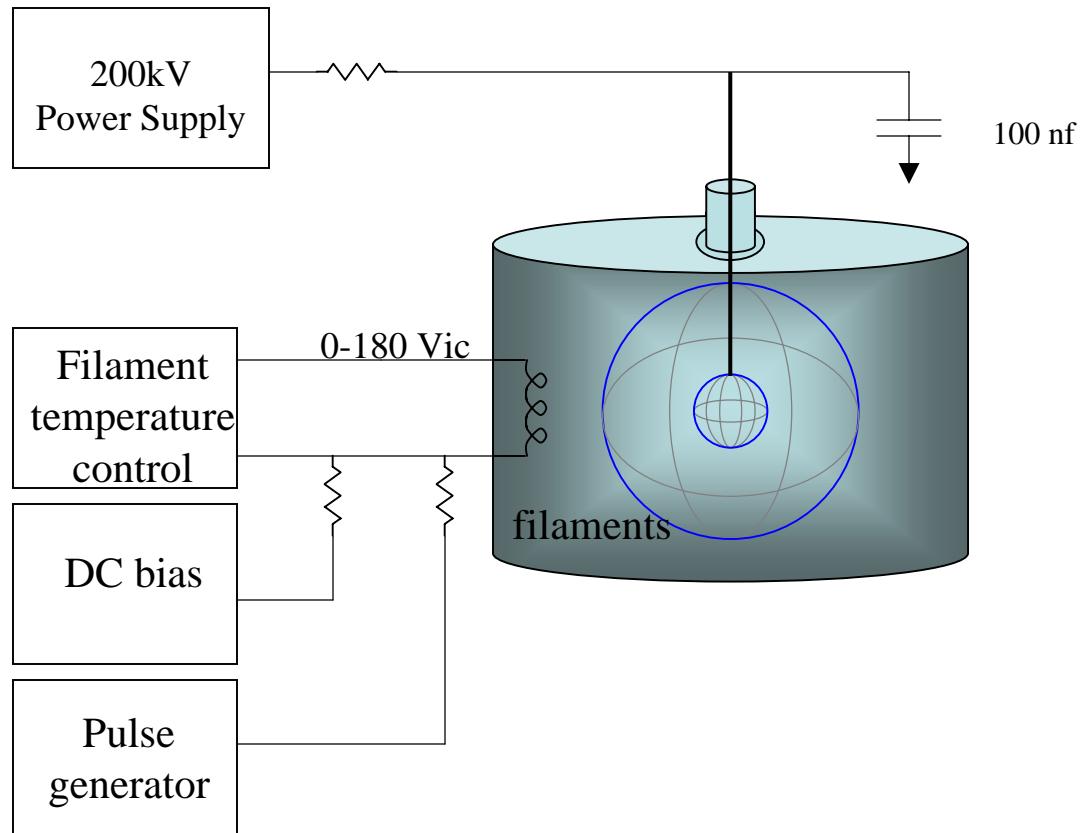


Explosives Containment and Detection Assembly
21

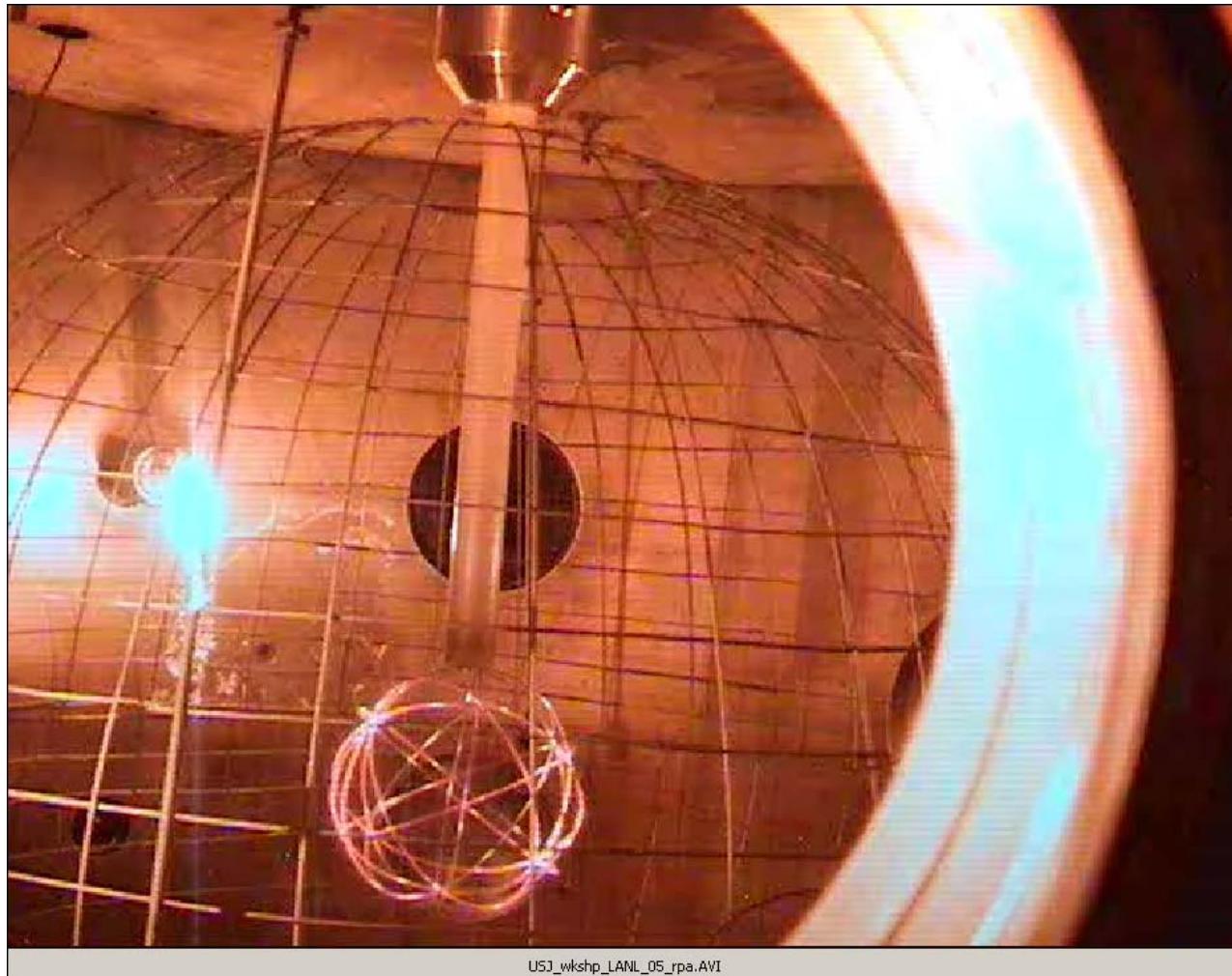
UW IEC History Timeline



Pulsed Operation of the Ion Source Has Been Demonstrated

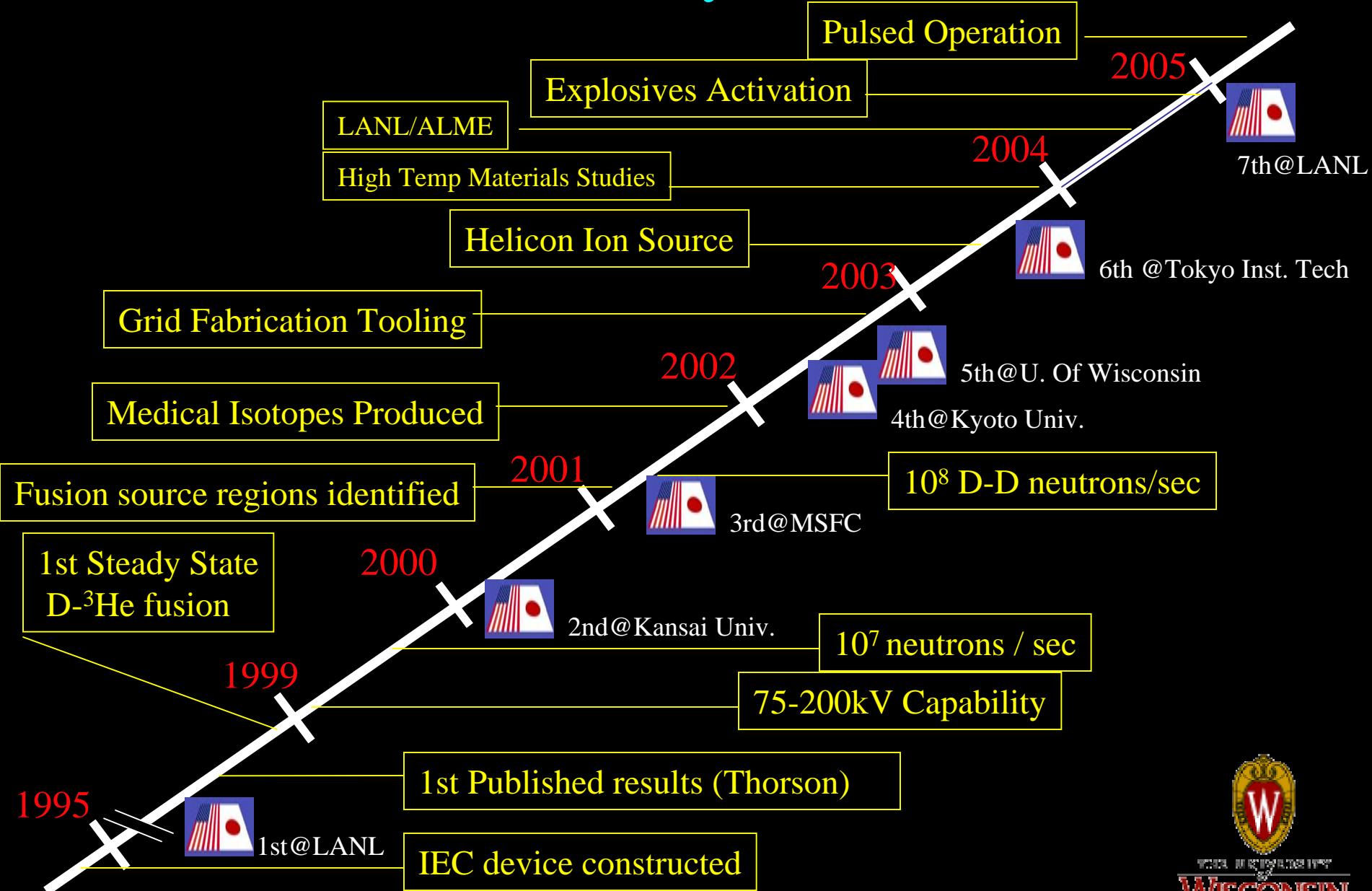


Pulsing at 1 Hz Shows Plasma and Grid Wire Response



USJ_wkshp_LANL_05_rpa.AVI

UW IEC History Timeline



Upcoming Talks on IEC Activities At The University of Wisconsin

- Atomic Physics Effects on IEC Ion Radial Flow
 - Gil Emmert (Monday, 3:45 Pm)
- Helicon Ion Source
 - Greg Piefer (Tuesday, 8:30 Am)
- Neutron Activation of Explosives
 - Alex Wehmeyer (Tuesday, 9:30 Am)
- Implantation of Fusion First Wall Materials
 - Ross Radel (Tuesday, 10:45 Am)

Questions?

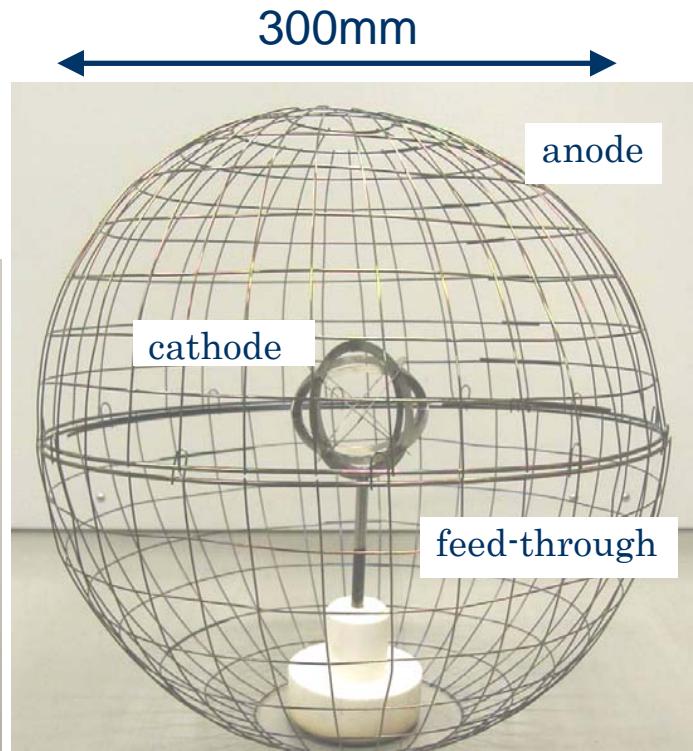
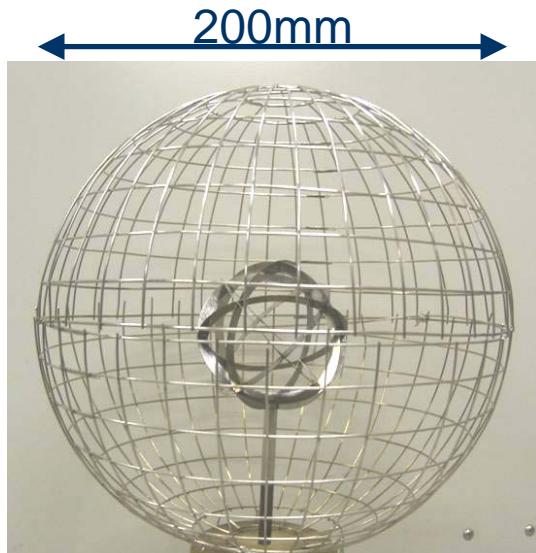
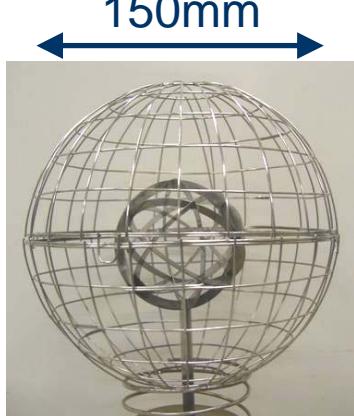
Neutron Yield in Inertial Electrostatic Confinement Fusion

Masami Ohnishi, Hodaka Osawa,
Takehiro Tabata, Shigehisa
Yoshimura
Faculty of Engineering Kansai
University
Osaka, Japan

Motivations of the study

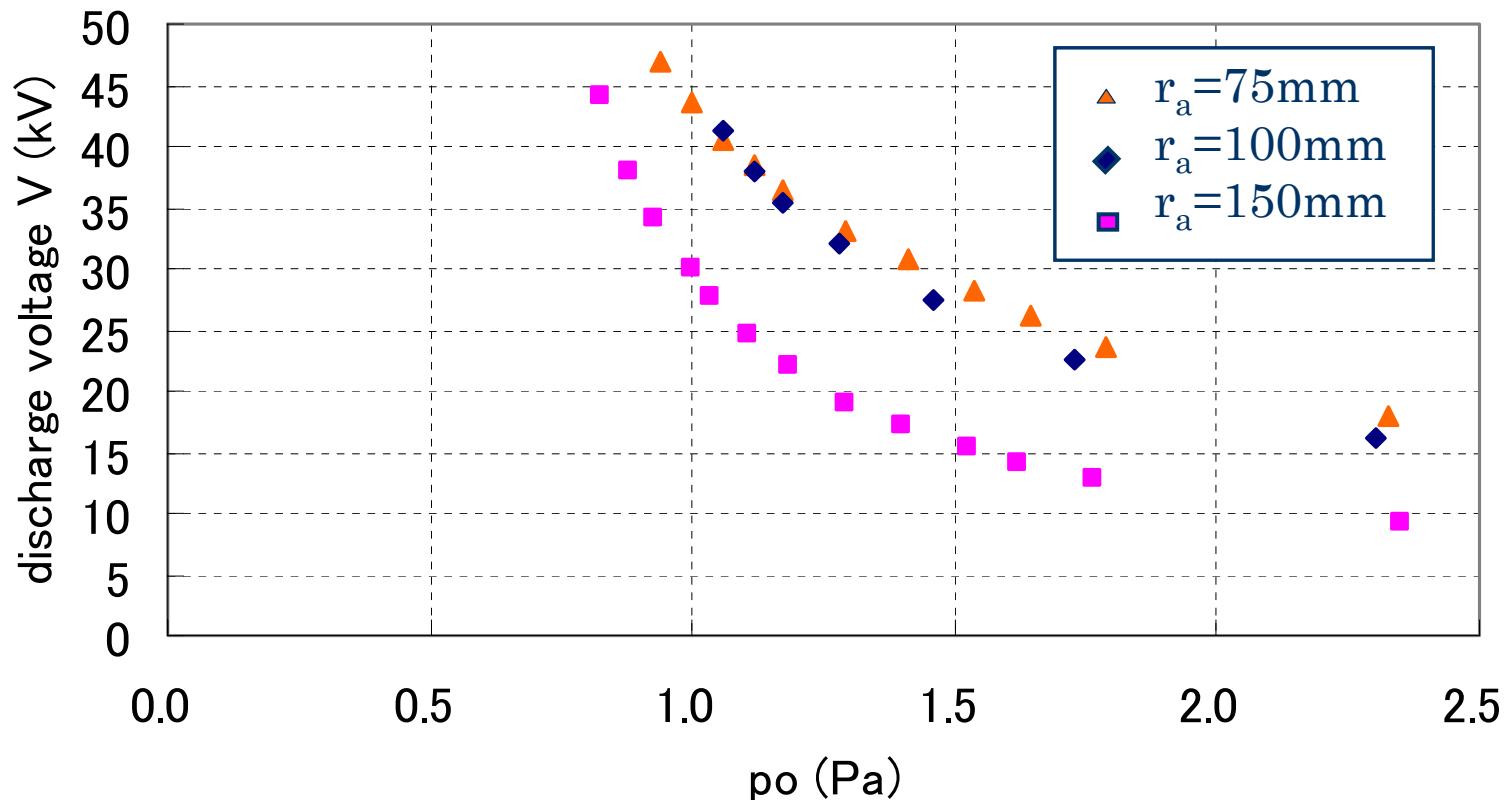
- The evaluation of neutron yield has previously been obscure with respect to the species of the particles that participate in the D-D fusion reaction.
- The present study is to determine the fraction of D^+ ions to D_2^+ from the experimental neutron yield.
- The dependence of radius of anode on neutron yield is studied experimentally.
- We derive a simple expression that provides a neutron yield consistent with that observed experimentally

Photos of anode and cathode



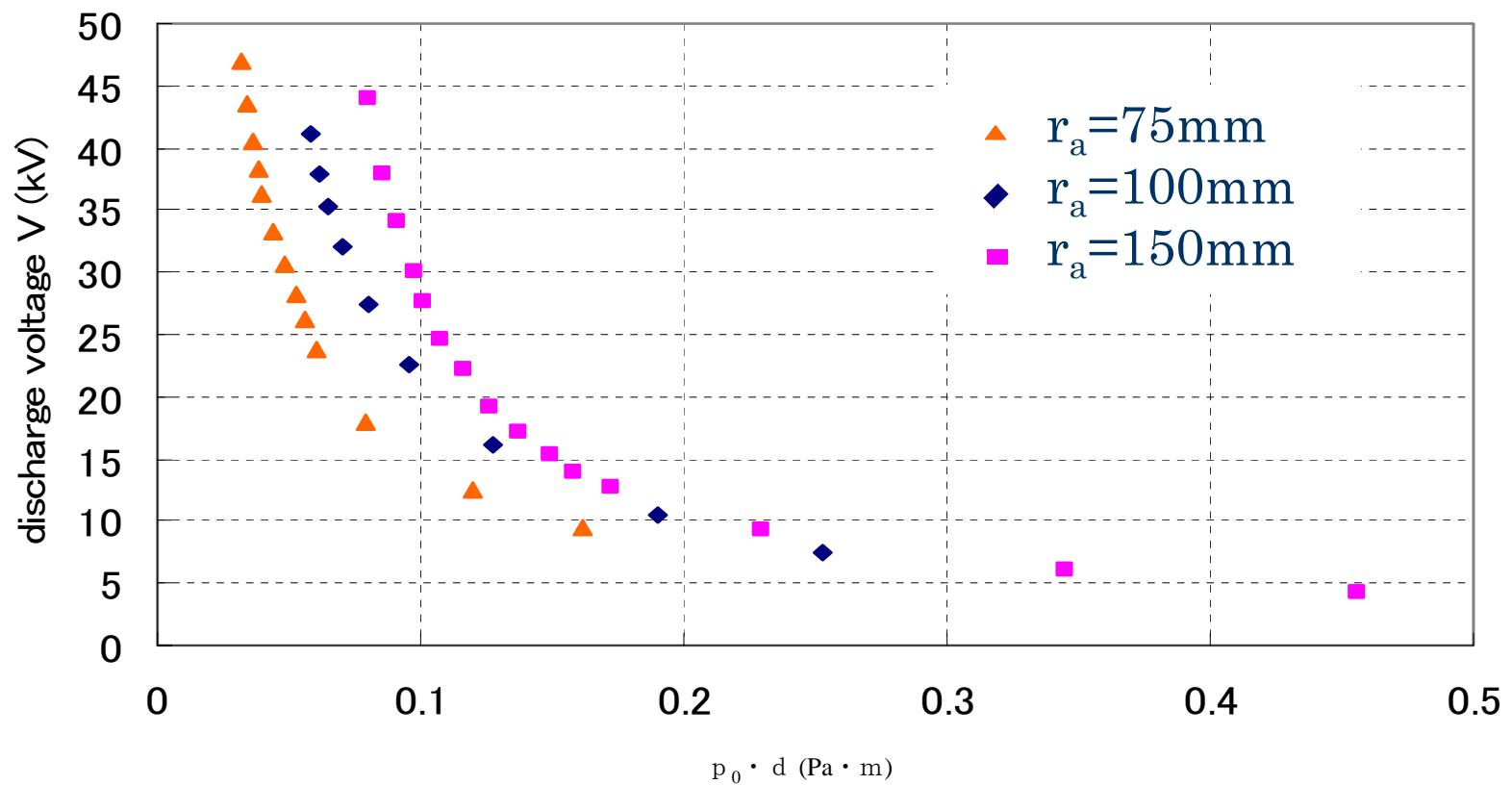
Gas pressure vs. Applied voltage

- Anode radius dependence



Gas Pressure times distance vs. applied voltage

- Anode radius dependence



Averaged fusion cross section

$$\frac{\text{NPR}}{p_0 \cdot I_{\text{meas}}} \propto \langle \sigma_{\text{DD}} \rangle = \frac{\sigma_1 v_1 (1-\alpha) + \sigma_2 v_2 \alpha}{v_1 (1-\alpha) + v_2 \alpha}$$

$$\alpha = n_2 / (n_1 + n_2)$$

n_1 : density of D^+

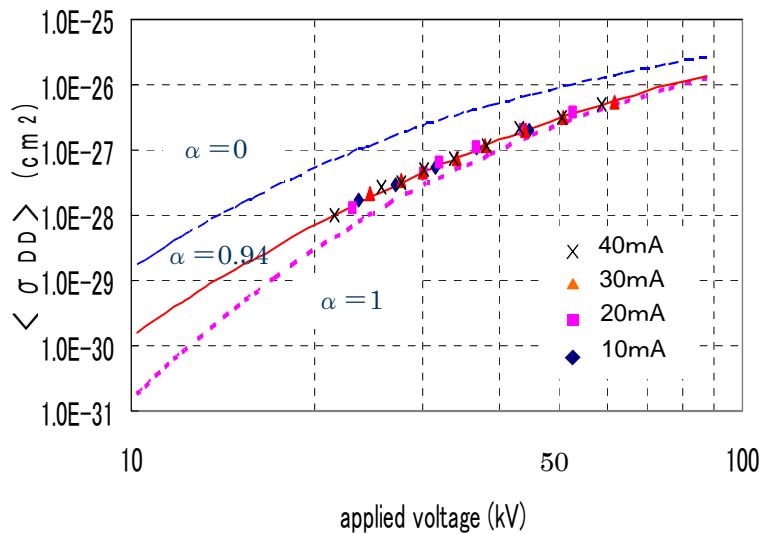
n_2 : density of D_2^+

v_1, v_2 : velocities of D^+ and D_2^+

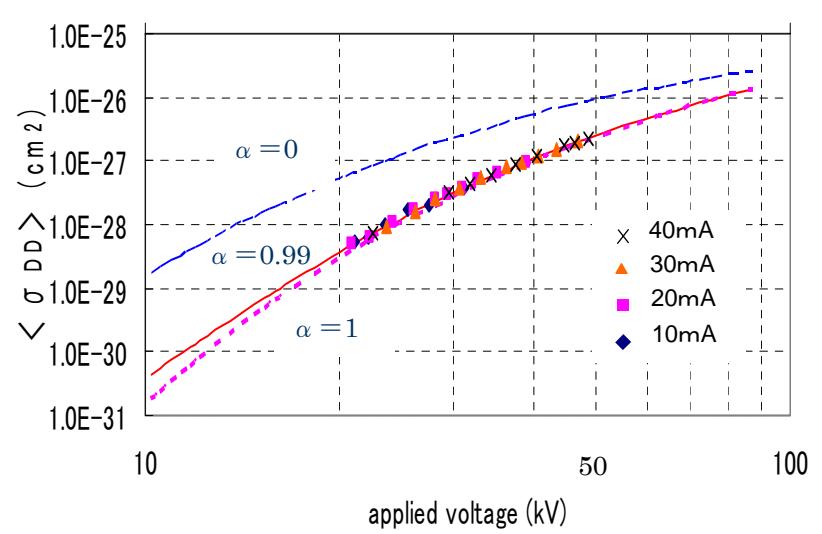
σ_1, σ_2 : fusion cross sections of D^+, D_2^+ and neutrals D_2^0

Fitting experimental data

(a) $r_a=150\text{mm}$

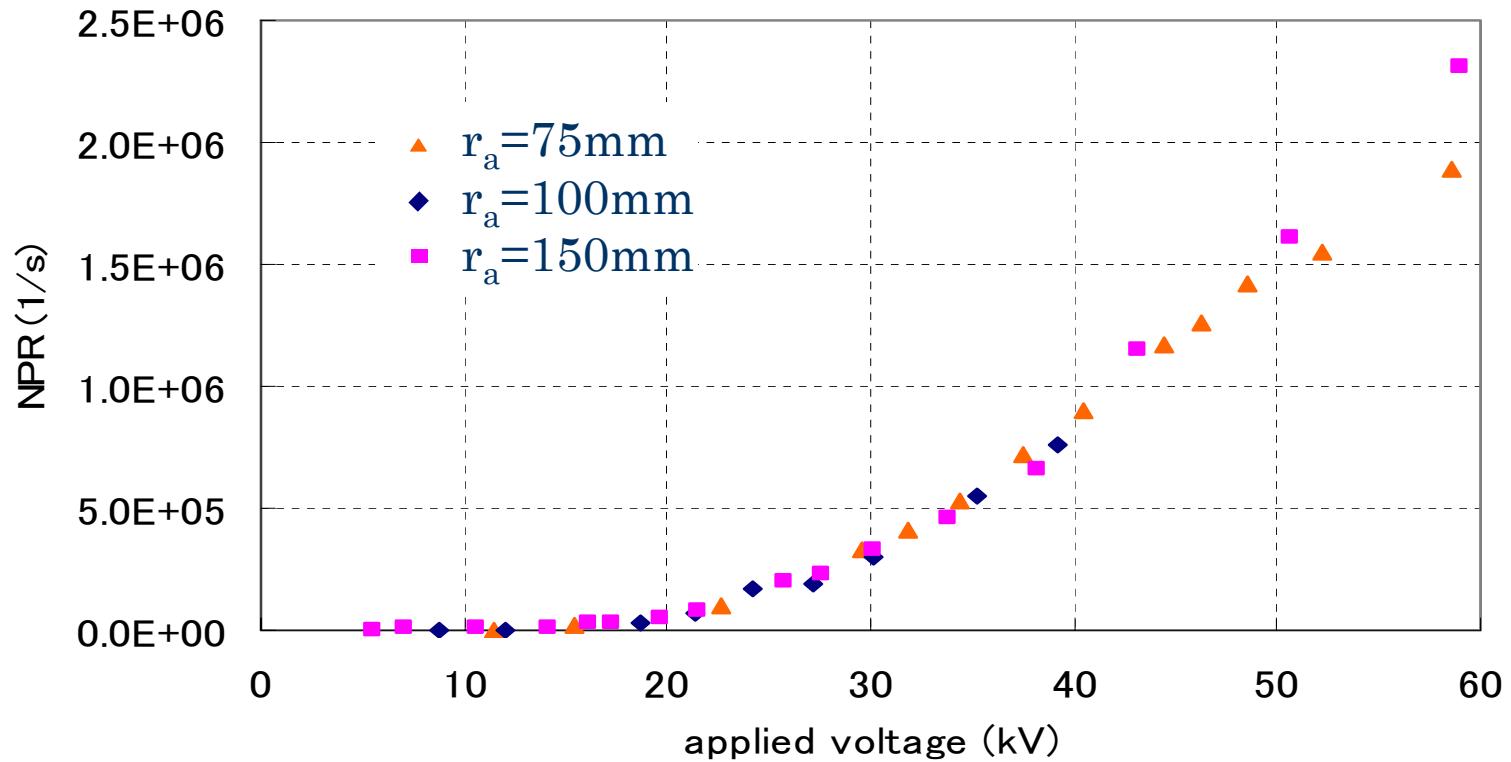


(b) $r_a=75\text{mm}$



Dependence of NPR on anode radius

- NPR vs. applied voltage for three anode radii 30 mA



Theoretical model to estimate neutron yield analytically

- Fusion reaction occur between accelerated ions and background neutrals in addition to between charge-exchanged fast neutrals and background neutrals.
- All accelerated ions possess an energy equal to applied potential at any position.
- Charge-exchange collisions occur only at the moment of entering the hollow cathode, and that the energy of fast neutral is equal to that of accelerated ions.
- Fusion reactions takes place within the whole region inside the anode.

NPR calculation

$$\text{NPR} = \sum_{i=D_2^+, D^+} \int_0^{r_a} n_0 n_i \sigma_{iD} v_i 4\pi r^2 dr + \sum_{i=D_0^2, D_0} \int_0^{r_a} n_0 n_{0icx} \sigma_{iD} v_{0i} 4\pi r^2 dr$$

Neutral particles charge-exchanged:

$$n_{0D^0} = n_{D^+} \left\{ 1 - \exp \left(-\frac{2r_c}{\lambda_1} \right) \right\} \quad n_{0D_2^0} = n_{D_2^+} \left\{ 1 - \exp \left(-\frac{2r_c}{\lambda_2} \right) \right\}$$

The continuities of currents and neutral particle flows:

$$\sum_{i=D_2^+, D^+} n_i v_i 4\pi r^2 = \sum_{i=D_2^+, D^+} n_{ic} v_{ic} 4\pi r_c^2 \quad \sum_{i=D_2^0, D^0} n_{0i} v_{0i} 4\pi r^2 = \sum_{i=D_2^0, D^0} n_{0ic} v_{0ic} 4\pi r_c^2$$

Simple expression of NPR

$$NPR = 2n_0 \frac{I_{\text{meas}}}{e(1 + \delta_e)(1 - t^2)} r_a$$

$$\times \left[2\alpha v_{D_2^+c} \sigma_{DD}(V/2) \left\{ 2 - \exp\left(-\frac{2r_c}{\lambda_2}\right) \right\} + (1 - \alpha) v_{D^+c} \sigma_{DD}(V) \left\{ 2 - \exp\left(-\frac{2r_c}{\lambda_1}\right) \right\} \right]$$

I_{meas} : current

δ_e : coefficient of secondary electrons

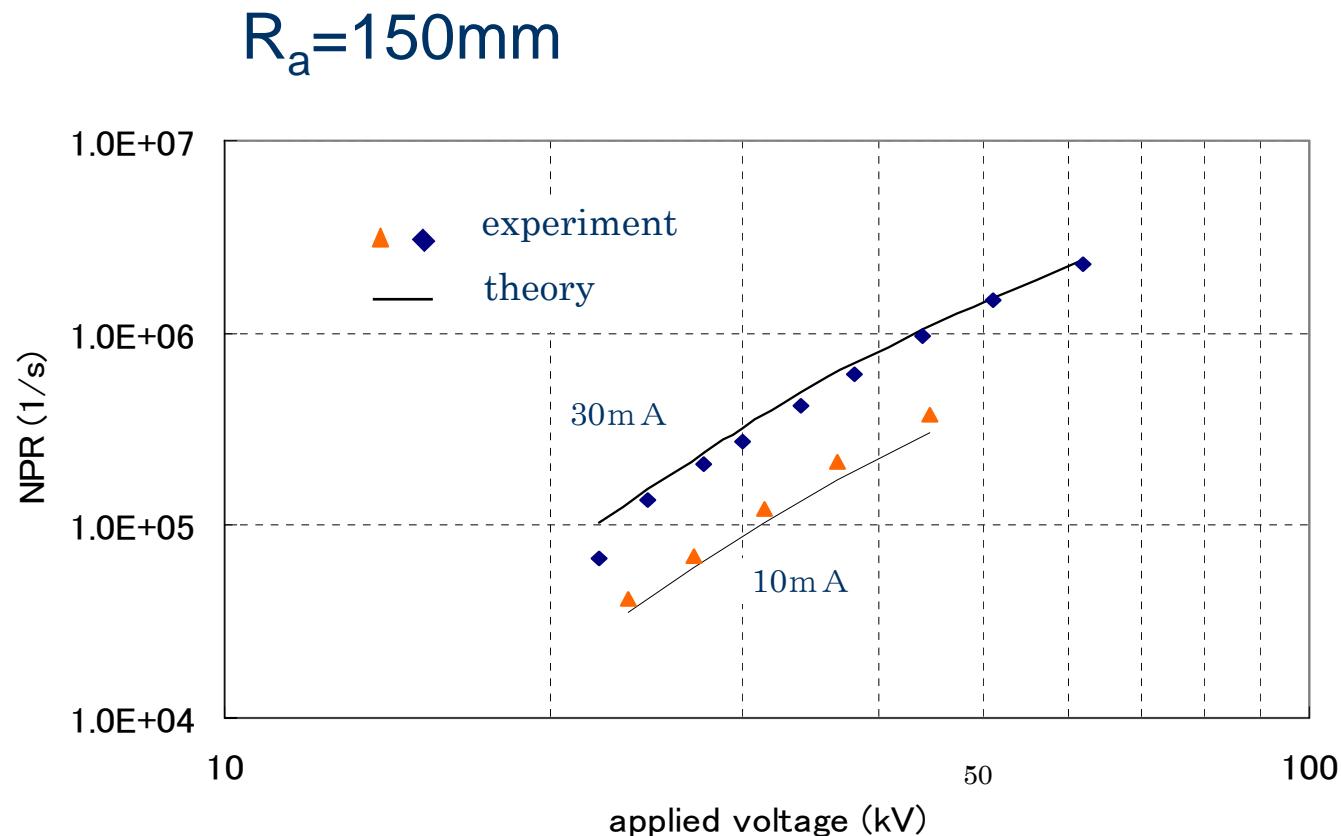
r_a, r_c : radii of anode and cathode

t : transparency ($t=0.6$)

λ_1, λ_2 : mean free paths for charge exchange

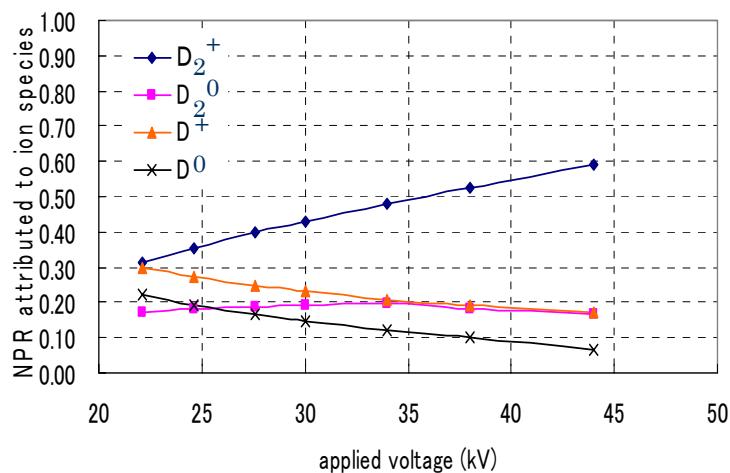
n_0 : neutral gas density

Comparison between experiment and theoretical estimation

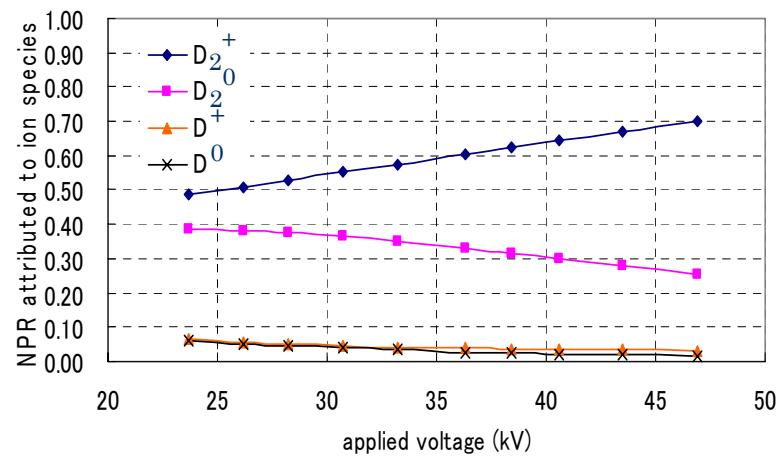


NPR attributed to particle species

(a) $r_a=75\text{mm}$



(b) $r_a=150\text{mm}$



Summary and Conclusions (1)

- We derived the fraction of ion species such as D^+ plus D^0 vs. D_2^+ plus D_2^0 from the experimentally measured NPR. ($D_2^+ + D_2^0$:94% for $r_a=150\text{mm}$)
- The NPR is well explained by the fusion events between the full accelerated D^+ and D_2^+ ions and the background neutrals and the charge exchanged fast neutrals and background neutrals.

Summary and Conclusions (2)

- We have derived a simple expression to explain the NPR observed in the experiments..
- The dependence of NPR on anode radius is very week.
- In order to apply our expression , it is necessary to know the relationship among the voltage, current and gas pressure.

Summary and Conclusions (3)

- In order to increase NPR, D^+ ions must be increased relative to D_2^+ .
- In an ordinary IEC device, the current, applied voltage and gas pressure are tightly coupled, i.e., no one of them can be independently changed, without the other two changing.
- It seems to be preferable that the ion gun be equipped with the device, so that more D^+ ions may be produced by ionizing deuterium gas by supplying hot electron using ECR etc.



Dipole Assisted Inertial Electrostatic Confinement

Yoshikazu Takeyama, Robert Thomas, G.H. Miley

Fusion Studies Laboratory
University of Illinois at Urbana - Champaign

US-Japan Workshop on IEC, Los Alamos, NM, March 14-16, 2005

Contents

- Introduction
 - Motivation of DaIEC
 - Theory of DaIEC
 - Experimental Setup

 - Plasma Diagnostics
 - Double probe
 - Triple probe
 - Preliminary Results and Analysis

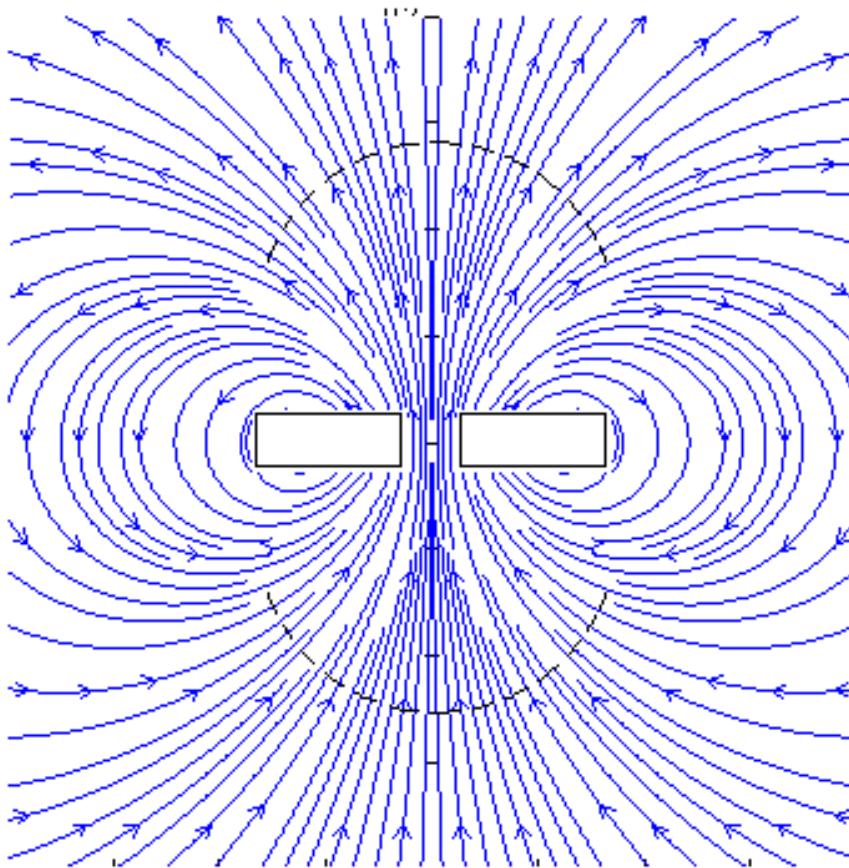
 - Conclusion
-



Objectives

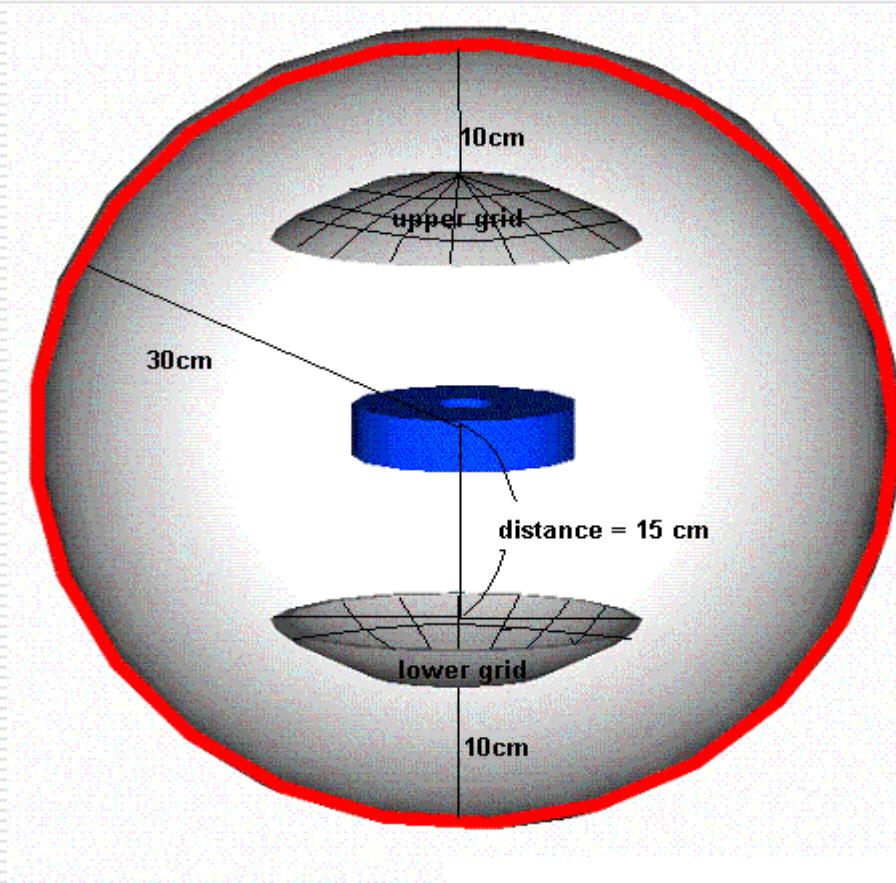
- Dipole Fields Enhance Plasma Density in the Center Region of the IEC
 - Combined IEC and Dipole Confinement Properties Reduce Plasma Losses
 - Provides Control of potential at the center region of IEC
 - Compliments aspects of Levitated Dipole Experiment (LDX) Being Conducted at MIT and Columbia
-

Dipole Field Produced by Coil provides the focus of ion beam



- 12 gage of Square magnet wire
• (copper)
- 17 x 26 turns of Coil.
- Current varied in the range of 0~20Amp.
- Maximum field strength of 0.1 T
At the center of dipole

Dipole Assisted IEC Schematic



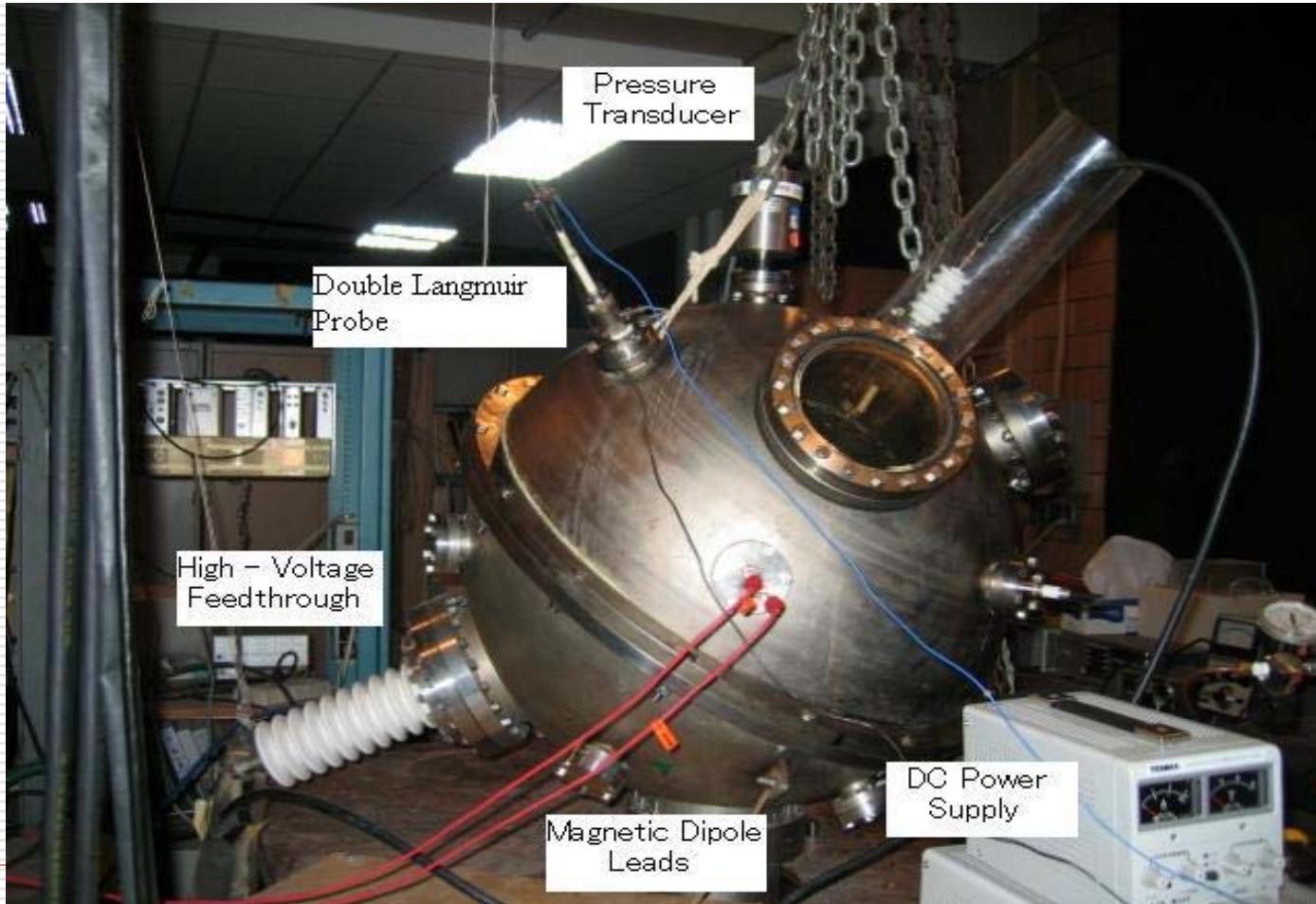
Coil

Inner Radius = 2 cm
Outer Radius = 8cm
Height = 4cm

Grid

20cm radius
2cm x 1cm spacing

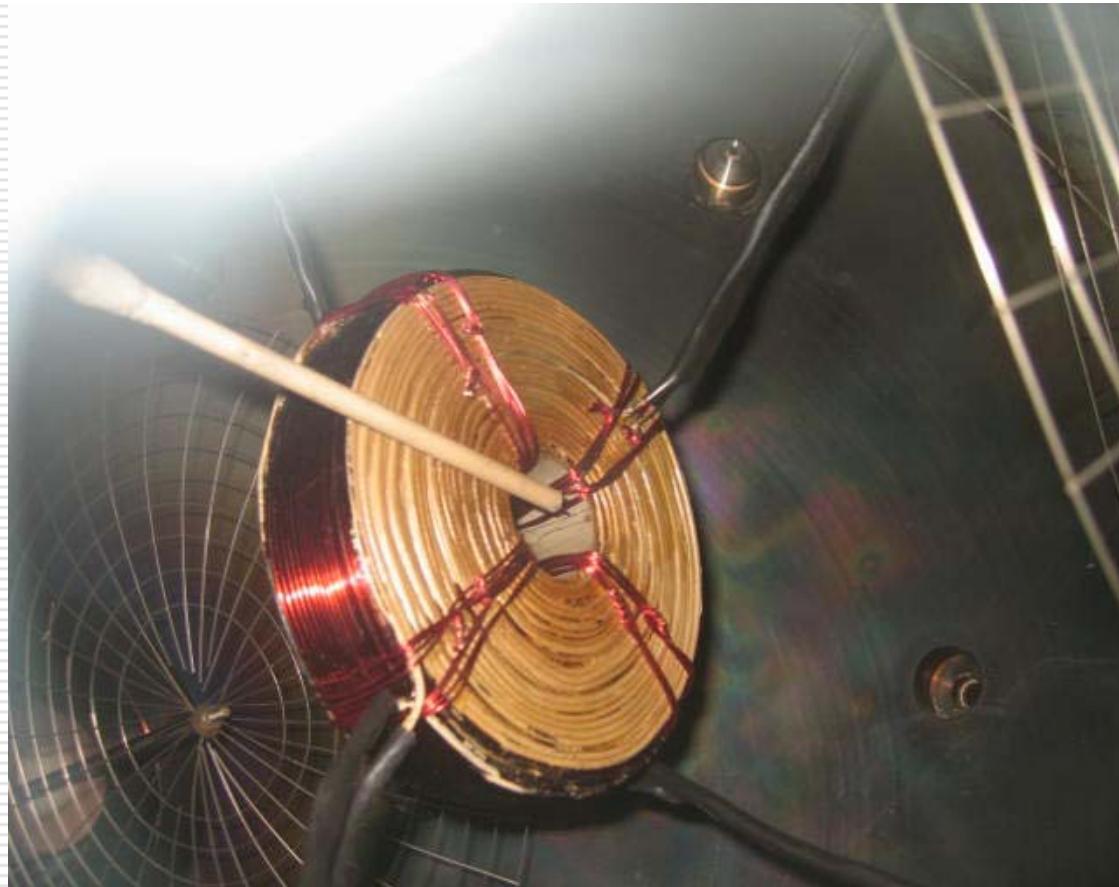
Dipole IEC Experimental Device



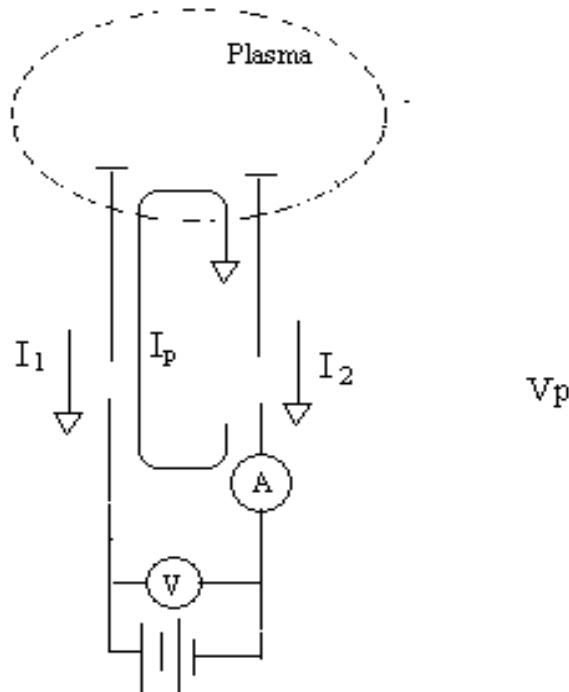
Copper ring is mounted on coil to control central potential



Probe is inserted to measure the density at the center

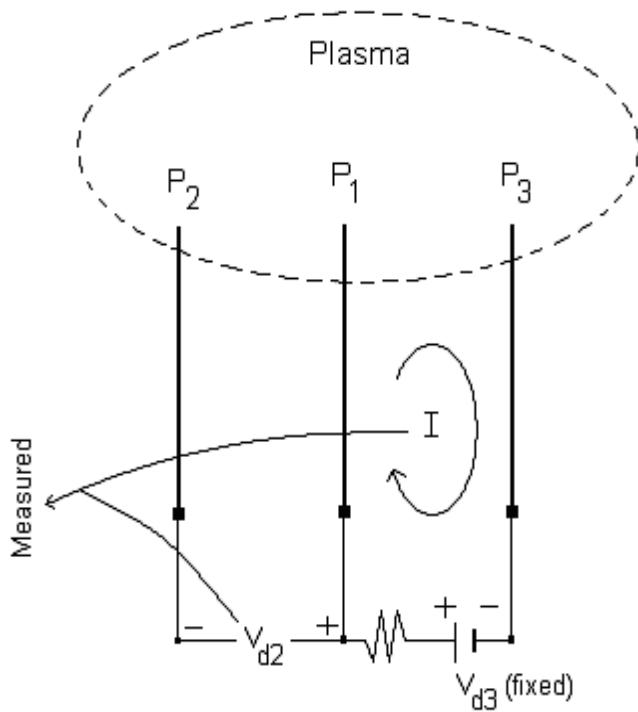


Double Probe Used to observe the electron distribution function



- Less disturbance of Plasma than single probe
- Well suited for IEC operating condition with presence of magnetic field
- Capable of measuring properties of non-Maxwellian plasma.

Triple Probe Used to Determine Values of T_e and n_e

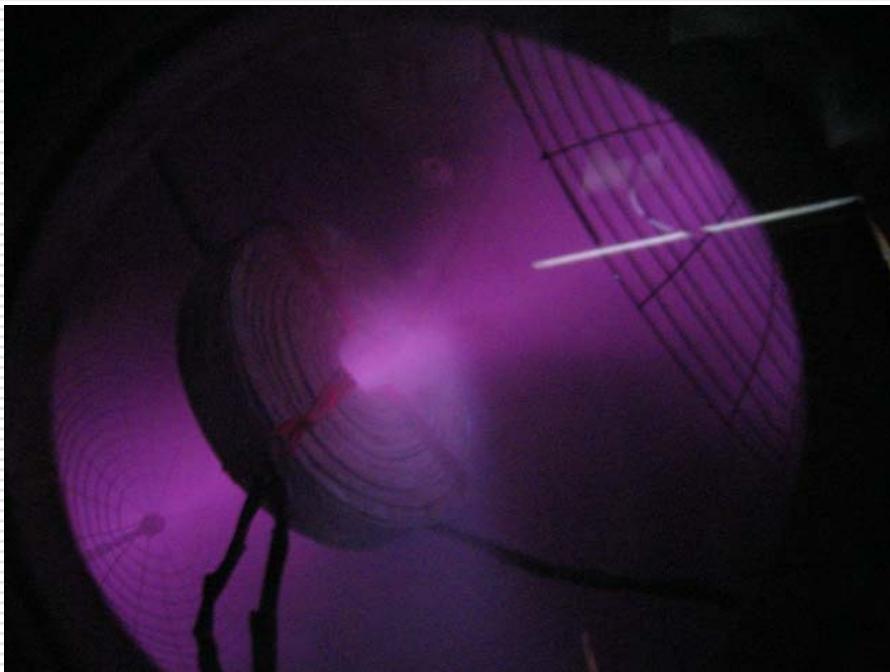


- Less disturbance plasma than single probe.
- Relatively simple set up
- Instantaneous measurements of T_e and n_e .

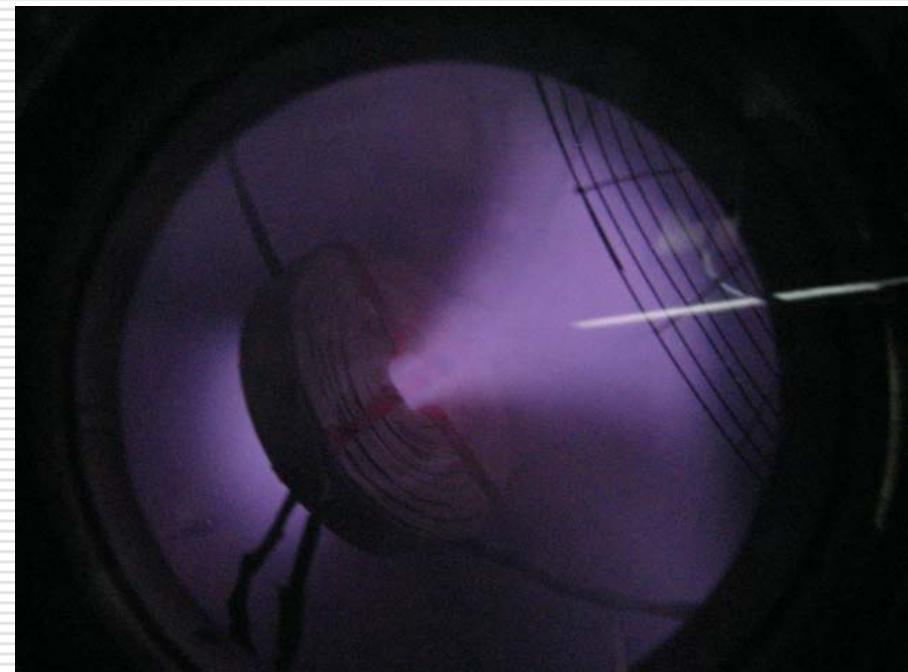
Operating Conditions

- Pressure Varied from 20 – 80 mTorr
 - Discharge Voltage 3 kV – 500 V
 - Central Potential Bias up to +- 120 V
 - Magnetic Field at measurement point is varied from 0 – 700 Gauss
-

Plasma More Focused Through Center With Field On



B-Field Off



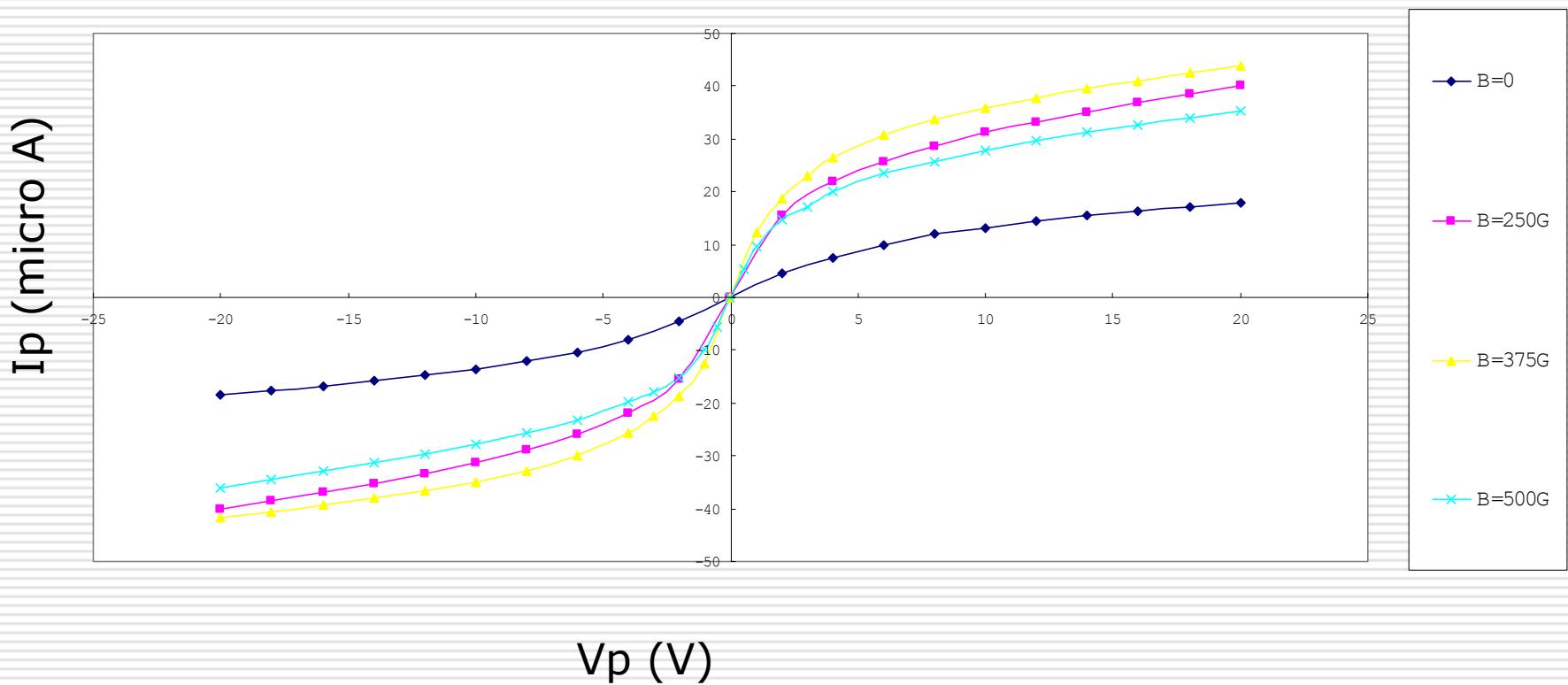
B-Field On

Shape of curves characteristic of Maxwellian electron distribution.

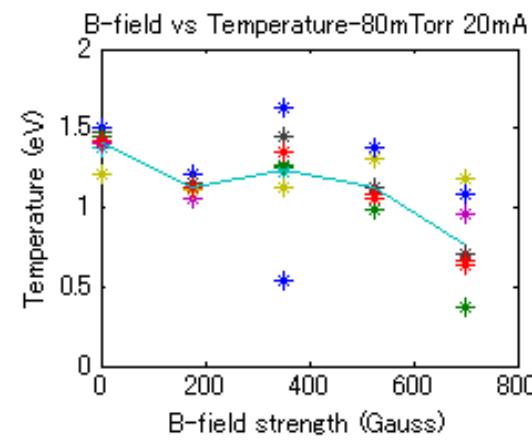
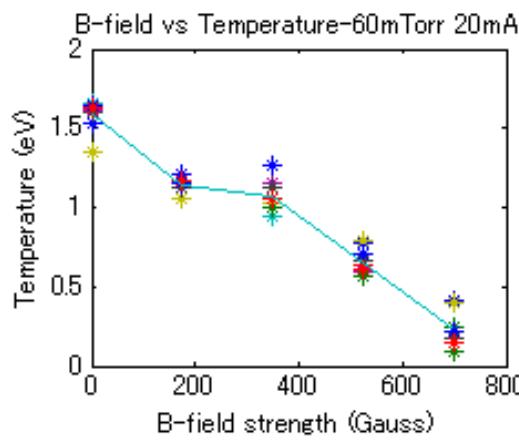
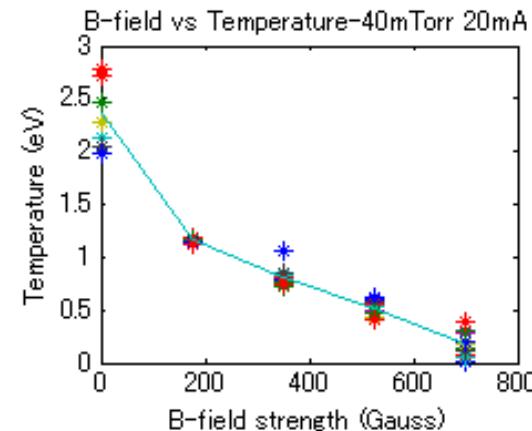
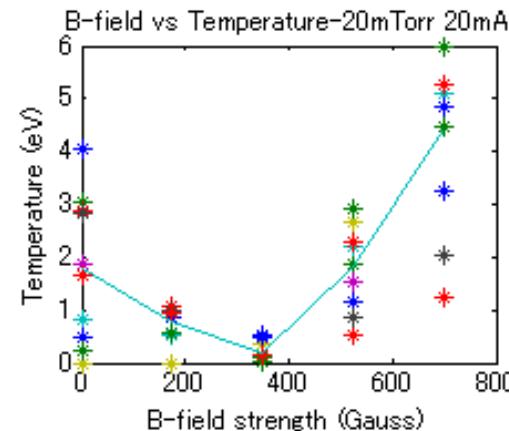


Maximum density at 375 G. ($V_c=0$)

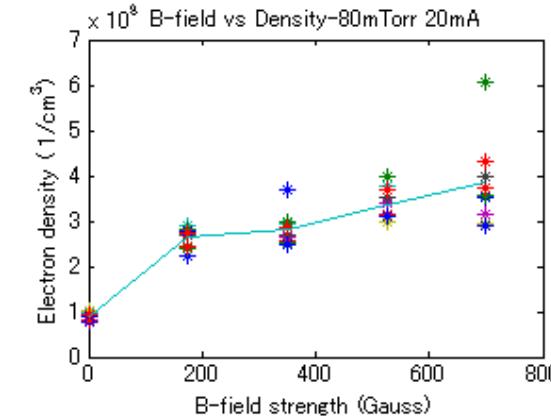
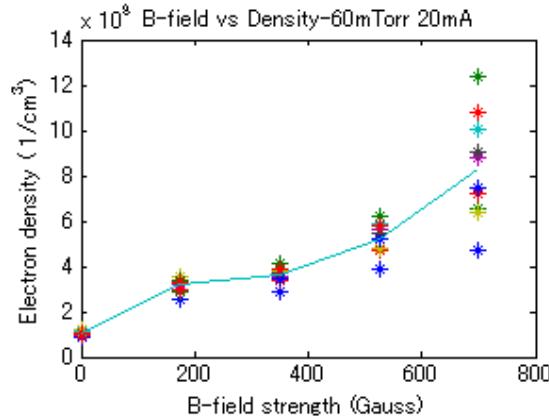
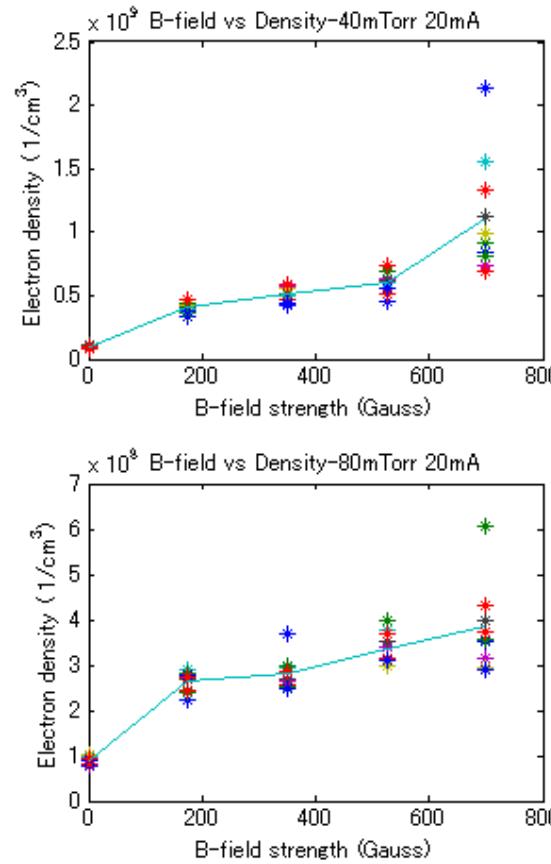
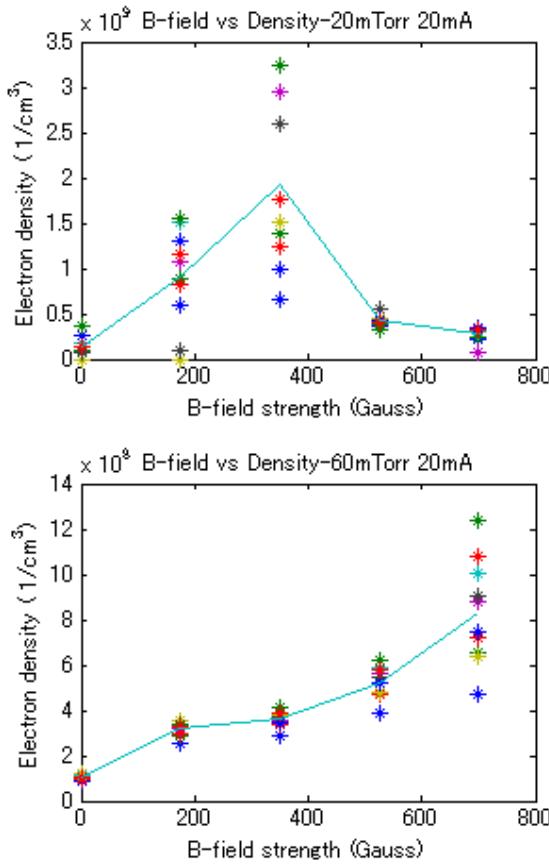
I-V curves with different B-field (25mTorr)



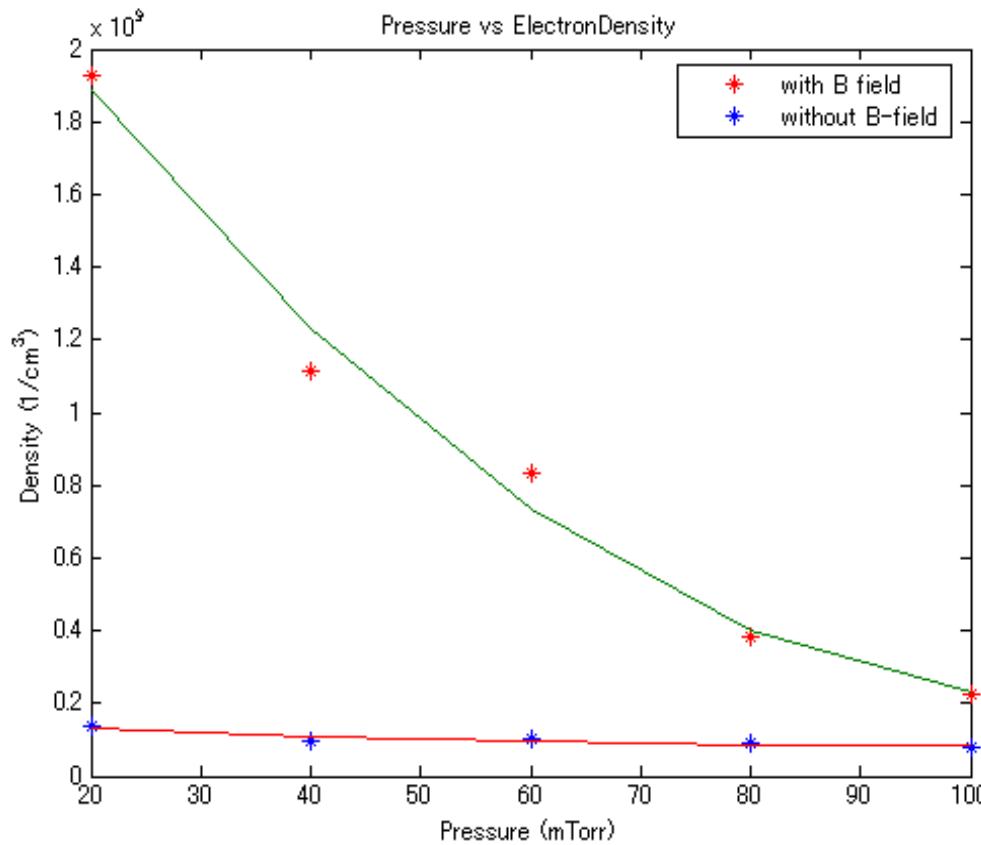
Triple probe shows Te increases with B at low pressure only.



Triple probe::at high pressure, ne increases with B. at 20mTorr, possible peak at 370 G like double probe



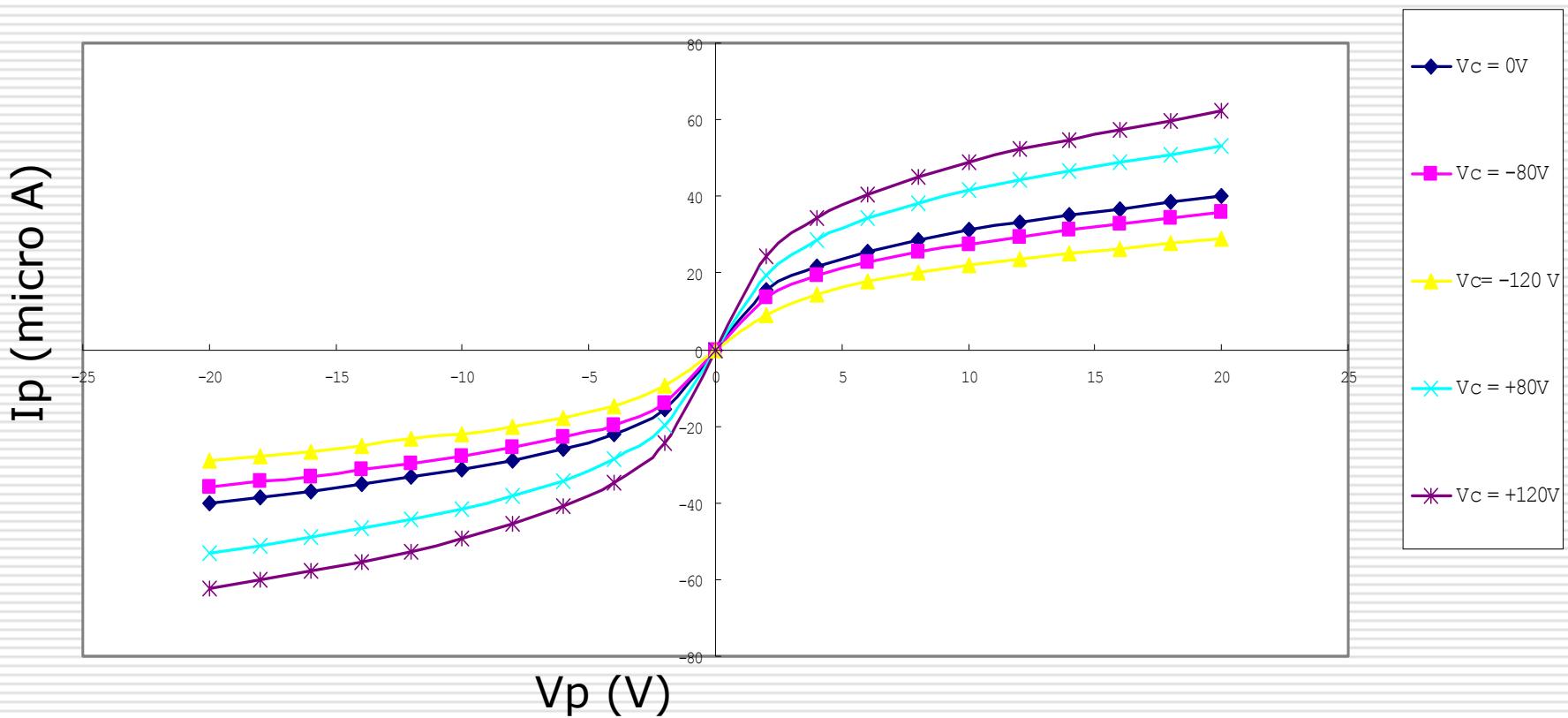
Optimal magnetic field increases ne
 $\sim 15 \times$ higher than that of no B-field
 at 20mT, $\sim 2 \times$ at 100mT.



P(mTorr)	ne (B-field)	ne (0 field)	Increase
20	1.97E+09	1.39E+08	14
40	1.10E+09	9.48E+07	12
60	8.33E+08	1.03E+08	8
80	3.84E+08	9.03E+07	4

$V_c = +120$ roughly triples ne at.
20mTorr-but potential control yet to
be demonstrated

I-V curve with varying central potential



Conclusions

- Results confirmed that Dipole Fields Enhance Plasma Density in the Center Region of the IEC
 - Presence of B-Field(350 G) increases the electron density at the center by a factor of 15.
 - Presence of bias +120 V enhances the electron density by factor of about 3. (DC discharge of 3kV)
 - Encouraging results suggest future scale up of experiment to higher grid voltage and fusion conditions.
-

Thank you

□ Yoshikazu Takeyama
■ ytakeya2@uiuc.edu



Performance Characteristics of Ion-Source-Assisted Cylindrical IEC Fusion Neutron/Proton Source

Kunihito YAMAUCHI, Atsushi TASHIRO, Sonoe OHURA,
Masato WATANABE, Akitoshi OKINO, Toshiyuki KOHNO,
Eiki HOTTA, and Morimasa YUURA*

Dept. of Energy Sciences, Tokyo Institute of Technology
**Pulse Electronic Engineering Co.,Ltd.*

Outline

- **Introduction**
- **DC Operation**
 - Basic IECF Setup
 - IECF Setup with Cusp Magnetic Field
 - IECF Setup with Cusp Magnetic Field & Biased Anode
- **Pulsed Operation**
 - IECF Setup with Cusp Magnetic Field
 - IECF Setup with Cusp Magnetic Field & Biased Anode
 - IECF Setup with Bucket-type Ion Source
- **Conclusions**
- **Future Plans**



Objective

- IEC fusion has been studied for practical use. However, some problems remain for the practical use, and the most critical one is the insufficiency of absolute neutron/proton yields.
 - Landmine Detection $>10^8$ n/s
 - Medical PET $>10^9$ n/s
- To obtain high neutron/proton yields, a new IECF device was designed and tested.



Key Features of New IECF Device

■ Cylindrical Configuration

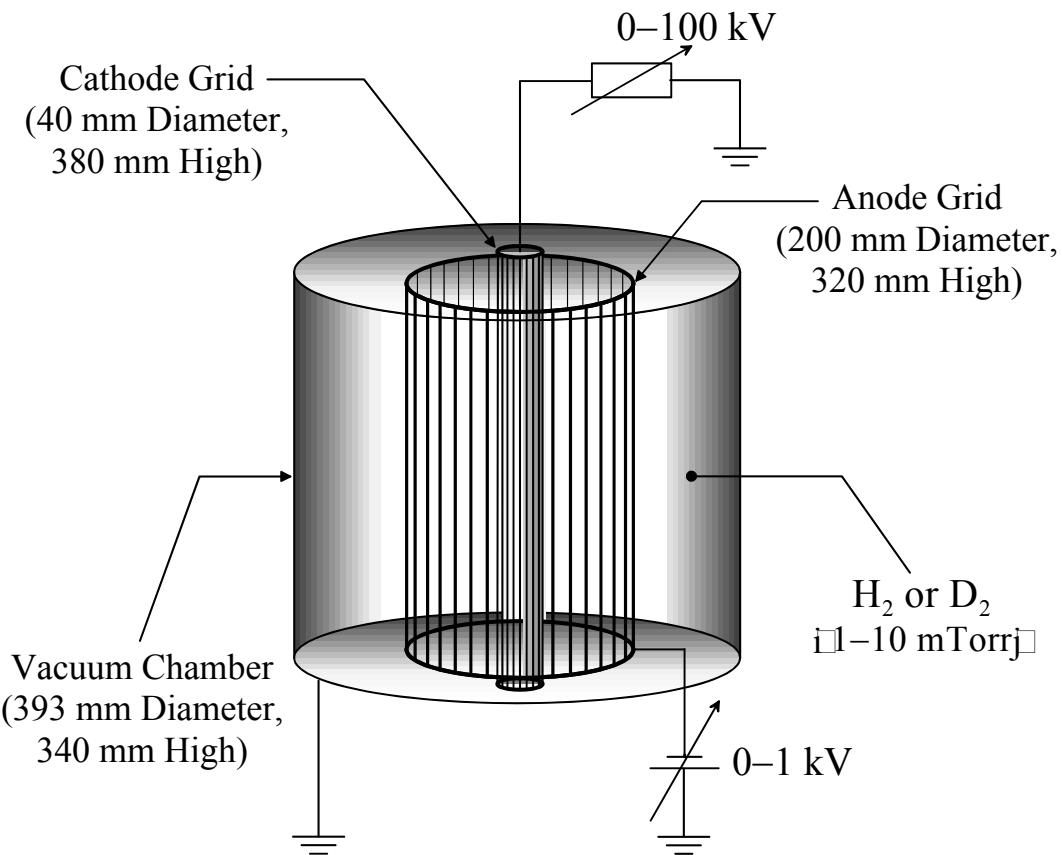
- Better electrostatic confinement of ions**
 - The influence of feedthrough can be reduced.**
- Efficient extraction of proton beams**
 - High flux can be obtained at the axial direction.**

■ Integrated Bucket-type Ion Source

- Simple configuration**
- High neutron/proton production rate**



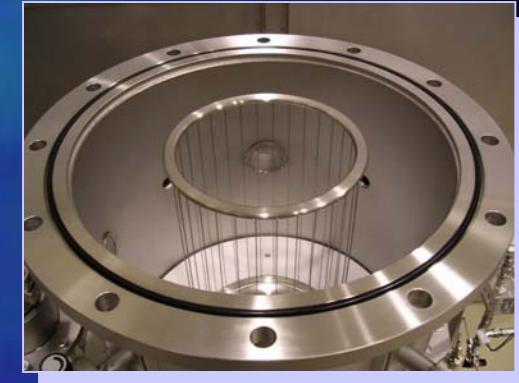
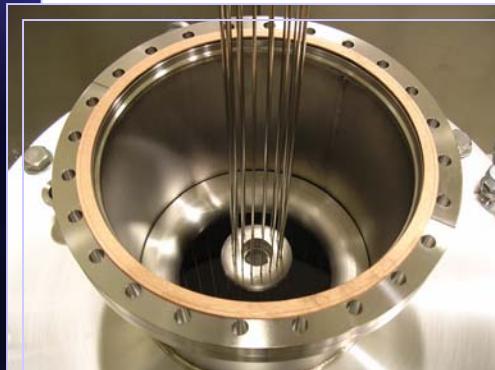
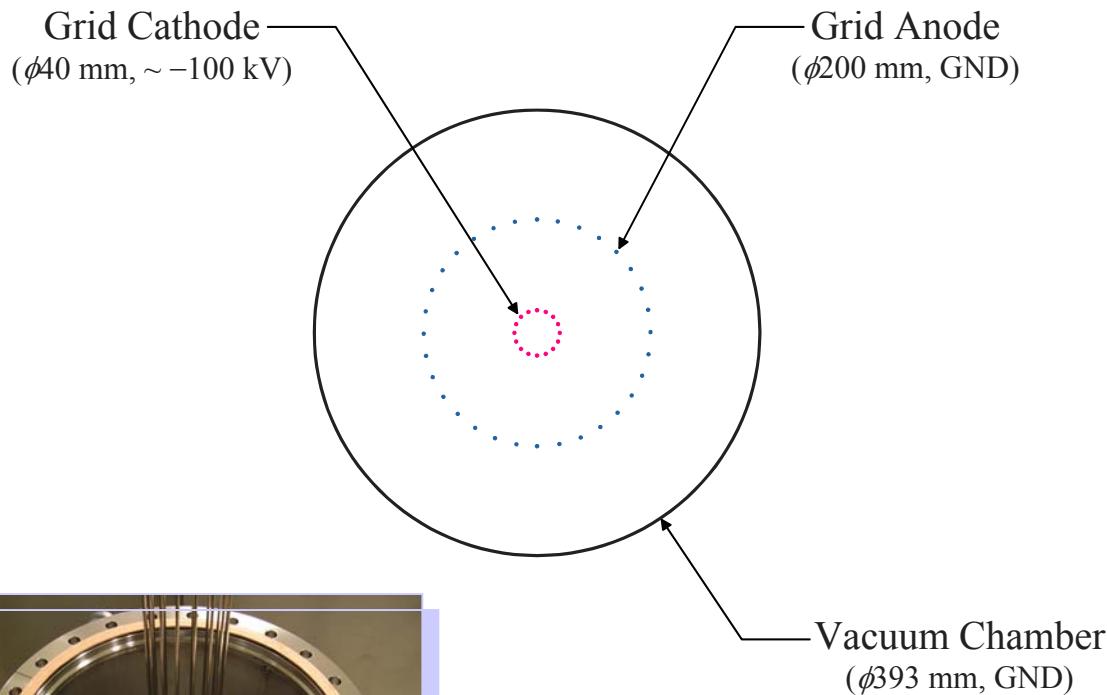
Schematic of New IECF Device



Cathode: ϕ 1.6-mm Stainless Steel Rod x16

Anode: ϕ 1.2-mm Stainless Steel Rod x32

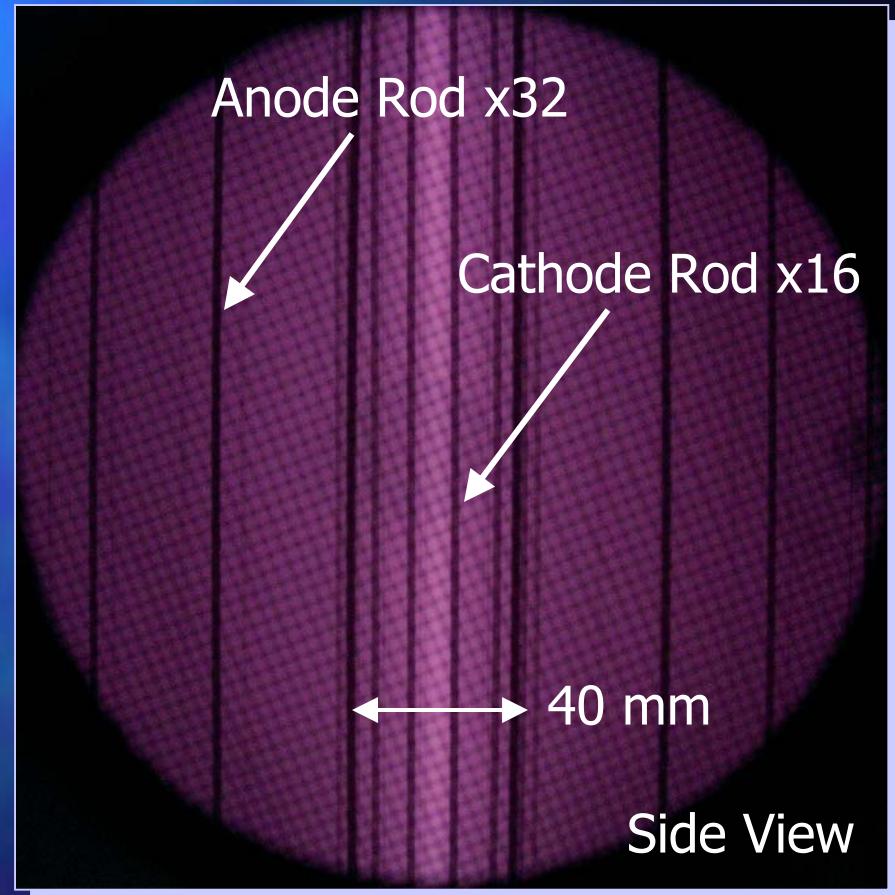
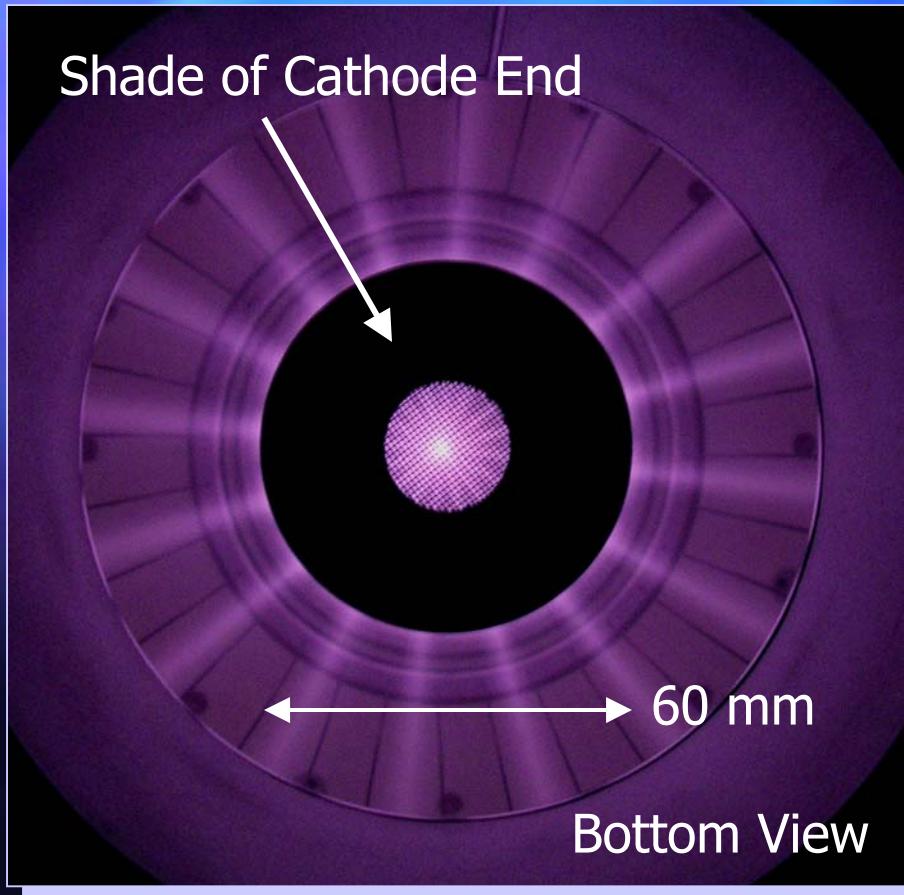
Basic IECF Setup



Cathode: $\phi 1.6$ -mm Stainless Steel Rod x16
Anode: $\phi 1.2$ -mm Stainless Steel Rod x32

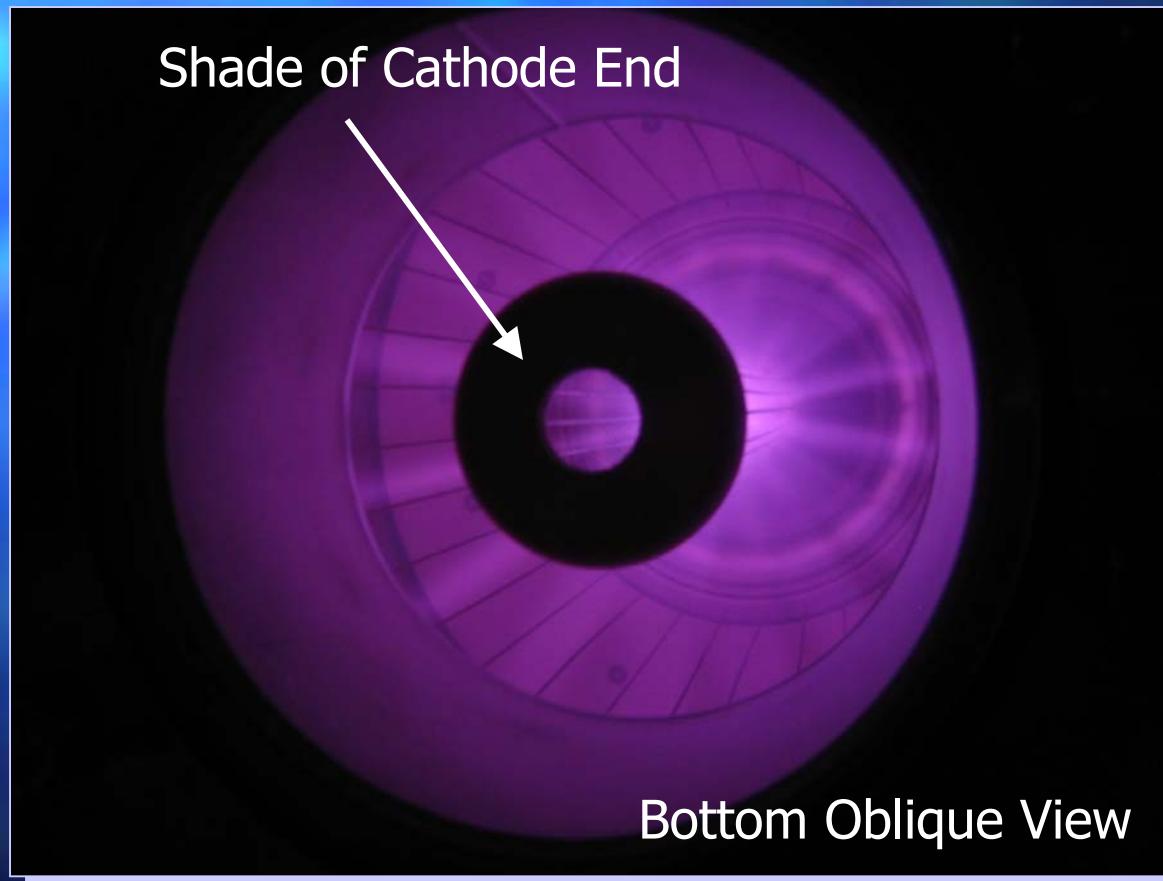
Photograph of Discharge Plasma

Star Mode: 10.0 mTorr H₂, 20.0 mA, -7.2 kV

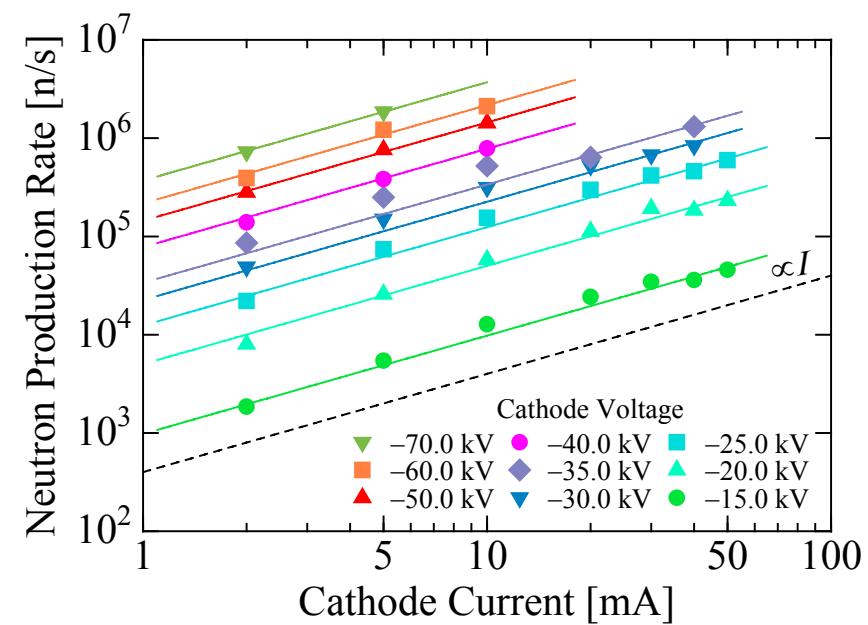
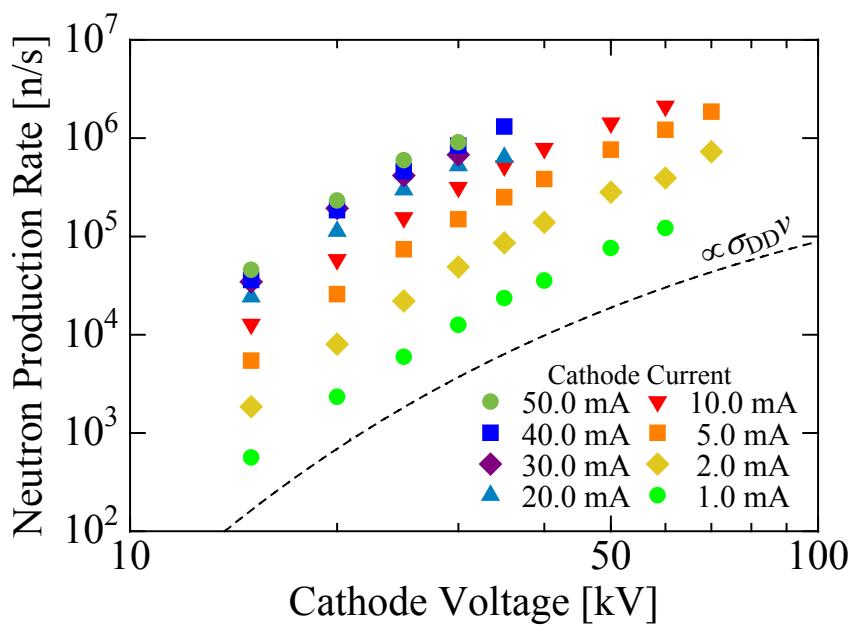


Photograph of Discharge Plasma

Star Mode: 10.0 mTorr H₂, 20.0 mA, -7.2 kV



Neutron Production Rate

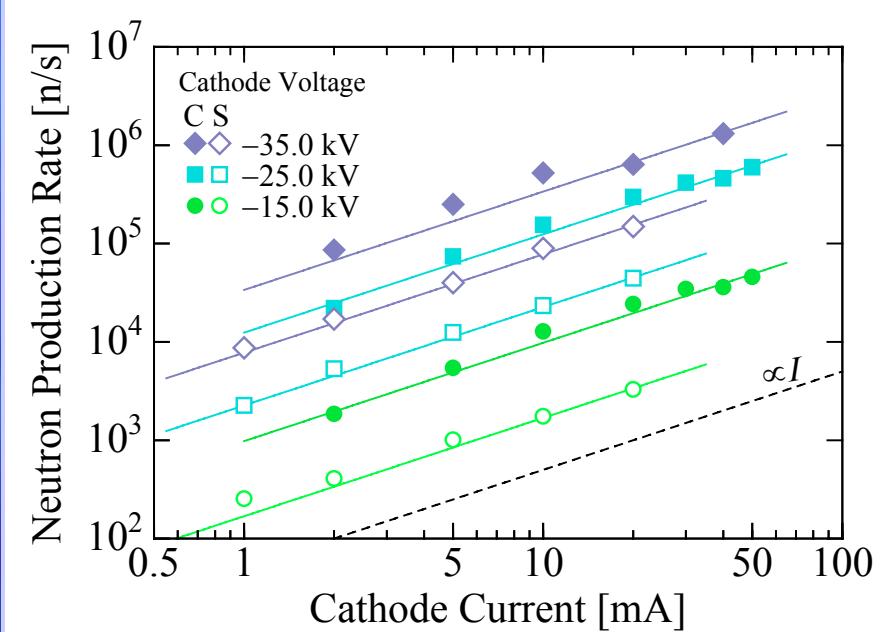
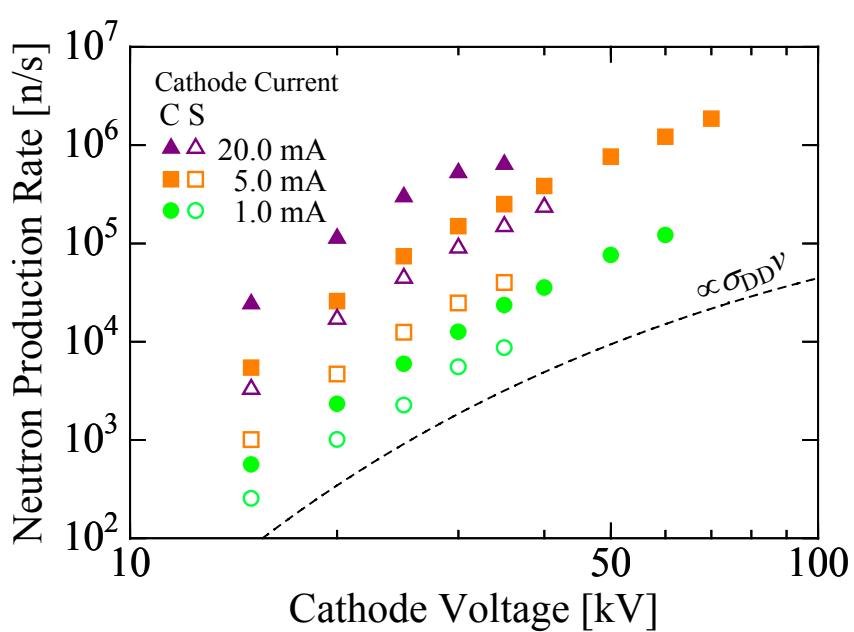


- The neutron production tendency of new cylindrical device is almost the same as that of conventional spherical device.
 - Beam-background reaction is dominant.
- The maximum neutron production rate of 2.1×10^6 n/s was obtained at a discharge of -60 kV, 10 mA.



Comparison with Spherical Device

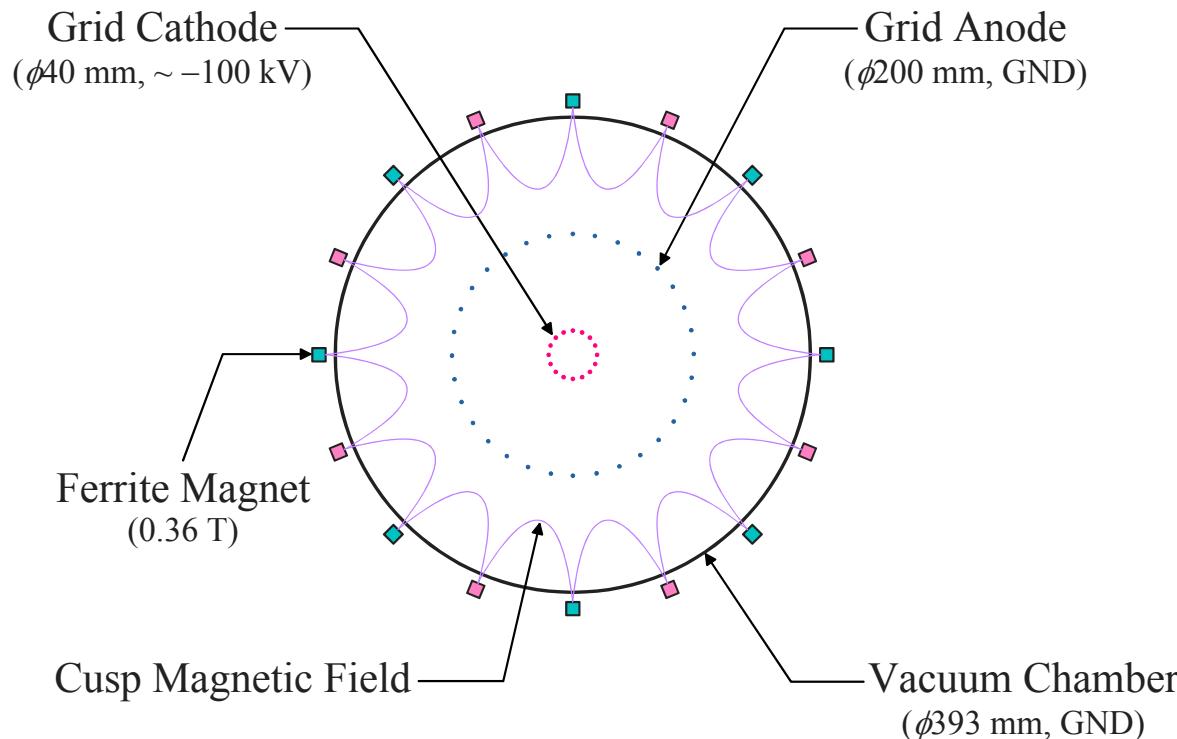
C: Cylindrical Device S: Spherical Device



- New cylindrical device can generate several times higher neutron yield than conventional spherical device.
- This may be caused by the better electrostatic confinement of ions.



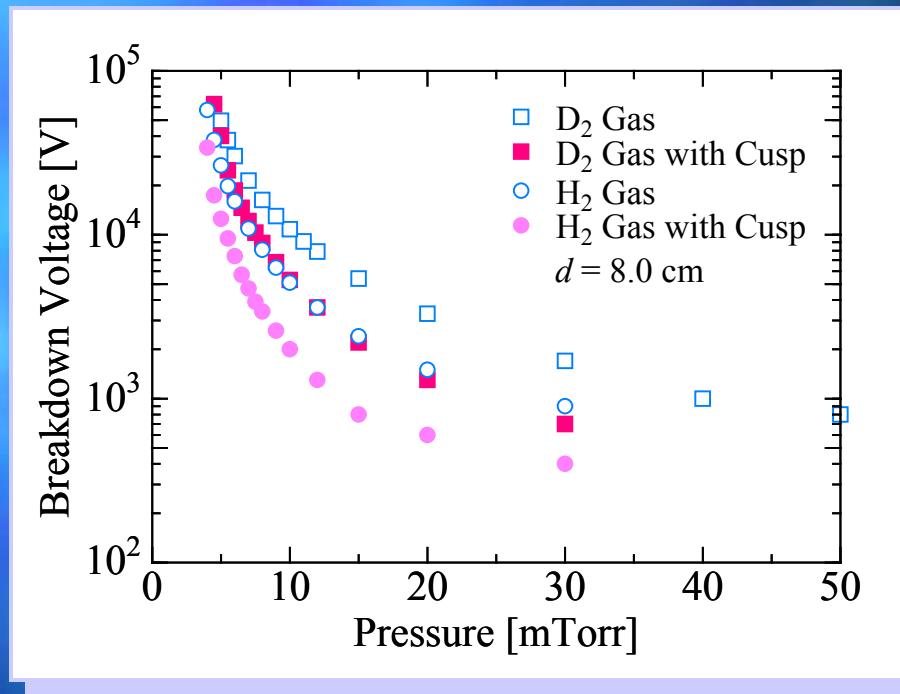
IECF Setup with Cusp Magnetic Field



Generated ions are extracted toward the center by the electric field leaked through the grounded grid anode.

- Electrons are trapped in the cusp magnetic field.
→ The path and life of electrons are elongated.

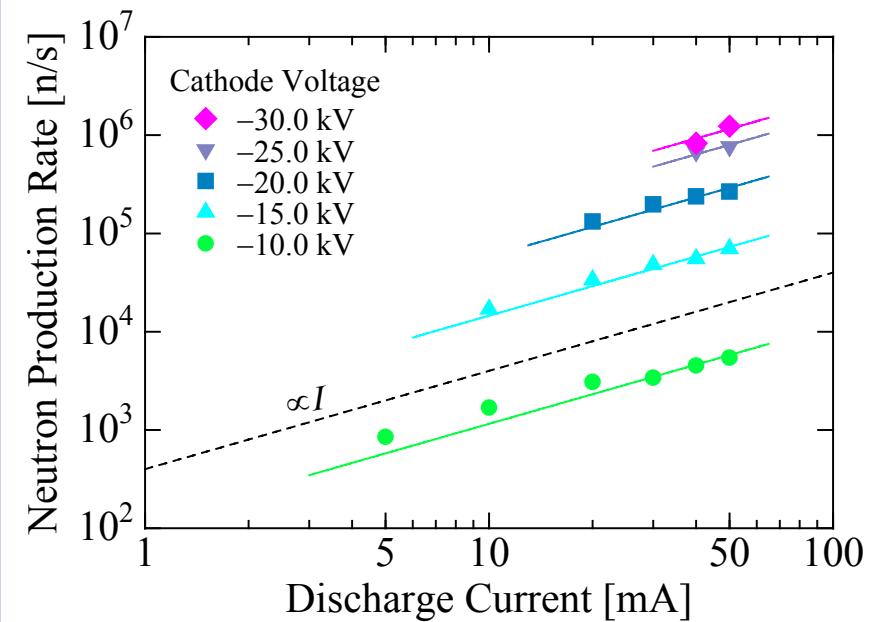
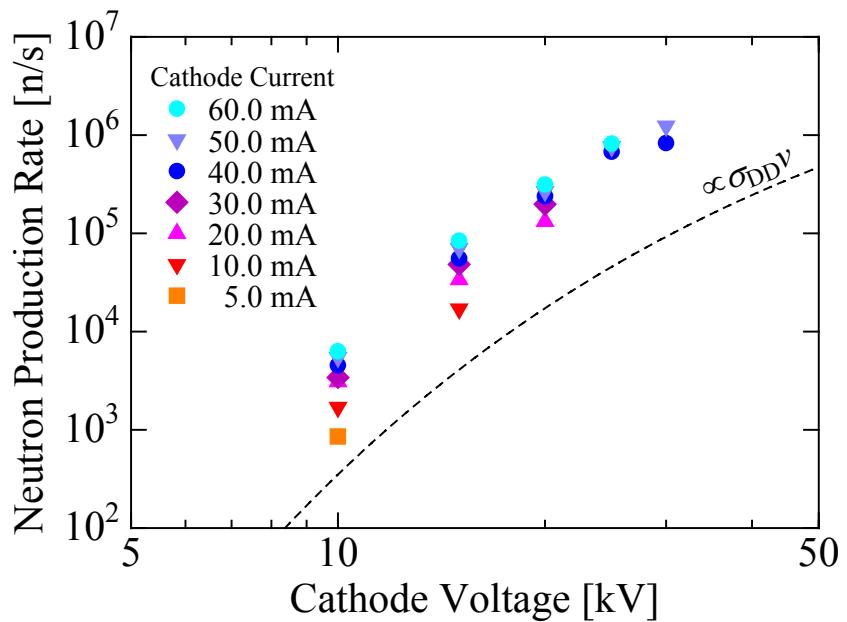
Breakdown Voltage Characteristics



- Breakdown voltage was reduced to a half with applying cusp magnetic field.
→ The cusp magnetic field works effectively as an ion source.



Neutron Production Rate

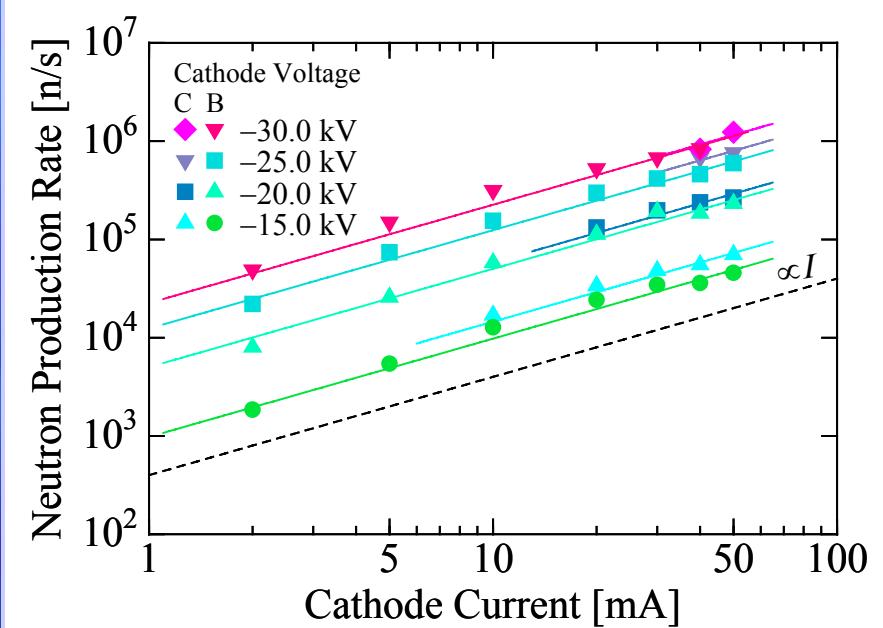
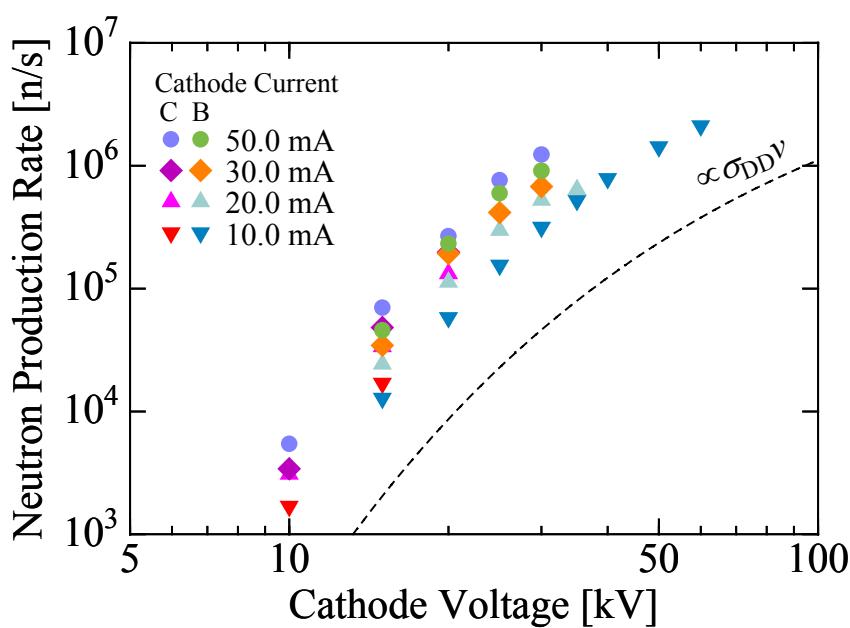


- The neutron production tendency of new cylindrical device is almost the same as that of conventional spherical device.
 - Beam-background reaction is dominant.



Comparison with Basic IECF Setup

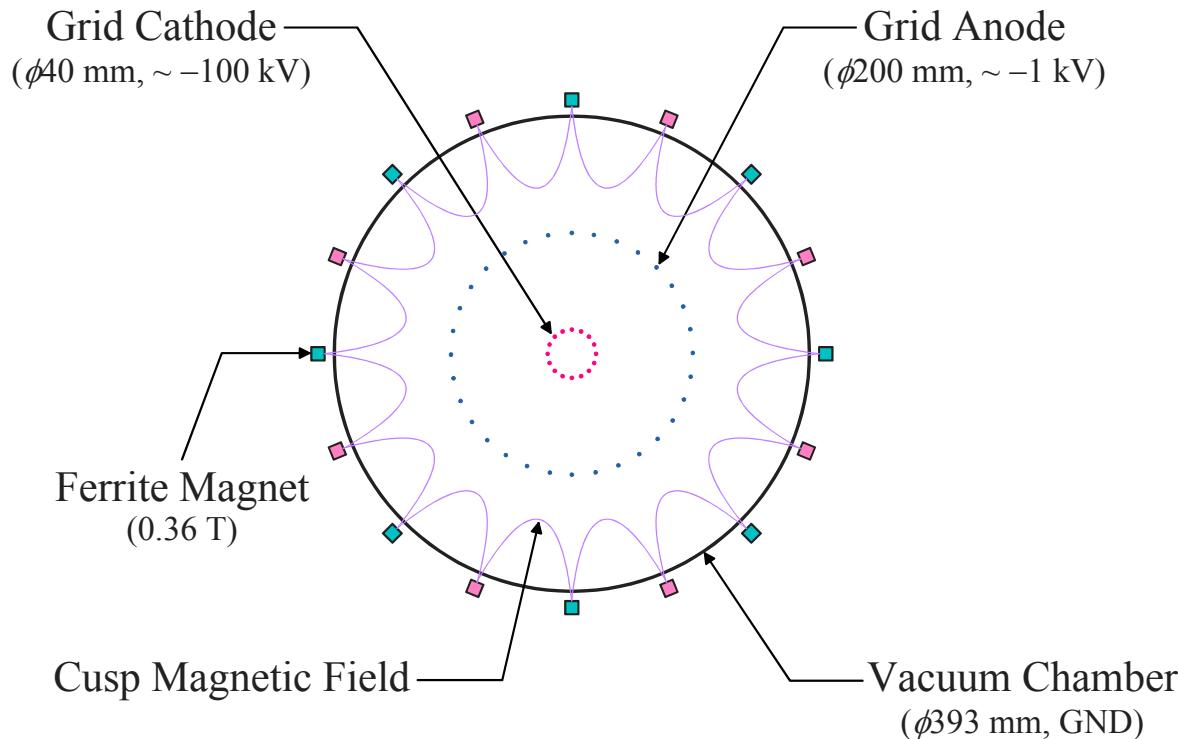
C: with Cusp Magnetic Field B: Basic Setup



- Neutron production rate was enhanced by a factor of about 1.5 with applying cusp magnetic field.
 - The cusp magnetic field works effectively as an ion source.



IECF Setup with Cusp Magnetic Field & Biased Anode

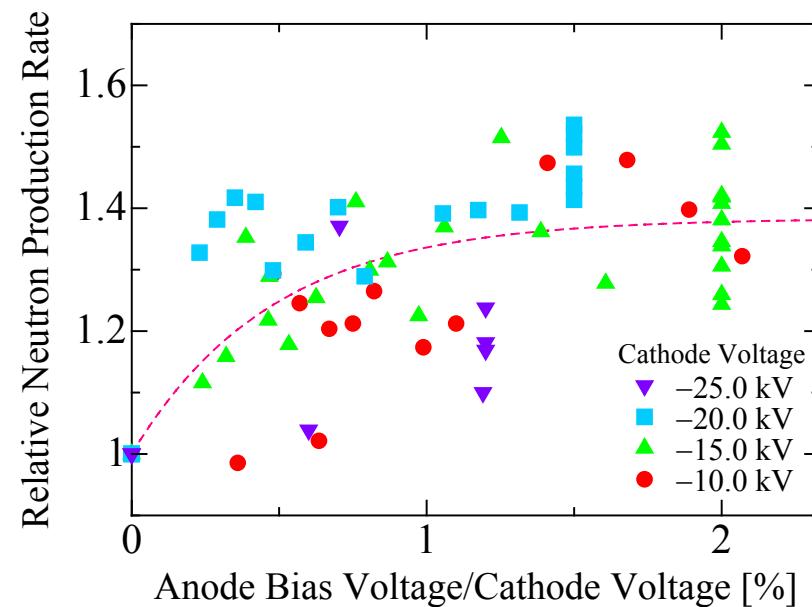
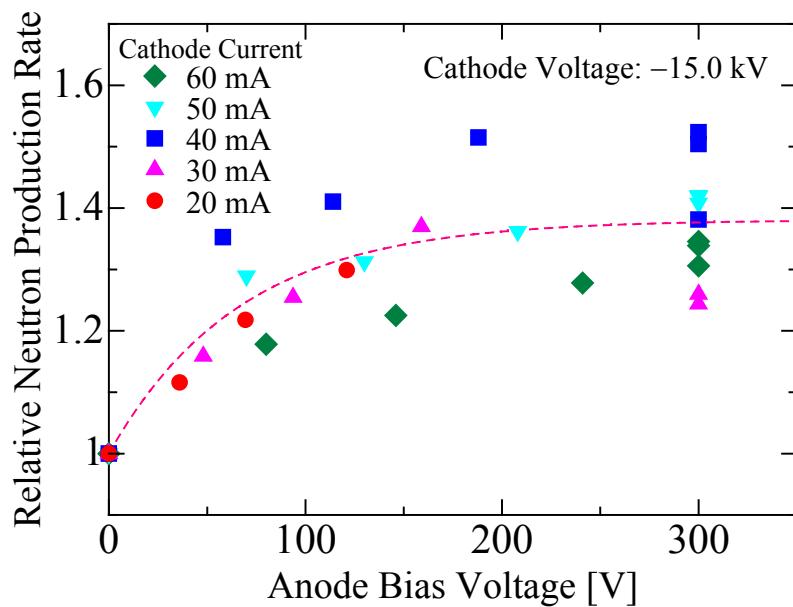


Three shunt resistors of 20, 50, 100 $k\Omega$ and a dc power supply were used for biasing the anode.

- Generated ions are efficiently extracted toward the center by the biased anode.



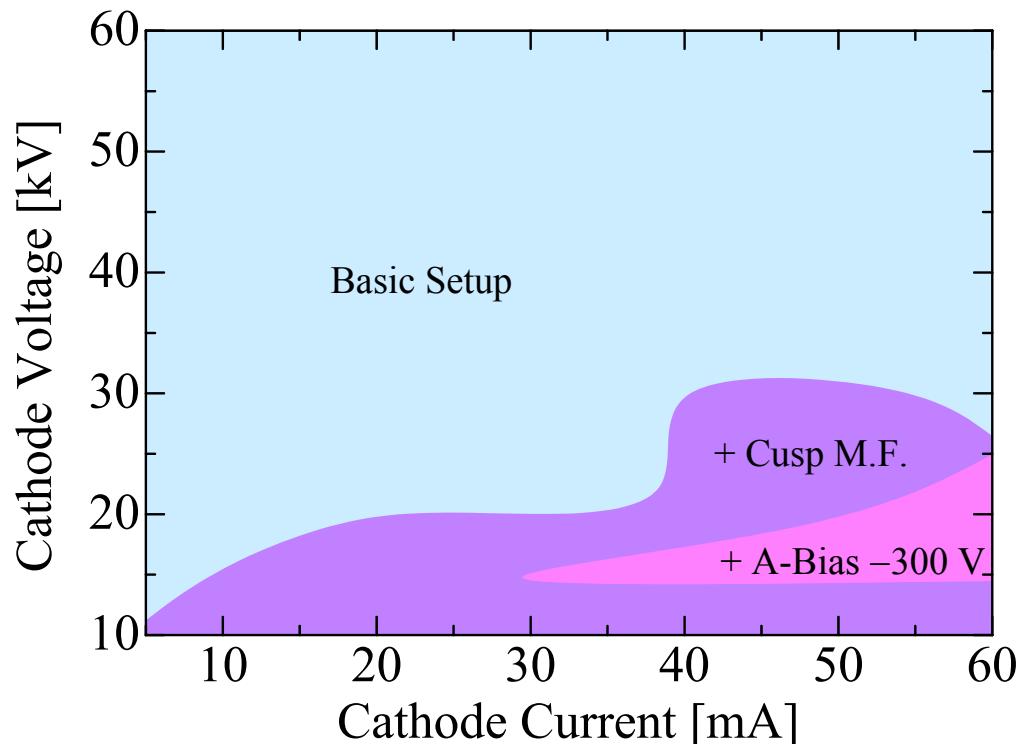
Neutron Production Rate



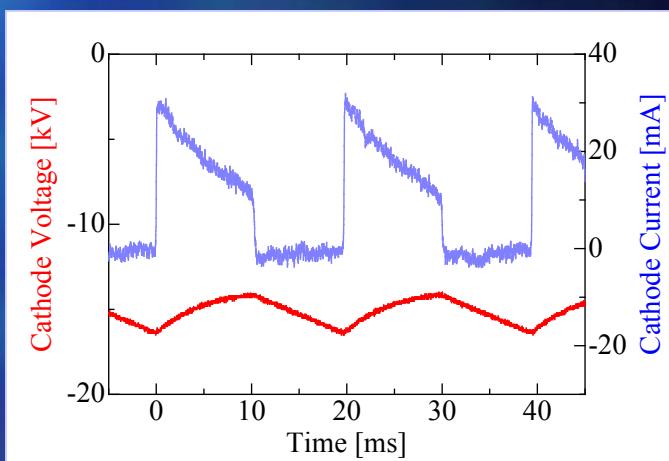
- Neutron production rate was enhanced by a factor of about 1.4 with biasing the anode.
 - The biased anode extracts the generated ions effectively.



Region of Stable DC Operation



Periodic discharge occurs by using ion source.



6.65 mTorr, 10.0 mA, -15.0 kV

- Stable region shifts to higher current and lower voltage side by using ion source.



Problem of Ion-Source-Assisted DC Operation

- Stable dc operation can hardly be obtained with enhancement of ion source effect.
 - CVCC control can not follow the rapid decrease of impedance.
 - Three CVCC power supply were tried.

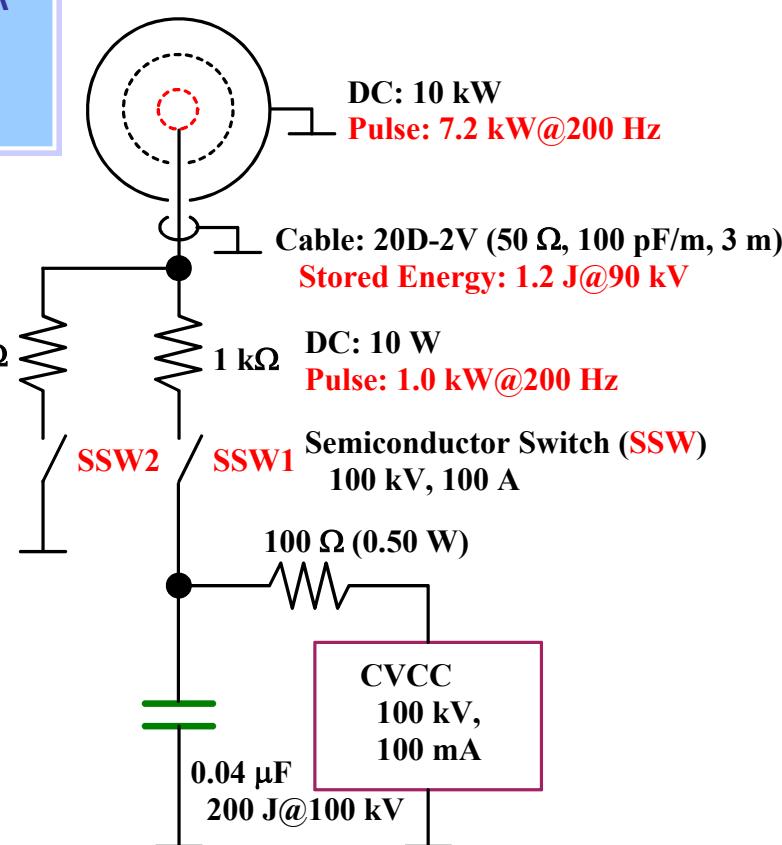
- 
- The ion-source-assisted IECF device is suitable for **Pulsed Operation**.



Circuit for Pulsed Operation

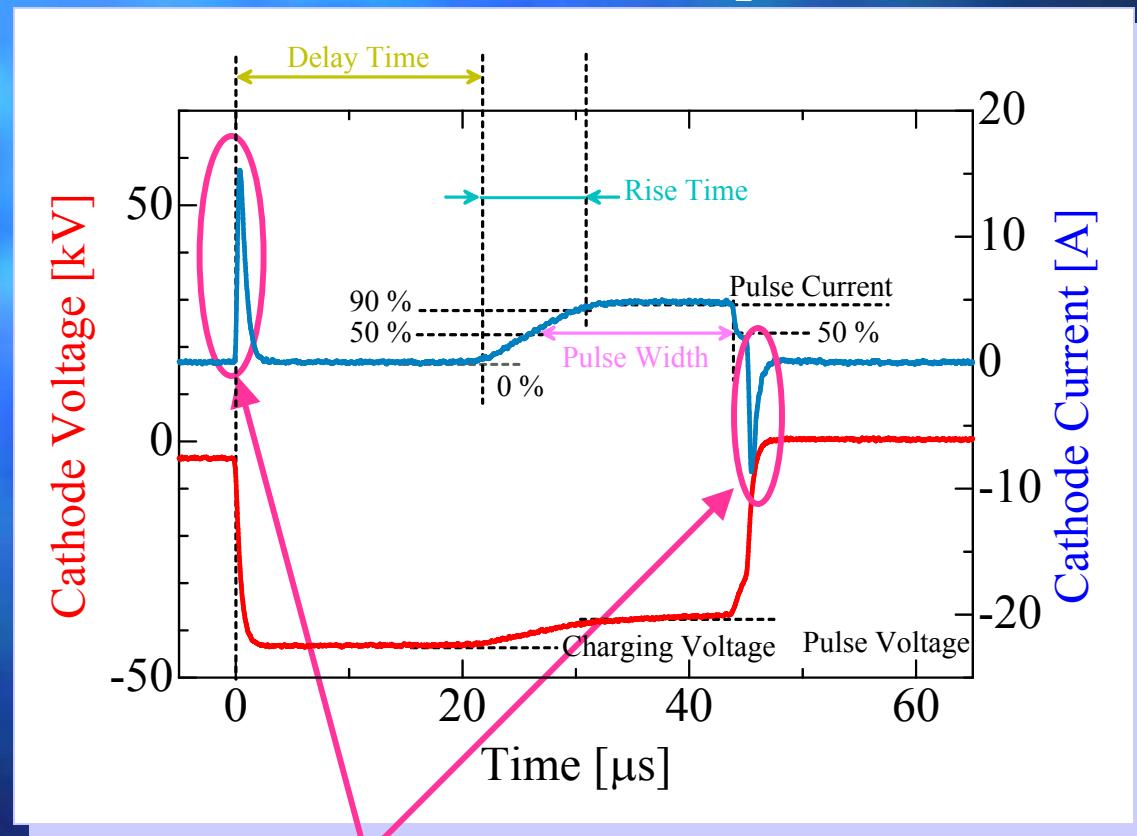
CW Discharge: -100 kV.100 mA
Pulsed Discharge: -90 kV.10 A.
40 μ s.200 Hz

Mode	SSW1	SSW2
DC	ON	OFF
Pulse	ON→OFF	OFF→ON
GND	ON	ON



Typical Waveforms

Pressure: 8.08 mTorr (D_2), Charging Voltage: -43 kV



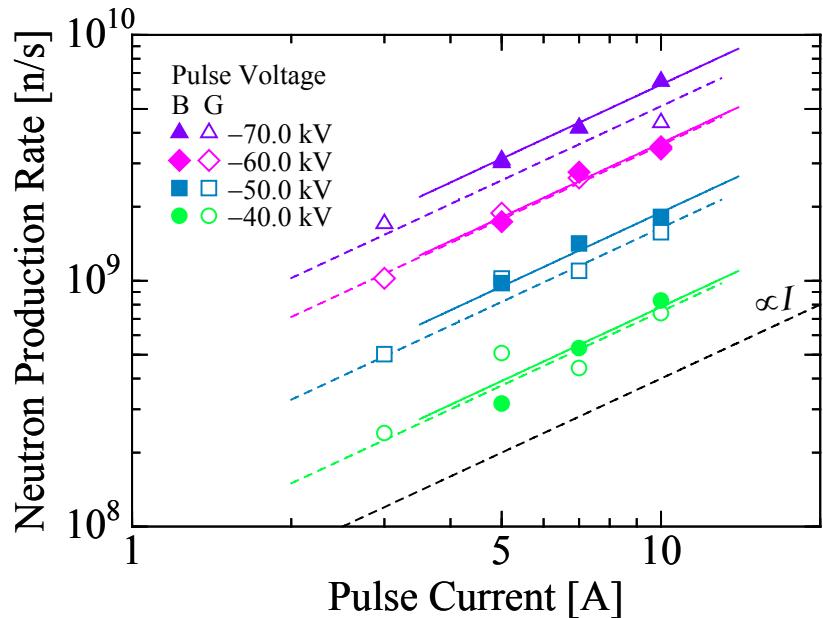
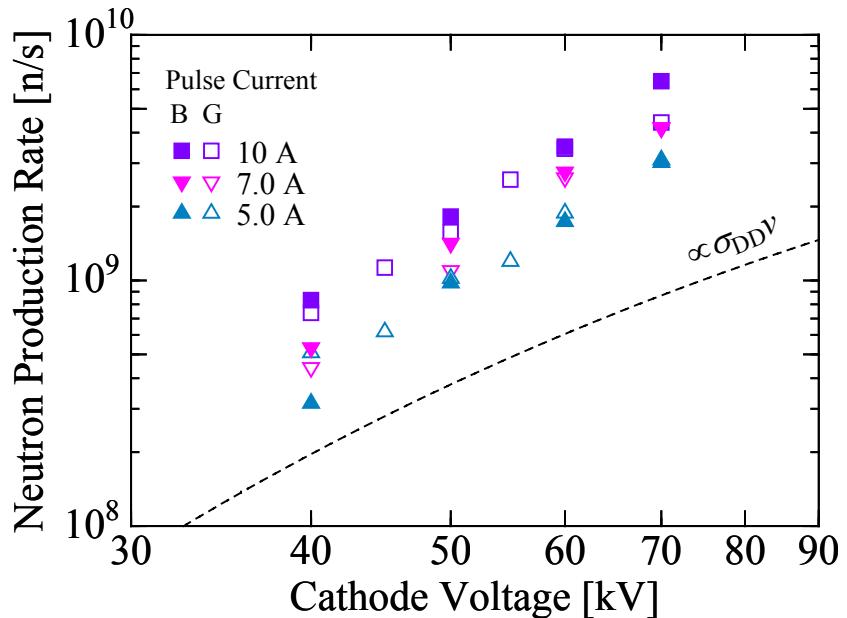
Charging and discharging currents of the coaxial cable(20D-2V, 3 m)



Pulsed Neutron Production Rate

B: Initial Bias Voltage -1.0 kV G: GND

Pulse Width: $20\text{ }\mu\text{s}$, Rep. Rate: 4 Hz

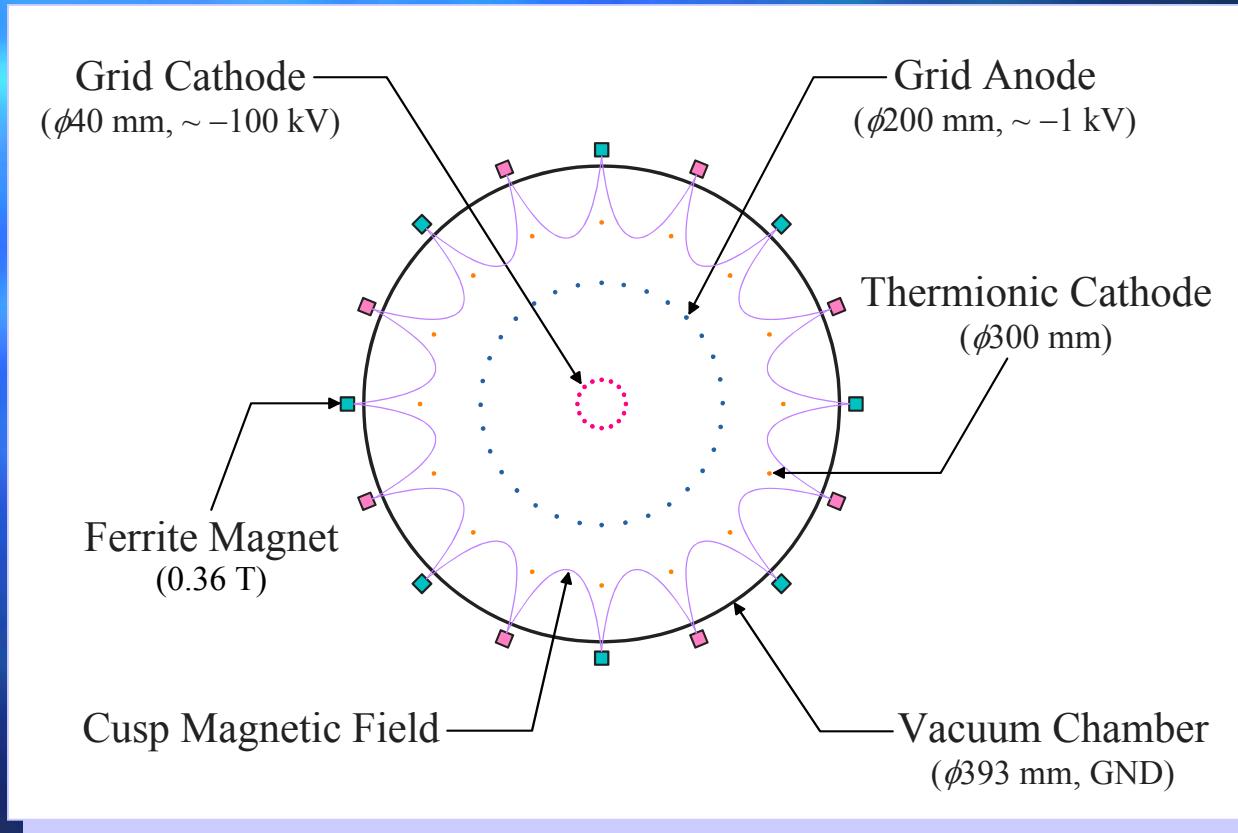


- The biased anode is also effective in pulsed operation.
- The maximum neutron production rate of $6.8 \times 10^9\text{ n/s}$ was obtained at a pulsed discharge of -70 kV , 10 A with bias voltage of -1.0 kV .



IECF Setup with Bucket-type Ion Source

Filament: $\phi 0.15\text{-mm}$ Thoriated Tungsten Wire



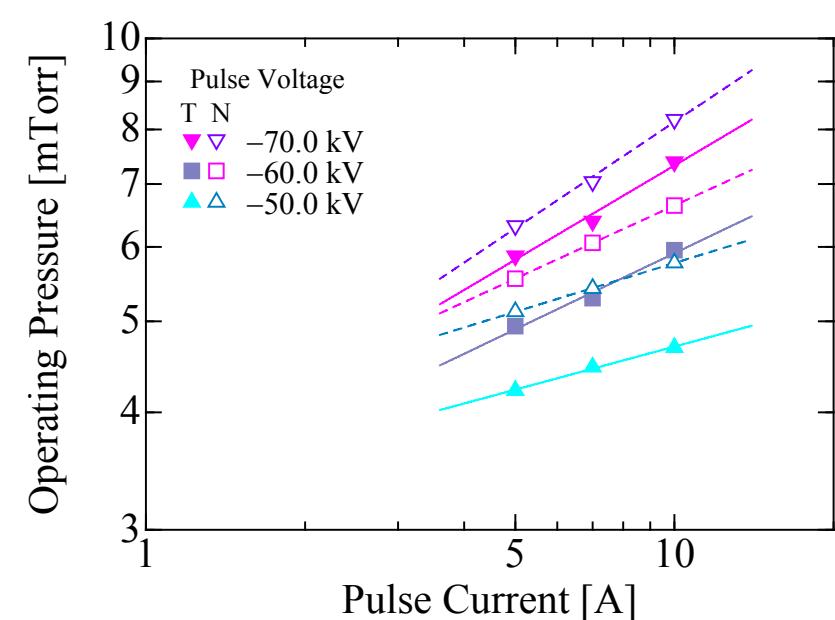
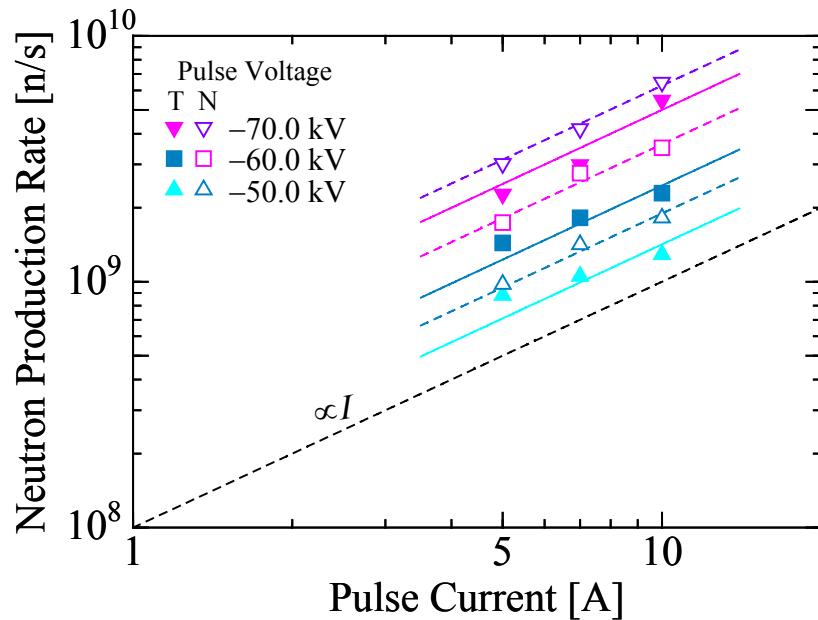
- Emitted thermionic electrons generate ions actively.



Pulsed Neutron Production Rate and Operating Pressure

T: with Thermionic Cathode (80 W)
N: w/o Thermionic Cathode

Pulse Width: 20 μ s, Rep. Rate: 10 Hz,
Initial Anode Bias Voltage: -1.0 kV



- Neutron production rate was decreased by a factor of about 0.8 with using thermionic cathode.
 - This may be caused by the over-reduced gas pressure.



Conclusions

- A new cylindrical IECF device with an ion source was designed and tested.
- The cylindrical device can generate several times higher neutron yield than conventional device.
- It was confirmed that the bucket-type ion source works effectively.
- The optimum strength of ion source exists.
- The maximum neutron production rate of 6.8×10^9 n/s was obtained at a pulsed discharge of -70 kV, 10 A, bias voltage of -1.0 kV.
 - The maximum neutron production rate of 2.1×10^6 n/s was obtained at a dc discharge of -60 kV, 10 mA.

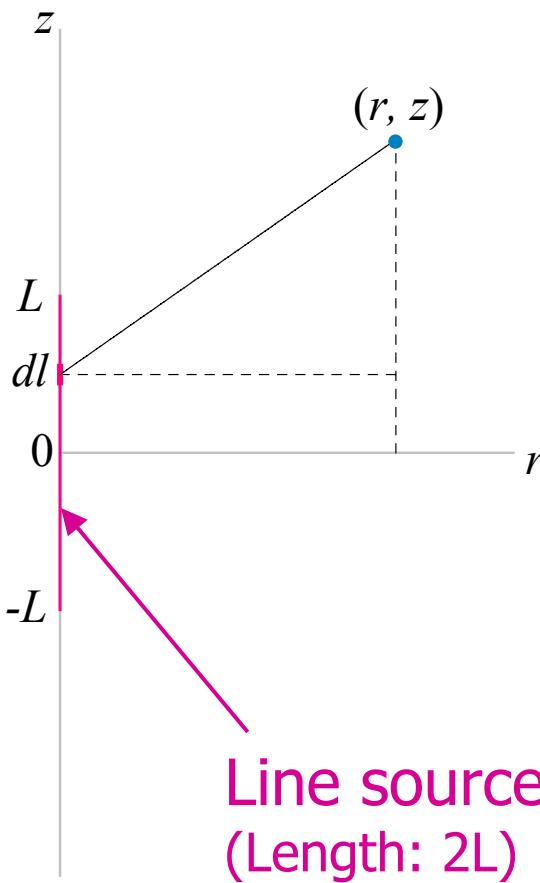


Future Plans

- Measurements of the characteristics in detail
 - There are many parameters in the ion-source-assisted IECF.
- Proton measurements
 - Proton was not measured in this work.
- D-³He reaction
 - High-energy proton for PET application can be obtained.



(Appendix) Neutron/Proton Flux of Cylindrical IEKF



$$\begin{aligned}\phi &= \int_{-L}^L \frac{N / 2L}{4\pi \{r^2 + (z - l)^2\}} dl \\ &= \frac{N}{4\pi L^2} \frac{L}{2r} \left(\tan^{-1} \frac{z + L}{r} - \tan^{-1} \frac{z - L}{r} \right)\end{aligned}$$

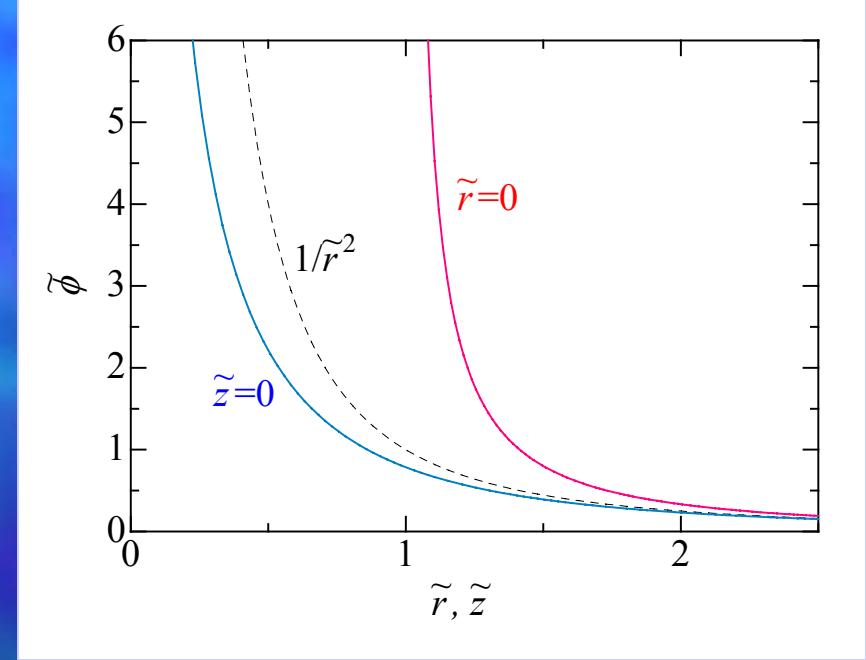
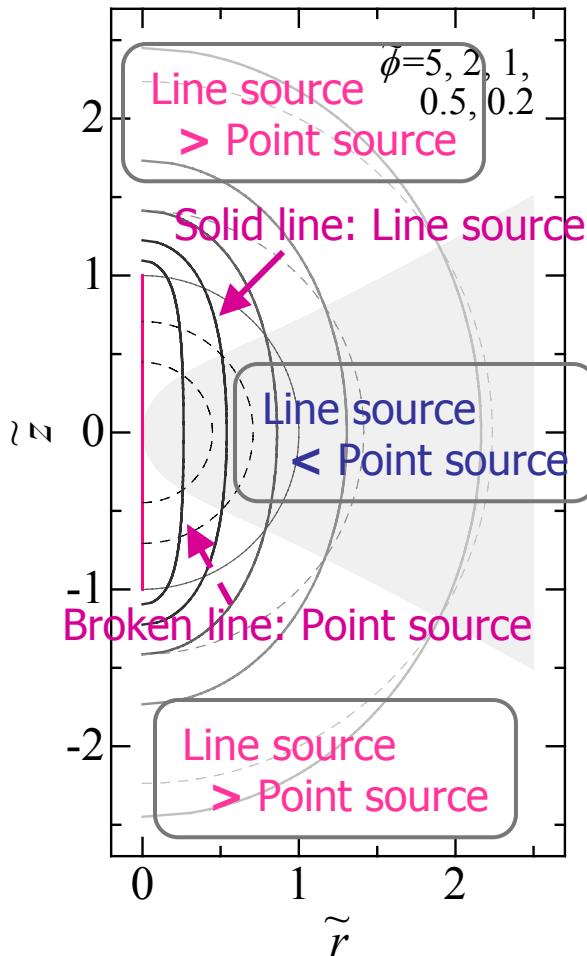
Normalization

$$\begin{cases} \tilde{r} = \frac{r}{L} \\ \tilde{z} = \frac{z}{L} \\ \tilde{\phi} = \frac{\phi}{N / 4\pi L^2} \end{cases}$$



(Appendix) Neutron/Proton Flux of Cylindrical IECF

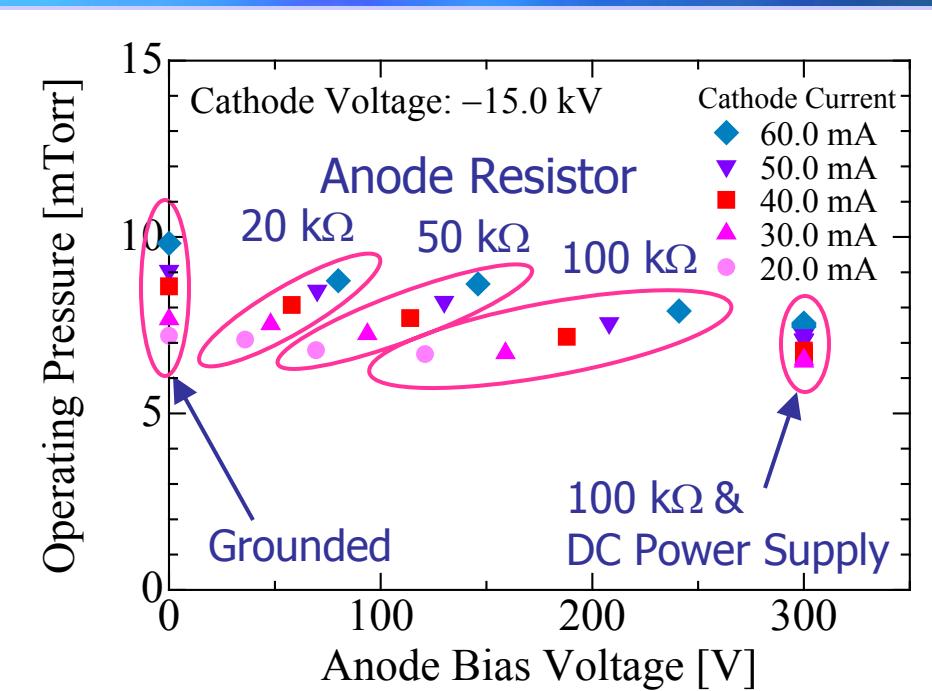
Equiflux Line



- High flux is obtained in the axial direction.
 - Better for extraction of proton beams



Operating Pressure vs. Anode Bias Voltage



- Operating pressure slightly decreases with increasing the anode bias voltage.
→ The biased anode extracts the generated ions effectively



Atomic Physics Effects on IEC Ion Radial Flow

*G.A. Emmert & J.F. Santarius
Fusion Technology Institute
University of Wisconsin*

*7th US-Japan Workshop on Inertial Electrostatic Confinement Fusion
Los Alamos, NM, March 14-16, 2005*



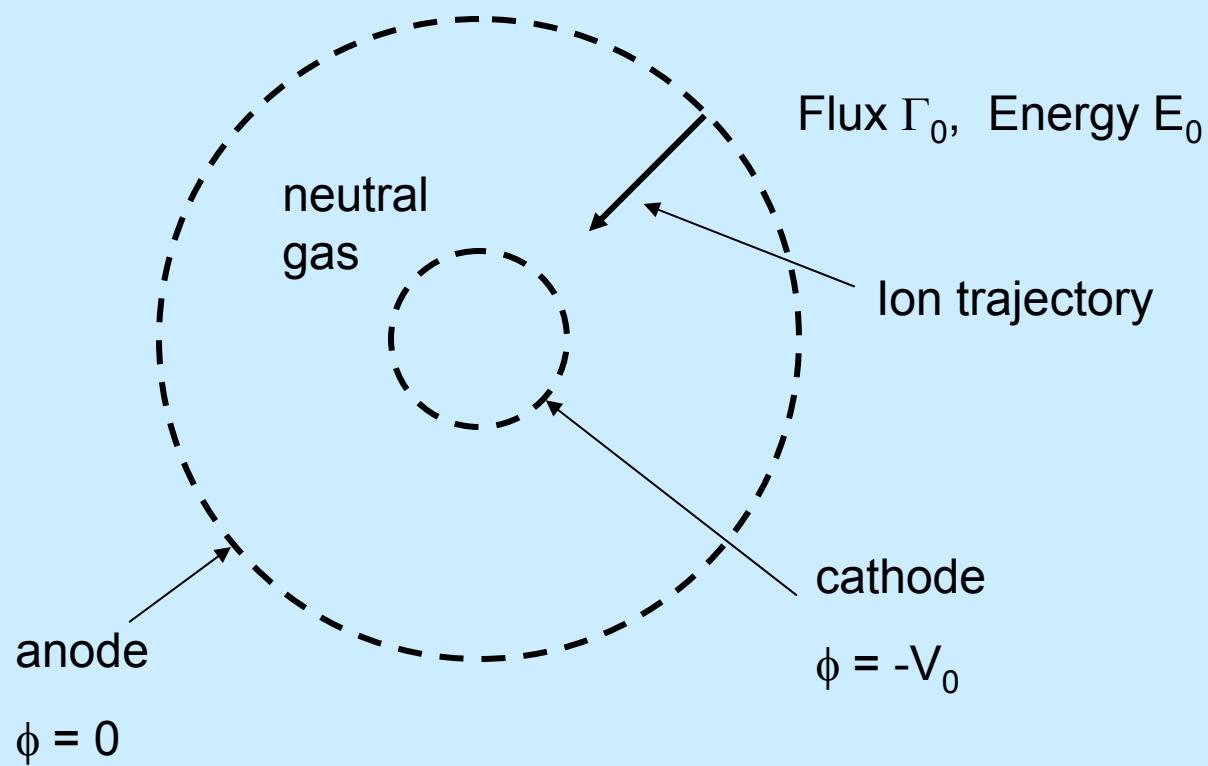
THE UNIVERSITY
WISCONSIN
MADISON



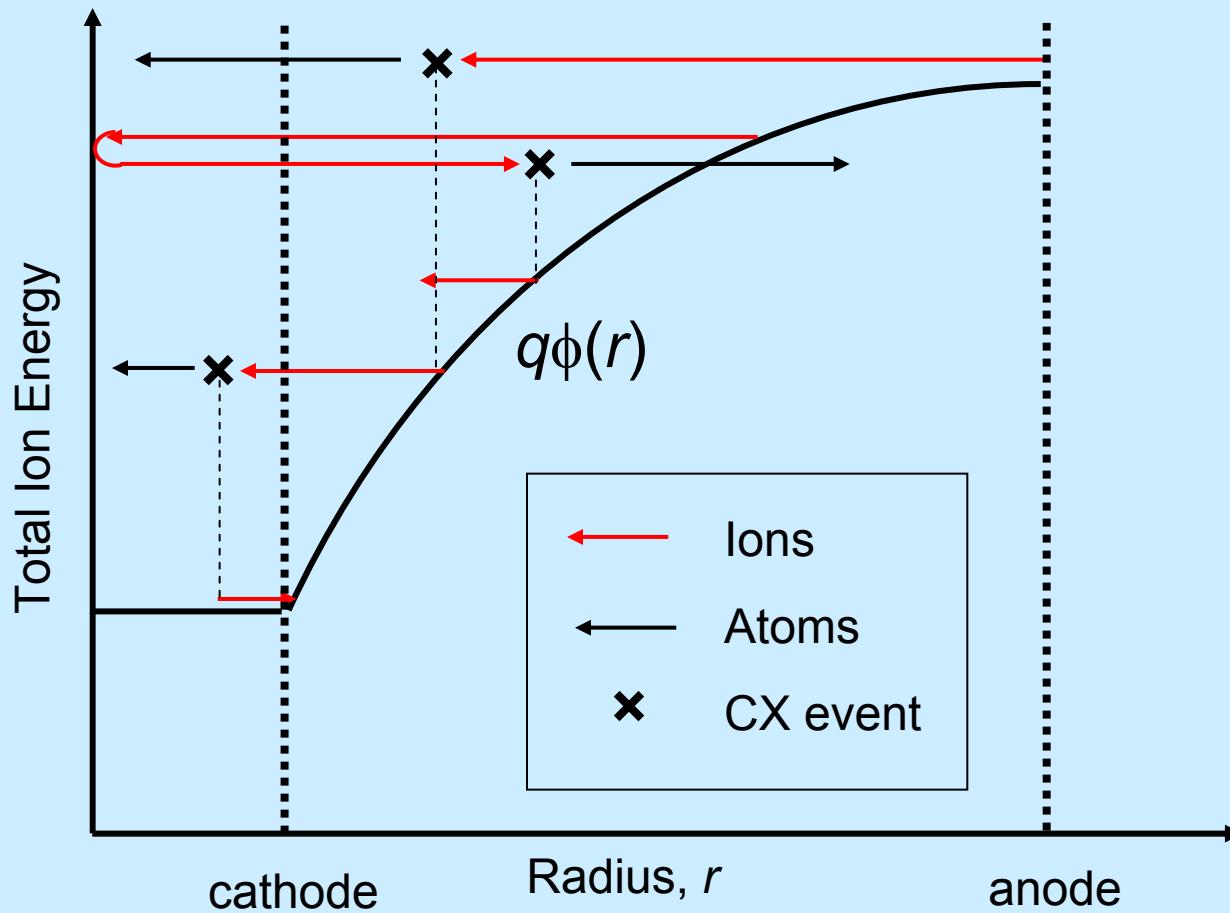
The Goal of this Research

- Understand the role of atomic physics on the flow of ions in gridded spherical IEC devices
- Develop a model to predict the performance of these devices

IEC Model

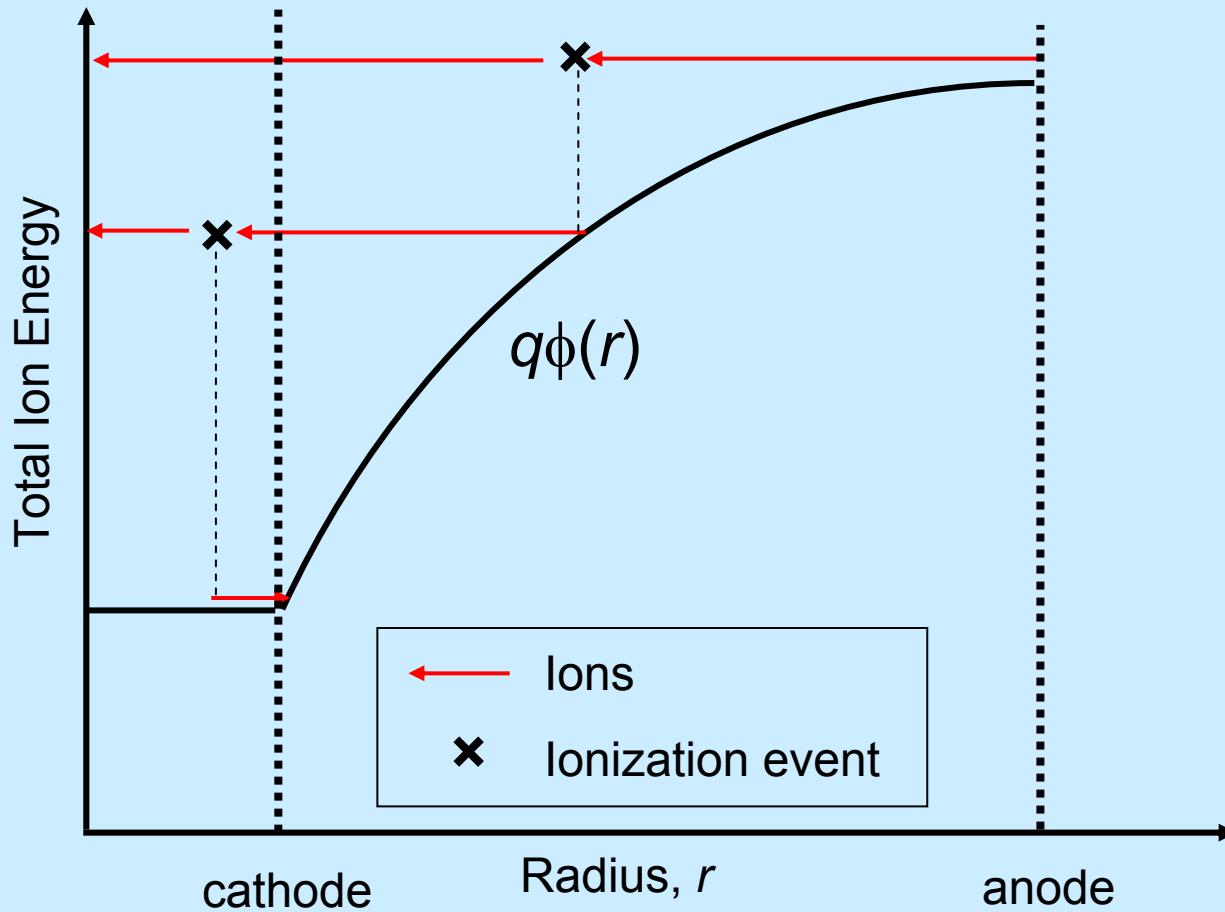


Charge Exchange Produces Fast Atoms and Cascading Down of the Ion Energy





Ionization Produces Cold Ions without Loss of Energy





Basic Assumptions of the Model

- Background D_2 gas
- Deuterium ions (no molecular ions)
 - Collisionless motion except for charge exchange and ion impact ionization interactions
- Fast deuterium atoms
 - Collisionless motion
- Prescribed electrostatic potential profile
 - Child-Langmuir or vacuum in intergrid region
 - Flat in the cathode region
- Spherical symmetry – ignore stalk and defocusing
- Electron – atom interactions neglected.



Formalism

- Cold ion source function = $S(r)$
 - Attenuation function = $g(r, r')$

- Ion flux $d\Gamma(r)$ at r due to ions born at r'

$$r^2 d\Gamma(r) = r'^2 g(r, r') S(r') dr'$$



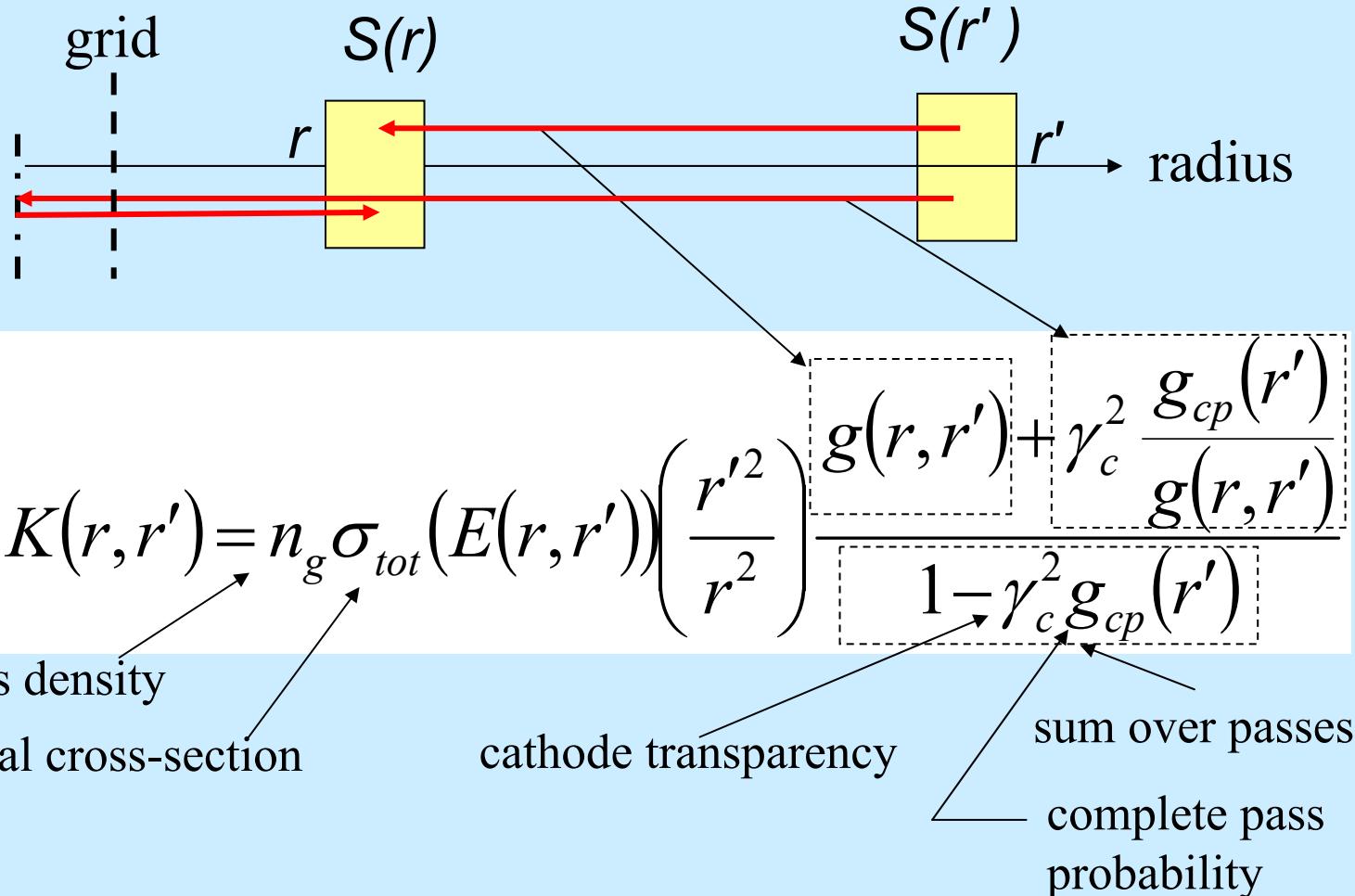
Particle Conservation in the Intergrid Region

Sum over all generations of cold ions and all ion passes

$$S(r) = A(r) + \int_r^{\text{anode}} K(r, r') S(r') dr'$$

$A(r)$ = cold ion source due to ions from the anode

Kernel relates the Source at one Radius to the Source at another Radius



$$K(r, r') = n_g \sigma_{tot}(E(r, r')) \left(\frac{r'^2}{r^2} \right) \frac{g(r, r') + \gamma_c^2 \frac{g_{cp}(r')}{g(r, r')}}{1 - \gamma_c^2 g_{cp}(r')}$$

gas density

total cross-section

cathode transparency

sum over passes

complete pass probability



Solution Method

- Set up a mesh in the intergrid region (the Volterra equation is only defined there)
- Calculate the attenuation coefficients in the intergrid region numerically and in the cathode region analytically
- Solve the Volterra equation by finite difference methods



Given $S(r)$ We Can Calculate:

- Energy spectrum of the fast ion flux, $f_i(r,E)$
- Energy spectrum of the fast neutral flux, $f_n(r,E)$
- Ion current collected by the cathode
- Neutron production rate
- etc



The “Catch”

- The ion current Γ_0 leaving the anode is unknown experimentally and therefore is an adjustable parameter.
- We adjust it to match the calculated cathode current with the measured value.
- We then compare calculated and measured neutron generation rates.

Example Calculation

Input:

Cathode voltage	166 kV
Gas pressure	2 mTorr
Inward anode current	12.3 mA

Cathode Current:

energetic ion current striking cathode	16.4 mA
cold ion current striking cathode	23.7 mA
secondary electron emission	27.8 mA
Total Cathode Current	68 mA

Example Calculation - II

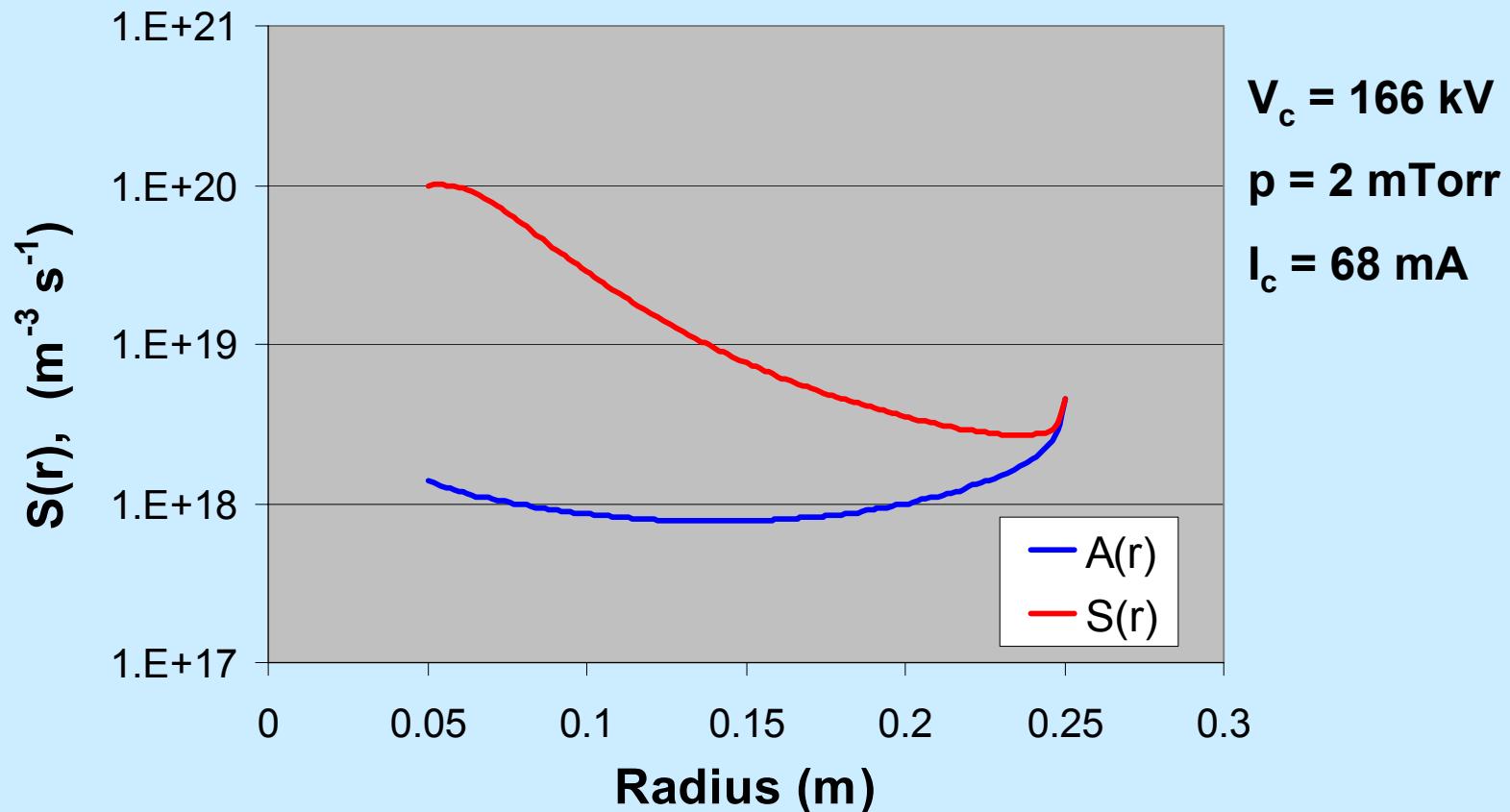
- Neutron Generation (model)
 - by ion-gas fusion 8.1×10^6 n/s
 - By fast atom-gas fusion 3.8×10^7 n/s
 - Total **4.6×10^7 n/s**
- Neutron Generation (exp.) **1.8×10^8 n/s**

Neutron generation processes not calculated:

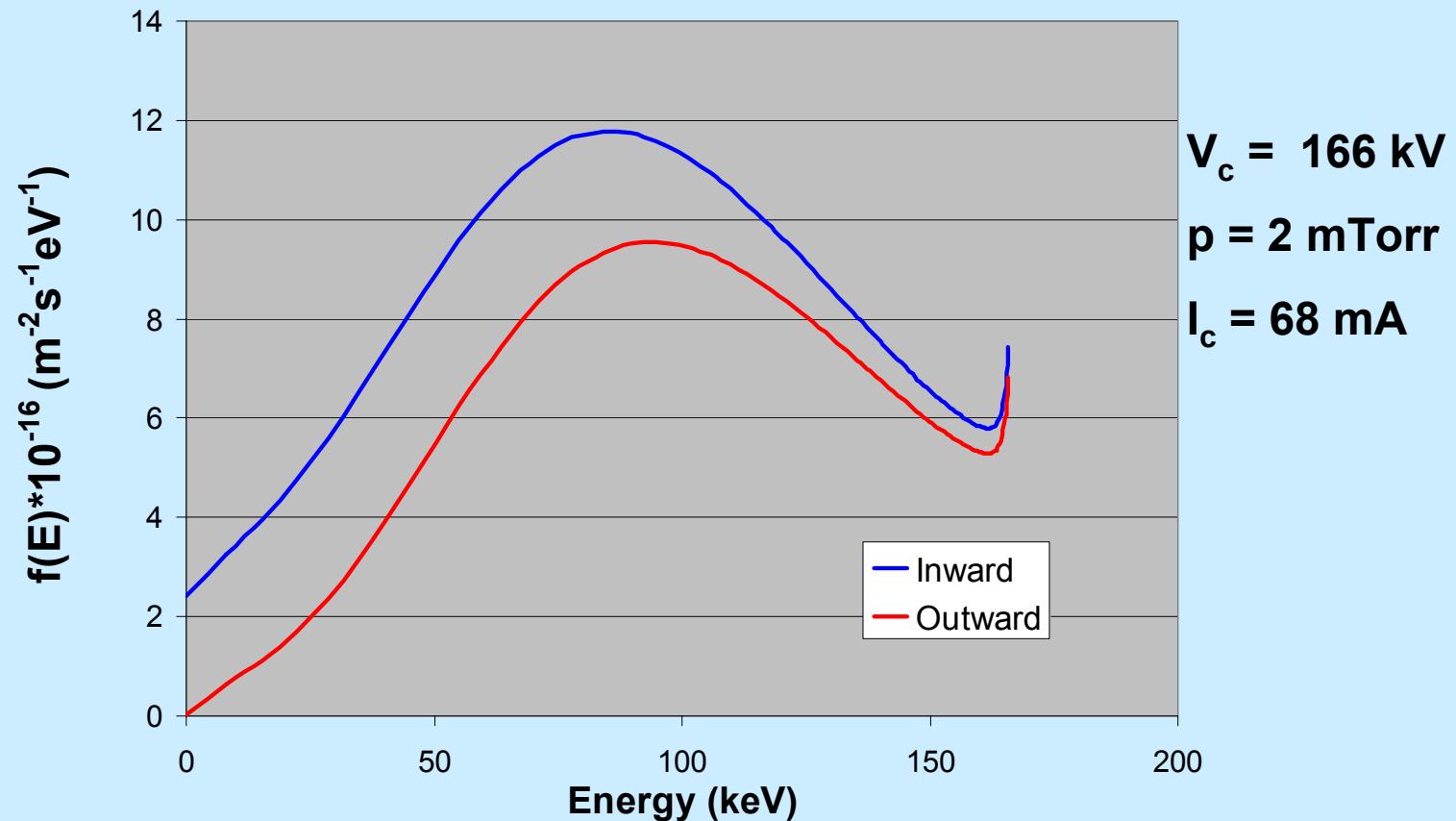
Ion-ion fusion

Implantation in cathode grid

Cold Ion Source Function

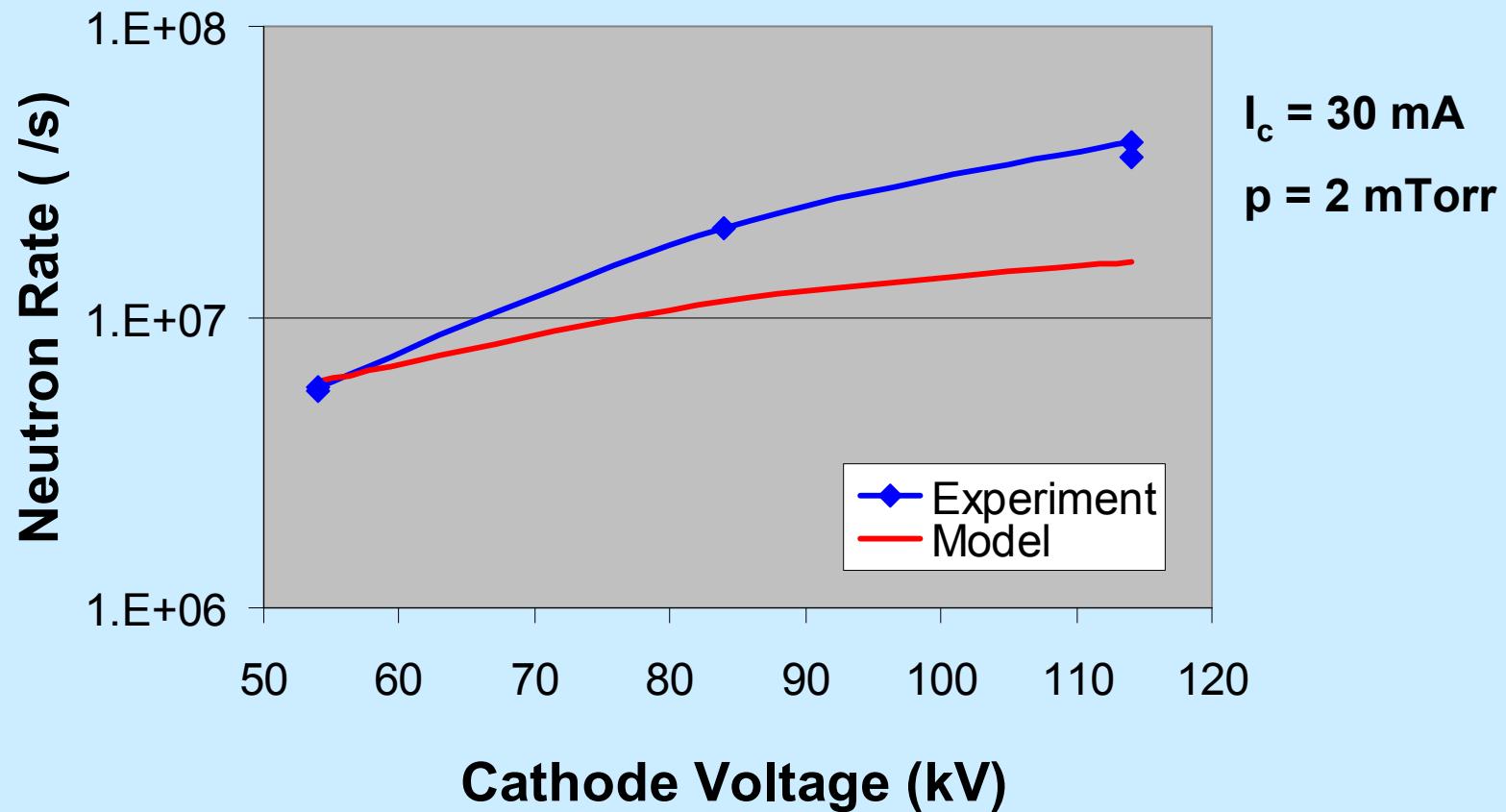


Energy Spectrum at Cathode

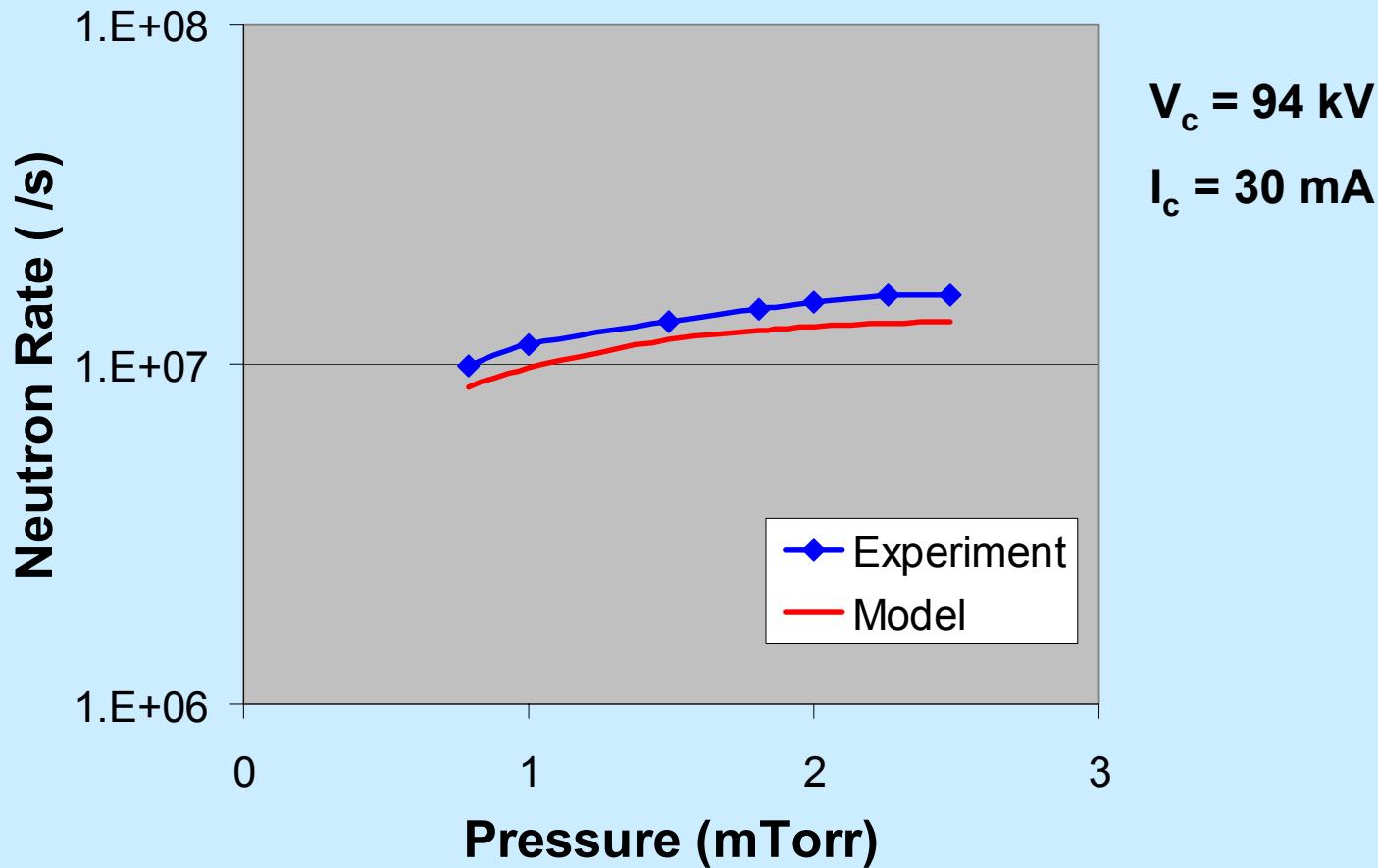




Voltage Scan

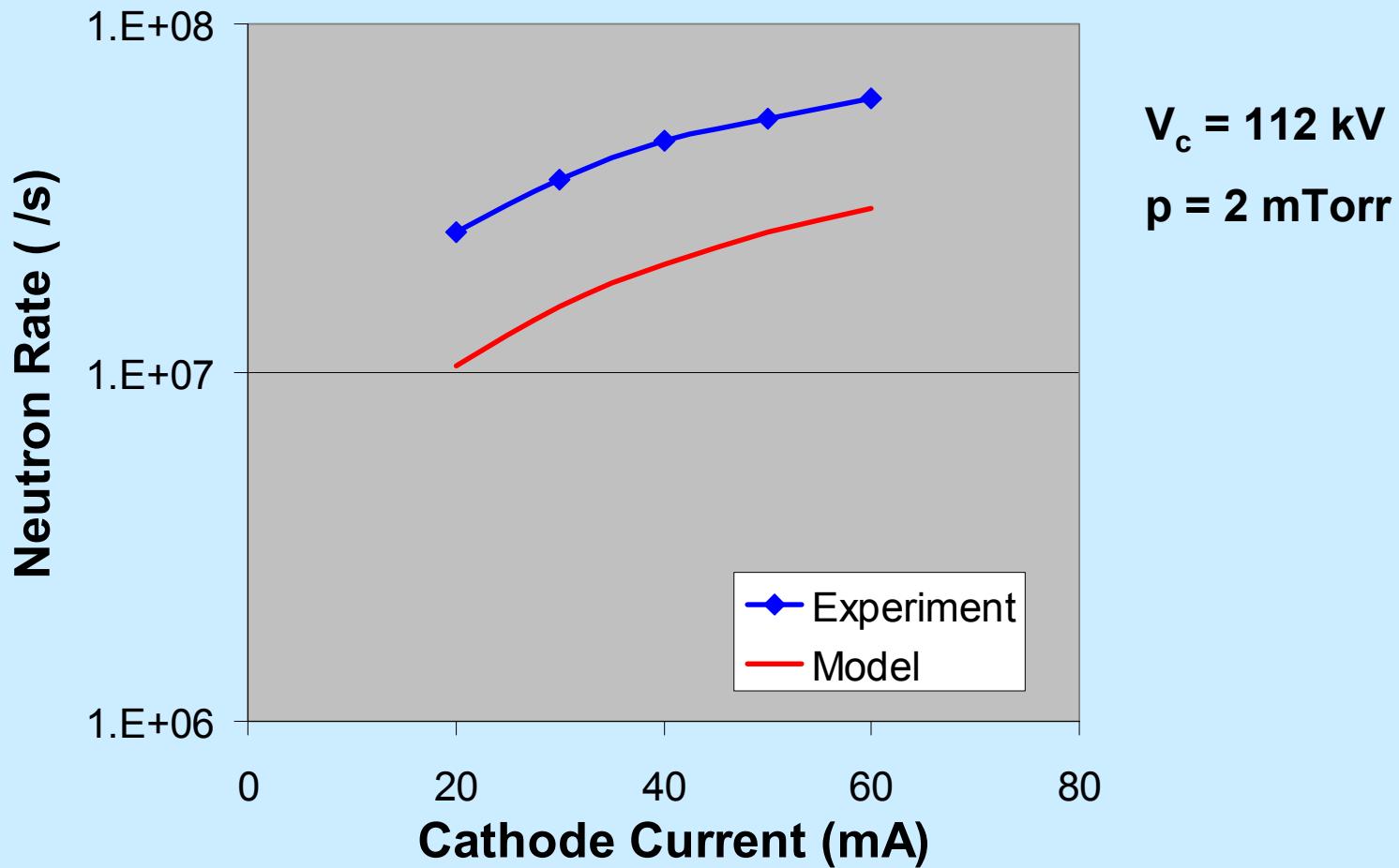


Pressure Scan





Current Scan



Conclusions

- The model reproduces the general trends of neutron production rate with changes in cathode current, cathode voltage, and gas pressure.
- The calculated neutron production rates are close to the measured values at low voltage and about a factor of 4 low at high voltage.

Possible Improvements

- Add molecular effects
- Calculate potential profile self-consistently
- Add potential “hill” in the cathode region
- Add multi-species, e.g. D-³He
- Other suggestions?



Acknowledgement

Thanks to the experimental group,
especially Alex Wehmeyer, for sharing
their experimental data.



Development of Low Energetic Metastable Helium Beam Injector for Electric Field Diagnostics through Laser Induced Fluorescence

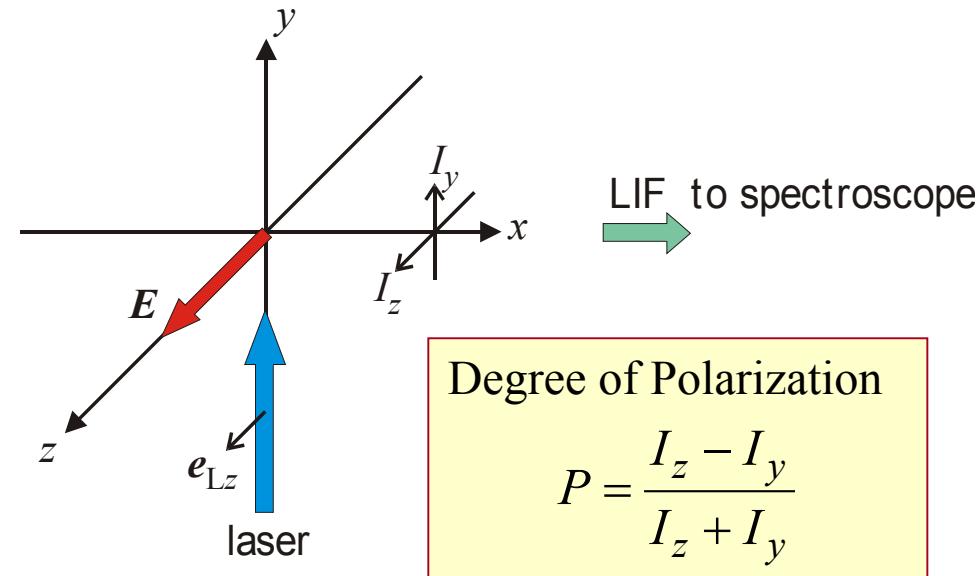
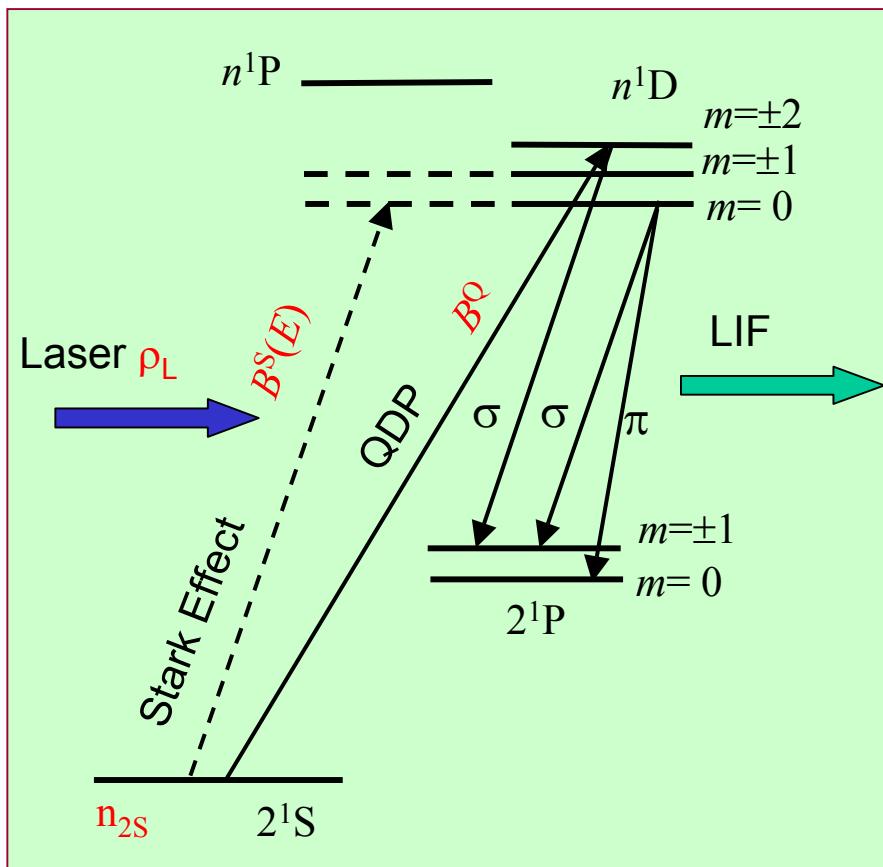
The 7th US-Japan Workshop on Inertial Electrostatic Confinement Fusion
Los Alamos, New Mexico, US
March 14-16, 2005

Inst. of Advanced Energy, Kyoto Univ.
Kai Masuda, T. Ando, T. Nishi, H. Toku and K. Yoshikawa



Determination of Electric Field by the Degree of LIF Polarization

K. Takiyama *et al.*, Proc. 8th Int. Sympo. Laser-Aided Plasma Diagnostics, Doorwerth, The Netherlands, 1997, pp. 81-84.



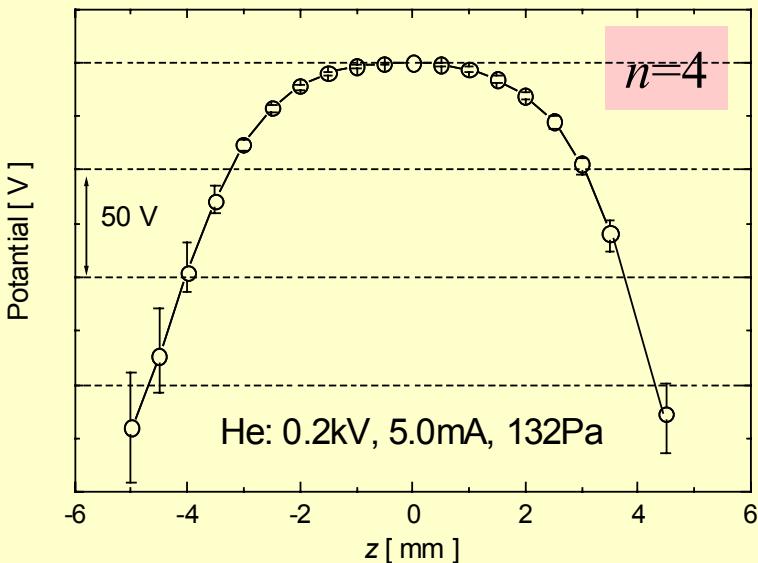
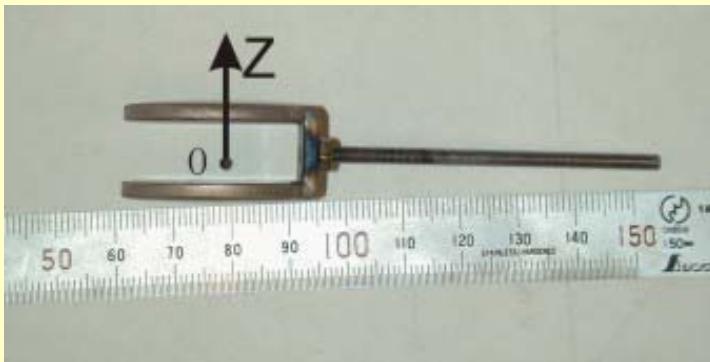
$$E = C \sqrt{\frac{I^S}{I^Q}} = C \sqrt{\frac{I_\pi^S + 2I_\sigma^S}{I_\pi^Q + 2I_\sigma^Q}} = C \sqrt{f(P)}$$

$$\text{where } f(p) = \frac{6P}{3 - 5P}$$

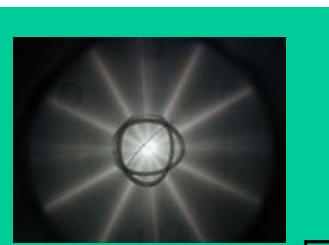
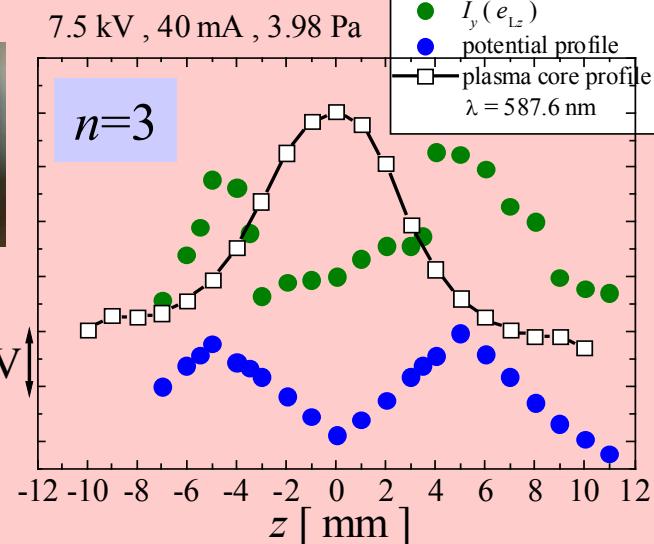
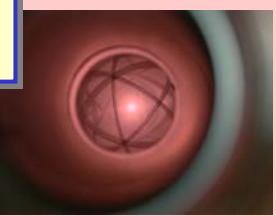


What We Could & Could not Measure by the LIF Method

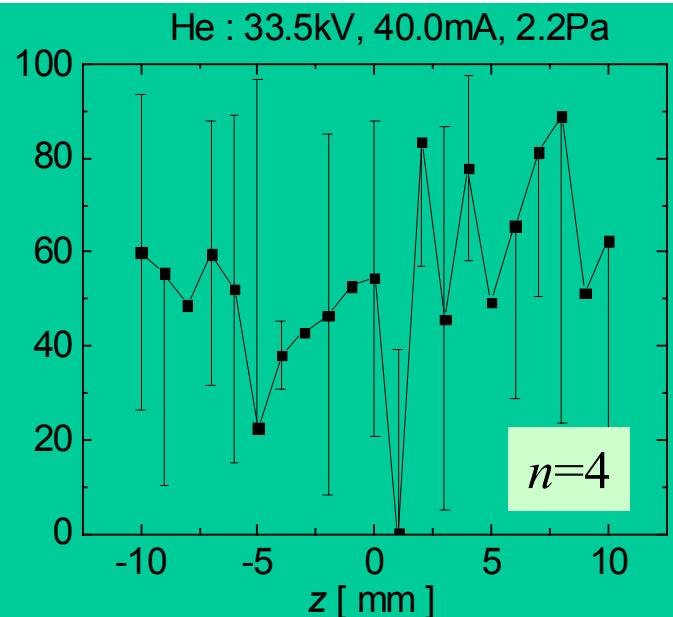
U-shaped hollow cathode plasma



center-spot mode IEC plasma

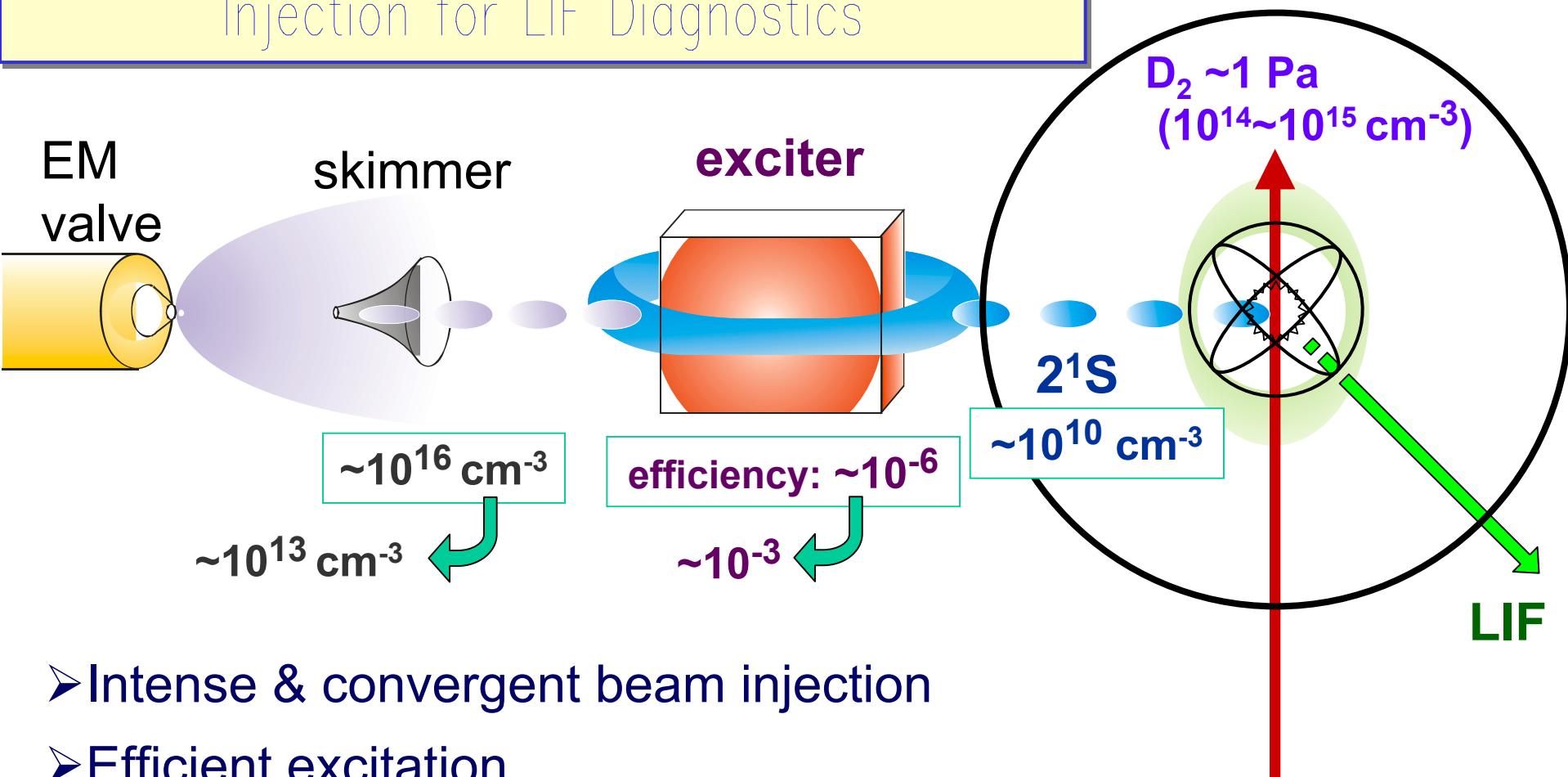


star mode IEC plasma





Low Energetic Metastable Helium Beam Injection for LIF Diagnostics



- Intense & convergent beam injection
- Efficient excitation
- Low background pressure in exciter
(plasma production by the beam itself)

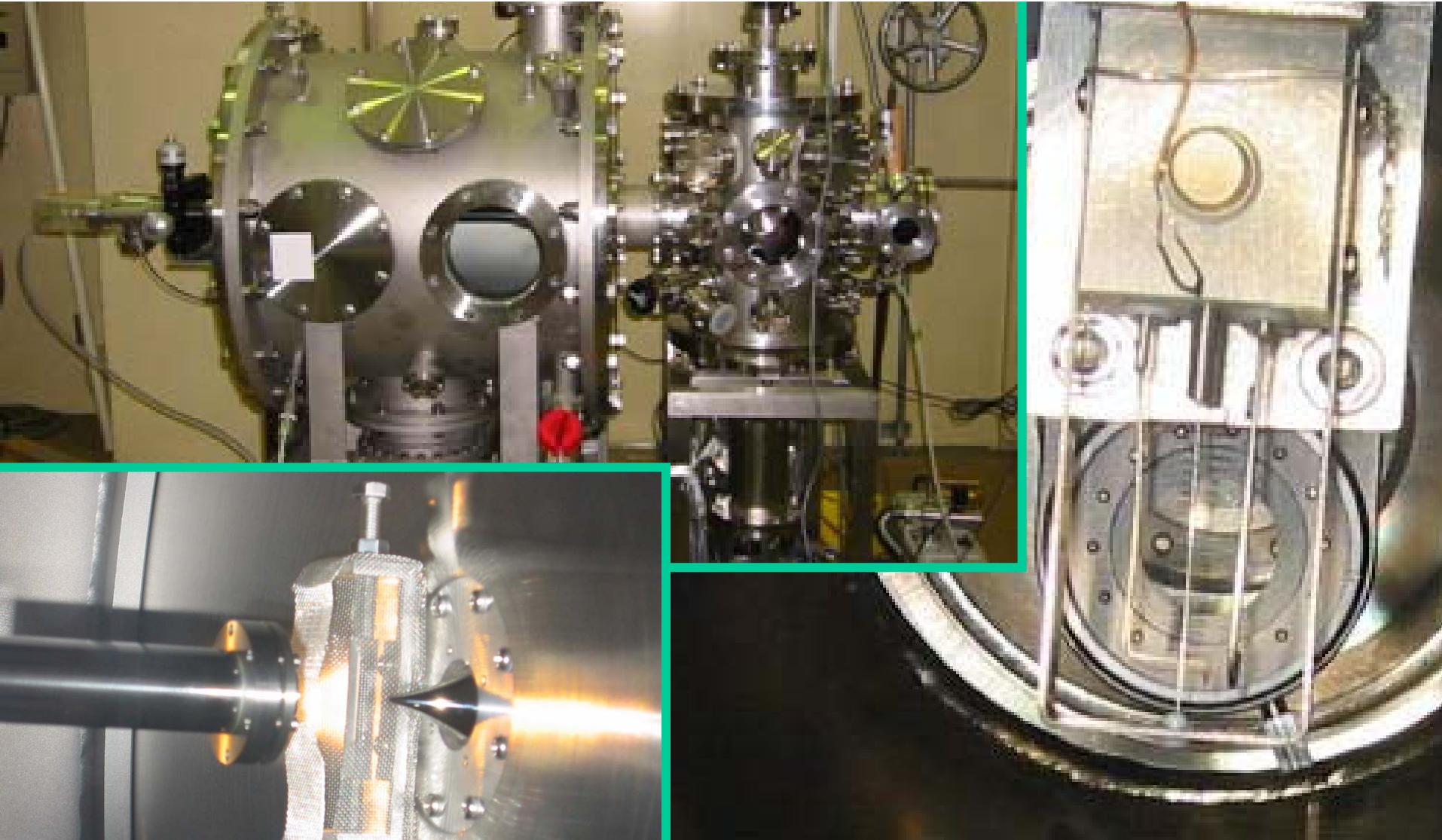
laser
5 nsec
650 mJ/pulse



The 7th US-Japan Workshop on IEC Fusion, Los Alamos, March 14-16, 2005

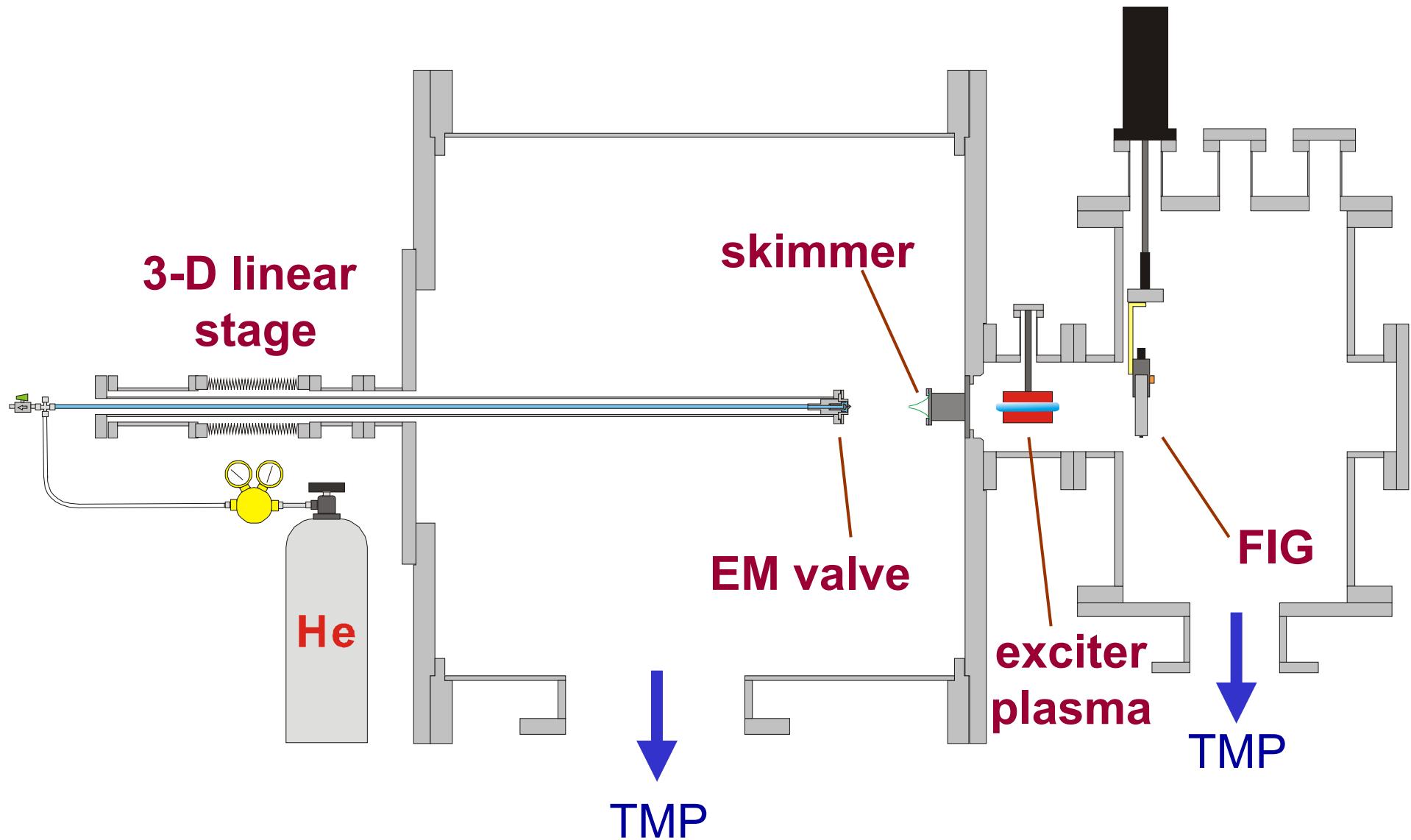
Development of Low-Energetic Metastable Helium Beam Injector for Electric Field Diagnostics through LIF, Kai Masuda, IAE, Kyoto Univ.

Low Energetic Metastable Helium Pulsed Beam Injector for LIF Diagnostics





Experimental Setup





R&D Targets and Achievements before the Last Workshop

Low-Energetic Neutral Helium Pulsed Beam Injection

<u>Density at the Beam Center</u> $\geq 10^{13} \text{ cm}^{-3}$	<u>Not Achieved</u> $2 \times 10^{12} \text{ cm}^{-3}$
<u>Longitudinal Length</u> as short as possible	150 μsec
<u>Transverse Diameter</u> as small as possible	$\leq 15 \text{ mm (FWHM)}$
<u>Repetition Rate</u> $\geq 1 \text{ Hz}$ (no degradation in transverse profile)	<u>Achieved</u> 5 Hz @ $2 \times 10^{12} \text{ cm}^{-3}$

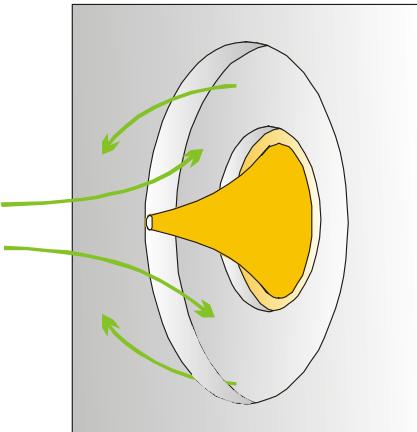
Exciter Plasma Production

<u>Longitudinal Plasma Length</u> optimal for maximal excitation efficiency	<u>Expected to be Achieved</u> by the race-track-shaped magnetron scheme
<u>Electron Density and Temperature</u> as high as possible	<u>Not Measured</u>
<u>Operating Gas Pressure (Density)</u> $\leq 0.04 \text{ Pa (} 10^{13} \text{ cm}^{-3} \text{)}$	<u>Achieved</u> $0.035 \text{ Pa (} 8.8 \times 10^{12} \text{ cm}^{-3} \text{)}$

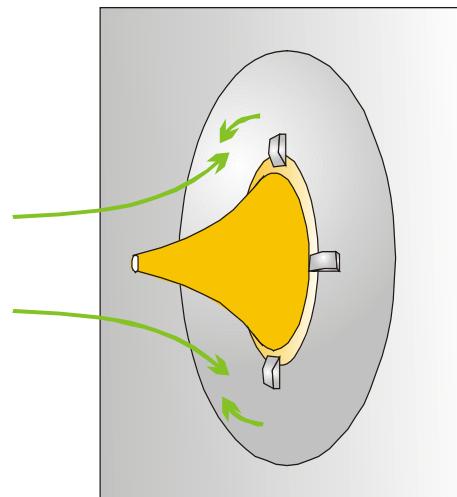


Skimmer Setup Affects Beam Density by means of Beam Reflection and Scattering

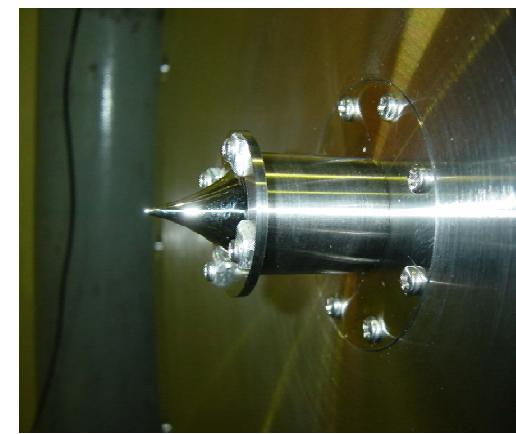
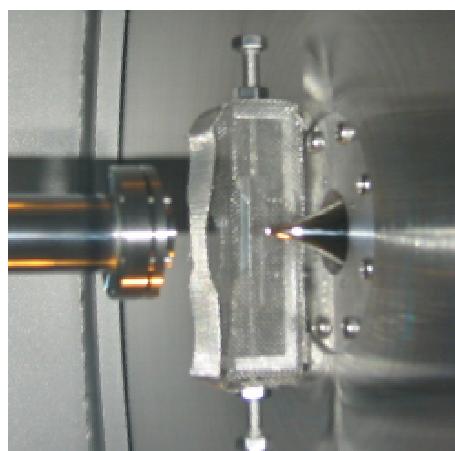
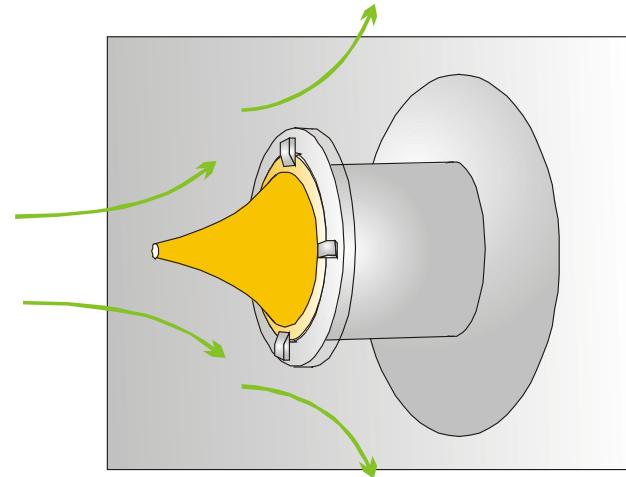
basic



refined I

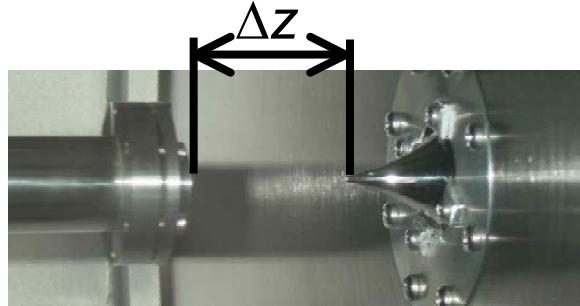
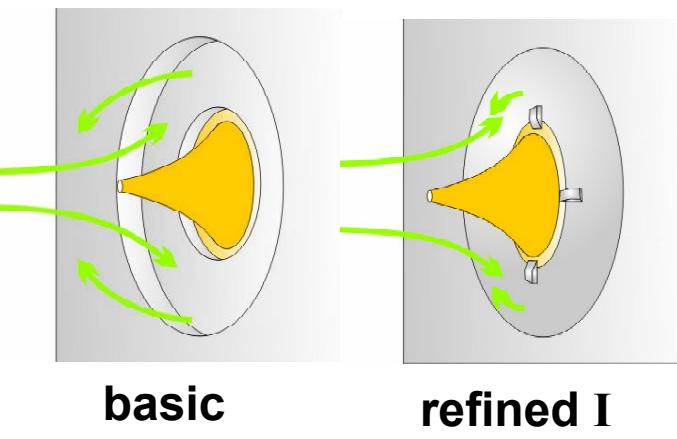
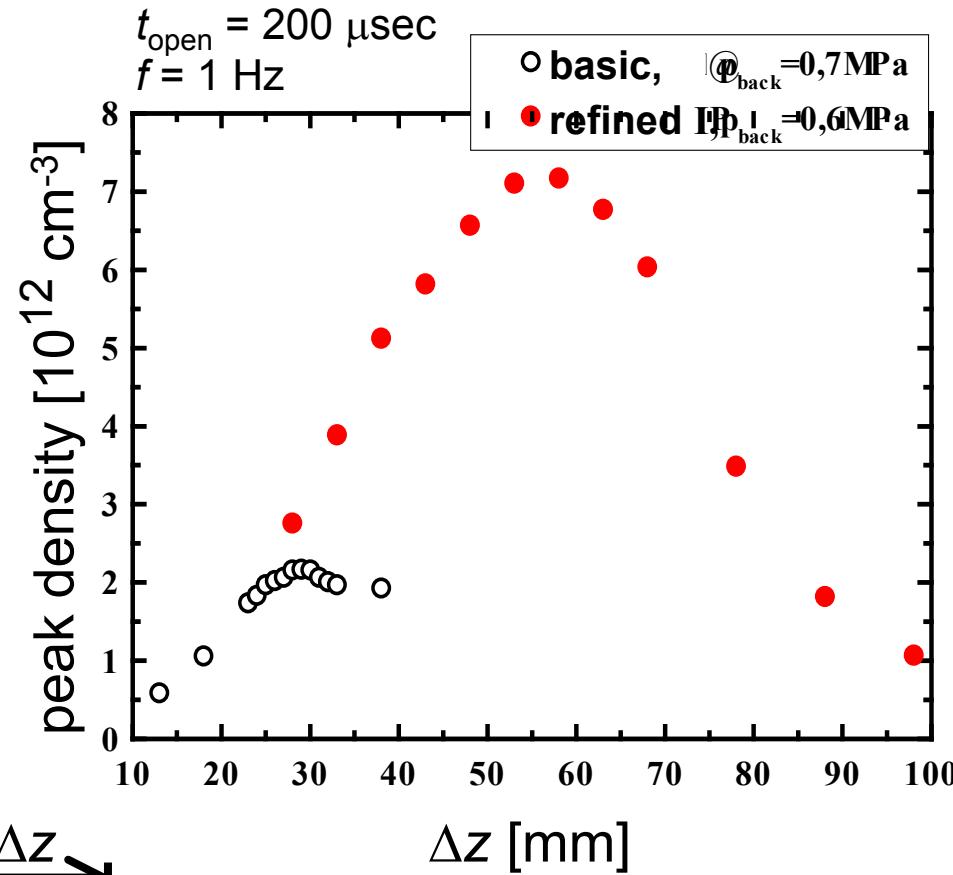
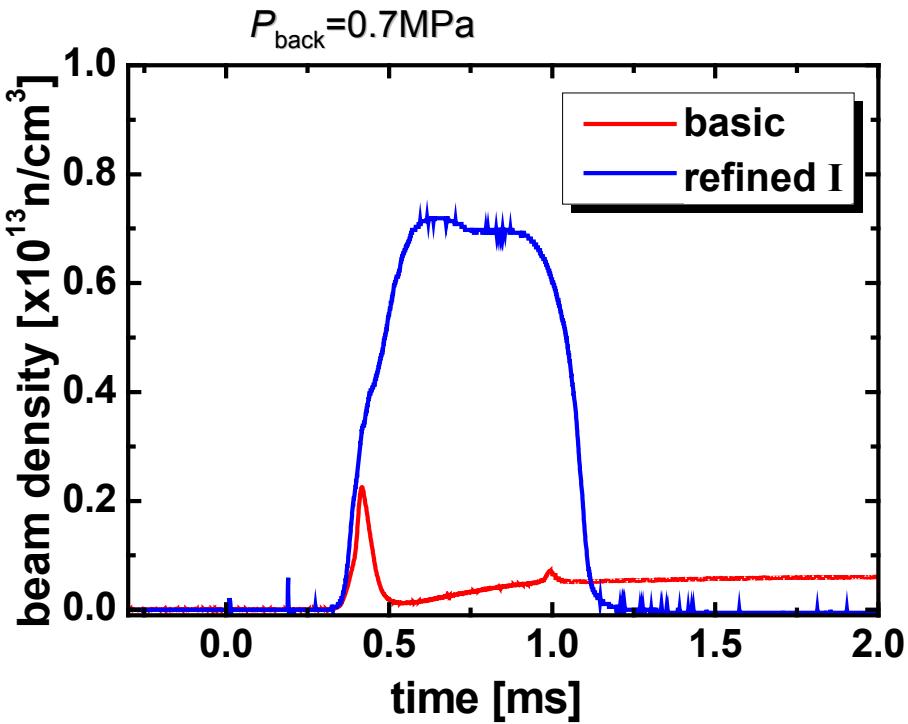


refined II



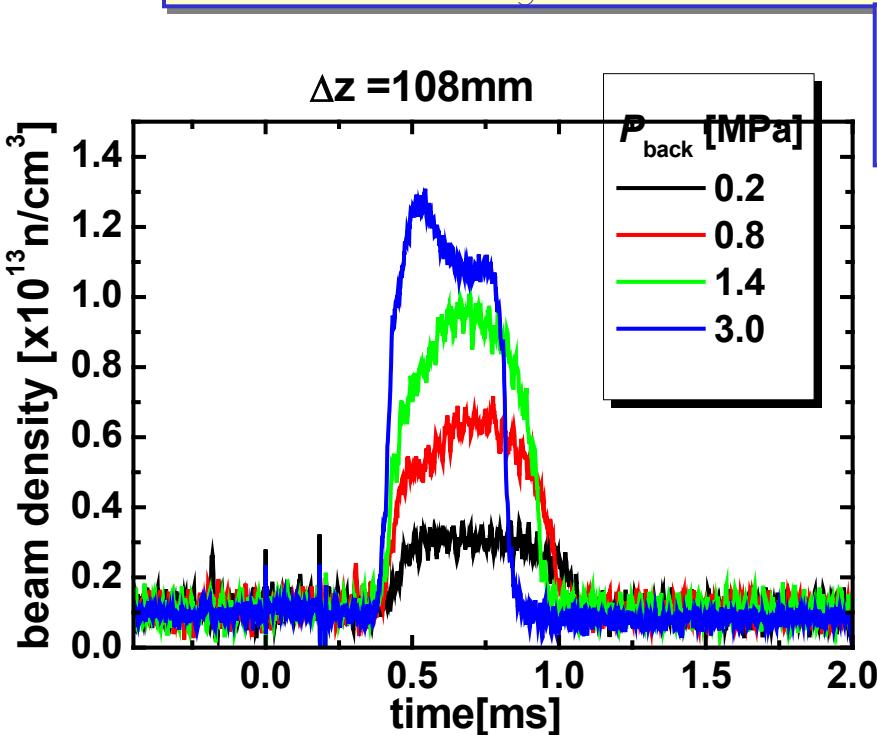


Refined Skimmer Setup Led to Drastic Enhancement

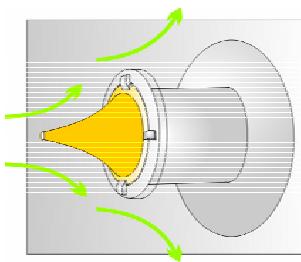
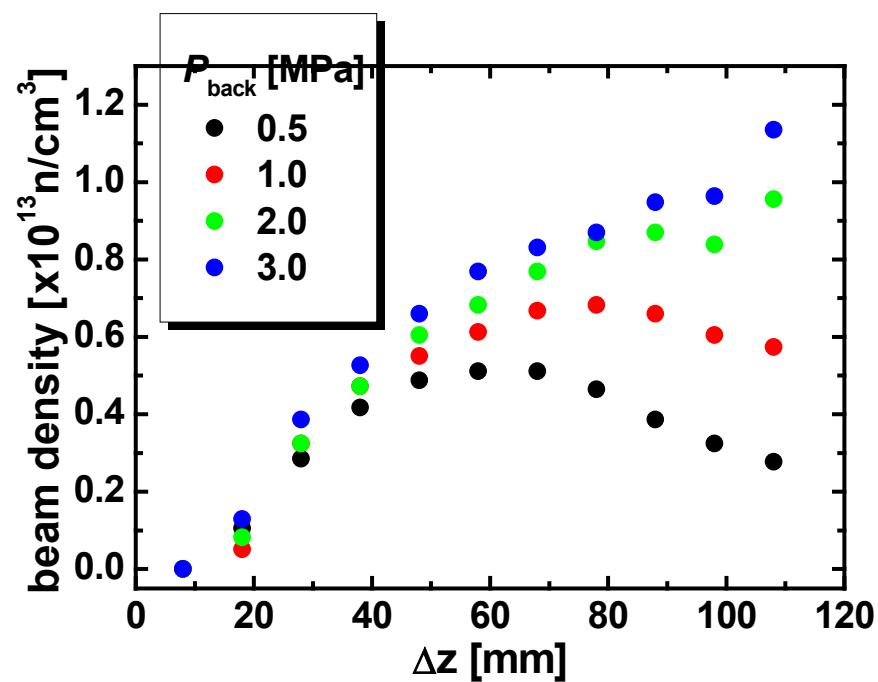




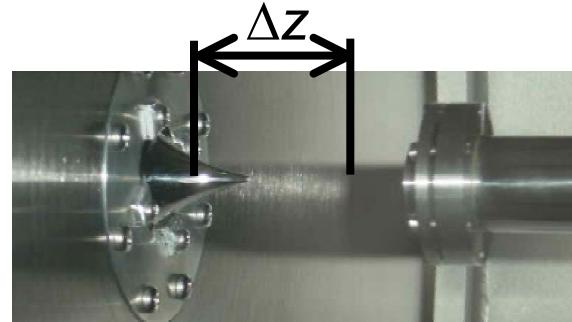
Refined Skimmer Setup Made High Pressure Operation Possible



and made the optimal valve-skimmer spacing Δz long!



refined II

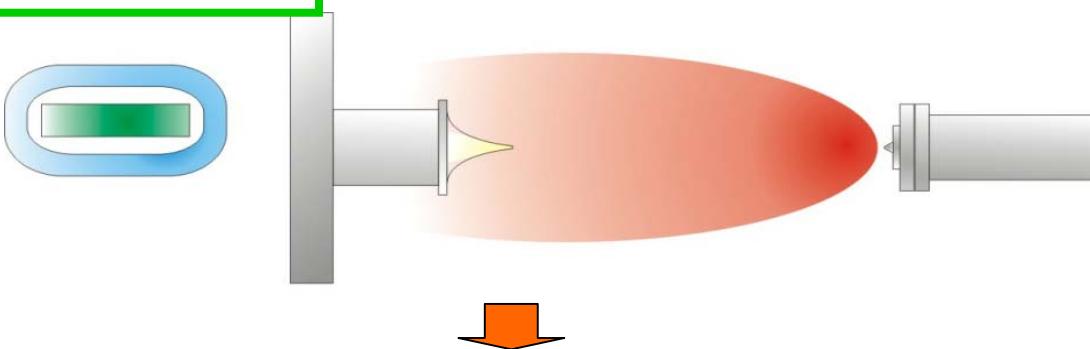




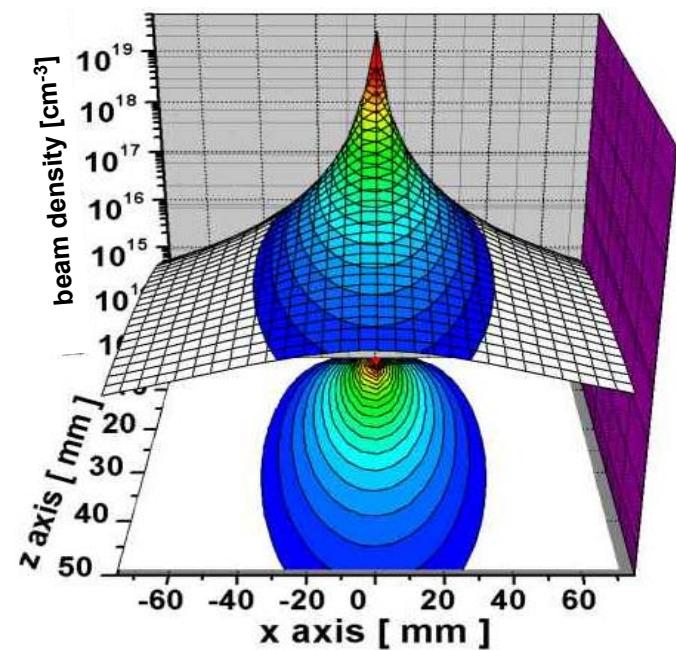
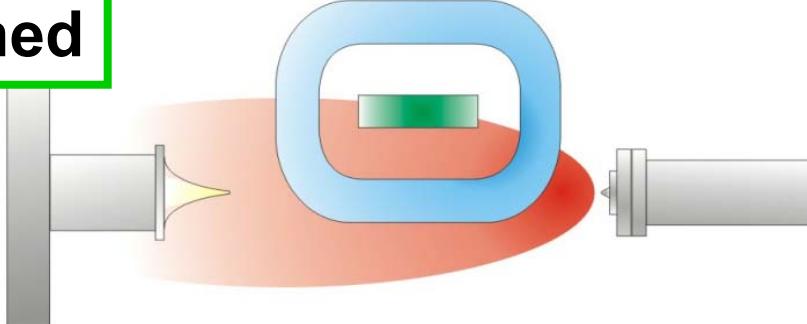
Future Plan

The optimal Δz turned out to be long enough to set the magnetron exciter between them.

At Present



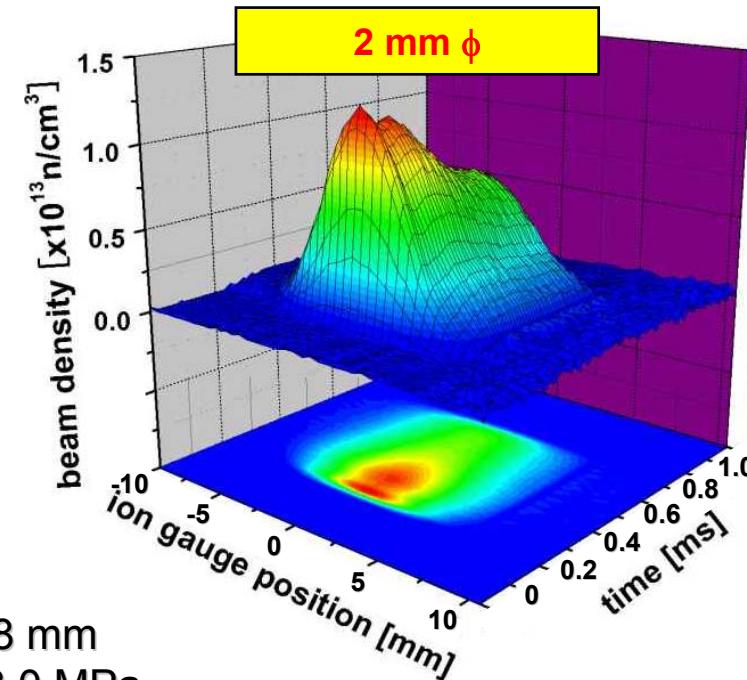
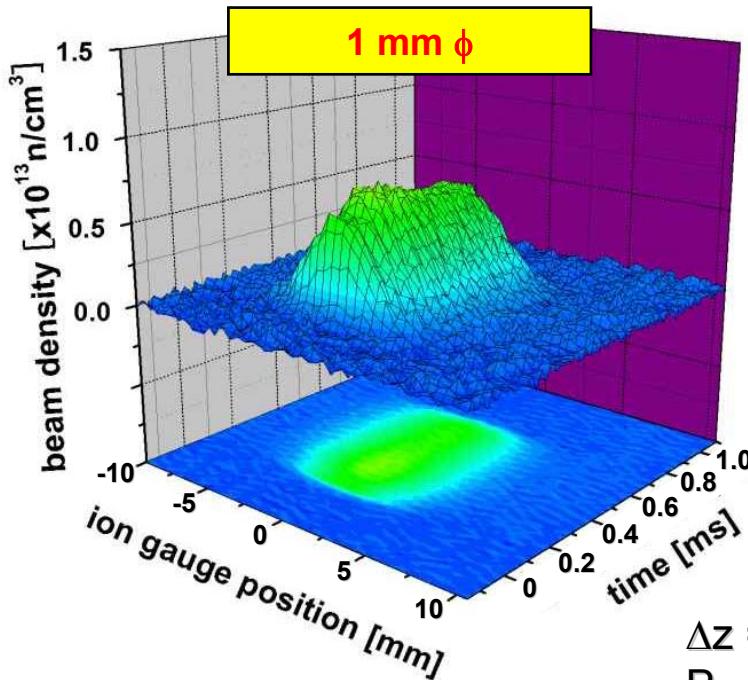
Refined





Comparison between 1 & 2 mm ϕ Skimmers

- Almost the same beam diameter
- Twice as high on-axis density with the 2 mm ϕ pin hole

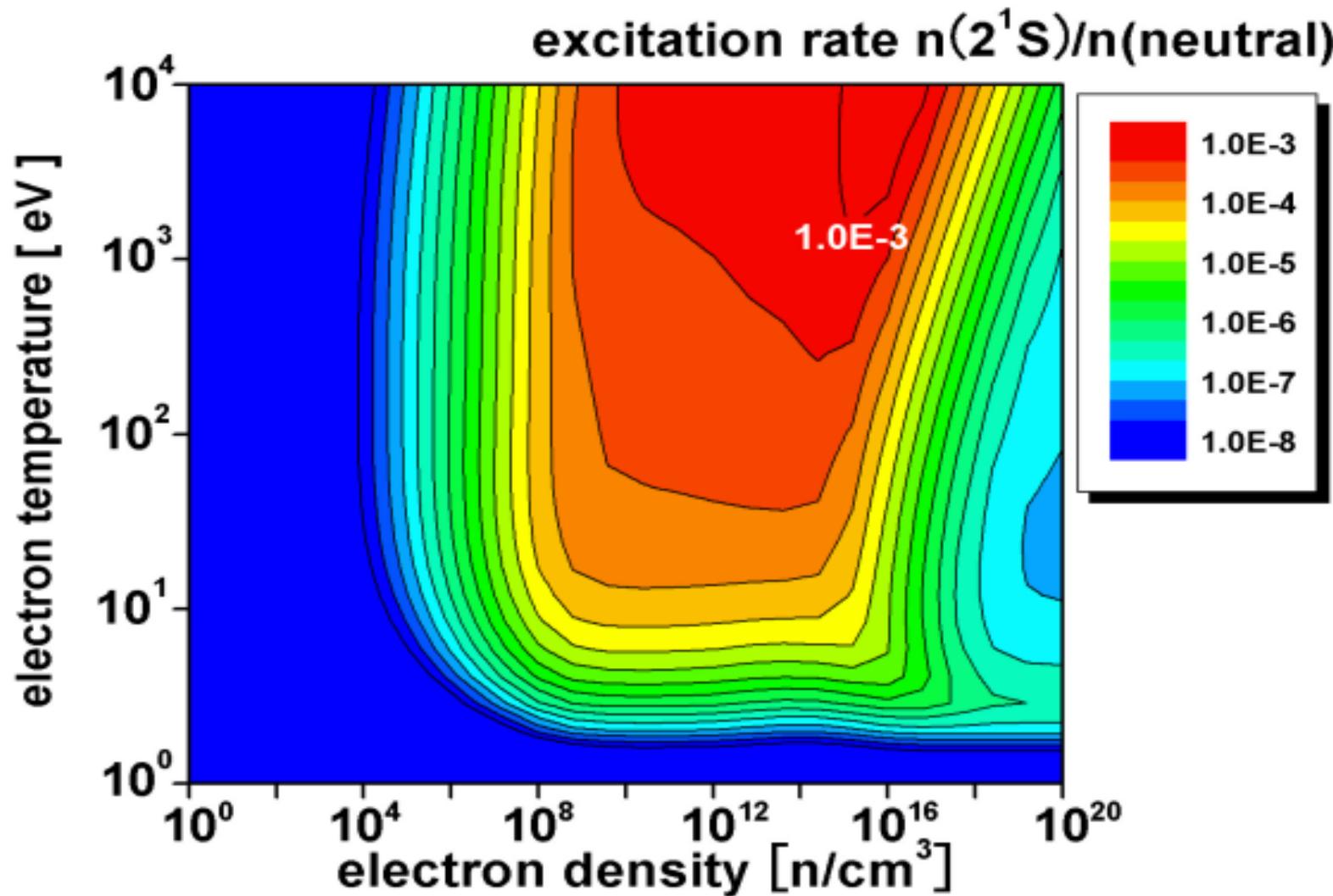


$\Delta z = 128 \text{ mm}$
 $P_{\text{back}} = 3.0 \text{ MPa}$



Excitation Rate as functions of Electron Density & Temperature in the Exciter Plasma

Calculated by use of “CR-Model” by M. Goto and T. Fujimoto, NIFS-DATA-43 (1997)





R&D Targets and Achievements before the Last Workshop

Low-Energetic Neutral Helium Pulsed Beam Injection

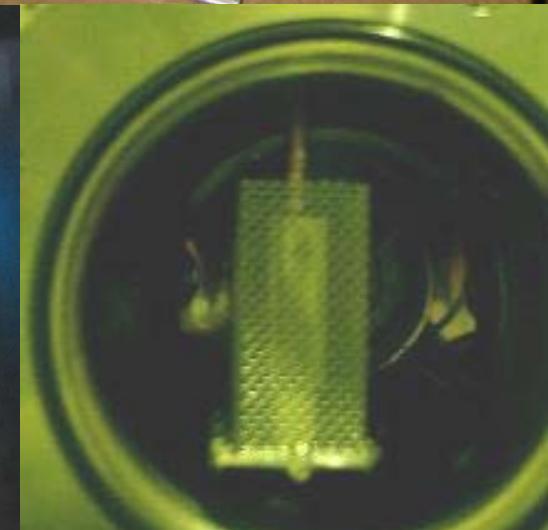
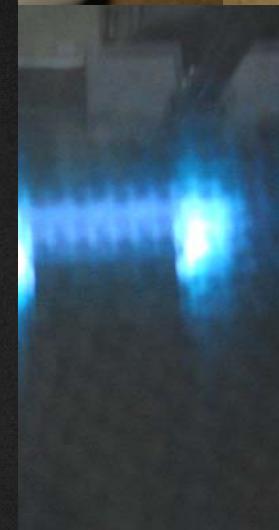
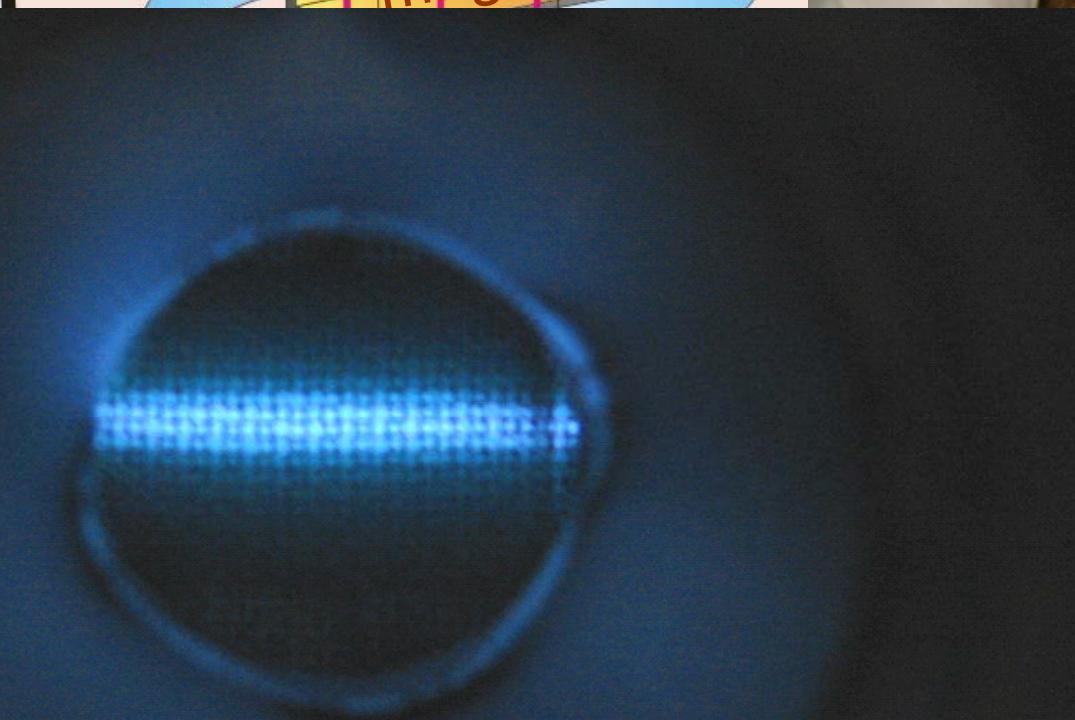
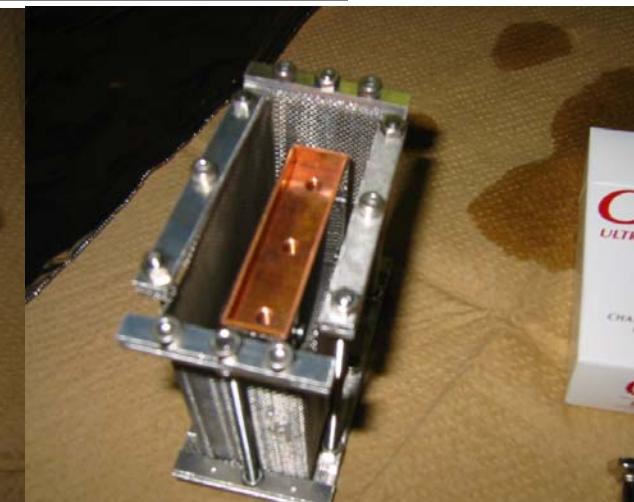
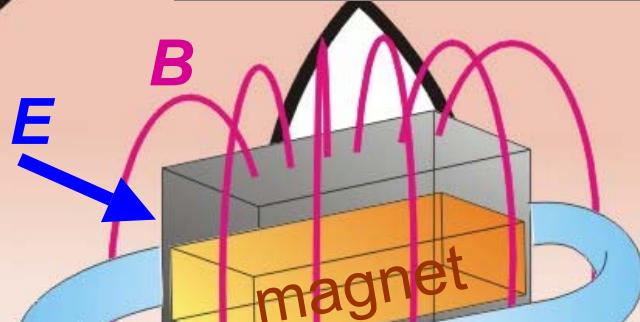
Density at the Beam Center $\geq 10^{13} \text{ cm}^{-3}$	Not Achieved $2 \times 10^{12} \text{ cm}^{-3}$
Longitudinal Length as short as possible	150 μsec
Transverse Diameter as small as possible	$\leq 15 \text{ mm (FWHM)}$
Repetition Rate $\geq 1 \text{ Hz}$ (no degradation in transverse profile)	Achieved 5 Hz @ $2 \times 10^{12} \text{ cm}^{-3}$

Exciter Plasma Production

Longitudinal Plasma Length optimal for maximal excitation efficiency	Expected to be Achieved by the race-track-shaped magnetron scheme
Electron Density and Temperature as high as possible	Not Measured
Operating Gas Pressure (Density) $\leq 0.04 \text{ Pa (} 10^{13} \text{ cm}^{-3} \text{)}$	Achieved $0.035 \text{ Pa (} 8.8 \times 10^{12} \text{ cm}^{-3} \text{)}$



Race-Track-Shaped Exciter Plasma by Magnetron Discharge

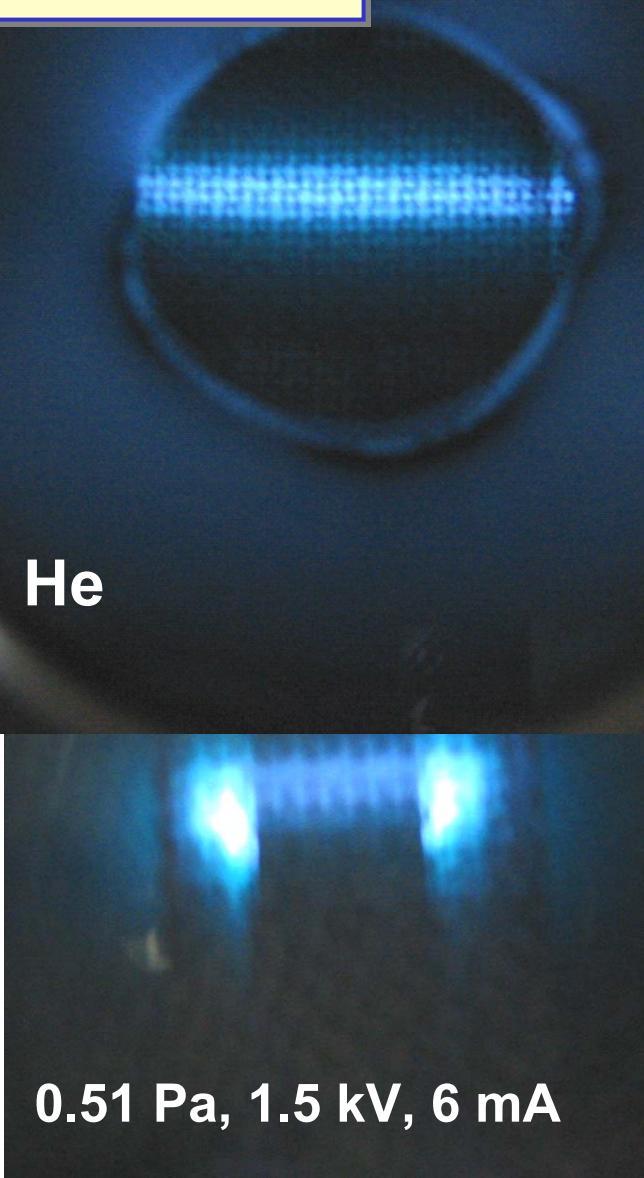
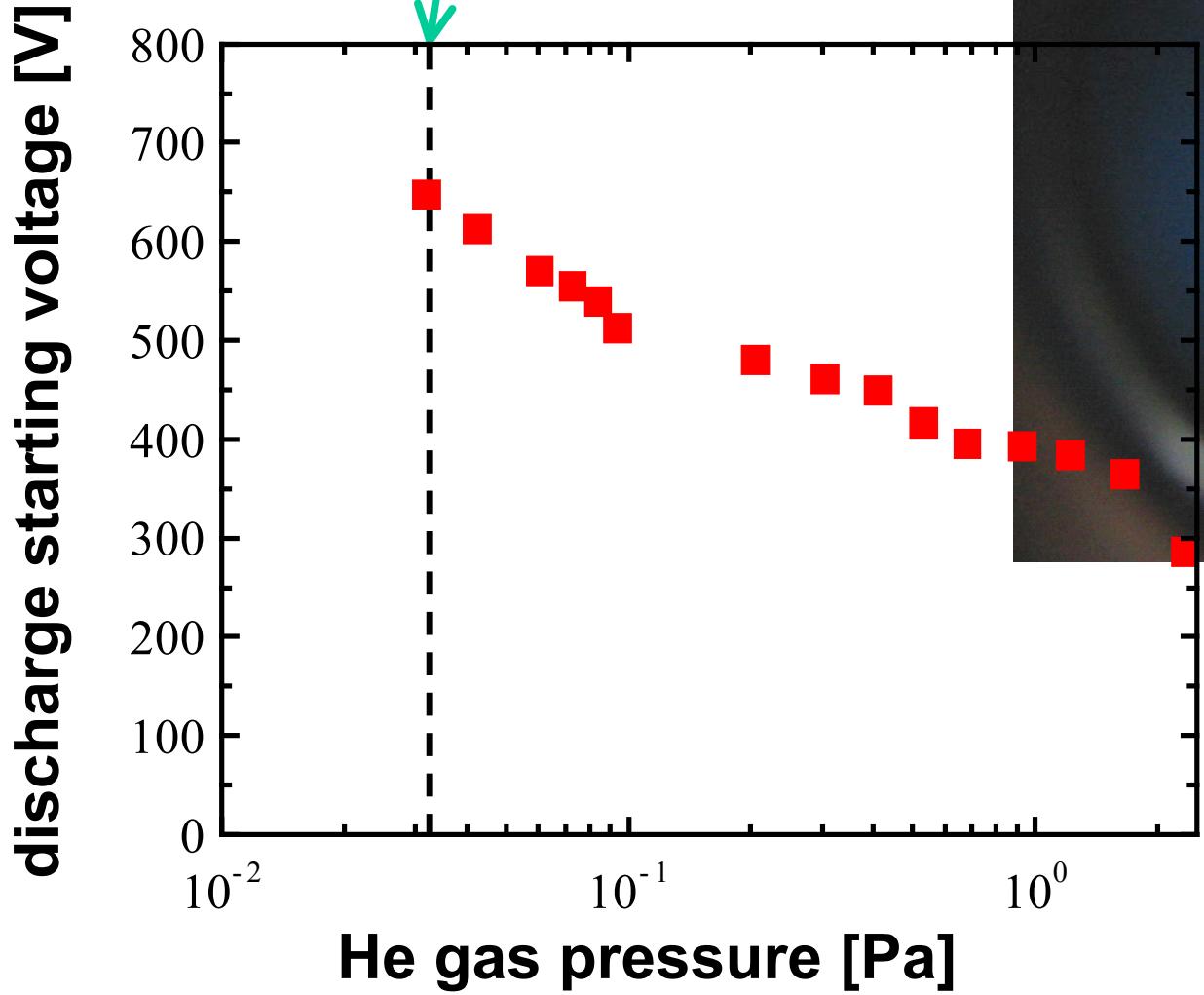


0.51 Pa (He), 1.5 kV, 6 mA



We had reached the required
accessible operating gas pressure

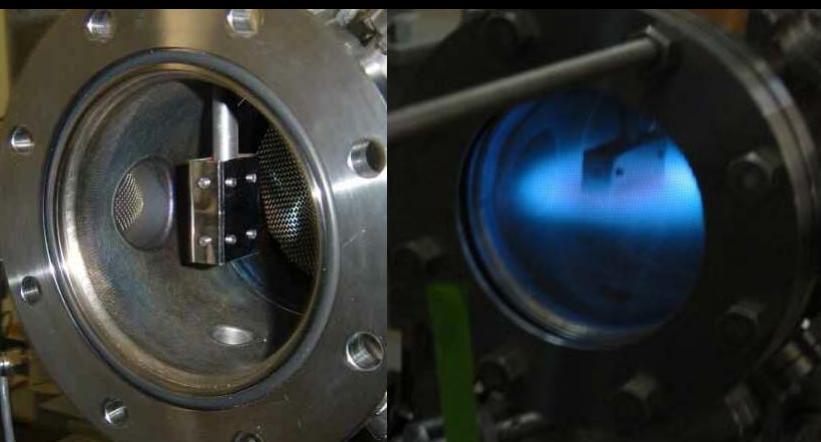
0.035 Pa $8.4 \times 10^{12} \text{ cm}^{-3}$





Refinements for Further Lower Pressure

The gridded anode was removed.



And Comparison between Two with
Different Lengths of the Race-
Track Shape

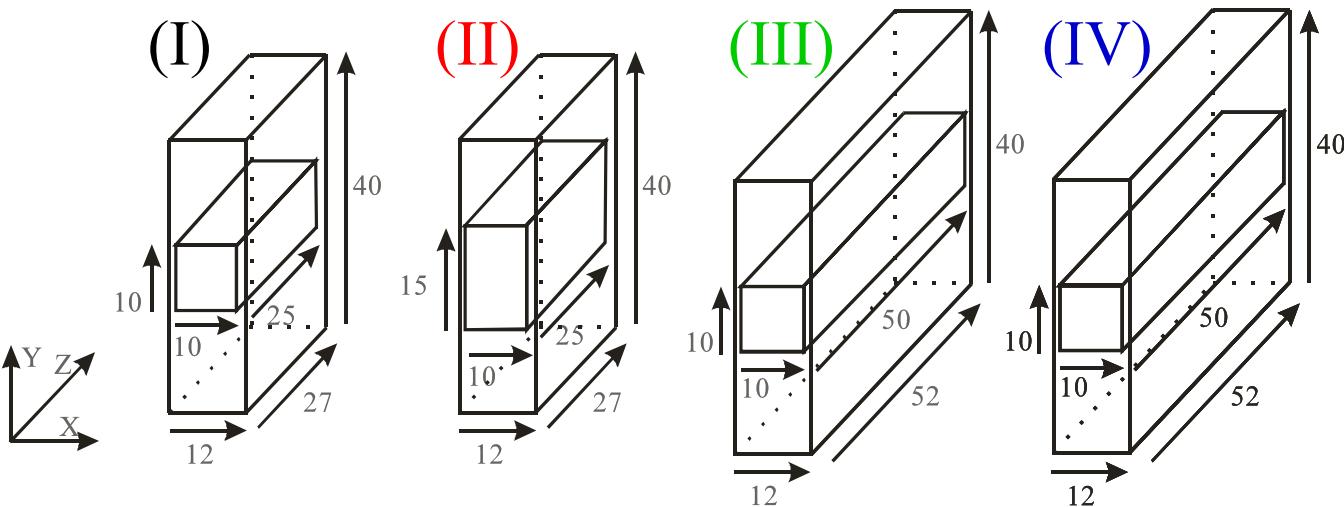
X × Y × Z =

(I) 10×10×25mm
Sm-Co:0.4T

(II) 10×15×25mm
Sm-Co:0.4T

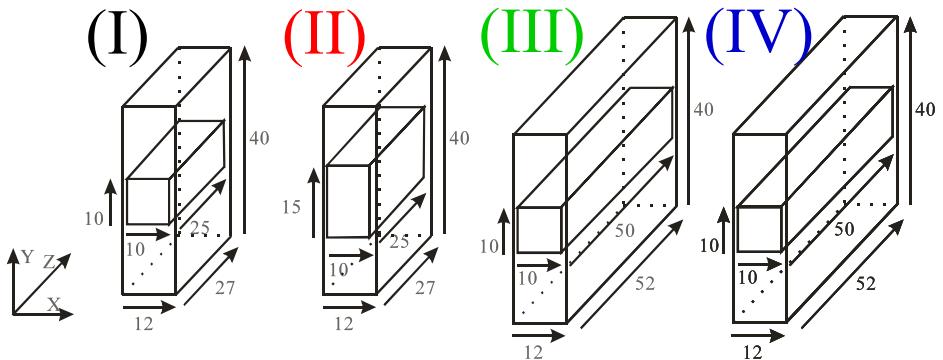
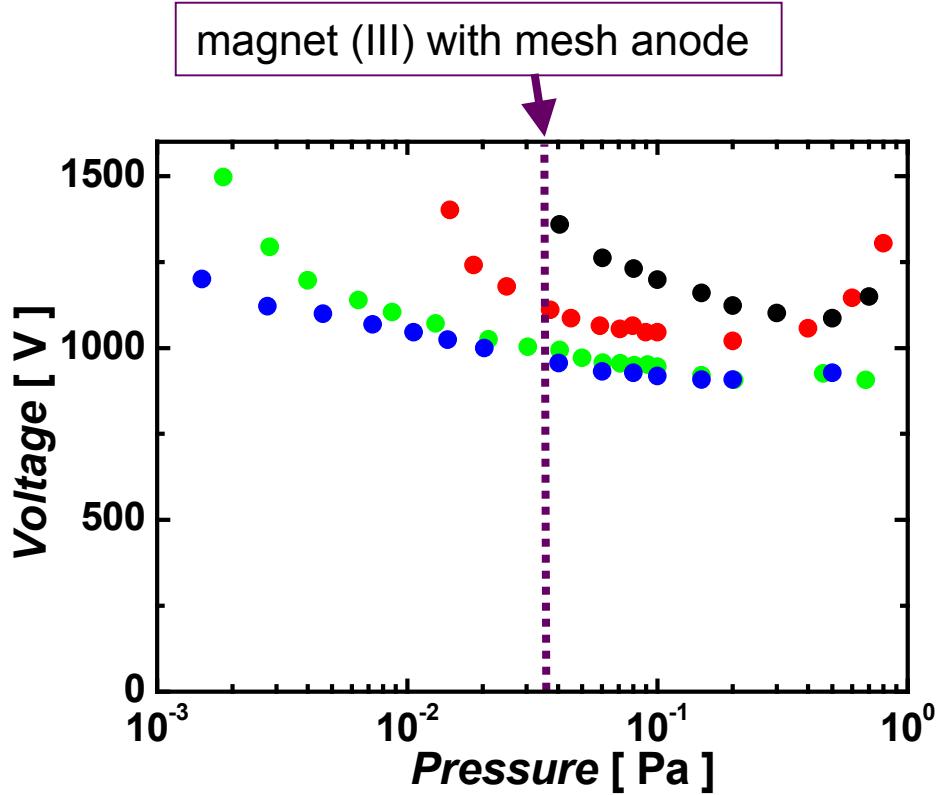
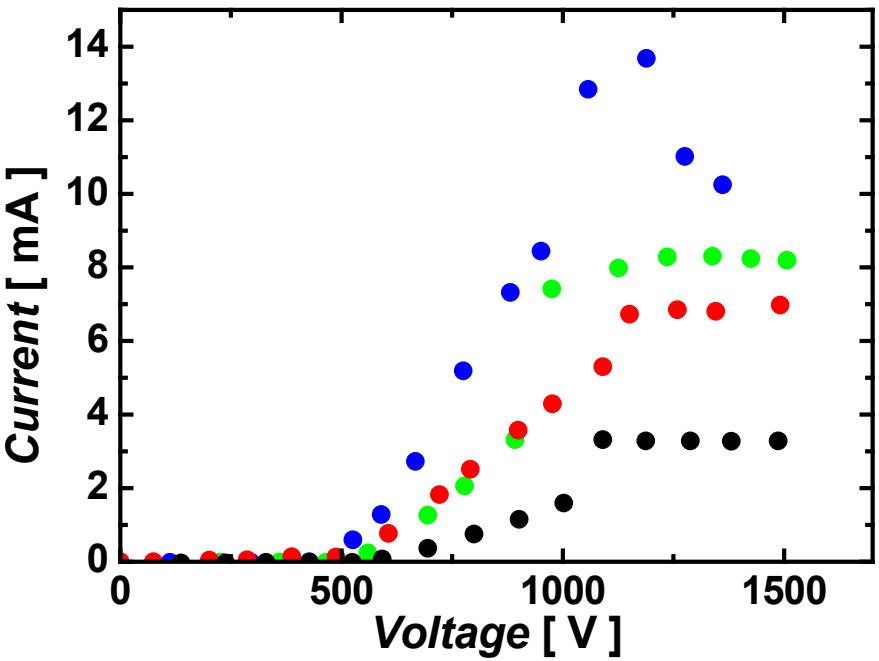
(III) 10×10×50mm
Sm-Co:0.4T

(IV) 10×10×50mm
Nd-Fe-B:0.6T





Comparisons among the Four Different Magnets



- ✓ No performance degradation was seen with the longer magnet (III).
- ✓ Accessible pressure was extended greatly down to 1.5 mPa.



Collisional-Radiative Model

for Calculating Population Densities of Helium Atoms in Plasmas

by M. Goto and T. Fujimoto, NIFS-DATA-43 (1997)

$$\frac{dn(p)}{dt} = - \left\{ \sum_{q \neq p} C(p,q) n_e + \sum_{q < p} A(p,q) + S(p) n_e \right\} n(p) \\ + \sum_{q \neq p} \{C(p,q) n_e + A(p,q)\} n(q) \\ + \{\alpha(p) n_e + \beta(p) + \beta_d(p)\} n_i n_e$$

$n(p)$: population density of level p

t : time

$A(p,q)$: spontaneous transition probability from level p to q

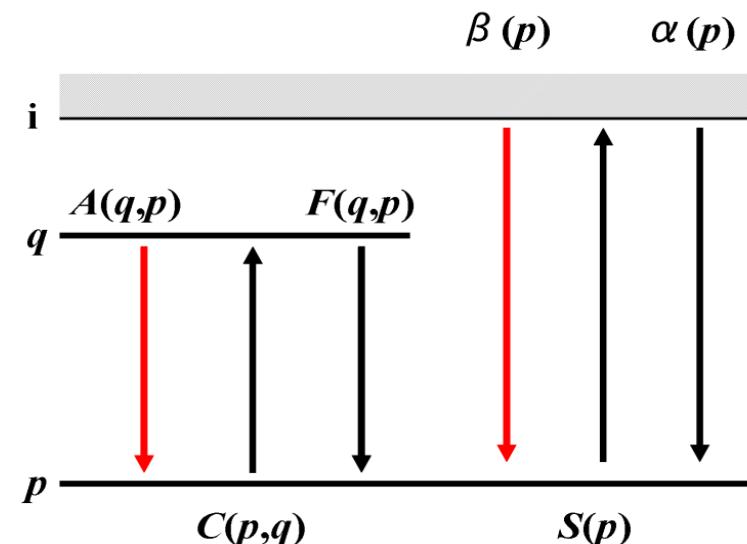
$C(p,q)$: rate coefficient for electron impact transition from level p to q

$S(p)$: rate coefficient for electron impact ionization for level p

$\alpha(p)$: rate coefficient for three-body recombination for level p

$\beta(p)$: rate coefficient for radiative recombination for level p

$\beta_d(p)$: rate coefficient for dielectronic recombination for level p





Collisional-Radiative Model (Cont.)

for Calculating Population Densities of Helium Atoms in Plasmas

by M. Goto and T. Fujimoto, NIFS-DATA-43 (1997)

Energy level structure:

Several levels are grouped.

$$1 \leq n \leq 7$$

levels with $l \geq 3$ are grouped

$$8 \leq n \leq 10$$

all of S, P, D ... levels are grouped

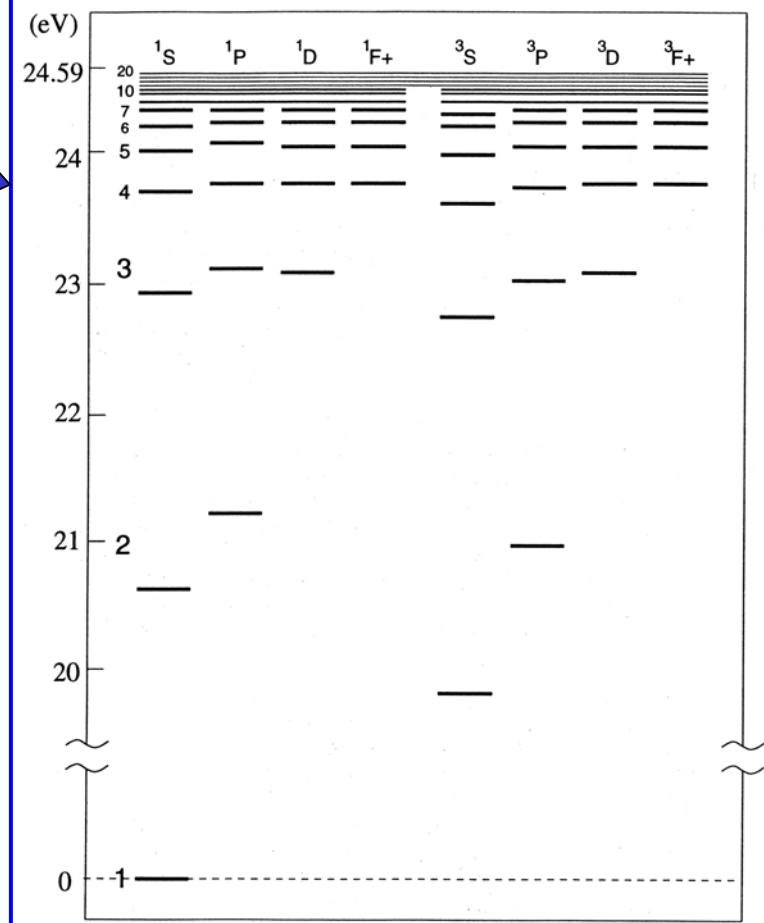
$$11 \leq n \leq 20$$

approximated by hydrogenic levels

Steady state approximation

(in our calculations):

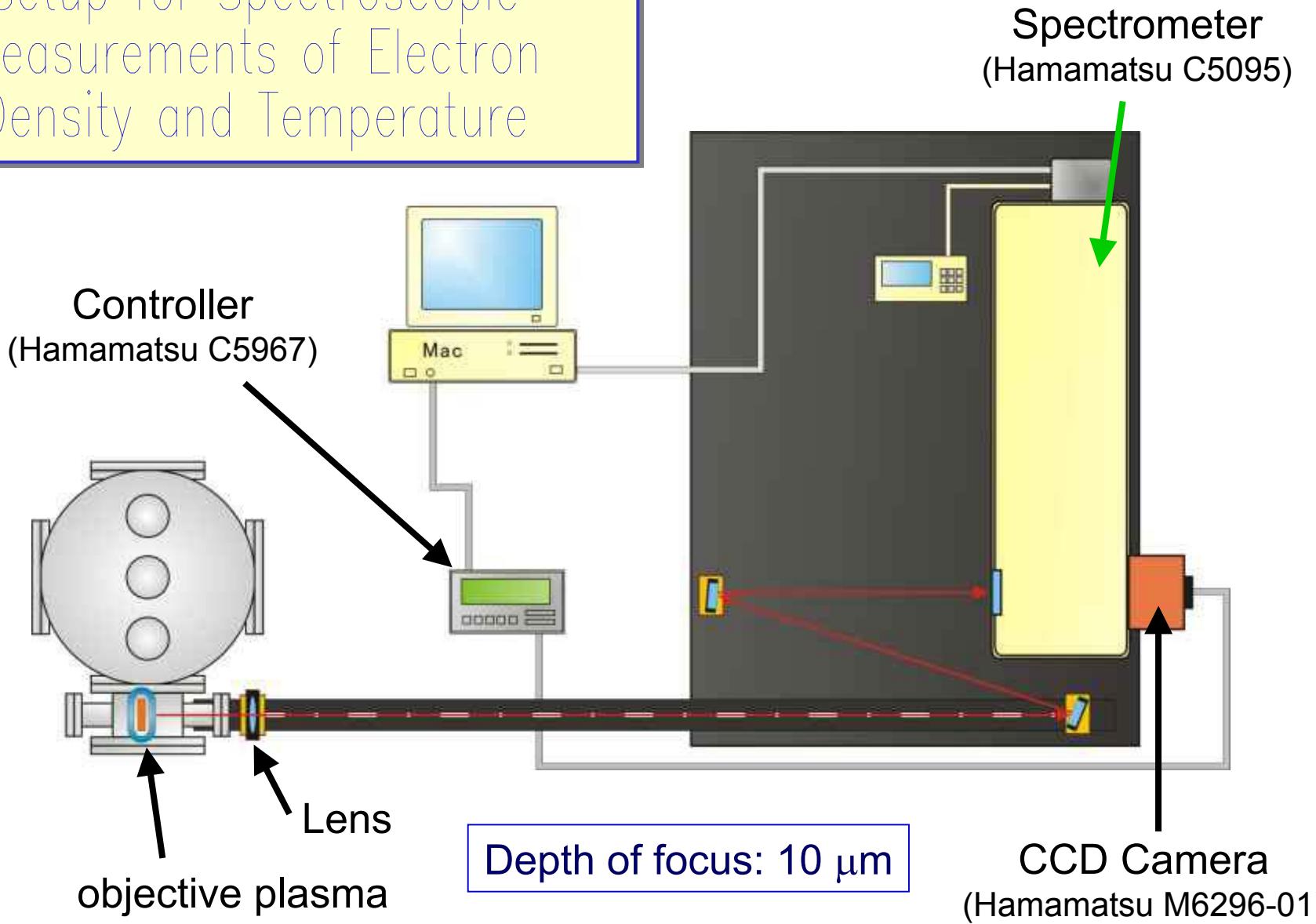
$$\frac{dn(p)}{dt} = 0 \rightarrow \frac{n(p)}{n(1^1S)}, \frac{n_i}{n(1^1S)}$$



are given as functions of n_e and T_e

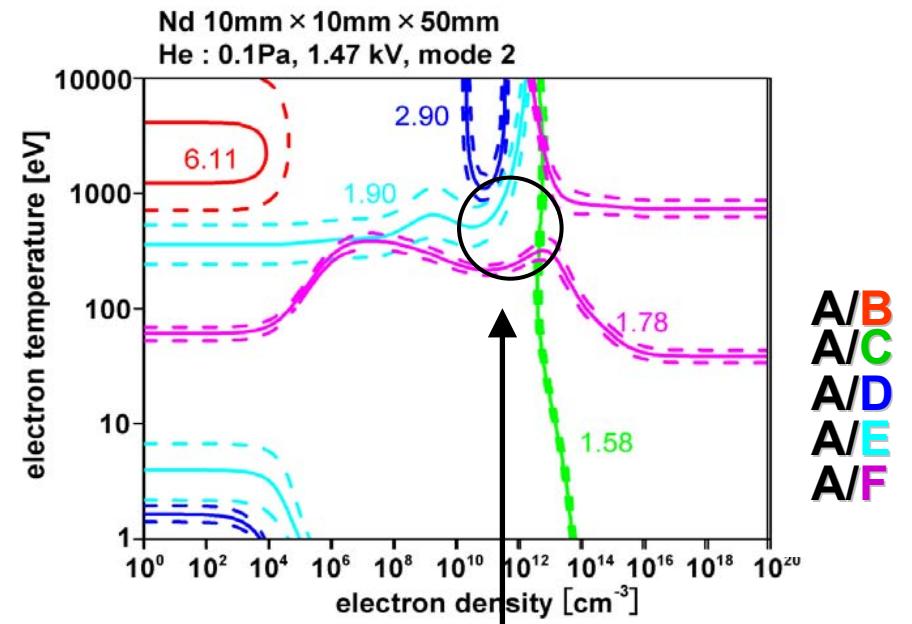
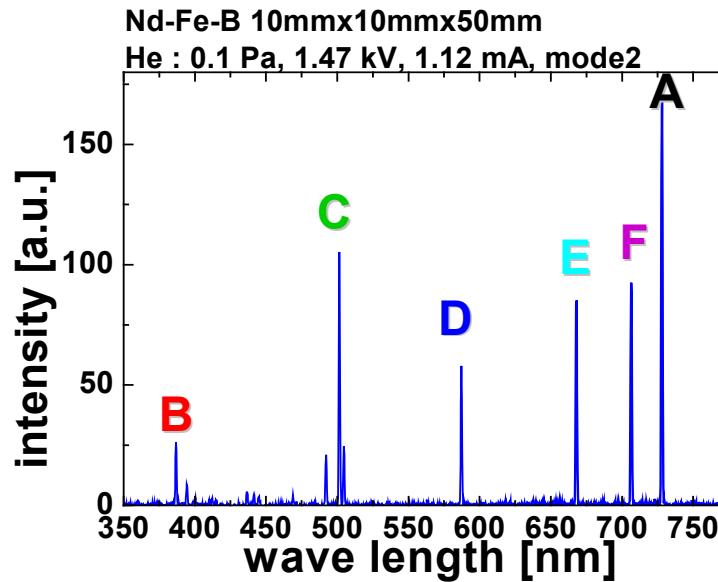


Setup for Spectroscopic Measurements of Electron Density and Temperature





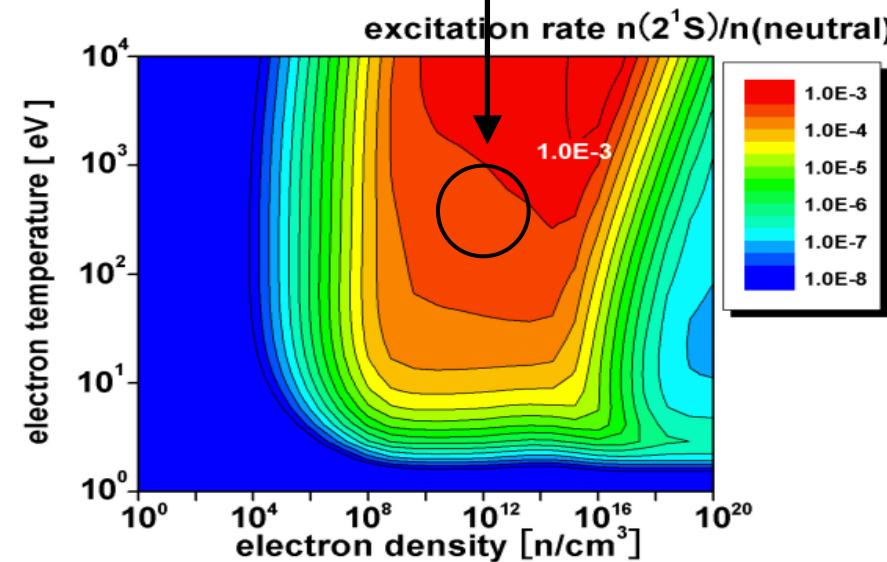
Spectroscopic Measurement Results



electron temperature >100 eV
electron density > 10^{11} cm^{-3}

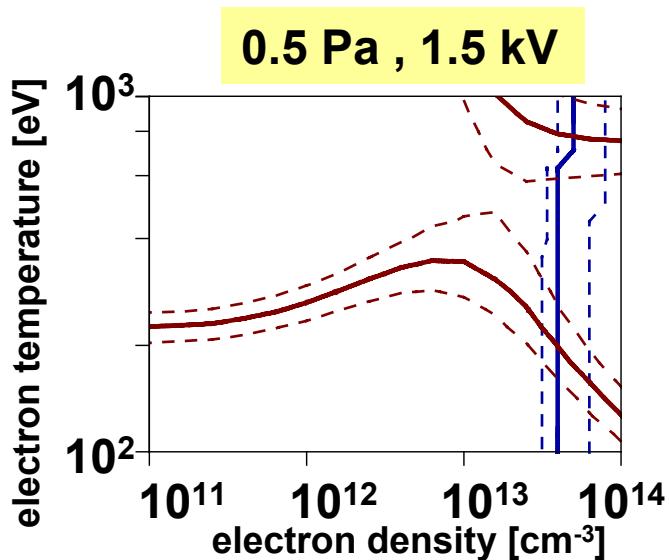
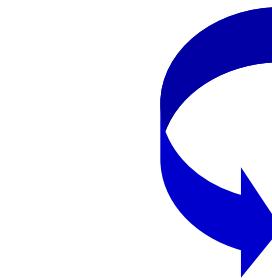
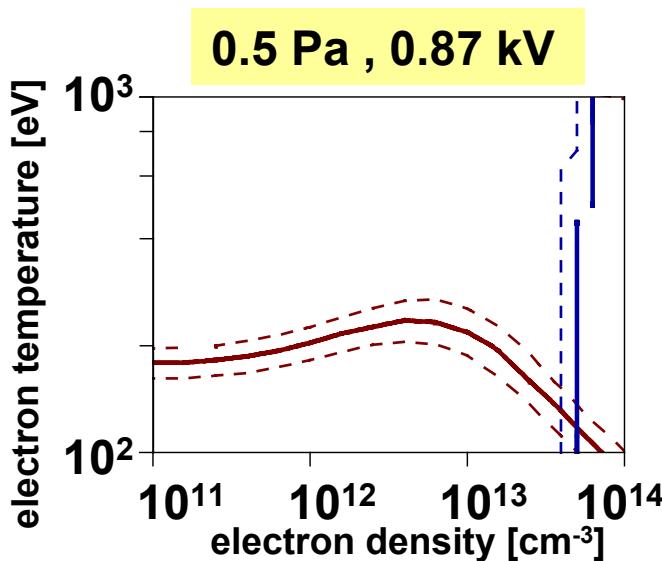
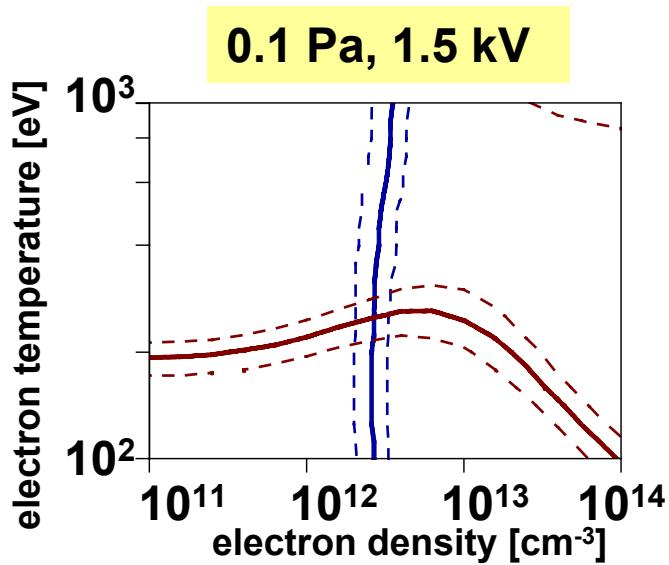
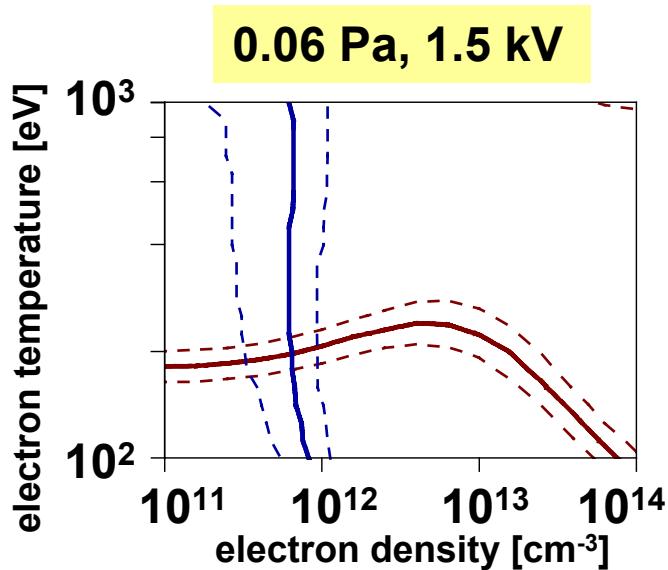


$$n(2^1\text{S}) / n(1^1\text{S}) > 5 \times 10^{-4}$$





Dependences of Ratios, A/C & A/F, on V & P





Summary R&D Targets and Achievements before This Workshop

Low-Energetic Neutral Helium Pulsed Beam Injection

Density at the Beam Center $\geq 10^{13} \text{ cm}^{-3}$	Achieved $1.5 \times 10^{13} \text{ cm}^{-3}$
Longitudinal Length as short as possible	300 - 400 μsec
Transverse Diameter as small as possible	7 - 8 mm (FWHM)
Repetition Rate $\geq 1 \text{ Hz}$ (no degradation in transverse profile)	Achieved 1 Hz @ $1.5 \times 10^{13} \text{ cm}^{-3}$

Exciter Plasma Production

Longitudinal Plasma Length optimal for maximal excitation efficiency	Can Be Achieved by the race-track-shaped magnetron scheme
Electron Density and Temperature as high as possible	$> 100 \text{ eV}, > 10^{11} \text{ cm}^{-3}$?
Operating Gas Pressure (Density) $\leq 0.04 \text{ Pa} (10^{13} \text{ cm}^{-3})$	Achieved $0.0015 \text{ Pa} (3.8 \times 10^{11} \text{ cm}^{-3})$

MEIEC (Microwave Enhancement of Inertial Electrostatic Confinement)

Plasmas: Theory and Experiment

John Brandenburg

Marin Racic

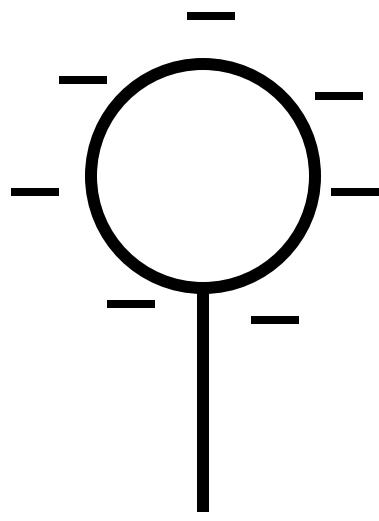
Florida Space Institute



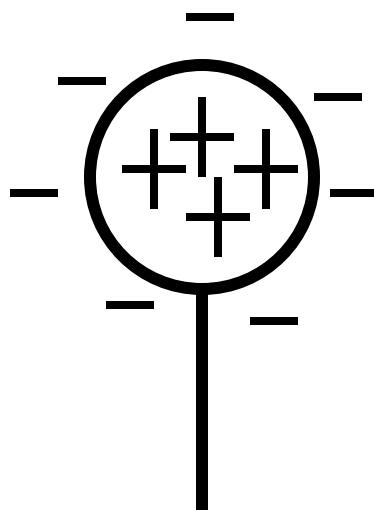
Agenda

- Theory of IEC (Inertial Electrostatic Confinement) of Plasmas
- Motivation : IEC Plasmas for Fusion
- Theory of MEIEC (Microwave Enhancement of IEC)
- Experiment
- Summary

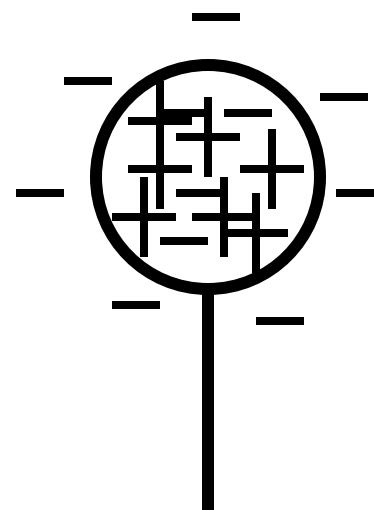
IEC (Inertial Electrostatic Confinement) of Plasmas



Porous
cathode

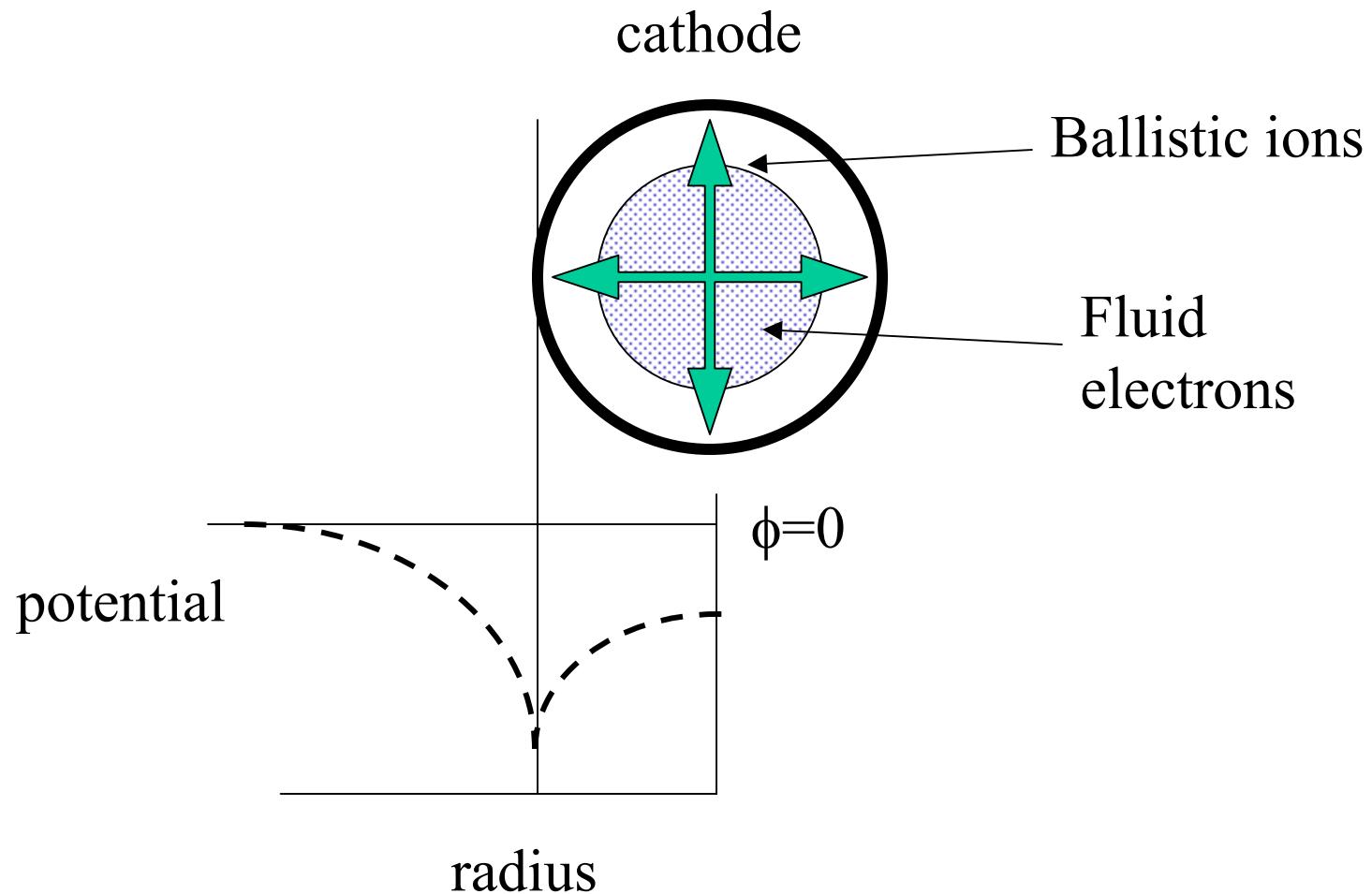


Trapped
ions



Trapped
dense
plasma

IEC : Cathode Potentials



Theory of IEC (Inertial Electrostatic Confinement) of Plasmas

$$\rho + \nabla \bullet (\rho v) = 0$$

$$\rho(\nabla + v \bullet \nabla) v = \nabla P$$

steady state combined equation

$$\nabla \bullet (\rho v v) - \nabla P = 0$$

Theory of IEC (Inertial Electrostatic Confinement) of Plasmas Cont.

electron equation

$$\nabla P_e - en_e E = 0$$

ion equation

$$\nabla \bullet (\rho_i \vec{v} \vec{v}) + en_i E = 0$$

summed

$$\nabla P_e + \nabla \bullet (\rho_i \vec{v} \vec{v}) + e(n_i - n_e) E = 0$$

Theory of IEC (Inertial Electrostatic Confinement) of Plasmas Cont.

summed

$$\nabla P_e + \nabla \bullet (\rho_i \overset{\rho\rho}{vv}) + \varepsilon_o \overset{\rho}{E} (\nabla \bullet \overset{\rho}{E}) = \nabla \bullet \overset{\tau}{T} = 0$$

$$\overset{\tau}{T} = \rho_i \overset{\rho\rho}{vv} + I P_e + \varepsilon_o (\overset{\rho\rho}{EE} - \frac{1}{2} I E^2)$$

Virial equation

$$\nabla \bullet (\overset{\tau}{T} \bullet \overset{\rho}{x}) = \nabla \overset{\rho}{x} : \overset{\tau}{T} + \overset{\rho}{x} \bullet \nabla \bullet \overset{\tau}{T} = tr \overset{\tau}{T}$$

Integrated with Gauss's Theorem

$$\oint \overset{\tau}{T} \bullet \overset{\rho}{x} \bullet dS = \int tr \overset{\tau}{T} dx^3$$

Theory of IEC (Inertial Electrostatic Confinement) of Plasmas Cont.

$$\nabla P_e + \nabla \bullet (\rho_i v v) + \varepsilon_o E \nabla \bullet E = \nabla \bullet T = 0$$

$$\oint \tau \bullet x \bullet dS = \int tr T dx^3$$

$$T = \rho_i v v + IP_e + \varepsilon_o (EE - \frac{1}{2} IE^2)$$

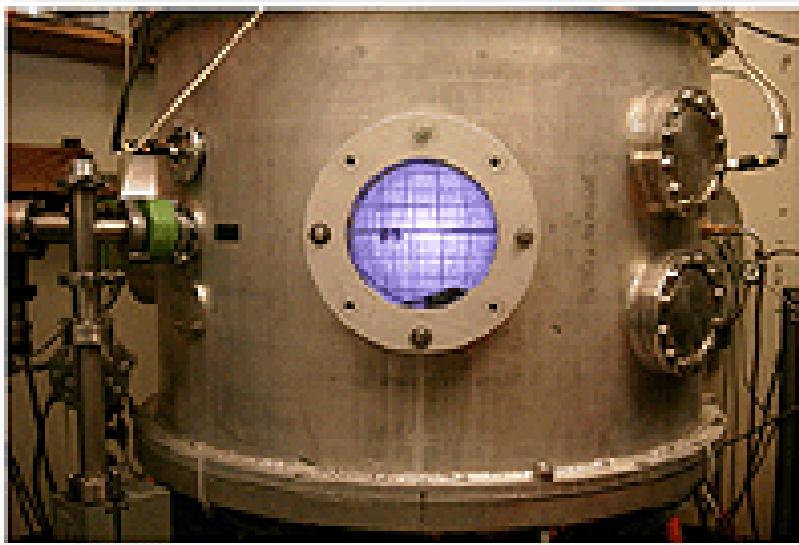
Virial equation with vaccum cathode surface

$$2\pi \varepsilon_o E_c^2 R_c^3 = \int tr T dx^3 = 4\pi R_c^3 \left\langle \rho_i v^2 + 3P_e + \frac{1}{2} \varepsilon_o E^2 \right\rangle$$

Momentum Flux Balance

$$\varepsilon_o E_c^2 = \left\langle \rho_i v^2 + 3P_e + \frac{1}{2} \varepsilon_o E^2 \right\rangle$$

Motivation: IEC for Fusion Plasmas



IEC Fusion is cheap , simple , but limited by cathode heating

Theory of MEIEC (Microwave Enhanced IEC)Plasmas

Microwaves induce electron motion

$$\overset{\circ}{E}_m = \overset{\circ}{E}_o \exp(i\omega t), \quad \overset{\circ}{v}_e = \frac{-i\overset{\circ}{E}_m}{m\omega}$$

new electron equation

$$\nabla \bullet (\rho_e \overset{\circ}{v}_e \overset{\circ}{v}_e) + \nabla P_e - en_e E = \nabla \bullet \left(\frac{e^2 n_e}{2m_e \omega^2} \overset{\circ}{E}_m \overset{\circ}{E}_m \right) + \nabla P_e - en_e E = 0$$

ponderomotive force (absolute value of Harmonic fields)

$$\nabla \bullet \left(\frac{\omega_p^2}{2\omega^2} \epsilon_o \overset{\circ}{E}_m \overset{\circ}{E}_m \right) + \nabla P_e - en_e E = 0$$

electron plasma frequency ω_p^2

Theory of IEC (Inertial Electrostatic Confinement) of Plasmas Cont.

new equation

$$T = \rho_i v^2 + IP_e + \varepsilon_o (E^2 - \frac{\omega_p^2}{2\omega^2} E_m^2 - \frac{1}{2} IE^2)$$

Virial equation with vaccum

cathode surface excluding microwaves

$$\varepsilon_o (E_c^2 + \frac{\omega_p^2}{2\omega^2} E_m^2) = \langle \rho_i v^2 + 3P_e + \frac{1}{2} \varepsilon_o E^2 \rangle$$

microwaves allow higher plasma pressures

at same E_c (Cathode Voltage)

Experiment



Experimental Demonstration



Without microwaves



With microwaves

Proposed Experiment

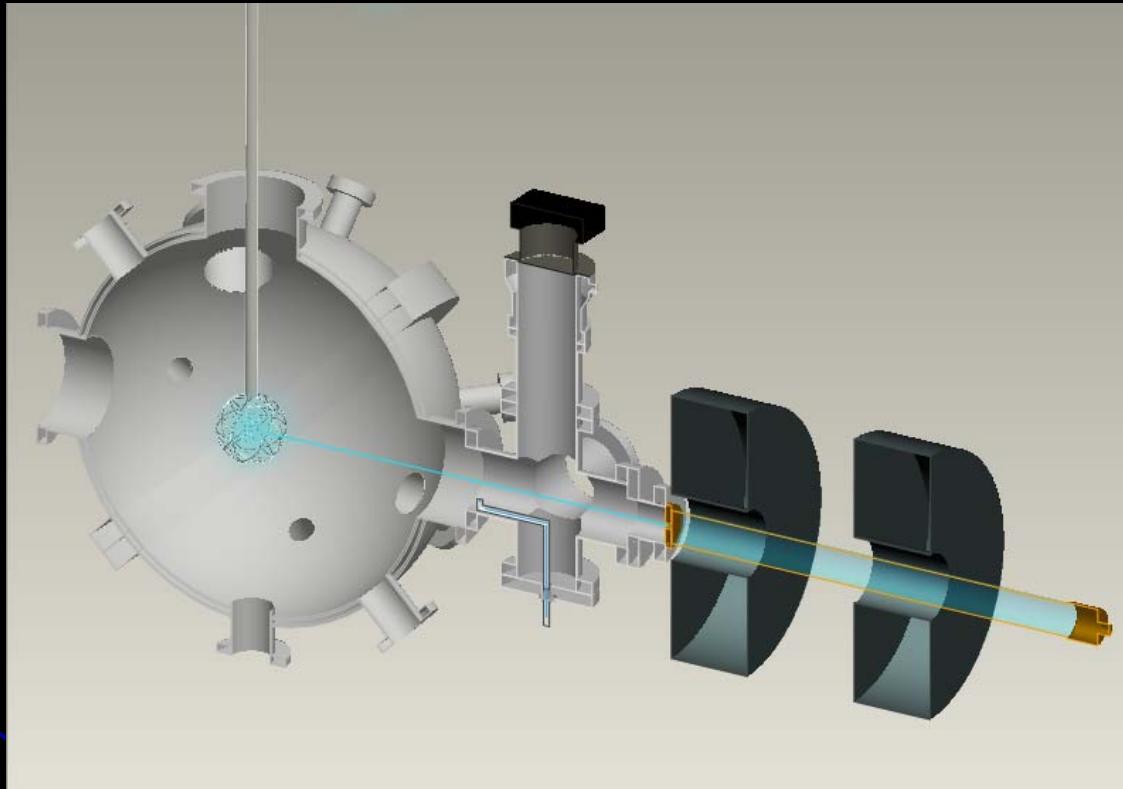
- MEIEC should be tested by others
- MEIEC should be tested in a fusion configuration to see if it enhances fusion rates (approximately 1kW per KV should be needed to enhance confinement))
- A 75KW experiment at 915MHz to enhance fusion rates at 75KV is being proposed
- Pulsed sources of High Power microwaves should be considered

MEIEC Summary

- Theory indicates that microwaves can enhance plasma confinement of EIC plasma
- Microwave fields require high power to effective ($\sim 1\text{kW per KV}$)
- Enhancement of confining pressure is due to electron pondromotive force
- Initial demonstration of effect suggests it has been successful-*is it possible nature allows cheap fusion power?*
- Further experiments are being conducted and data is being analyzed



Progress in the Development of a ${}^3\text{He}$ Ion Source for IEC Fusion



G.R. Piefer, E.A. Alderson, R.P. Ashley, D.R. Boris, G.A. Emmert, R.C. Giar, G.L. Kulcinski, R.F. Radel, T.E. Radel, J.F. Santarius, A.L. Wehmeyer

US-Japan Workshop on IEC Devices
March 14-16, 2005 Los Alamos National Lab
Los Alamos, New Mexico



Outline

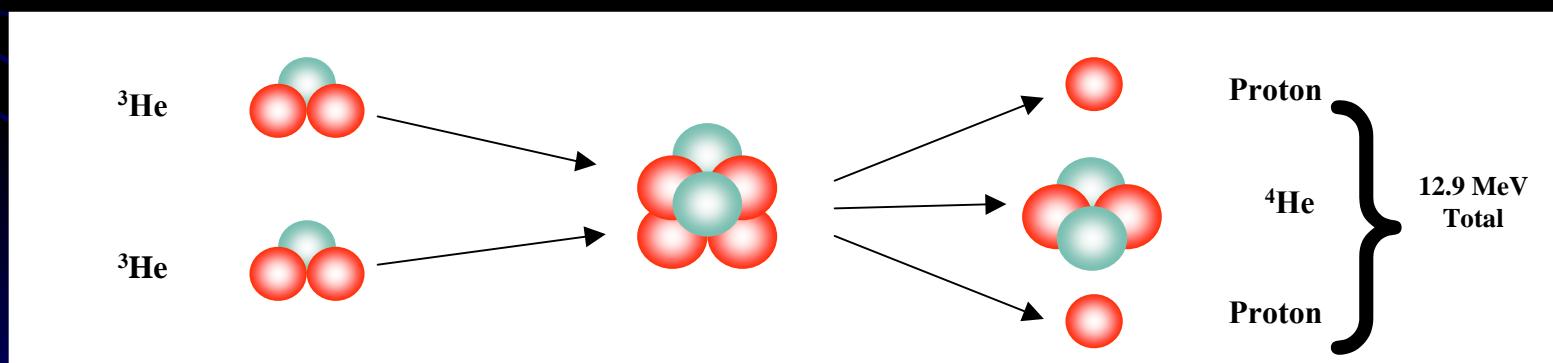
- ^3He - ^3He Fusion
 - Rationale for experiments
 - Reaction physics
 - IEC beam-background reaction rate estimate
 - Detectability
- Ion source development
 - Status as of the last meeting
 - Progress since the last meeting
 - Summary



Purpose of ^3He - ^3He Fusion in an IEC

- Benefits of ^3He - ^3He Fusion

- No Radioactive fuels or products
- Possibility of direct energy conversion
- Minimal or no activation of reactor vessel

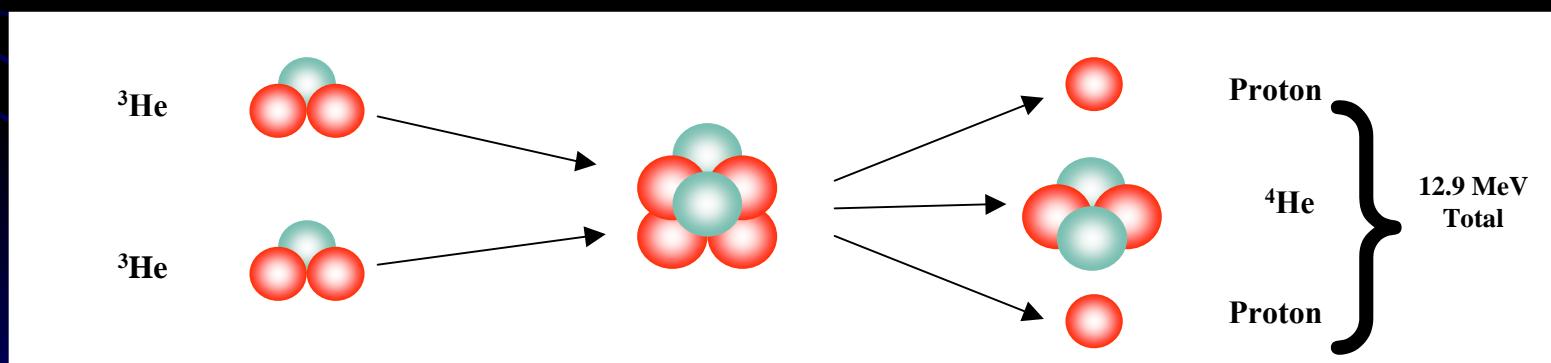


The ^3He - ^3He fusion reaction



Purpose of ^3He - ^3He Fusion in an IEC

- IEC offers some advantages over other research experiments
 - Higher energy capability than MFE or ICF devices
 - Higher current capability than accelerators
 - Allows for study of cross sections where counting statistics are currently poor

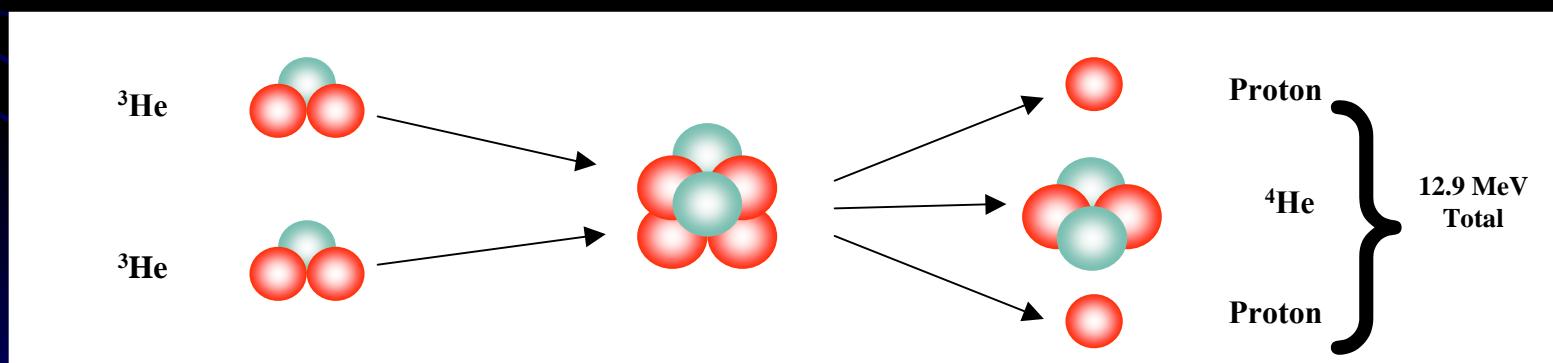


The ^3He - ^3He fusion reaction



Purpose of ^3He - ^3He Fusion in an IEC

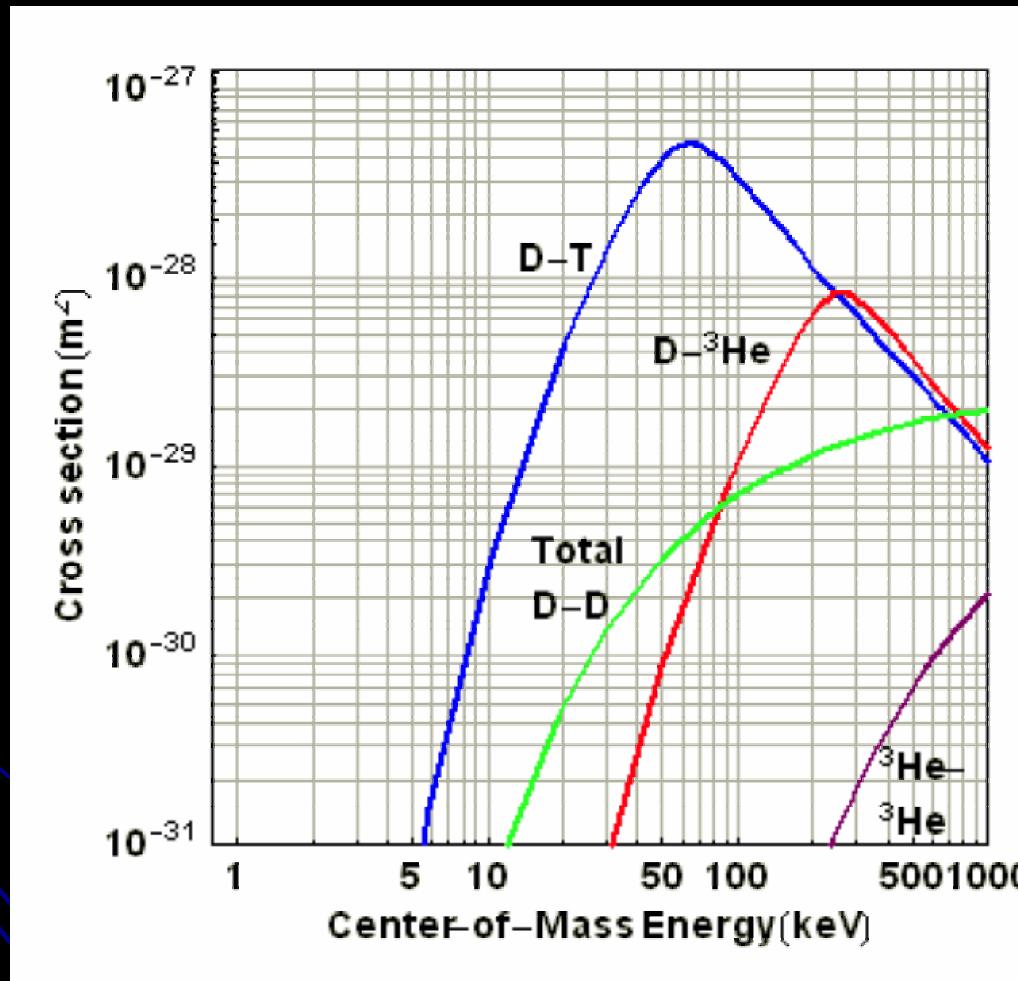
- ^3He - ^3He fusion has some significant disadvantages
 - Very small cross section at low voltages
 - Relatively difficult to obtain fuel in large quantities



The ^3He - ^3He fusion reaction

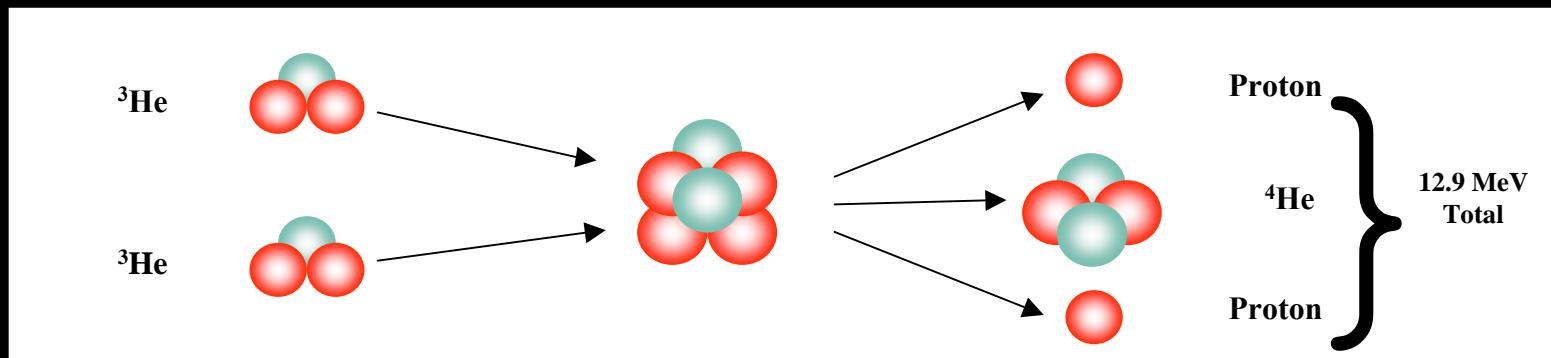


^3He - ^3He Fusion Cross Section is Substantially Lower than D-D



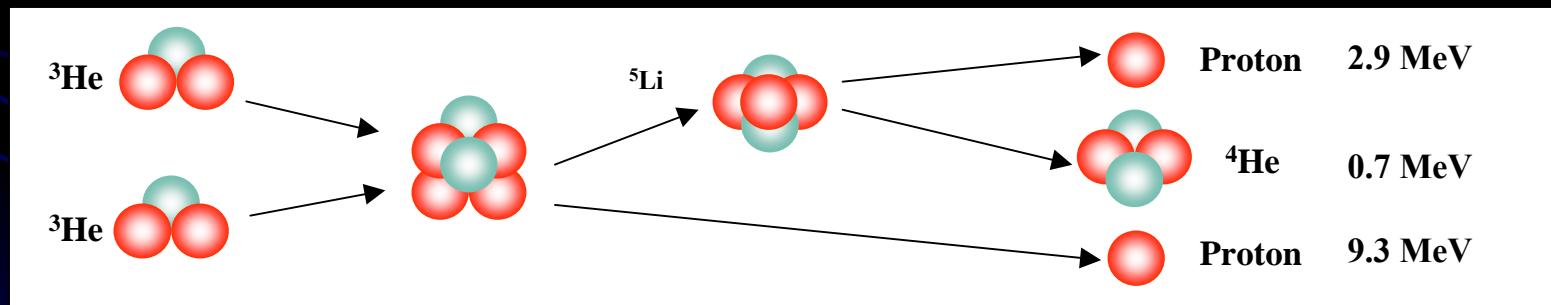


^3He - ^3He Reaction has Two Possible Reaction Sequences



The 3-body ^3He - ^3He reaction (~90% of reactions at 190keV CM energy)

- The three body reaction gives a relatively flat continuum of proton energies, which will be difficult to separate from noise



The two 2-body ^3He - ^3He reaction (~10% of reactions at 190keV CM energy)

- The 2-body reaction however, gives discrete proton energies, which will appear as a peak on top of the continuum at 9.3 MeV

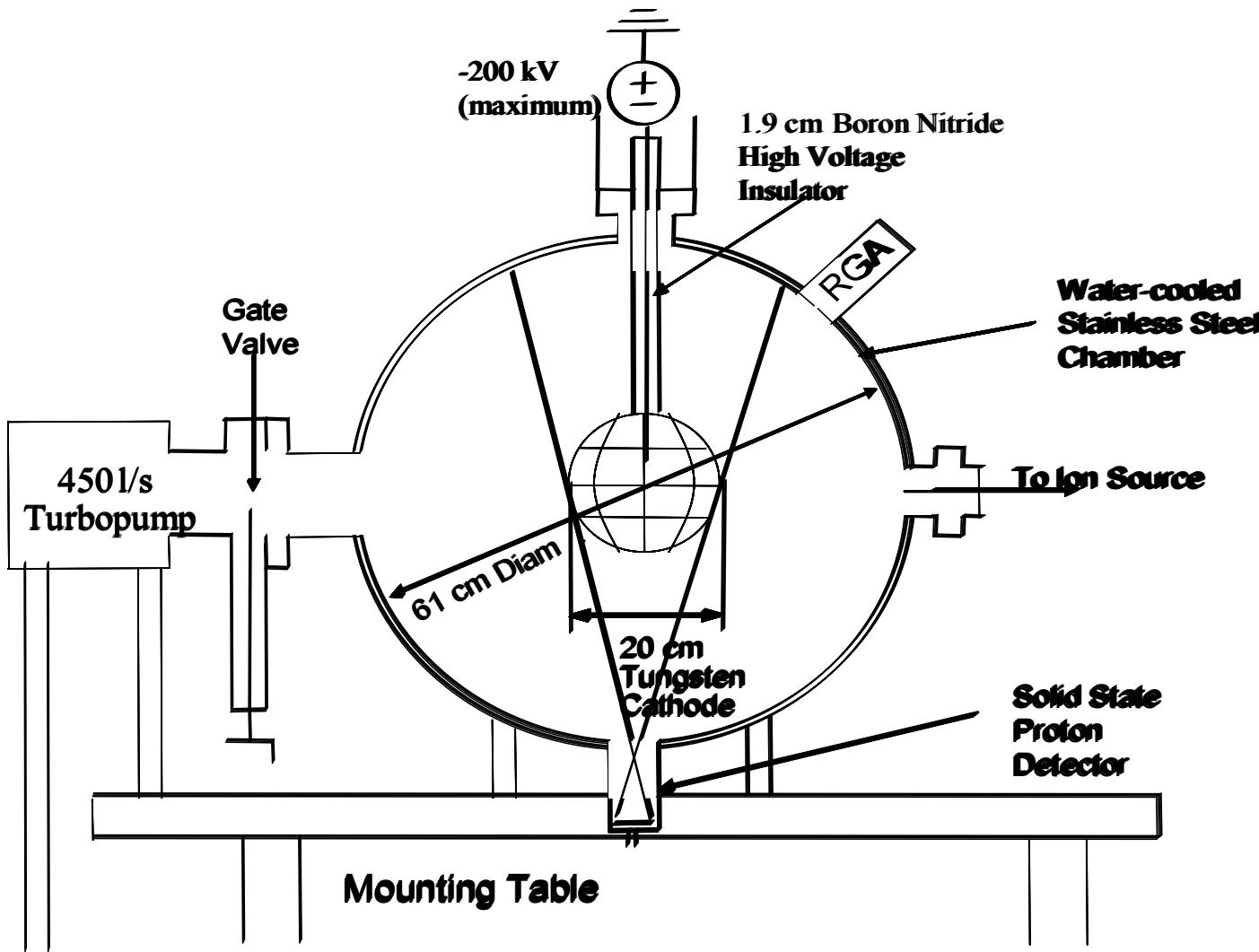


Reactivity in IEC will be Modeled as a Monoenergetic Beam-Background Source

- Beam currents low enough so that converged-core reactions are assumed to be insignificant
- Background gas pressure kept low enough such that ion charge exchange time is long compared to ion lifetime
- Model assumes proton detector observes reactions only inside of the cathode

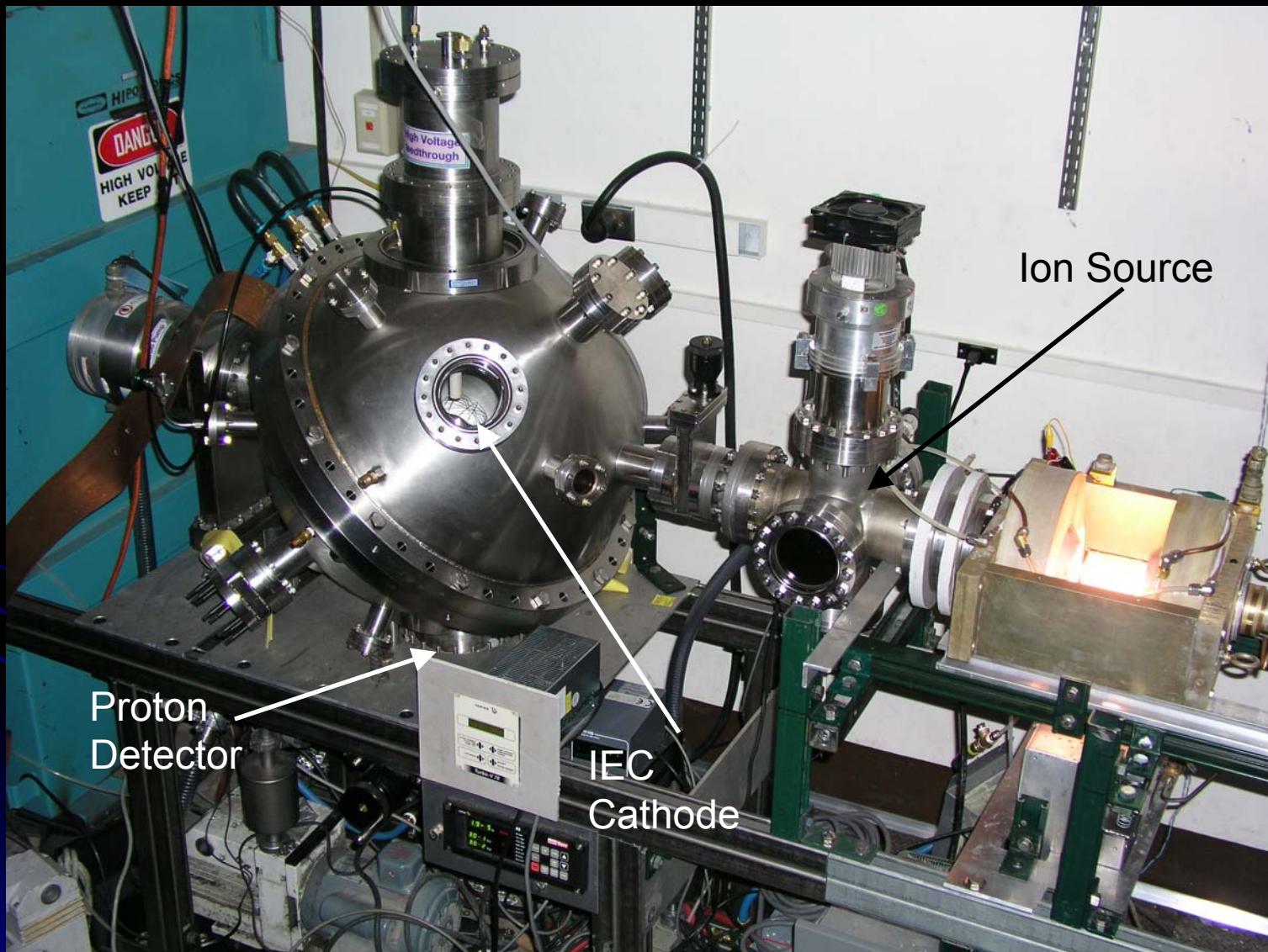


Setup for ${}^3\text{He}$ - ${}^3\text{He}$ Experiments





Setup for ${}^3\text{He}$ - ${}^3\text{He}$ Experiments





Assumptions for Rate Calculation

- Cathode current ~ 10 mA
- Cathode voltage = 200 kV
 - ${}^3\text{He}$ singly ionized \rightarrow Center of mass energy = 200 keV
- Cathode Transparency = 99%
- Average secondary emission coefficient = 2
- Background gas pressure = 0.2 mtorr (27 mPa)
- Cathode/anode radius ratio sufficiently small such that full ion current can be drawn



Fusion Rate can be Calculated from Assumed Parameters

- The fusion rate for a beam-background mono-energetic system can be calculated by the following equation:

$$F = n_b * \frac{I_{cath} * 2R_{cath}}{e(1 - \gamma)(1 + \sigma_{se})} * \sigma(E)$$

n_b is the background gas density, I_{cath} is the measured cathode current, R_{cath} is the cathode radius, $\sigma(E)$ is the fusion cross section, e is electron charge, γ is the grid transparency, and σ_{se} is the average secondary emission coefficient



Fusion Rate can be Calculated from Assumed Parameters

- The fusion rate for a beam-background mono-energetic system can be calculated by the following equation:

$$F = n_b * \frac{I_{cath} * 2R_{cath}}{e(1 - \gamma)(1 + \sigma_{se})} * \sigma(E)$$

- Using existing data for ${}^3\text{He}-{}^3\text{He}$ cross sections, this gives a fusion rate of $2*10^5$ fusions/second



Detection Rate Should be Observable

- Detector is ~ 50 cm from center of device
- Detector area = 1200 mm²
- The number of detected counts can be expressed as:

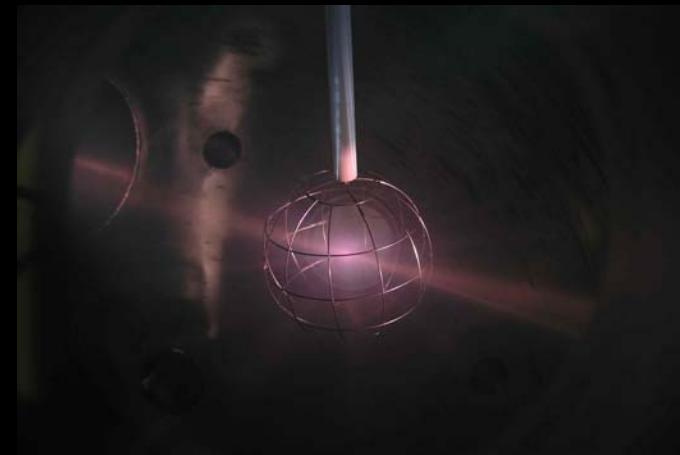
$$D = \frac{F}{4\pi R_{\text{det}}^2} A_{\text{det}}$$

- Detection rate ~ 76 counts/sec
- If 10% of these are 2-body reactions, the 9.3 MeV peak will have 7.6 counts/sec



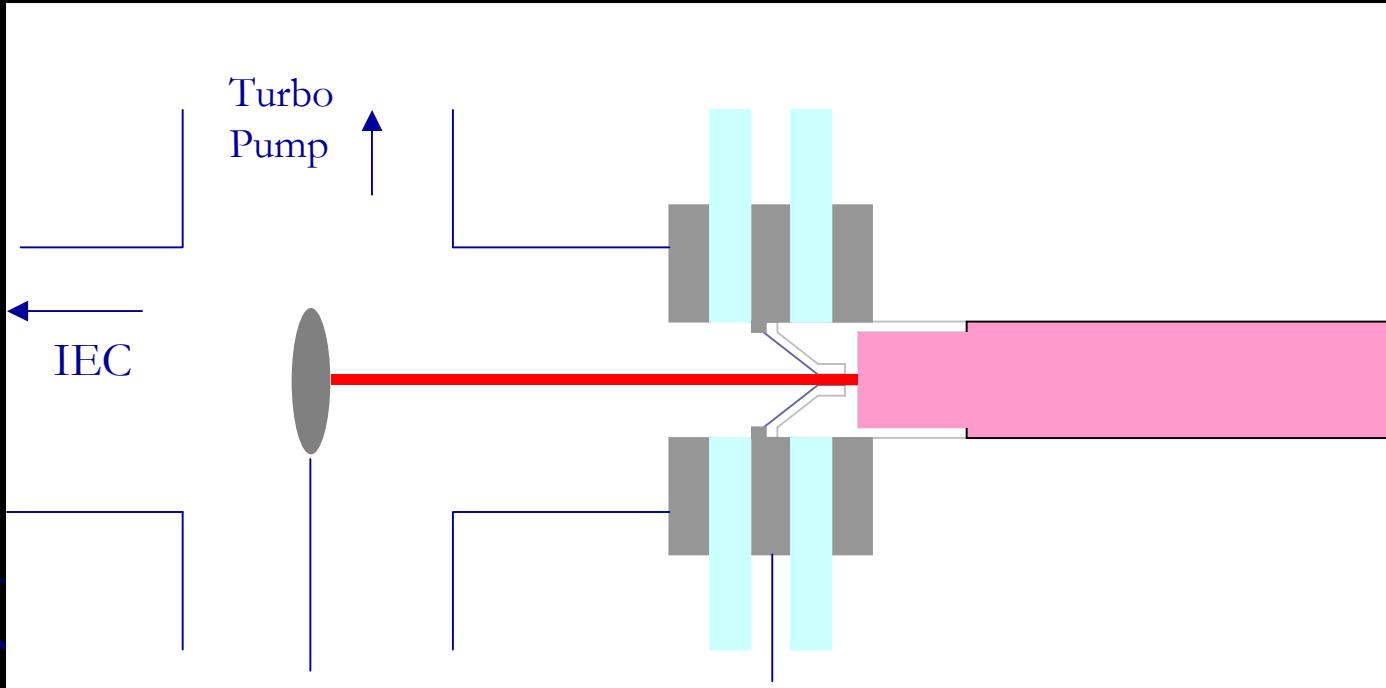
Ion Source Status as of Last Workshop— October 2003, Tokyo, Japan

- Helicon source on-line with ${}^4\text{He}$
- 2 mA cathode current observed in main system at modest voltage (~ 35 kV)
- Extraction system not yet constructed
- Ion current difficult to control
- Helicon fringing fields affected extracted beam





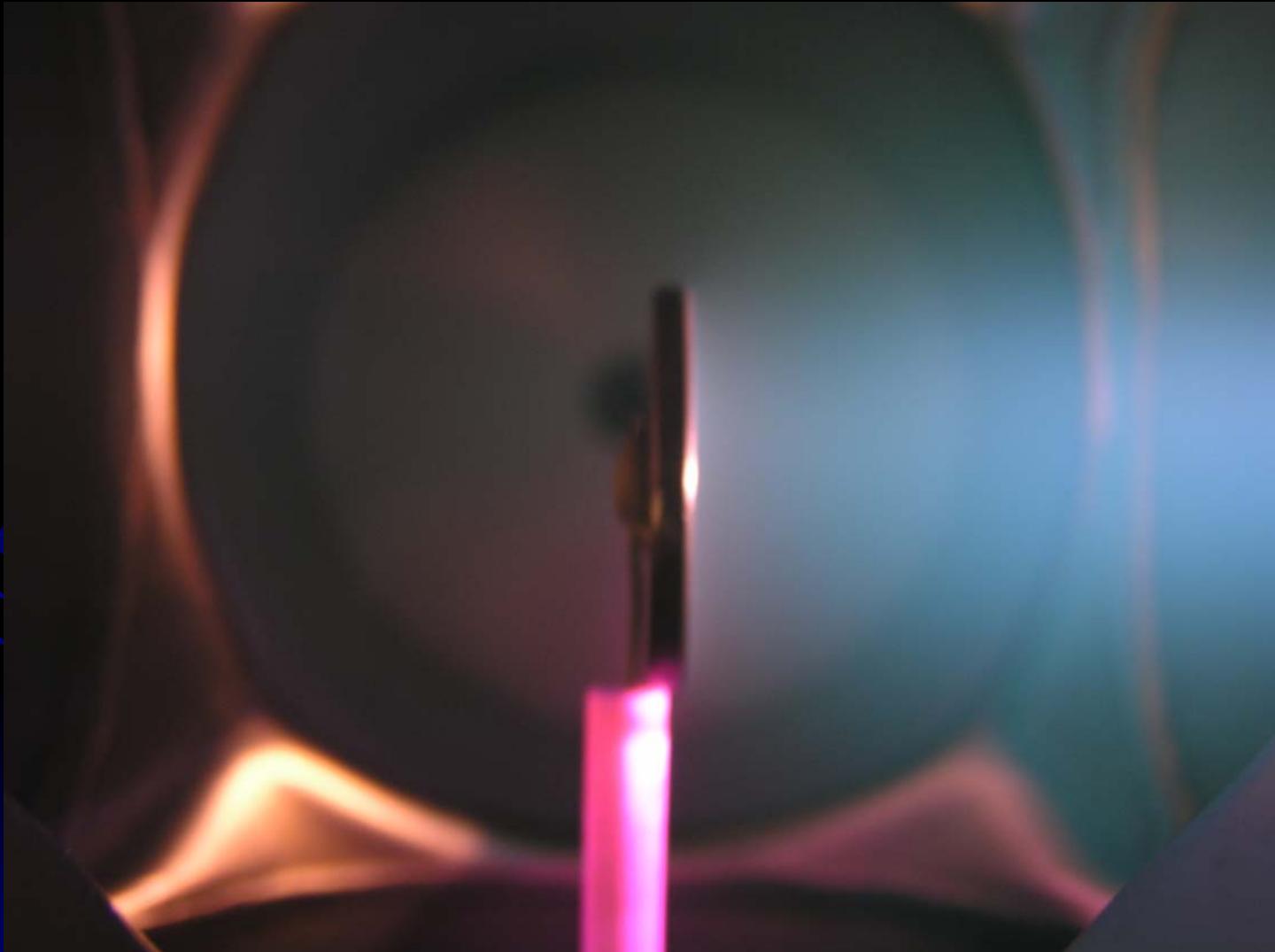
Ion Extraction Region Completed and Operational



- New electrode designed to minimize erosion
- Beam collection plate diagnostic added

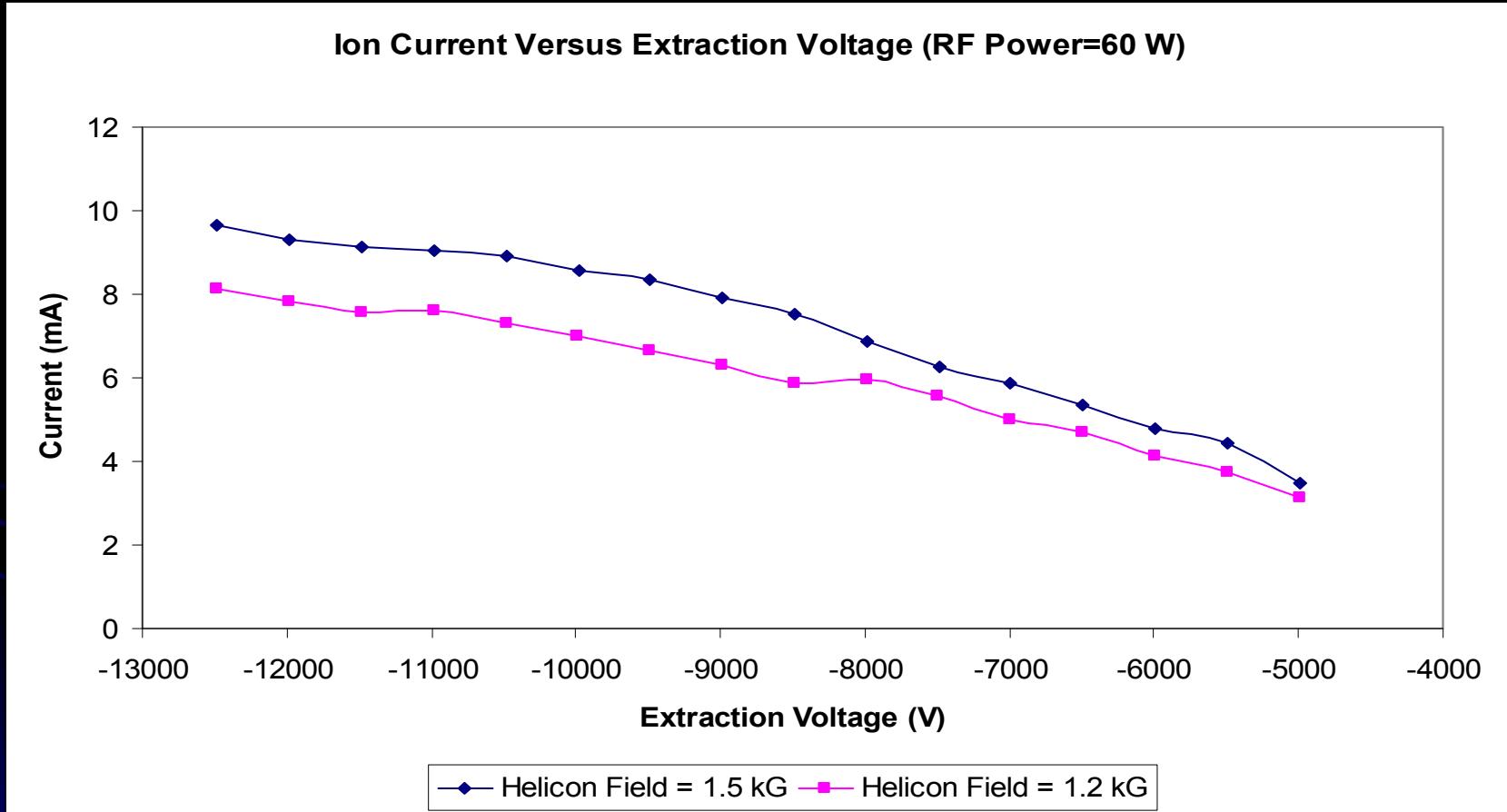


Extraction System Tested in ^4He with Collection Plate



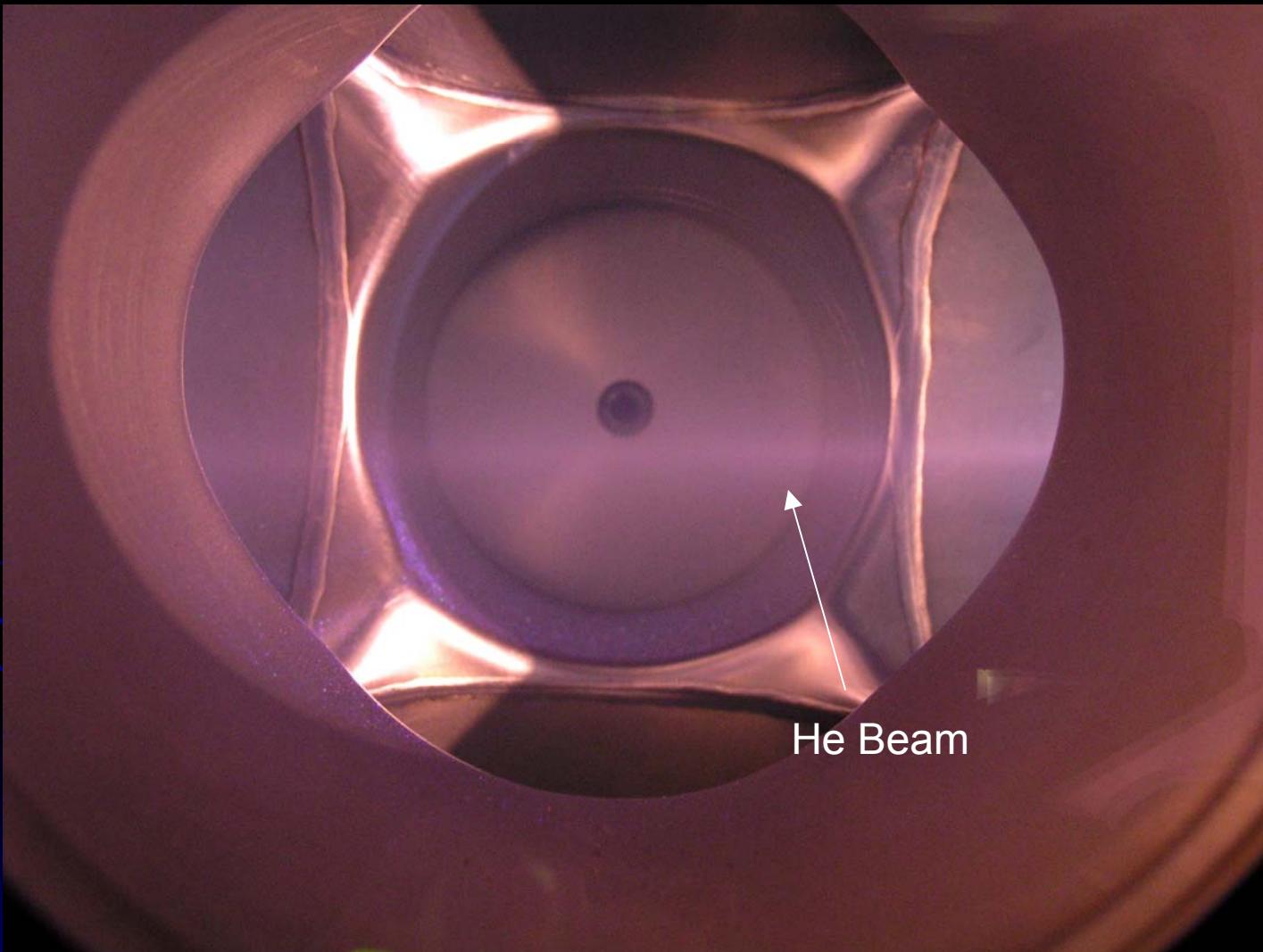


Ion Extraction Current Versus Extraction Voltage Shows Good Current Capability



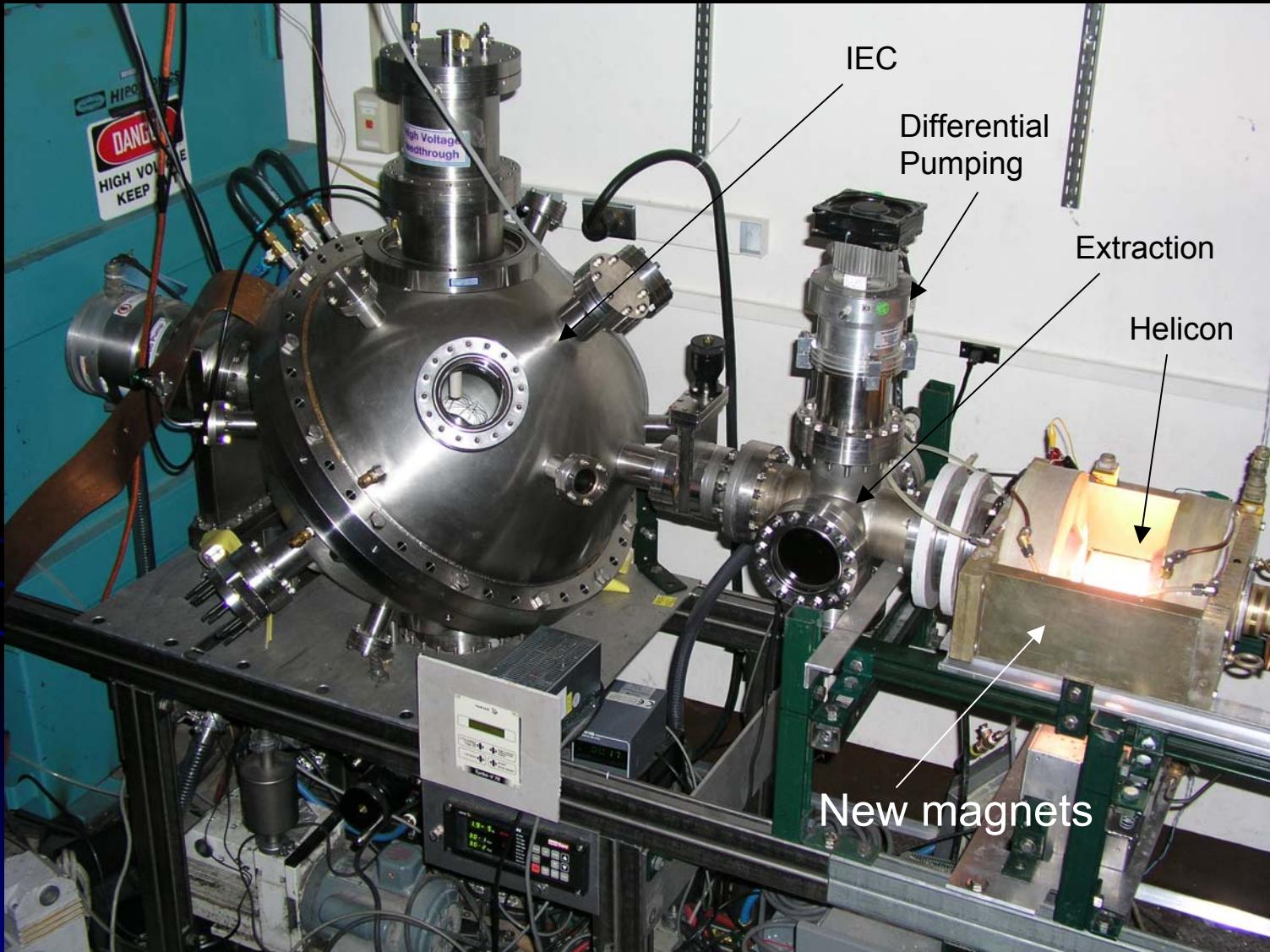


Stray Fields from Helicon Source Appear to Cause Beam Deflection



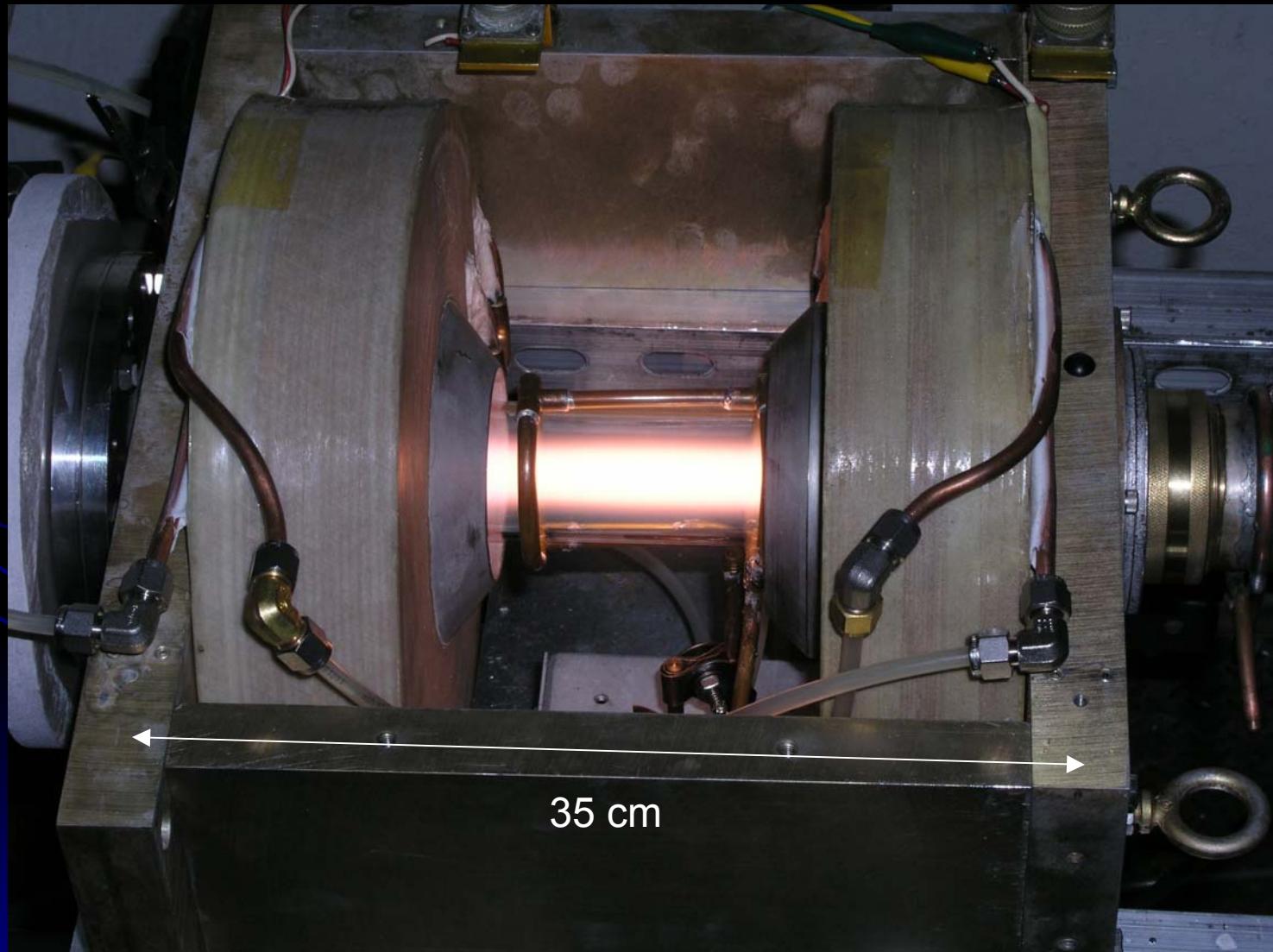


New Helicon Magnets are Installed and Now Being Tested





Fringing Fields Shunted Through Magnetic Circuit



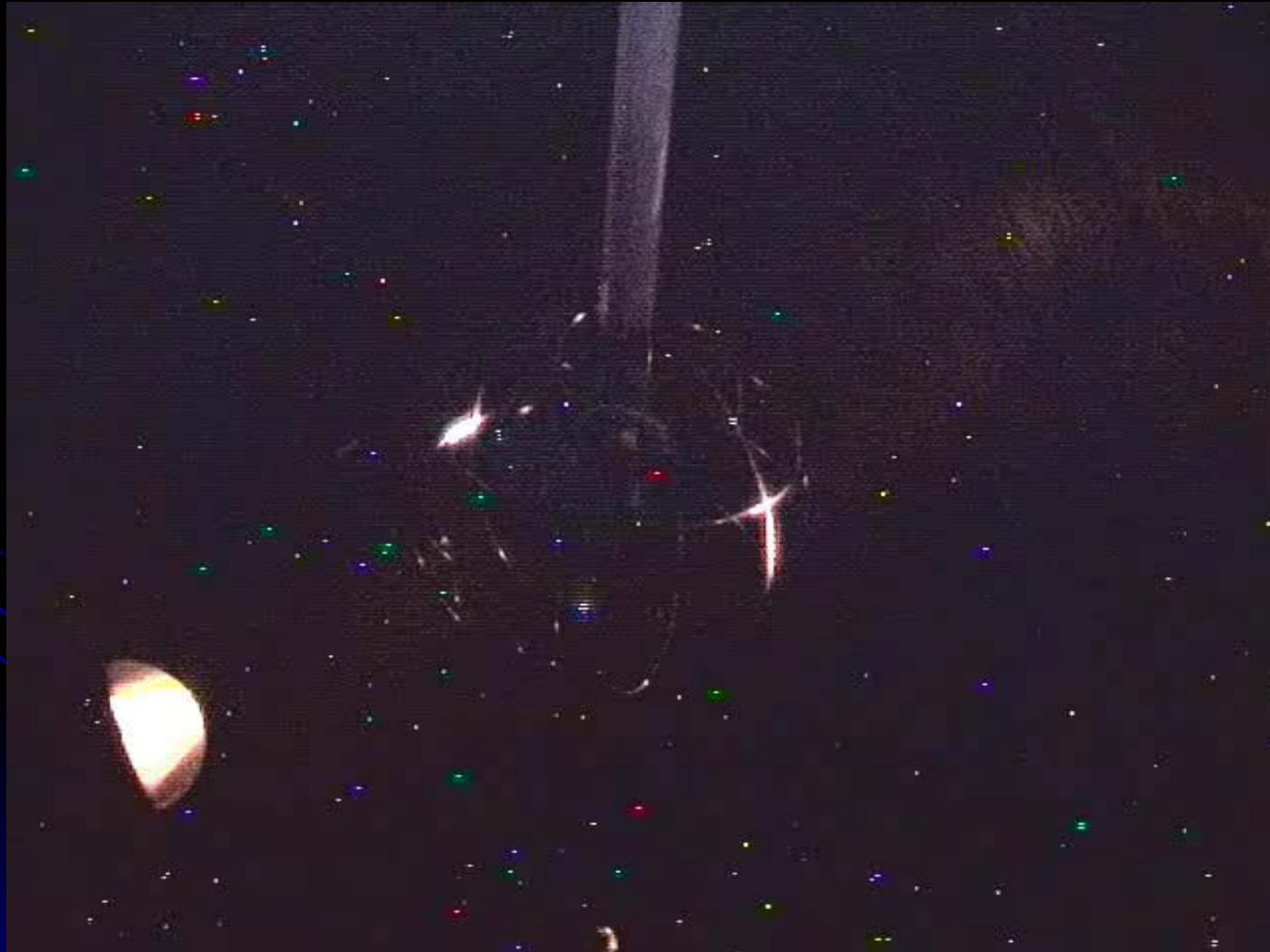


IEC Operation with Ion Source is Improving

- Operation at voltages up to 130 kV
- Operation at cathode currents up to 10 mA
- Operation at pressures as low as 50 μ torr, and as high as 0.5 mtorr



Some Instability in High Voltage Discharges



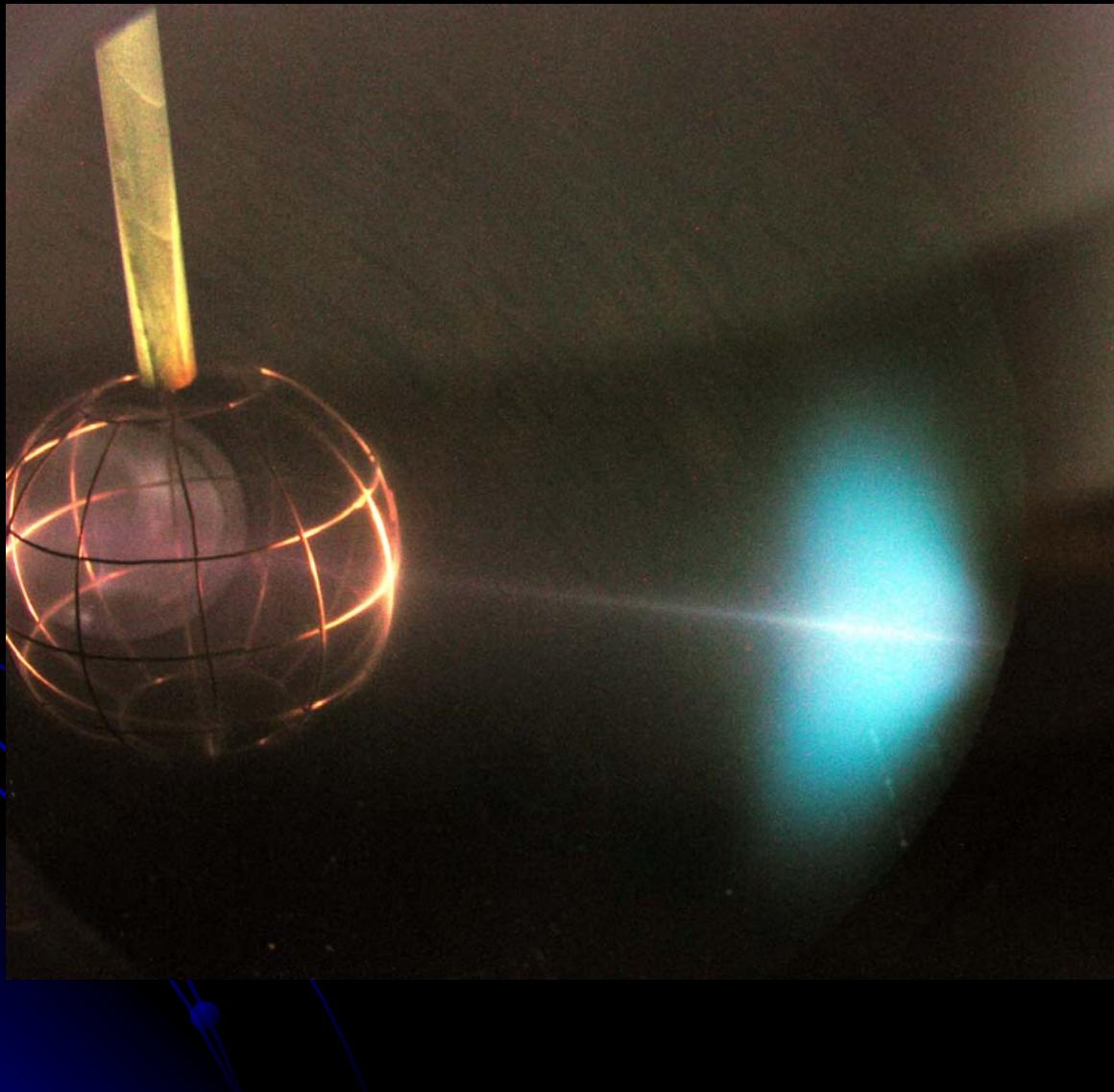


Conclusions

- IEC experiments looking for ${}^3\text{He}$ - ${}^3\text{He}$ fusion reactions are underway
- Good results so far with ${}^4\text{He}$, and some with ${}^3\text{He}$
- Ion source and IEC operation with source have improved markedly
 - Extraction region online
 - Helicon fringe fields reduced
 - IEC operating voltage up to 130 kV
- Still some problems to overcome
 - HV breakdown at high cathode voltages
 - He beam deflection



Questions?





Measurement of D-³He Protons in an Inertial Electrostatic Confinement Fusion

Satoshi Ogawa, Takeshi Hama, Teruhisa Takamatsu,
Kai Masuda, Hisayuki Toku, Kiyoshi Yoshikawa

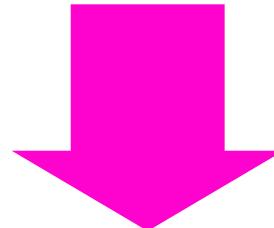
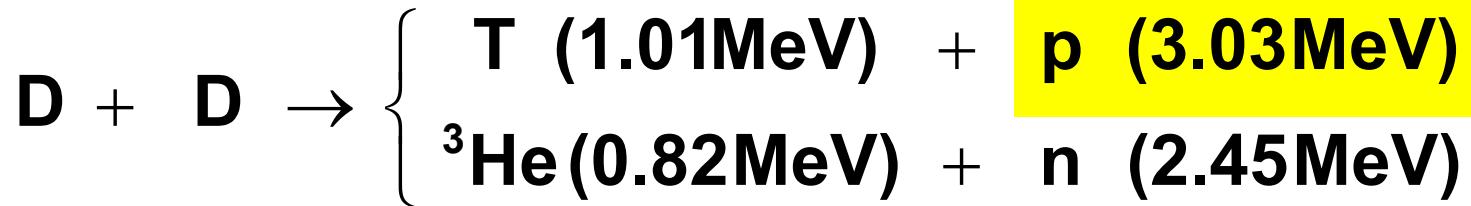
Institute of Advanced Energy, Kyoto University.

7th US/Japan IEC Workshop
at Los Alamos National Laboratory

March 15. 2005



D-D and D-3He fusion reaction



PET (Positron Emission Tomography)



Objective

3.03MeV D-D Protons

Noise



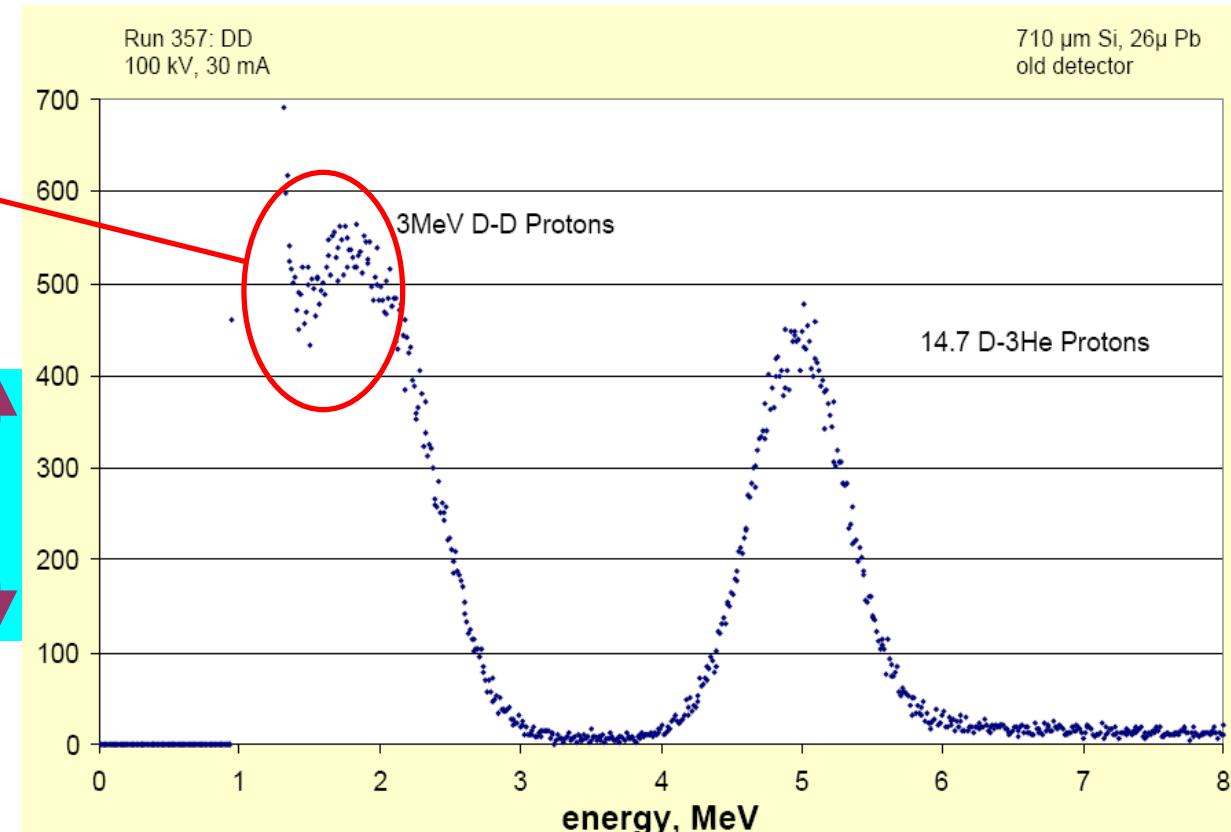
Improve

3.03MeV
D-D Protons energy

Noise



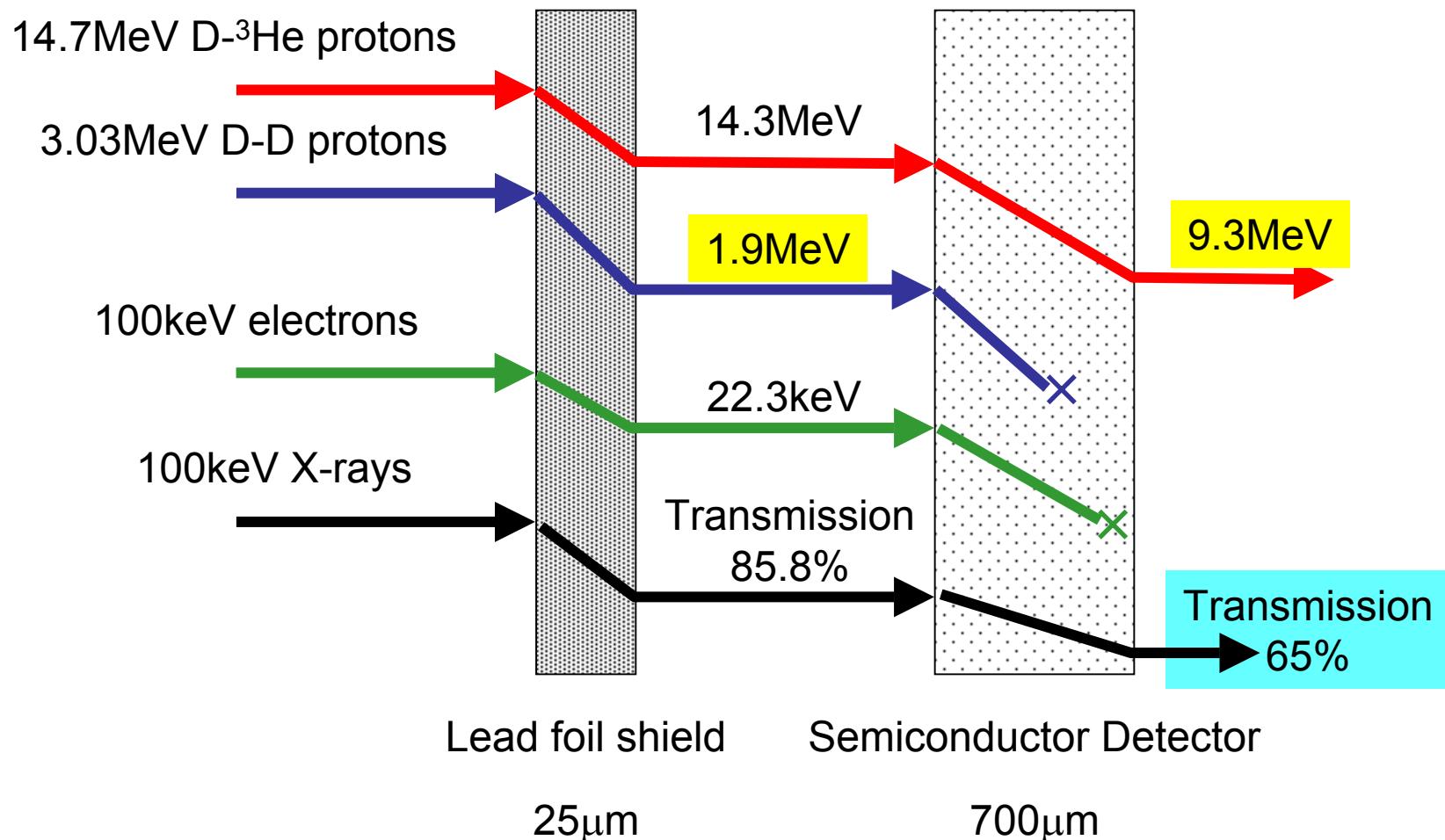
3.03MeV D-D Protons
can be measured
more clearly



R. P. Ashley, et al., "Fusion Product Source Regions in the IEC Fusion Reactor",
US-Japan Workshop on Inertial Electrostatic Confinement Fusion, Madison, Wisconsin
October 9-10, 2002.

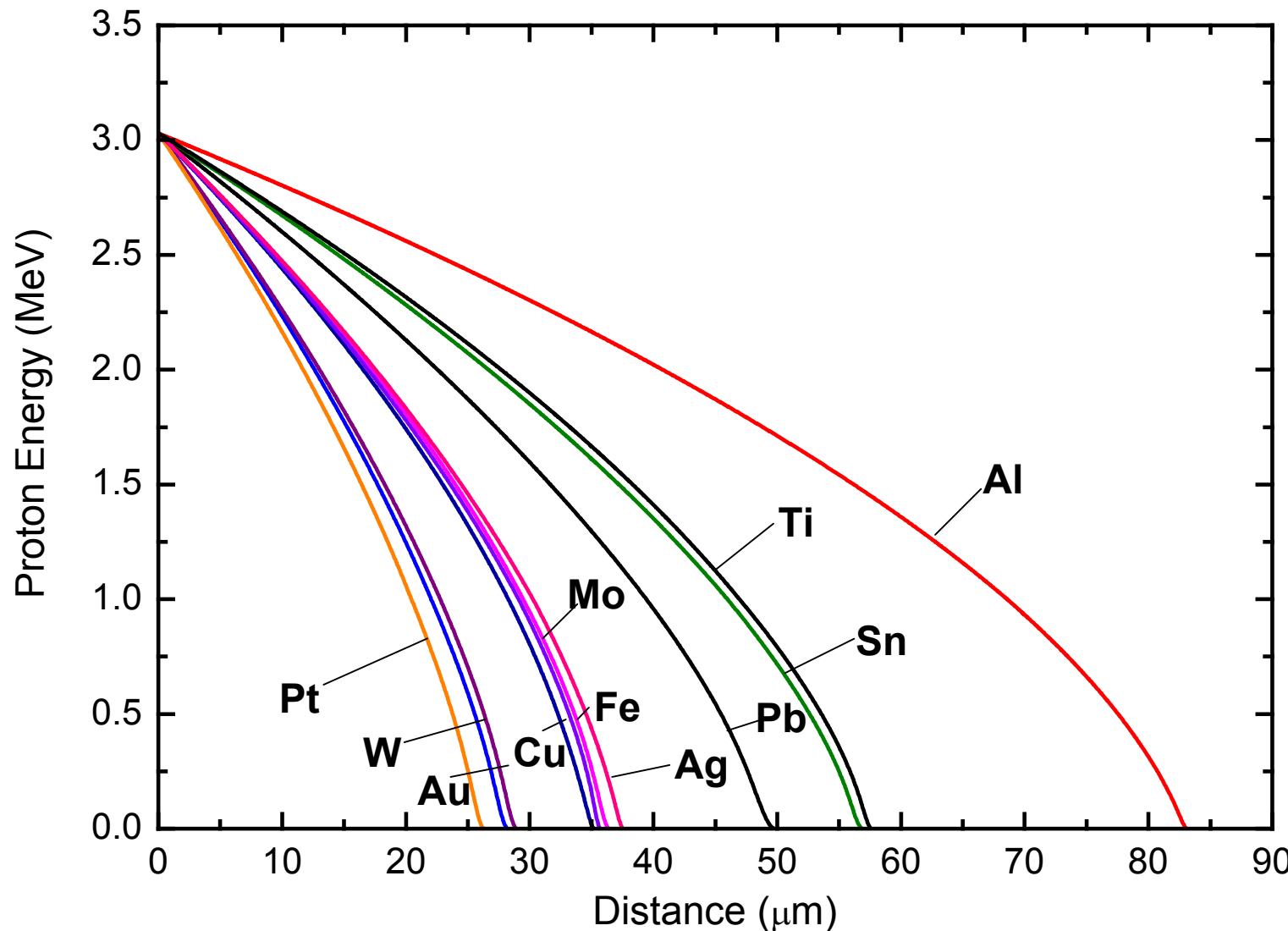


Lead foil 25 μ m and the Si detector



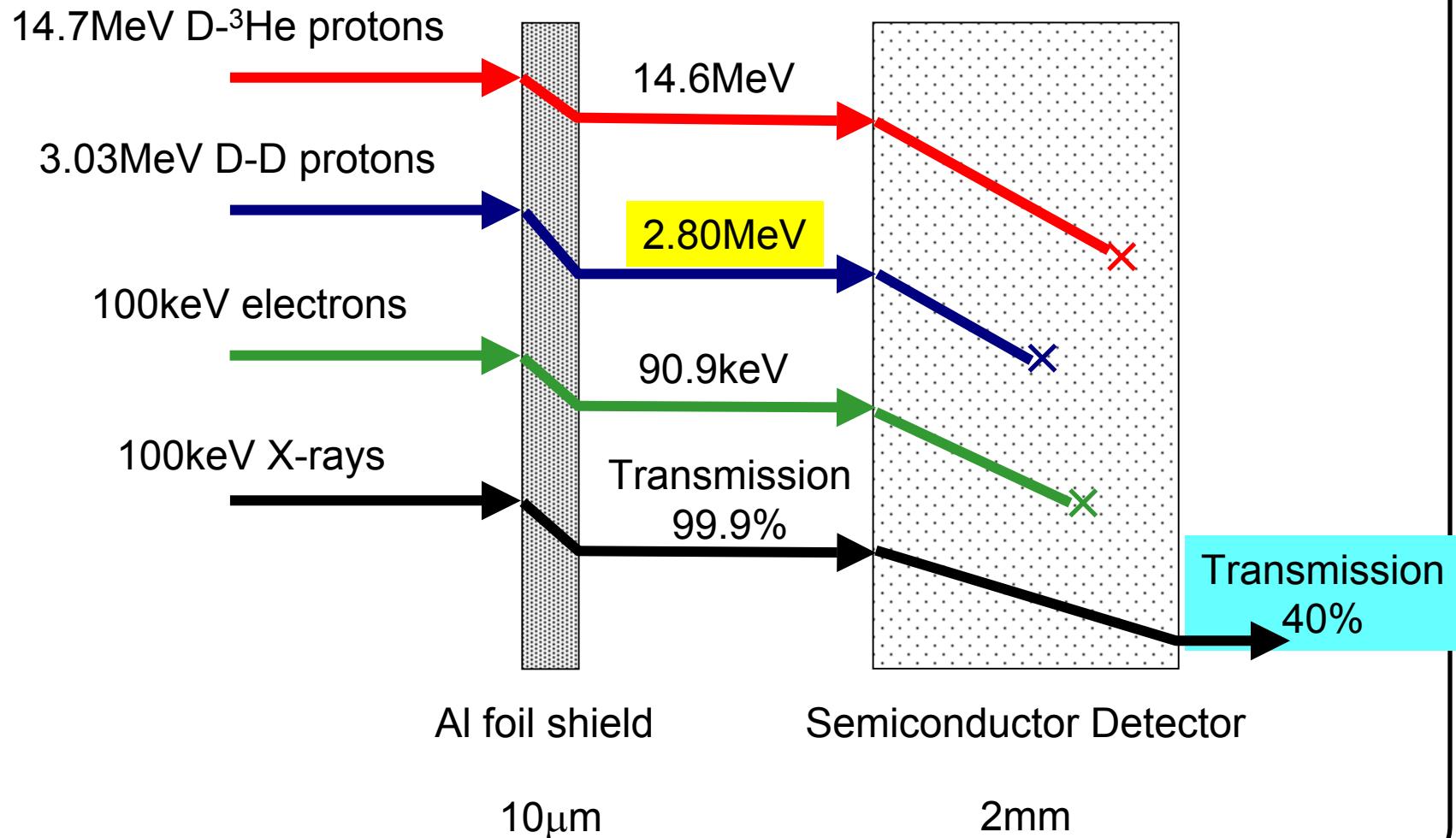


Attenuation of D-D Proton Energy with various foil thickness and material





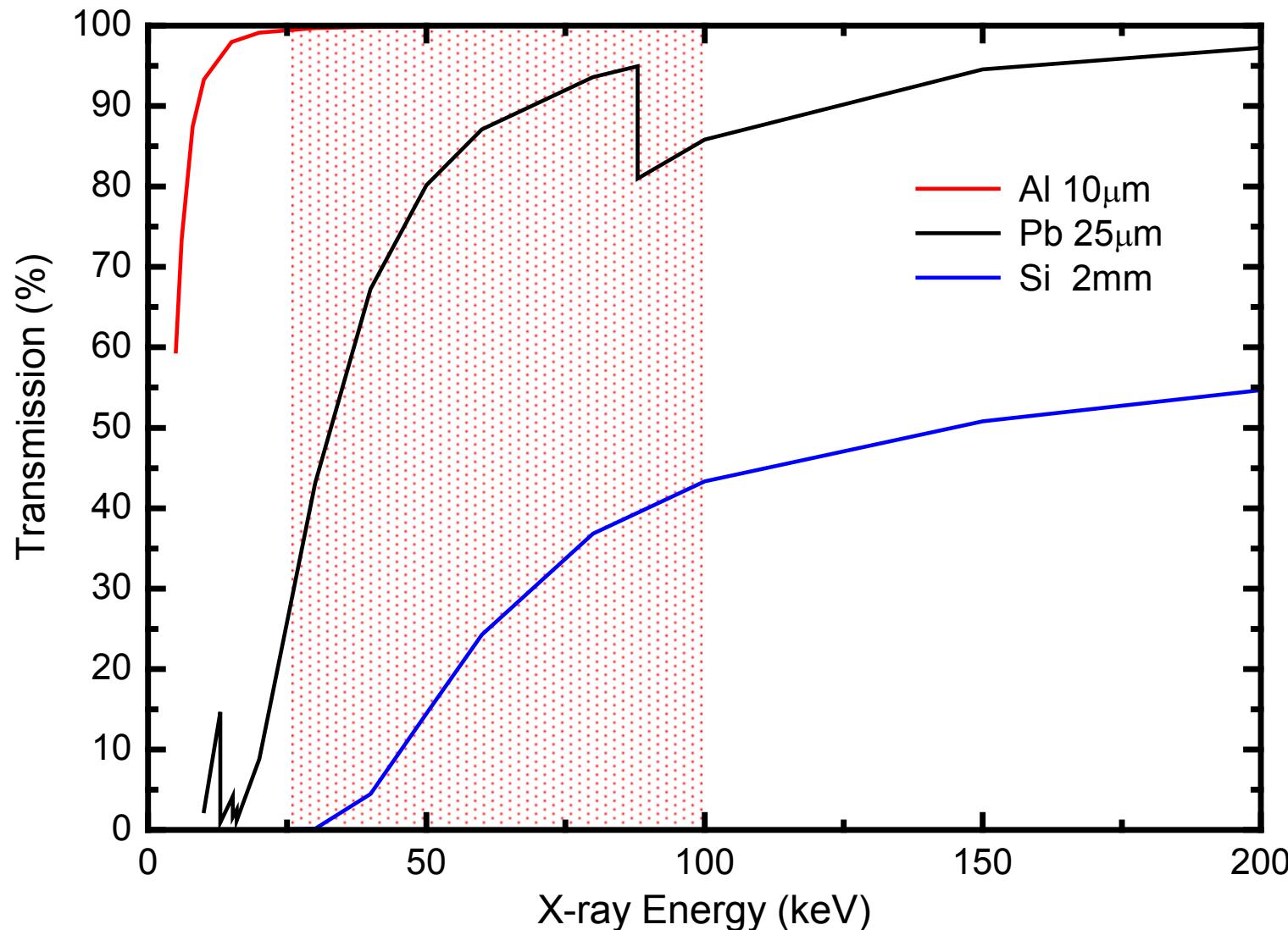
Al foil 10 μ m and the Si detector





Transmission of X-rays

with Al 10 μ m, Pb 25 μ m, Si 2mm



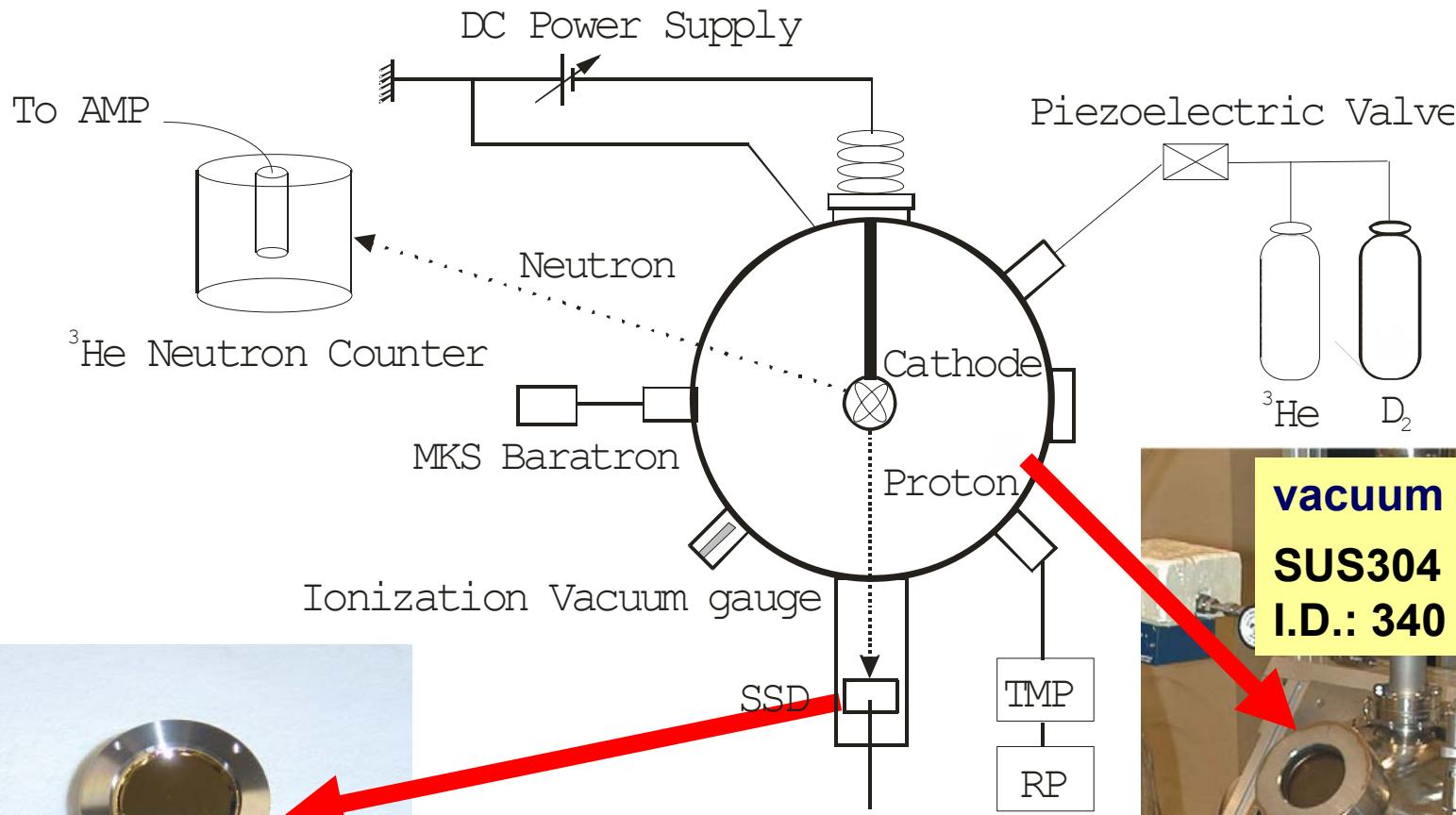


Foil shielding characteristics

	3.03MeV Proton (MeV)	14. 7MeV Proton (MeV)	100keV Electron (keV)	100keV X-ray (%)
Pb 25μm	1.87	14.3	22.3	85.8
Al 10μm	2.80	14.6	90.9	99.9
W 15μm	1.77	14.3	11.2	88.5



Experimental setup



Solid-State Detector (SSD)

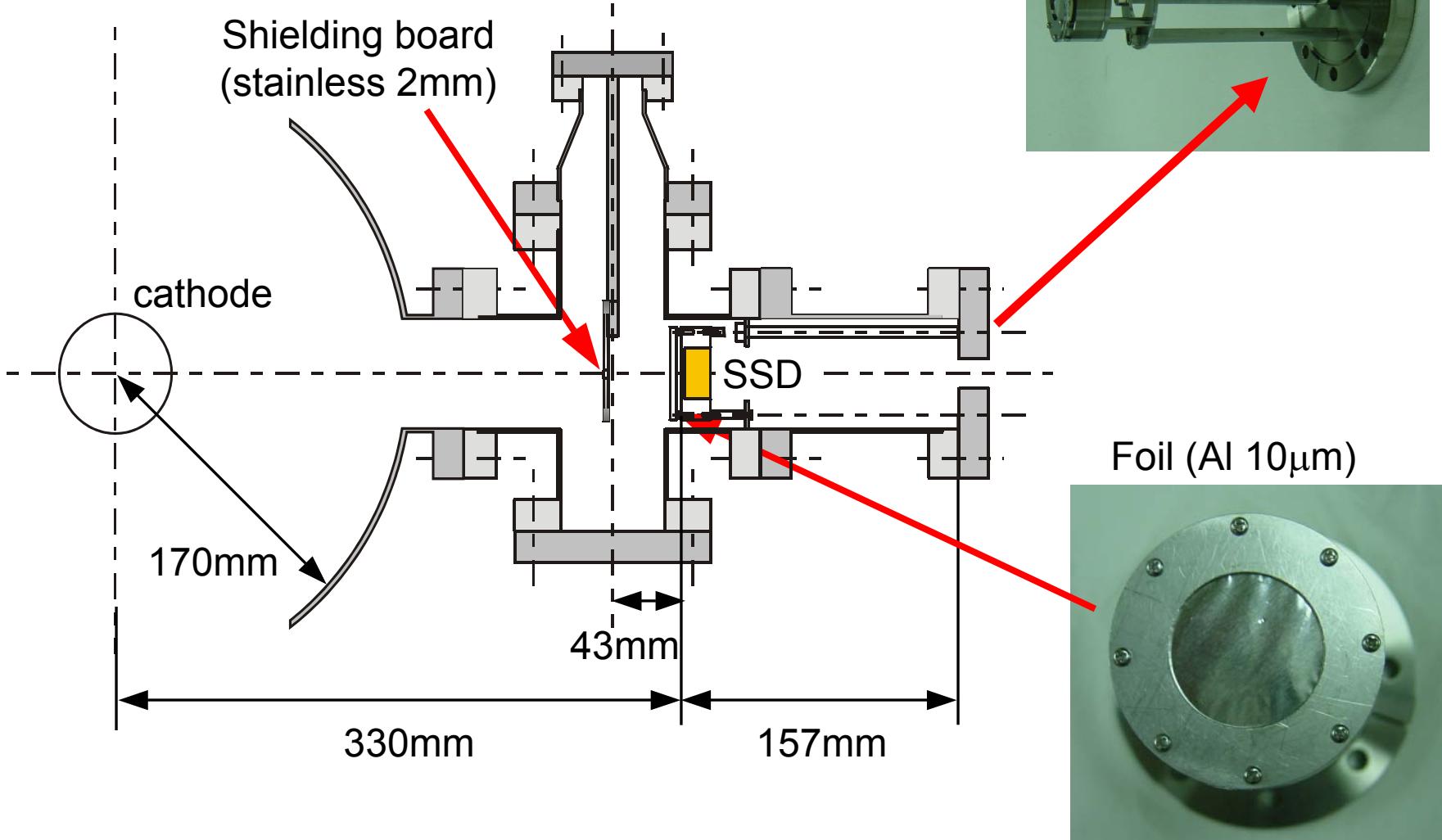
Depletion region thickness: 2 mm
Active area: 600 mm²



vacuum chamber
SUS304
I.D.: 340 mm

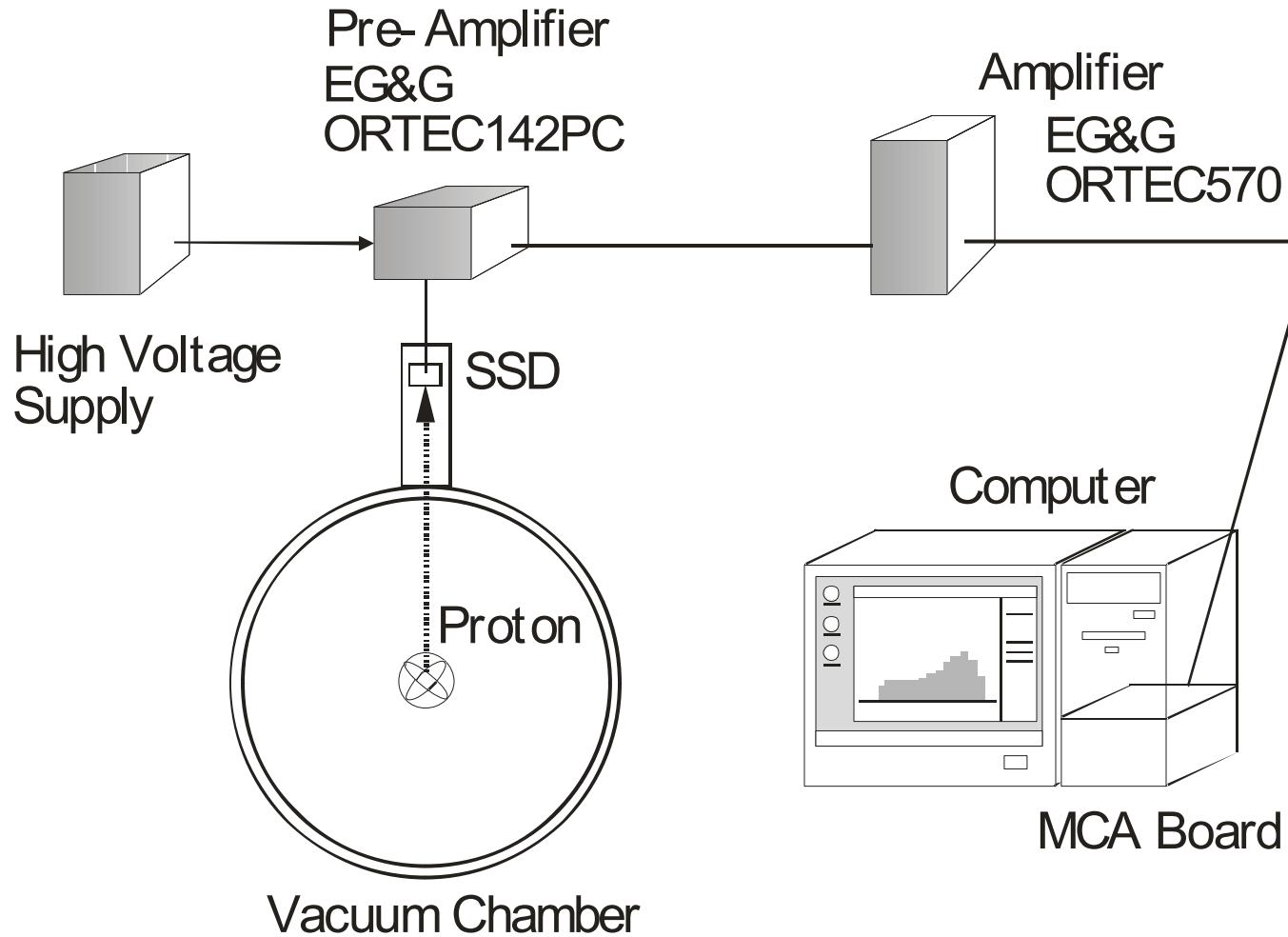


Schematic configuration of a Proton counting system



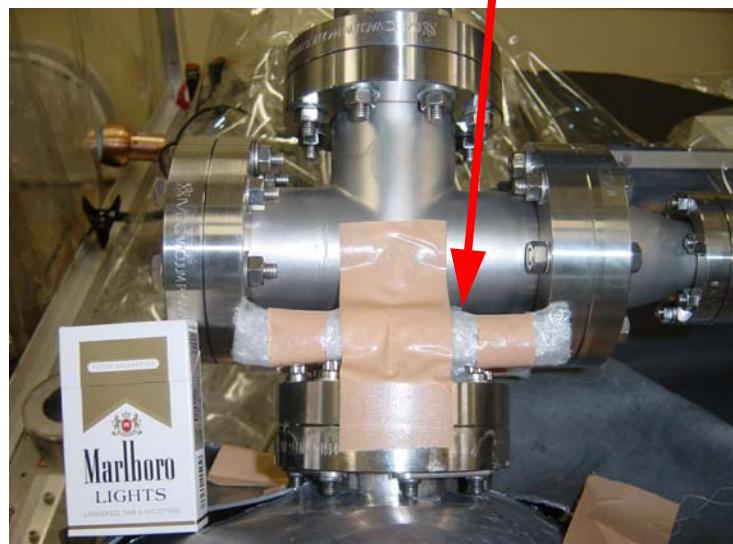
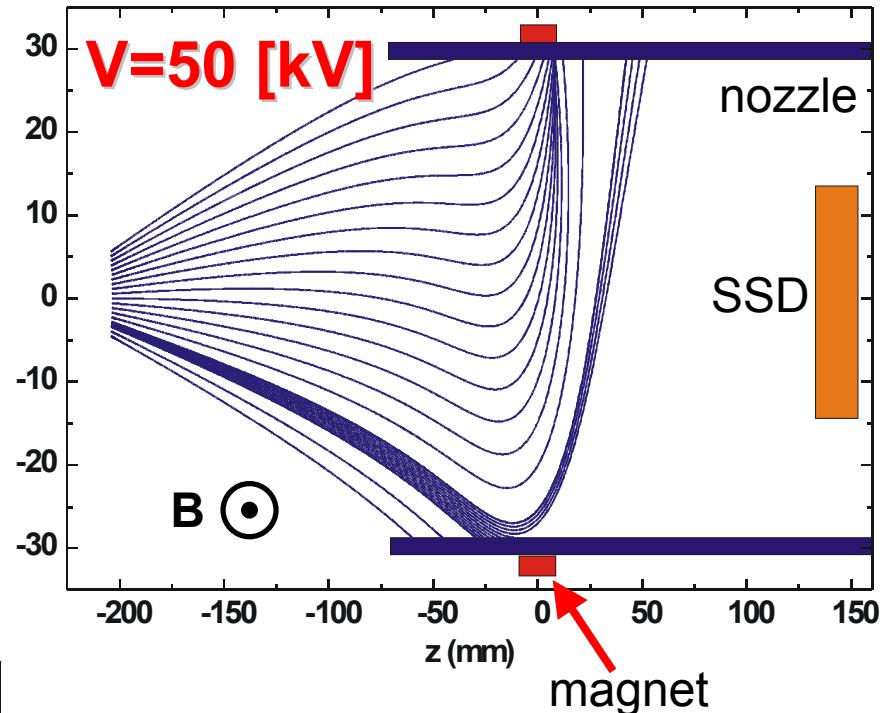
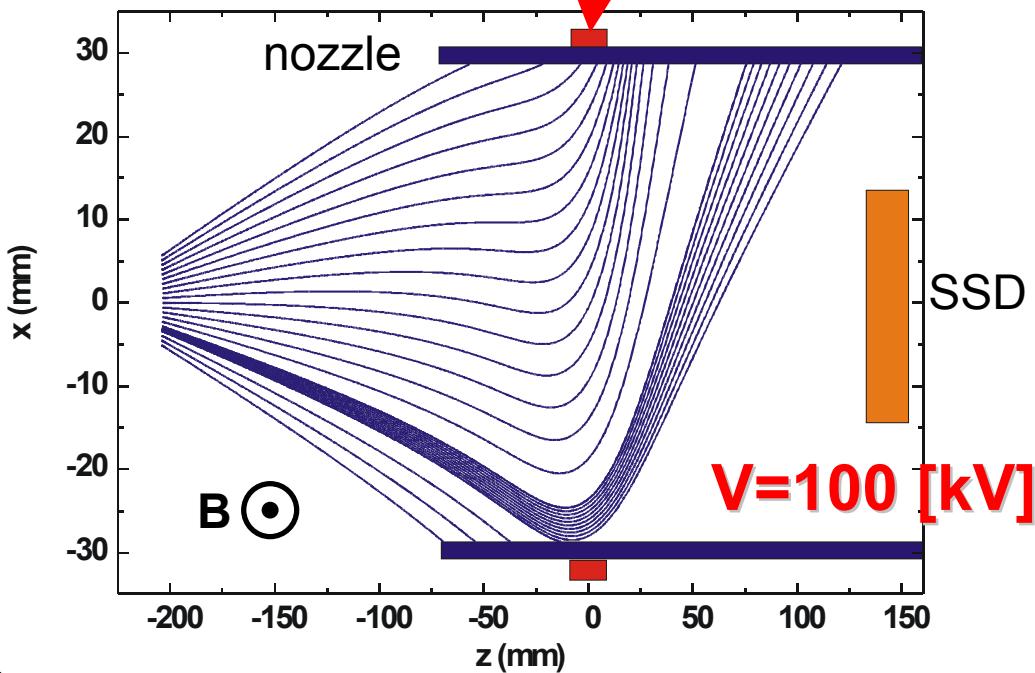
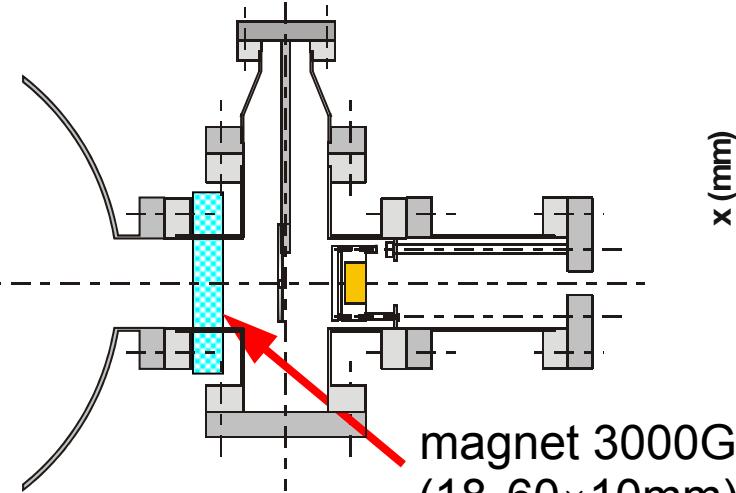


Diagnostics for proton counting



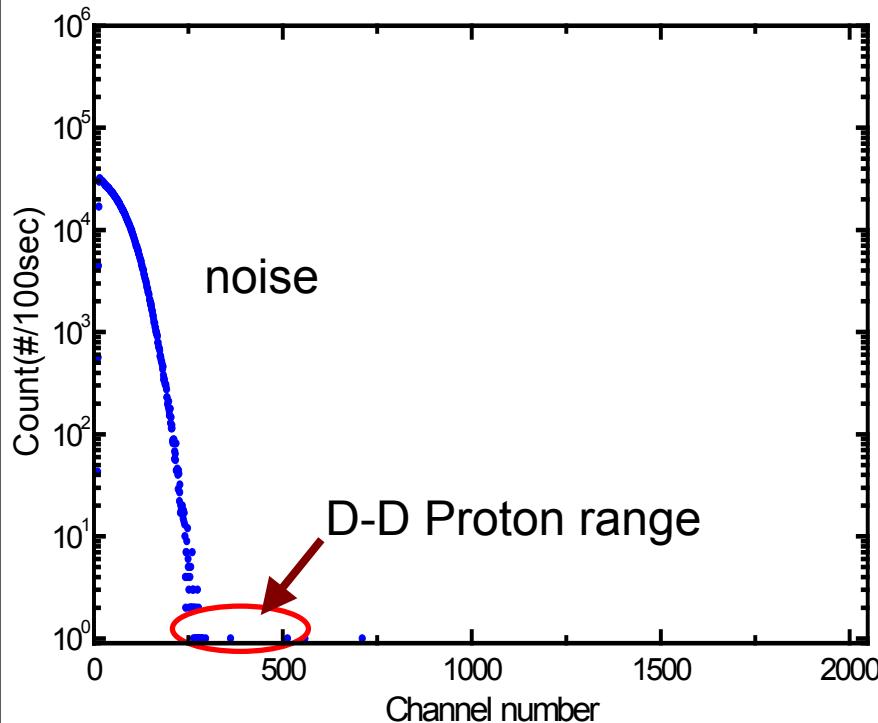


Electron Trajectory



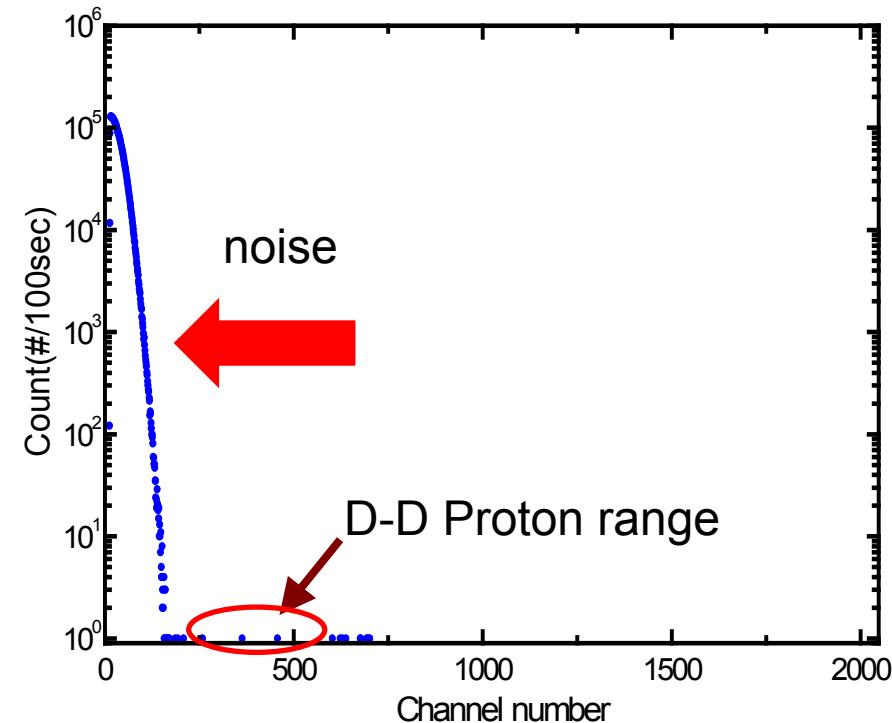


Proton count with or without magnet



$I=1\text{mA}$, $V=30\text{kV}$, $P=1.0\text{Pa}$, 100sec

Without magnet

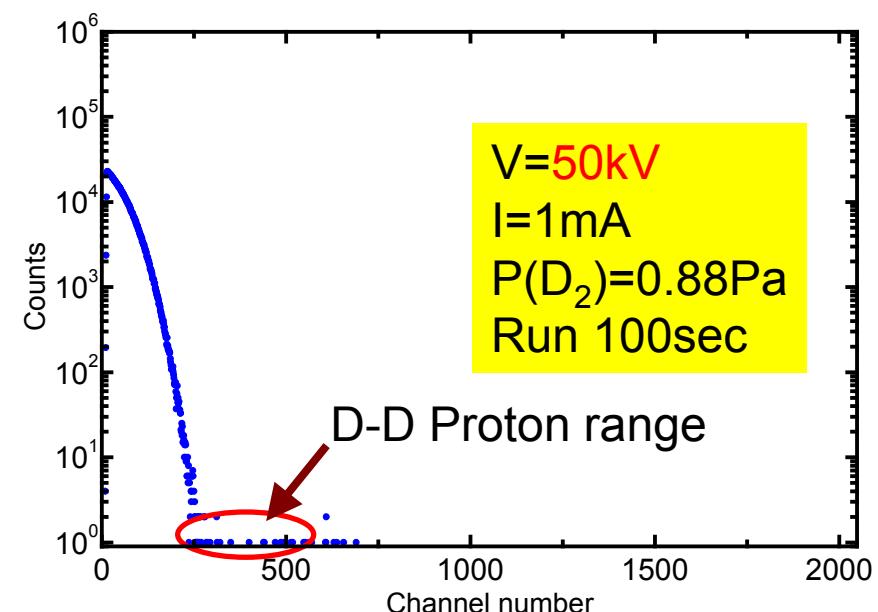
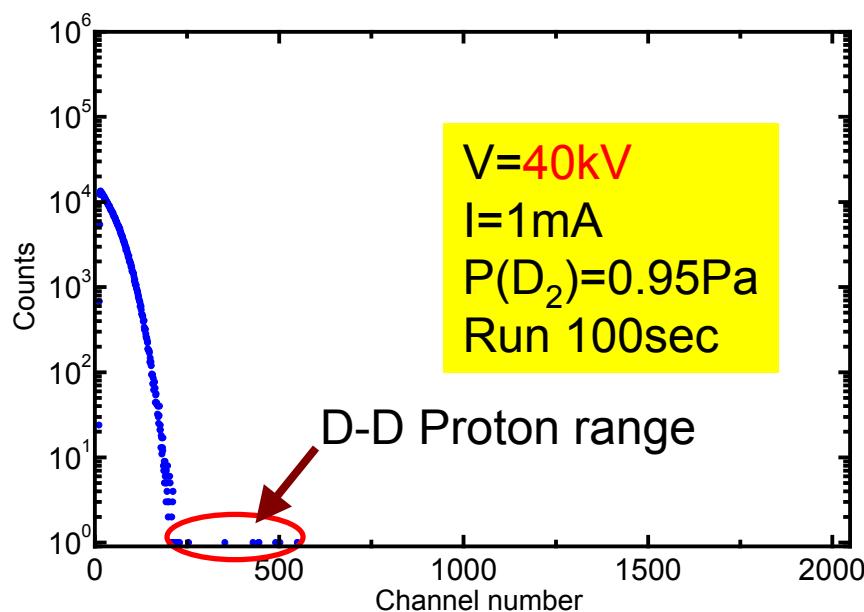
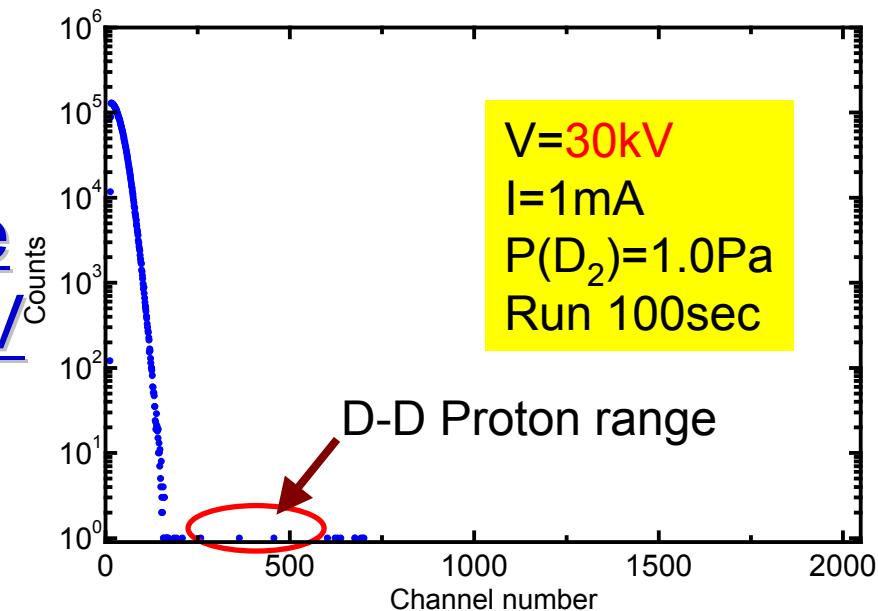


$I=1\text{mA}$, $V=30\text{kV}$, $P=1.0\text{Pa}$, 100sec

With magnet

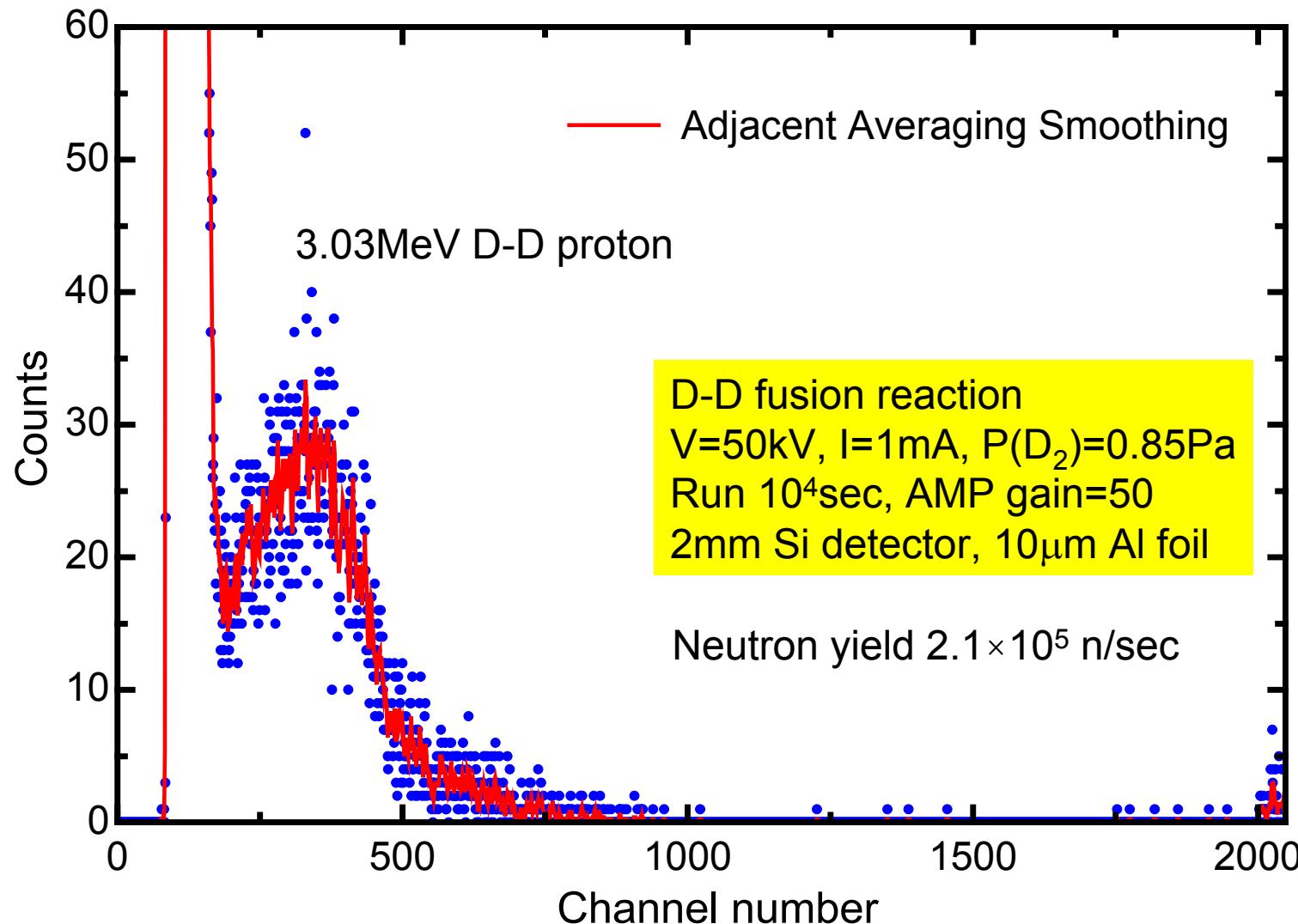


Proton count at IEC cathode voltages of 30, 40, and 50kV



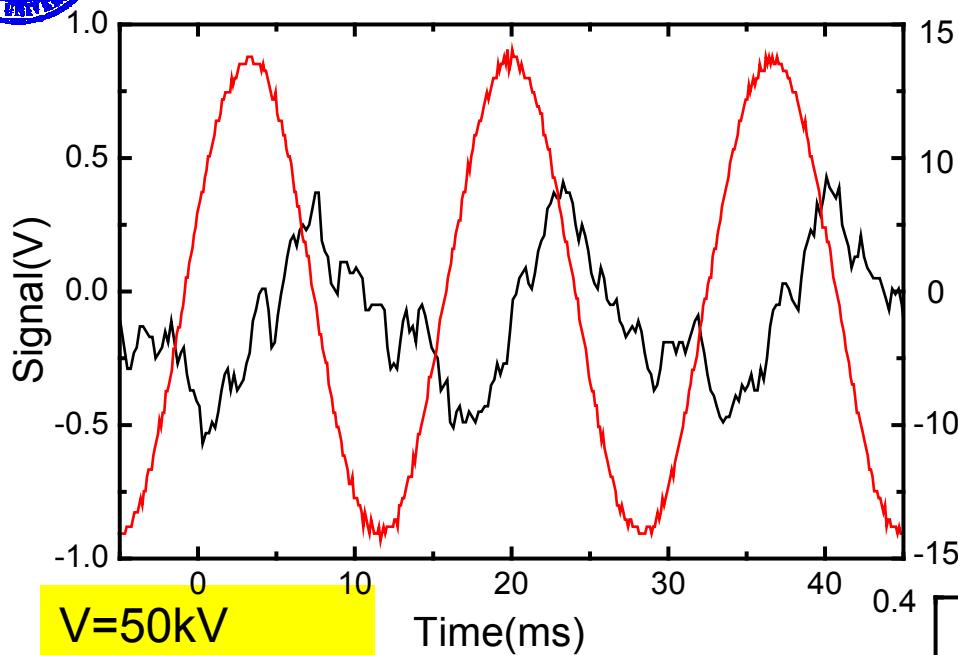


Proton count for 10^4 seconds





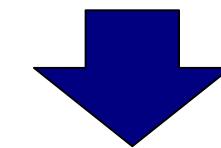
SSD signal from Preamplifier



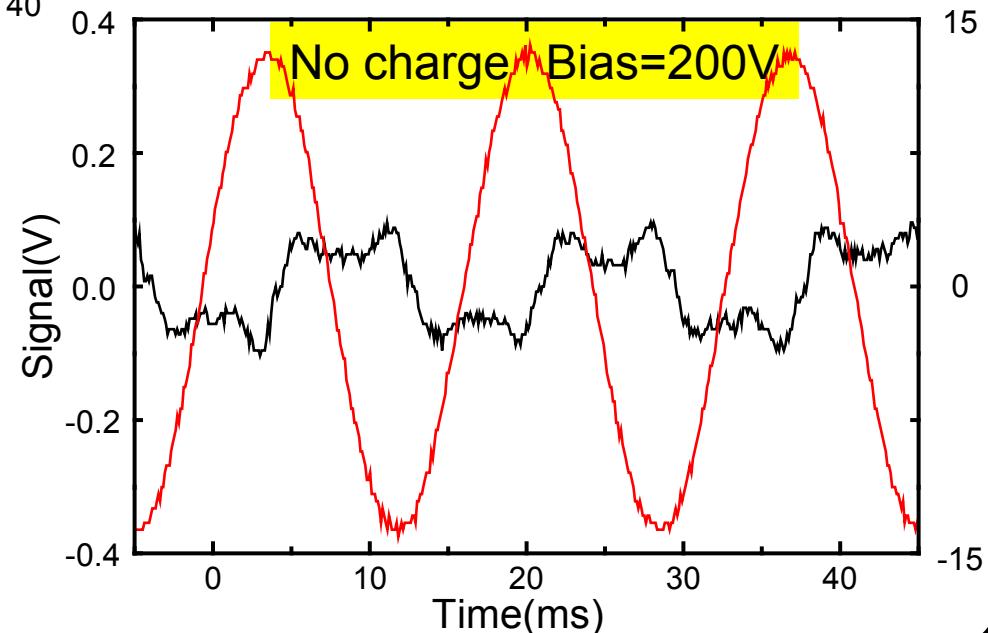
V=50kV
I=1mA
 $P(D_2)=0.85\text{Pa}$
Bias=200V

— AC signal 60Hz
— Preamplifier signal

noise on preamplifier signal

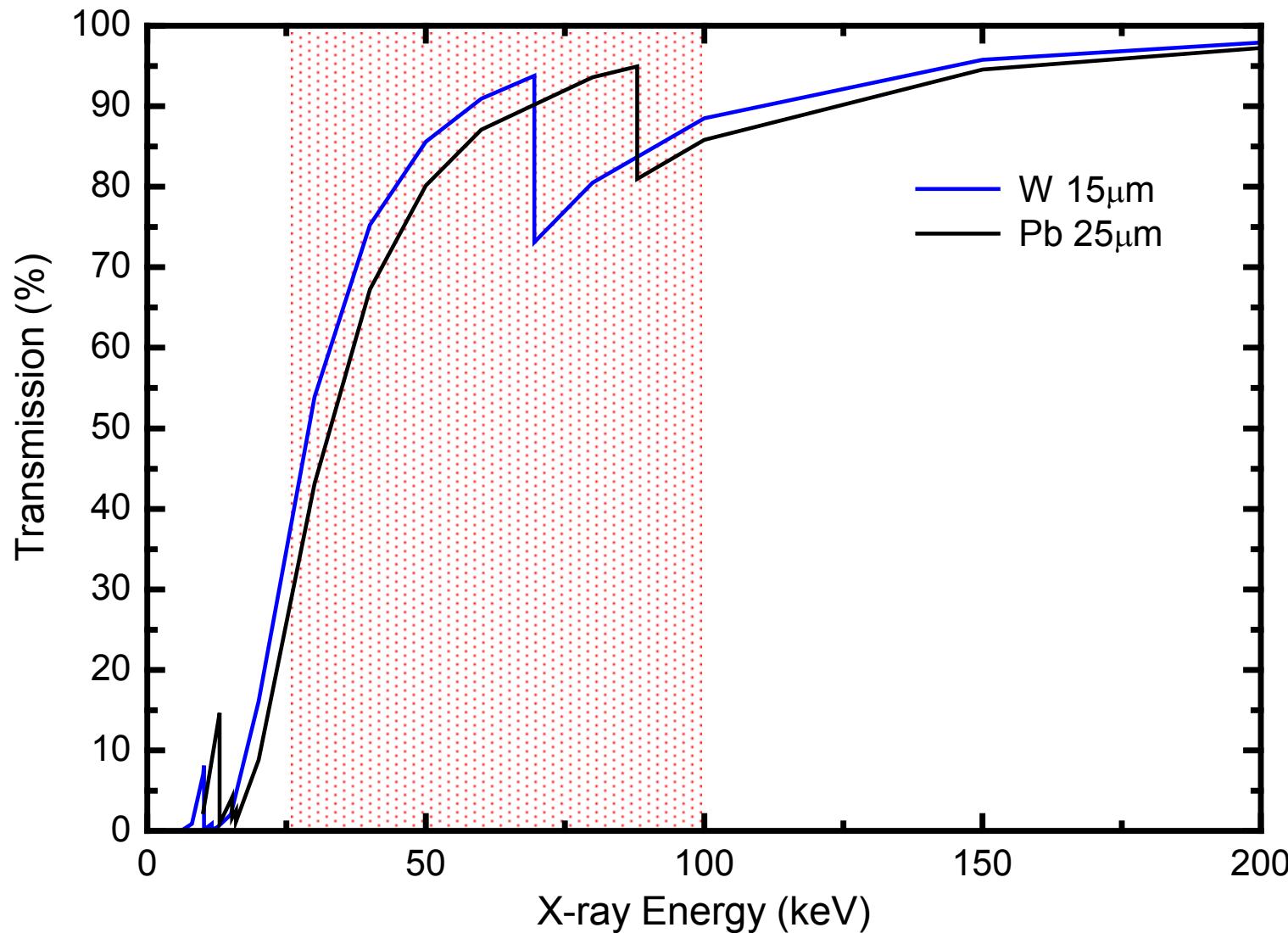


FWHM → wide
S/N ratio → bad





Attenuation of X-rays with Pb 25 μ m, W 15 μ m





Foil shielding characteristics

	3.03MeV Proton (MeV)	14. 7MeV Proton (MeV)	100keV Electron (keV)	100keV X-ray (%)
Pb 25μm	1.87	14.3	22.3	85.8
Al 10μm	2.80	14.6	90.9	99.9
W 15μm	1.77	14.3	11.2	88.5



Summary

Proton count using SSD was made.

We examined an optimal shielding foil thickness and material.

The noise is reduced by using deflection magnetic field.



Future work

Reduce 60Hz noise on preamplifier signal

Examine W 15mm or Pb 25mm foil to know effect of X-rays noise.

Count proton through D-³He reaction.

For more information contact
Satoshi OGAWA
satoshi@iae.kyoto-u.ac.jp

Progress in Explosives Detection using D-D Fusion

at the University of Wisconsin-Madison

A.L. Wehmeyer

**E.C. Alderson, R.P. Ashley, D.R. Boris, G.A. Emmert,
R.C. Giar, G.L. Kulcinski, G.R. Piefer,
R.F. Radel, T.E. Radel, and J.F. Santarius**

*Fusion Technology Institute
University of Wisconsin
Madison, WI*

Outline

- Background
- Experimental Objective
- Theory of Explosives Detection
- Experimental Setup
- Modeling Experiment in MCNP5
- MCNP5 Calculational Results
- Experimental Results without Explosives
- Summary
- Future Work



Background Information

- Thermal neutron activation analysis (TNAA) can be used for detecting common explosives.
- Typical explosive compositions contain low Z material (C, H, N, O).
- Composition 4 (C-4), a military plastic explosive, is approximately 90% RDX by weight (RDX – $\text{C}_3\text{H}_6\text{N}_6\text{O}_6$).

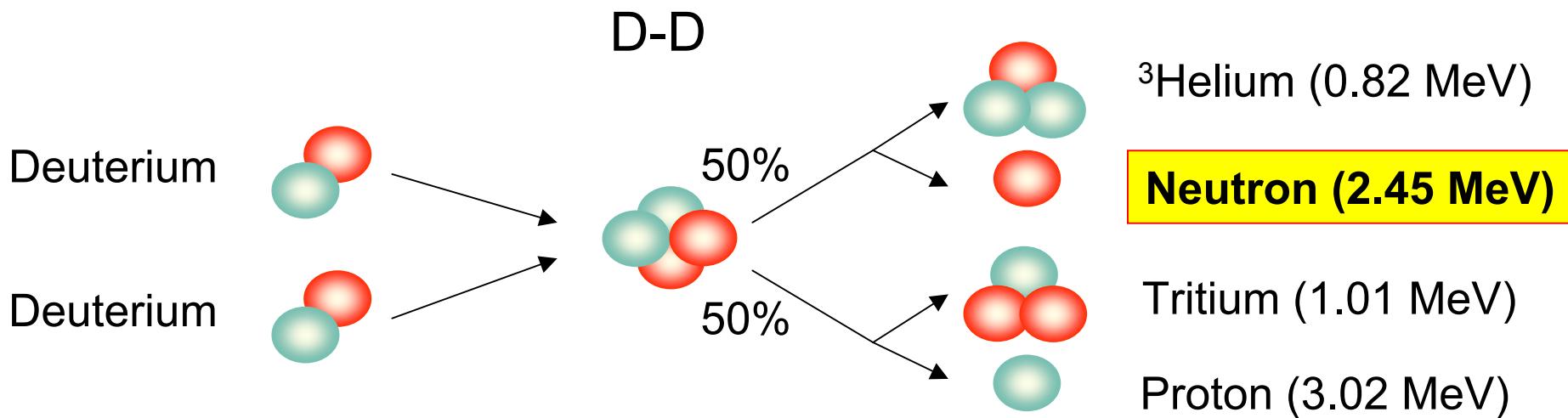


Package Containing 24 –
20g vials
of Composition 4 (C-4)

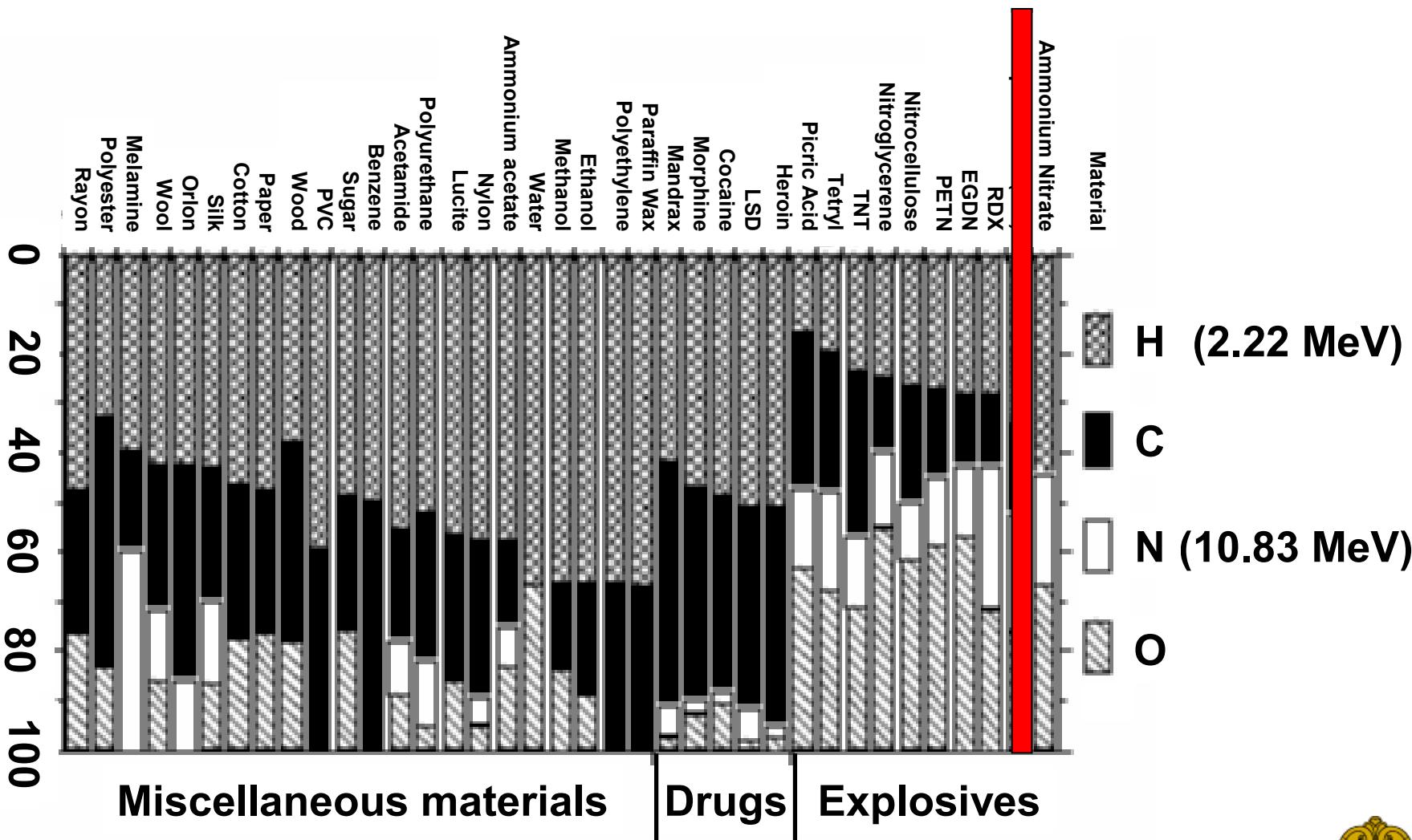


Experimental Objective

- Proof-of-principle experiment to detect explosives using the D-D fusion reaction in an IEC device.



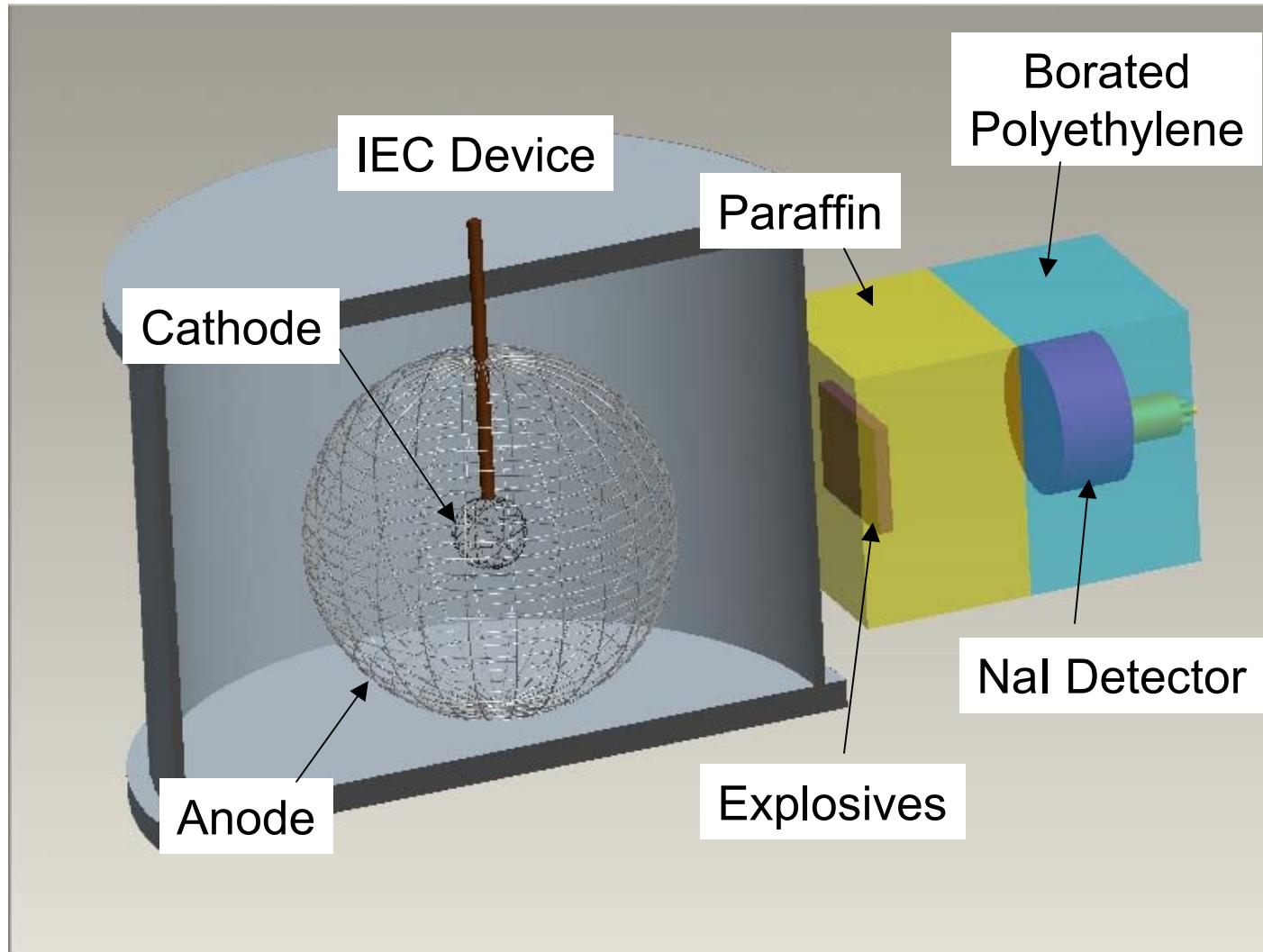
Characteristic gamma rays from hydrogen and nitrogen can be detected using TNAA



Source: A. Buffler, "Contraband Detection by Fast Neutron Scattering," presented at the 2nd National Nuclear Technology Conference, NAC, South Africa, May 14-15, 2001.



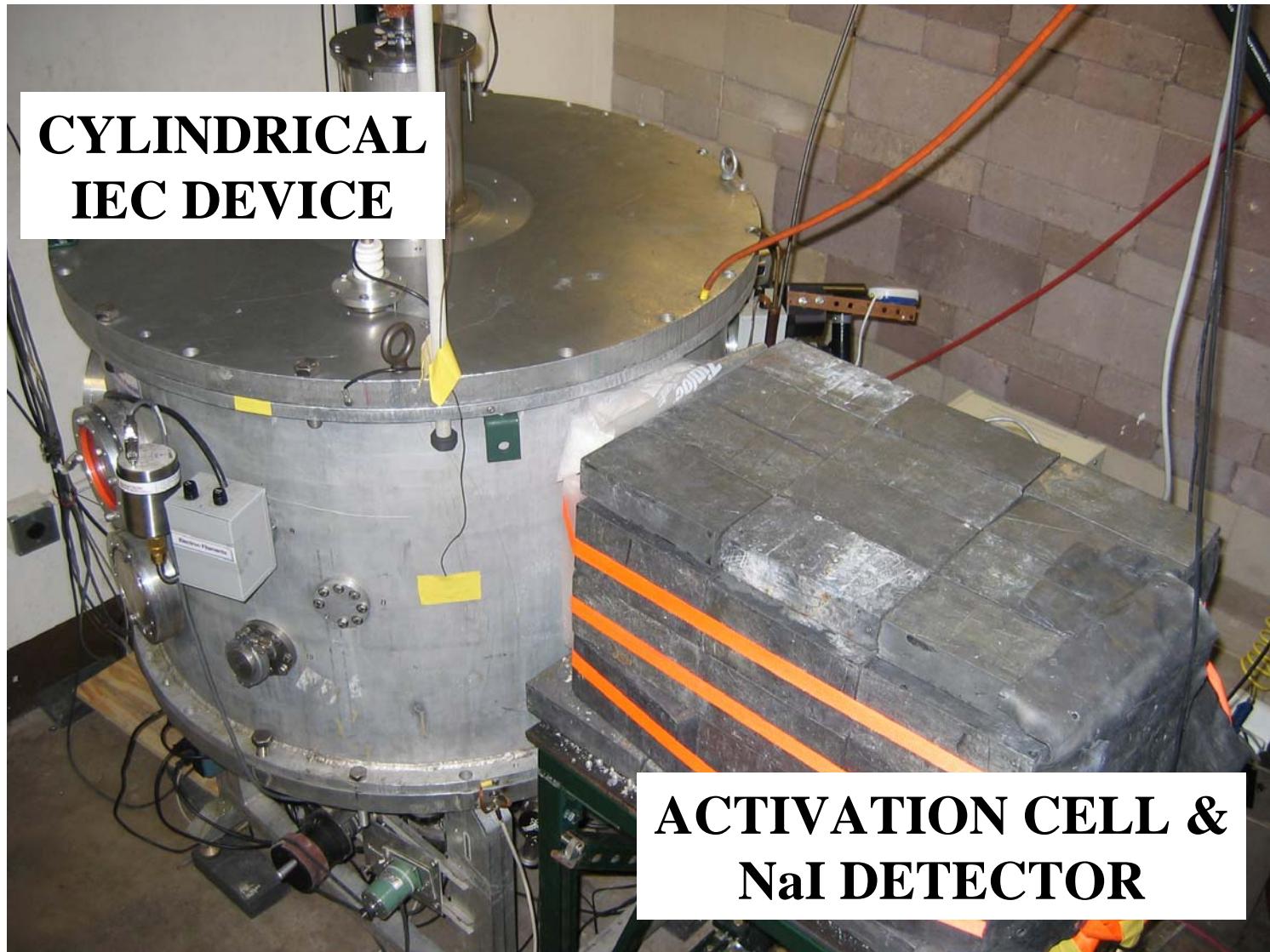
CAD Representation of UW Experimental Setup for Explosives Detection



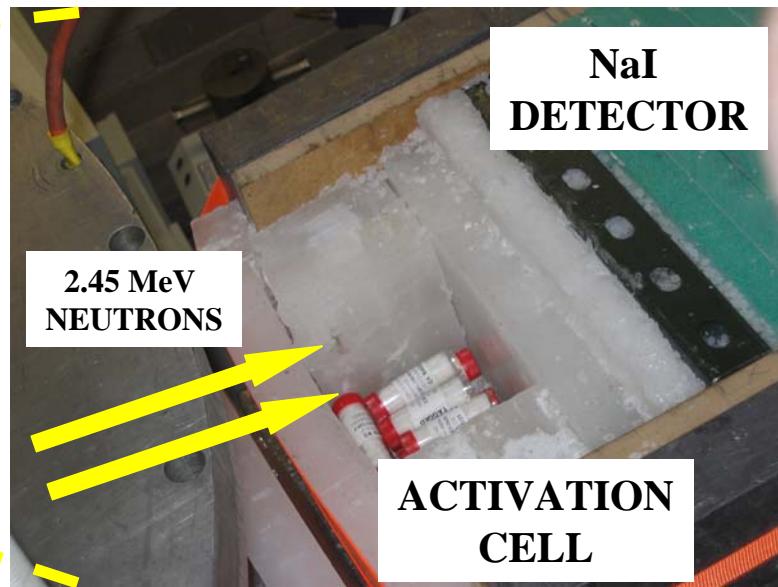
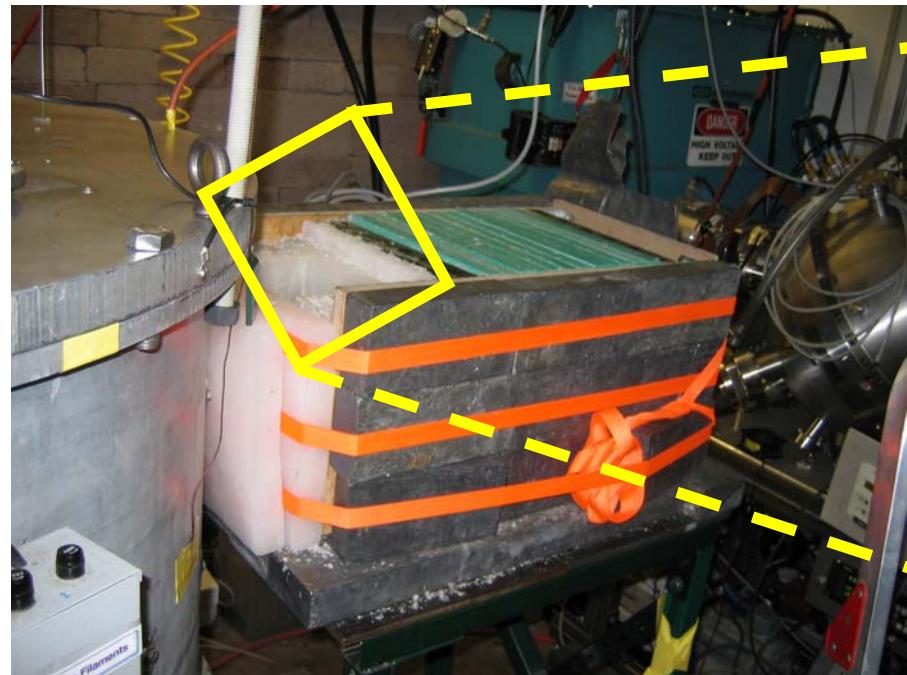
Source: Greg Sviatoslavsky, FTI, University of Wisconsin



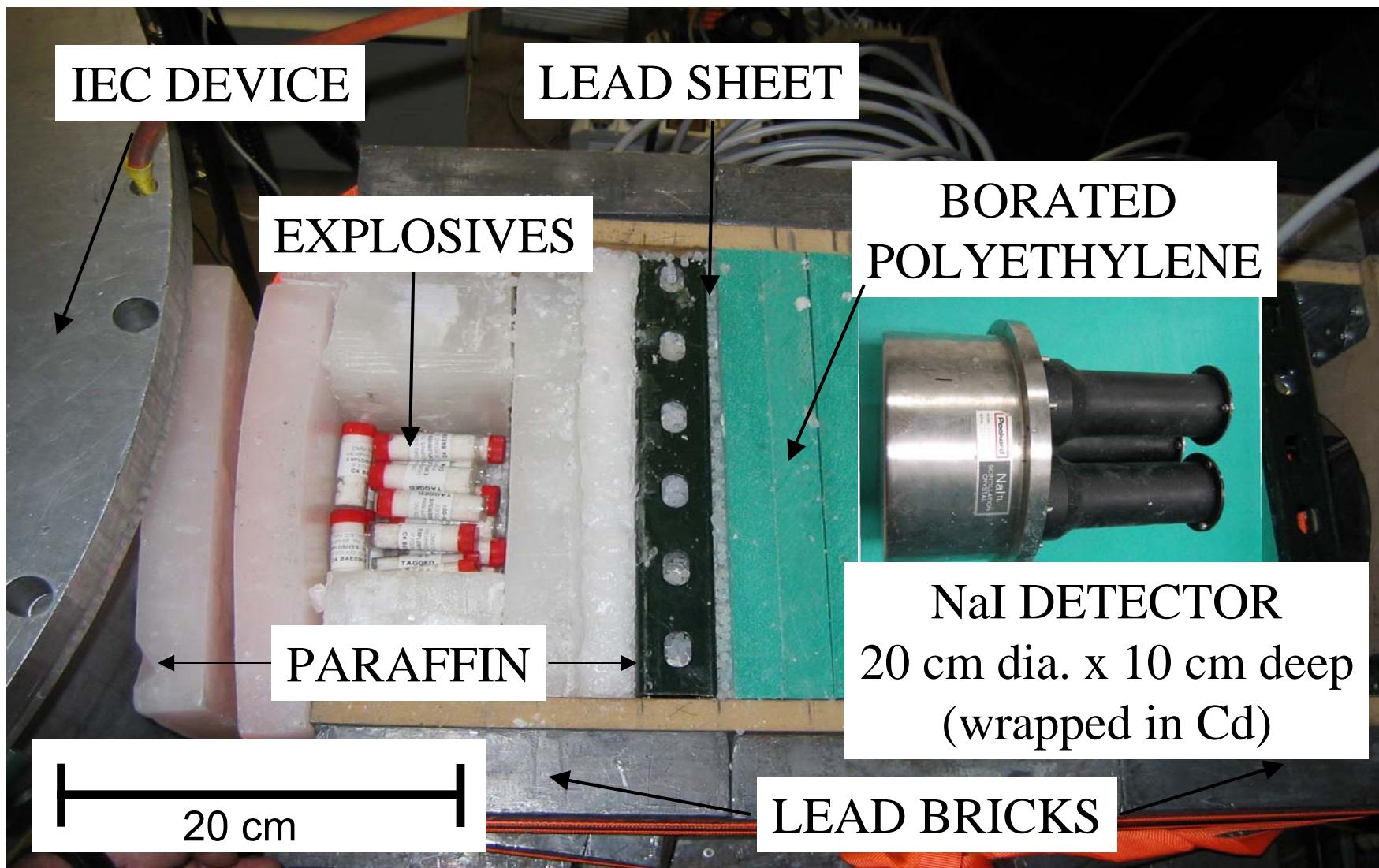
UW Experimental Setup for Explosives Detection using IEC Fusion



UW Experimental Setup for Explosives Detection using IEC Fusion (cont.)

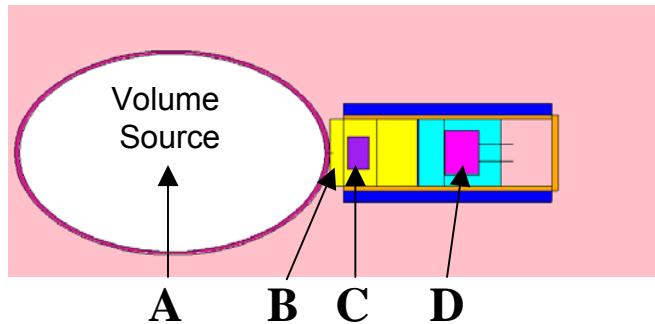


UW Experimental Setup for Explosives Detection using IEC Fusion (cont.)

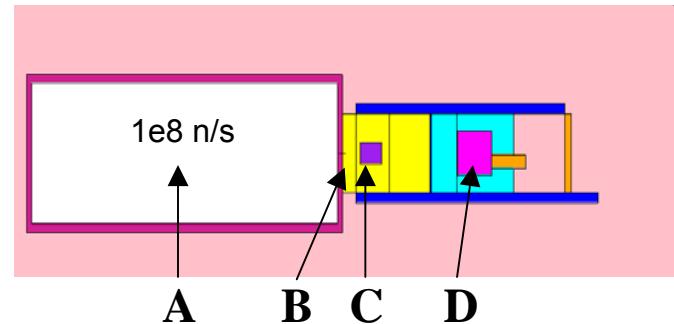


MCNP Model of UW Experimental Setup for Explosives Detection and MCNP Results

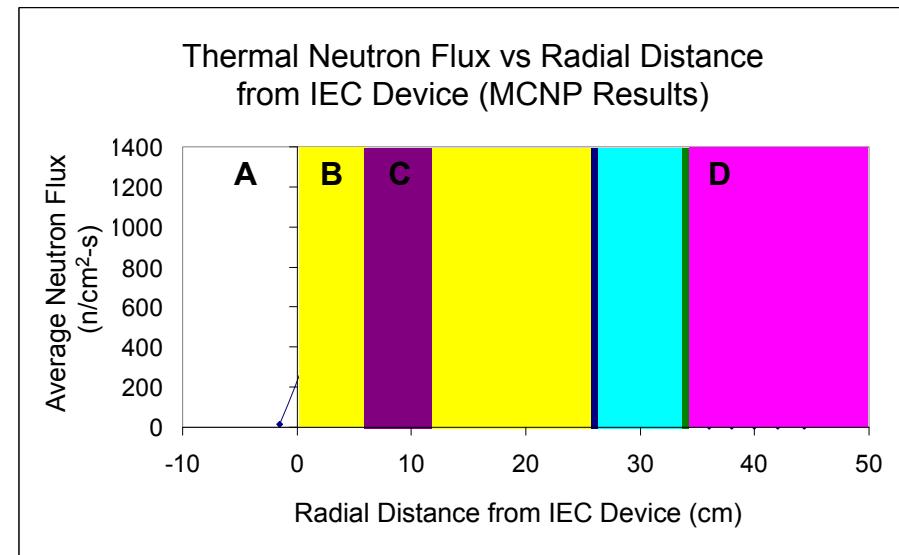
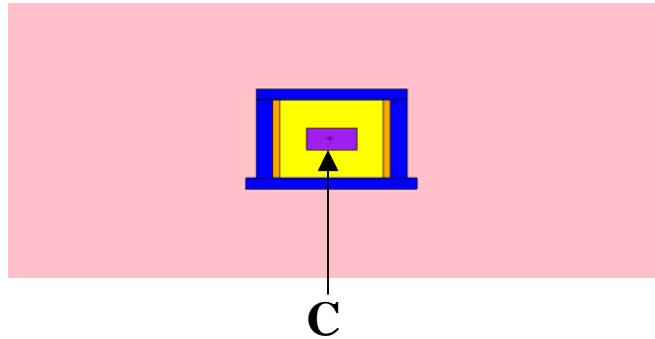
TOP VIEW



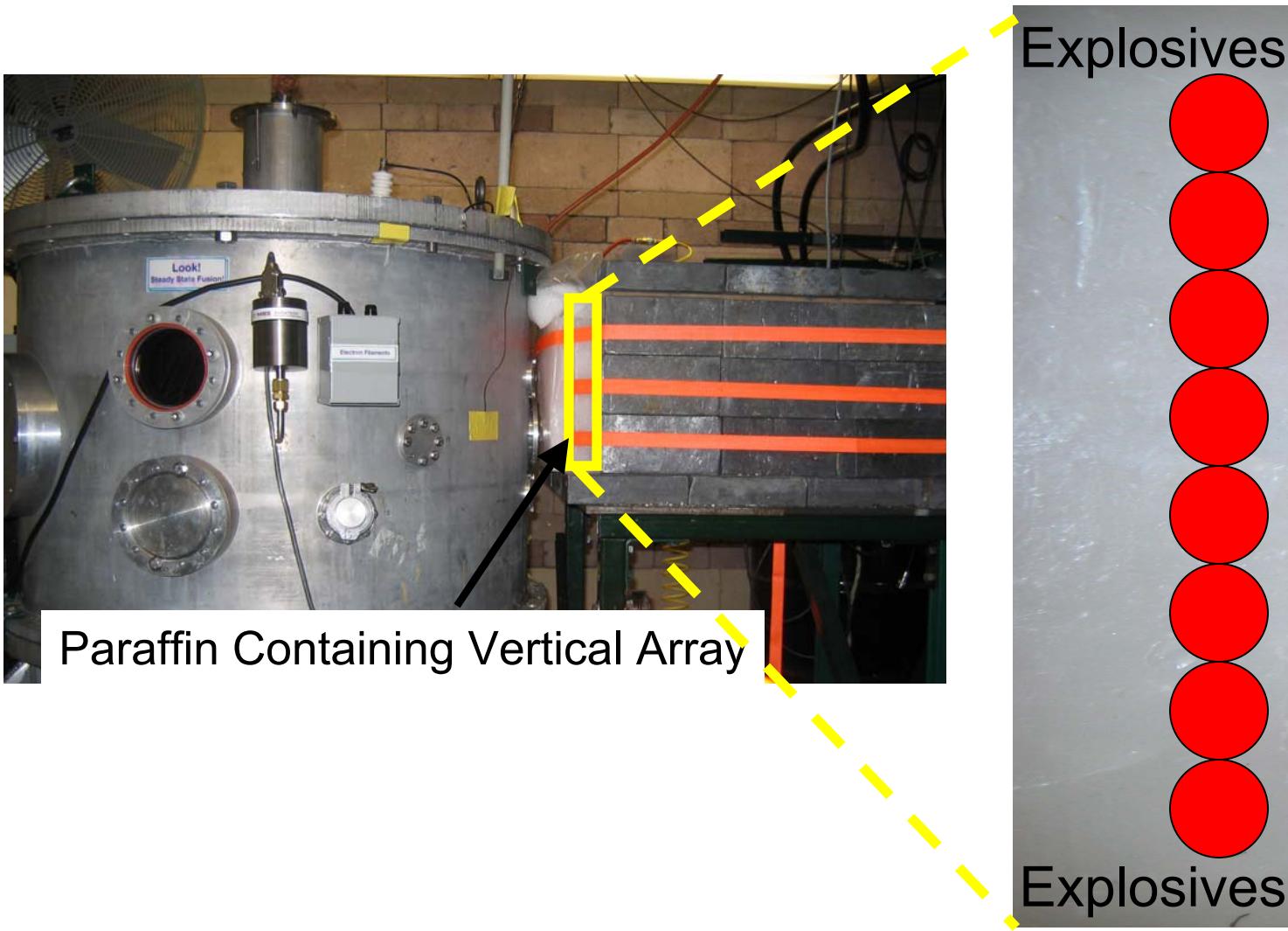
SIDE VIEW



FROM CENTER OF
EXPLOSIVES

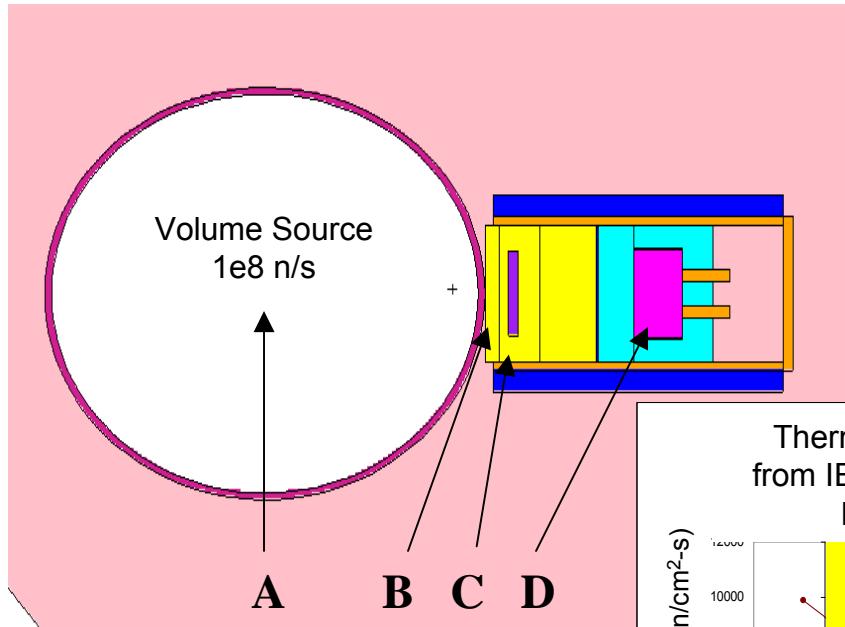


Changed to Vertical Explosives Array Configuration based on MCNP Results

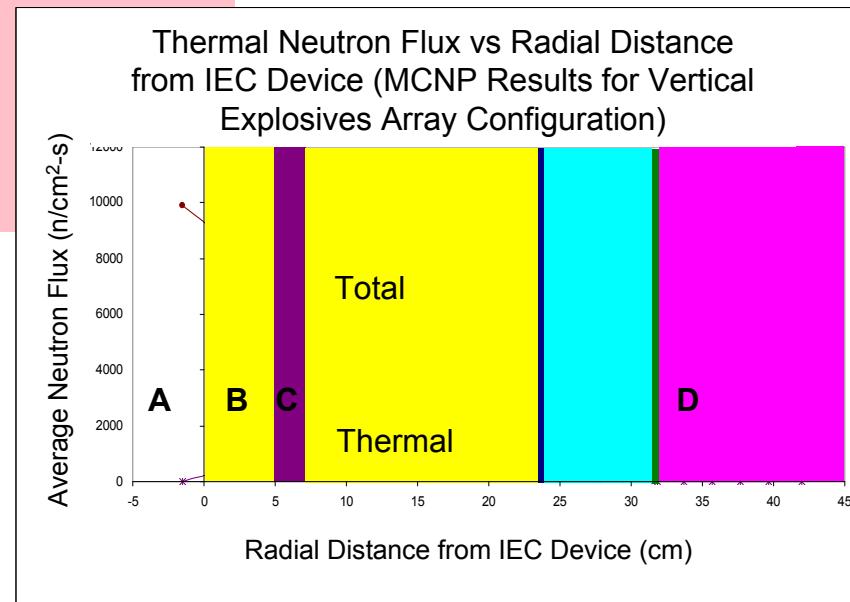


MCNP Model and Results from Vertical Explosives Array Configuration

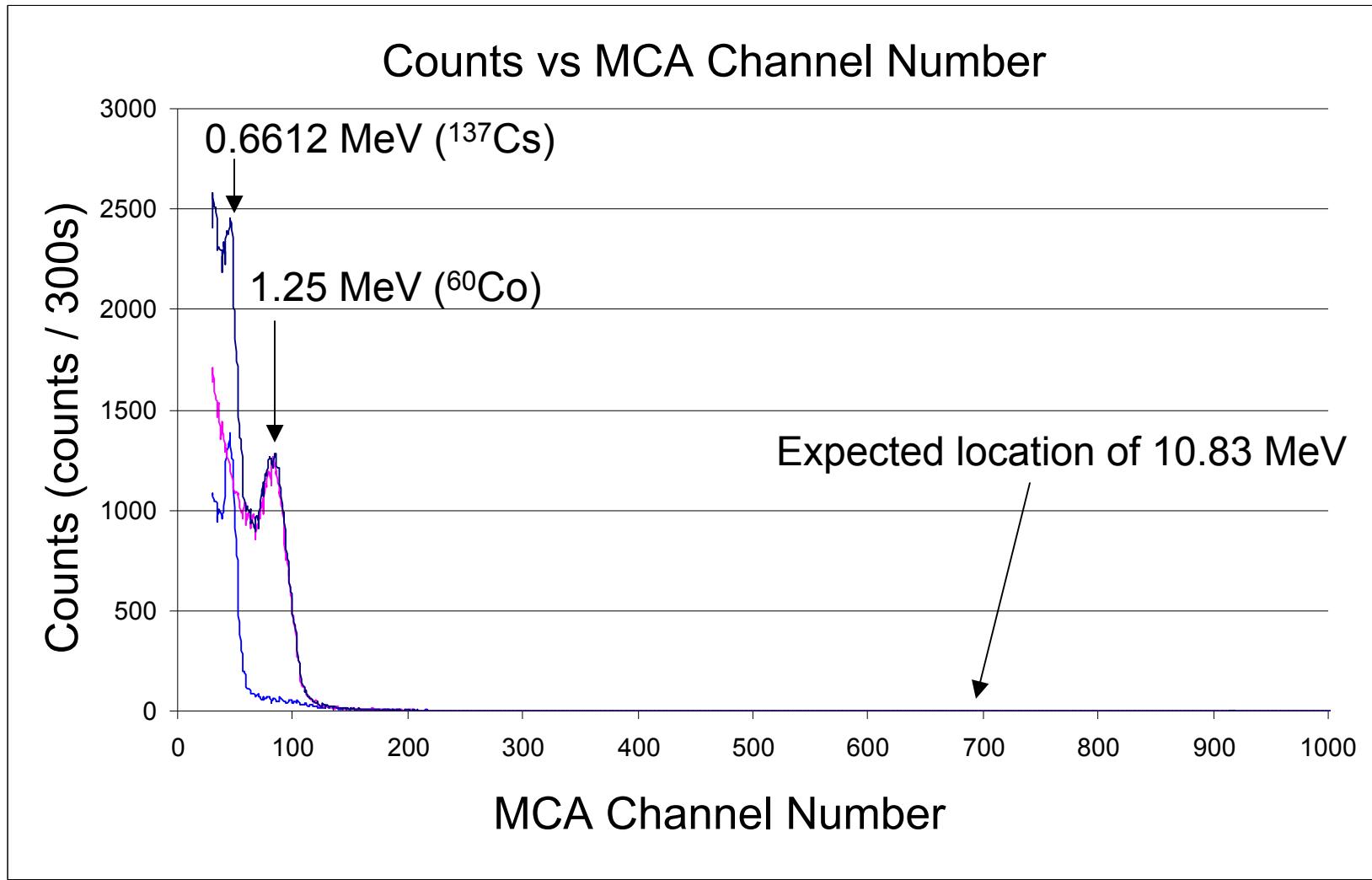
TOP VIEW



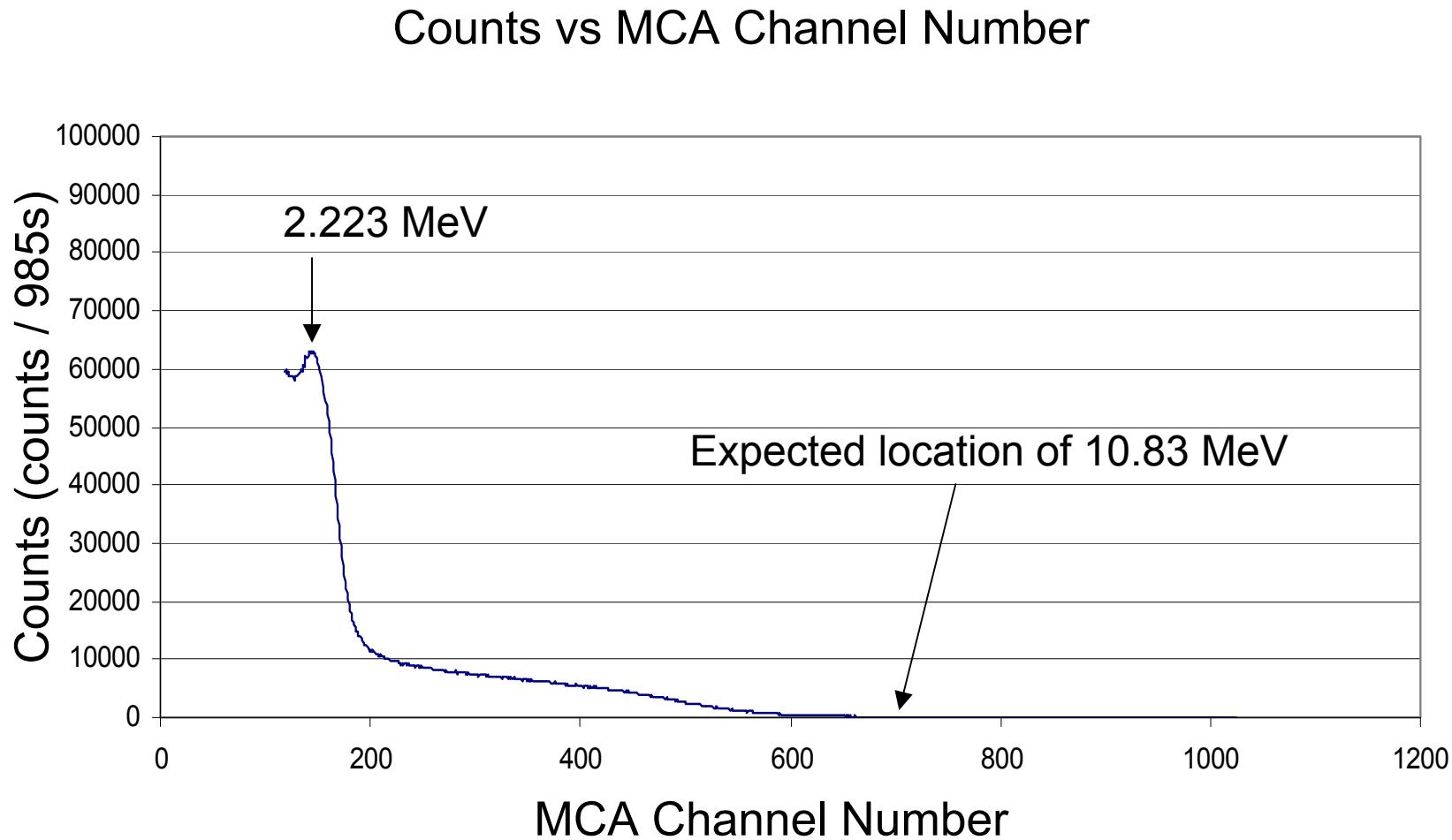
Avg thermal neutron flux increased from $856 \text{ n/cm}^2\text{-s}$ to $1220 \text{ n/cm}^2\text{-s}$ within the C-4



NaI Detector Calibration with two known sources (^{137}Cs and ^{60}Co)



Experimental Results from D-D Fusion Neutrons without Explosives



Summary

- Completed preliminary UW experimental setup for explosives detection.
- Completed preliminary MCNP5 model of UW experimental setup for explosives detection.
- Optimized placement of explosives within activation cell based on MCNP5 calculations.
- Successfully calibrated NaI detector and performed initial experiments without explosives



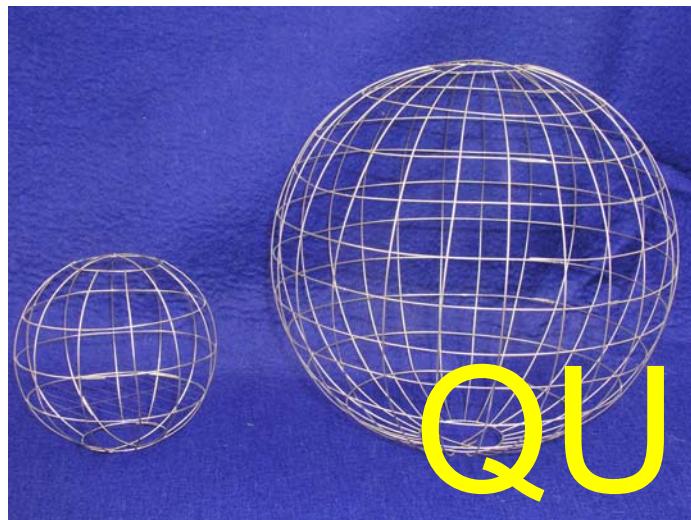
Future Work

- Conduct experiments with explosives (C-4, TNT, Urea fertilizer)
- Further refinement of MCNP5 model to include tally for (n,γ) reactions for ^{14}N and tally for pulse height detector output
- Increase shielding on backside of experimental setup and move detector closer to explosives
- Increase neutron production rates
 - Increase cathode voltage and current
 - Vary cathode size
 - Vary cathode to anode distance



Preliminary work has begun on studying different factors which might affect neutron production rates

Cathode Size



Cathode Geometry



QUESTIONS?

Cathode Material

Atomic Number	75	186.21	Atomic Weight
	Re		
Crystal Lattice	HCP	2,13,32, 18,8,2	Electron Shells

10 cm Inner Cathode Grid (Re)

Atomic Number	74	183.85	Atomic Weight
	W		
Crystal Lattice	BCC	2,8,18,3, 2,12,2	Electron Shells

10 cm Inner Cathode Grid (WRe)



Coaxial Neutron Generators Using RF-driven Plasmas

K. J. Chung, M. J. Park, H.D. Jung, J. Y. Park, S. H. Kim,
I. J. Kim, H.D. Choi and Yong-Seok Hwang

*Dept. of Nuclear Eng., Seoul National University
San 56-1, Shillim-dong, Gwanak-gu, Seoul, 151-744, KOREA*

E-mail: yhwang@snu.ac.kr

*7th US-Japan IEC Workshop
Los Alamos National Lab., USA
March 14-15, 2005*

Outline

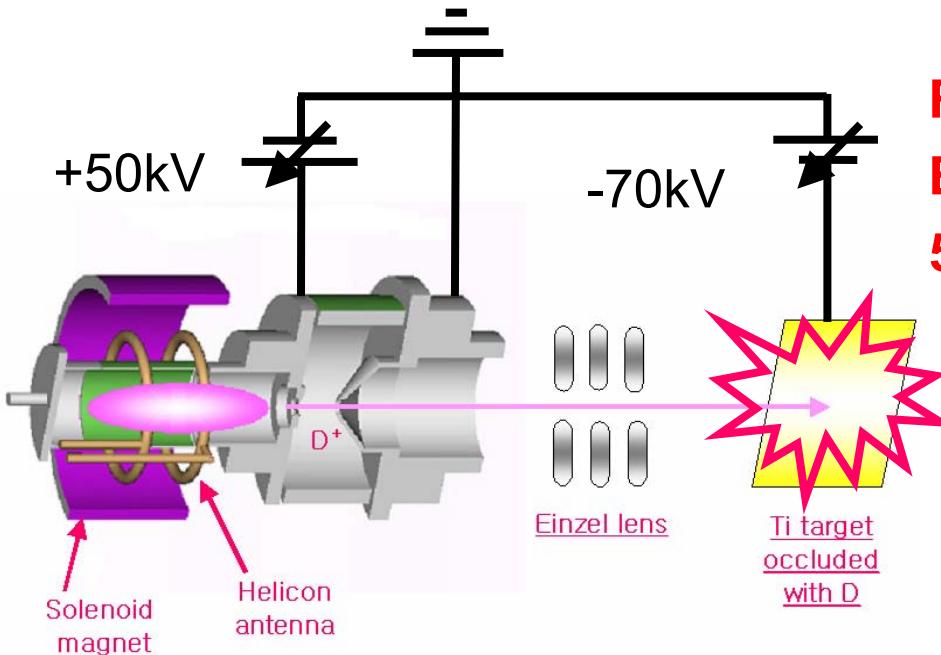
- ❑ *RF plasma ion sources for neutron generation?*
- ❑ *Neutron Generation and Detection with Helicon Ion Source*
- ❑ *Cylindrical Coaxial Neutron Generator*
 - *Experimental Setup*
 - *CW and Pulse Operation Results*
 - *PBGUNS Simulations and Discussions*
 - *Design Requirements for Cylindrical Device Upgrade*
- ❑ *Summary*

Why RF plasma ion source for neutron generation?

- **Low pressure & high density plasma generation**
→ *Reduced charge exchange reaction & high current density*
- **Independent control of plasma generation & acceleration**
→ *Convenient control of plasma & beam parameters*
- **High yield of mono-atomic species(D⁺)**
→ *High fusion reaction cross section*
- **Long lifetime**
- Both CW & pulsed operation
- Versatile utilization of magnetic field configuration
→ *Enhanced flexibility*

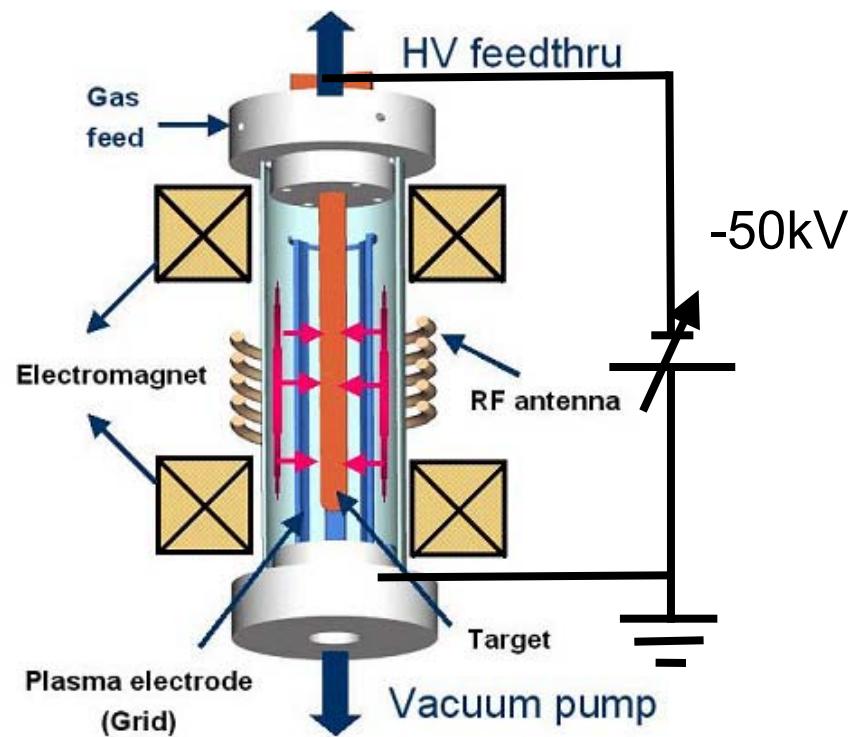
Efficient & high yield neutron generation

Neutron Generators Based on RF Plasma Ion Sources

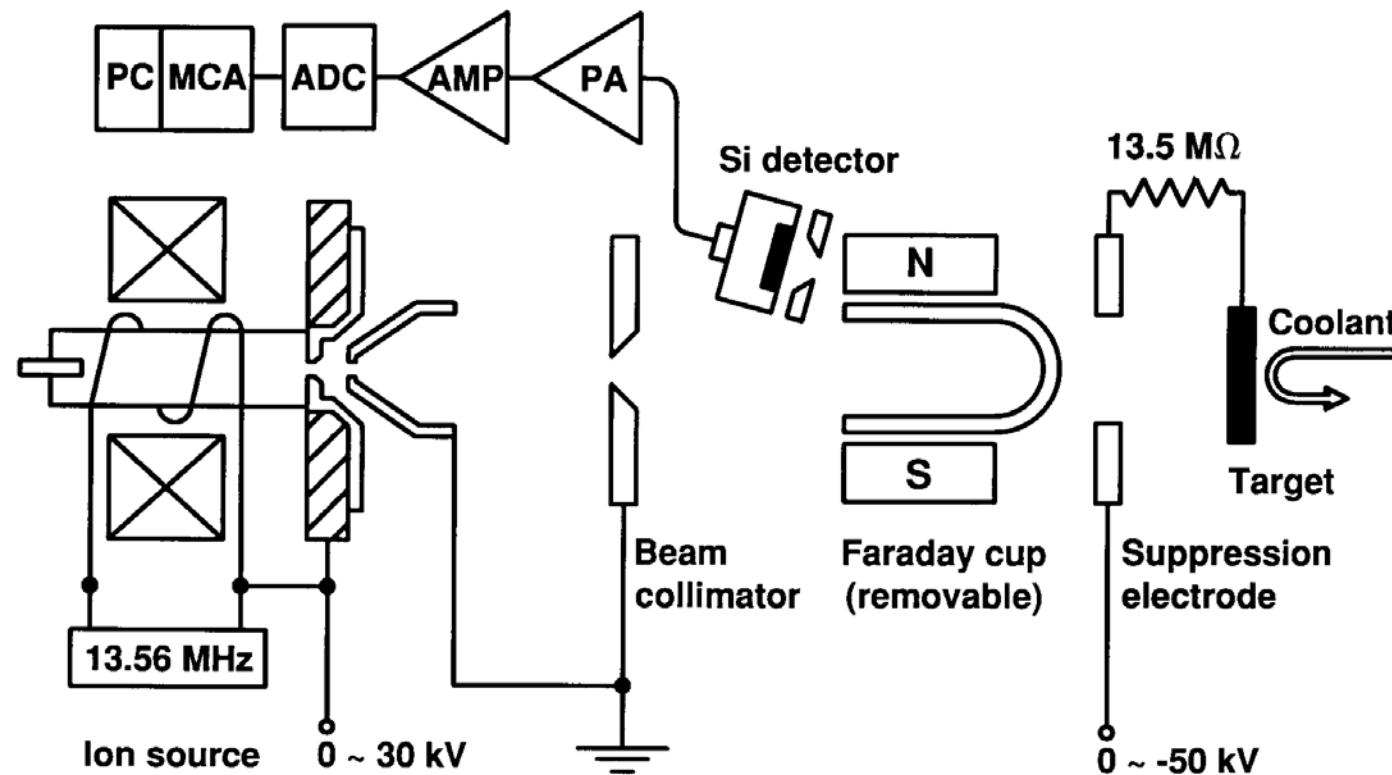


Radial Extraction
Beam-Target/Beam-Beam Type
50keV(B-T), 100keV(B-B), >50mA D⁺

Axial Extraction
Beam-Target Type
120keV, 50mA D⁺
Expected neutron yield : > 10⁸ n/s

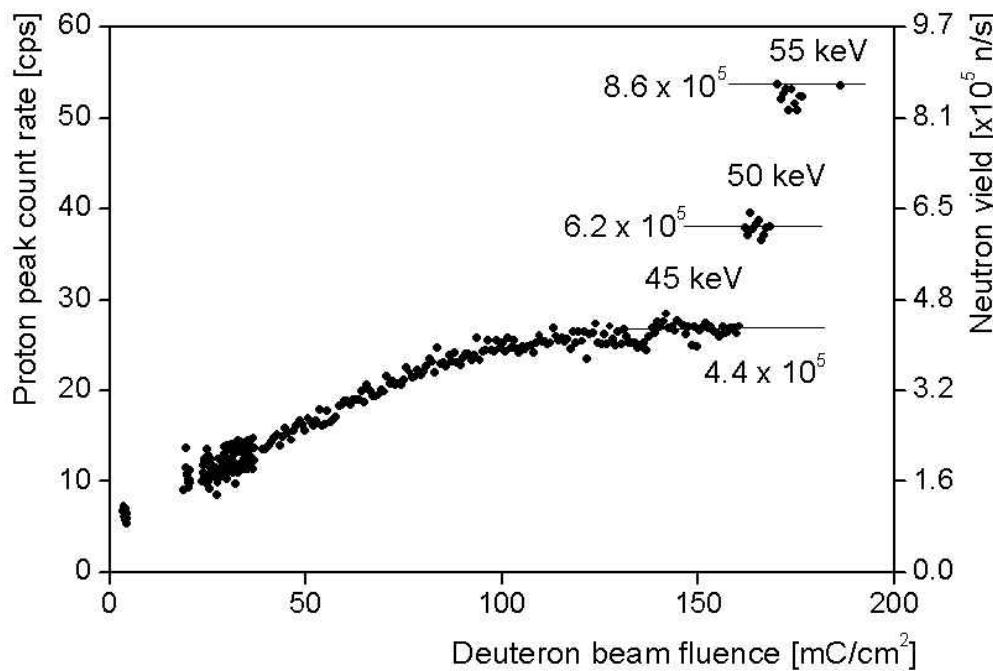


Neutron Generation and Detection System



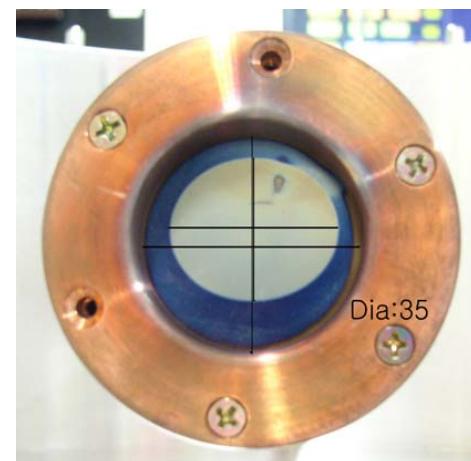
- Charged particle detection (using Si semiconductor detector)
- Proton detection
- Effective detection for low neutron yield

Neutron Generation and Measurements with Prototype Helicon Ion Source

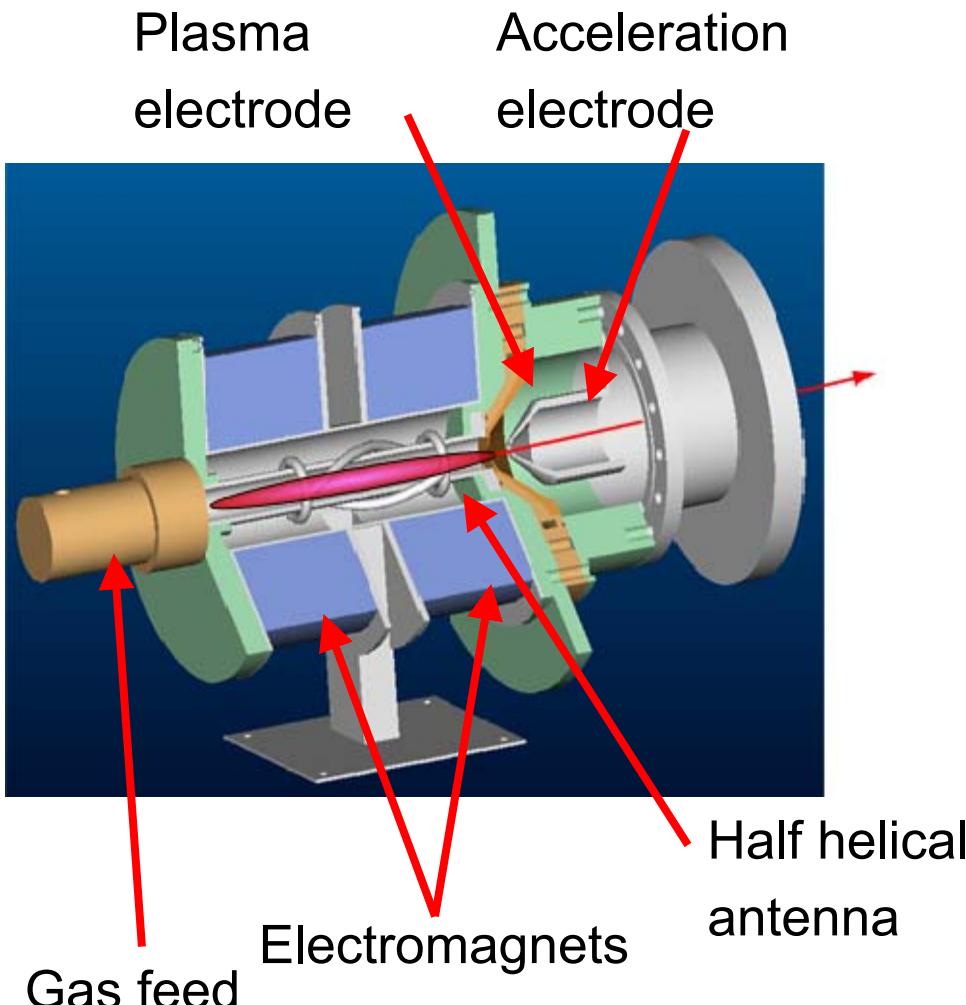


- 55kV, 57 μA
- $8.6 \times 10^5 \text{ n/s}$
- 4h 10m CW
- Expected D/Ti : 0.75
- RF : 1.2kW
- Detector solid angle: $1 \times 10^{-3} \text{ str}$

Image of beam mark left on target surface



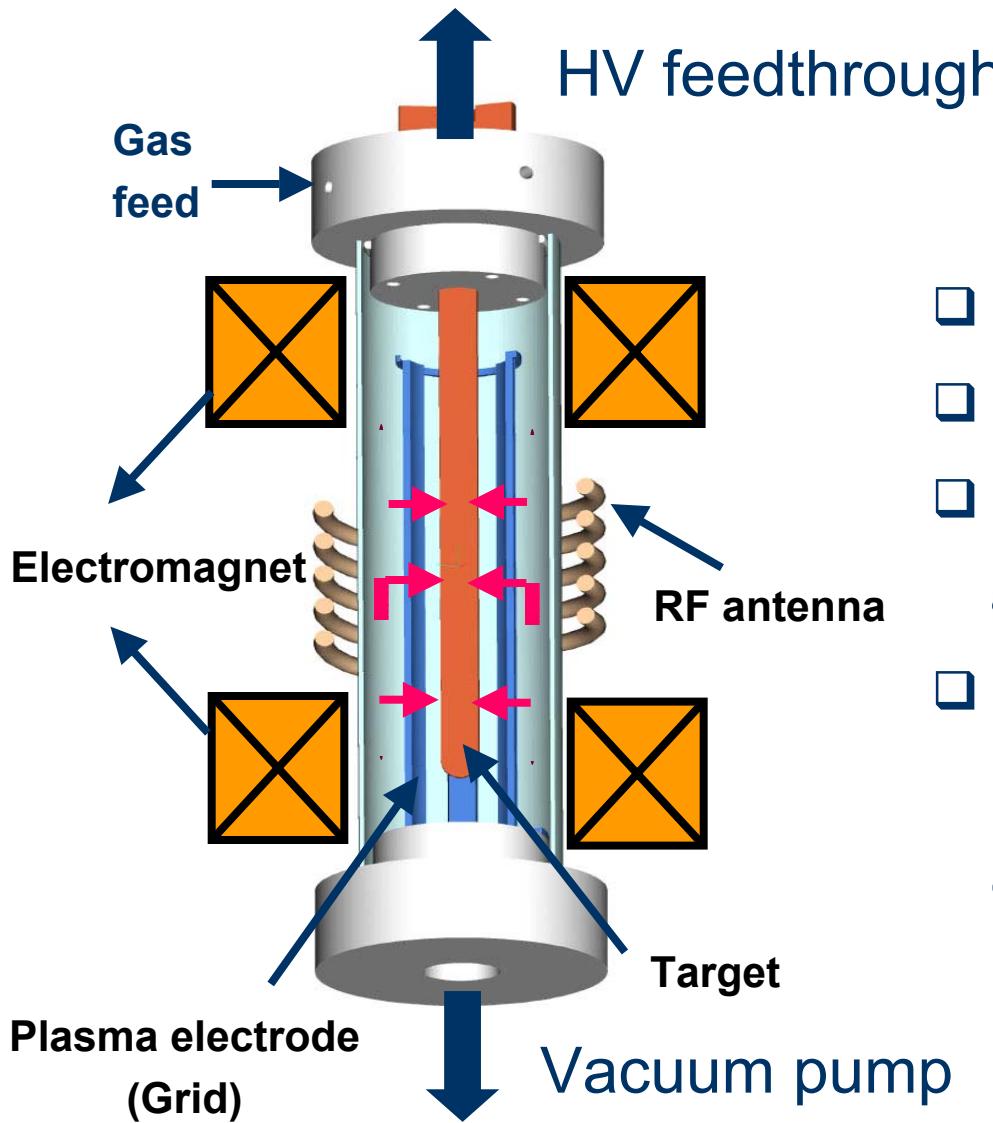
50kV, 50mA Helicon Plasma Ion Source



B Configuration	Uniform
Antenna	HH 9cm
Power	1000W
Plasma region pressure	26mtorr
Main chamber pressure	0.1mtorr
Magnetic field	200G
Hole size	4mm(D)
Gap distance	7mm
Measurement position	190mm

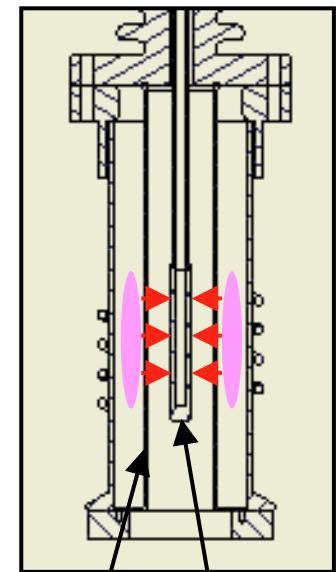
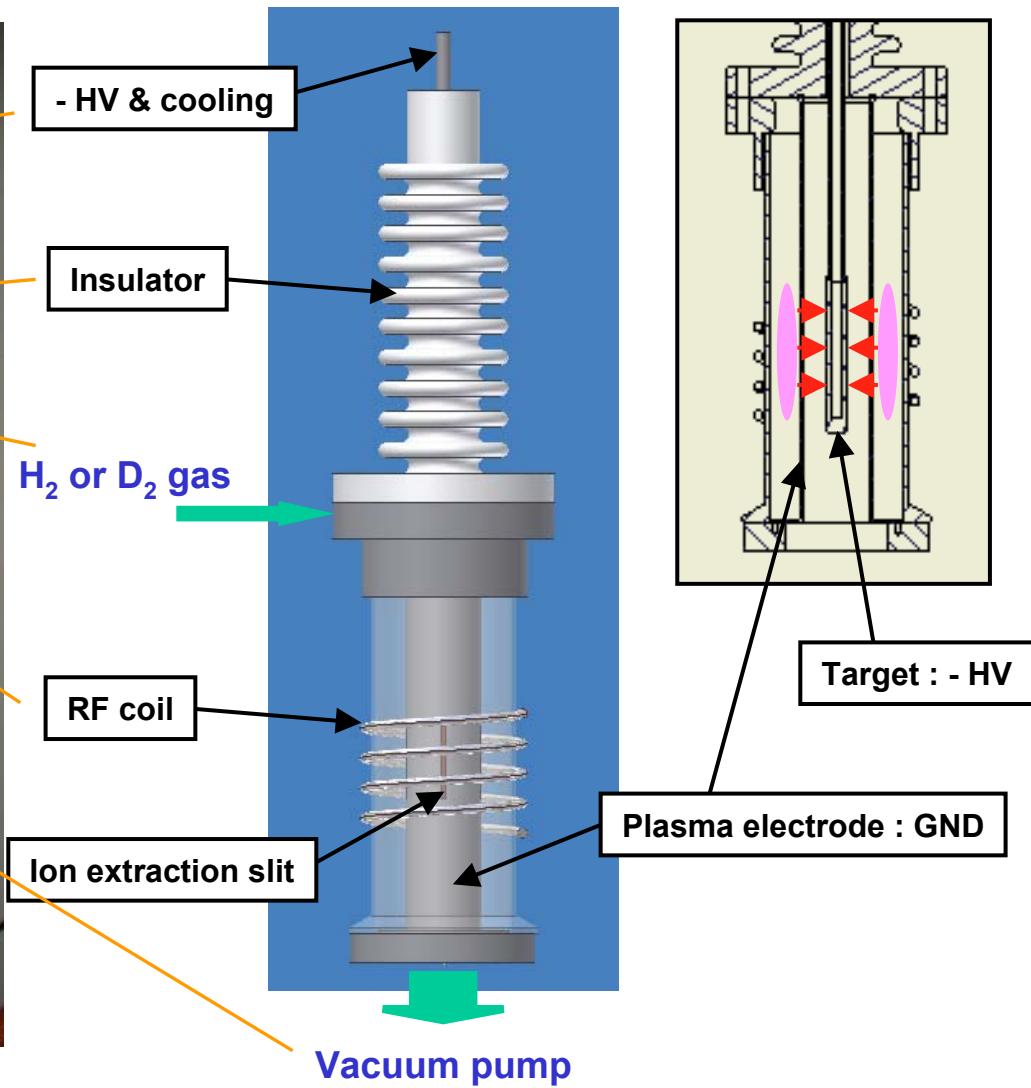
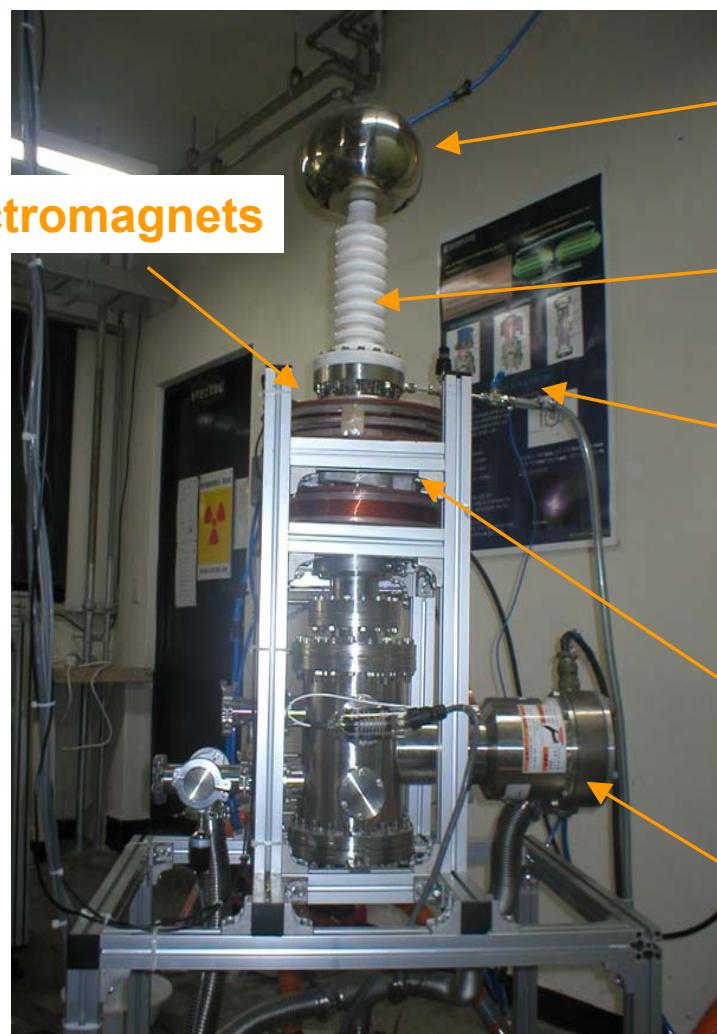
Max. beam current of 30mA at 37kV
Max. beam current density of 215mA/cm²

Cylindrical Coaxial Neutron Generator



- Compact
- High current with multi slots
- Neutron yield can increase as axial length increases
- Beam-beam type is also possible if a target is replaced with other grids

Picture and Schematic of Prototype Device

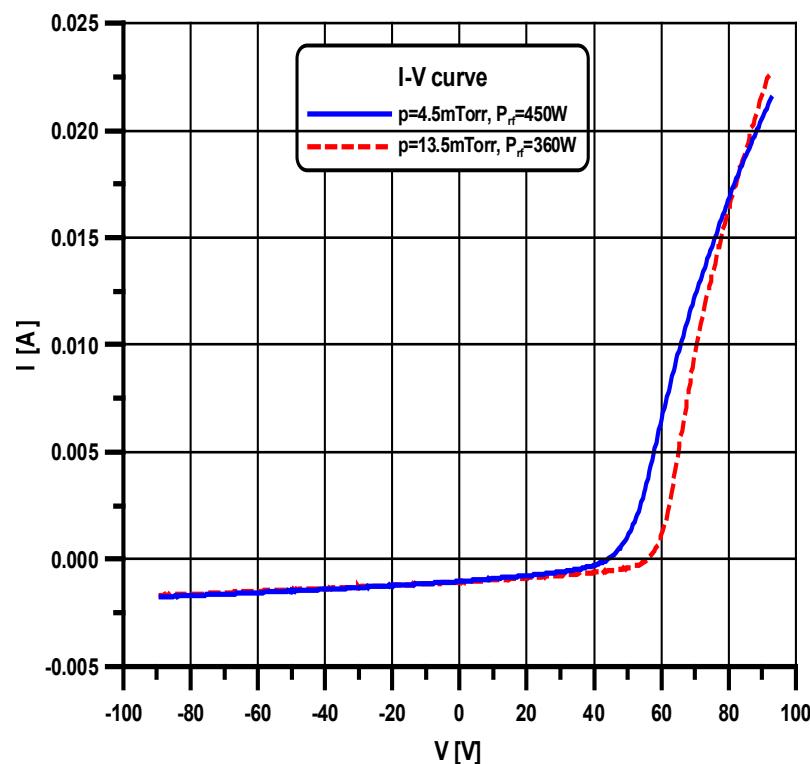


Langmuir Probe Measurements of RF Plasmas

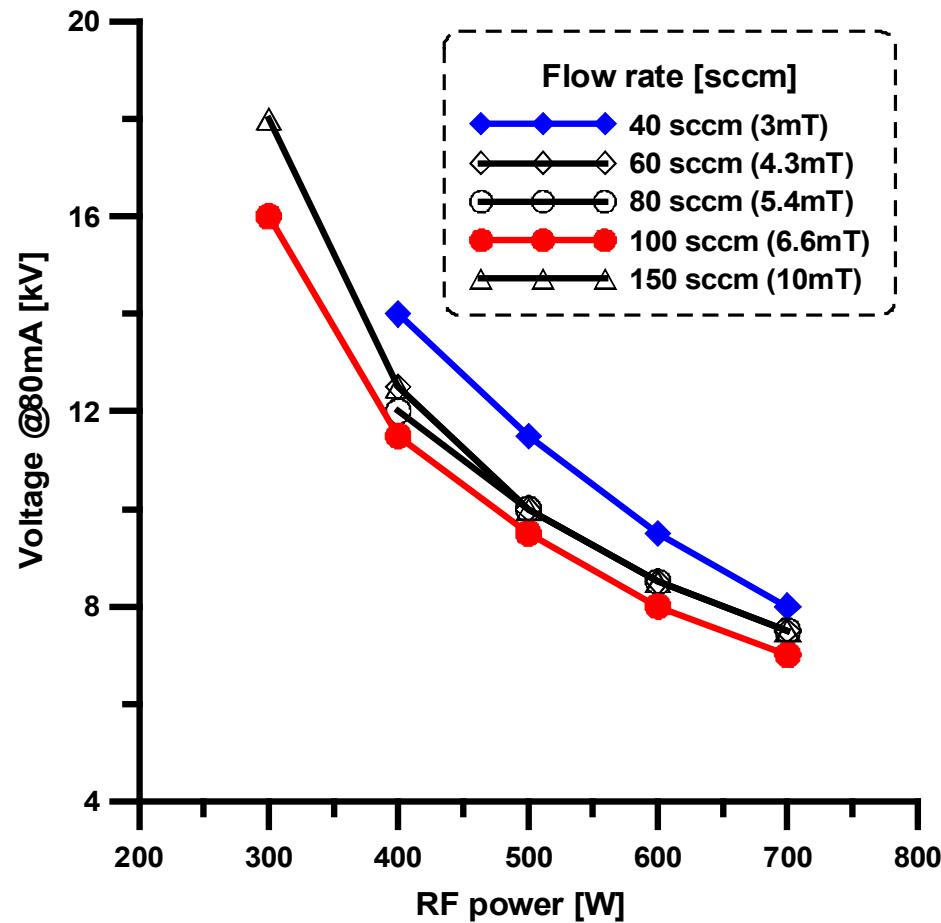
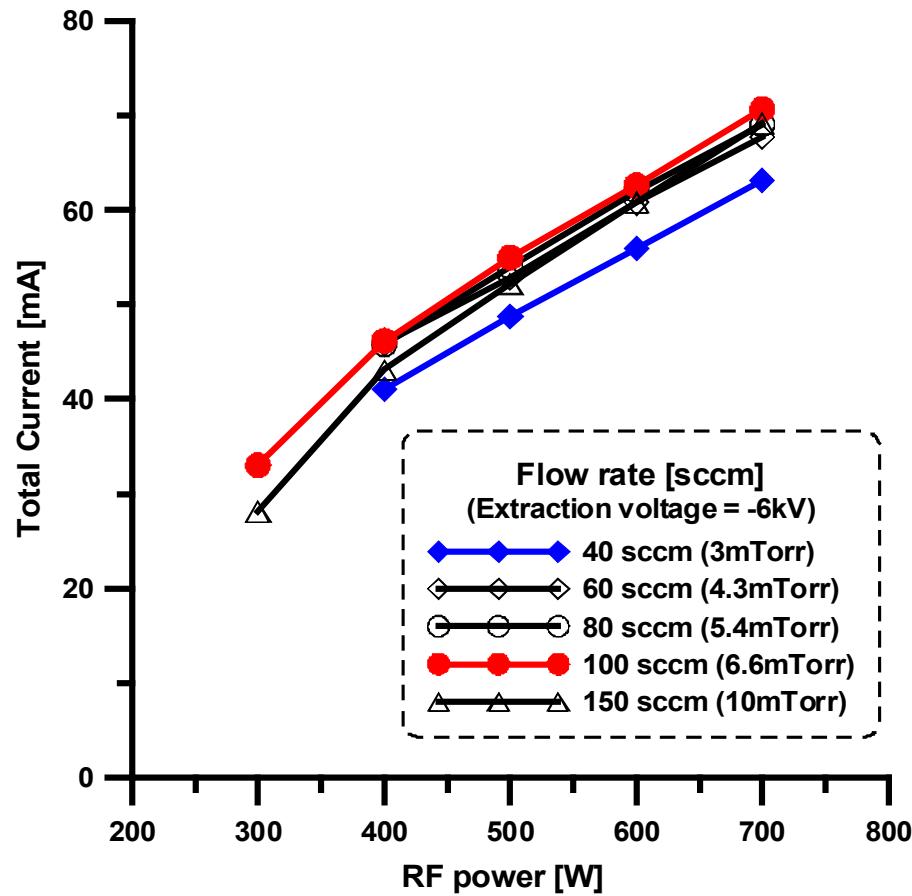
- Quartz tube only (no plasma electrode and target)
- 1-turn antenna

	Case 1	Case 2	Unit
Gas	H ₂	H ₂	-
Flow rate	100	200	sccm
Pressure	4.5	13.5	mTorr
RF Power	450	360	W
I _s	0.47	0.46	mA
V _f	44.5	56.3	V
V _p	58	67	V
T _e	4.8	4.0	eV
n _e	4.8E10	5.1E10	cm ⁻³

* Probe tip : Tungsten, D=0.3mm, L=5mm



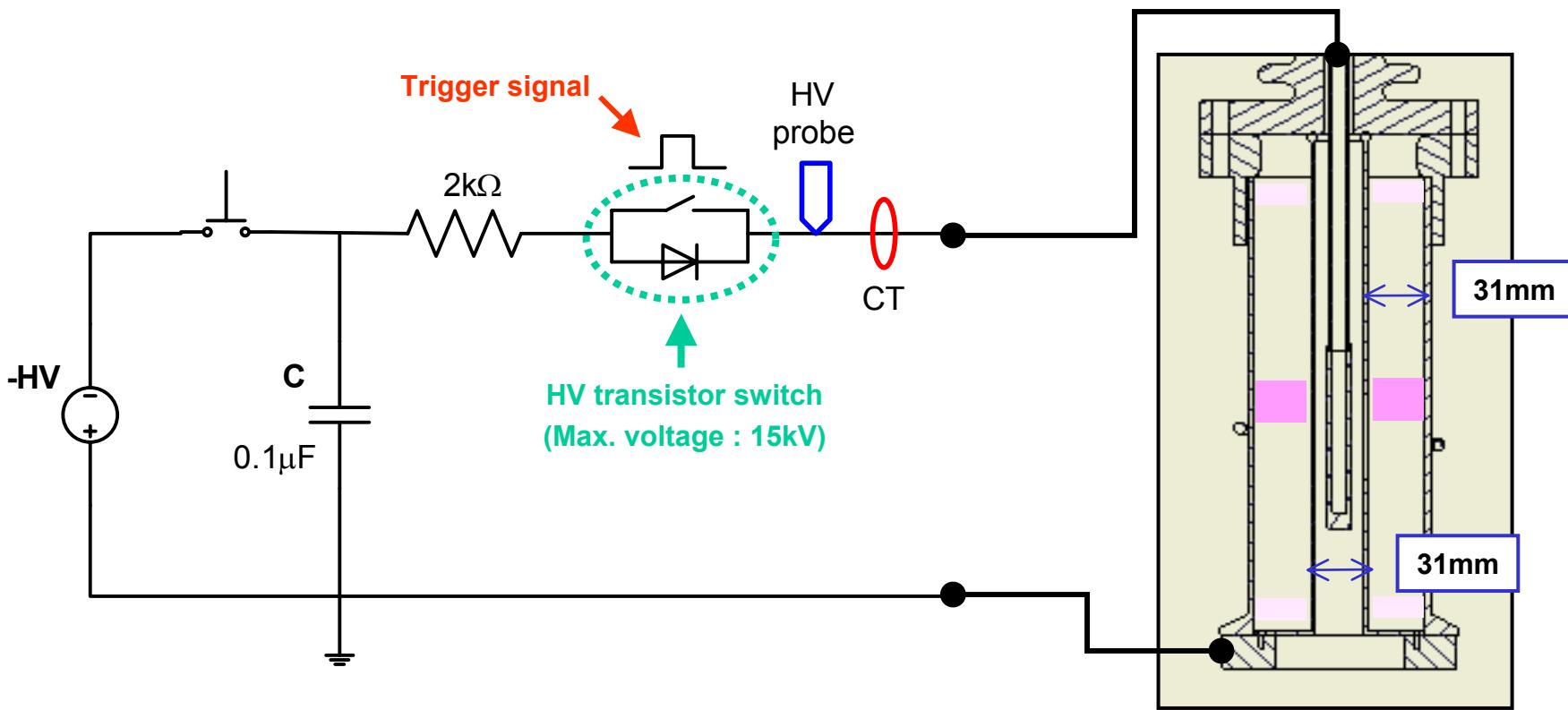
CW Discharge and Beam Characteristics



**Relatively strong RF power dependency
with less gas pressure dependency**

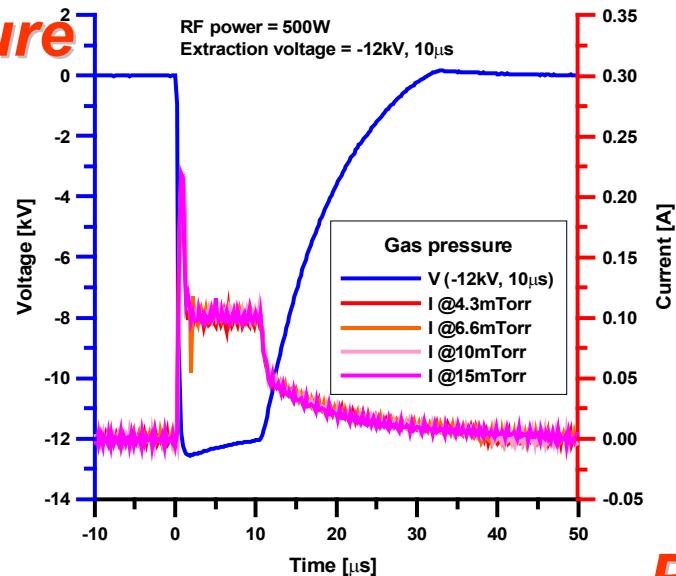
Experimental Setup of Pulsed Extraction

- Plasma electrode : **OD=31mm**, 2t, slits=2mmx50mmx4ea
- Extraction area = **4cm²**
- Target : **OD=14mm**, Cu, water cooling
- 1-turn antenna
- Inductive mode operation

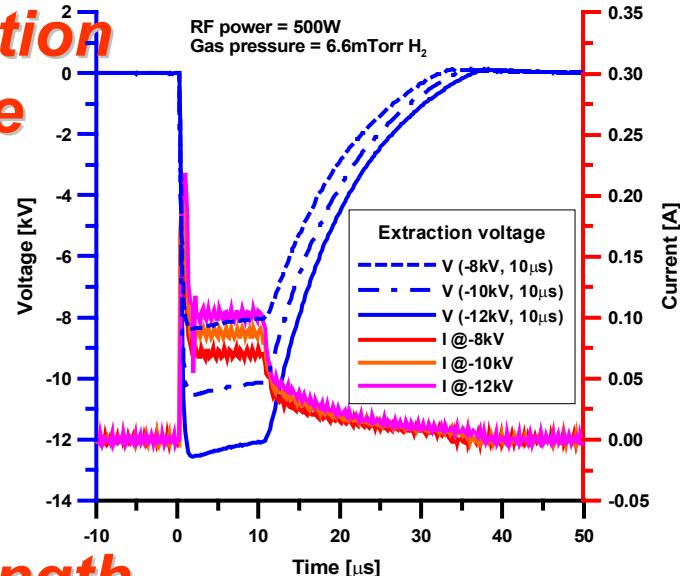


Pulse Discharge and Beam Characteristics

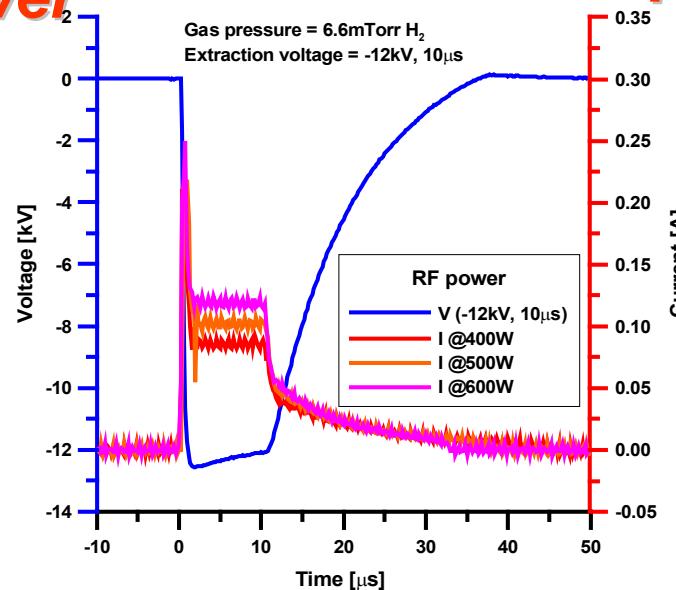
Pressure



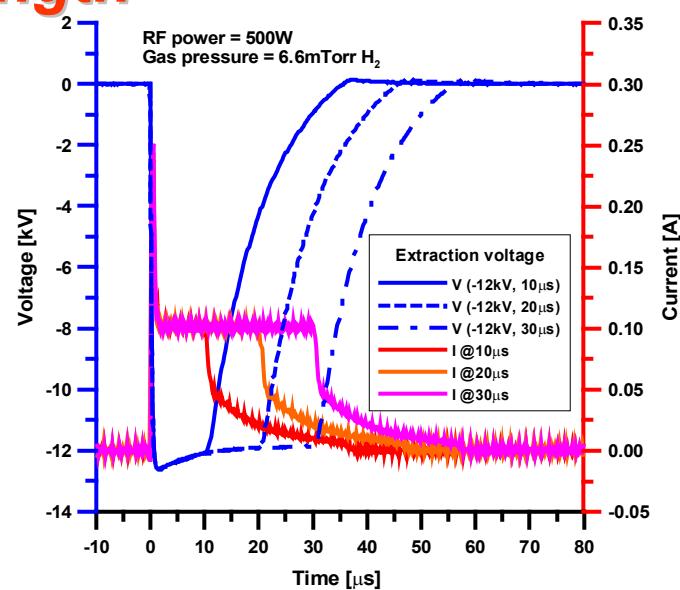
Extraction voltage



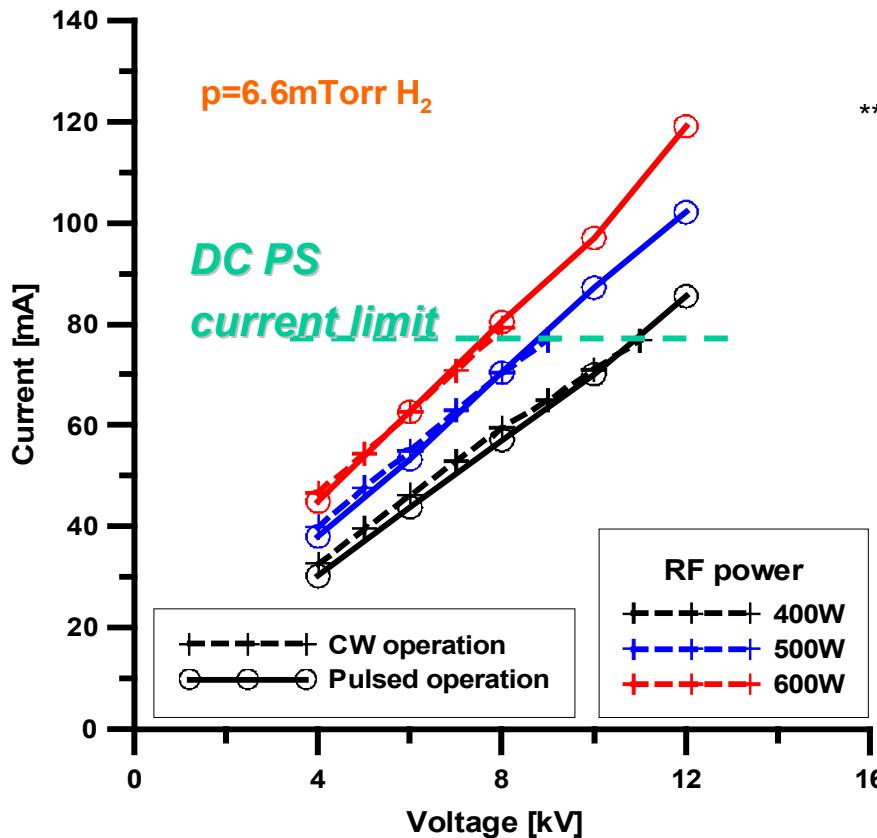
RF power



Pulse length

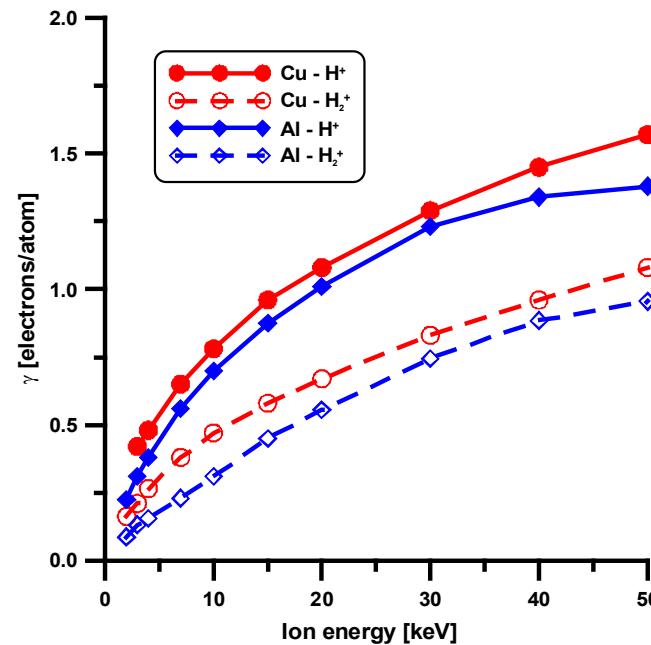


I-V Characteristics of CW and Pulsed Beams



Secondary electron emission coefficient**

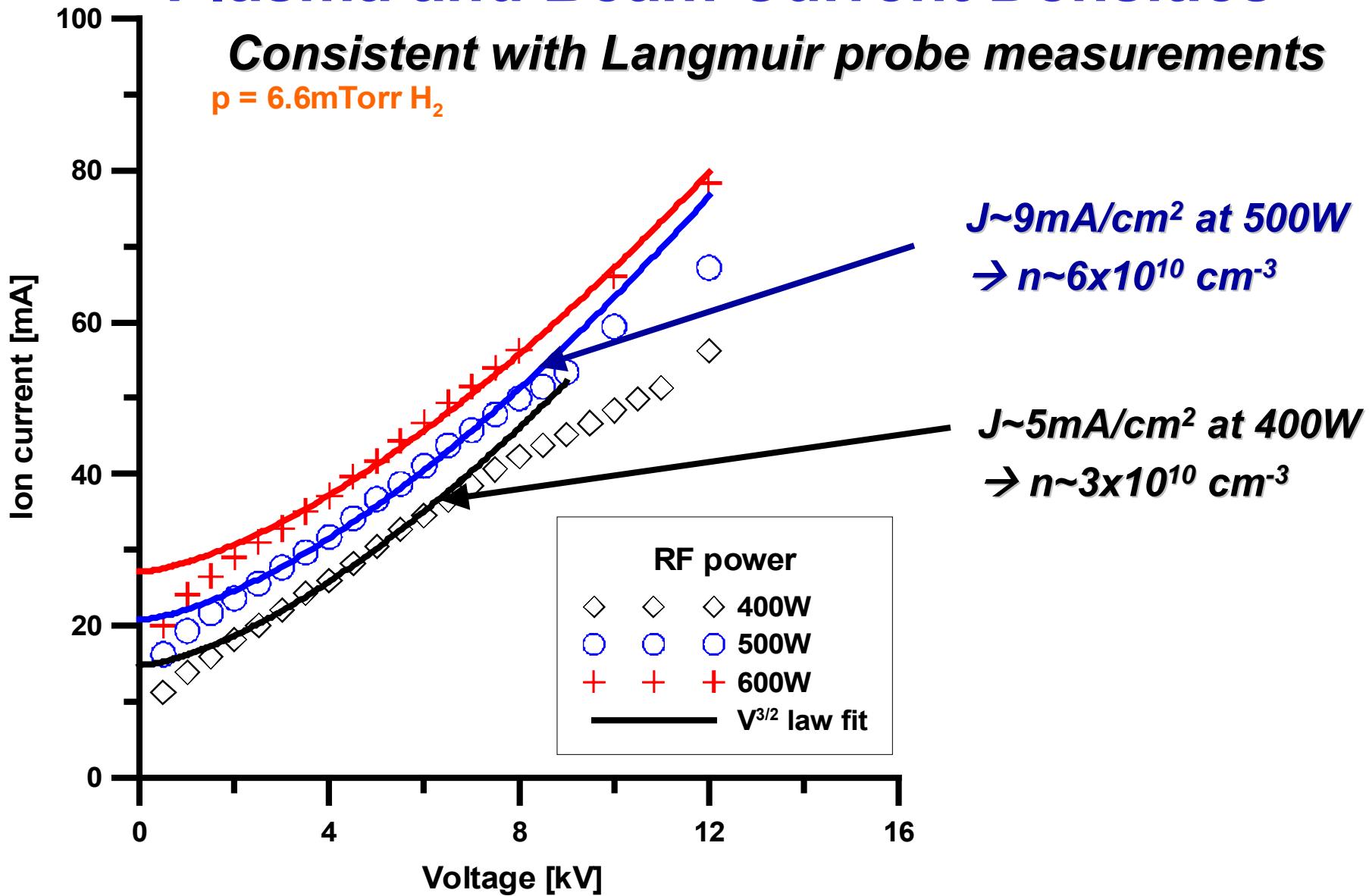
** R. A. Baragiola, et al., Physical Review B 19 (1979) 121-129



- Both CW and pulse beam currents depends extraction voltages for the given RF power, i.e. plasma density
- CW extraction is limited by DC power supply current limits
- Pulsed operation is limited by the specifications of switch (15kV)
- Need secondary electron current correction

Plasma and Beam Current Densities

Consistent with Langmuir probe measurements
 $p = 6.6\text{mTorr H}_2$

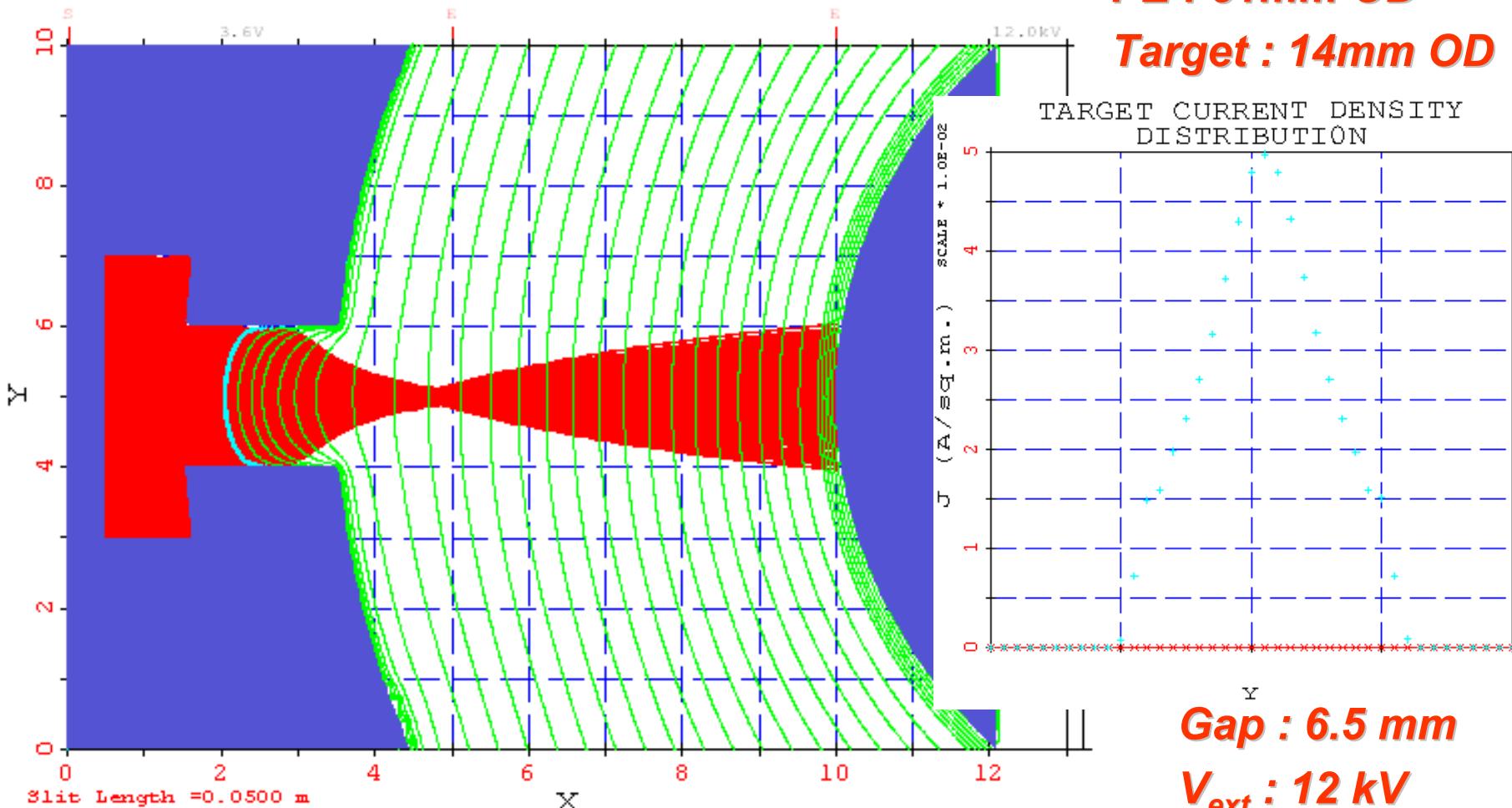


PBGUNS Simulations

10-MAR-05 AT 15:23:44

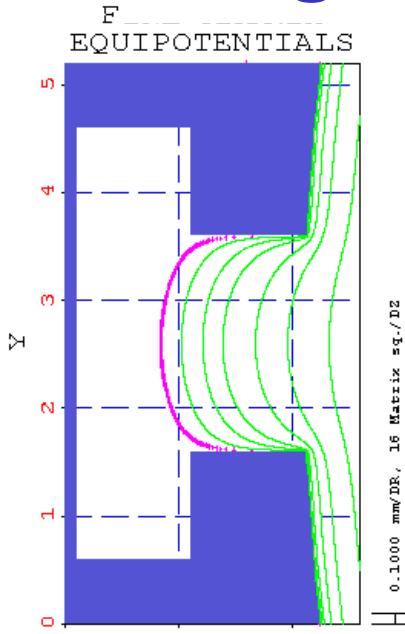
POSITIVE ION BEAM extracted radially in cylindrical geometry, solid t.

TRAJECTORIES AND EQUIPOTENTIALS

**Slit : 2mmx50mm****PE : 31mm OD****Target : 14mm OD****TARGET CURRENT DENSITY DISTRIBUTION****Gap : 6.5 mm** **$V_{ext} : 12 \text{ kV}$** **$I : 29.5 \text{ mA}$**

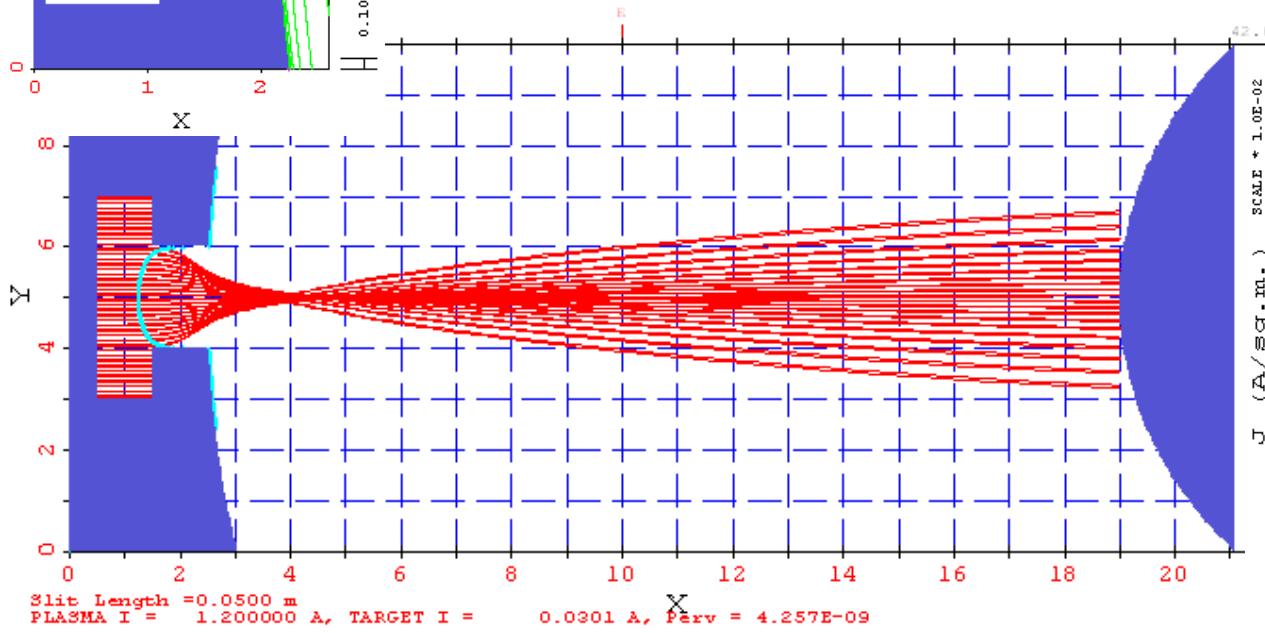
Larger Gap for High Voltage Operation

How to get high energy beam with this setup ?



POSITIVE ION BEAM extracted radially in cylindrical geometry, 51mm +14mm target

TRAJECTORIES



Gap : 16.5mm

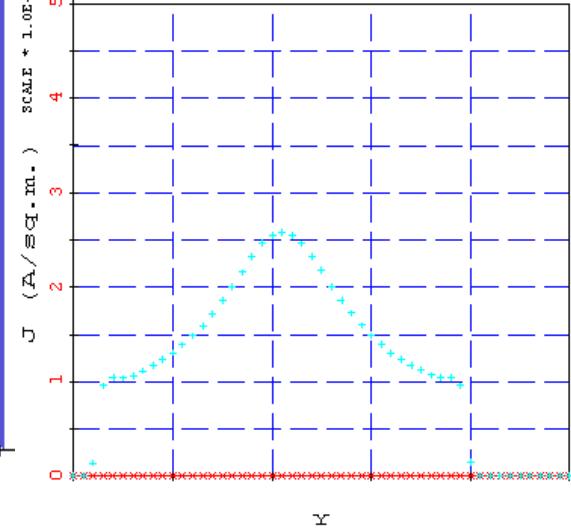
V_{ext} : 42 kV

I : 30.1 mA



2×10^8 n/s

TARGET CURRENT DENSITY DISTRIBUTION



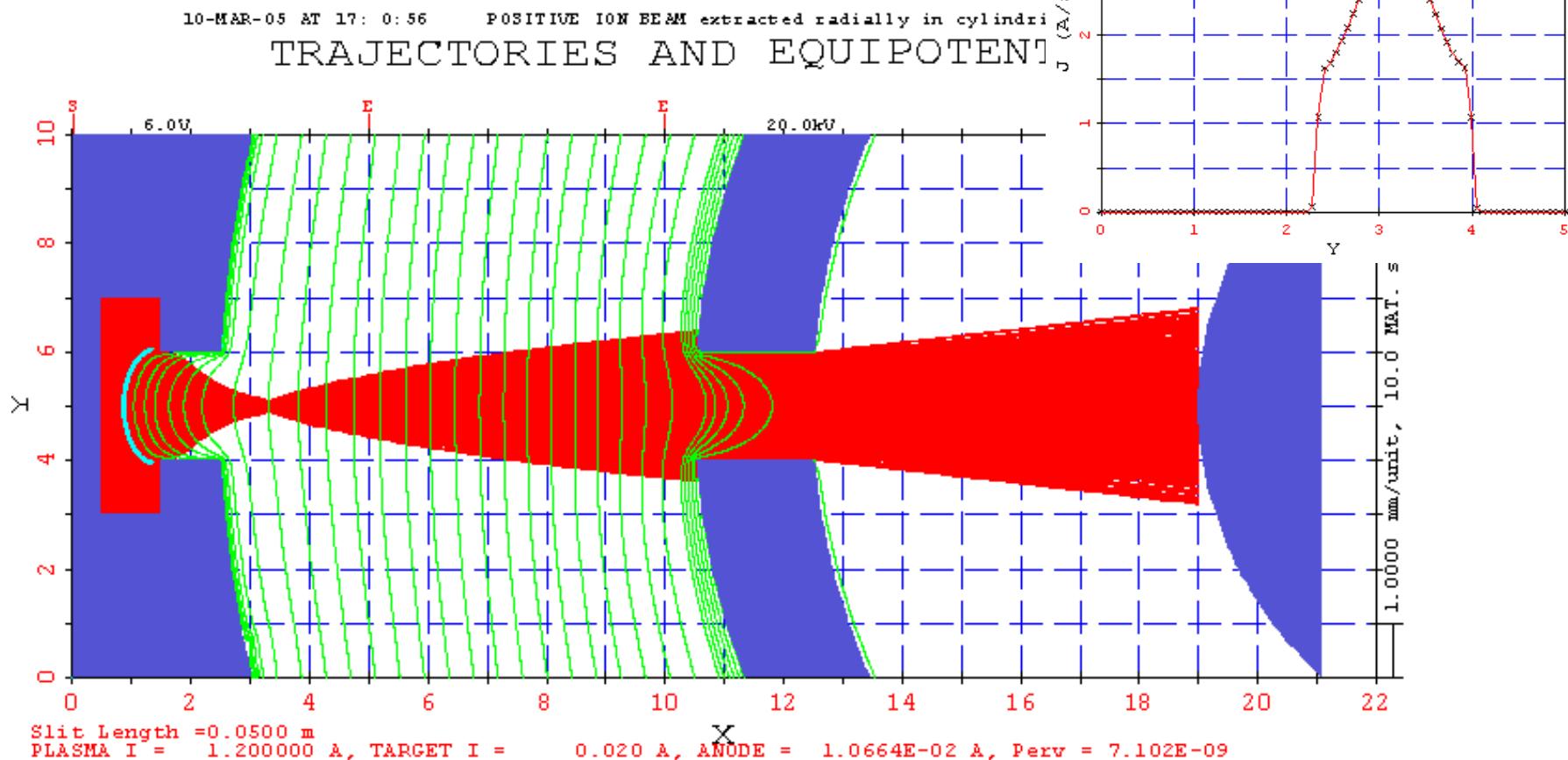
Suppression of Secondary Emission Currents

Slit : 2 mm x 50 mm

Gaps : 8 mm – 6.5 mm

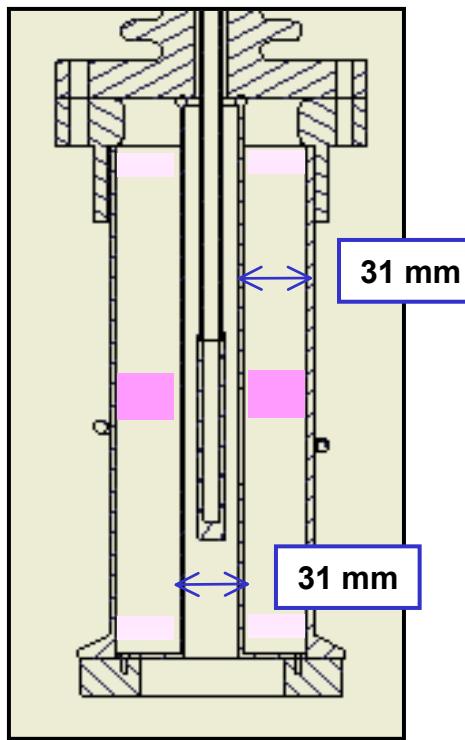
V_s : 20 kV – 19.8 kV

I : 20 mA at target

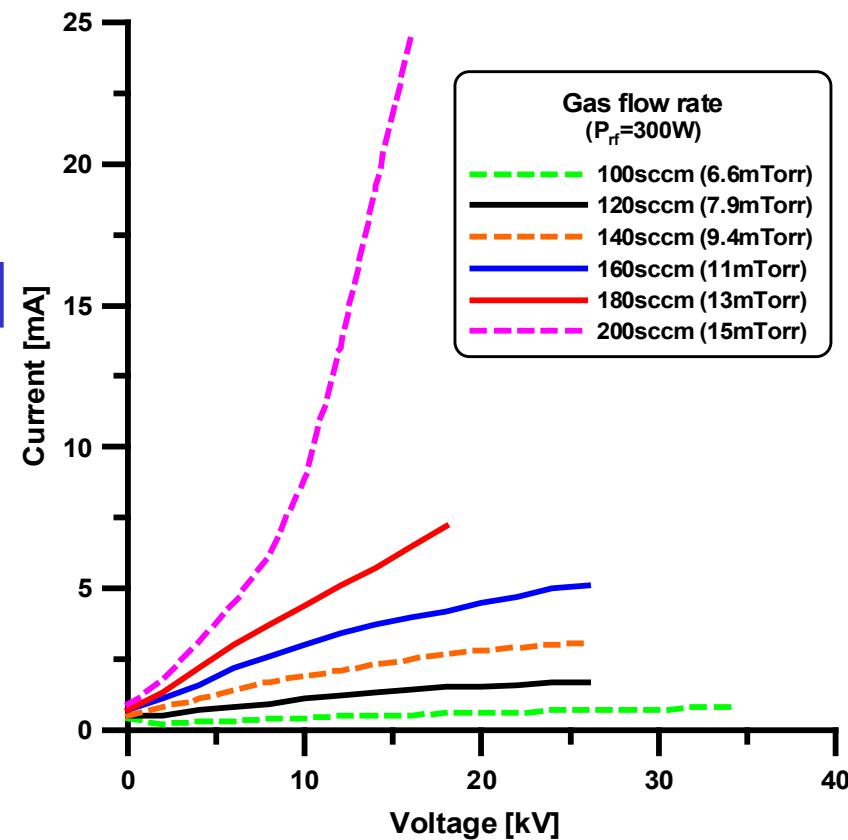
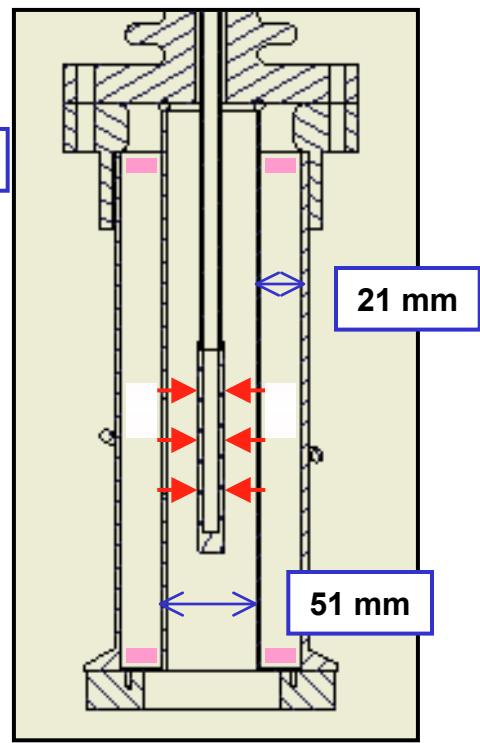


Electrode Size and Skin Depth Issues

OD=31mm Plasma Electrode

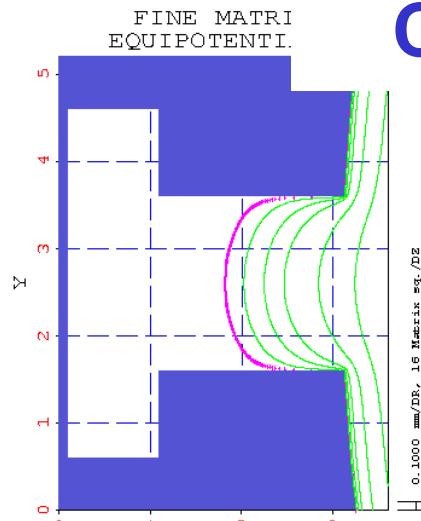


OD=51mm Plasma Electrode



Operable only at high pressures (eddy currents at electrode)
→ Unstable extraction → Need larger plasma chamber

Cylindrical IEC Configuration



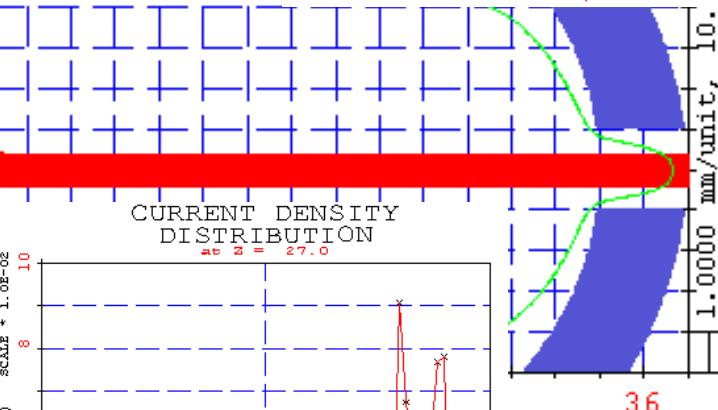
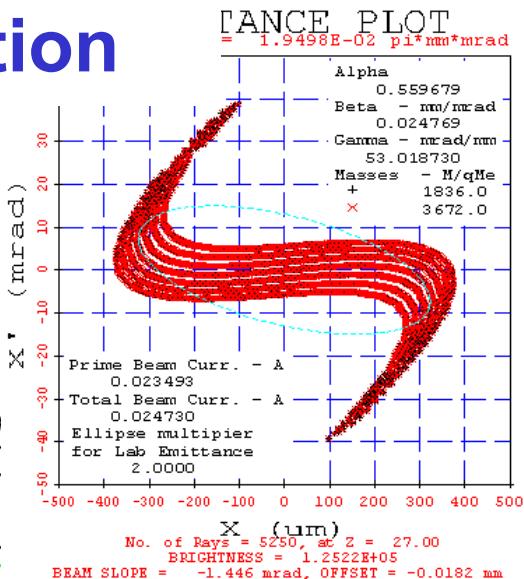
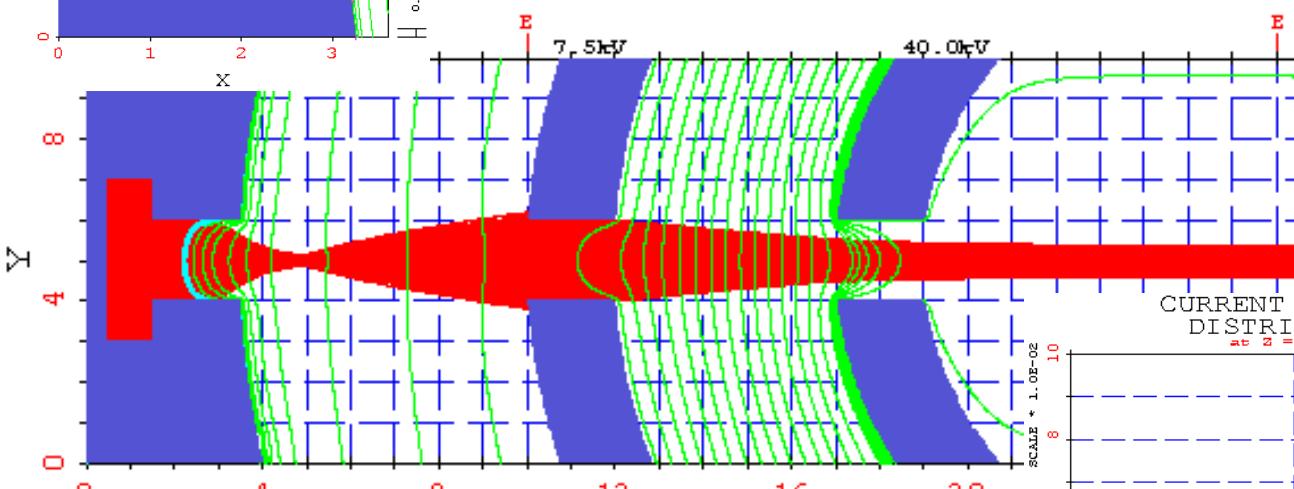
Slit : 2 mm x 50 mm

Gaps : 6.5 mm – 5 mm

V_s : 7.5 kV – 40 kV

I : 25mA, No Target

JECTORIES AND EQUIPOTENTI



Focusing electrodes are required!

Summary

- **Neutron yield measurements with Si detector : measure D-D protons from the target bombarded by a helicon ion source**
- **Radial beam extraction from cylindrical RF plasmas in cw and pulse mode**
 - **CW beam extraction limited by DC power supply current limit of 80mA : larger gap required for higher beam energy**
 - **Pulsed beam extraction up to 12kV without current limit : high voltage switch under preparation**
- **PBGUNS simulation in cylindrical geometry :**
new design requires larger plasma chamber to accommodate focusing grids for beam-beam reactions as well as a secondary electron suppression electrode



A Magnetron Discharge Ion Source for an Inertial Electrostatic Confinement Fusion Device

7th U.S.-Japan IEC WORKSHOP March 14-16, 2005

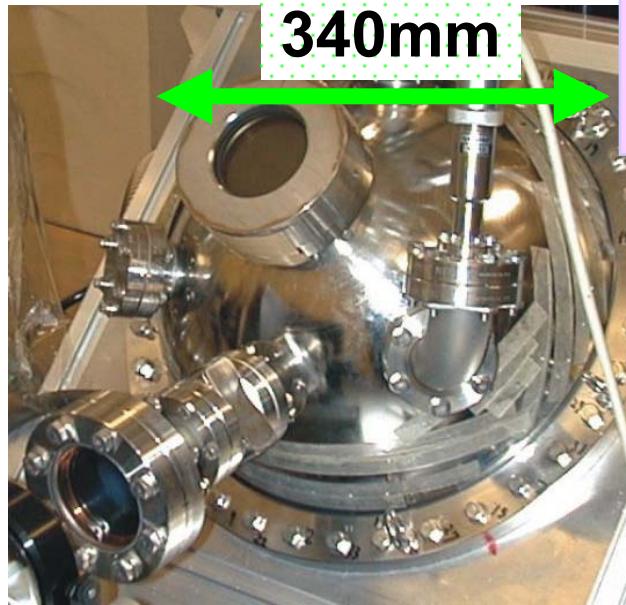
Teruhisa Takamatsu, Toshiyuki Kyunai, Satoshi Ogawa,
Kai Masuda, Hisayuki Toku, and Kiyoshi Yoshikawa
Inst. of Advanced Technology, Kyoto Univ.



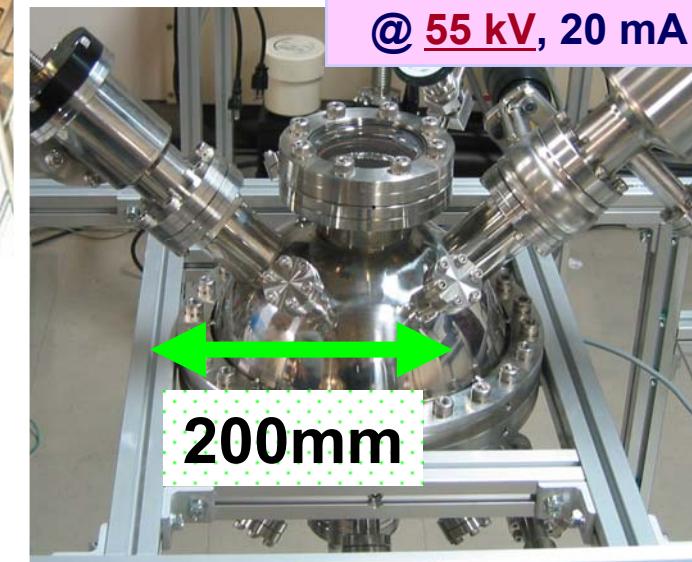
Outline

- Our IEC devices
- Landmine detection using IEC neutron source
- Magnetron discharge type ion source for IEC device
- Numerical analysis of magnetron ion source
- summary

IECF Neutron Source



Neutron
 $1 \times 10^7 \text{ sec}^{-1}$ (DC)
@ 63 kV, 30 mA



IEC20 device

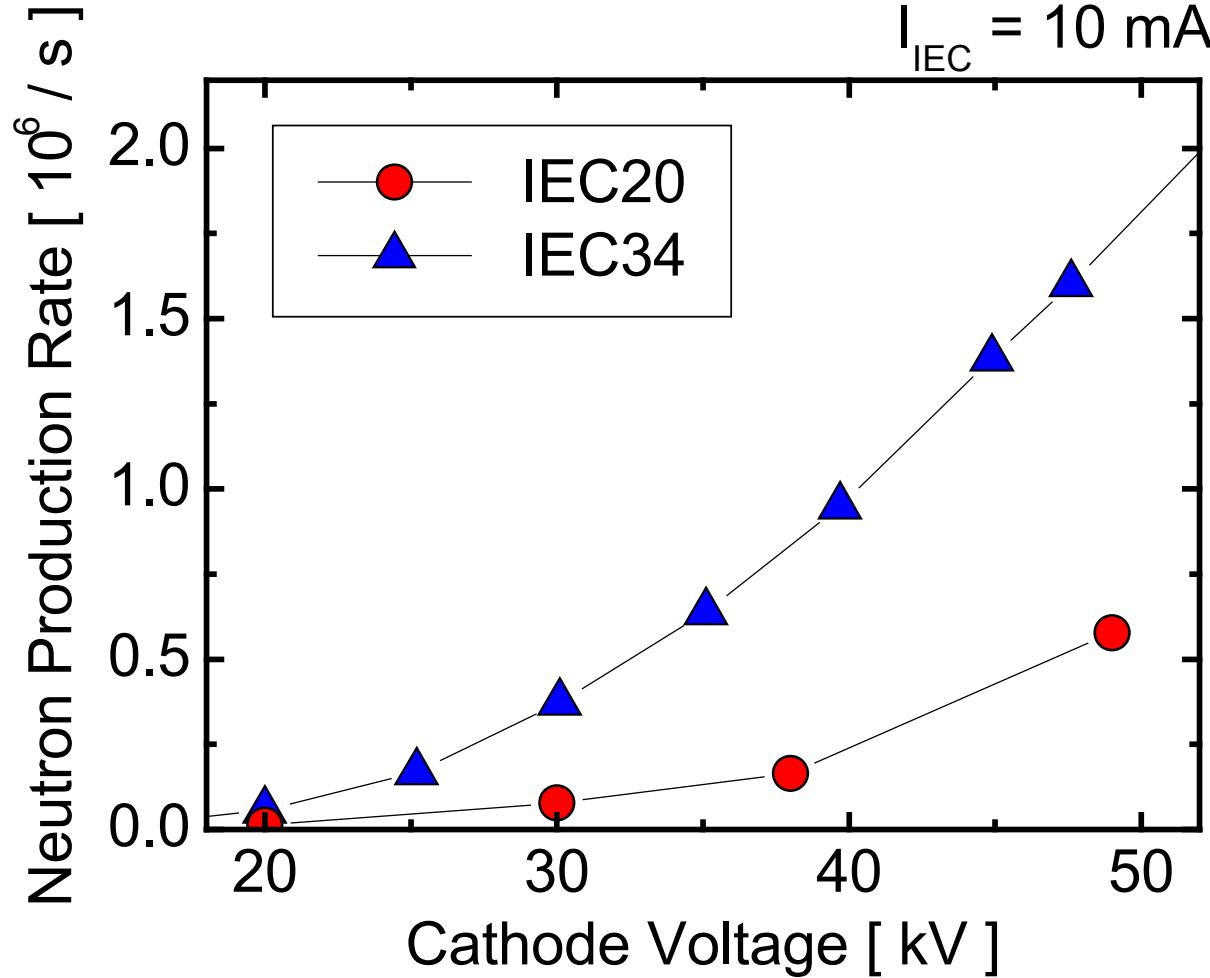


feedthru and cathode

IEC34 device



Neutron Yield

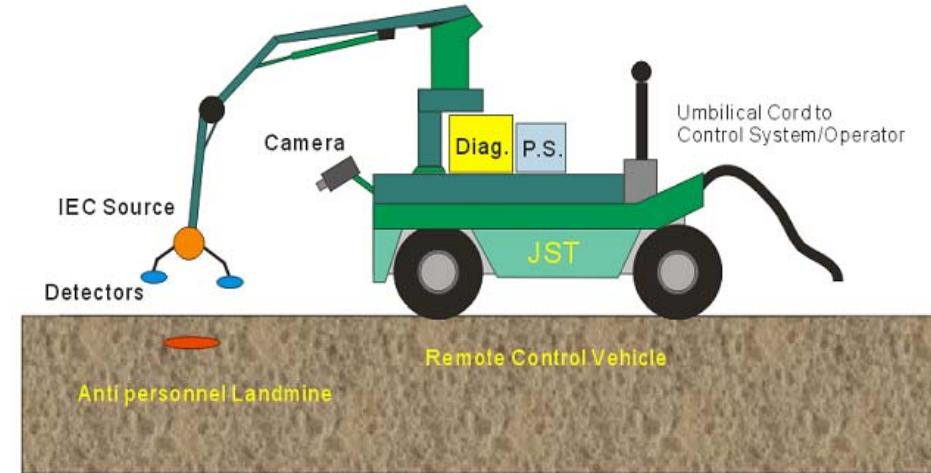
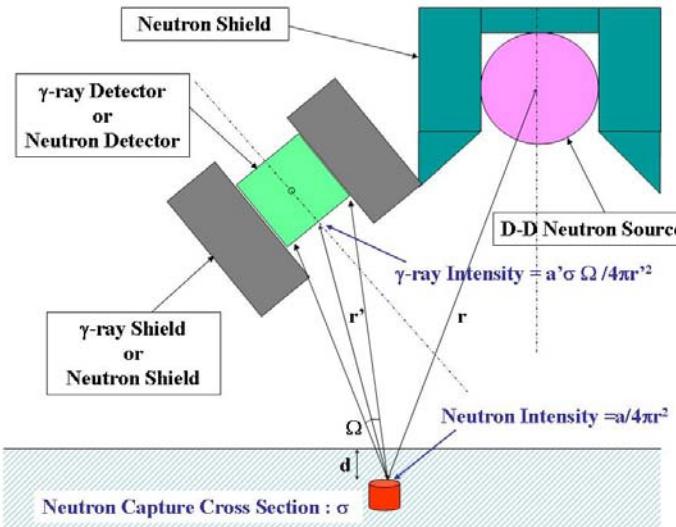


Small device IEC20 obtains almost quarter neutron yield of IEC34





Project of Landmine Detection



R&D of LM Detection

- Diagnostics;
Kyoto-U., TIT, Kyushuu-U.
- Tomography;
Kyoto-U., JAERI, Wakasa-bay Energy Res. Center,
- Total system;
Kyoto-U., Nikki Co.

R&D of compact IEC

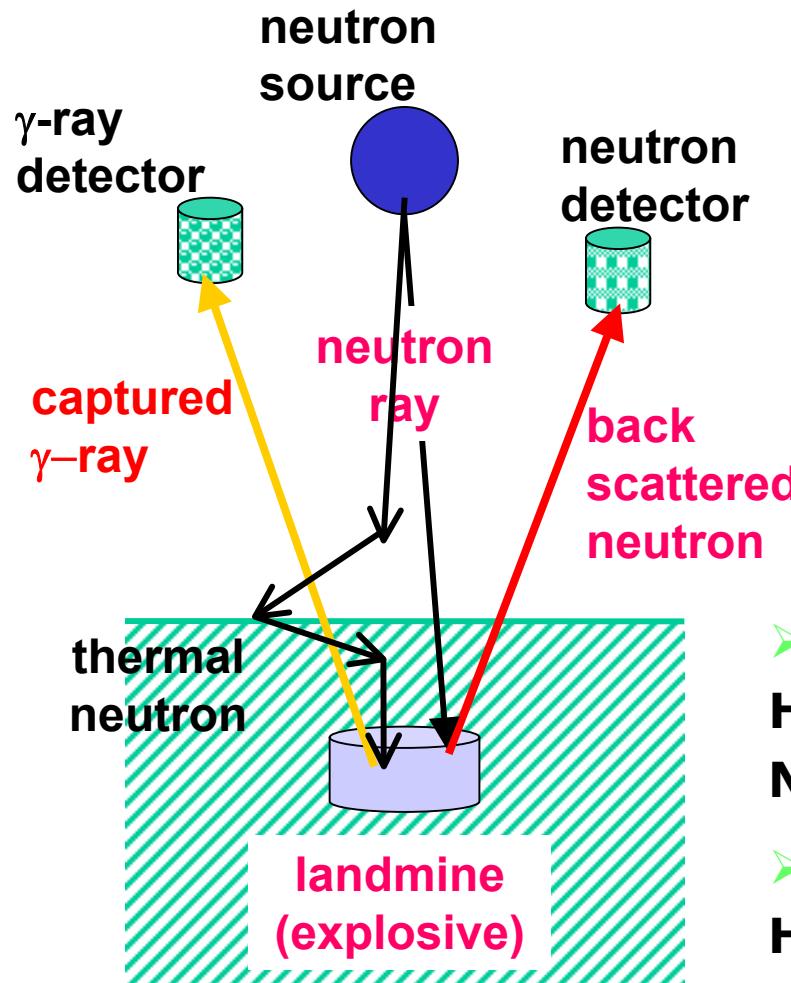
- CW/pulse IEC;
Kyoto-U., Kansai-U.
- CW/Pulse power supply ; TIT



The project is supported by Japan Science and Technology Agency

How to Detect Landmine

Neutron yield of $\sim 10^8$ is required



Atomic ratio of TNT explosive

H	C	N	O
3	7	3	6

Atomic ratio of explosives fixed

- **neutron-captured γ ray (kind of LM)**
 $H(n,\gamma) \cdots 2.22 \text{ MeV } \gamma \text{ ray emission}$
- **$N(n, \gamma) \cdots 10.83 \text{ MeV } \gamma \text{ ray emission}$**
- **back-scattered neutron (existence of LM)**
 $H(n, n') \cdots H \text{ scatter neutron}$

Landmine Detection Field Test



GPR detection system

We are planning to take our test using IEC neutron source until 2007

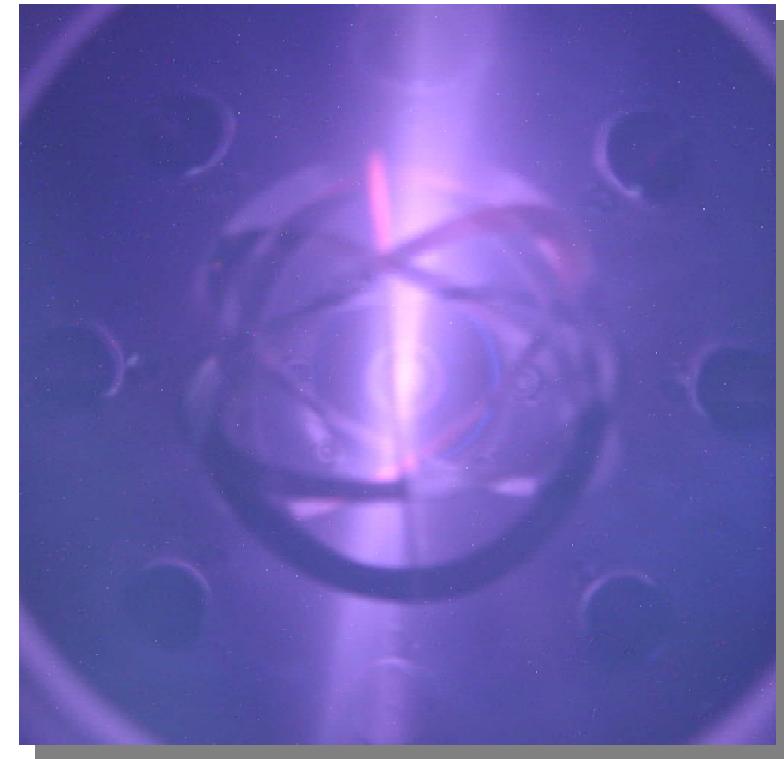
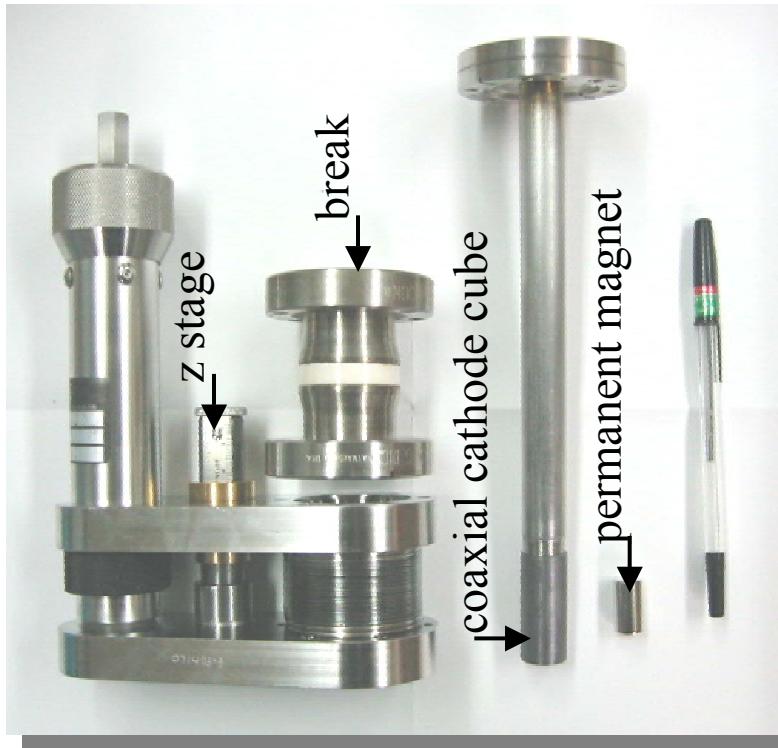
Landmine detection Field Test
25 Feb '05 at Kagawa, Japan

The vehicle has a detection system attached at the end of the long arm



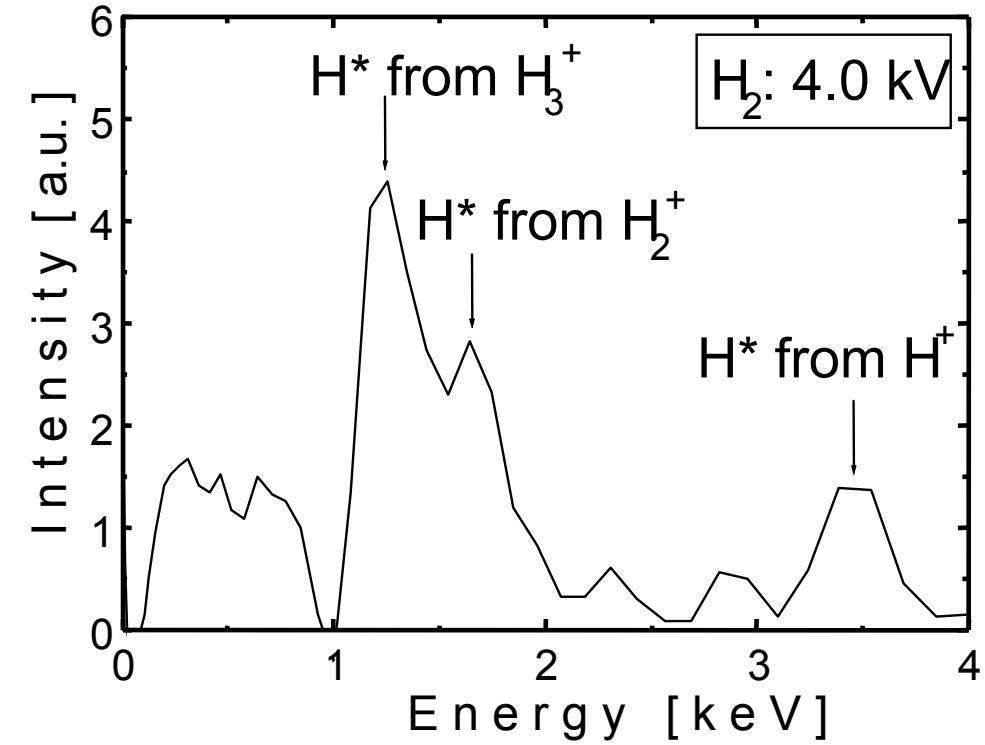
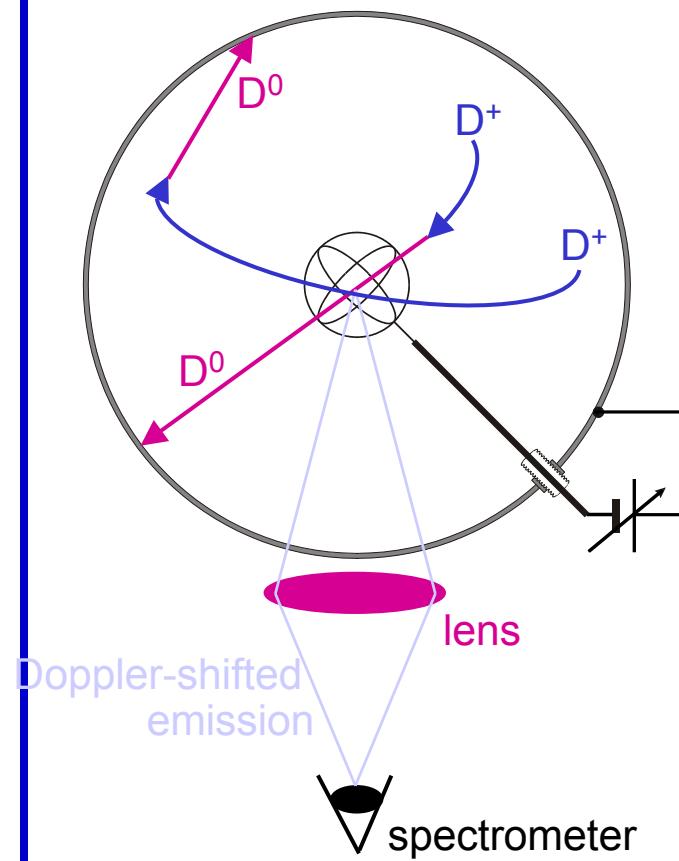


Magnetron Discharge Ion Source for IEC



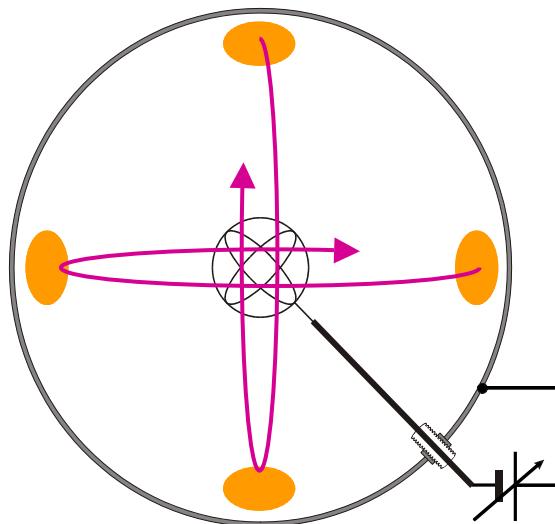
Problems to be Coped With Inherent in Glow-Discharge Based IECF

- Diverse energies of converging ions
- Too short mean free path of ions for envisaged re-circulation



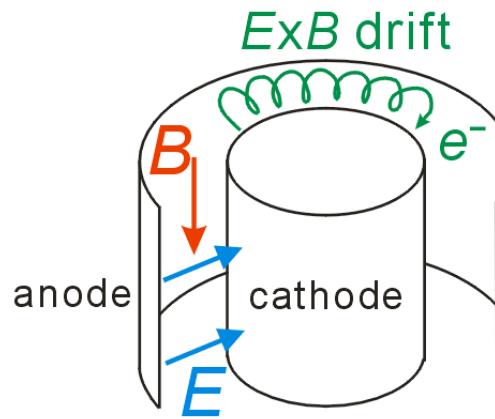
observed energy spectrum of fast hydrogen neutrals originating from converging ions

What We Expect with Ion Sources



- localized birthplace of ions
 - reduced operating gas pressure
-
- ✧ enhanced ion energy
 - ✧ recirculation of ion current

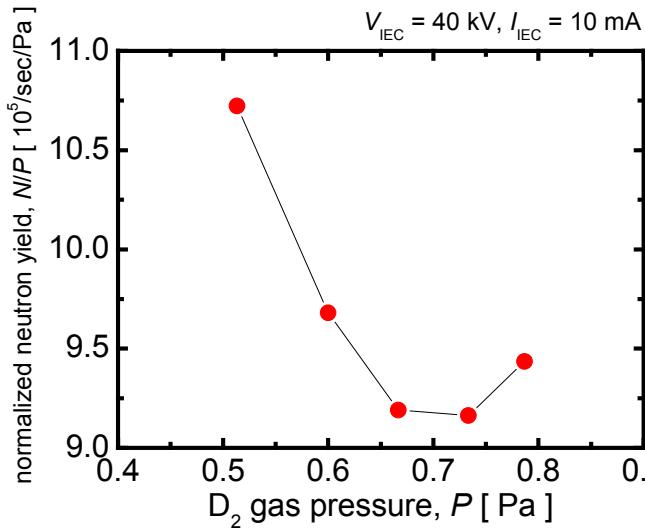
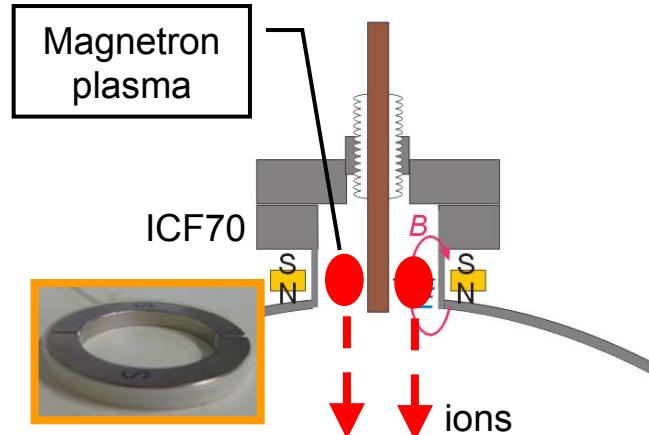
Why We have Chosen DC Magnetron Discharge



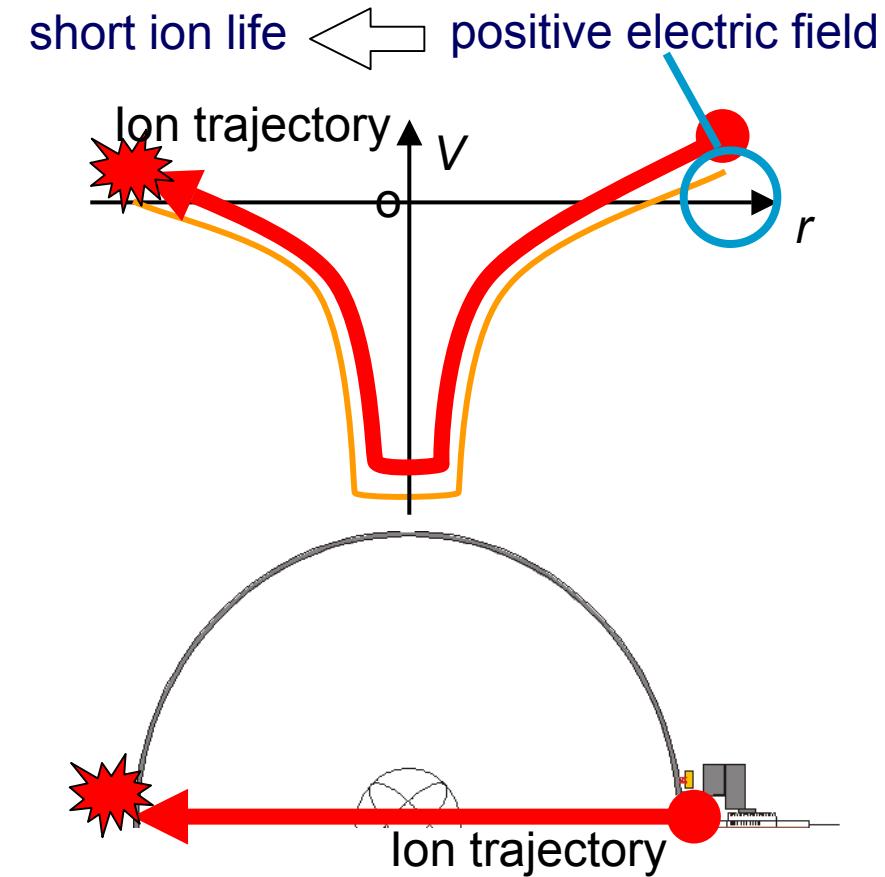
- ✓ simple configuration
- ✓ compactness
- ✓ ample current supply under low gas pressure condition



Previous Magnetron-Type Ion Source Experiment

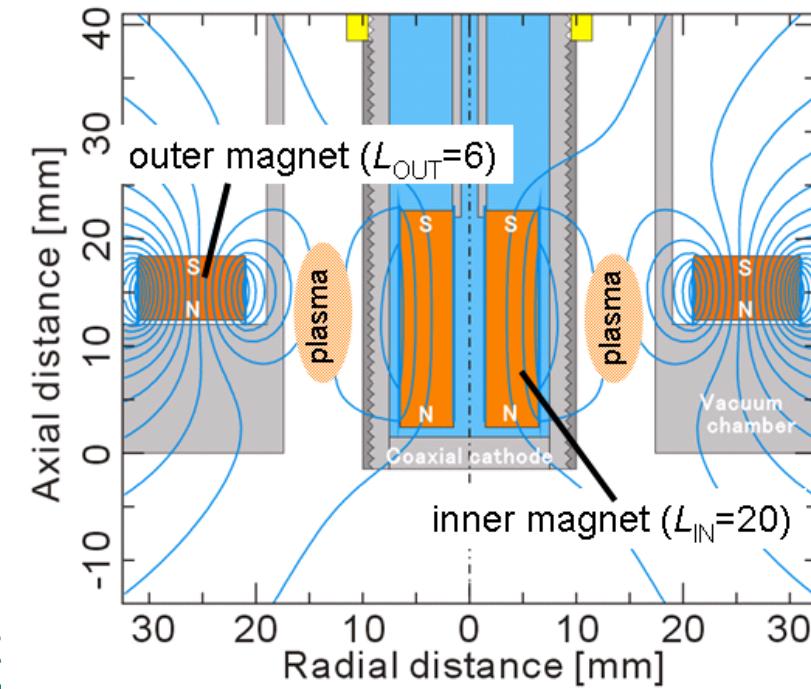
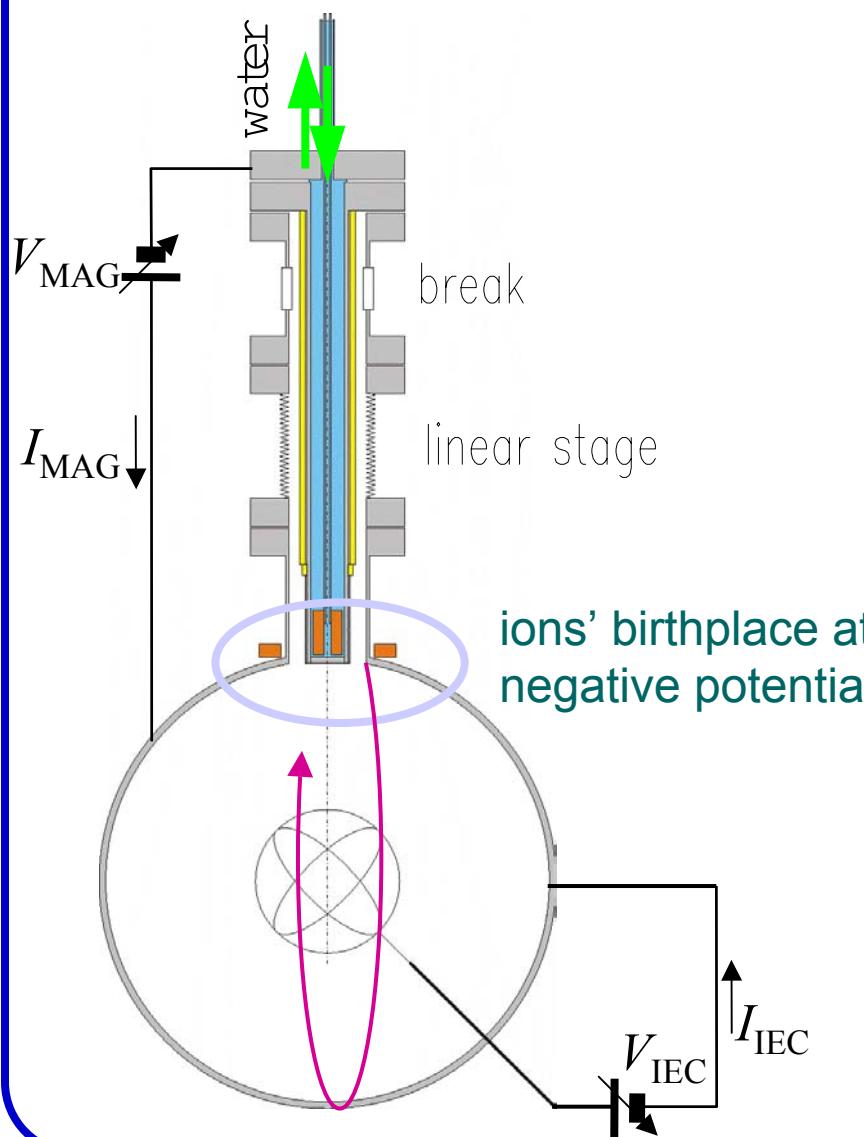


Problem of the original
magnetron ion source





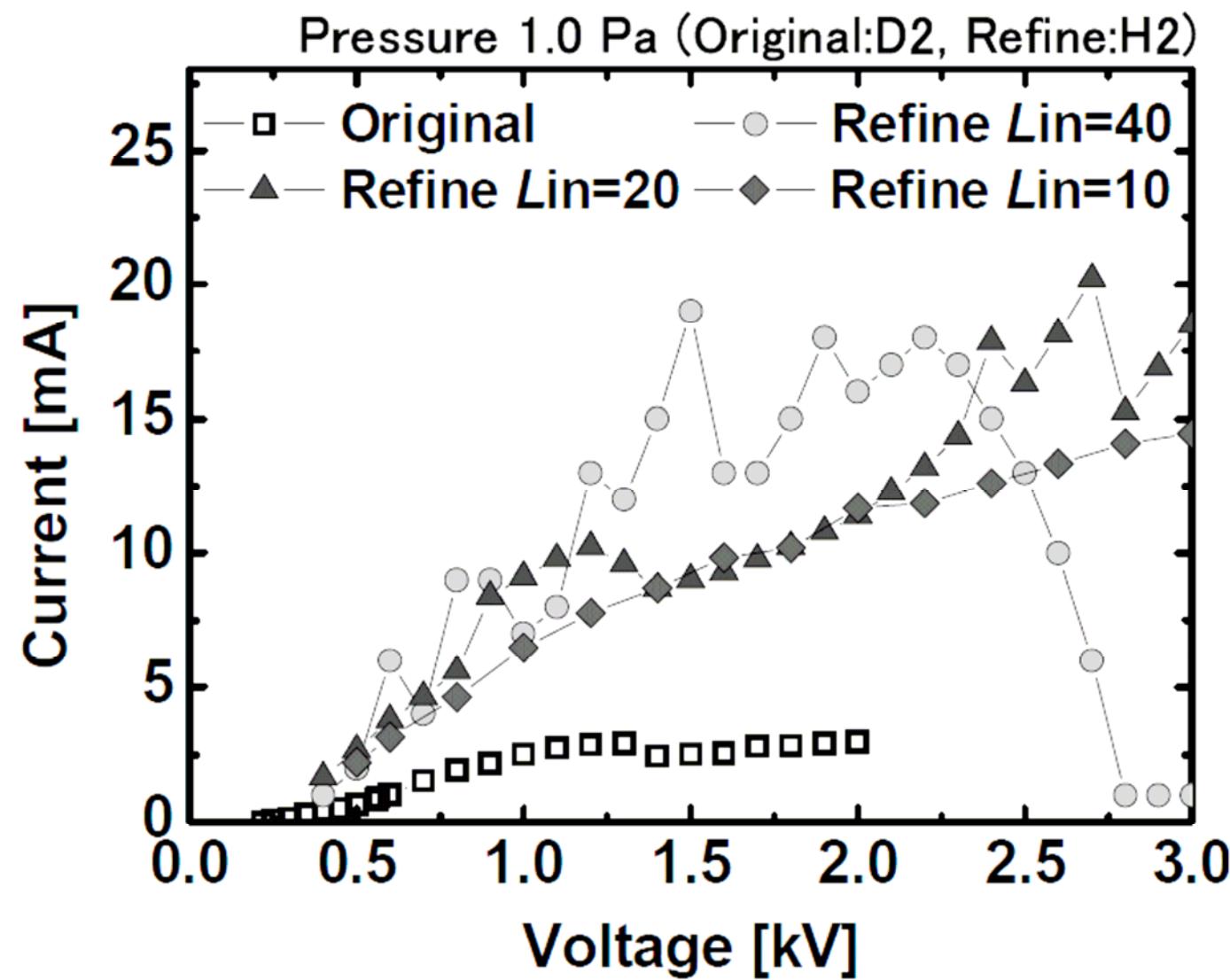
Setup for Glow–Magnetron Hybrid Discharge



$P(\text{H}_2)=3.0 \text{ Pa}$, $V=3.0 \text{ kV}$

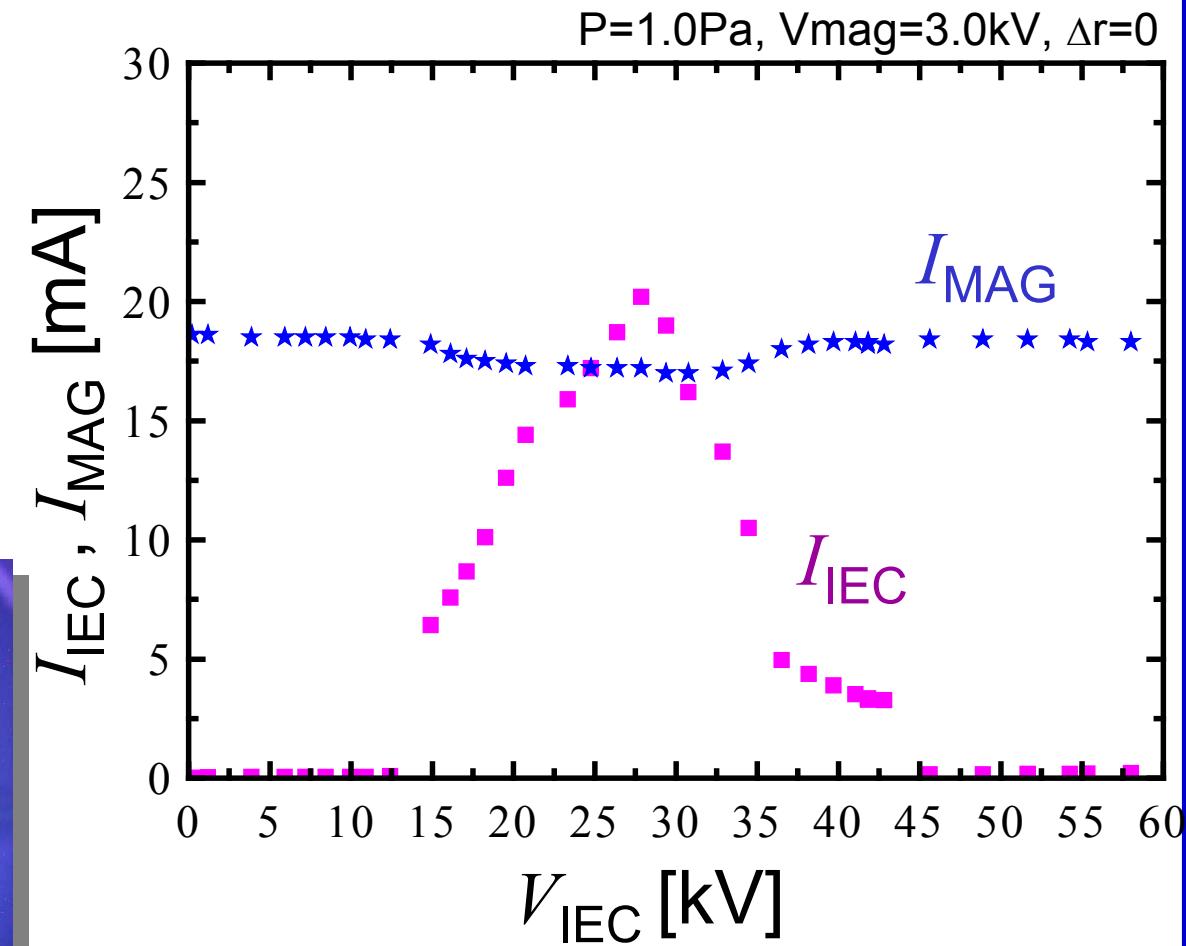
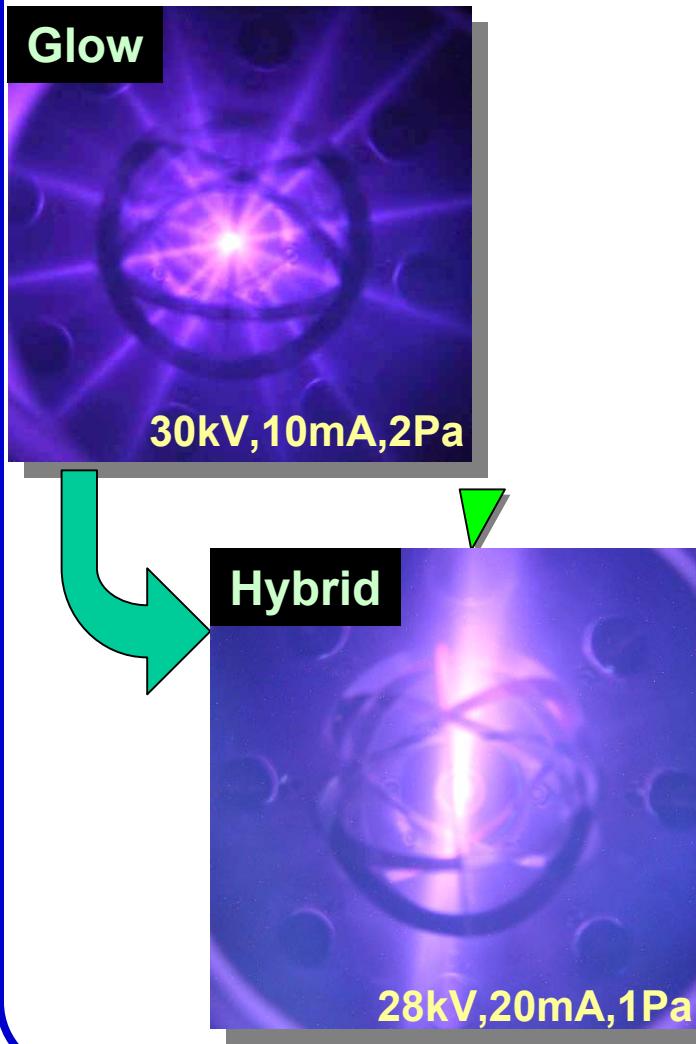


Manetron Discharge Current



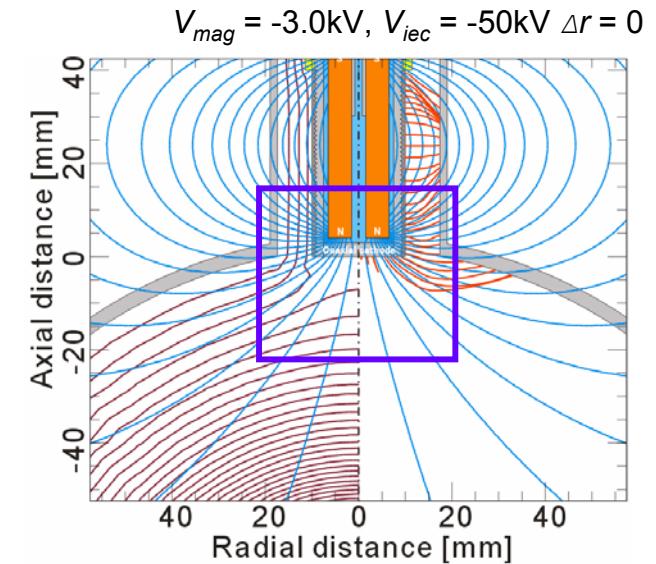
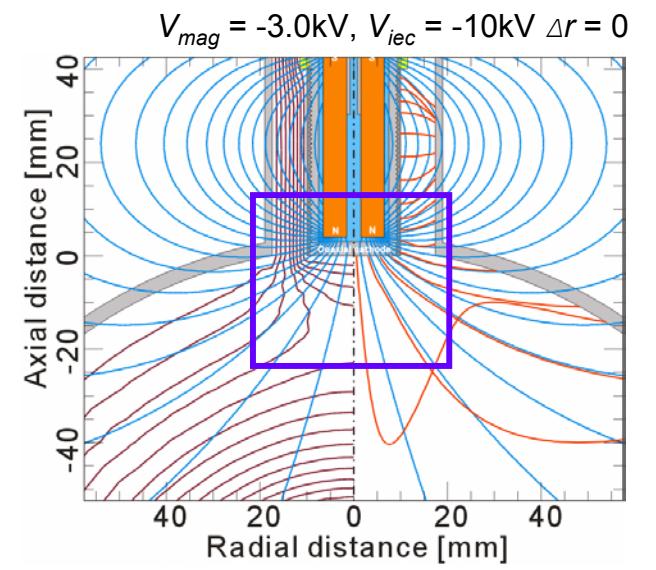
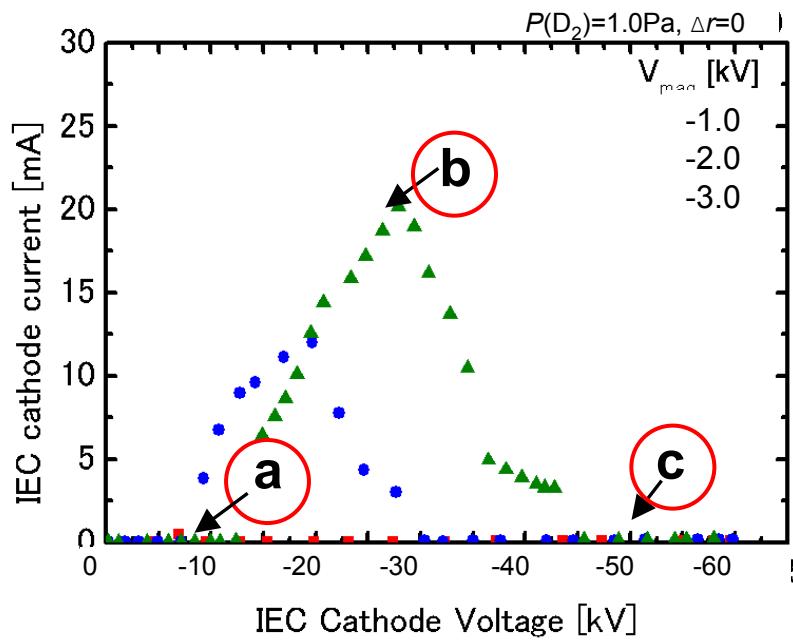


Glow-Magnetron Hybrid Discharge



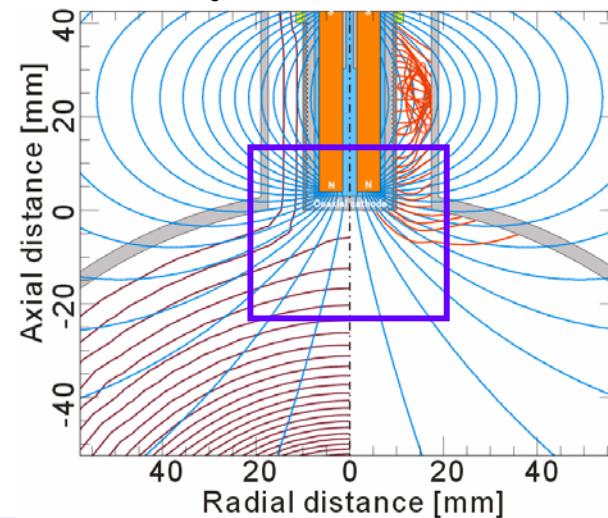
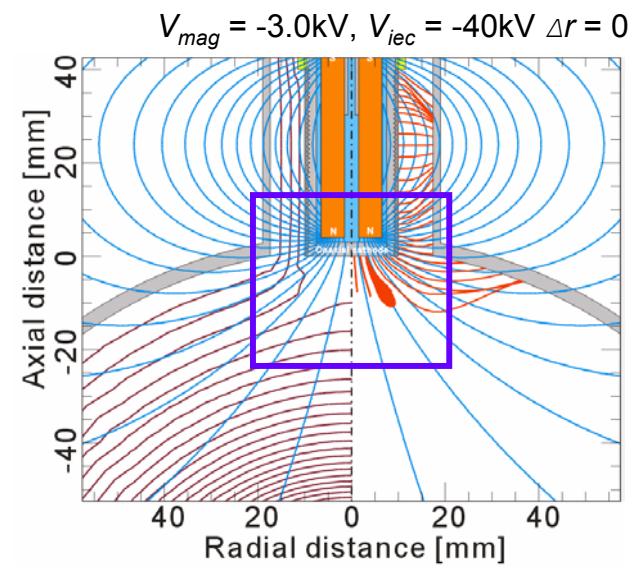
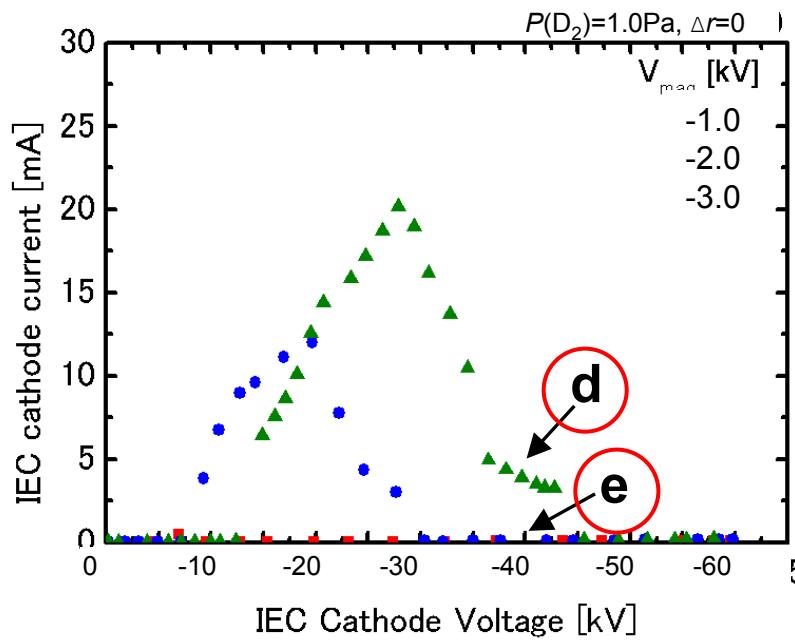


2-D Simulation Electron Trajectories





2-D Simulation Electron Trajectories



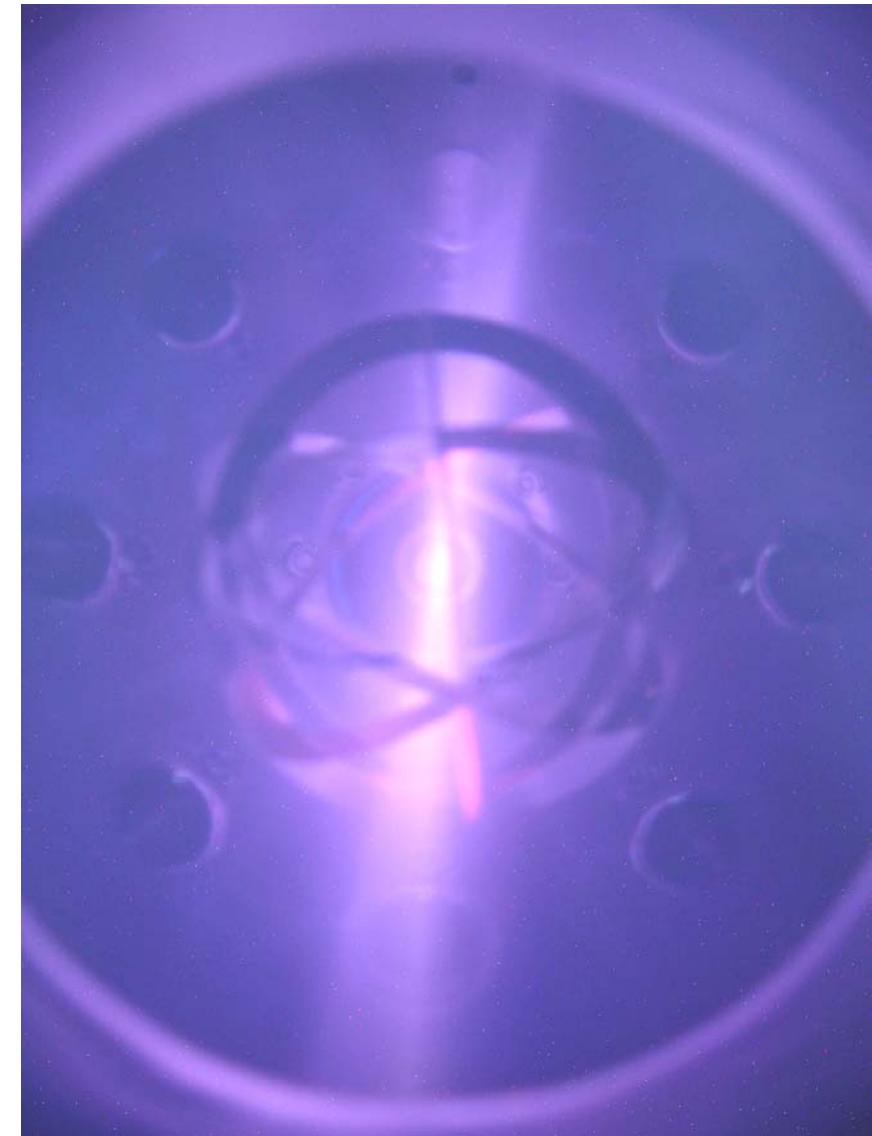
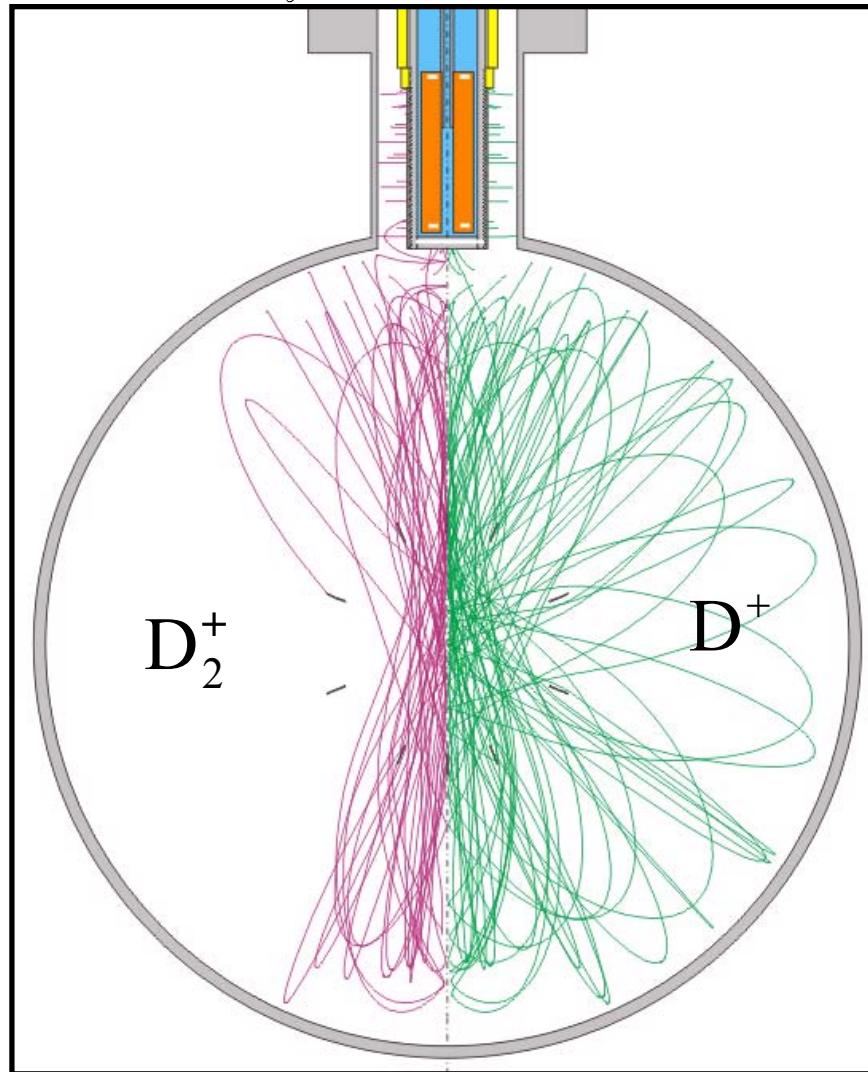
Trapped electrons at the top of coaxial cathode play an important part of hybrid discharge mode?





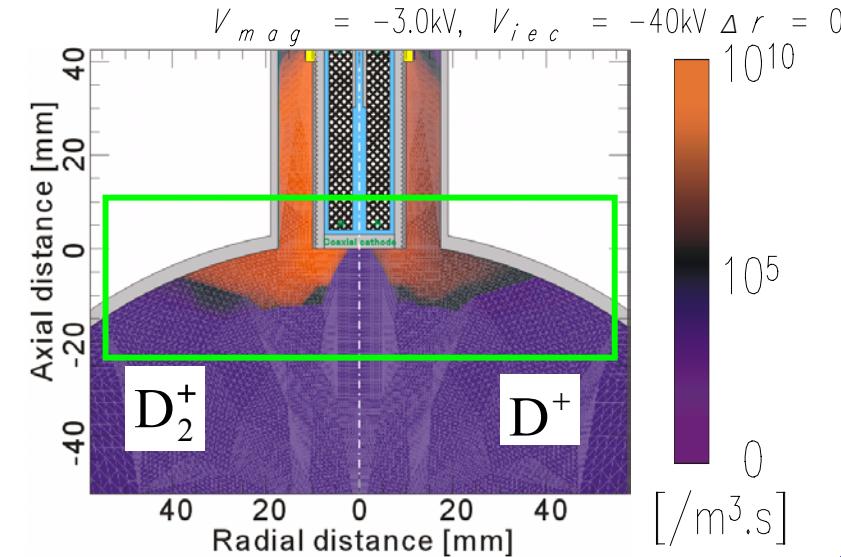
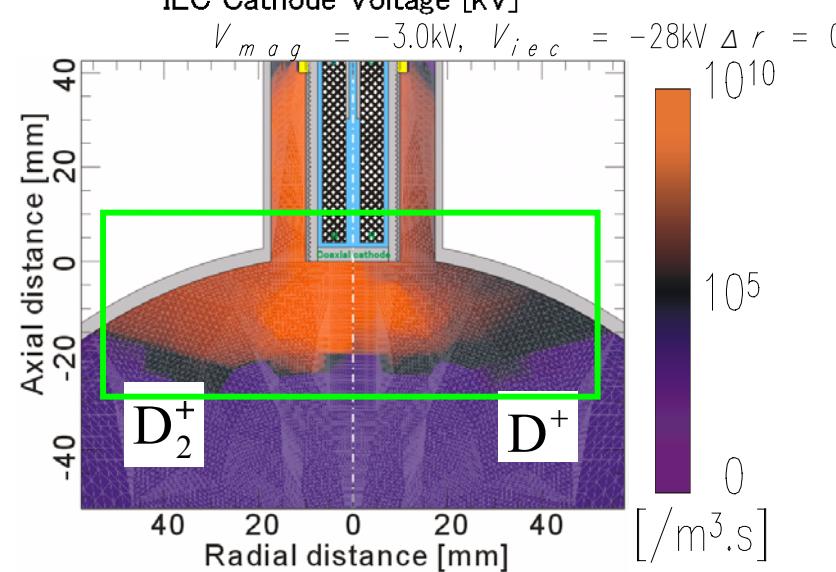
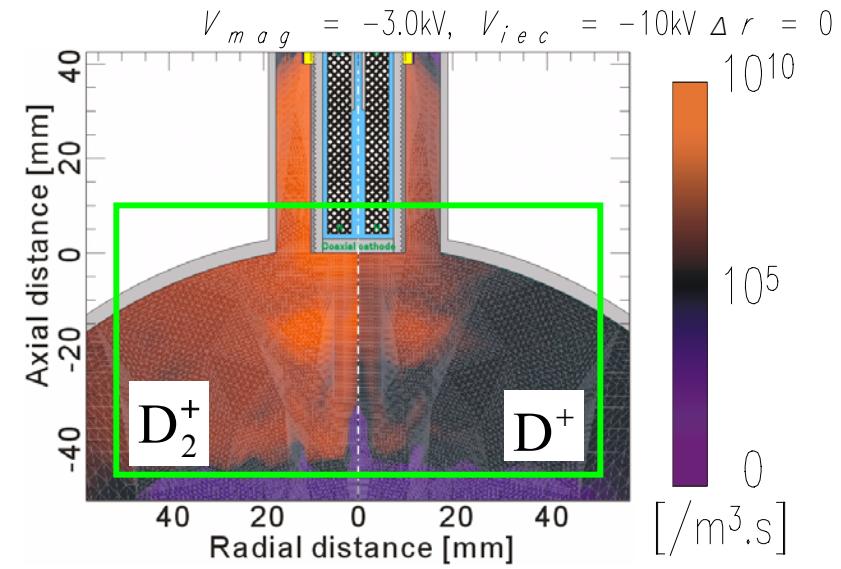
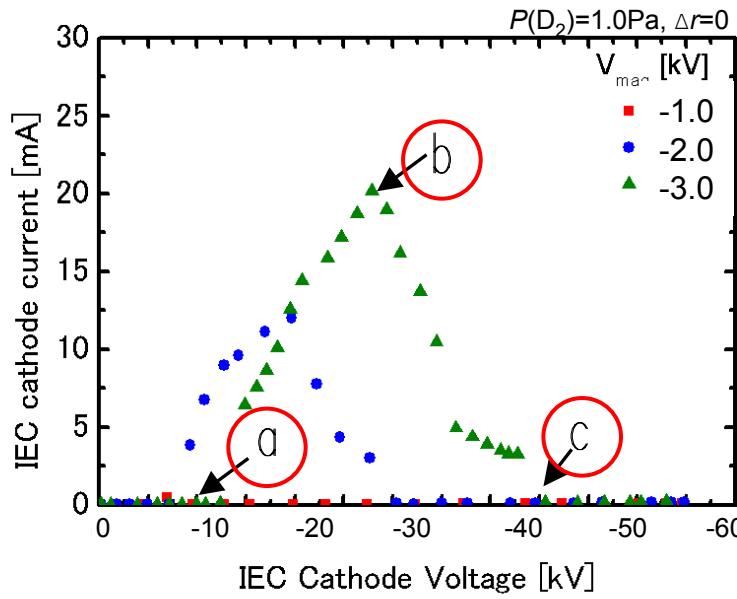
2-D Simulation .Ion Trajectories.

$$V_{mag} = -3.0 \text{ kV}, V_{iec} = -28 \text{ kV}$$





2-D Simulation . Ion Production.





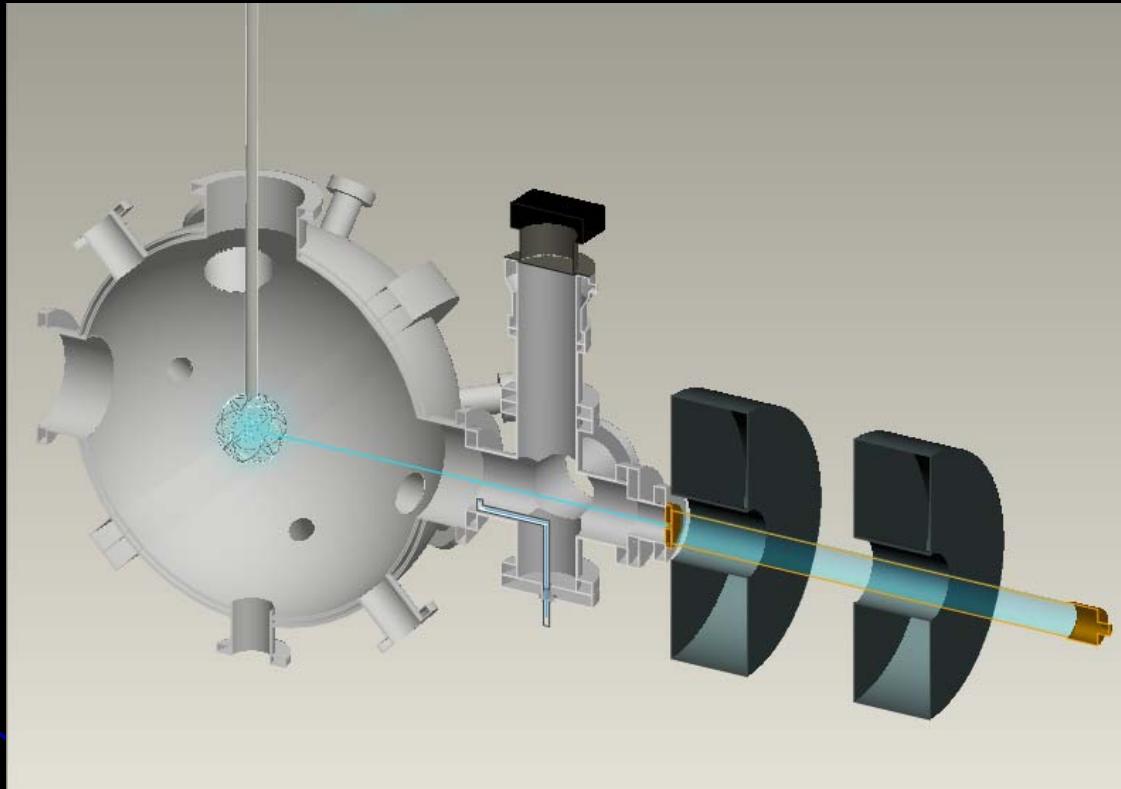
Summary

- We have developed refined magnetron-type ion source
- In glow-magnetron hybrid discharge, a decline in IEC cathode current was observed in high IEC cathode voltage region
- Numerical analyses suggest an influence of unexpected discharge mode

For more information please contact
Teruhisa Takamatsu: teruhisa@iae.kyoto-u.ac.jp



Progress in the Development of a ${}^3\text{He}$ Ion Source for IEC Fusion



G.R. Piefer, E.A. Alderson, R.P. Ashley, D.R. Boris, G.A. Emmert, R.C. Giar, G.L. Kulcinski, R.F. Radel, T.E. Radel, J.F. Santarius, A.L. Wehmeyer

US-Japan Workshop on IEC Devices
March 14-16, 2005 Los Alamos National Lab
Los Alamos, New Mexico



Outline

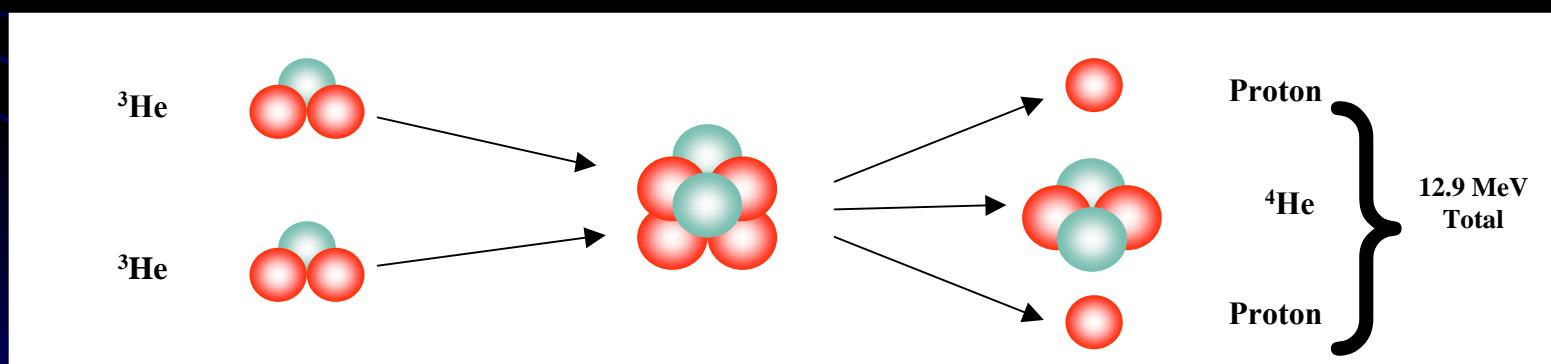
- ^3He - ^3He Fusion
 - Rationale for experiments
 - Reaction physics
 - IEC beam-background reaction rate estimate
 - Detectability
- Ion source development
 - Status as of the last meeting
 - Progress since the last meeting
 - Summary



Purpose of ^3He - ^3He Fusion in an IEC

- Benefits of ^3He - ^3He Fusion

- No Radioactive fuels or products
- Possibility of direct energy conversion
- Minimal or no activation of reactor vessel

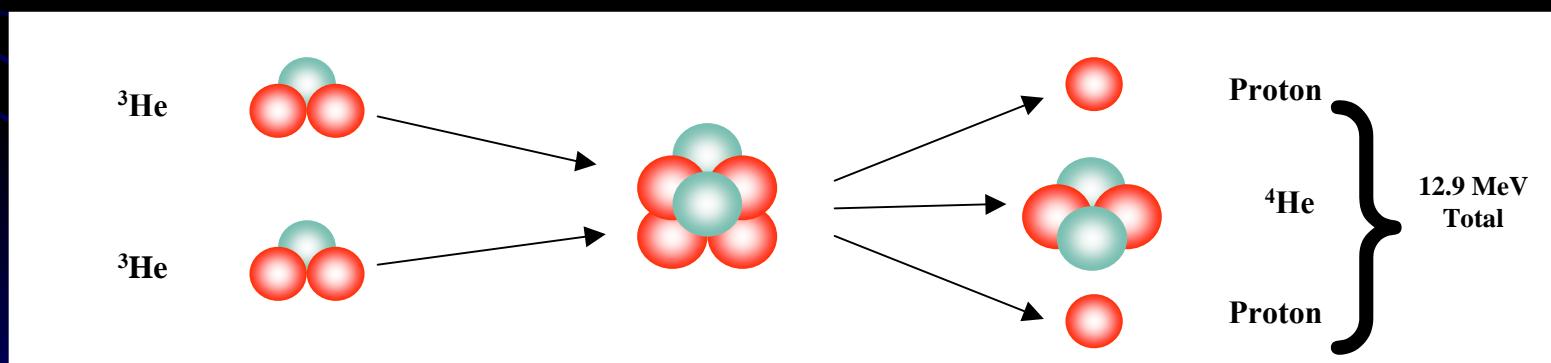


The ^3He - ^3He fusion reaction



Purpose of ^3He - ^3He Fusion in an IEC

- IEC offers some advantages over other research experiments
 - Higher energy capability than MFE or ICF devices
 - Higher current capability than accelerators
 - Allows for study of cross sections where counting statistics are currently poor

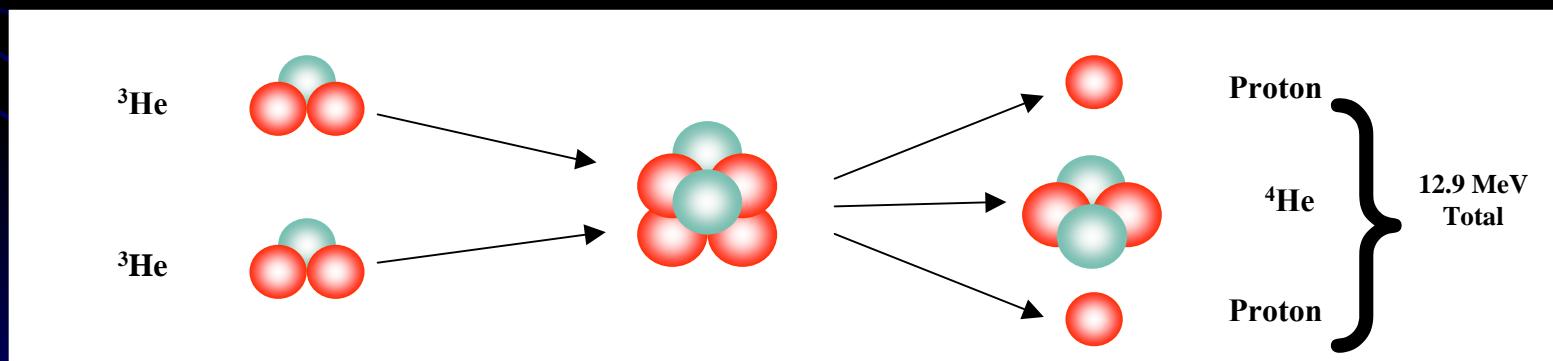


The ^3He - ^3He fusion reaction



Purpose of ^3He - ^3He Fusion in an IEC

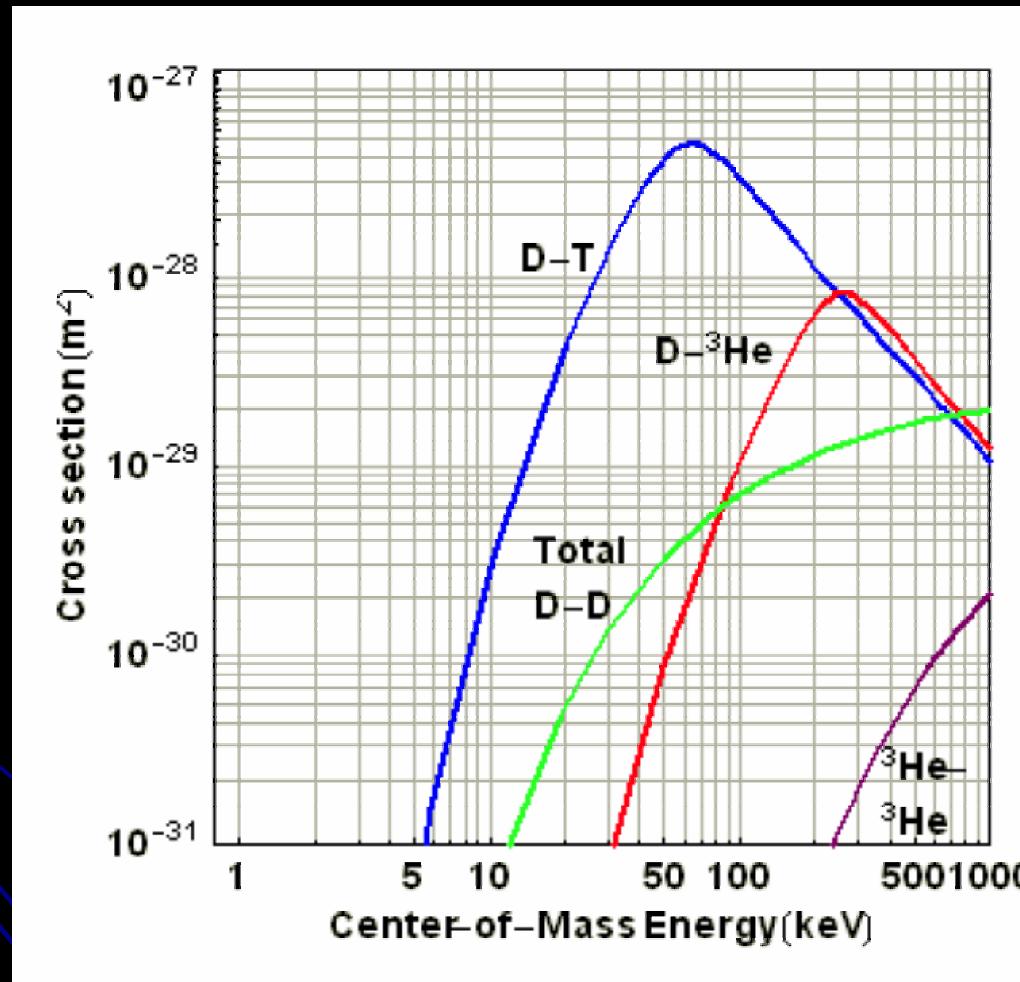
- ^3He - ^3He fusion has some significant disadvantages
 - Very small cross section at low voltages
 - Relatively difficult to obtain fuel in large quantities



The ^3He - ^3He fusion reaction

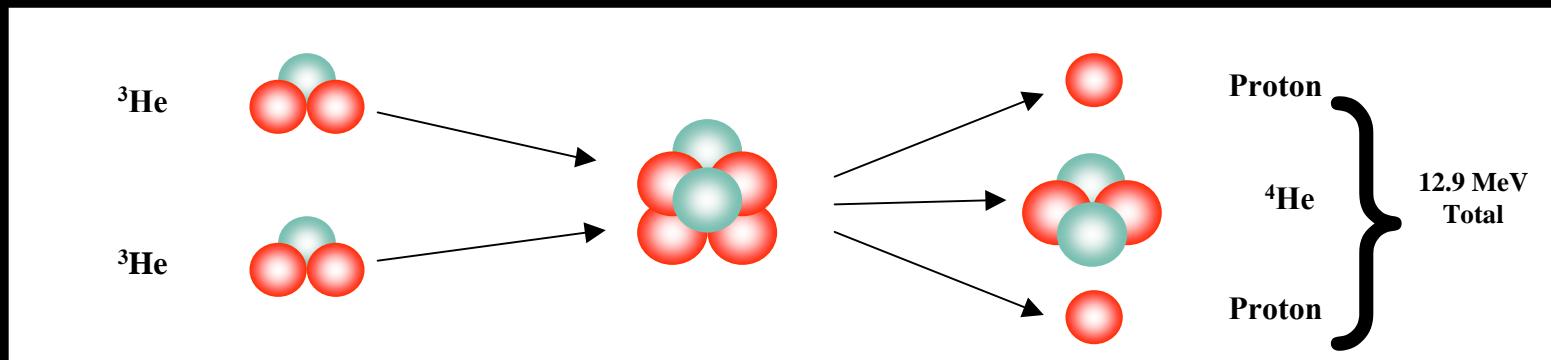


^3He - ^3He Fusion Cross Section is Substantially Lower than D-D



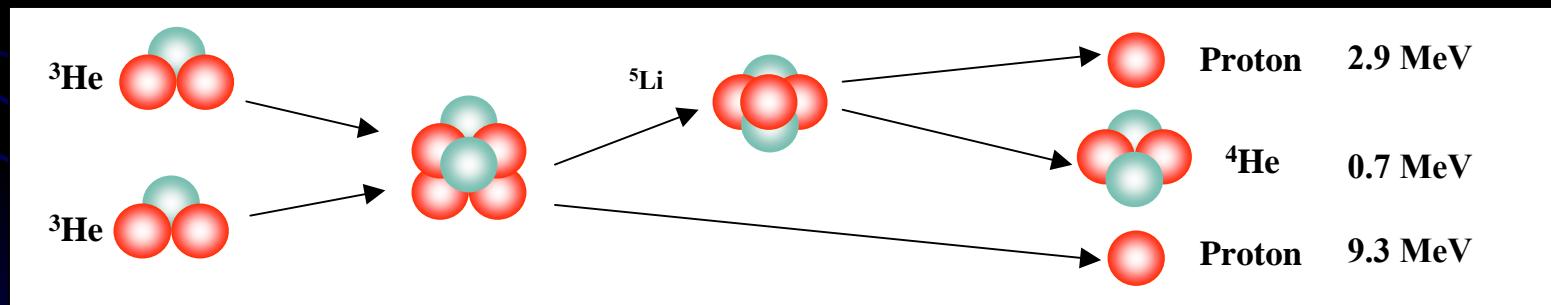


^3He - ^3He Reaction has Two Possible Reaction Sequences



The 3-body ^3He - ^3He reaction (~90% of reactions at 190keV CM energy)

- The three body reaction gives a relatively flat continuum of proton energies, which will be difficult to separate from noise



The two 2-body ^3He - ^3He reaction (~10% of reactions at 190keV CM energy)

- The 2-body reaction however, gives discrete proton energies, which will appear as a peak on top of the continuum at 9.3 MeV

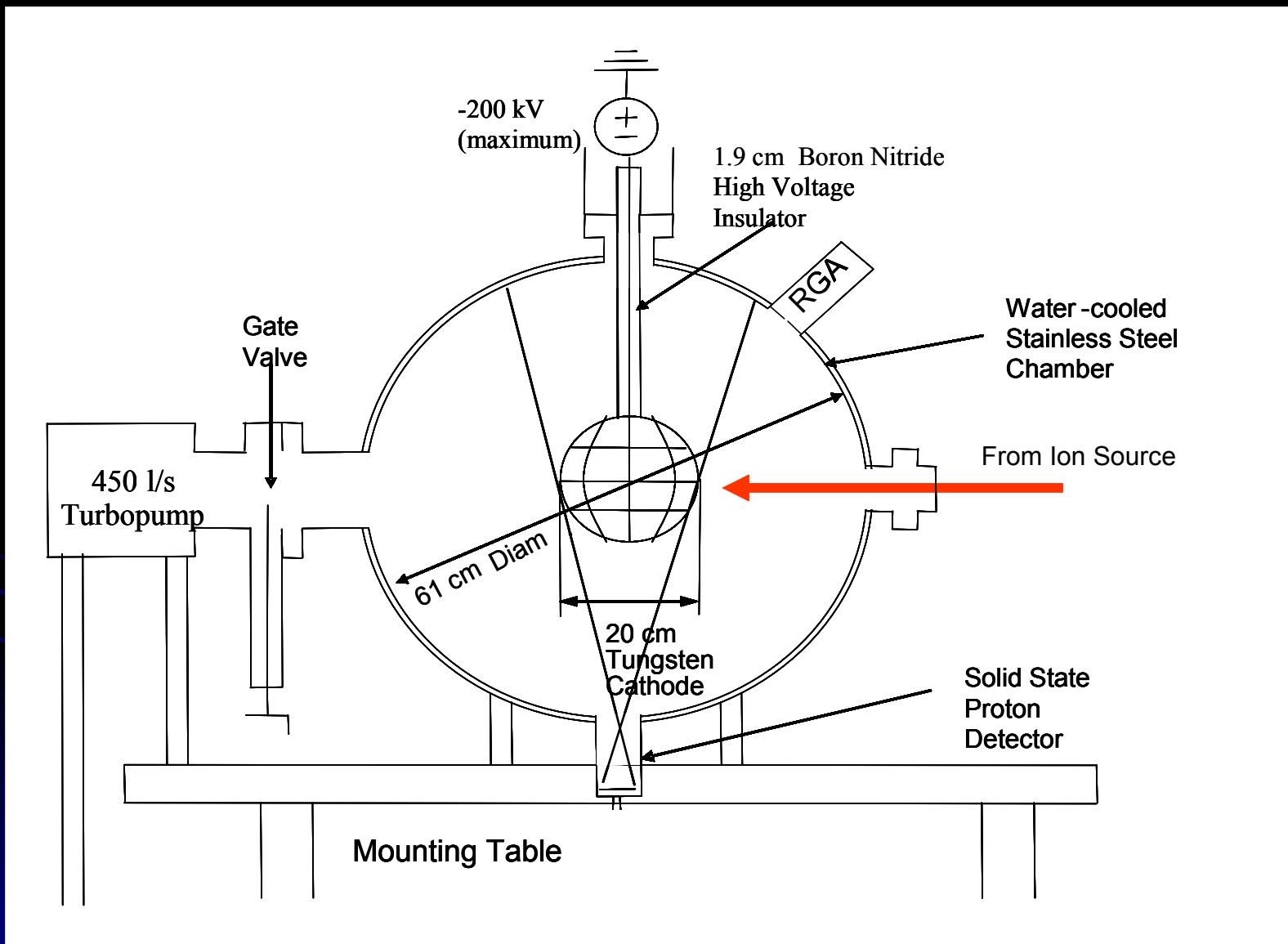


Reactivity in IEC will be Modeled as a Monoenergetic Beam-Background Source

- Beam currents low enough so that converged-core reactions are assumed to be insignificant
- Background gas pressure kept low enough such that ion charge exchange time is long compared to ion lifetime
- Model assumes proton detector observes reactions only inside of the cathode

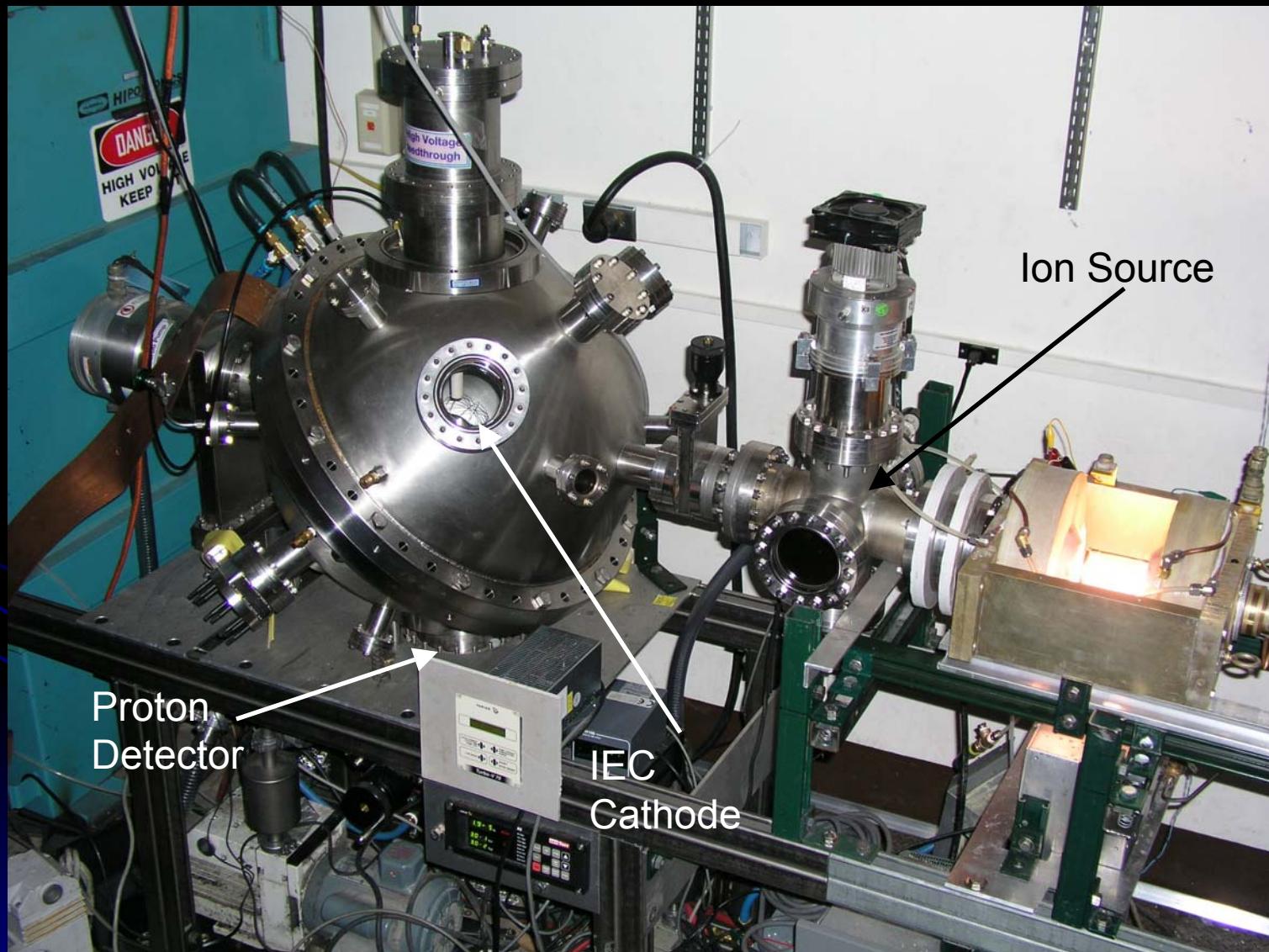


Setup for ${}^3\text{He}$ - ${}^3\text{He}$ Experiments





Setup for ${}^3\text{He}$ - ${}^3\text{He}$ Experiments





Assumptions for Rate Calculation

- Cathode current ~ 10 mA
- Cathode voltage = 200 kV
 - ${}^3\text{He}$ singly ionized \rightarrow Center of mass energy = 200 keV
- Cathode Transparency = 99%
- Average secondary emission coefficient = 2
- Background gas pressure = 0.2 mtorr (27 mPa)
- Cathode/anode radius ratio sufficiently small such that full ion current can be drawn



Fusion Rate can be Calculated from Assumed Parameters

- The fusion rate for a beam-background mono-energetic system can be calculated by the following equation:

$$F = n_b * \frac{I_{cath} * 2R_{cath}}{e(1 - \gamma)(1 + \sigma_{se})} * \sigma(E)$$

n_b is the background gas density, I_{cath} is the measured cathode current, R_{cath} is the cathode radius, $\sigma(E)$ is the fusion cross section, e is electron charge, γ is the grid transparency, and σ_{se} is the average secondary emission coefficient



Fusion Rate can be Calculated from Assumed Parameters

- The fusion rate for a beam-background mono-energetic system can be calculated by the following equation:

$$F = n_b * \frac{I_{cath} * 2R_{cath}}{e(1 - \gamma)(1 + \sigma_{se})} * \sigma(E)$$

- Using existing data for ${}^3\text{He}-{}^3\text{He}$ cross sections, this gives a fusion rate of $2*10^5$ fusions/second



Detection Rate Should be Observable

- Detector is ~ 50 cm from center of device
- Detector area = 1200 mm²
- The number of detected counts can be expressed as:

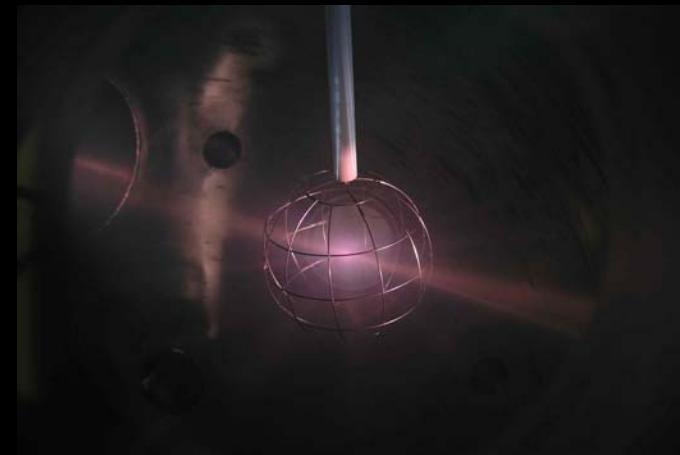
$$D = \frac{F}{4\pi R_{\text{det}}^2} A_{\text{det}}$$

- Detection rate ~ 76 counts/sec
- If 10% of these are 2-body reactions, the 9.3 MeV peak will have 7.6 counts/sec



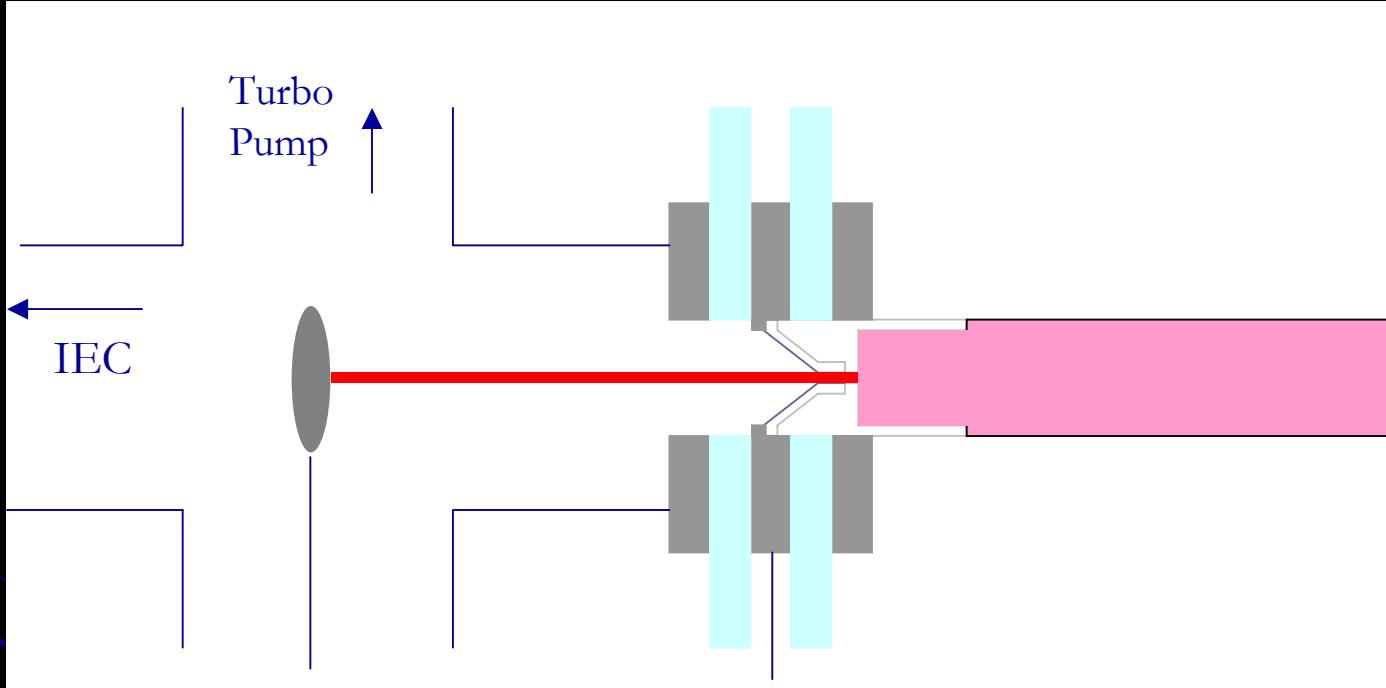
Ion Source Status as of Last Workshop— October 2003, Tokyo, Japan

- Helicon source on-line with ${}^4\text{He}$
- 2 mA cathode current observed in main system at modest voltage (~ 35 kV)
- Extraction system not yet constructed
- Ion current difficult to control
- Helicon fringing fields affected extracted beam





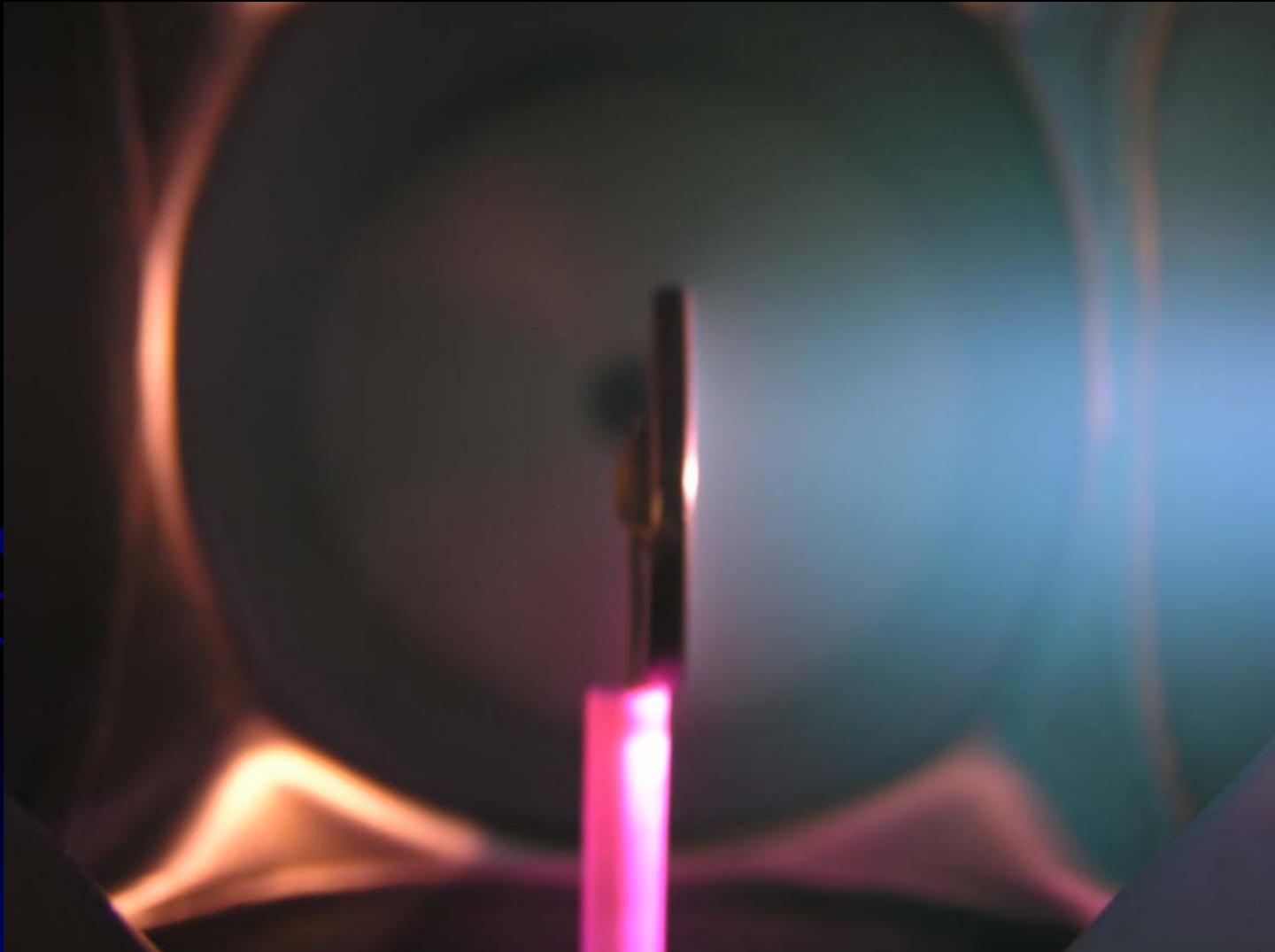
Ion Extraction Region Completed and Operational



- New electrode designed to minimize erosion
- Beam collection plate diagnostic added

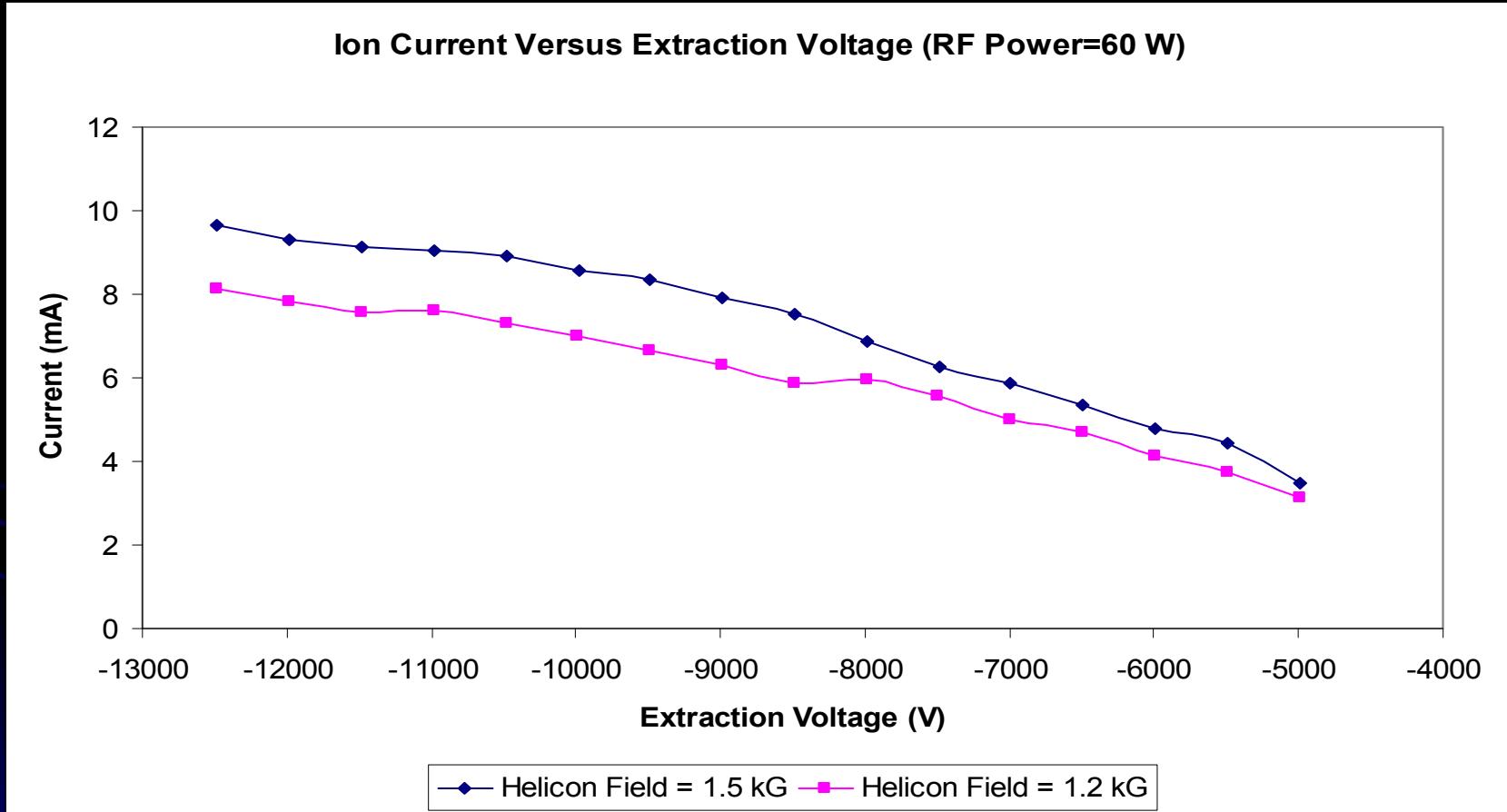


Extraction System Tested in ^4He with Collection Plate



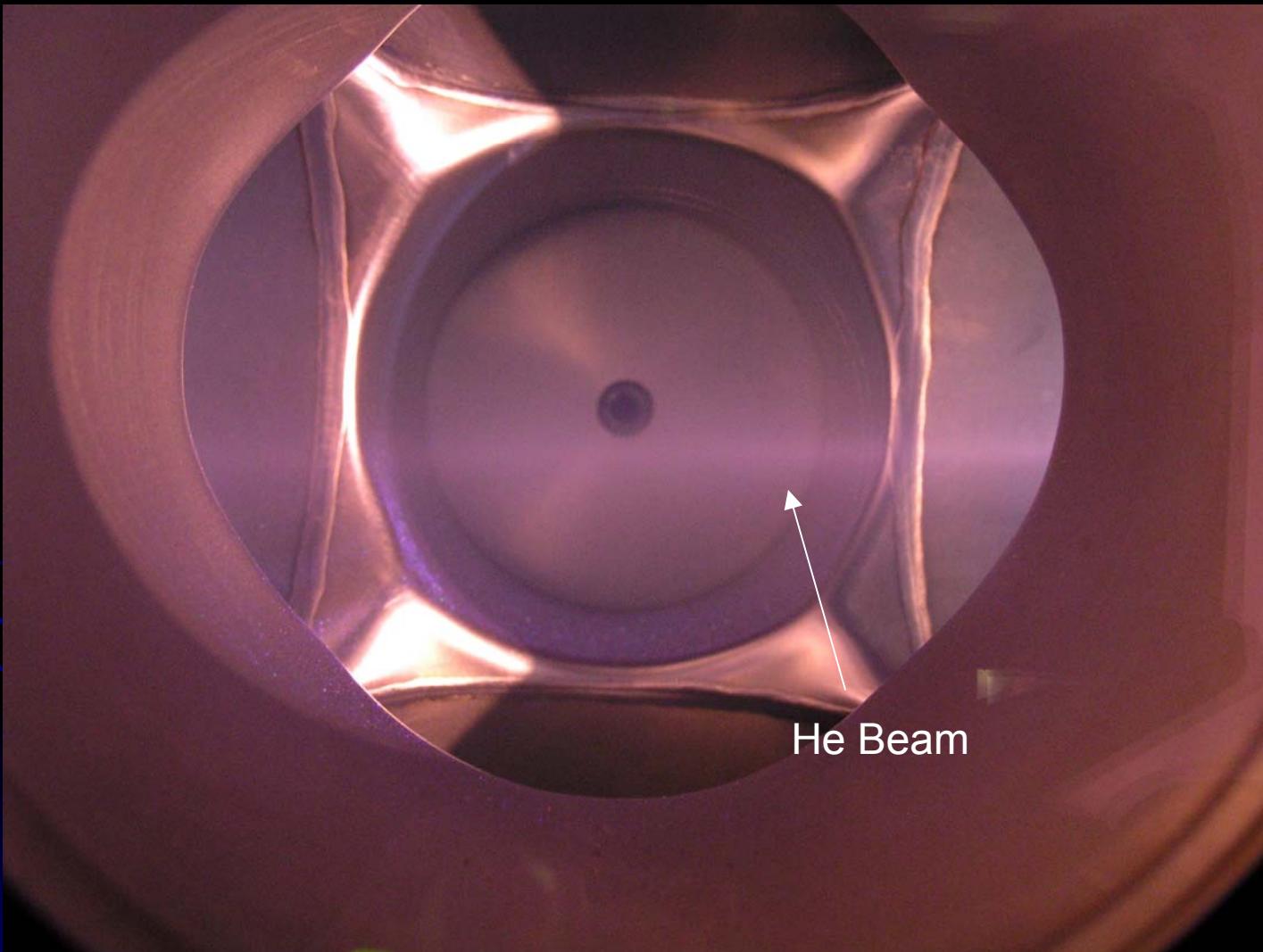


Ion Extraction Current Versus Extraction Voltage Shows Good Current Capability



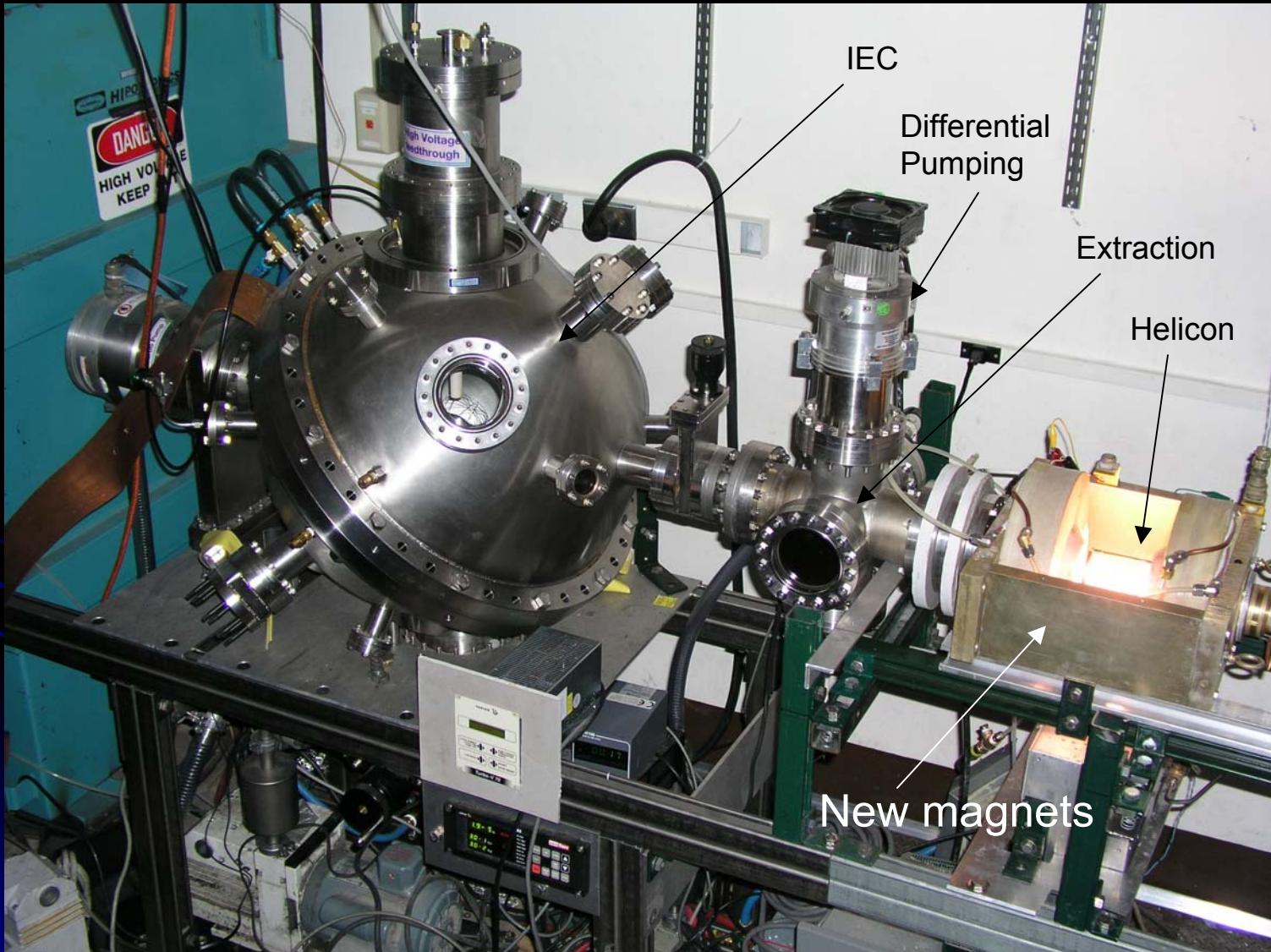


Stray Fields from Helicon Source Appear to Cause Beam Deflection



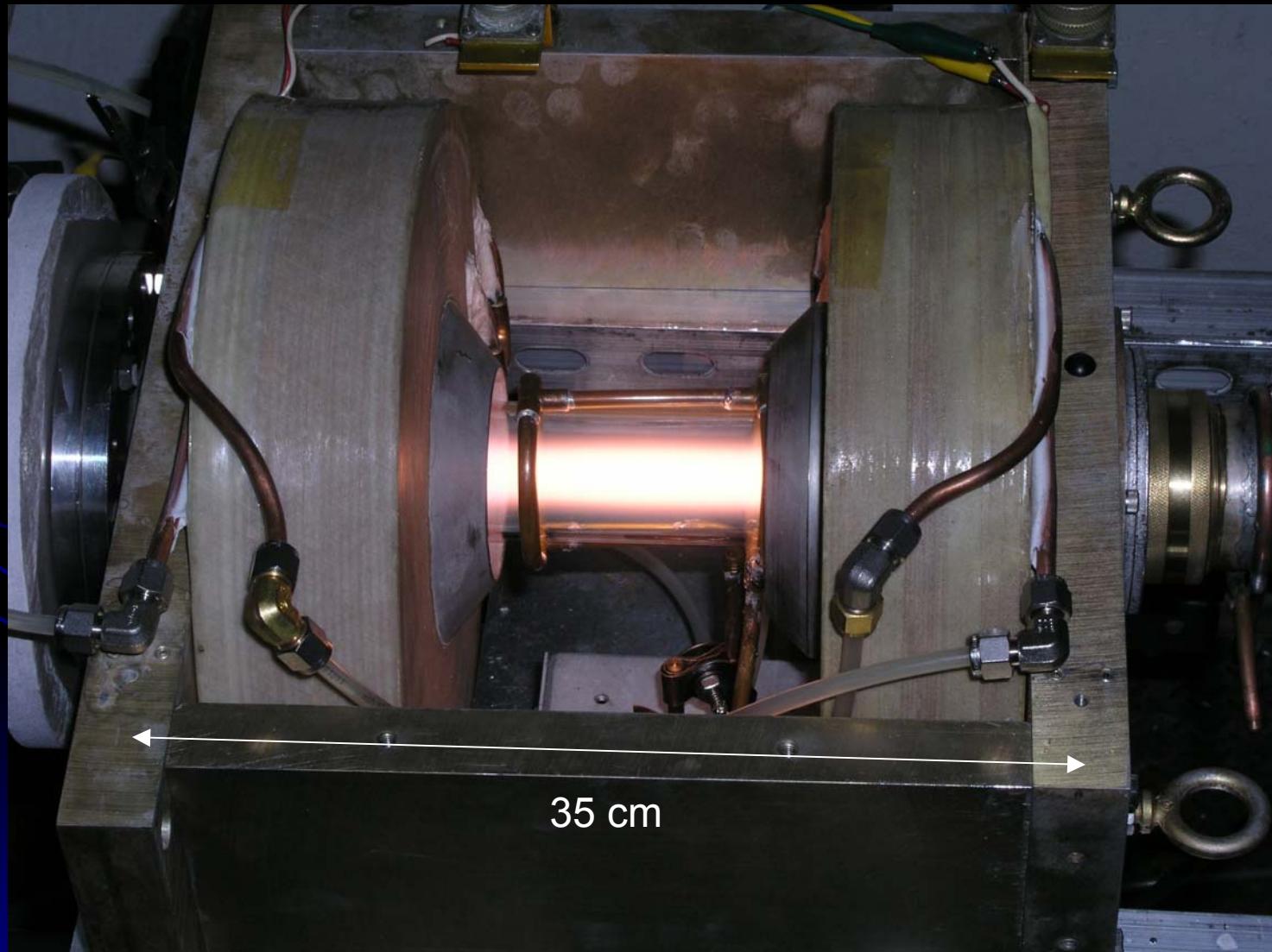


New Helicon Magnets are Installed and Now Being Tested





Fringing Fields Shunted Through Magnetic Circuit



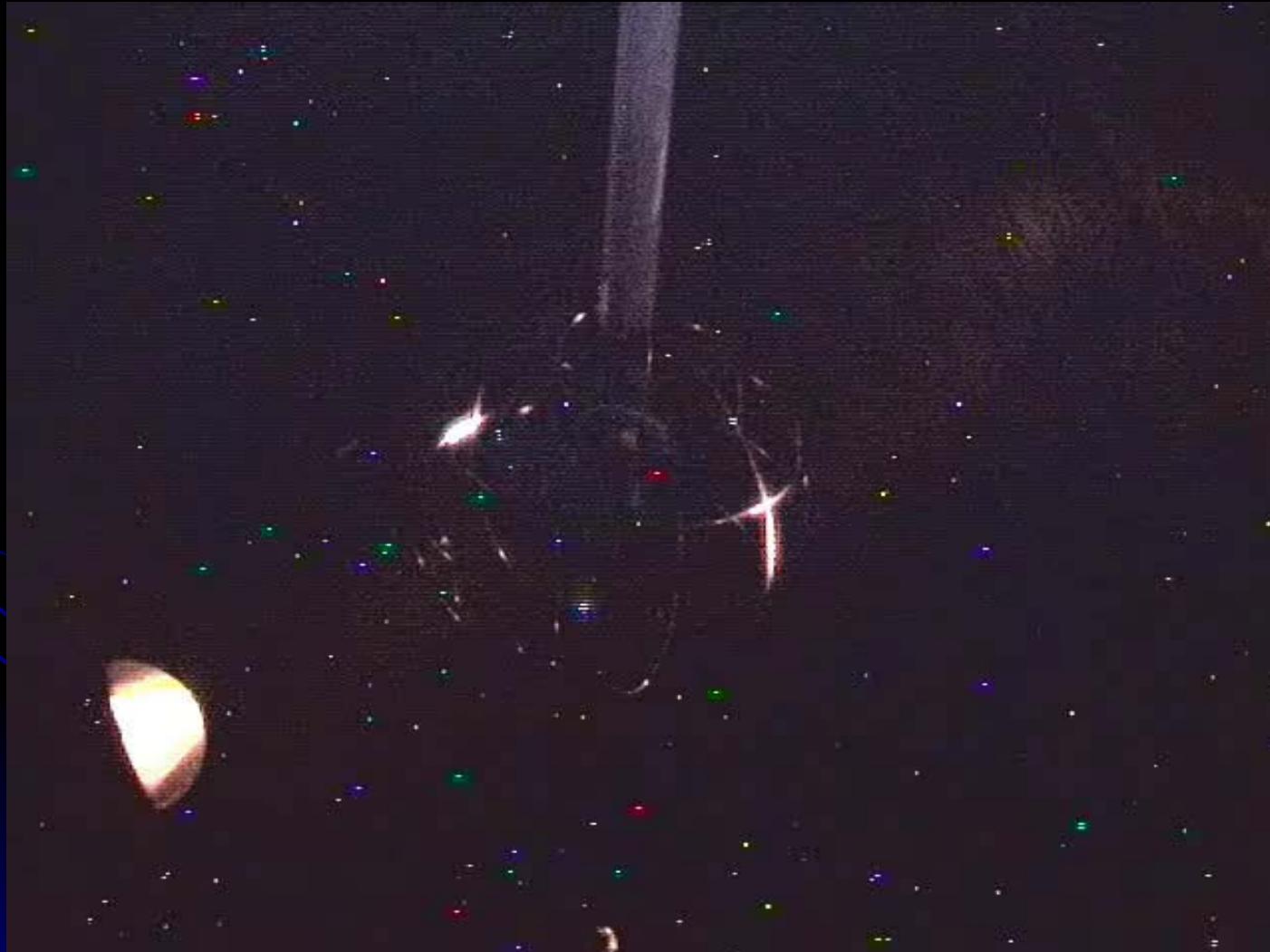


IEC Operation with Ion Source is Improving

- Operation at voltages up to 130 kV
- Operation at cathode currents up to 10 mA
- Operation at pressures as low as 50 μ torr, and as high as 0.5 mtorr



Some Instability in High Voltage Discharges



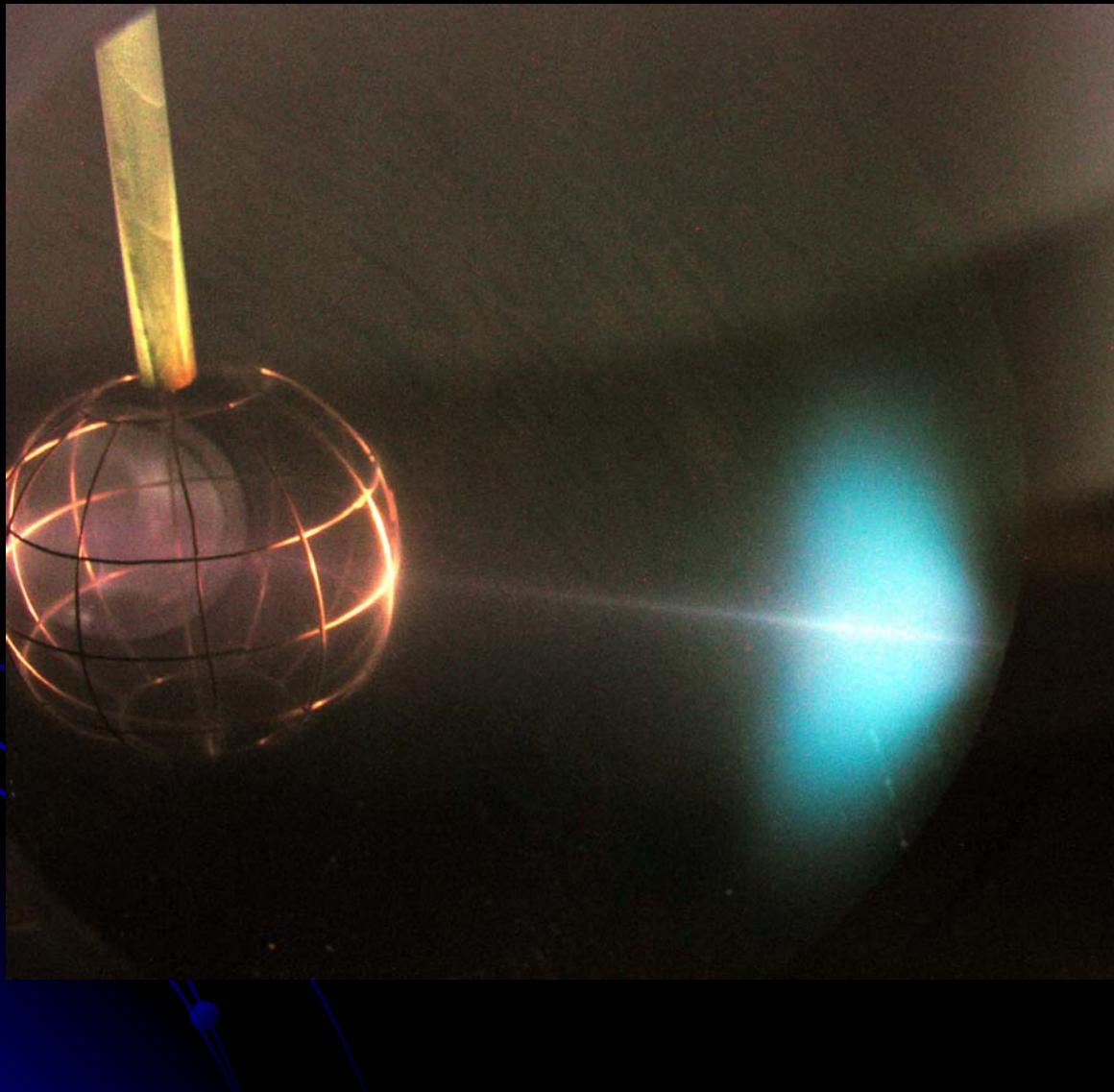


Conclusions

- IEC experiments looking for ${}^3\text{He}$ - ${}^3\text{He}$ fusion reactions are underway
- Good results so far with ${}^4\text{He}$, and some with ${}^3\text{He}$
- Ion source and IEC operation with source have improved markedly
 - Extraction region online
 - Helicon fringe fields reduced
 - IEC operating voltage up to 130 kV
- Still some problems to overcome
 - HV breakdown at high cathode voltages
 - He beam deflection



Questions?





Neutron Production through Beam-Beam Collision at Low Gas Pressure and Large Current Operation

K. Noborio, Y. Yamamoto, Y. Ueno and S. Konishi

Institute of Advanced Energy, Kyoto University

Gokasho, Uji, Kyoto, 611-0011, Japan



Outline

- Previous works and objectives
- Simulation code
- Results
- Summary



Our previous works

One dimensional simulation of the spherical IECF

- “Normal” glow discharge.(without ion source, self sustaining)
 - ✓ Self sustaining discharge mechanism:
Charge-exchange and re-ionization cycle
 - ✓ Spatial distribution of NPR: Ion-background - near the cathode
Neutral-background - uniformly
- “Assisted” discharge enabling low pressure operation
 - ✓ Discharge characteristics: V and I can be controlled independently
 - ✓ NPR (through beam-background reaction): does not increase with reducing of the P



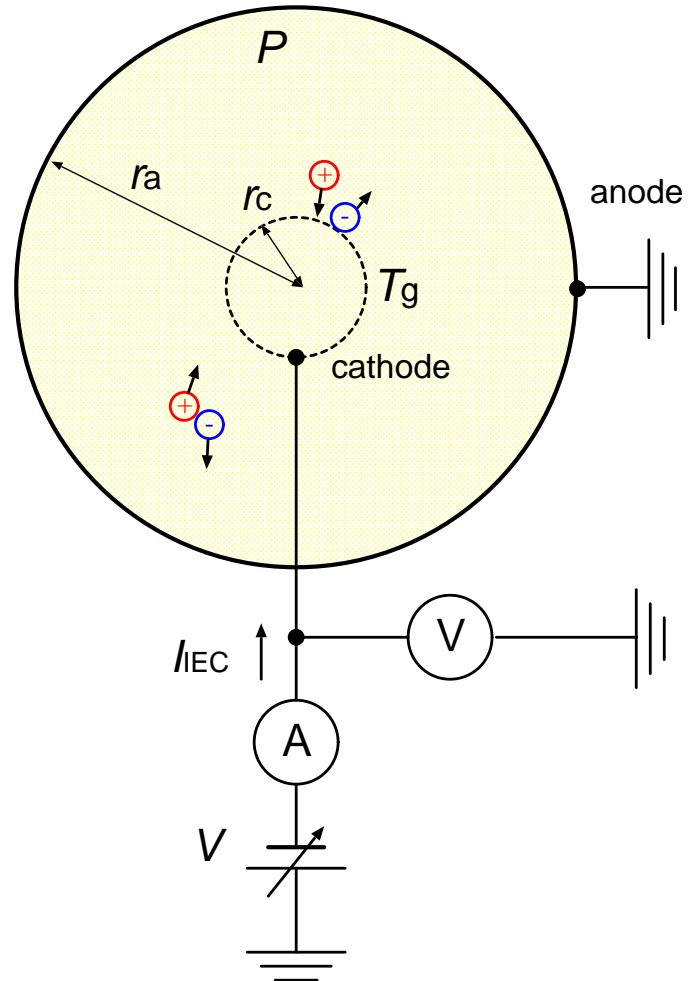
Objectives

Evaluation of

- Characteristics on low pressure ($\sim 0.1\text{mPa}$)
- Confinement level of energetic particles
- NPR through beam-beam collision at large current operation

Simulation code

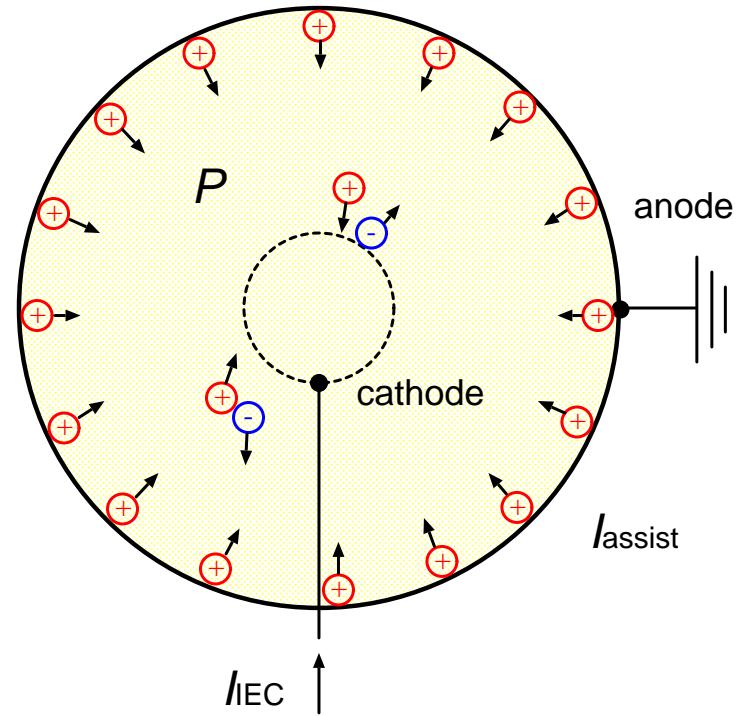
- Particle-in-Cell (PIC) model
- One-dimensional coordinate (r)
- Two-dimensional velocity (v_r , v_θ)
- Energetic ion, neutral, & electron (= “beam” particles)
- Atomic processes between beam particle and background gas particle with Monte Carlo scheme
- Fusion reaction rate through beam-neutral collision and beam-beam collision
- Life span of each super-particle



Simulation of “assisted” discharge

Injecting ions to sustain glow discharge in low pressure

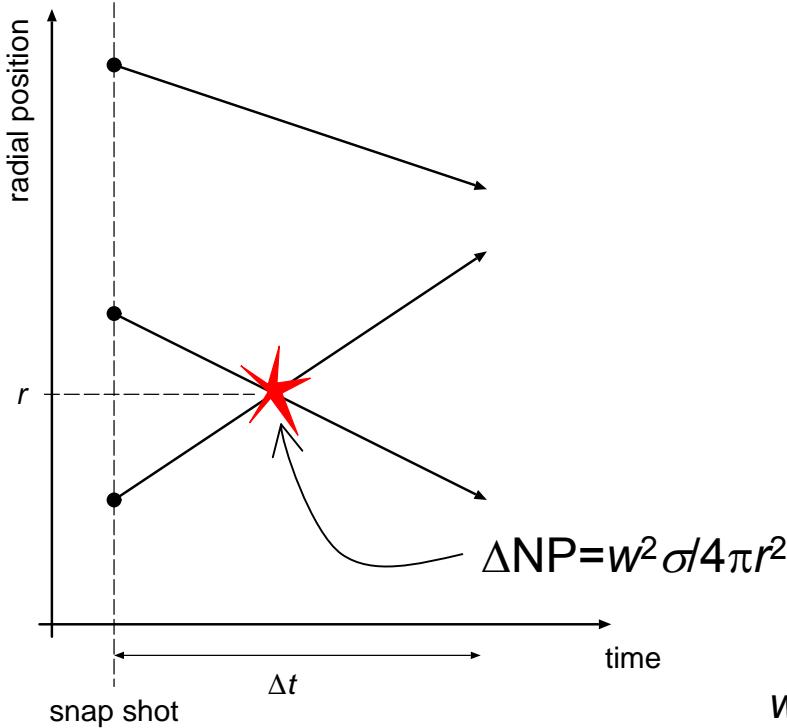
- D_2^+
- From the position of the anode
- Constant injection current (I_{assist} , 2mA-200mA)
- Low energy (0.5% of the applied voltage)



Calculation of Beam-Beam fusion

From snap shot of velocity distribution (r, v_r) (independent from main flow)

- Considering all possible combination



```

for (all pairs of particles)
  if (the trajectories intersect){
    calculate  $\Delta NP$ 
     $NP = NP + \Delta NP$ 
  }
}
 $NPR_{BB} = NP / \Delta t$ 

```

w : weigh of super-particle

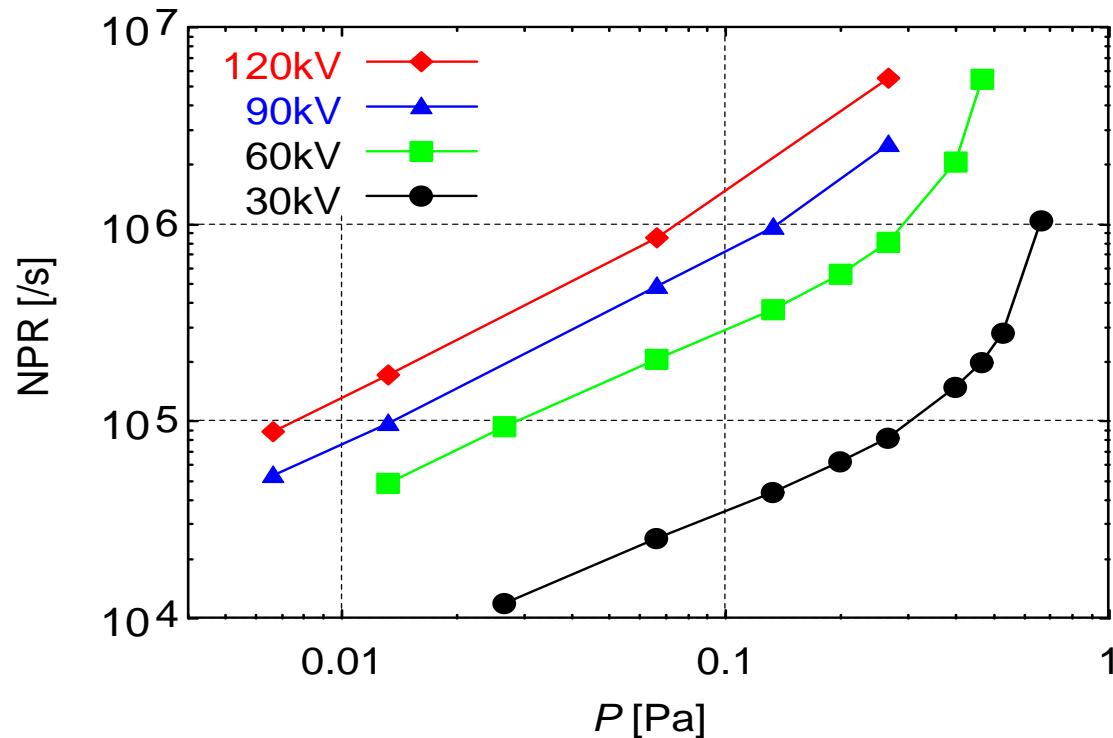


Simulation parameters

• Anode radius	$r_a = 17\text{cm}, 10\text{cm}$
• Cathode radius	$r_c = 3\text{cm}$
• Transparency of the cathode	$T_g = 0.92, 0.98$
• Gas pressure	$P = 0.1\text{mPa} \sim 1\text{Pa}$
• Discharge voltage	$V = 60\text{kV} \sim 120\text{kV}$
• Discharge current	$I_{IEC} = \sim 5\text{A}$
• Injected ion current	$I_{assist} = 2\text{mA} \sim 200\text{mA}$
• Time step	$\Delta t = 2\text{ps}$
• Spatial mesh width	$\Delta r = 0.2\text{mm}$

NPR vs. gas pressure

NPR vs. gas pressure



- Discharge voltage } given
- Injected current
- Discharge current calculated

NPR does not increase as expected when the pressure decreases.

$$(I_{\text{assist}} = 2 \text{mA}, r_a = 17 \text{cm}, T_g = 0.98)$$



Confinement of energetic particles

$$\text{NPR}_{\text{BN}} = \int n_i n_g \sigma_{\text{fusion}} v dV$$

n_i : Density of beam particles
 n_g : Density of background
 σ_{fusion} : X-section
 v : Ion velocity

Low pressure

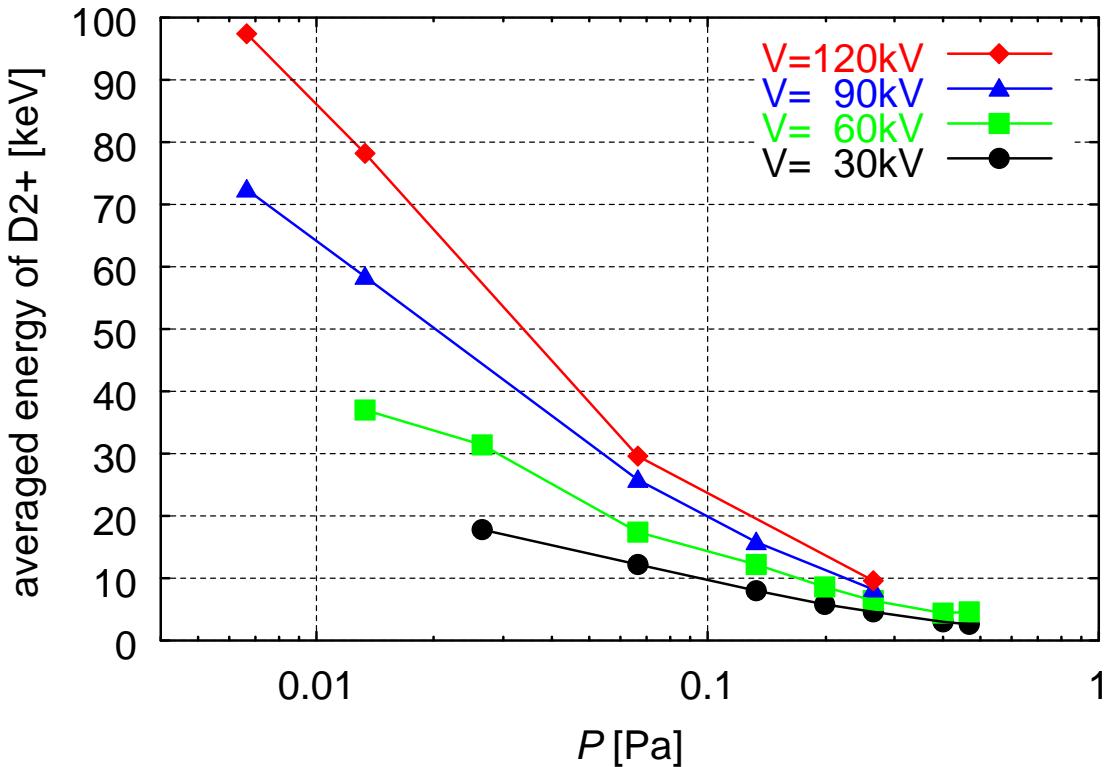


n_g : decrease

σv : increase \leftarrow ion energy

n_i :
 { increase \leftarrow circulation
 decrease \leftarrow multiplication (ionization)

Averaged energy of ions (within the cathode)

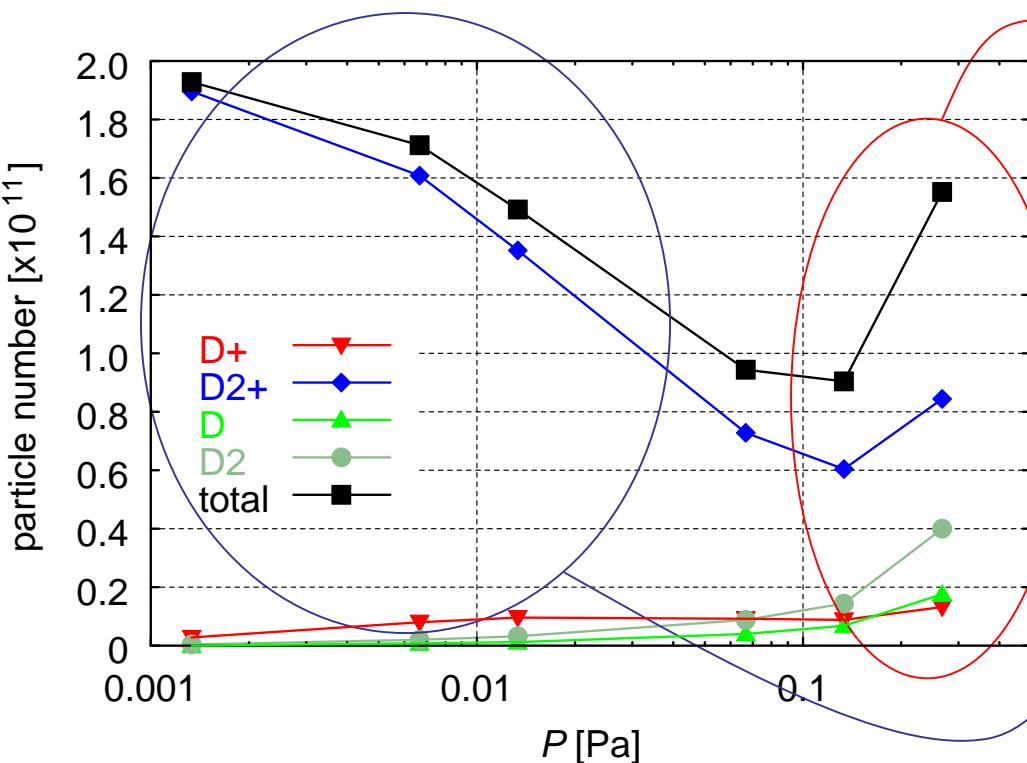


- Averaged energy of ions increases as the pressure decreases.
- Averaged energy does not reach the energy responding to the applied voltage less than 0.01Pa
→more reduction is expected to be efficient

($I_{\text{assist}}=2\text{mA}$, $r_a=17\text{cm}$, $T_g=0.98$)

Confinement of energetic particles

particle number vs. gas pressure



$P > 0.1 \text{ Pa}$:

number of each species increases with increase of P
(multiplication effect)

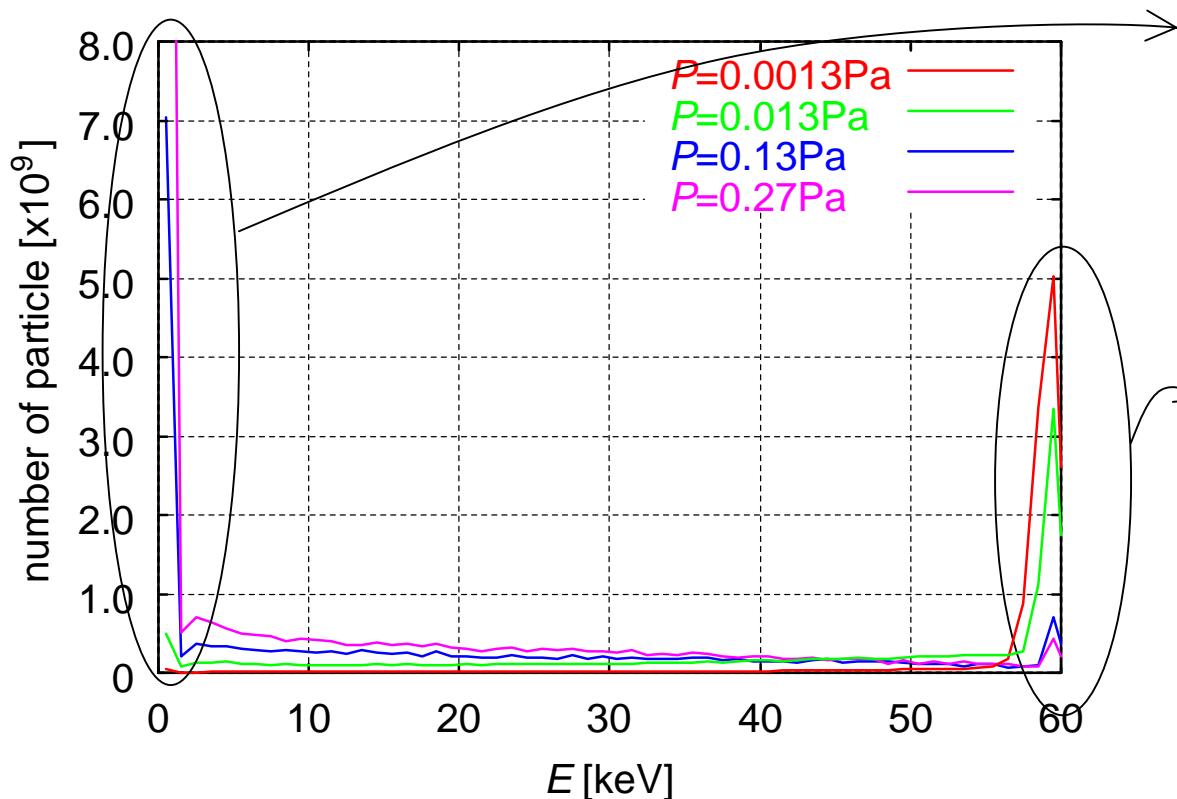
$P < 0.1 \text{ Pa}$:

number of D_2^+ increases with decreasing of P
(circulation effect)

$$V=60\text{kV}, I_{\text{assist}}=2\text{mA}, r_a=17\text{cm}, T_g=0.98$$

Multiplication effect through ionization

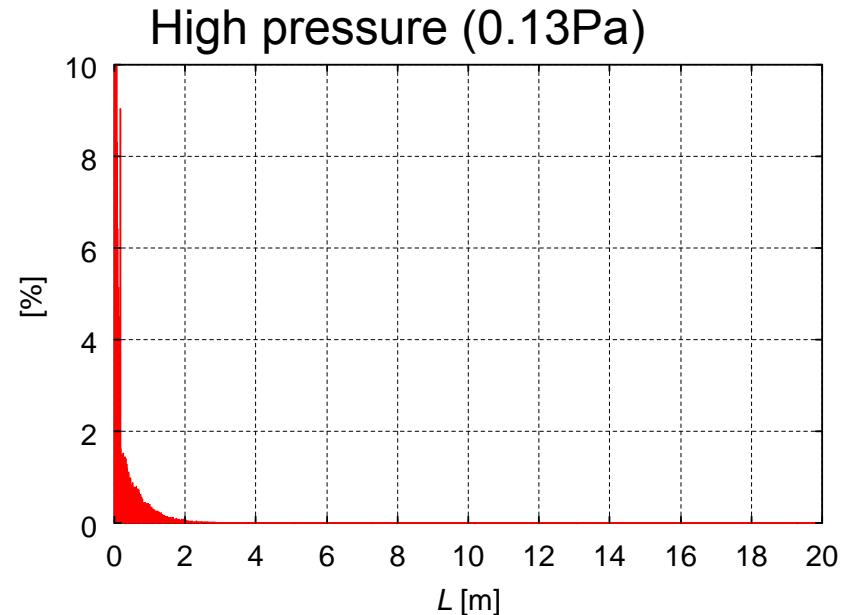
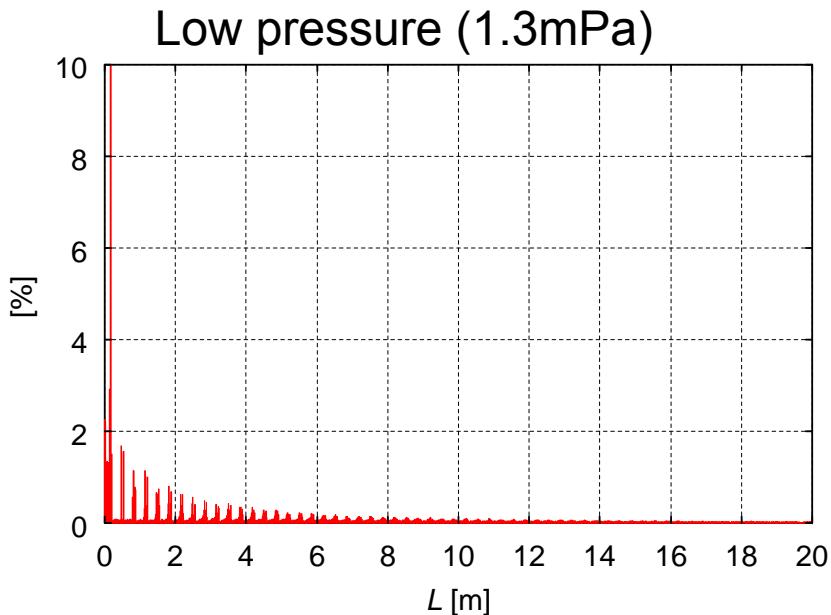
Energy distribution of D_2^+ within the cathode



- Low energy:
 $\text{Low } P \rightarrow \text{decrease}$
 (Multiplication through ionization reaction within the cathode)
- High energy:
 $\text{Low } P \rightarrow \text{increase}$
 (fully accelerated from the anode to the cathode)

$$V=60\text{kV}, I_{\text{assist}}=2\text{mA}, r_a=17\text{cm}, T_g=0.98$$

The life span of injected ions

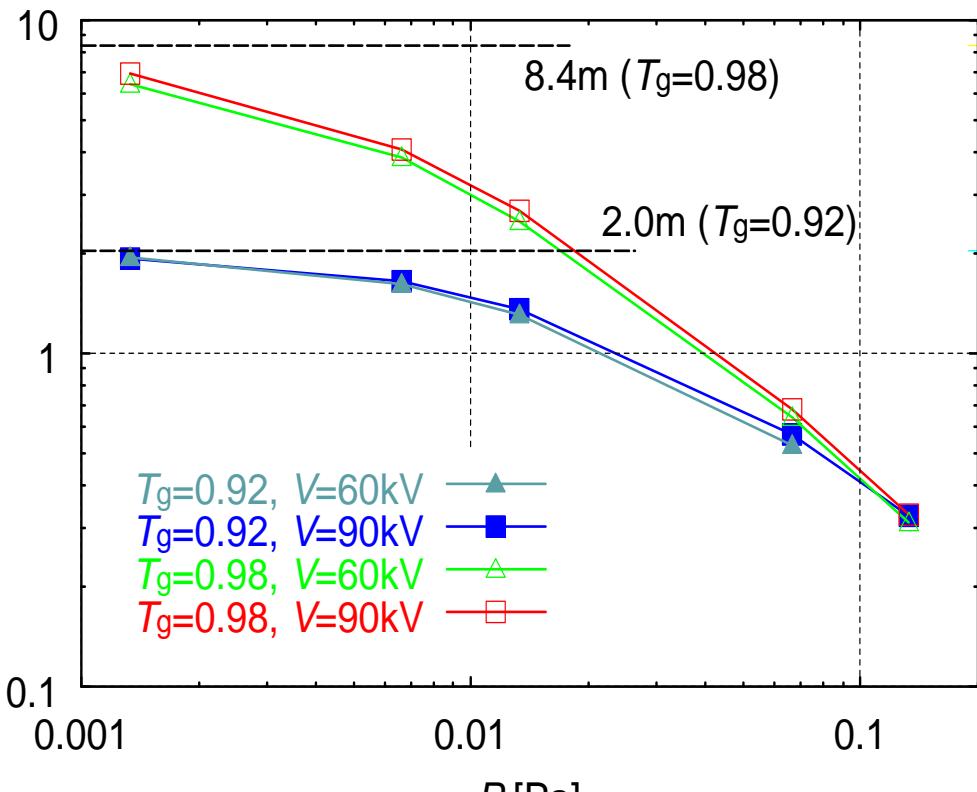


- Almost all injected ions disappear at the position of the cathode
- Averaged life span is long (6.9m, 20times longer than the device size)

- Many ions collide with background gas
- Few ions hit the cathode
- Averaged life span is short (33cm, ~device size)

$$V=90\text{kV}, I_{\text{assist}}=2\text{mA}, r_a=17\text{cm}, T_g=0.98$$

Influence of P and T_g on the averaged L



$I_{\text{assist}} = 2\text{mA}$, $r_a = 17\text{cm}$

- With decrease of P , averaged L increases as mean free path of CX increases.
- Averaged L converges to a value corresponding to T_g

$T_g = 0.92 \rightarrow 2.0\text{m}$

$T_g = 0.98 \rightarrow 8.4\text{m}$



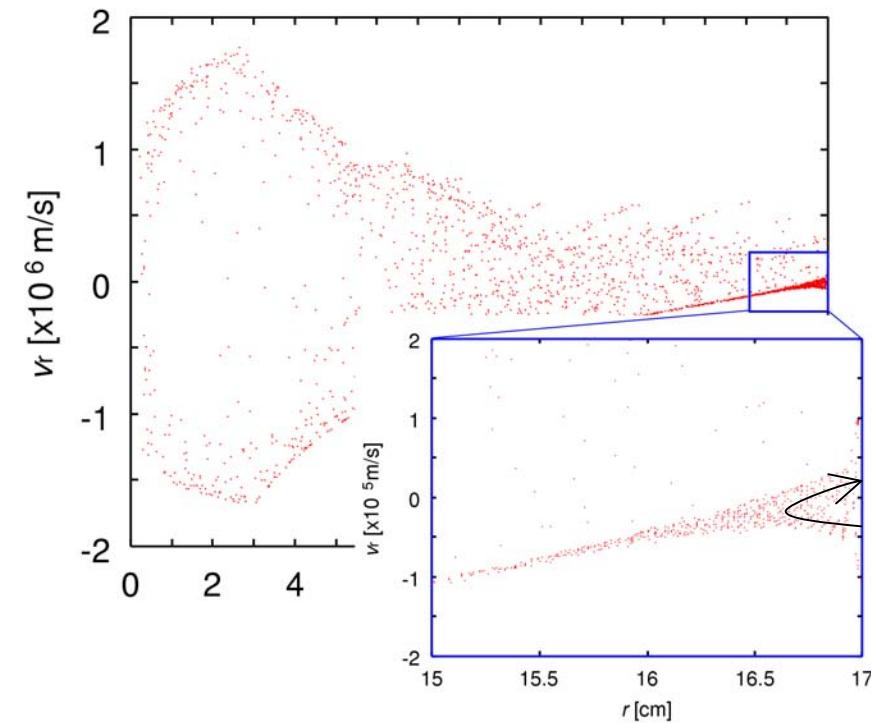
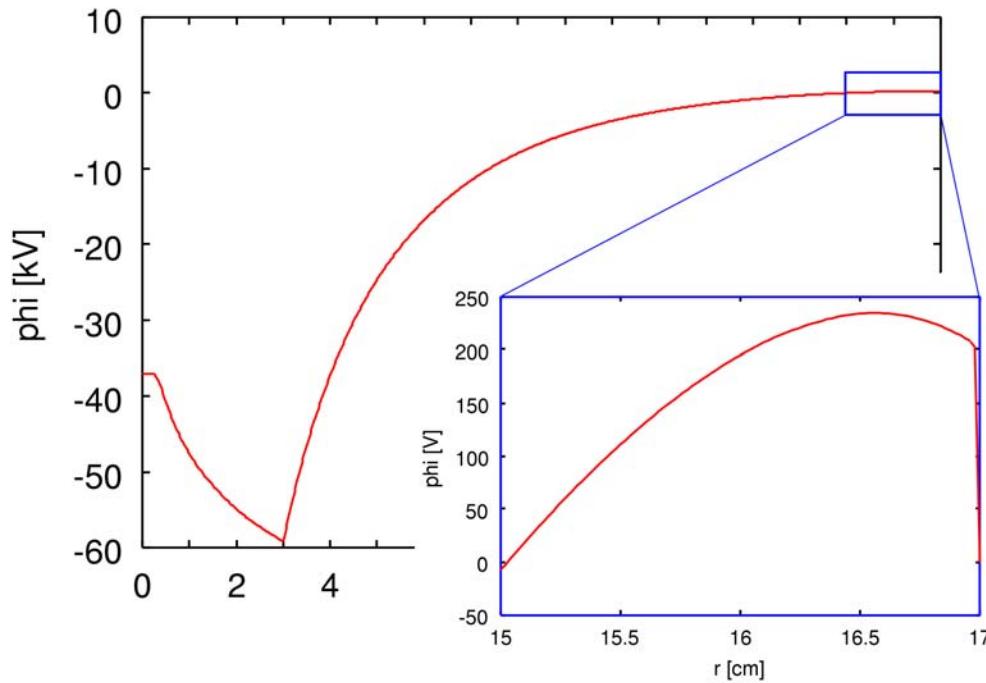
Beam-background fusion is limited by T_g



Beam-beam fusion
(large current operation)

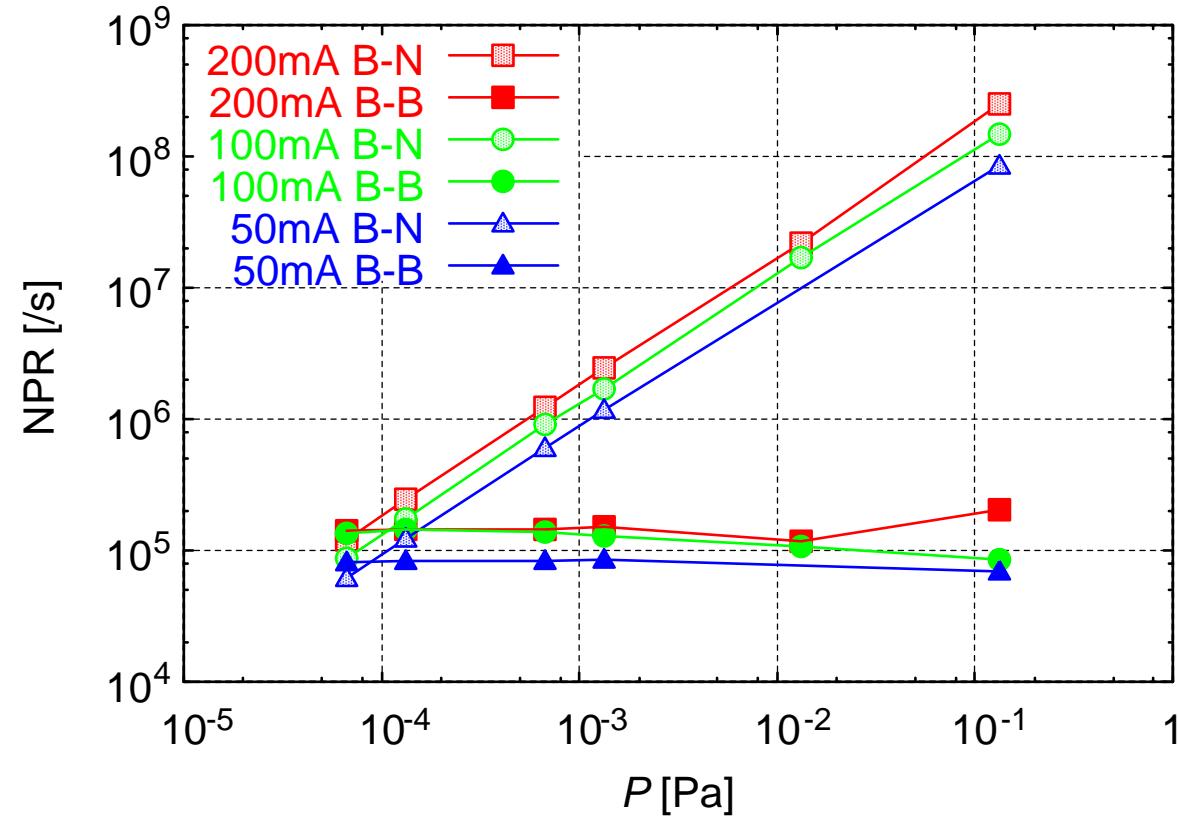
Large current injection

Large current injection: Space charge of injected ion restricts new ion



Applying high electric field by reducing anode radius ($r_a = 17\text{cm} \rightarrow 10\text{cm}$)
 → Maximum $I_{\text{assist}} = 200\text{mA}$, $I_{\text{IEC}} = 5\text{A}$

NPR characteristics -1- change with gas pressure



With decrease of P ...

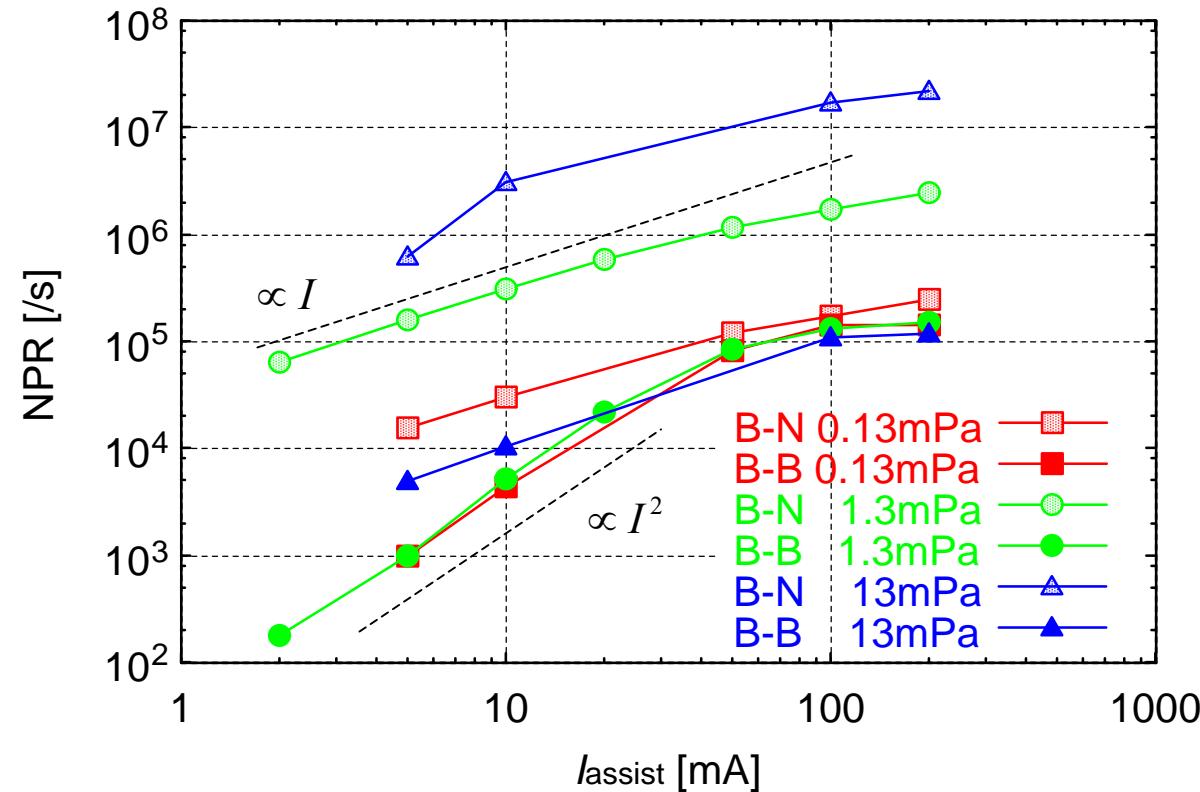
- NPR_{BN} decreases in proportion to P .
- NPR_{BB} hardly changes (slightly increases).
- $P < 0.1\text{mPa} \rightarrow NPR_{BB} > NPR_{BN}$

B-N: Beam-Neutral (background) collision

B-B: Beam-Beam collision

($V=120\text{kV}$, $r_a=10\text{cm}$, $T_g=0.98$)

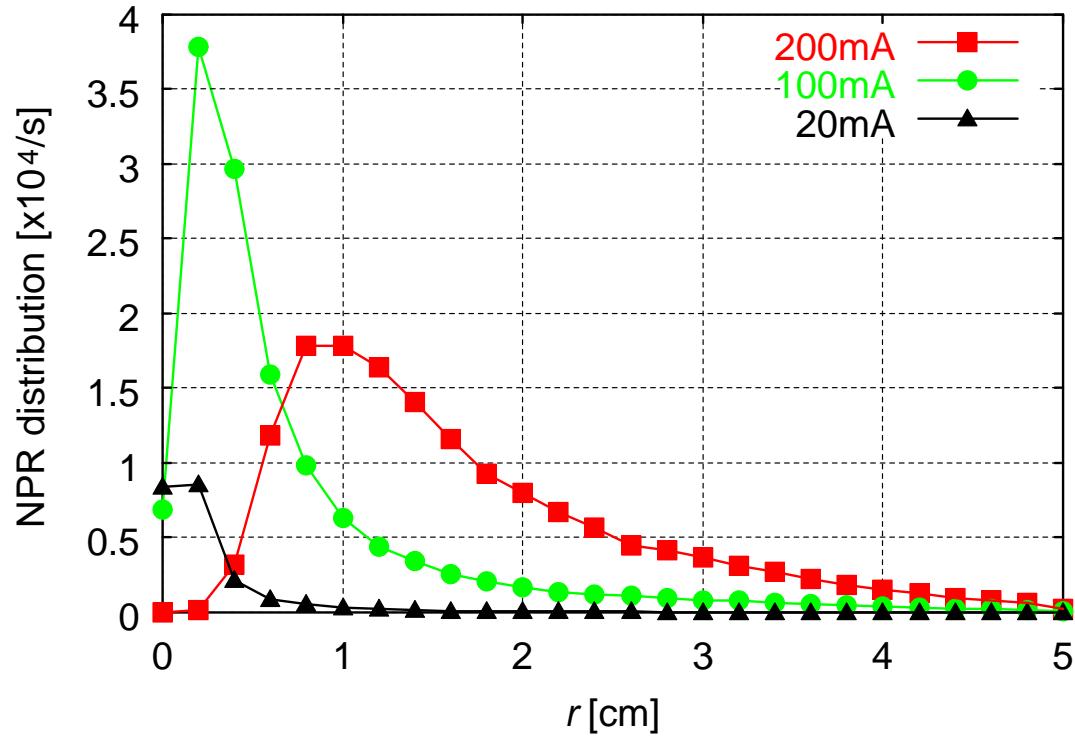
NPR characteristics -2- change with injected current



- NPR_{BN} is almost proportional to I_{assist} .
- NPR_{BB} is proportional to I_{assist}^2 in small current and low pressure region.
- In large current region, NPR_{BB} saturates.

$V=120\text{kV}$, $r_a=10\text{cm}$, $T_g=0.98$

Spatial distributions of NPR_{BB}

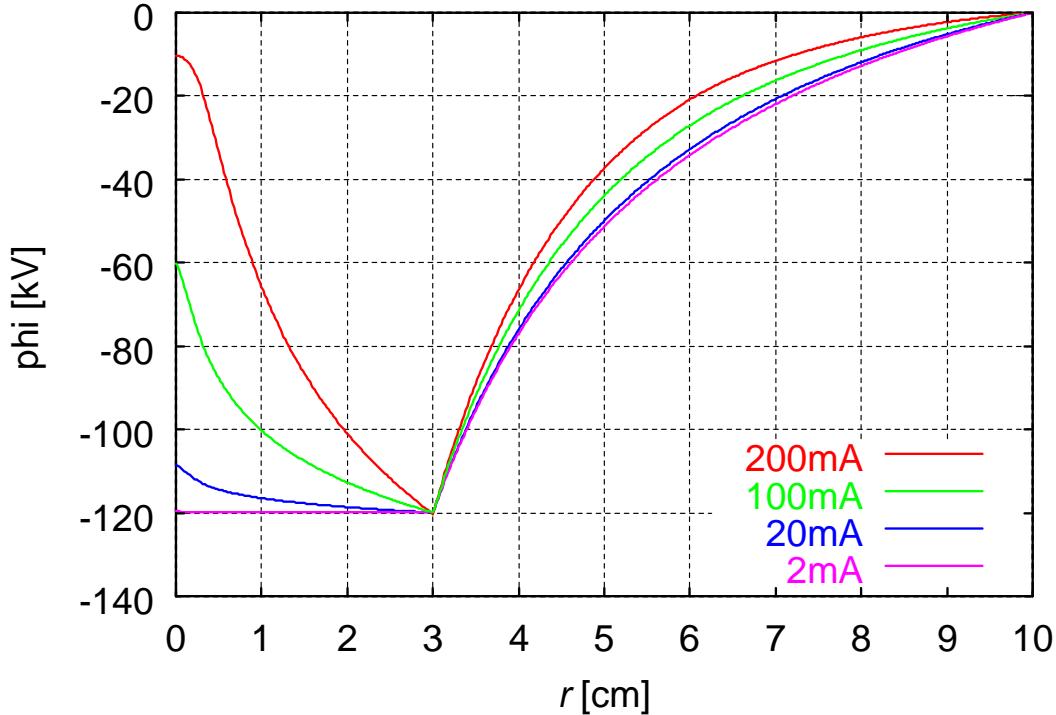


$V=120\text{kV}$, $r_a=10\text{cm}$, $T_g=0.98$

As I_{assist} increases ,
the position where NPR_{BB}
takes peak value shifts
outward.

(The energy of ion in
center region is reduced.)

Potential profiles



$V=120\text{kV}$, $r_a=10\text{cm}$, $T_g=0.98$

- Converged ions make potential structure in center region (single-well)
- Ions are decelerated within the cathode by the well.
- Peak of NPR is shifted outward

Canceling the center potential or creating multi potential structure are needed to increase NPR_{BB}



Summary

One dimensional simulation of assisted discharge in the spherical IECF on low pressure and large current has been done.

- Neutron yield through beam-background collision does not increase with decrease of the gas pressure.
- Averaged energy of ion and life span are enhanced.
- By reducing the anode radius, simulation of large current injection can be carried out.
- Neutron yield through beam-beam collision increases slightly as the pressure is reduced.
- It increases in proportion to I_{assist}^2 while the current is small, but saturates because potential peak of center decelerates ions.

Plasma Compression in the Periodically Oscillating Plasma Sphere

R. A. Nebel, L. Chacon, J. Park, E. Evstati
Los Alamos National Laboratory
Los Alamos, New Mexico 87545

Outline

I. Background for IECs and POPS.

II. Stability of Virtual Cathodes.

III. POPS and Cathode Stability.

IV. Plasma Compression.

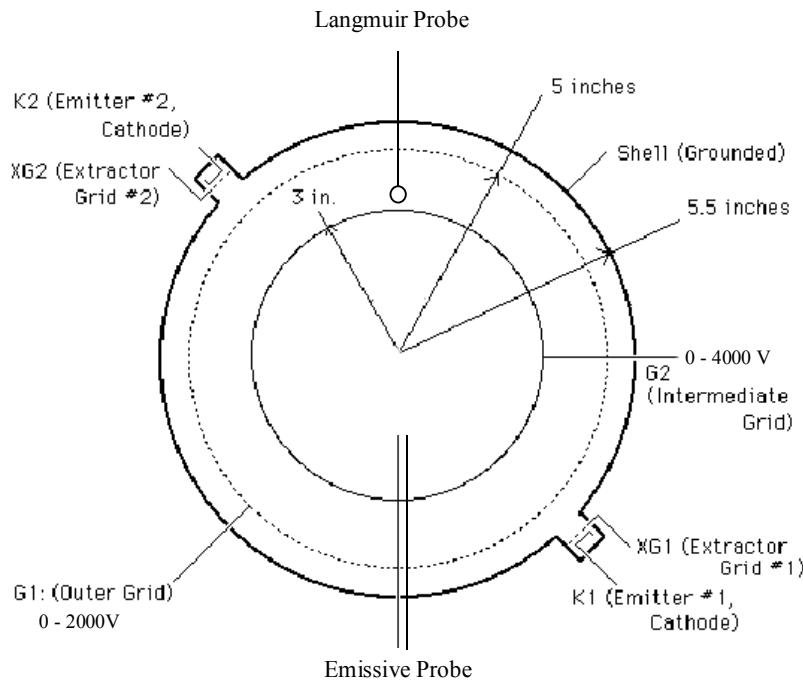
V. Conclusions

INS-e Device



INS-e Device

Electrostatic Grids



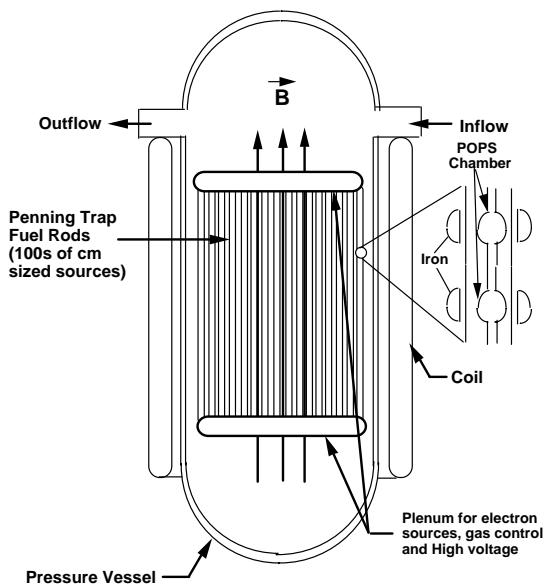
INS-e Device Configuration

- Virtual cathode formed by electron injection.
- Virtual cathode confines ions electrostatically.

Electrostatic Basics

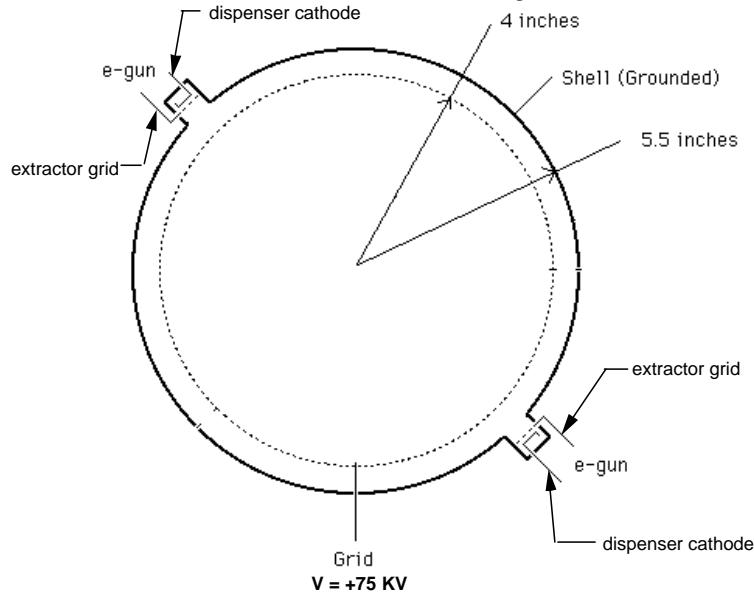
- Fusion parameters
 - $T \sim V_{\text{applied}}$ (easy).
 - $\tau_{\text{classical}} \rightarrow \infty$ (not too bad).
 - Density limited by $\lambda_{\text{Deff}}/a \sim 1$ (difficult).
- Power scaling
 - $P \sim 1/a$.
 - Massively modular reactor.

Penning Trap Reactor Vessel

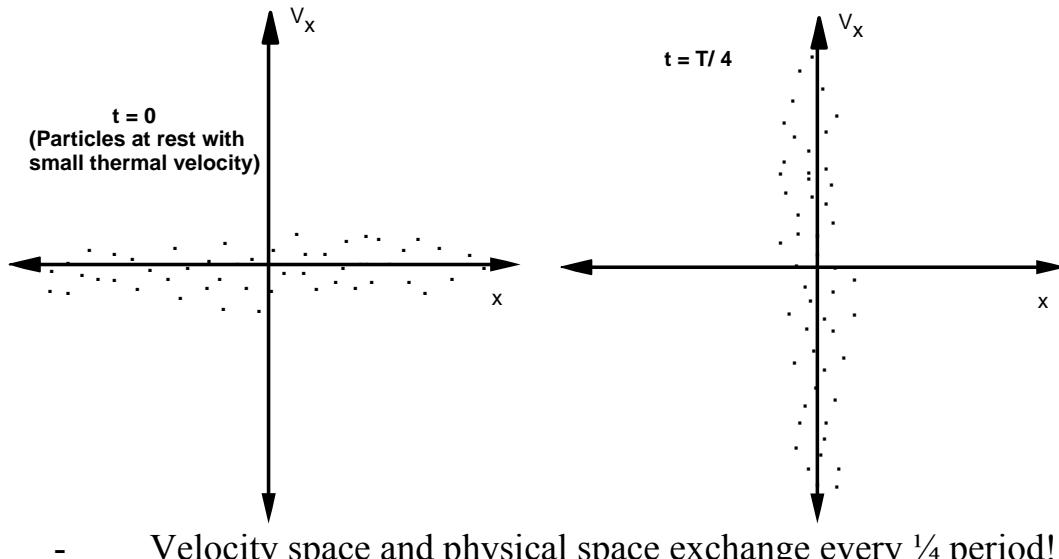


- Mass Power Density 100-1000 times larger than magnetic confinement systems.
- ITER grade plasmas for $\sim \$100k$ (single cell).

POPS Ion Physics

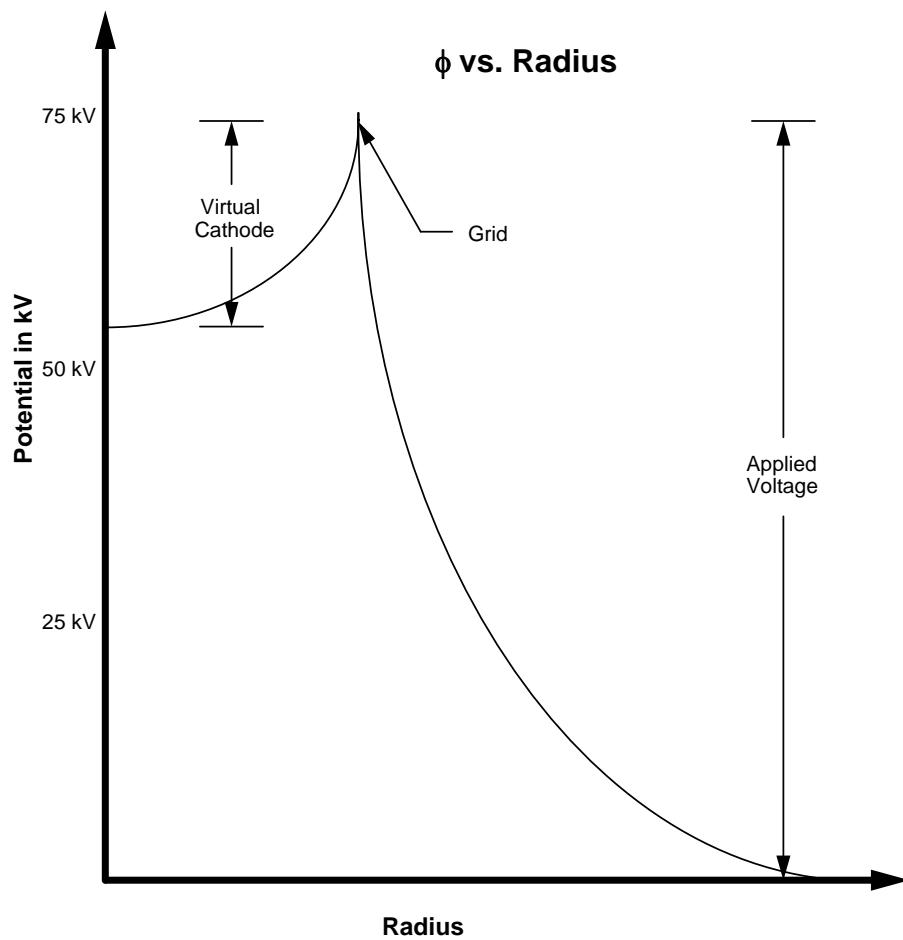


- Characteristics of POPS solutions
 - 1-D Time and space separable
 - Stable to multidimensional perturbations
 - Profiles remain in l.t.e. throughout oscillation
 - High compression is possible
 - Density profile is Gaussian in radius, Maxwellian in velocity.
- Ion phase space motion in a harmonic oscillator
 - $d^2x/dt^2 + kx = 0, d^2y/dt^2 + ky = 0, d^2z/dt^2 + kz = 0$



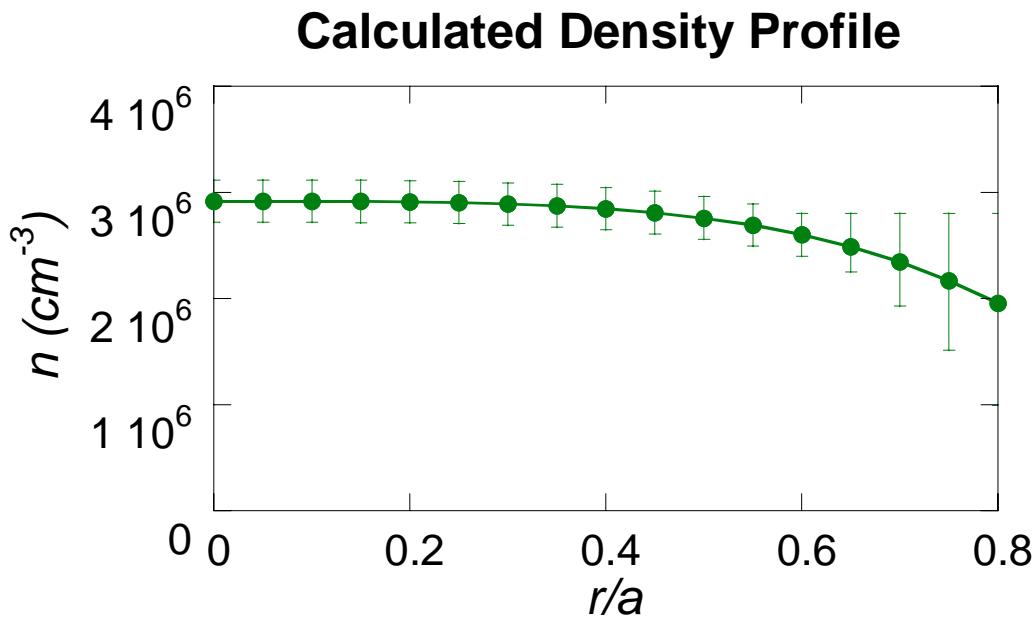
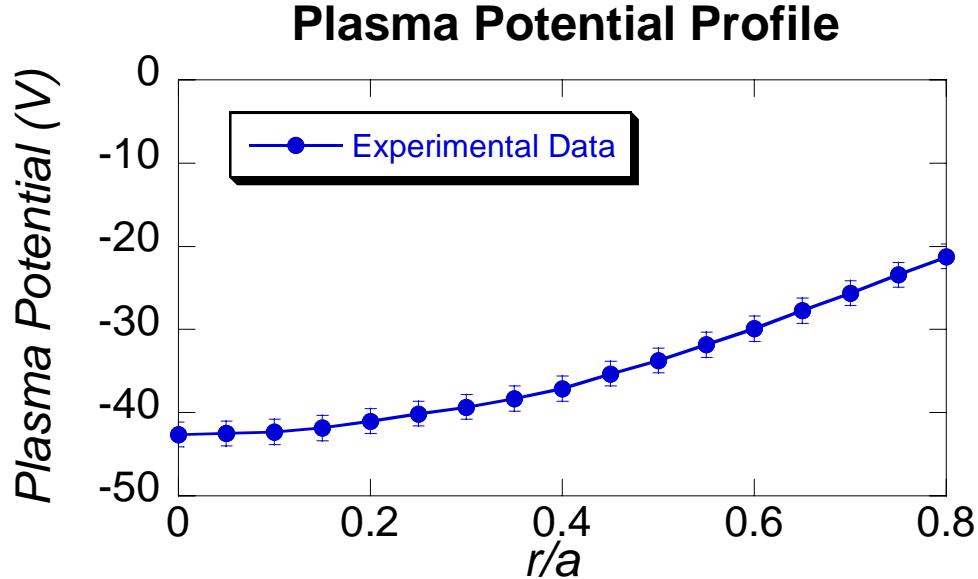
Virtual Cathode Stability

- Previous results
 - Cathode stability limit determined by the electron-electron two stream stability limit.
 - For slab model $\lambda_D/a > 1 \Rightarrow$ stable
- Equilibrium implications
 - $|\phi_{\text{applied}}| / |\phi_{\text{virtual}}| \sim (\lambda_D/a)^2$
 - If $(\lambda_D/a)^2 = 1$ then $|\phi_{\text{applied}}| / |\phi_{\text{virtual}}| = 7$



Experimental Program

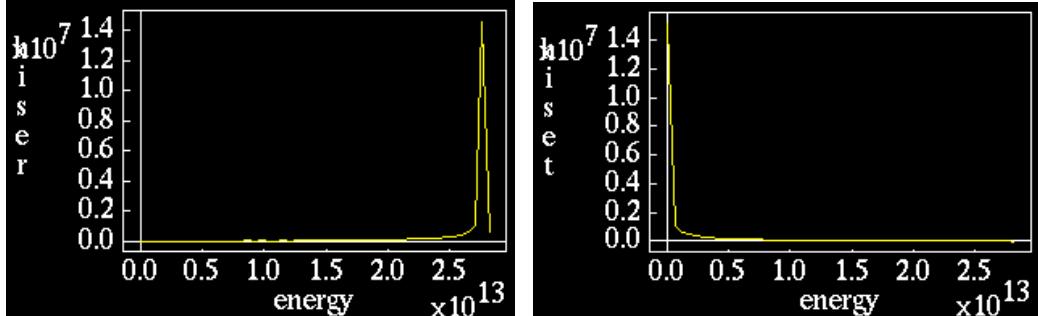
- Determine virtual cathode stability limit



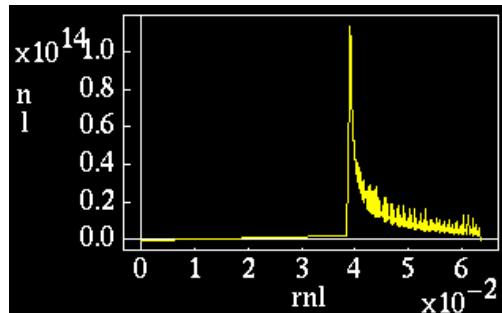
- Well depths of 60% [or $(\lambda_{\text{Deff}}/a) = .5$] have been achieved with flat density profiles and no evidence of instability.
- Slab theory is clearly too conservative.

Electron-Electron Two-Stream Stability in a Sphere

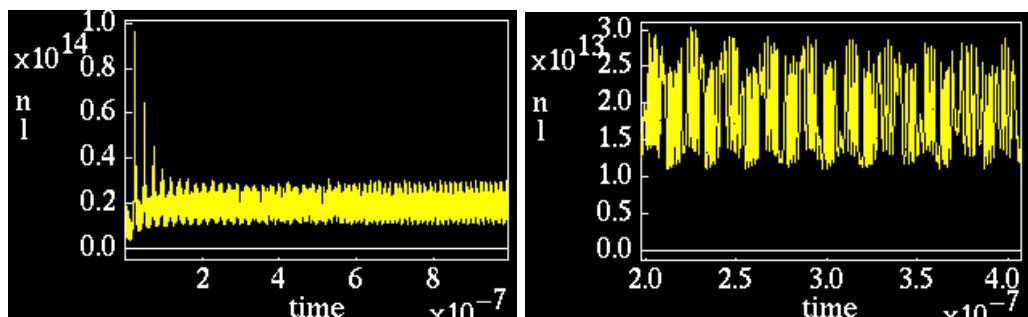
- Simulations use 1-D Gridless Particle code (including finite angular momentum).
- Force on a particle is determined by Gauss's law.



Radial and poloidal distribution functions at plasma boundary



Kinetic equilibrium: Electron Density vs. Radius ($n_e \sim 1/r$)

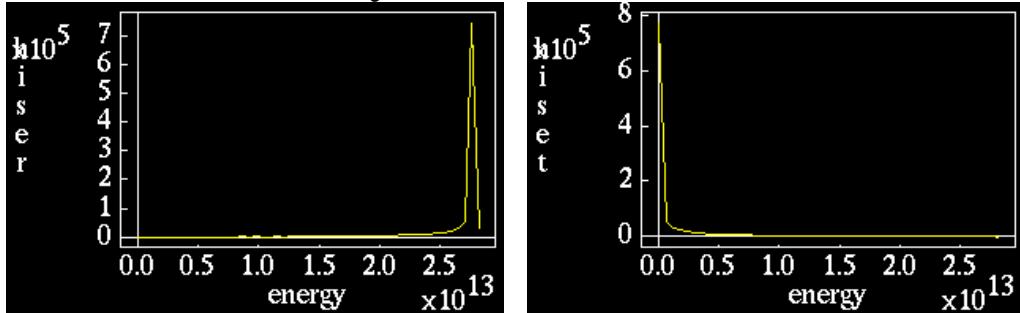


Density Fluctuations vs. Time

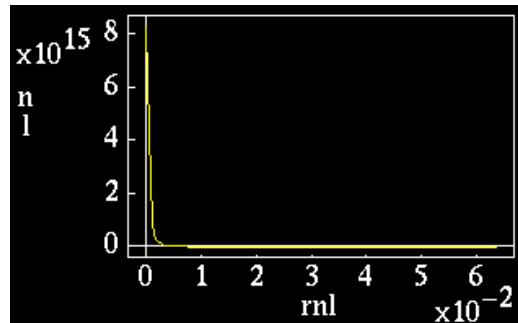
- $\omega_{pe} \sim 3.99 \times 10^8 \text{ s}^{-1}$, $\omega_{\text{meas.}} \sim 2.98 \times 10^8 \text{ s}^{-1} - 5.03 \times 10^{-8} \text{ s}^{-1}$,
- $\delta n/n \sim 50\%$: Two stream present

Two-Stream Stability Continued

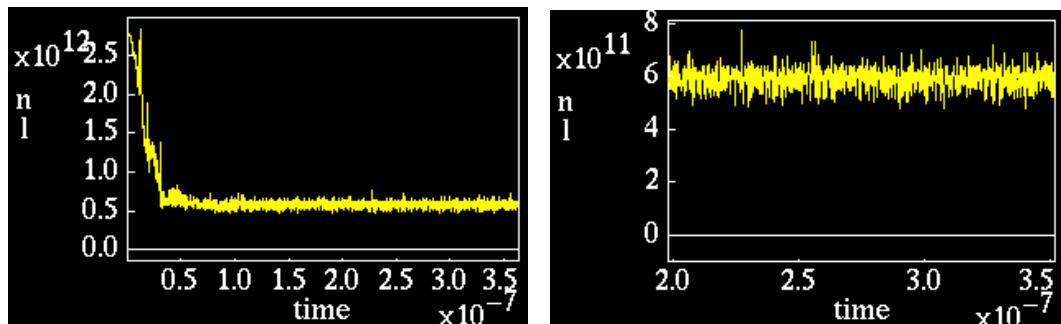
- Particle reflection required to observe the two-stream instability.



Distribution functions (same as previous case, lower current)



Kinetic equilibrium: Electron Density vs. Radius ($n_e \sim 1/r$)

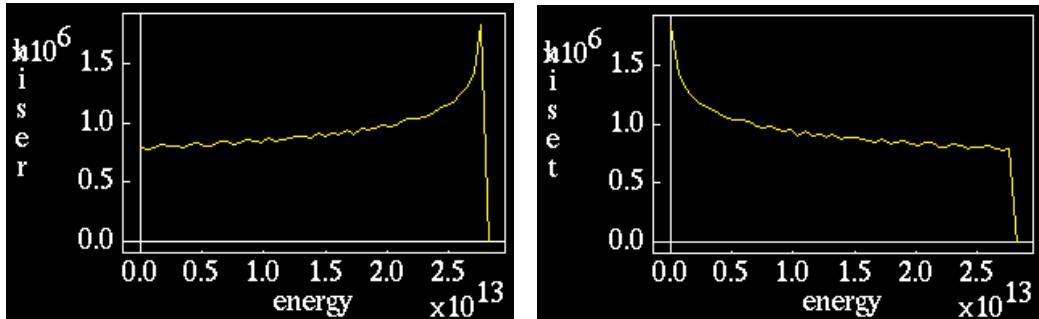


Density Fluctuations vs. Time

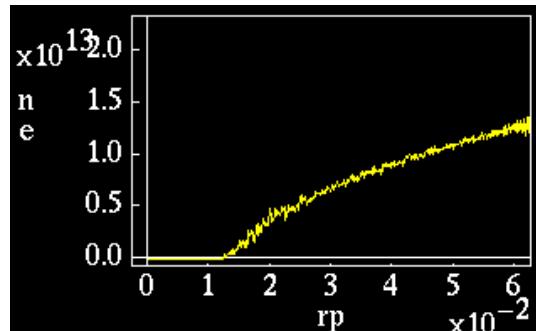
- $\delta n/n \sim 15\%$, no coherent oscillations (just shot noise).
- No two-stream instability.
- Coherence appears as soon as the density peak moves off-axis.
- Particle reflection makes two-stream resonant at some point.

Two-Stream Stability Continued

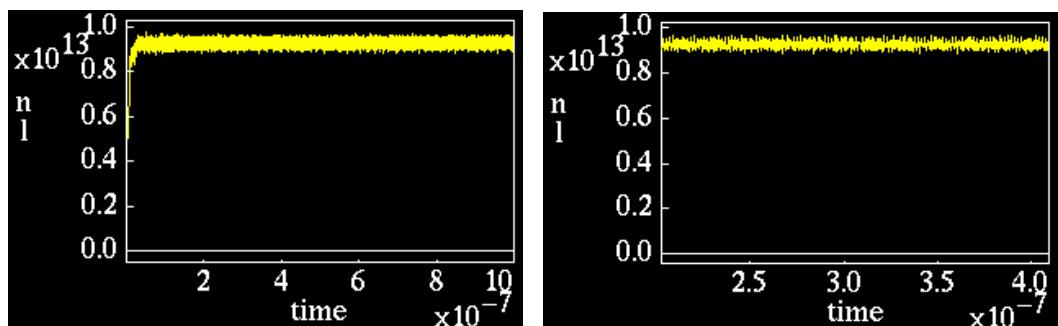
- Finite angular momentum (temperature) stabilizes two-stream.



Distribution functions almost isotropic (high angular momentum).



Hollow density profiles achieved by high current injection

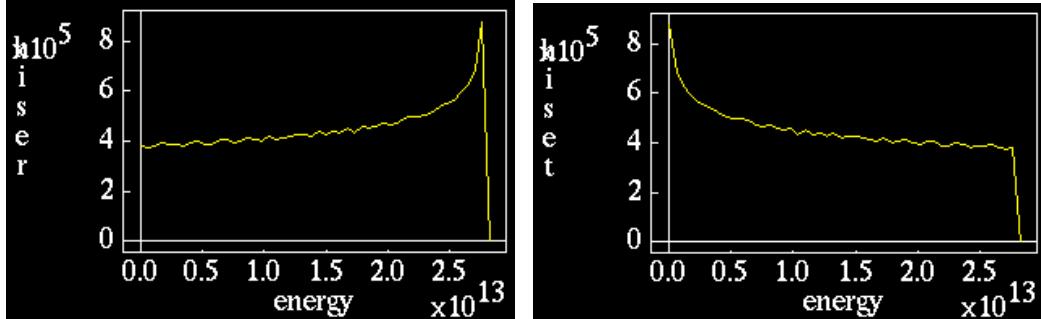


Density Fluctuations vs. Time

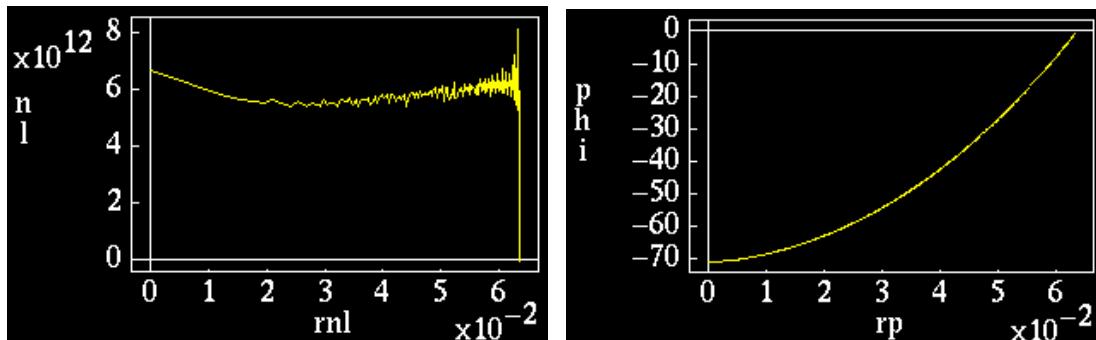
- $\delta n/n \sim 5\%$, no coherent oscillations (just shot noise).
- No two-stream instability.
- Finite angular momentum stabilizes two-stream

Two-Stream Stability for POPS Case

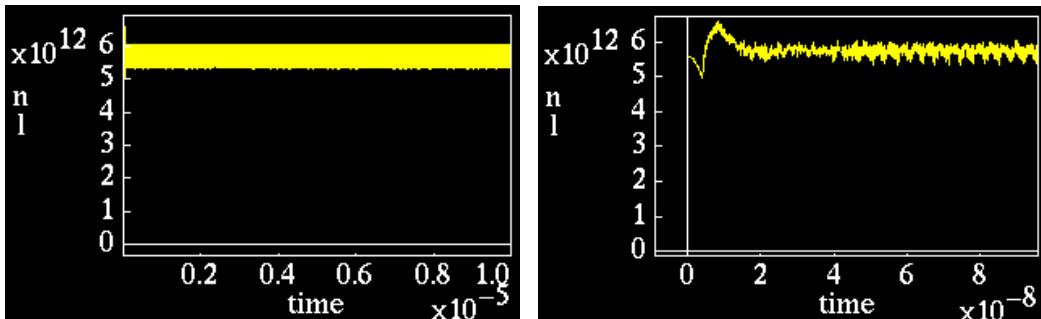
- Harmonic oscillator case is stable for almost 100% fractional well depths!



- Distribution functions almost isotropic as in previous case



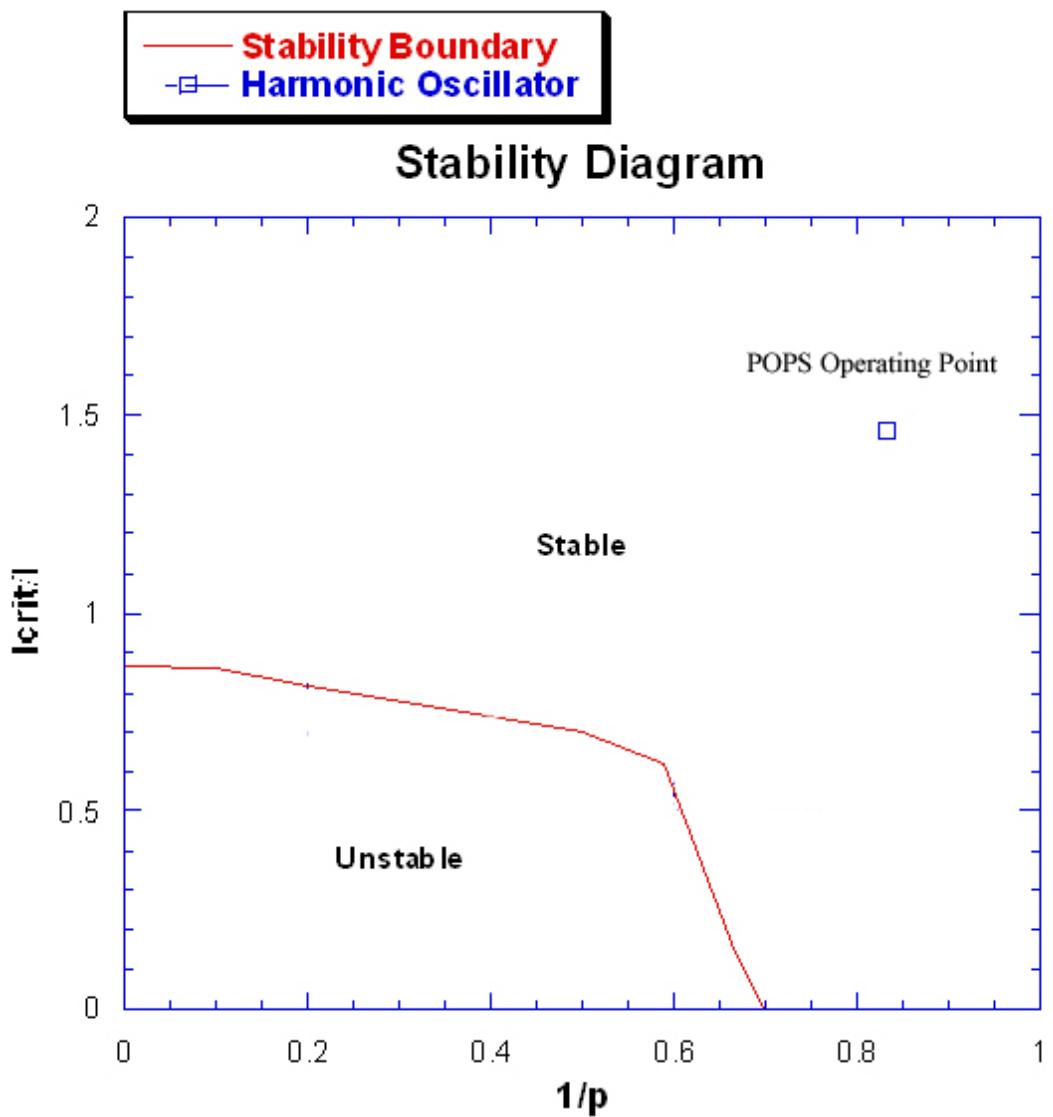
- Kinetic equilibrium: electron density and electrostatic potential vs. radius for electron injection energy of 80 eV.



Density Fluctuations vs. Time

- $\omega_{pe} \sim 1.35 \times 10^8 \text{ s}^{-1}$, $\omega_{\text{measured}} \sim 2.2 \times 10^9 \text{ s}^{-1}$, $\delta n/n \sim 4\%$
- **No sign of electron-electron two-stream instability even with a 90% fractional well depth.**

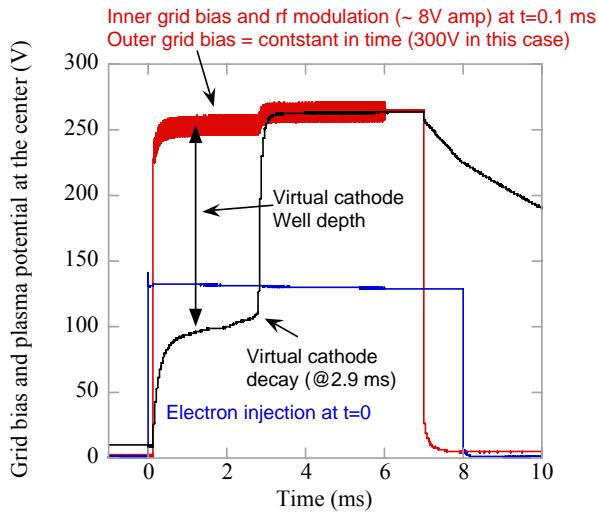
Two Stream Stability Diagram



Summary

- Virtual cathode stability
 - Experimental results
 - * Fractional well depths of 60% have been achieved with flat density profiles and no evidence of instability.
 - * These wells depths are four times deeper than predicted by the electron-electron two stream limit in a slab.
 - Theoretical results
 - * The two-stream stability limit is much higher in a sphere than a slab.
 - * Stabilization is provided by a combination of finite angular momentum (temperature) and decoherence by particle streaming.
 - * Fractional well depths greater than 90% have been achieved with no sign of instability.
 - * Caveat: Results are 1-D. Multi-dimensional stability work is presently being done.

POPS measurement

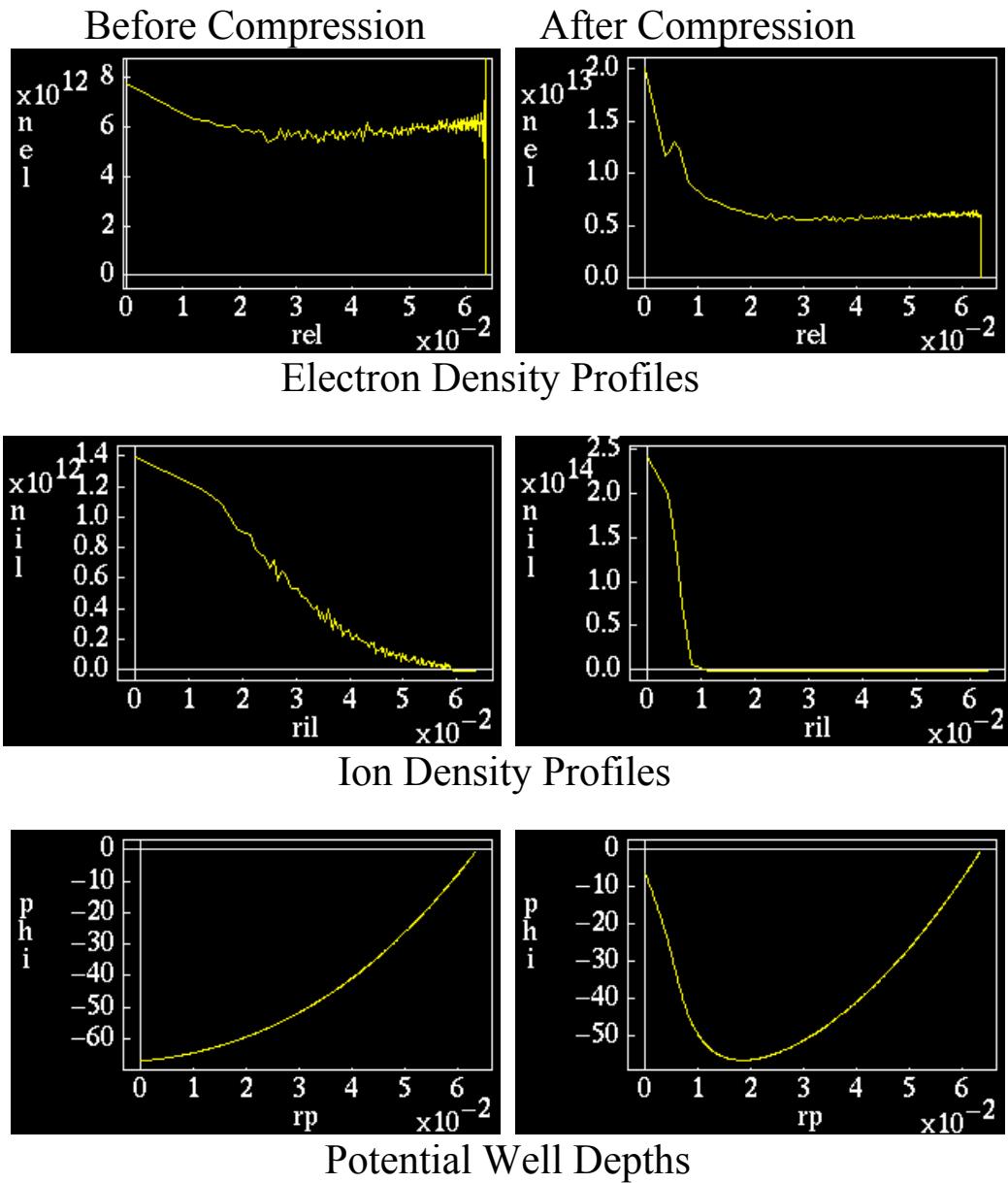


- Impose rf oscillation of plasma potential by modulating inner grid bias
- Driven POPS oscillation is mathematically equivalent to Mathieu Equation (forced harmonic oscillator).
- POPS oscillation will affect the ion confinement (increase ion loss term) --> delay the virtual cathode decay.
- Measure the virtual cathode decay time using emissive probe.

- **Transition is likely caused by multidimensional instability**
- **It depends on ions in the well**
- **Lapenta and Evstati are looking at this with multidimensional PIC code (CELESTE).**

POPS Simulations With Kinetic Ions and Electrons

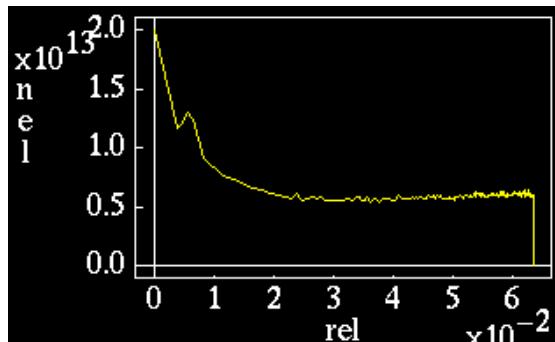
- Does ion repulsion limit achievable compression?



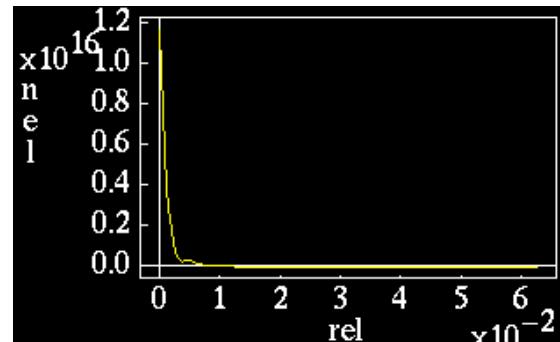
- Electrons follow ions into center, but not enough to achieve total space charge neutralization.
- 6.3:1 compression ratio.

POPS Simulations With Focused Electrons

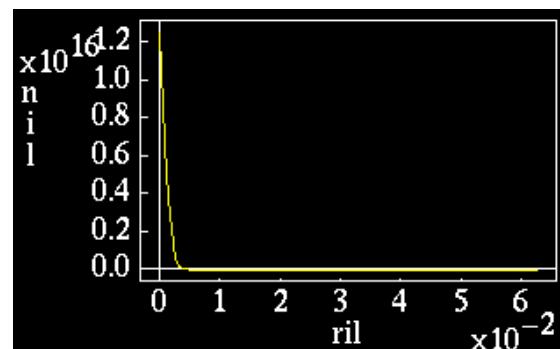
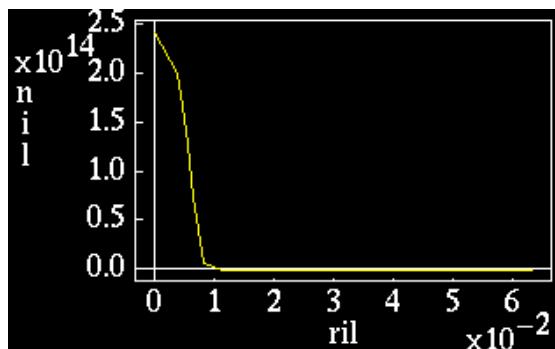
Unfocused Electrons



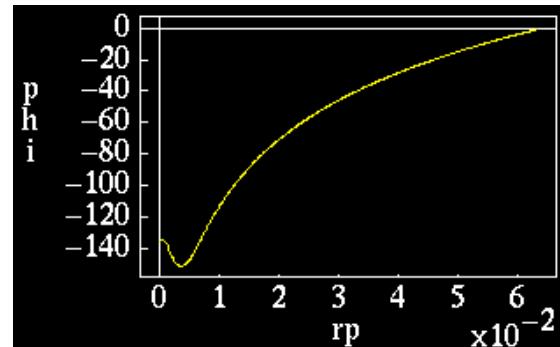
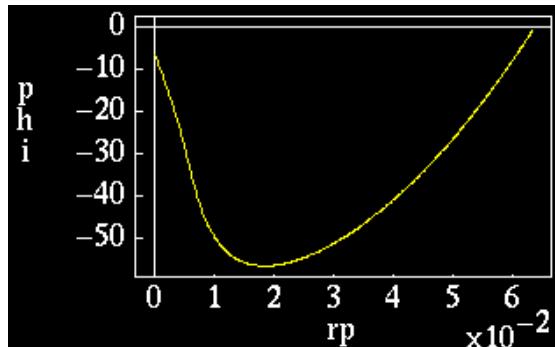
Focused Electrons



Electron Density Profiles



Ion Density Profiles



Potential Well Depths

- Ion density improves by a factor of 50.
- 23.2:1 compression ratio

Space Charge Neutralization

Extending the work of Barnes, Chacon and Finn¹

we find that:

$$n(r) = \int_{e\phi}^{\infty} dE \int_0^{L_m} \frac{g(E_0, L)}{V_r} L dL$$

where

$$L_m \equiv r \sqrt{2m_e(E_0 - e\phi)}$$

and

$$V_r = \sqrt{\frac{2}{m_e}(E_0 - e\phi) - \frac{L^2}{m_e^2 r^2}}$$

and

$$\phi = -\phi_0 \frac{r^2}{2a^2} \quad \text{and } E_0 \text{ is the electron energy}$$

Using an inverse Abel transform yields:

$$g(E_0, L) = \frac{1}{\pi r} \frac{d}{dy} \left[\int_0^y \frac{G(x)}{\sqrt{y-x}} dx \right]_{y=L}$$

where

$$G(y) = \frac{n(y)}{2\pi r} \sqrt{\frac{\sqrt{E_0^2 + \frac{e\phi_0 y}{m_e a^2}} - E_0}{e\phi_0/a^2}}$$

and

$$y = r^2 2m_e (E_0 + \frac{e\phi_0 r^2}{a^2})$$

- We now have a formula to calculate the required edge distribution function to yield arbitrary electron density profile
- This removes the requirement that $\langle n_i \rangle < n_{e0}$!

1. D.C. Barnes, L. Chacon, J.M. Finn, Phys. Plasmas 9, 4448 (2002).

Space Charge Neutralization Continued

Now choose:

$$n_e(r, t) = n_{eo} + n_{io} e^{-r/\lambda(t)}$$

where $\lambda(t)$ is the radial scale length function of Barnes and Nebel². $\lambda(t)$ comes from the similarity solutions.

- In principle, this allows arbitrarily high plasma density
- This formalism is being incorporated in the 1-D Particle code.
- Why is this important?
 -

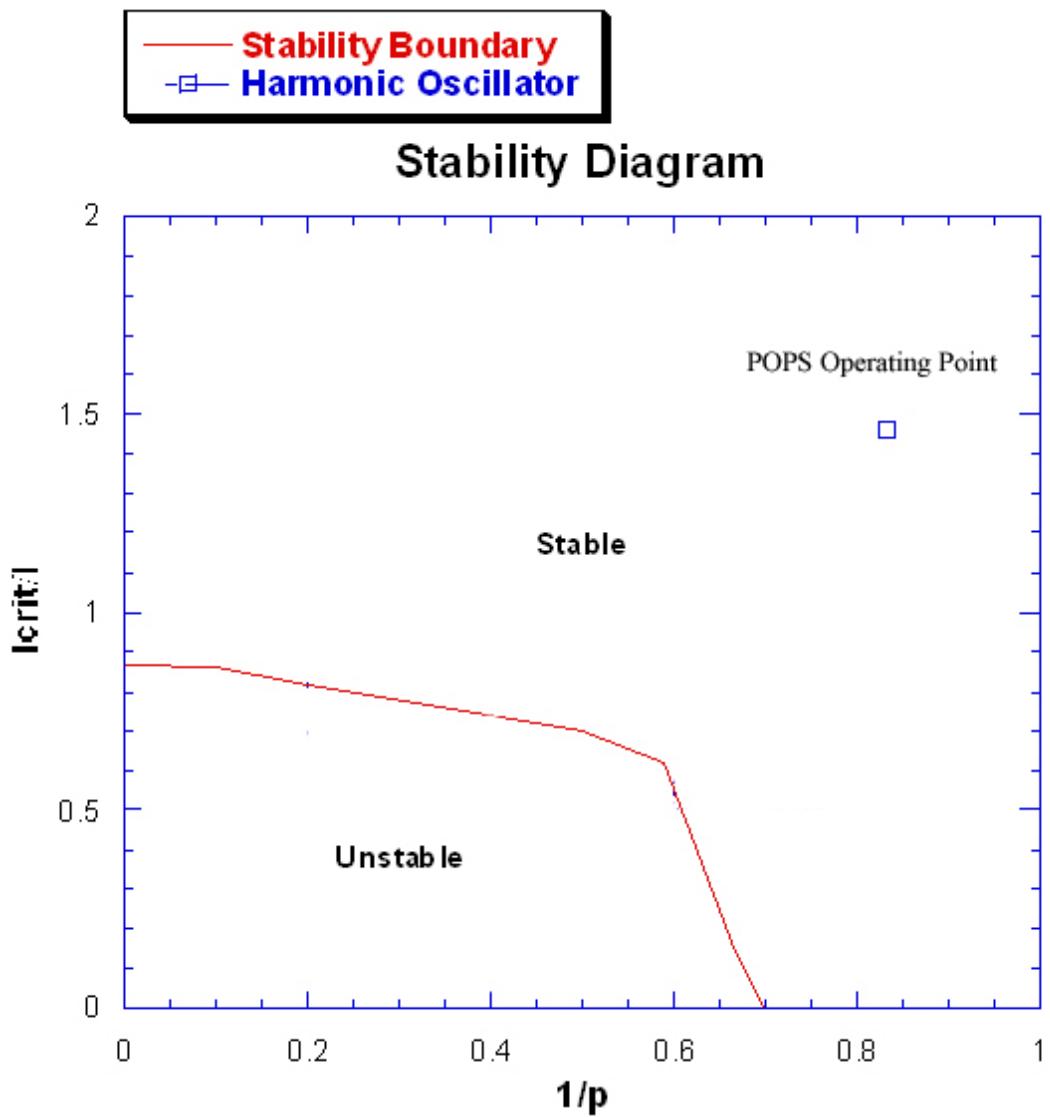
$$- P_{\text{fusion}} \sim \frac{3 \left(\frac{n_{io}}{n_{eo}} \right)^2 \phi_0^2 \theta^2 \langle \text{cov} \rangle}{2 \pi e^2 a}$$

- This can be a huge effect.

- What limits the achievable density?
 - Virtual Cathode Stability?
 - Accuracy of distribution function?
 - Ionization rate

2. D.C. Barnes, R.A. Nebel, Physics of Plasmas 5, 2498 (1998),

Two Stream Stability Diagram



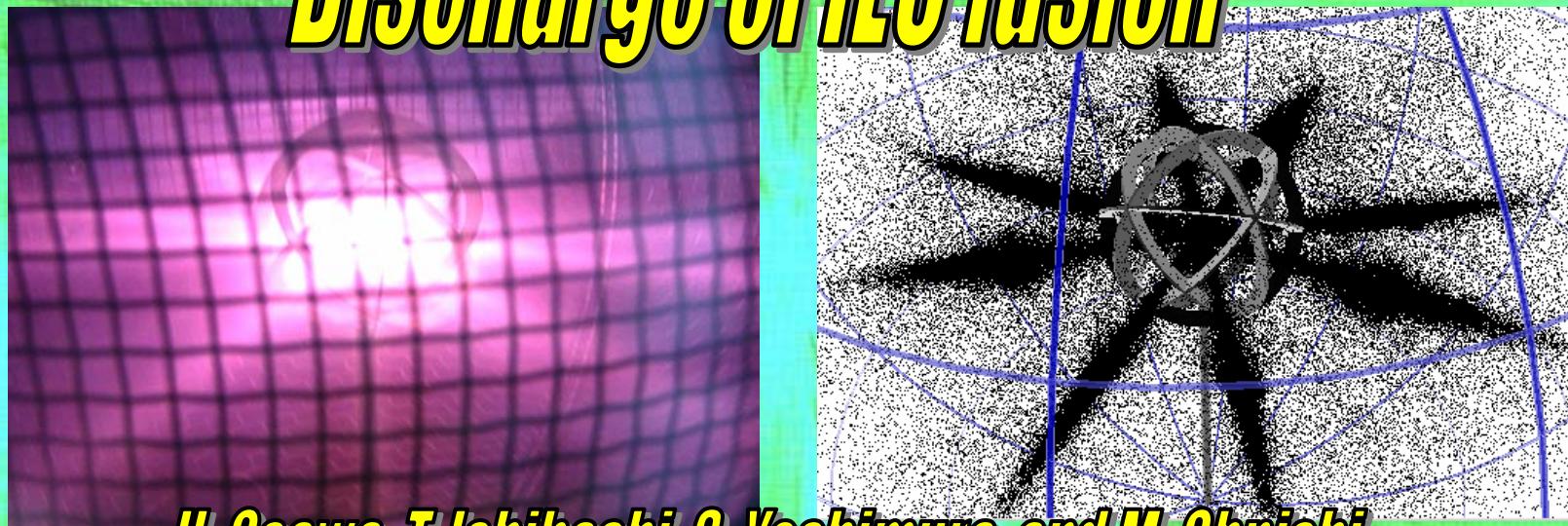
Conclusions

- Virtual cathode stability
 - Experimental results
 - * Fractional well depths of 60% have been achieved with flat density profiles and no evidence of instability.
 - * These wells depths are four times deeper than predicted by the electron-electron two stream limit in a slab.
 - Theoretical results
 - * The two-stream stability limit is much higher in a sphere than a slab.
 - * Stabilization is provided by a combination of finite angular momentum (temperature) and decoherence by particle streaming.
 - * Fractional well depths greater than 90% have been achieved with no sign of instability.
 - * Caveat: Results are 1-D. Multi-dimensional stability work is presently being done.

Conclusions Continued

- Space charge neutralization
 - Fully kinetic PIC simulations of POPS indicate that space charge neutralization is a significant issue.
 - Space charge neutralization can be mitigated by proper programming of the electron distribution function.
 - Chacon formalism can completely eliminate space charge problem and allow for arbitrarily high densities.
 - Theoretical density limits likely to be set by virtual cathode stability constraints.

Numerical Study on Hollow Cathode Discharge of IEC fusion



*H. Osawa, T. Ishibashi, S. Yoshimura, and M. Ohnishi
Faculty of Engineering, Department of Electrical Engineering,
Kansai University, Yamate 3-3-35, Suita, Osaka 564-8680, Japan*

Introduction

In IEC device, neutron production is more efficient in the discharge of high voltage and low pressure.

It is difficult to maintain the steady discharge in a low pressure, since the glow discharge becomes unstable in the condition.

We made the full 3-dimensional Monte Carlo PIC code including atomic processes to investigate the glow discharge.

Numerical Model (Discharge Simulation)

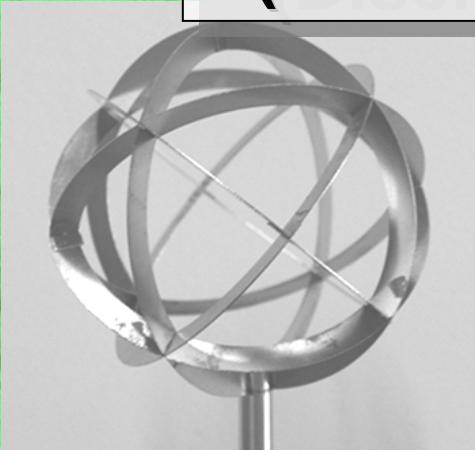
Deuterium ions (D^+ , D_2^+ , D_3^+), fast neutrals (D^0 , D_2^0) and electrons (e^-) are used as tracking particles.

We use 1000 particles of each ion species and 3000 electrons distributed uniformly within the anode initially.

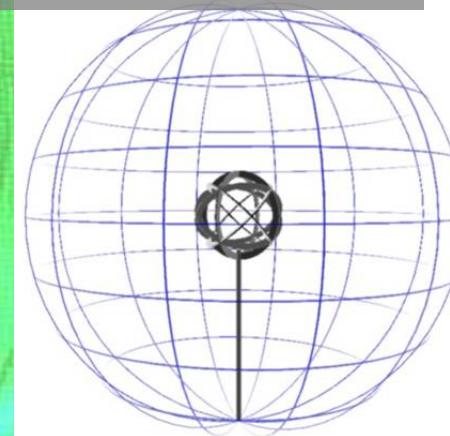
We trace the trajectory of each particles by the Runge-Kutta method in 3-D space. They move in the 3-D vacuum potential calculated by the finite difference method with the 1 mm spatial 6,750,000 meshes.

After pushing each particle, the atomic and molecular collisions and elastic collisions are taken into account by Monte Carlo method.

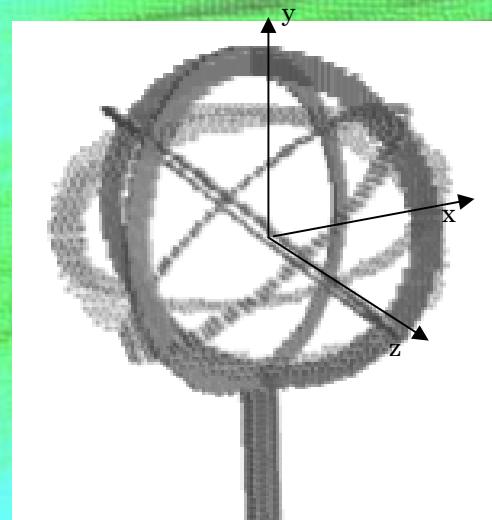
Numerical Model (Discharge Simulation)



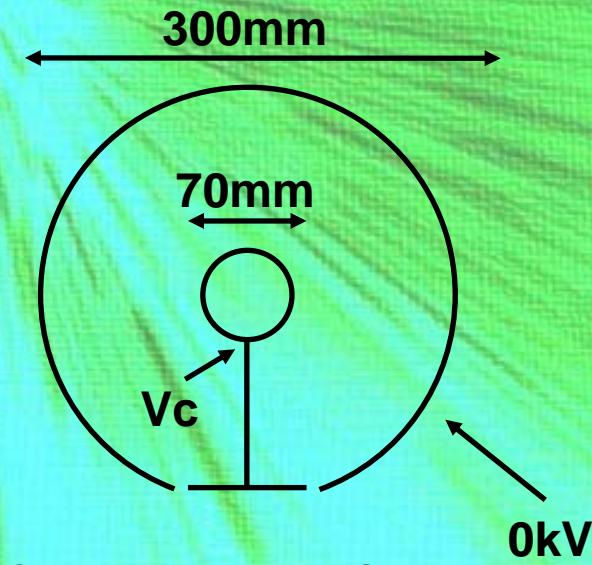
Photo(6ring cathode)



Simulation Area Image

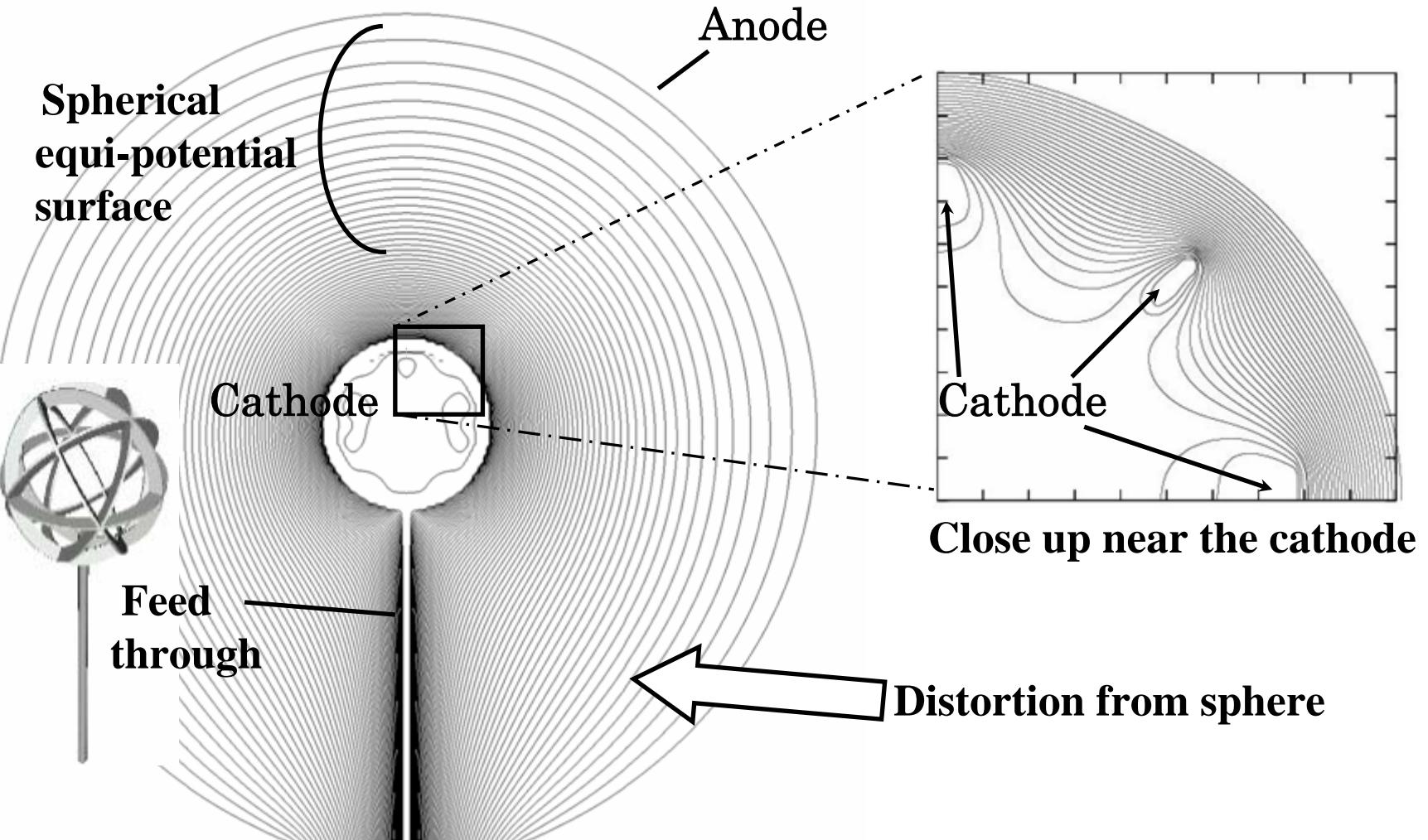


FDM model cathode



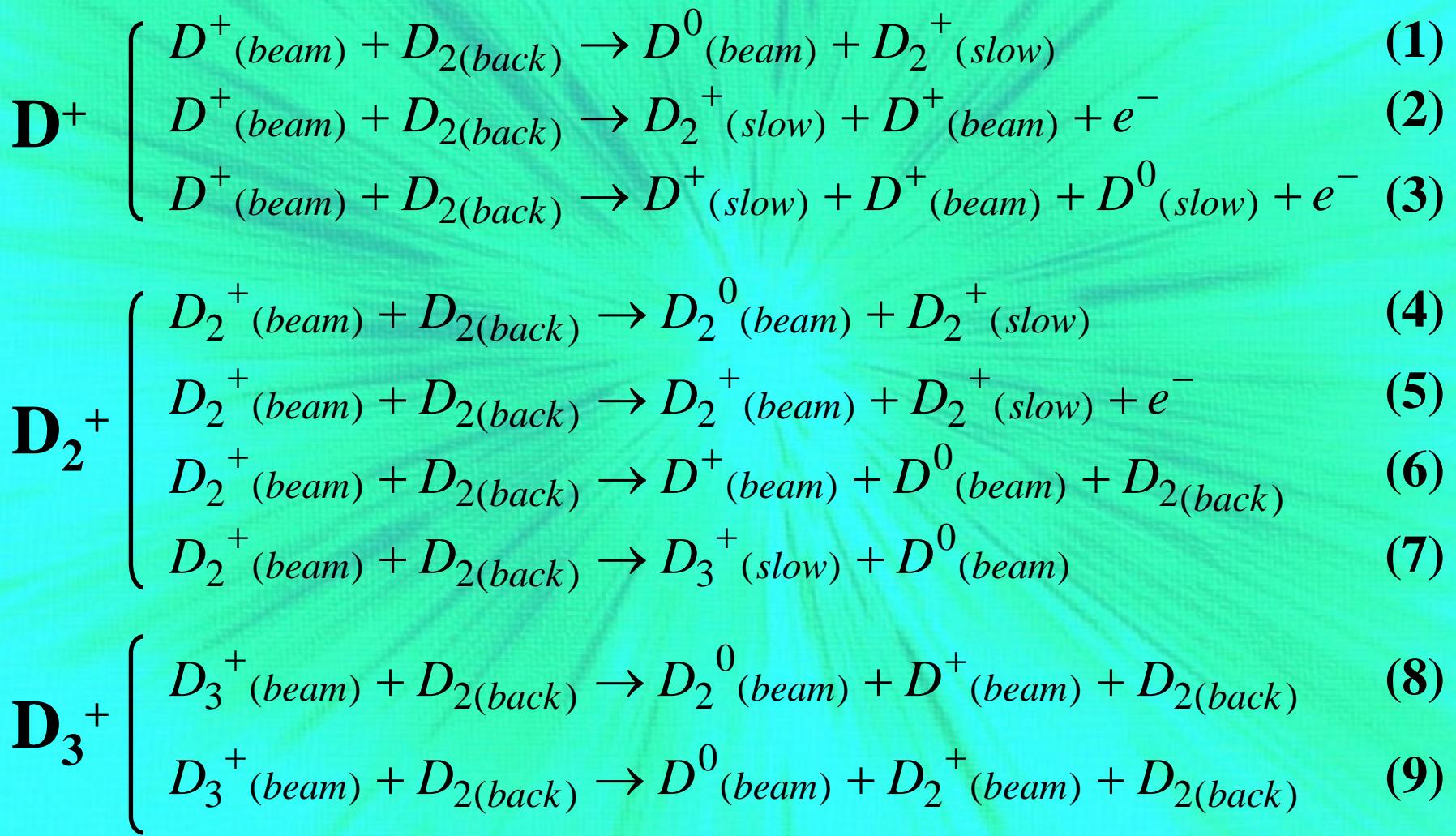
Computational Setup

Equi-potential Surface with Feed Through



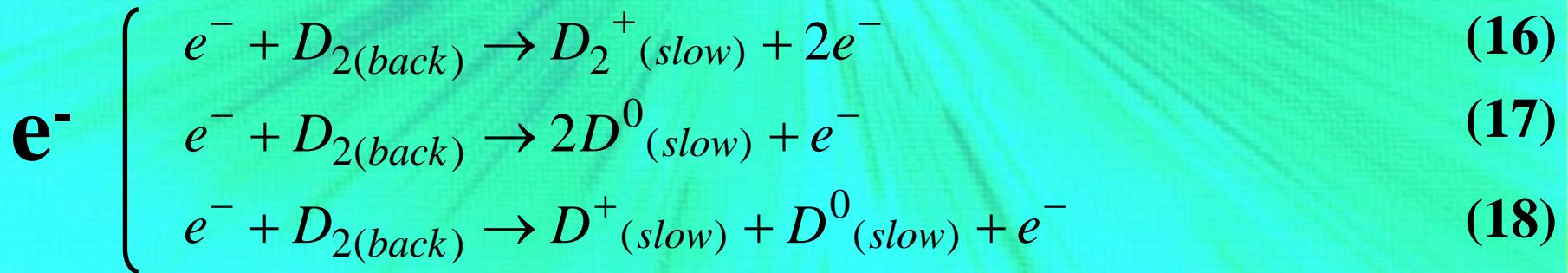
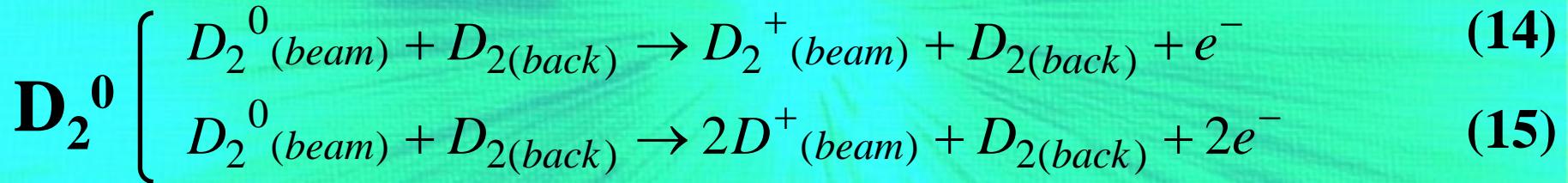
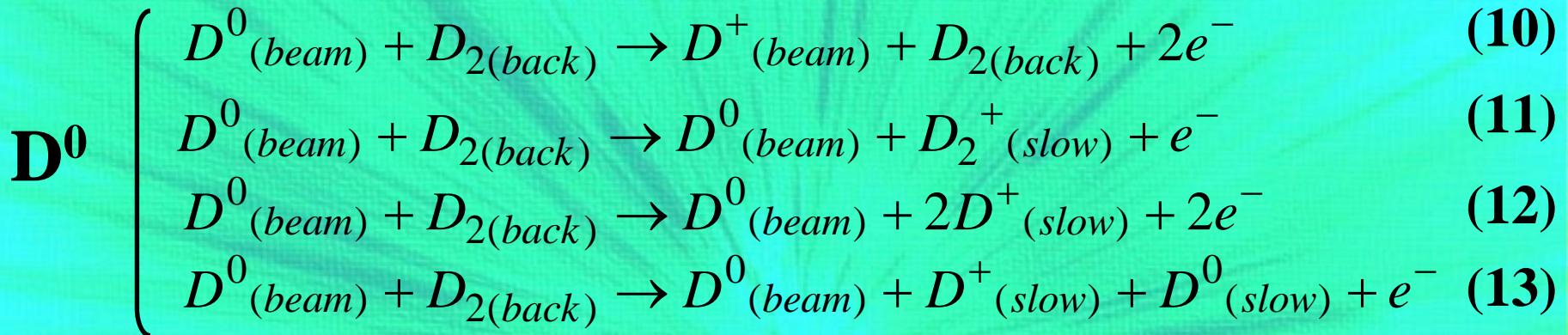
Atomic and Molecular Processes 1

(Discharge Simulation)

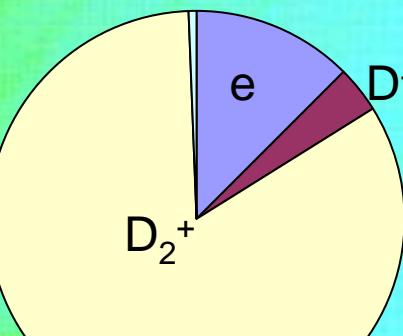
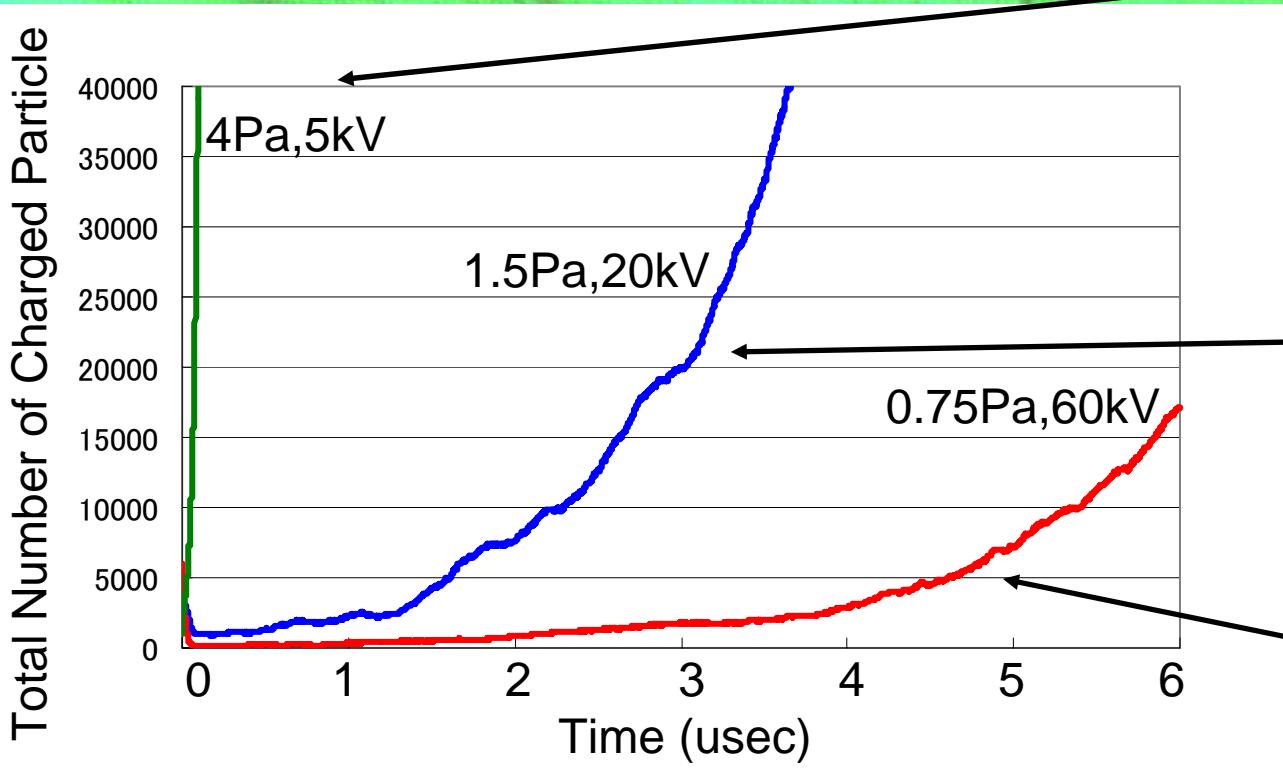


Atomic and Molecular Processes 2

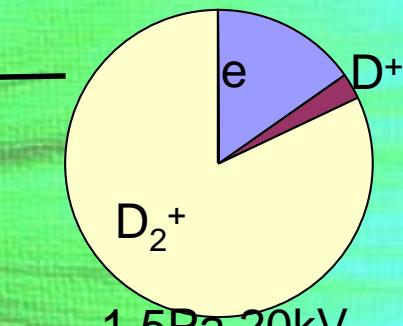
(Discharge Simulation)



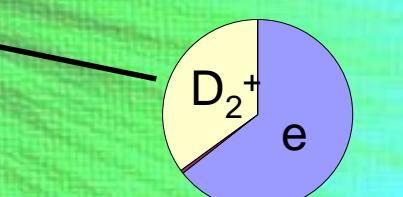
Growth of Particle Number (Discharge Simulation)



4Pa, 5kV



1.5Pa, 20kV



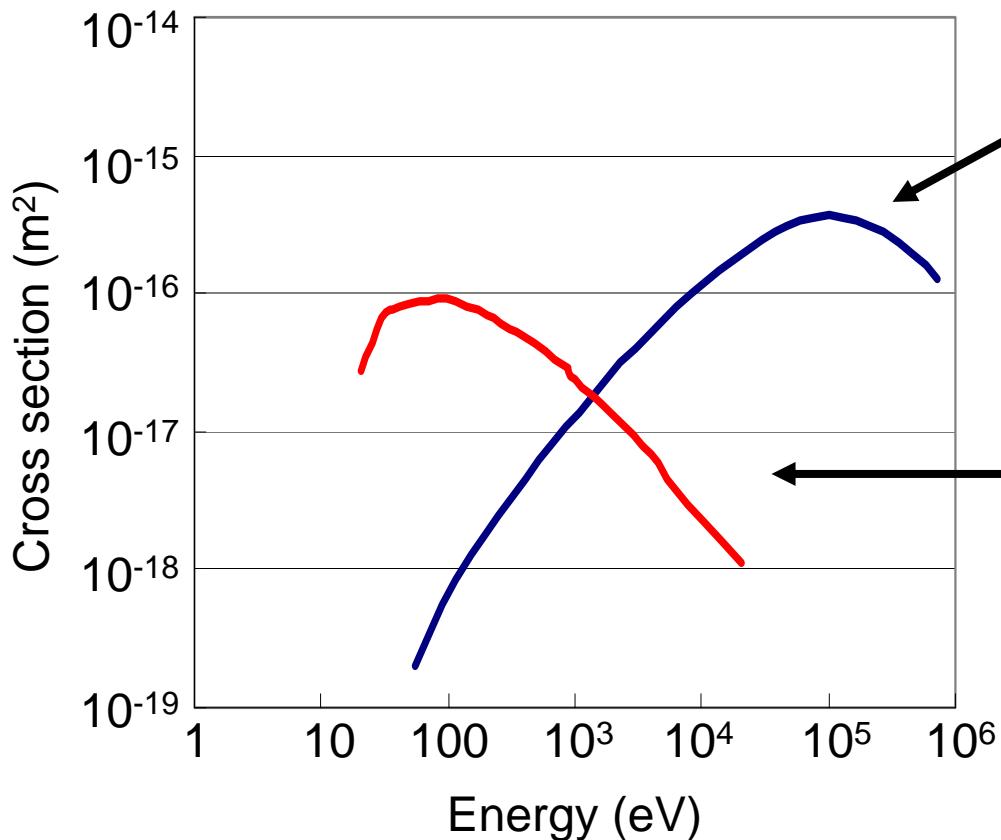
0.75Pa, 60kV

Charged particle increase at the much larger rate.

The multiplication of ions is larger at the higher pressure.

Main reaction of discharge

(Discharge Simulation)



Self-Multiplication of D₂⁺

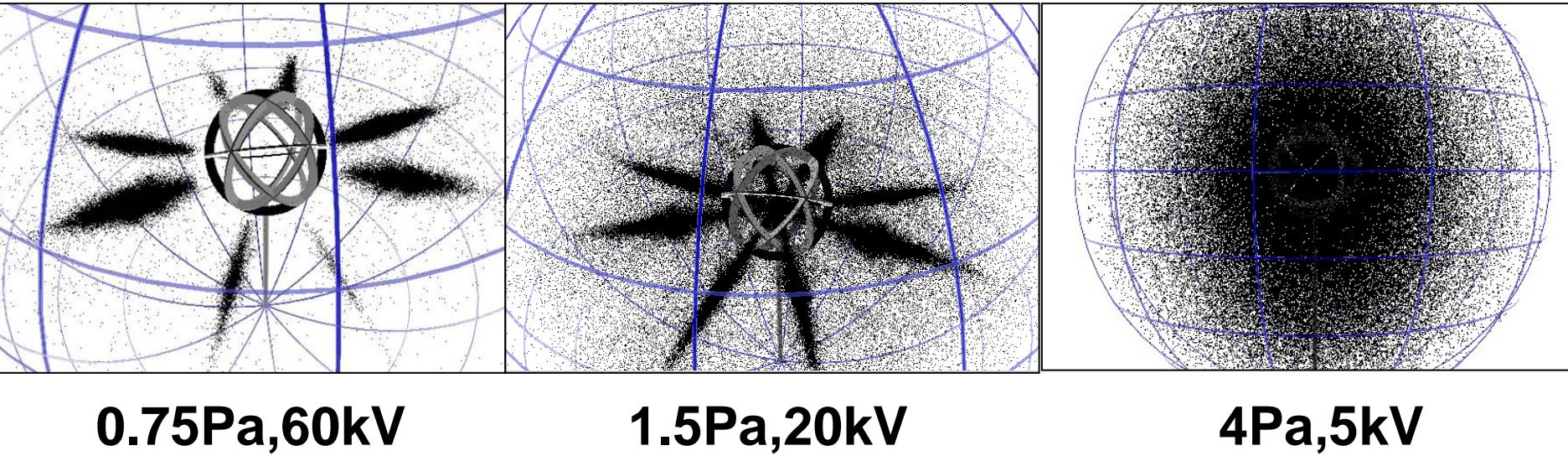


Self-Multiplication of e⁻



Ionization place

(Discharge Simulation)



Star Mode Discharge (1.5Pa, 20kV)

(Discharge Simulation)

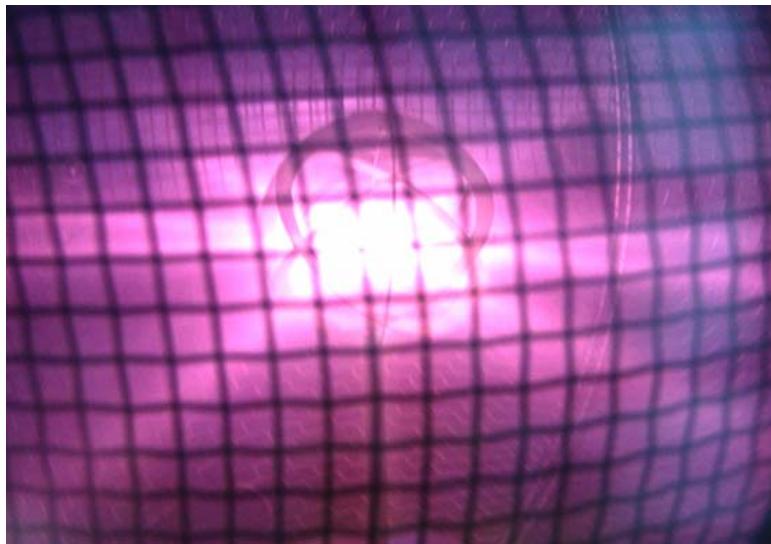
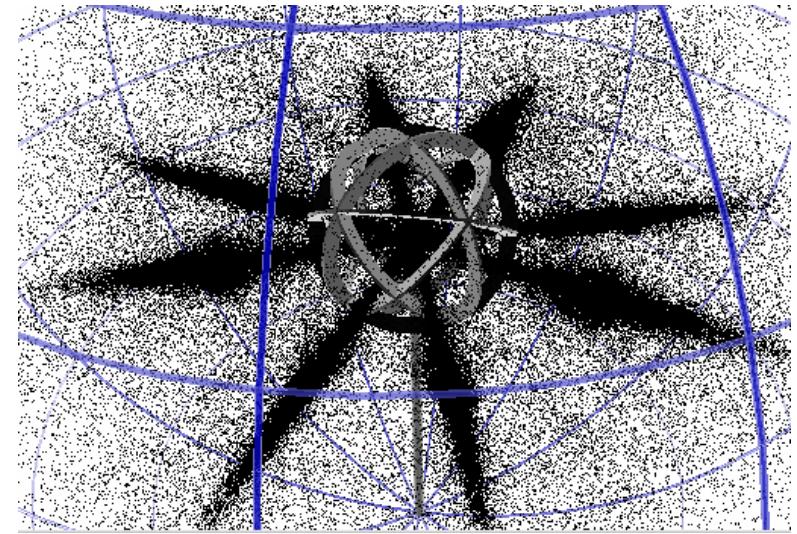


Photo of Star mode



Ionization by calculation

It is difficult to produce enough amounts of ions through a glow discharge at low pressure.

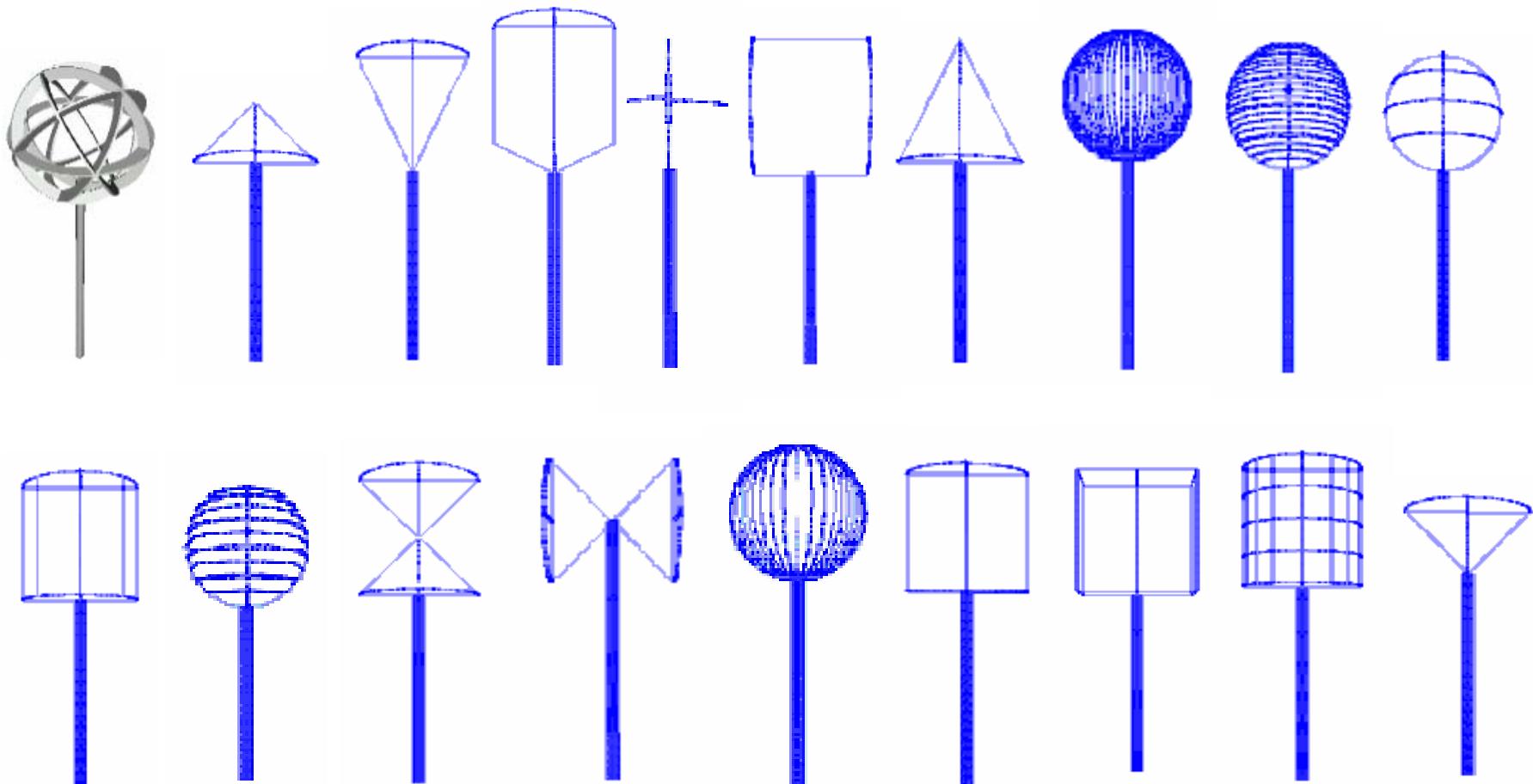
One of the solutions is to equip the ion source such as a magnetron near the anode.

However, The original cathode dose not have good performance of focusing for ion beam from ion source.

Numerical Model 2 (Orbital simulations)

We trace the trajectory of D_2^+ from ion source with the same code to test the various shape of the cathode.

Various Shapes of cathode (Orbital simulations)



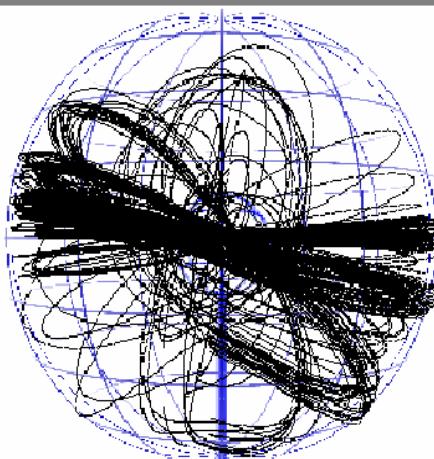
and more...

Ion Trajectories from Ion Source

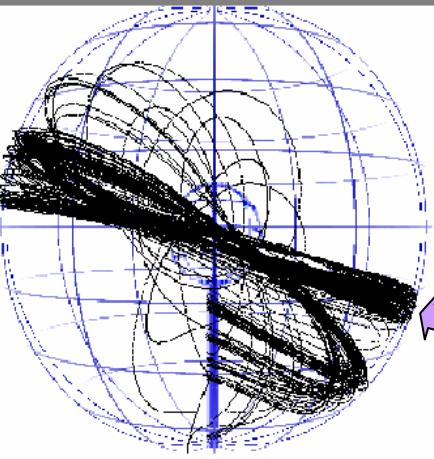
(Orbital simulations)



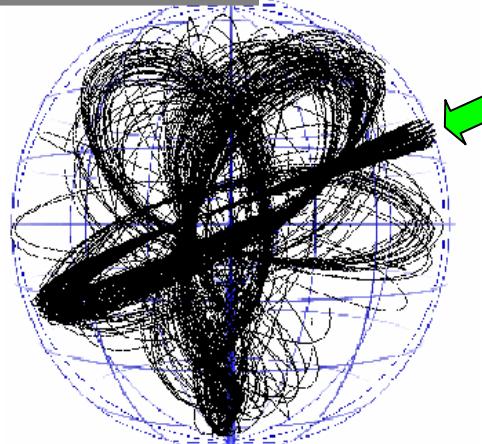
Original
Cathode



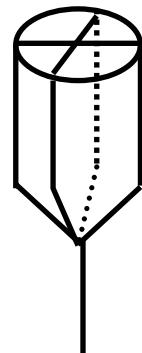
(2.54)



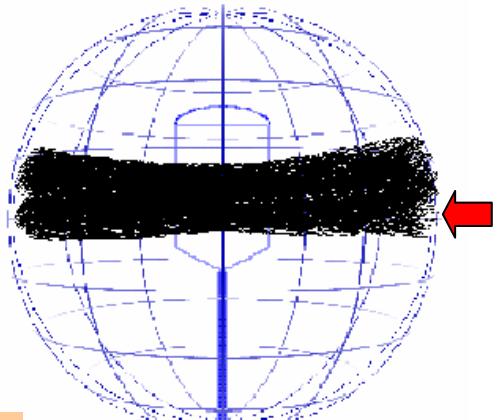
(1.50)



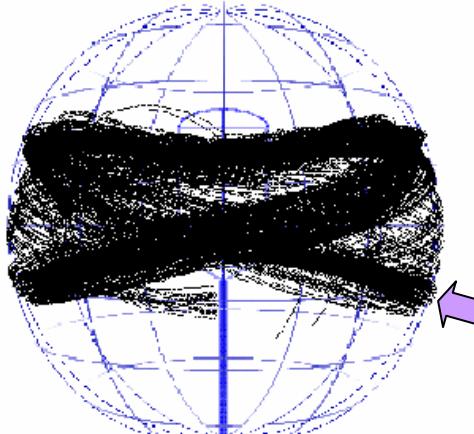
(2.01)



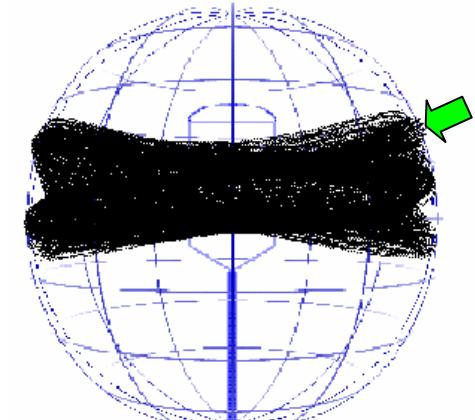
Improved
Cathode



(3.83)



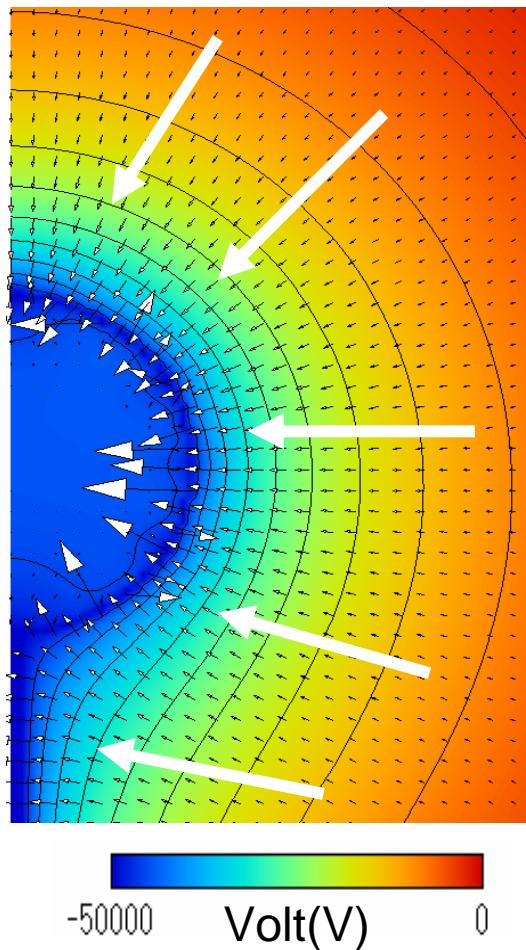
(3.75)



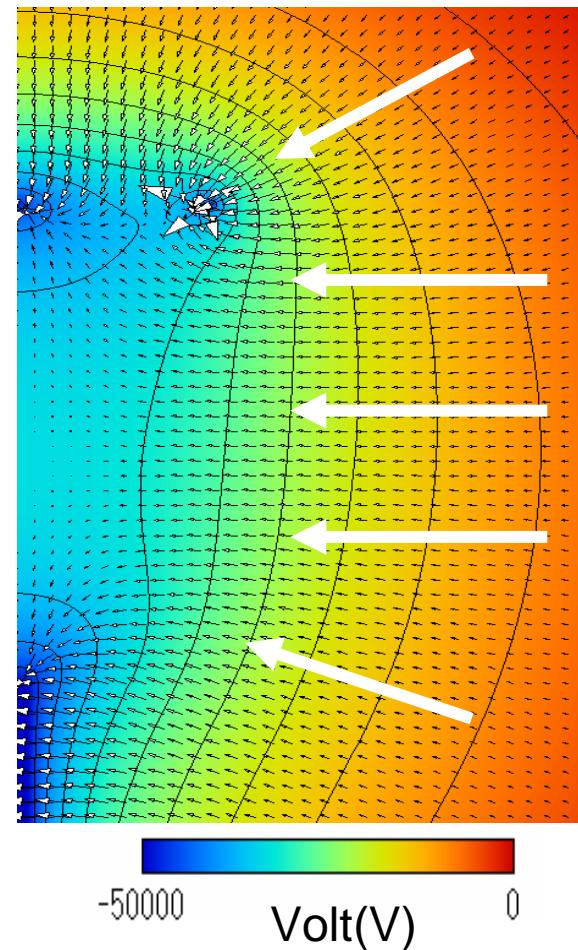
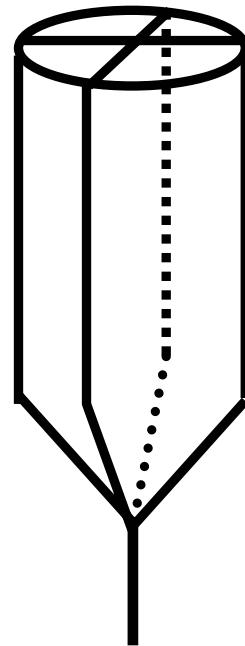
(3.81)

Equi-potential Surface near Cathode

(Orbital simulations)



Original Cathode



Improved Cathode

The area have horizontal electric field is enlarged.

Conclusions

The glow discharge pattern with several light spokes called “star mode” observed in the experiments is numerically demonstrated.

The main reaction which plays a main role of the discharge is the combination of self-multiplication reactions which produce D_2^+ ions and electrons.

The fact that the discharge at a low pressure is unstable is explained by the less multiplication rate of ions and electrons.

The improved cathode have good performance of ion beam stability for the horizontal direction.

UNCLASSIFIED

PIC Simulation of the IEC Experiment at LANL

G. Lapenta, R. Nebel, J. Park

Los Alamos National Laboratory



The World's Greatest Science Protecting America

UNCLASSIFIED



Outline

- Numerical Scheme:
 - Equations
 - Implicit Formulation
 - Immersed Boundary Method
 - Adaptation
- IEC Simulation
 - Setup of our code
 - Verification

Fundamental equations

- We consider collisionless plasmas
- Vlasov-Poisson model

- Maxwell equation

$$\begin{cases} \nabla \cdot \mathbf{E} = 4\pi\rho \\ \nabla \cdot \mathbf{B} = 0 \\ \nabla \times \mathbf{E} + \frac{1}{c} \frac{\partial \mathbf{B}}{\partial t} = 0 \\ \nabla \times \mathbf{B} - \frac{1}{c} \frac{\partial \mathbf{E}}{\partial t} = \frac{4\pi}{c} \mathbf{J} \end{cases}$$

Vlasov equation

$$\frac{\partial f}{\partial t} + \mathbf{v} \frac{\partial f}{\partial \mathbf{x}} + q(\mathbf{E} + \mathbf{v} \times \mathbf{B}) \frac{\partial f}{\partial \mathbf{p}} = 0$$

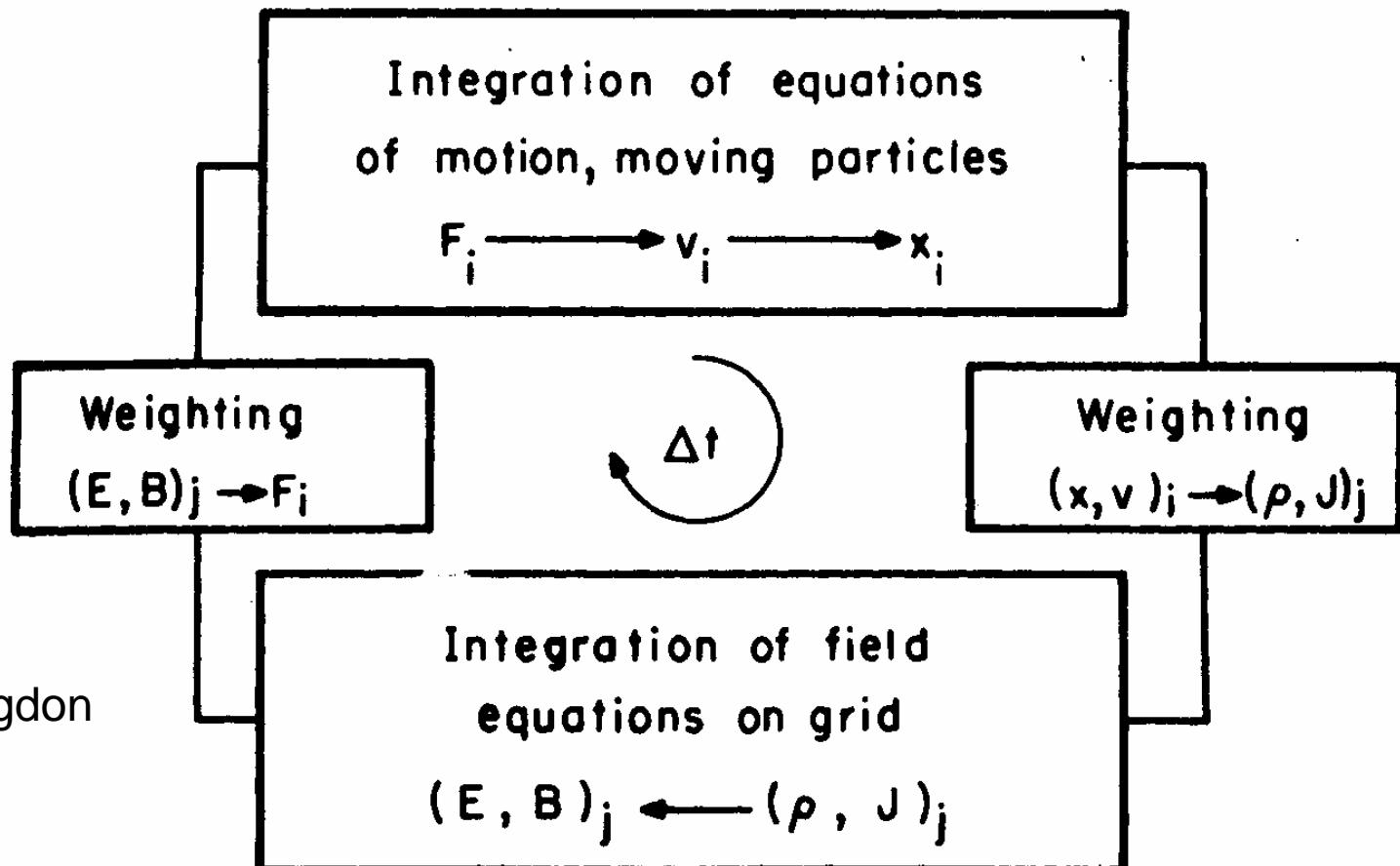
Eulerian formulation

Newton equation

$$\begin{cases} \frac{d \mathbf{x}_i}{dt} = \mathbf{v}_i \\ \frac{d \mathbf{v}_i}{dt} = \frac{q_i}{m_i} (\mathbf{E} + \mathbf{v}_i \times \mathbf{B}) \end{cases}$$

Lagrangian formulation

Explicit PIC Scheme



Birdsall & Langdon

Summary of the Stability constraints

- Time step and grid spacing limit:

- Explicit stability constraints

$$\omega_{pe} \Delta t < 2 \quad \Delta x < \lambda_{De} \quad c \Delta t < \Delta x$$

- Implicit accuracy conditions

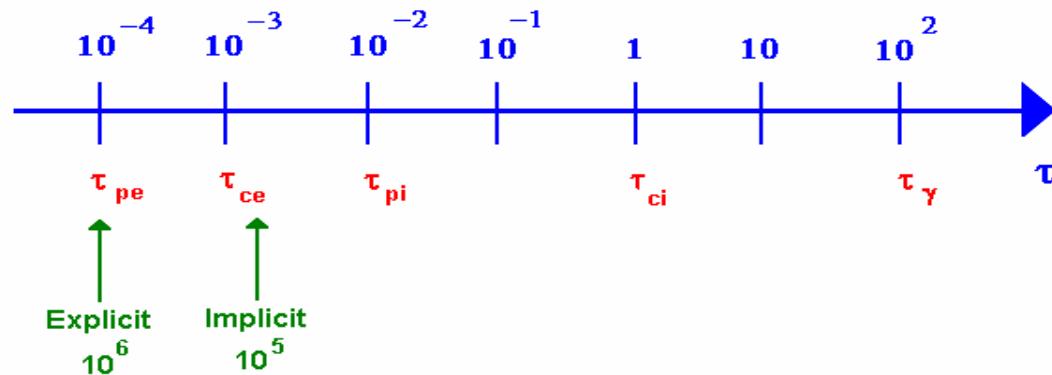
$$v_{th,e} \frac{\Delta t}{\Delta x} \quad \lambda_{De} \omega_{pe} \frac{\Delta t}{\Delta x} < 1$$

- Scaling of relative cost of explicit and implicit simulations:

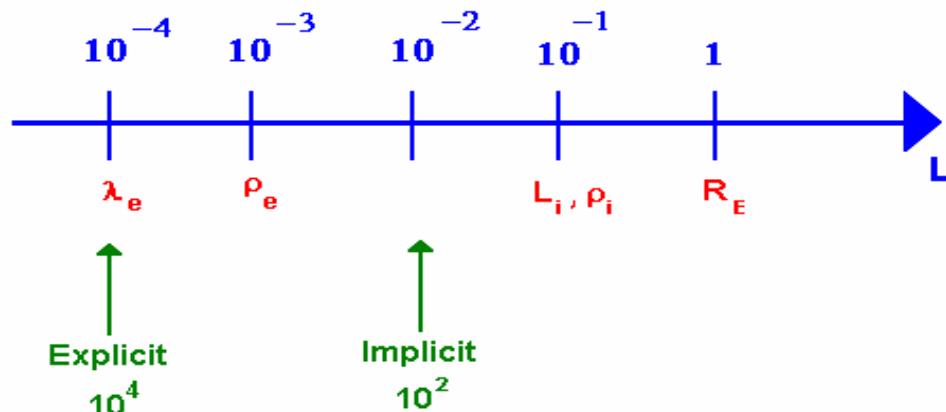
$$\left(\frac{m_i}{m_e} \right)^{\frac{d+1}{2}}$$

Scales in Implicit & Explicit PIC

- Time scales:



- Spatial scales:



Implicit PIC: Celeste

- With an implicit PIC code we adopt
 - Maxwell equations: implicit second order formulation for \mathbf{E}
 - Newton equations: implicit form
- The stability constraints of explicit PIC are removed:

$$\omega_{pe}\Delta t < 2 \quad \longrightarrow \quad \frac{\omega_{pe}\Delta t}{\Delta x/\lambda_{De}} < 1$$

$$\Delta x < \zeta \lambda_{De} \quad \longrightarrow \quad \frac{\Delta x/\lambda_{De}}{\omega_{pe}\Delta t} < \zeta$$

Divergence Equations

$$\nabla \cdot \mathbf{E}^\theta = 4\pi n^\theta$$

$$\nabla \cdot \mathbf{B}^0 = 0$$

Ampere's Law

$$\nabla \times \mathbf{B}^\theta = \frac{1}{c} \frac{\mathbf{E}^1 - \mathbf{E}^0}{\Delta t} + \frac{4\pi}{c} \mathbf{J}^{1/2}$$

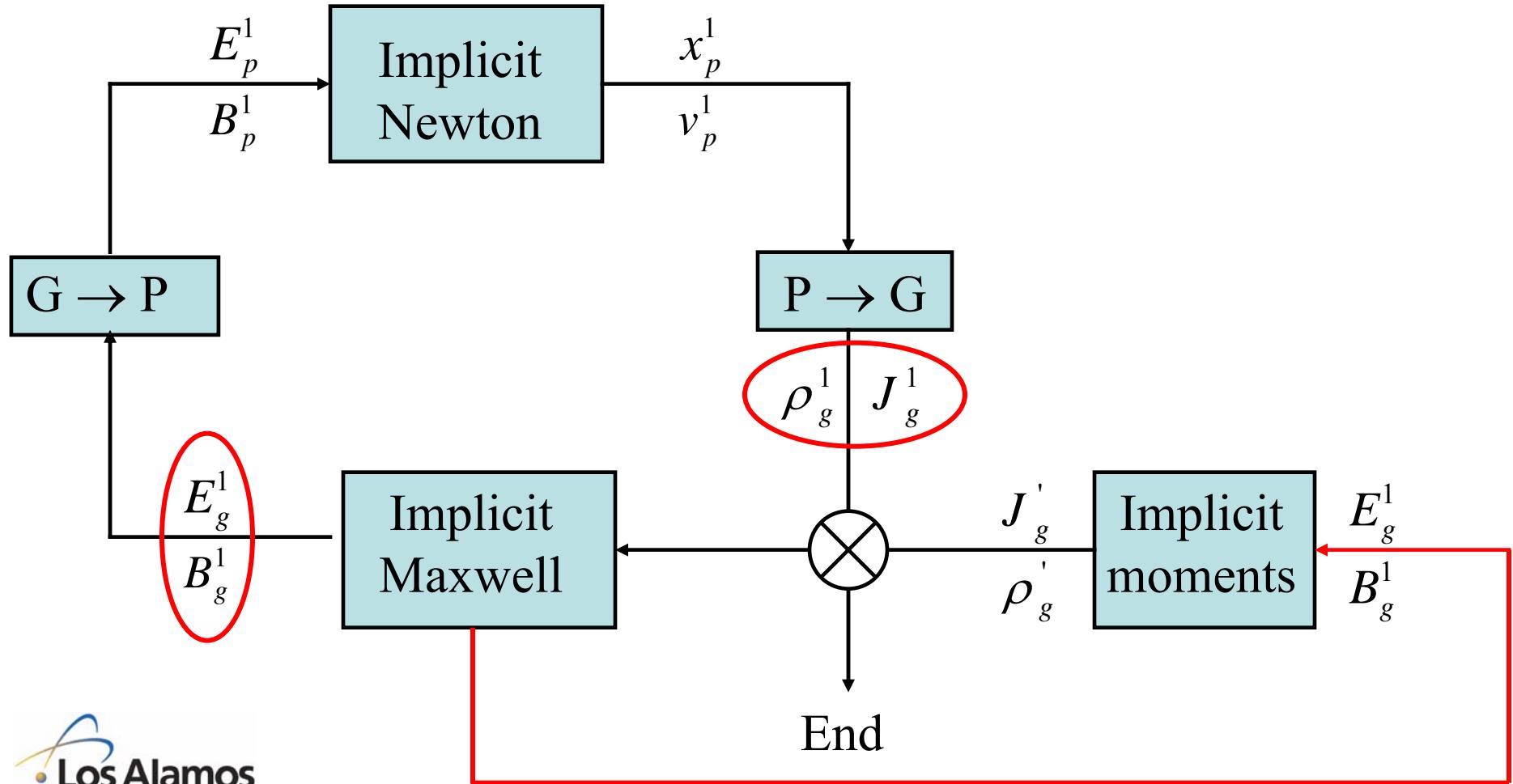
Faraday's Law

$$\nabla \times \mathbf{E}^\theta = -\frac{1}{c} \frac{\mathbf{B}^1 - \mathbf{B}^0}{\Delta t}$$

Charged Particle Equations of Motion

$$\begin{aligned} \mathbf{x}_p^1 &= \mathbf{x}_p^0 + \mathbf{u}_p^{1/2} \Delta t \\ \mathbf{u}_p^{1/2} &= \mathbf{u}_p^0 + \frac{q_s}{m_s} \left[\mathbf{E}^\theta + \frac{\mathbf{u}_p^{1/2} \times \mathbf{B}^0}{c} \right] \Delta t \end{aligned}$$

Implicit Moment method



Immersed boundary method

1. Any object in contact with a plasma is represented by particles
2. Object particles have properties to represent the real object



Objects \Rightarrow Set of object particles



Object properties \Rightarrow Properties of the object particles



Object boundary \Rightarrow Immersed boundary method

G. Lapenta et al., *IEEE Trans. Plasma Sci.*, **23**, 769, 1995.

Example: Electrostatic

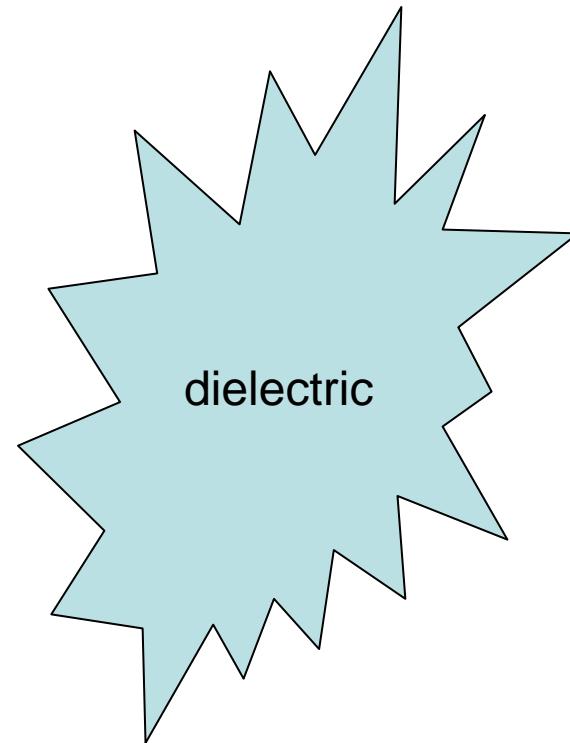
- Poisson's equation

$$\nabla \cdot \epsilon \nabla \varphi = \rho$$

- Solved everywhere
- Conductors:

$$\epsilon^{-1} \approx 0 \Rightarrow \nabla \varphi \approx 0$$

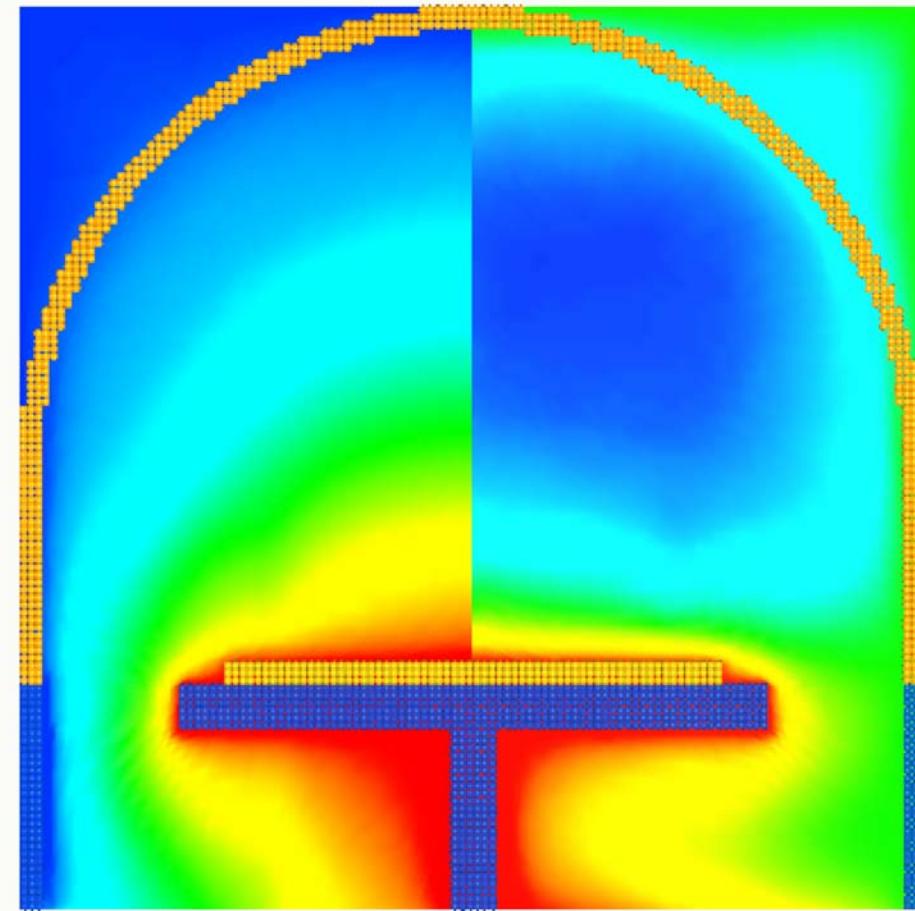
- ϵ generated by object particles



Represent object
with particles

UNCLASSIFIED

Plasma processing device



G. Lapenta et
al., *IEEE*
Trans. Plasma
Sci., **24**, 105,
1996.

UNCLASSIFIED

Grid Generation: Variational Formulation

$$\int_V e d^N x$$

THEOREM 2 In a optimal grid, defined as a grid that minimizes the local truncation error according to the minimzation principle (18), the product of the local truncation error in any cell i by the cell volume V_i (given by the Jacobian $J = \sqrt{g}$) is constant:

$$e_i V_i = \text{const} \quad (24)$$

G. Lapenta, JCP, 193, 159, 2004

UNCLASSIFIED

Equivalent Formulations

$$e(\mathbf{x}) = w(\mathbf{x})g^k \quad \frac{\partial}{\partial x^j} \left(w g^k g_{im} \frac{\partial \xi^m}{\partial x^j} \right) = 0$$

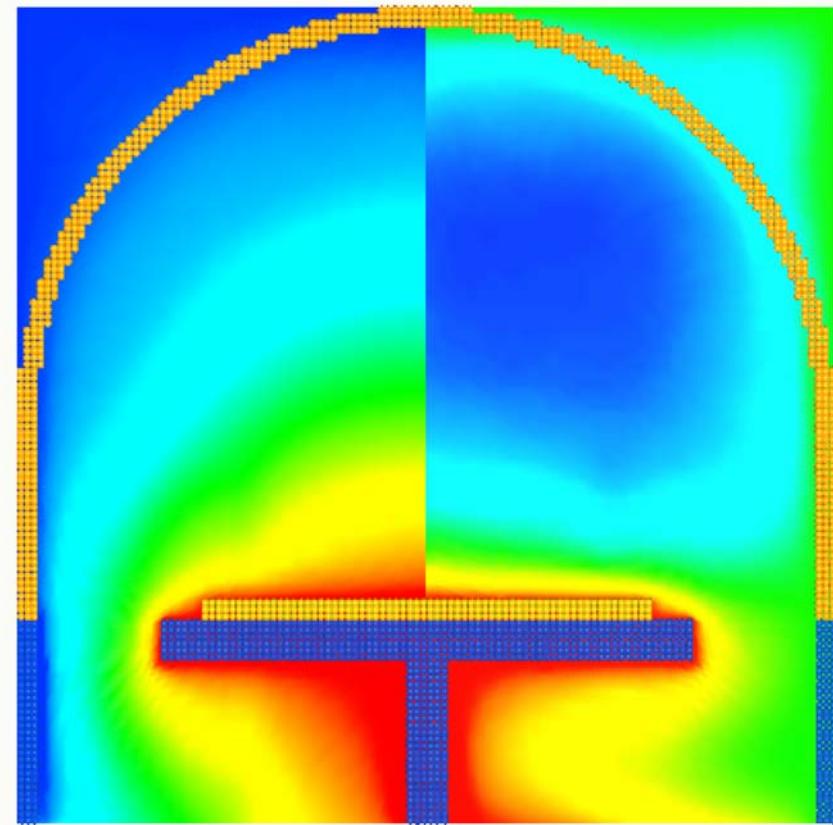
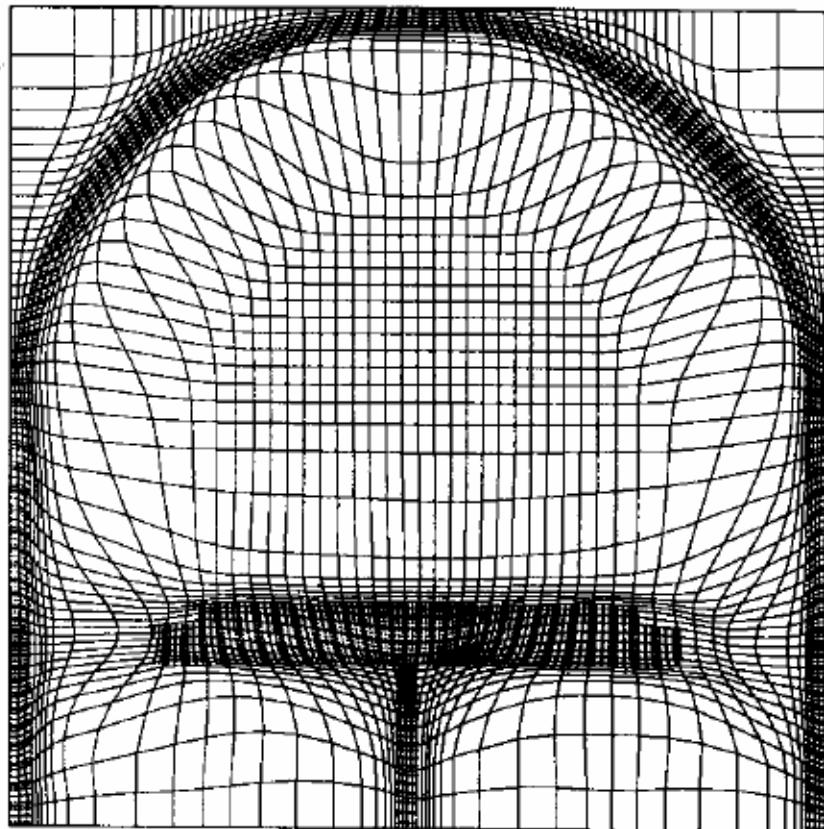
$$e(\mathbf{x}) = w_k(\mathbf{x})g^{kk} \quad \frac{\partial}{\partial x^j} \left(w_i \frac{\partial \xi^i}{\partial x^j} \right) = 0$$

$$e(\mathbf{x}) = w_{ij}(\mathbf{x})g^{ij} \quad \frac{\partial}{\partial x^j} \left(w_{ik} \frac{\partial \xi^k}{\partial x^j} \right) = 0$$

UNCLASSIFIED

UNCLASSIFIED

Example of grid adaptation



UNCLASSIFIED

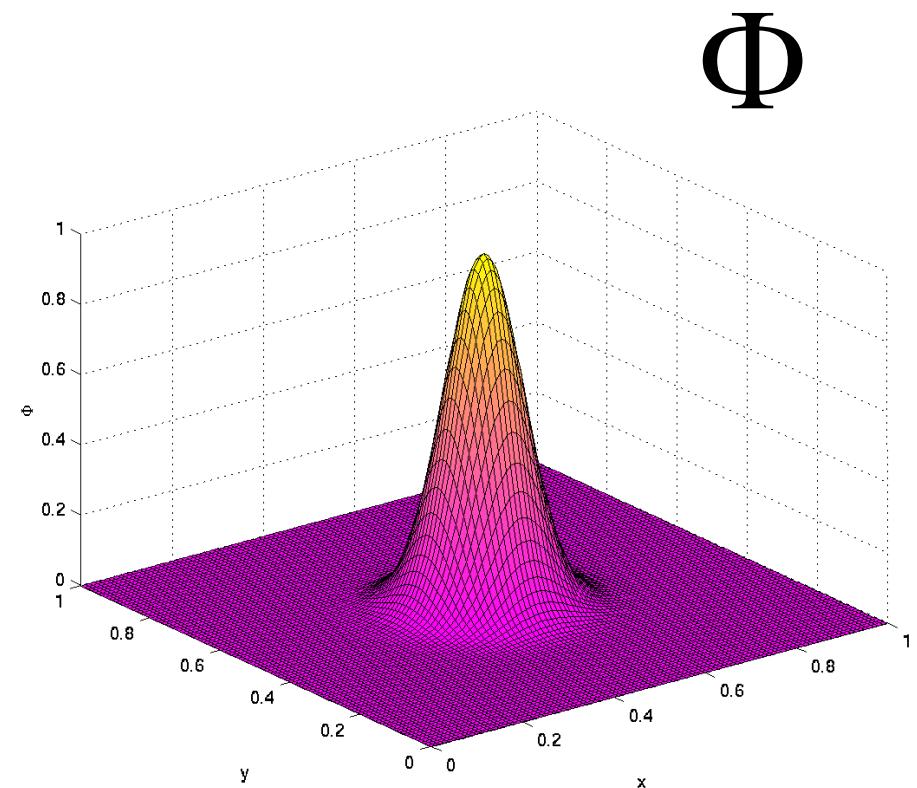
Test: Debye-Hückel

- Grid Adaptation based on
 - Error Detector
 - Heuristic guidance:

$$|\nabla \Phi| / \Phi$$

- Density considered:

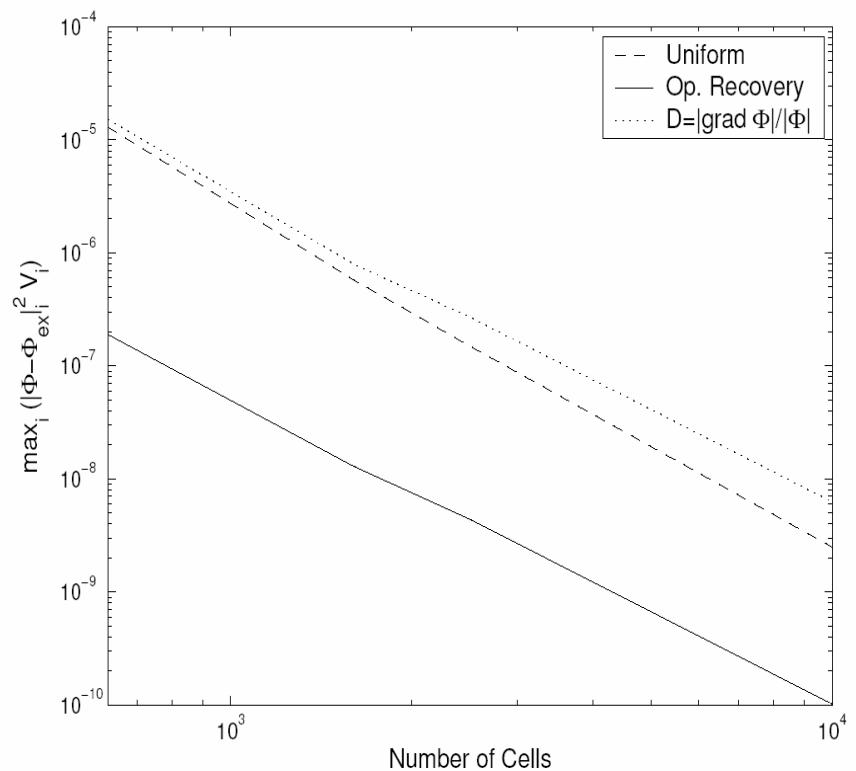
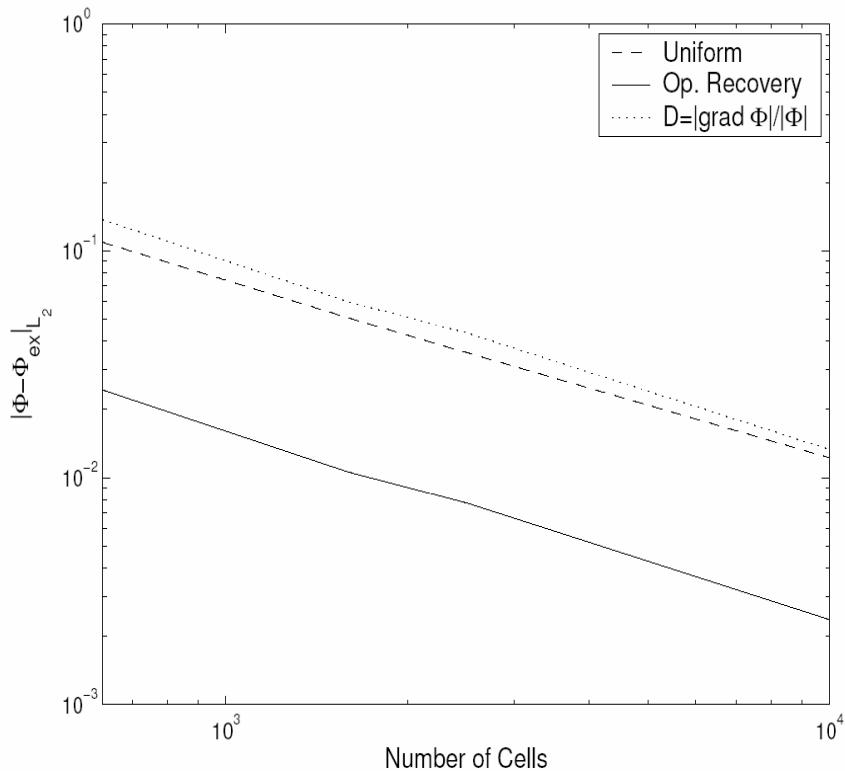
$$\rho = \left(4 \frac{\sigma^2 - r^2}{\sigma^4} - \frac{1}{\lambda_D^2} \right) e^{-r^2/\sigma^2}$$



UNCLASSIFIED

Convergence Rate

$\sigma = .1$



G. Lapenta, JCP, 193, 159, 2004

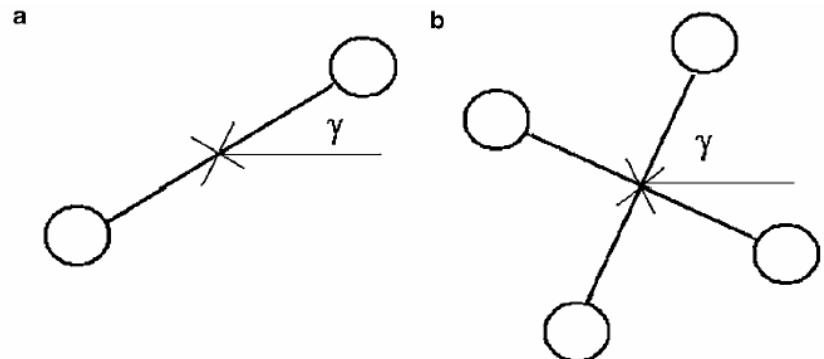
UNCLASSIFIED

Particle Adaptation

Constraints:

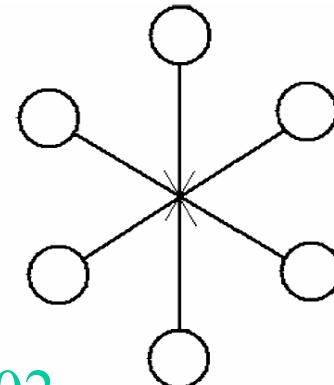
- Conservation of moments on the grid:

$$\sum_{p \in \mathcal{S}_N} \epsilon_p S_g(\mathbf{x}_p) = \sum_{p' \in \mathcal{S}_{N'}} S_g(\mathbf{x}_{p'}) \epsilon_{p'}$$



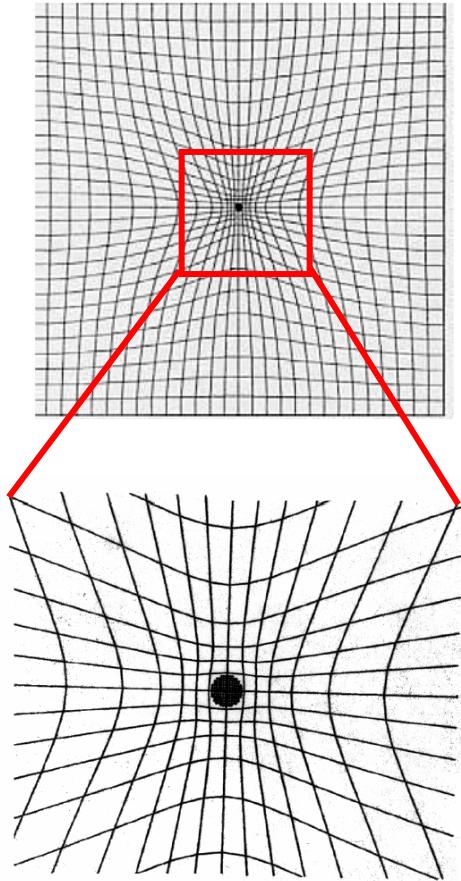
- Conservation of PdF:

$$\sum_{p \in \mathcal{S}_N} \mathbf{F}(\mathbf{v}_p) S_g(\mathbf{x}_p) q_p = \sum_{p' \in \mathcal{S}_{N'}} \mathbf{F}(\mathbf{v}'_{p'}) S_g(\mathbf{x}_{p'}) q_{p'}$$

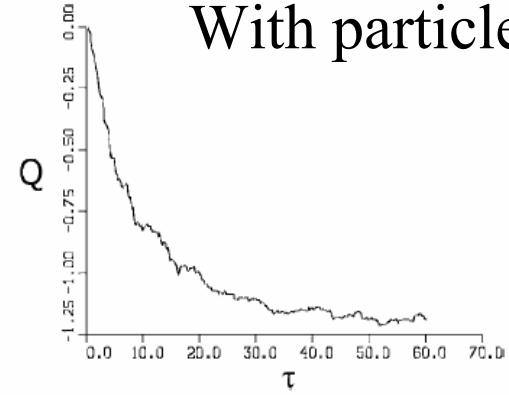


G. Lapenta, JCP, 181, 317, 2002

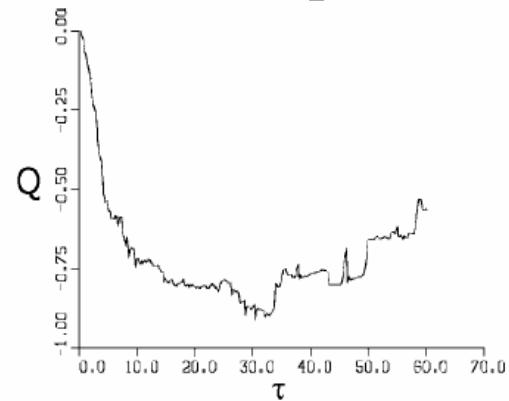
Example of particle adaptation: dust charging



With particle control



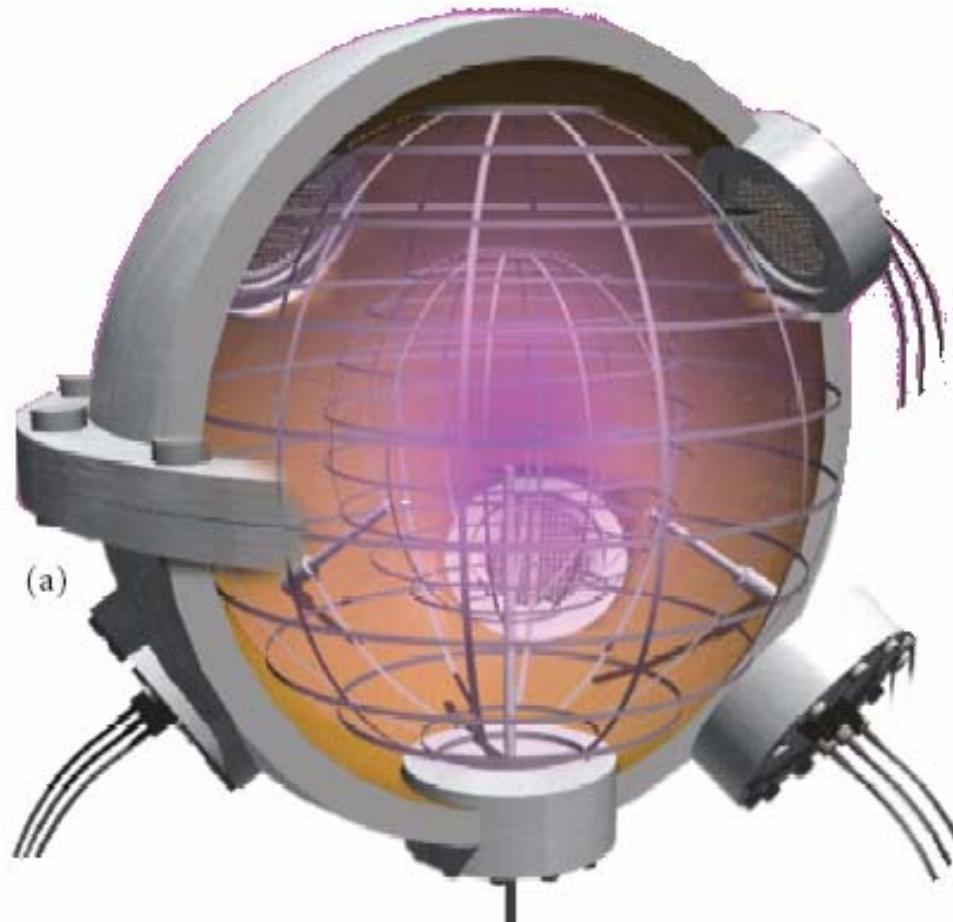
No particle control



UNCLASSIFIED

IEC @ LANL

Nebel, Barnes, Fusion Technol, **38**, 28, 1998
Nebel et al., PoP, **12**, 012701, 2005



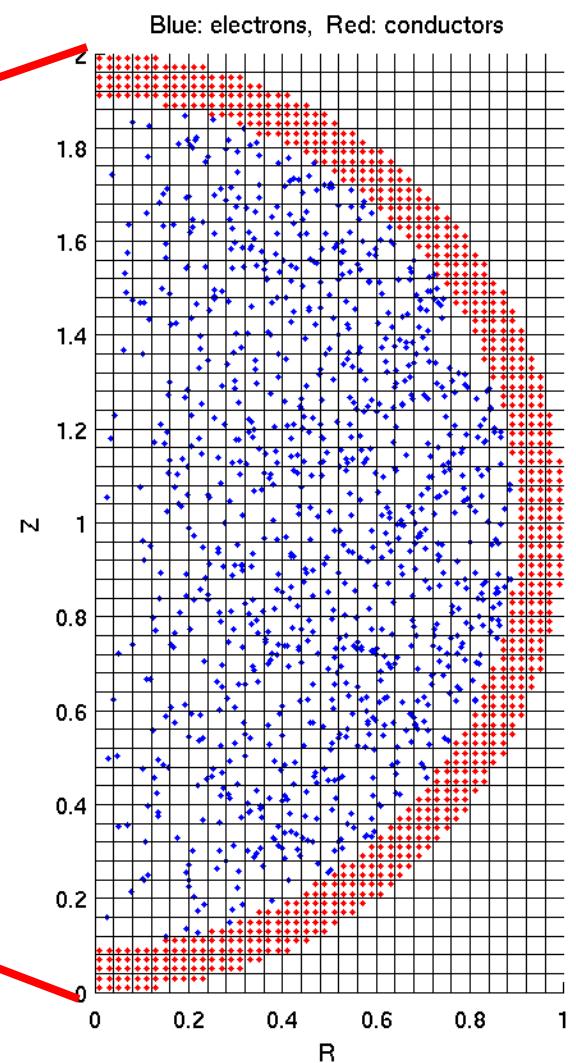
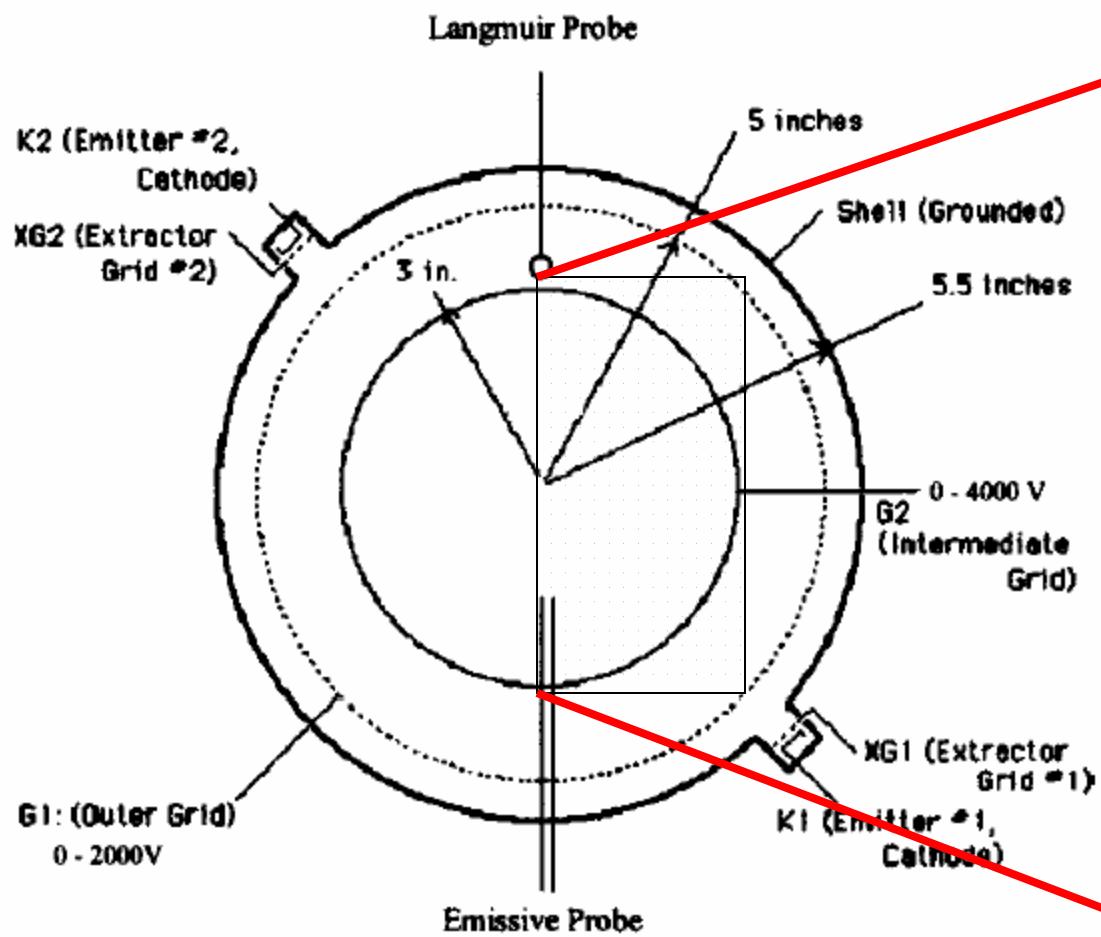
The World's Greatest Science Protecting America

UNCLASSIFIED



UNCLASSIFIED

IEC Simulation



© 2024 Sandia National Laboratories

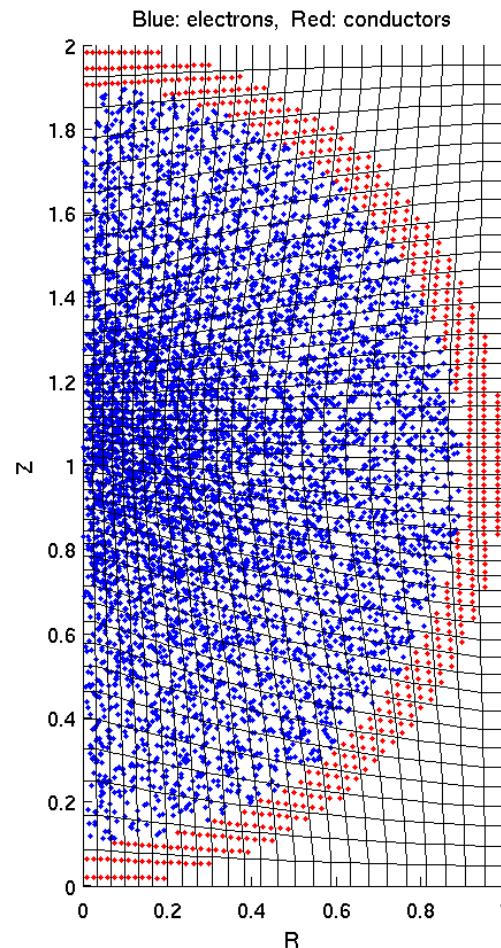
EST. 1943

The World's Greatest Science Protecting America

Self-Similar expansion of an electron cloud

- Nebel et al, PoP, 12, 012701 (2005)
- Initial uniform electron density
- Cold electrons (zero T and zero drift)
- Self-similar solution:

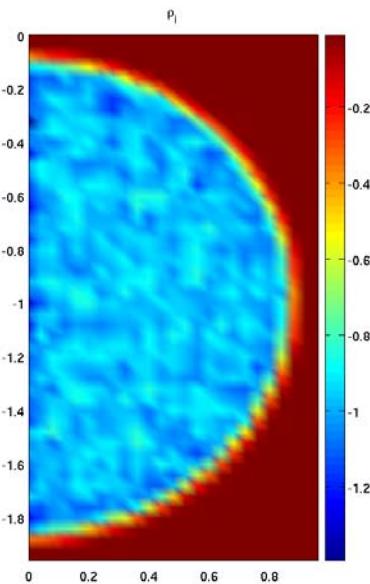
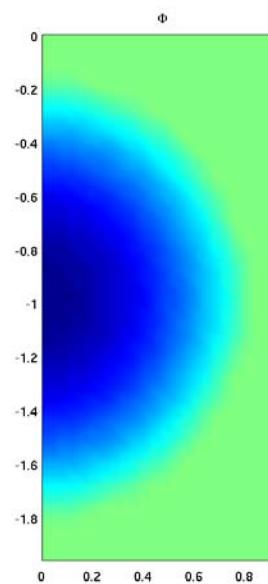
$$n_e(t) \rightarrow t^{-3}$$



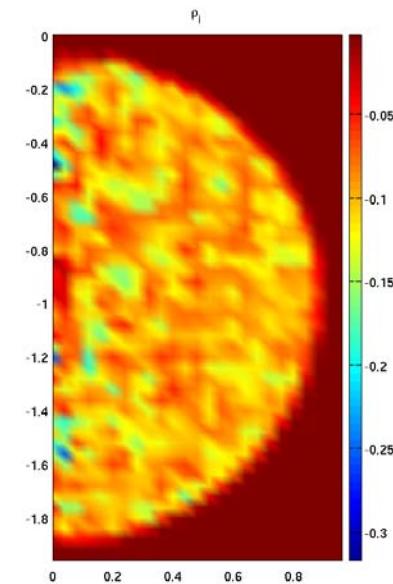
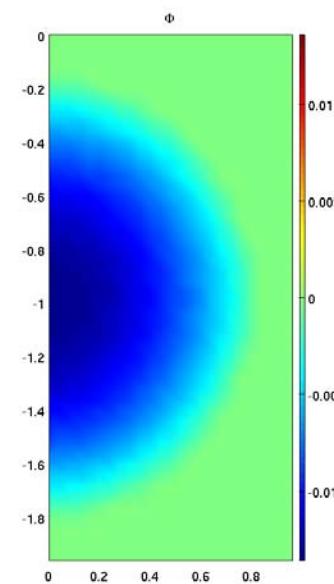
UNCLASSIFIED

End: potential and density

T=0



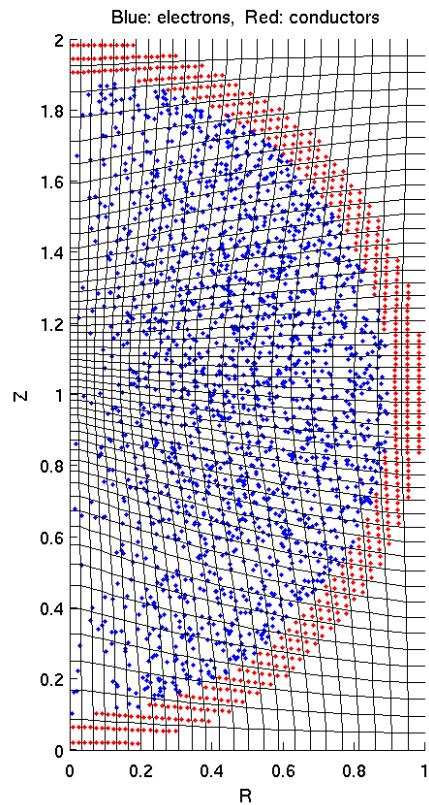
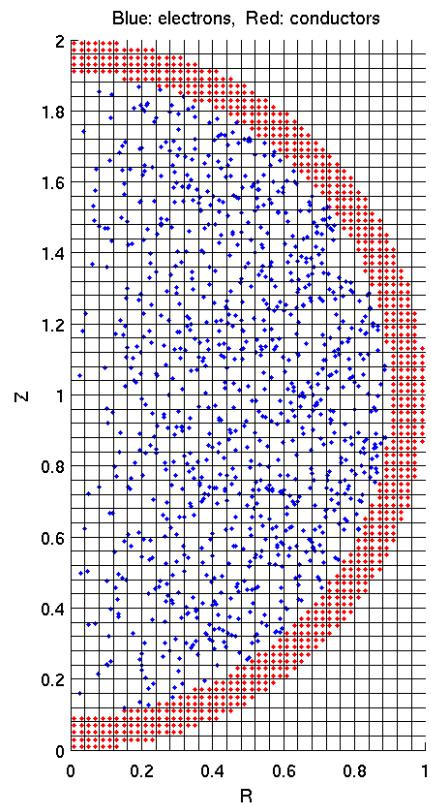
$\omega T = 6$



UNCLASSIFIED

UNCLASSIFIED

Adaptive Grid

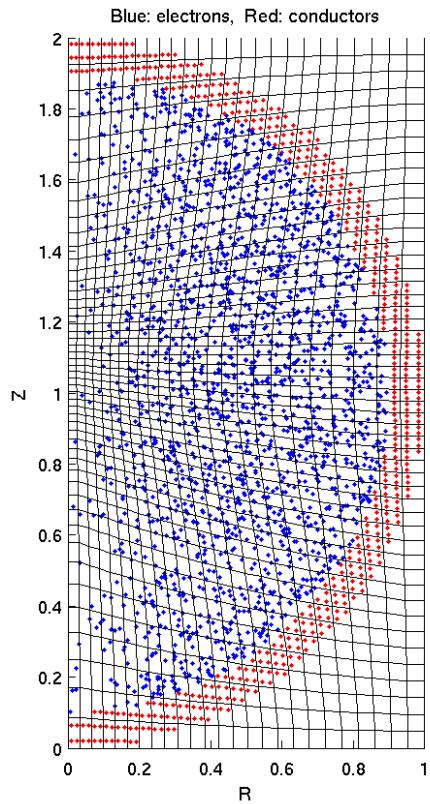


UNCLASSIFIED

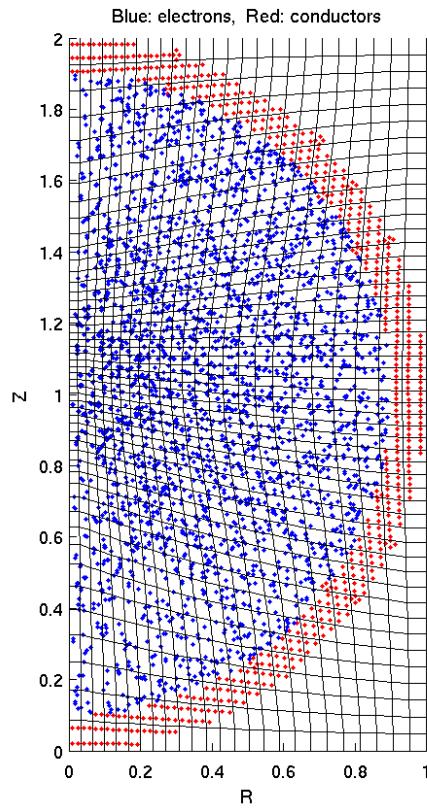
UNCLASSIFIED

Particle adaptation

Without
Particle
adaptation



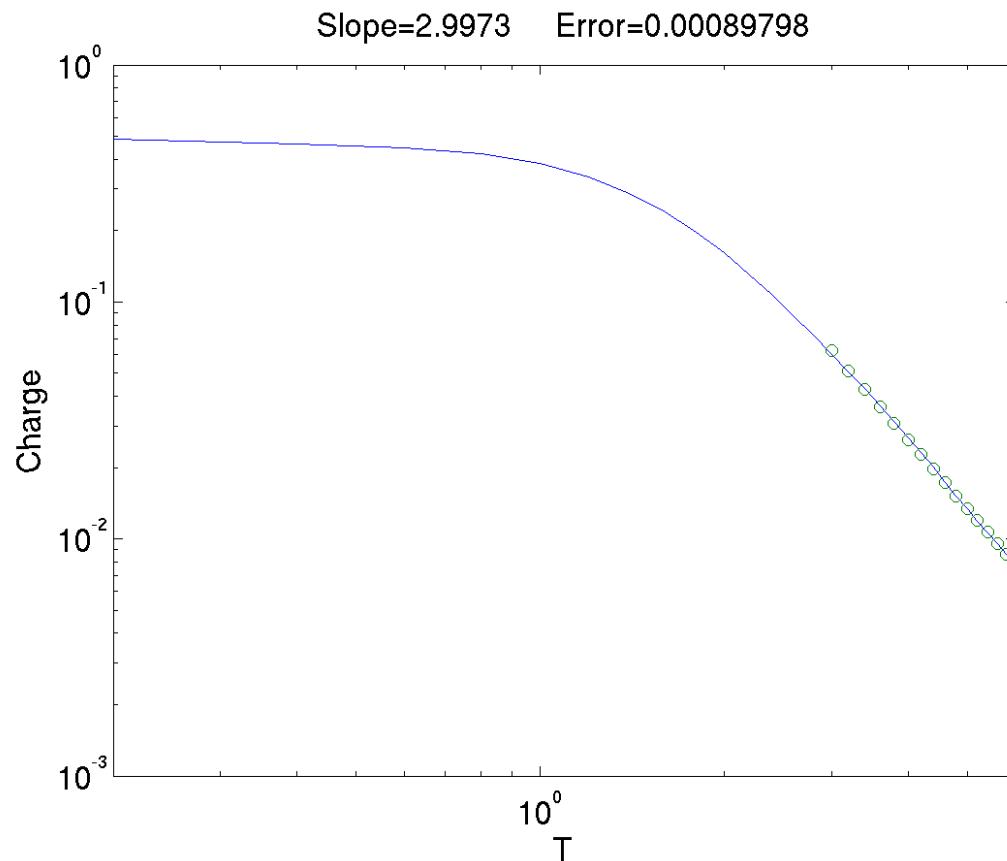
With
Particle
adaptation



UNCLASSIFIED

UNCLASSIFIED

Verification with self similar solution



Theoretical
Slope: 3

UNCLASSIFIED

Conclusions

- CELESTE is suitable to simulate IEC
 - Implicit to treat ions and electrons
 - Immersed boundary method to treat the geometry
 - Adaptive for accuracy
 - Injection for describing the electron input
- Verification
 - Unit testing
 - Longstanding use
 - IEC-relevant self-similar solution

7th U. S./Japan IEC Workshop - Perspectives



Professor Ohnishi
Professor Kulcinski

March 15, 2005



General Comments

- The ingenuity and collegiality of the IEC research groups in the U. S. and Japan continues and flourishes.
- The 10 students (out of 32 registrants) represent the continuing interest of the young generation in the development of advanced fusion concepts.
- The number of near term applications is increasing.
- The trend toward near term applications of IEC fusion technology continues with neutron interrogation of clandestine materials occupying the center of that activity.

Theory and Simulation

- More detailed models of IEC physics have been developed and are beginning to more closely describe the IEC performance. However, there is still significant work to be done.
- Important parameters that need to be measured include energy and temperature dependent secondary electron emission coefficients, ion source terms, and accurate transparency calculations.



Experimental Facilities

- Sophistication of experimental facilities is increasing.
- New cylindrical designs show promise for pulsing.
- Number of facilities with ion sources is increasing and experimental results are promising.

New Directions

- New D³He studies have been initiated.
- New ³He-³He studies are underway.
- Use of IEC facilities for fusion materials studies.



Issues

- The number of national “teams” is not increasing fast enough.
- Not enough thought (except for POPS) about ultimate power goal.
- Fusion not demonstrated in convergent core mode.
- National funding for IEC research still small.
- Need broader participation from women in IEC program.

Concluding Thoughts

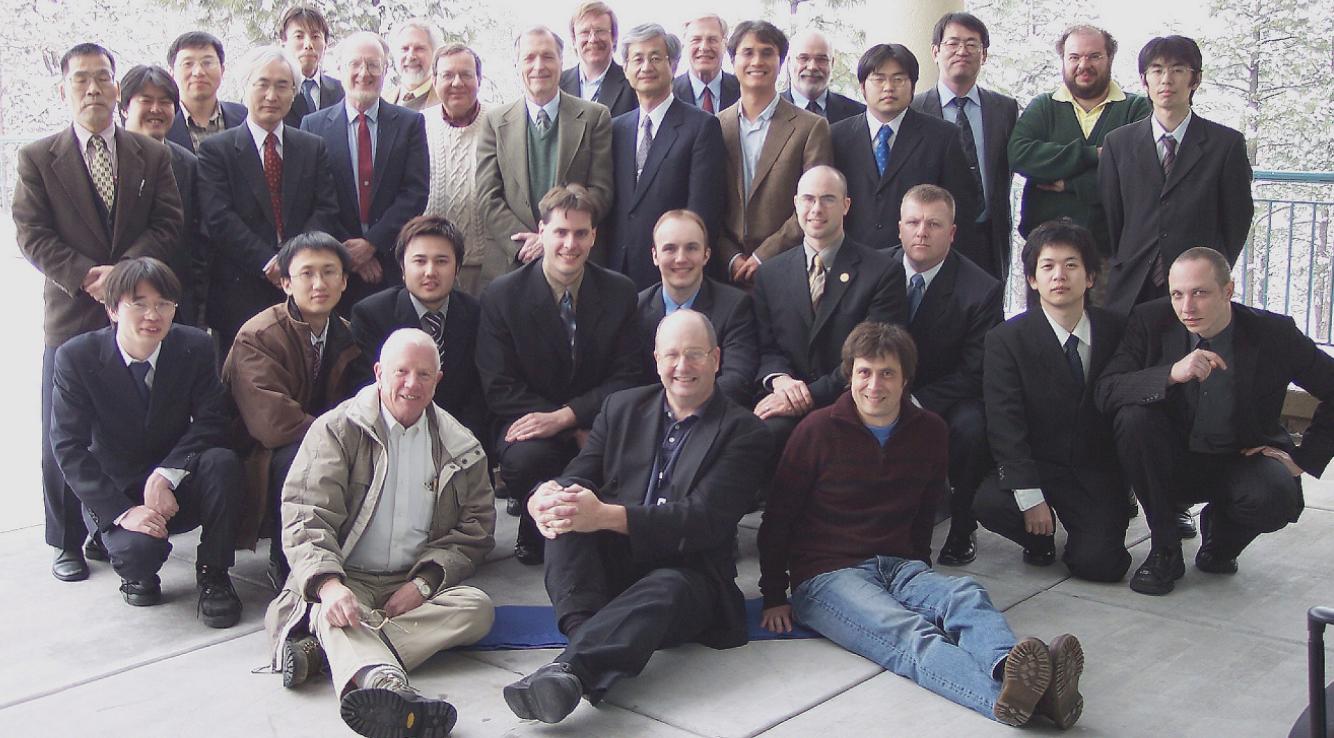
- An International IEC Project (Lab, experiment, IAEA, etc.).
- Continued communication between U. S. and Japan needs to be pursued.
- Bring in other national IEC partners?

Present Status and Future Direction of U. S./Japan Workshop

- All workshops (#1 thru #7) have been successful.
- Official title of future U. S./Japan workshop?
 - *Fusion Plasma neutron/proton and Power Generators.
 - *Near term applications of IEC fusion on the way to electrical power stations.
 - Others?

Next Workshop

- 8th workshop
- Two days in April, 2006
- At Kansai University, Osaka, Japan







Owned and Operated by
Los Alamos Commerce and Development Corporation





RANDE

